THE UNIVERSITY OF CHICAGO

DEVELOPMENT OF ENANTIOSELECTIVE REACTIONS UTILIZING NITRONES AS EFFECTIVE IMINIUM SURROGATES

A DISSERTATION SUBMITTED TO

THE FACULTY OF THE DIVISION OF THE PHYSICAL SCIENCES

IN CANDIDACY FOR THE DEGREE OF

DOCTOR OF PHILOSOPHY

DEPARTMENT OF CHEMISTRY

BY

TESSA LYNCH-COLAMETA

CHICAGO, ILLINOIS

JUNE 2021

ABSTRACT

Development of Enantioselective Reactions Utilizing Nitrones as Effective Iminium Surrogates

Tessa Lynch-Colameta

Natural products are the source of many valuable folk medicines and pharmaceutical agents used throughout the world every day. However, due to their structural complexity, short and efficient syntheses of natural products are still a challenge to perform in the laboratory setting. Thus, there is always a need for new methodology developments to enhance our ability to execute effective total syntheses. In the pursuit to construct biologically significant alkaloids and other nitrogen-containing compounds of importance, there are numerous synthetic problems that cannot be easily solved using traditional imine or iminium chemistry. Nevertheless, nitrones, which are rapidly prepared, relatively stable and quite reactive, are known to be competent imine or iminium cation surrogates in a range of reactions. In this dissertation, we detail our efforts to develop Mannich-type and Pictet–Spengler-type reactions by engaging nitrones to achieve superior results to their iminium congeners.

Hence, Chapter 1 will provide a brief introduction into nitrone chemistry. To begin, the methods commonly used for the synthesis of nitrones will be described. Then, while there are many types of transformations that nitrones can undergo, this section will focus on reactions of nitrones as electrophiles that lead to *N*,*N*-disubstituted hydroxylamines. More specifically, asymmetric reactions will be of particular interest. Our intent is not to comprehensively cover nitrone chemistry, but to highlight some useful examples to demonstrate the current state-of-the-art chemistry available and what general challenges still exist in this area.

Chapter 2 will present our investigations into Mannich-type reactions of cyclic nitrones. Though 2-substituted and 2,6-disubstituted piperidine moieties are found in an array of natural products and synthetic drugs, there are only a finite number of approaches for the synthesis of such compounds. Within, is described two distinct Mannich-type reactions capable of generating β-*N*-hydroxy-aminoketones in both a racemic and asymmetric format. The first procedure uses β-ketoacids under catalyst-free conditions, while the second employs methyl ketones in the presence of chiral thioureas. Both processes have broad scope, with the latter providing products with high enantioselectivity (up to 98% *ee*). The combination of these methods, along with other critical steps, has enabled 8-step total syntheses of the 2,6-disubstituted piperidine alkaloids (–)-lobeline and (–)-sedinone.

Next, in Chapter 3, we will detail our work on the synthesis of aza-quaternary centers via Pictet–Spengler reactions of ketonitrones. Despite substantial investigation into the synthesis of β-carbolines, due to their diverse medicinal properties and complex structures, effective methods to access aza-quaternary centers through direct Pictet–Spengler reactions remain limited. Herein, we report on the discovery of a facile procedure that utilizes a broad variety of ketonitrones activated by commercially available acyl chlorides to readily induce such Pictet–Spengler reactions. Notably, the reaction process is mild, fast, and high-yielding (54–97%) for a collection of >40 substrates. In addition, an asymmetric variant of the process with good levels of enantioselectivity (up to 83% *ee*) was established by deploying an acyl bromide in combination with a thiourea promoter. Lastly, the products can also be transformed in a number of distinct ways by taking advantage of the resultant N–O bond, affording valuable complementarity to existing Pictet–Spengler variants based on the use of imines.

Finally, Chapter 4 will reveal our current efforts in the exploration of iso-Pictet–Spengler reactions utilizing ketonitrones. During the last decade, iso-Pictet–Spengler reactions have been of interest to provide access to underexplored indole core structures, which may have considerable potential as drug candidates. In spite of this, much of the pioneering work focused on the formation of aza-tertiary centers, instead of the arguably more challenging aza-quaternary centers. The sparse examples that create aza-quaternary centers require stoichiometric chiral reagents and/or very specific substrate control for the cyclization to successfully occur with high enantioselectivity. Here, is proposed the development of several catalytic, enantioselective iso-Pictet–Spengler reactions that are capable of producing three distinct scaffolds with aza-quaternary centers and diverse substrate scopes. To achieve this, we envision employing the power of organocatalysis and the unique reactivity of nitrones.

TABLE OF CONTENTS

LIST OF FIGURES

LIST OF TABLES

LIST OF SCHEMES

LIST OF ABBREVIATIONS

Ac	acetyl
Ar	aryl
Bn	benzyl
Boc	*tert*-butyloxycarbonyl
Bz	benzoyl
CIDR	crystallization-induced dynamic resolution
COSY	correlated spectroscopy
DIAD	diisopropyl azodicarboxylate
4-DMAP	4-dimethylaminopyridine
DMSO	dimethyl sulfoxide
dr	diastereomeric ratio
ee	enantiomeric excess
Et	ethyl
***i*-Bu**	isobutyl
IBX	2-iodoxybenzoic acid

***i*-Pr**	isopropyl
IR	infrared spectroscopy
Me	methyl
MS	molecular sieves
MTBE	methyl *tert*-butyl ether
Nap	naphthalene
NMR	nuclear magnetic resonance
NOESY	nuclear Overhauser effect spectroscopy
Ph	phenyl
Piv	pivaloyl
TBDPS	*tert*-butyldiphenylsilyl
TBS	*tert*-butyldimethylsilyl
Tf	trifluoromethylsulfonyl
TFA	trifluoroacetic acid
THF	tetrahydrofuran
TMPDA	*N*,*N*,*N*′,*N*′-tetramethyl-1,3-propanediamine
TMS	trimethylsilyl
***p*-Tol**	*p*-tolyl

DEDICATION

This dissertation is dedicated to my mother, Mary Lynch-Colameta, in loving memory. She could not be here for the journey, but I know she would have been proud of each step along the way.

ACKNOWLEDGEMENTS

Although I would need many more pages to thank everyone who helped me get here, I would like to acknowledge the following people for their continued encouragement and support throughout my journey to and during my Ph.D. studies at the University of Chicago.

Prof. Scott Snyder for being a magnificent mentor and principal investigator during the last five years. Your empathy and dedication to all of your students inspires me every day. Without a committed mentor like you, I would not be where I am today and will forever be grateful for the time I had in your laboratory. Thank you for having faith in me during my "not optimal" times.

The Snyder Group for constantly enhancing my chemistry knowledge, providing a welcoming and fun work environment, and challenging me to grow as a person.

Dr. Charles Cole, Philipp Gemmel, Sohee Kim, Dr. Lilia Fuentes, Cooper Taylor, and Russell Kielawa for being the most supportive labmates and friends. I would have been lost without all of you. Additional thank you to **Charles, Phil, Cooper, and Russell** for editing chapters of my dissertation.

Dr. Samantha Maki, Cheng Peng, Pei Qu, Heng Yi, and Dr. Fangjie Yin for being exceptional labmates during a pandemic, I enjoyed our daily conversations during such a stressful time.

Dr. Yuan Zhang, Dr. Zhiyao Zhou, and Prof. Hyung Min Chi for going above and beyond as colleagues and friends, especially during my first year to help me prepare for my candidacy exam.

Dr. Alison Gao and Dr. Pei Gan for being my role models when I was a first year and all your guidance and friendship since then. Also, to **Alison** for being a wonderful host at visit weekend, which really helped me decide which school to attend for my graduate studies.

Dr. Vladislav Lisnyak for being a talented collaborator, having many productive discussions about my research, and introducing me to the beauty of nitrone chemistry.

Dr. Christoph Lentsch for being my first mentor in the Snyder group and greatly enhancing my scientific abilities to set me on a path for success.

Ian Hsu for being a great, hardworking undergraduate collaborator and friend during my first year.

Elizabeth Kelley and Josie Little for entrusting me as your mentor in your early studies.

Sarah Greta and Olivia Morales for being the best undergraduate collaborators that a graduate student could ask for. It was a delight to be your mentor and watch you both blossom into independent chemists. I wish you all the best in your future careers.

Prof. Guangbin Dong and Prof. Viresh Rawal for serving on my committee, reading my dissertation, and general guidance throughout my time in the program.

My collaborators Sarah Zinn, Prof. Greg Engel, Stephen Hansknecht, Prof. Steven Sibener, and Dr. Jeffrey Vieregg for allowing me to work on new and exciting chemistry with all of you that I otherwise would not have been exposed to.

Shinyoung Choi, Dr. Ki-Young Yoon, and Alexander Rago for your friendship throughout the years and help with late-night chemical borrowing. The collegiality between our groups dramatically enriched my experience at the University of Chicago.

Brooke Schuster and Tamara Schuster for giving me a home away from home and lasting friendships. I must also thank **Brooke** for bringing my cat, Fatty, into my life.

Laura Tociu and Kate Berger for being caring and fun friends during graduate school.

Women in Chemistry Board (Sarah Brown, Julia Murphy, and Nan Pon; 2018-2019) for working with me to create a more supportive environment for the non-male identifying members of the department. Our time on the board together was a highlight of my graduate career.

Directors of Graduate Student Initiatives (Sarah Brown, Ben Slaw, and Hannah Yi; 2019-2020) for being the most perfectly balanced team I ever had the pleasure of working with, and helping me survive the transition into quarantine. I truly believe our efforts made a difference.

Dr. Vera Dragisich for your honesty, advice, and laughs throughout my time in the program. Your dedication and hard work for the graduate students are appreciated more than you will ever know.

Prof. Andrei Tokmakoff for putting up with two years of quarterly, or even monthly, meetings with me when I was a "fiery" student leader. Your time and effort as Chair were greatly appreciated.

Dr. Antoni Jurkiewicz, Dr. Josh Kurutz, Dr. Jin Qin, Dr. Alex Filatov, Dr. Andrew McNeece and Kate Jesse for your help with NMR spectroscopy, mass spectrometry, and X-ray analysis.

Melinda Moore, Laura Luburich, and Mike Reedy for keeping department running.

Dr. Valerie Keller, Dr. Rebecca Loy, and Dr. Bruno Rubio for guiding me as I developed my teaching skills and always being available for a chat.

Prof. Aaron Beeler for allowing me to work in your lab as an undergraduate researcher throughout my time at Boston University. You opened the world of organic chemistry research to me.

Dr. Reem Telmesani for being my very first research mentor and inspiring me to pursue a Ph.D. in organic chemistry. You continue to inspire me with all your recent achievements.

Dr. Edwin Alfonzo, Dr. Alexis Courtney, Dr. Randolph Escobar, Kayla Myers, Rachel Rosen, and Jessie Zhen for your friendship and chemistry discussions while in the Beeler group, along

with our after-lab trips to Sunset Cantina or dancing at ‘90s nights. Also, thank you to **Rachel** for all the classes, graduate school applications, and accomplishments we experienced together.

Sam Duarte and Dr. Katie McGeough for the summer of a lifetime together as interns at Vertex Pharmaceuticals. As well as to **Sam** for being my supportive, fun roommate during our first year of graduate school. And, to **Katie** for being someone I could confide in anytime through my Ph.D.

Nathan Waal for your mentorship and guidance during my time as an intern at Vertex Pharmaceuticals and beyond. This experience was invaluable in shaping my career goals.

Dr. Jamie McCabe Dunn and Dr. Dani Schultz for your mentorship and advice during my time as an intern at Merck & Co. I aspire to be as talented and successful chemists as you both are one day and appreciate your continued support after my internship.

Ms. Lynsey Kraemer, Mr. Kraig Gustafson, and Ms. Kimberly Osborne for being outstanding educators and believing in me before I believed in myself. A special thank you to **Ms. Kraemer** for inspiring me to become a chemist when I was a high school student in your class.

Ms. Chris Hart for taking care of me and guiding me on the right path as a child.

Gabriela Aquino, Erika Dilbarian, Sasha Grodsky, Kip Strother, Stephen Wu, and Golshan Zaheri for being lifelong friends who constantly supported my dreams and brightened my darkest days. Our limited time together over the last five years was always treasured to me.

Ora Grodsky and Jonathan Rosenthal, Teri and Stephen Mitton for welcoming me into your lives and always caring for me throughout the years.

The Quarantine Four (Amanda Arnoff, Kylie Molter, and Shayla Titus) for being my number one support system through the COVID-19 pandemic. I really loved our weekly Zoom date nights.

Kiley Alpaugh for being there from the very beginning to end of this graduate school journey; there is no one else I would have wanted along for the ride. Your friendship is irreplaceable and I am lucky to have a best friend like you in my life.

My cats (Cricket, Fatty, and in memory of T.J.) for providing emotional support and joy.

My Dad (James Colameta) for encouraging my education and pursuit of a career in science.

My family for all their love and support when I was so far away from home.

CHAPTER 1

NITRONE CHEMISTRY

1.1 Synthesis of Nitrones

1.1.1 Oxidation Reactions

The term "nitrone" was first coined by Pfeiffer in 1916 as a contraction for "nitrogen ketone" due to their observed similarities with ketones.[1] Since their discovery over a century ago, nitrones (**1**) have proven to be a powerful synthetic tool.[2] In fact, there are numerous methods to access these desirable compounds. One of the most common approaches is through the use of oxidation reactions, as seen in Scheme 1.1, which are able to produce both cyclic and acyclic nitrones.

Scheme 1.1. Examples of common types of oxidation reactions utilized to form nitrones.

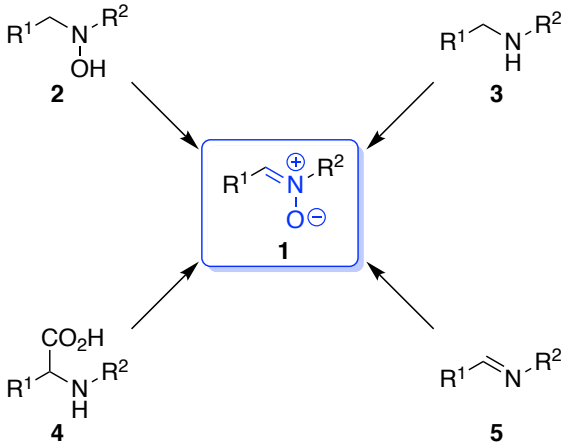

The oxidation of *N,N*-disubstituted hydroxylamines (**6**) can be easily performed using a variety of stoichiometric and catalytic oxidants (Scheme 1.2).[3] Traditionally, yellow mercury(II) oxide (HgO) has been utilized as an extraordinarily effective stoichiometric oxidant,[4] however, because of its toxicity other oxidants have been heavily explored in the last few decades. For example, manganese dioxide (MnO_2),[5] sodium hypochlorite (NaOCl),[6] 2,2,6,6-tetramethyl-1-piperidinyloxy (TEMPO),[7] and triphenylbismuth carbonate (Ph_3BiCO_3)[8] are more environmentally friendly options that can be applied on large scale. While all of these reagents can

provide good regiocontrol, 2-iodoxybenzoic acid (IBX), is typically the best oxidant for the preparation of aldonitrones in the absence of directing groups.[9]

Scheme 1.2. Oxidation of *N,N*-disubstituted hydroxylamines to nitrones.

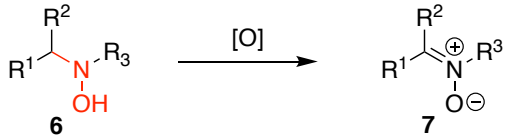

The first catalytic oxidation of *N,N*-disubstituted hydroxylamines, which deployed palladium black as the catalyst and air as the oxidant, was published by Murahashi and co-workers in 1983.[10] Since then, multiple highly efficient aerobic oxidations catalyzed by nanoparticles (such as gold nanoparticles supported on silica, unsupported nanoporous gold, and rhodium nanoparticles supported on carbon nanotube) have been reported.[11] In addition, the Goti group developed an aerobic oxidation using tetra-*n*-propylammonium perruthenate (*n*-Pr_4NRuO_4, TPAP) as a catalyst, based upon their earlier work where *N*-methylmorpholine *N*-oxide (NMO) was an oxidant with the same catalyst.[12] Another facile procedure used methyltrioxorhenium (MTO) as an exceptionally capable oxygen transfer catalyst with hydrogen peroxide (H_2O_2) or urea-hydrogen peroxide complex (UHP) as the terminal oxidant.[13]

Although the oxidation of *N,N*-disubstituted hydroxylamines has proven to be synthetically useful, the oxidation of secondary amines (**8**) to nitrones (**7**) is arguably more convenient due to the abundance of readily available amine starting materials (see Scheme 1.3). The first method for the oxidation of secondary amines was discovered by Murahashi and co-workers in 1984 utilizing stoichiometric aqueous 30% hydrogen peroxide in the presence of catalytic sodium tungstate dihydrate ($Na_2WO_4 \cdot 2H_2O$).[14] While hydrogen peroxide is cheap and environmentally friendly, it can cause issues during work-up because of the high solubility of some nitrone products in water. In those cases, UHP can be used as the oxidant instead to prevent this problem.[15] Multiple other

catalysts (1-10 mol %) can be substituted in the oxidation reaction with hydrogen peroxide, including selenium dioxide (SeO_2),[16] MTO,[17] Ti(IV) triphenolate amino complexes,[18] and Pt(II) complexes.[19] It was later reported that alkyl hydroperoxides (*tert*-butyl hydroperoxide or cumyl hydroperoxide) were also competent oxidants when combined with catalytic amounts of (trialkanolaminato)titanium(IV) complexes.[20] Though less common, it was demonstrated that the oxidation of secondary amines was possible by exploiting heterogeneous catalysts.[21] In addition, metal free versions can be executed using oxone,[22] dimethyldioxirane (DMDO),[23] Davis reagent,[24] and *m*-chloroperbenzoic acid (*m*-CPBA).[25] Finally, biomimetic flavin-[26] or cyclohexanone monooxygenase-catalyzed[27] reactions applying molecular oxygen as the oxidant have been established.

Scheme 1.3. Oxidation of secondary amines to nitrones.

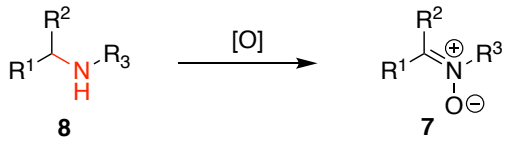

8 **7**

A method that is highly advantageous for the regioselective synthesis of nitrones (**1**) is the oxidation of *N*-alkyl-α-amino acids (**4**) (Scheme 1.4). This strategy employs hydrogen peroxide in the presence of Na_2WO_4, but also requires the addition of a phase transfer catalyst (tetraethylammonium chloride) and stoichiometric base (K_2CO_3) to succeed.[28] The ability to make a single regioisomer by way of decarboxylative oxidation allows for the synthesis of nitrones that would be quite challenging under other conventional oxidation conditions.[29]

Scheme 1.4. Oxidation of *N*-alkyl-α-amino acids to nitrones.

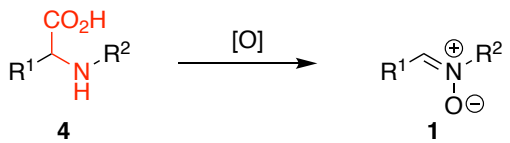

4 **1**

As shown in Scheme 1.5, the conversion of imines (**5**) to nitrones (**1**) can also be performed. For decades, the peroxyacid oxidation of imines was studied, but these reactions usually favored the formation of oxaziridines, with only a minority of cases obtaining nitrones as the major product.[30] Nonetheless, other oxidants, such as DMDO, have been found to be proficient in selectively synthesizing the corresponding nitrones.[31] The Jørgensen group also developed a method capable of oxidizing imines to nitrones in reasonable yields employing permanganate ion under phase-transfer conditions.[32]

Scheme 1.5. Oxidation of imines to nitrones.

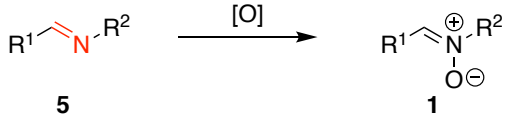

5 **1**

The first successful catalytic oxidation procedure for the oxidation of imines to nitrones was reported by Goti and co-workers in 2007.[33] This mild and high yielding method treats benzylic and cyclic imines with UHP in the presence of catalytic amounts of MTO to form the desired nitrones. They later extended this work to a one-pot protocol that promoted the condensation and oxidation of primary amines and aromatic aldehydes under the same conditions (UHP and MTO).[34]

It should be noted that there are several other less common oxidation methods available to forge nitrones, including, but not limited to, the oxidation of hydroxylamides[35] and isoxazolidines.[36]

1.1.2 Condensation Reactions

The condensation of *N*-monosubstituted hydroxylamines (**10**) with aldehydes or ketones (**9**) is a robust way to synthesize a diverse array of nitrones (**7**) (Scheme 1.6). One advantage of the condensation approach is the avoidance of poor regioselectivity observed with some oxidation

reactions. The simplest condensation procedure combines aldehydes and *N*-monosubstituted hydroxylamines in an organic solvent (typically CH_2Cl_2) in the presence of a heterogeneous drying agent (commonly $MgSO_4$).[37] Although the addition of acid can dramatically improve results, the reaction generally proceeds more smoothly with aldehydes or ketones with small R groups.[38] When trying to condense sterically encumbered ketones, it may be necessary to increase the temperature to form the corresponding nitrones.[39] Solvent-free condensation methods are also available via exploitation of a ball-mill[40] or microwave reactor.[41] Additionally, while condensation reactions are widely used to create acyclic nitrones, they can be utilized to make cyclic nitrones when the hydroxylamine and carbonyl components are appropriately placed in the same molecule.[42]

Scheme 1.6. Condensation of *N*-monosubstituted hydroxylamines with aldehydes or ketones.

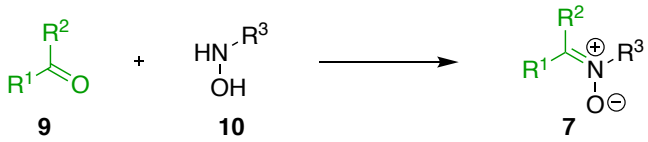

1.1.3 Other Reactions

There are various other methods available to construct nitrones, such as reactions of oximes with electrophiles and reactions of nitro compounds with aldehydes under reductive conditions, which have been comprehensively summarized in a recent review.[2e] Though relevant in their own right, these systems will not be detailed here due to their subsidiary synthetic utility in our own chemistry in comparison to oxidation or condensation reactions.

1.2 Reactions of Nitrones as Electrophiles

Despite the long history of synthetic applications of nitrones, new transformations of nitrones are continuously being disclosed. Nitrones are particularly useful in comparison with their corresponding imines or iminium ions because they are easily prepared, quite stable, and highly reactive. In addition, diastereoselective and enantioselective reactions are sometimes more facile due to the configurational stability and possible chelation effect of nitrones. Traditionally, reactions of nitrones as electrophiles[43] and 1,3-dipoles[44] were studied extensively (Figure 1.1). Yet, in the last two decades, several novel reaction classes involving nitrones have been discovered.[45] Three examples with considerable synthetic applicability are the formal [2+2] cycloaddition with terminal alkynes (the Kinugasa reaction),[46] formal [3+3]/[4+3] cycloaddition with cyclopropanes/cyclobutanes,[47,48] and SmI_2 coupling based on the umpolung reactivity nitrones.[49] However, since the focus of our work is on the reactions of nitrones as electrophiles to generate *N*,*N*-disubstituted hydroxylamine derivatives, this chapter will solely discuss that topic, with a particular emphasis on asymmetric methodology developments.

Figure 1.1. Traditional reaction types of nitrones.

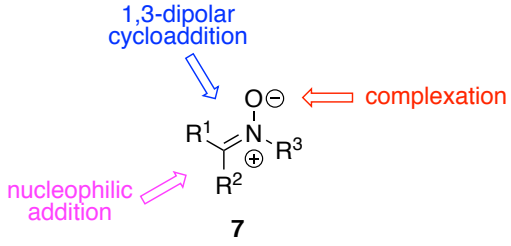

7

1.2.1 Hard and Soft Nucleophiles

The addition of nucleophiles into the highly electrophilic C=N double-bond of nitrones has been studied for well over a century now and has proven to be a formidable approach in the synthesis of biologically important nitrogen compounds (Scheme 1.7). In fact, the first report of a Grignard addition to a nitrone was published in 1911, which described the reaction of PhMgX with *N*,α-diphenyl nitrone.[50] Since then, a wide variety of nucleophiles have been investigated with prochiral nitrones, including other organometallic reagents, allylic organometallic reagents, silylated nucleophiles under Mukaiyama conditions, hydrogen cyanide, and more. Lombardo and Trombini have done an excellent job reviewing this topic.[43b]

Scheme 1.7. Nucleophilic additions to nitrones.

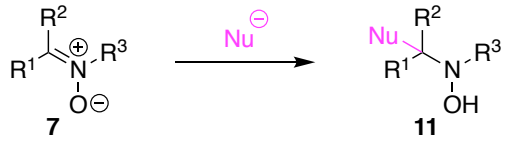

7 **11**

More impressive, though, are the investigations into stereocontrolled processes. Still, the application of asymmetric catalysis to nucleophilic additions to nitrones has proven to be a particular challenge. For instance, the incorporation of chiral additives in nucleophilic reactions with organometallic reagents was probed by the Ukaji group. They described how 3,4-dihydroisoquinoline *N*-oxide derivatives (**12**) could be reacted with dialkylzinc compounds (**13**) in the presence of catalytic chiral magnesium salts (**14** or **15**) to yield products of type **16** in high enantioselectivity (Scheme 1.8a).[51] These reactions benefit from the ability of the oxygen atom of the nitrone to strongly coordinate with metal complexes. Nevertheless, this tactic has limited applications and is very sensitive to the reaction conditions.[52] Another useful strategy is the addition of chiral nucleophiles to achiral nitrones. As shown in Scheme 1.8b, Murahashi and co-workers designed a highly diastereoselective reaction between nitrone **17** and lithiated (*R*)-(+)-

methyl *p*-tolyl sulfoxide **18** with stoichiometric quinidine as an additive for the synthesis of optically active tetrahydroquinoline alkaloids.[53]

Scheme 1.8. Stereocontrolled reactions: (a) chiral additives with organometallic compounds; (b) chiral nucleophiles.

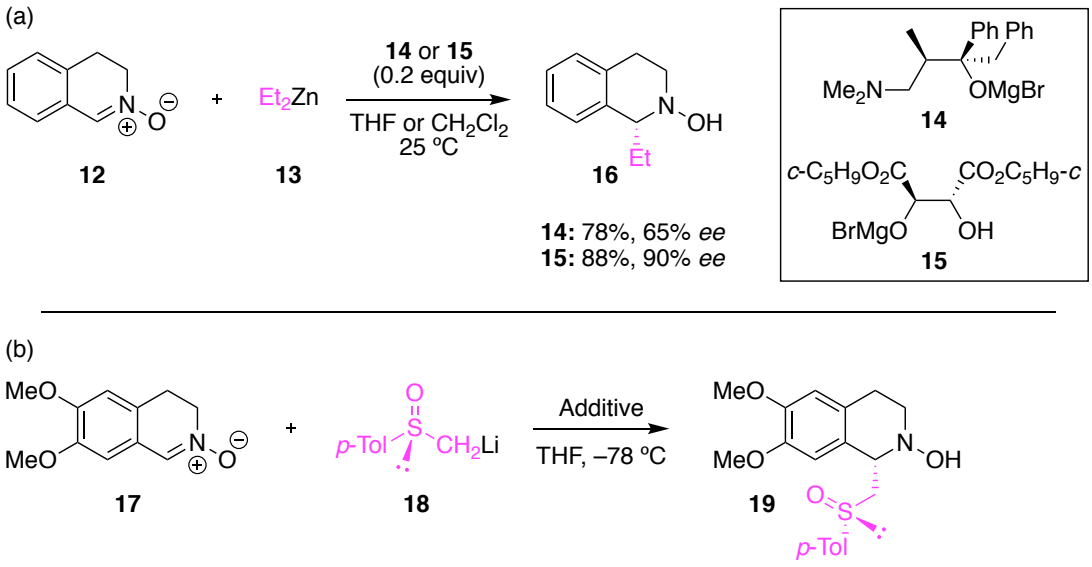

Entry	Additive	Yield (%)	*dr*
1	None	78%	64:36
2	Quinidine (1 equiv)	68%	92:8

Nonetheless, the most exhaustively studied approach for the stereocontrolled synthesis of enantiomerically pure hydroxylamines is via nucleophilic additions to chiral nitrones. In particular, Merino and Tejero heavily focused on three chiral nitrones **20**, **22a**, and **22b**, derived from protected versions of D-glyceraldehyde and L-serinal, respectively, to determine how to effectively control the diastereofacial induction for the addition of different nucleophiles (Scheme 1.9).[43] It was found that the reaction of α-alkoxynitrones (**20**) with a variety of organometallic reagents gave rise to the *syn* product. The same trend was noted when zinc (II) bromide ($ZnBr_2$), magnesium (II) bromide ($MgBr_2$), trimethylsilyl triflate (TMSOTf), or trimethylchlorosilanes (TMSCl) were utilized as promoters (α-chelation model, *Re* attack). Yet, when diethylaluminum chloride (Et_2AlCl), boron trifluoride etherate ($BF_3 \cdot OEt_2$), or titanium (IV) chloride ($TiCl_4$) were used as

precomplexing agents (at β-oxygen, *Si* attack), a reversal in selectivity was observed favoring the *anti* adduct. This Lewis acid modulated stereocontrol was extended to other α-alkoxynitrones as well. Unlike for **20**, the stereocontrol of α-aminonitrones (**22**) was not affected by different Lewis acids. Instead, the type of protection of the α-amino substituent dictated the stereochemical outcome of the reaction. Ultimately, it was determined that diprotected nitrones (**22a**) preferentially generated the *syn* product, while monoprotected nitrones (**22b**) greatly favored the formation of the *anti* product regardless of whether Lewis acid additives were included. This is just one example of the power of chiral nitrones in the synthesis of nitrogen-containing compounds of importance, but further information about reactions with chiral nitrones can be found in several exceptional reviews.[2c,43]

Scheme 1.9. Diastereoselectivity outcomes with chiral nitrones **20** and **22**.

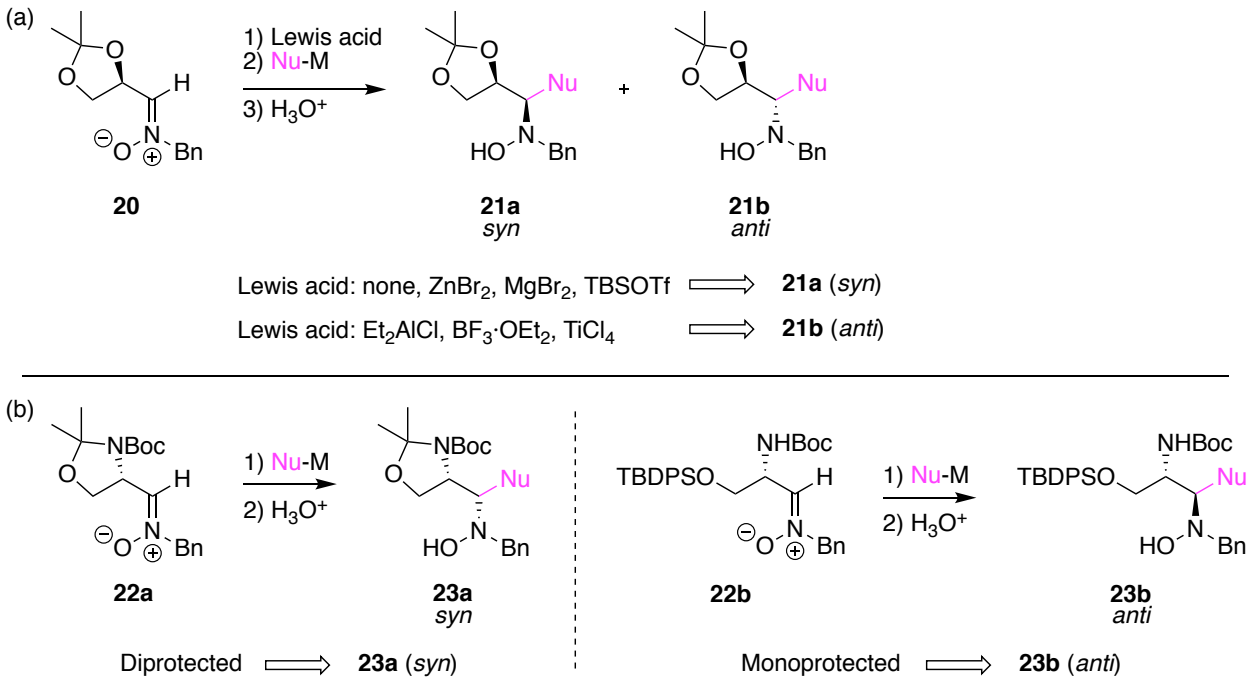

Table 1.1. Selected reactions of nitrones with nucleophiles *via N*-benyloxyiminium ions.

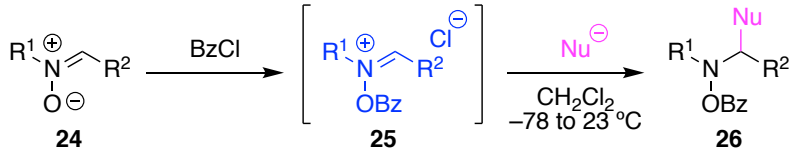

24 **25** **26**

Entry	Nitrone	Nucleophile	Product	Yield (%)
1	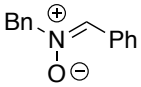 **27**	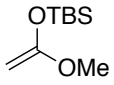 **28**	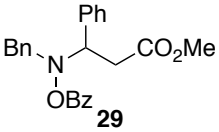 **29**	99
2	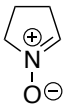 **30**	**28**	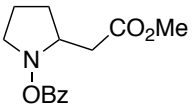 **31**	92
3	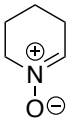 **32**	**28**	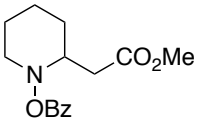 **33**	68
4	**27**	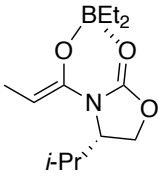 **34**	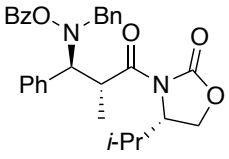 **35**	82 *anti* (80:20 *dr*)
5	**27**	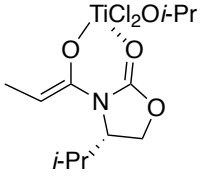 **36**	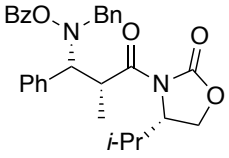 **37**	69 *syn* (84:16 *dr*)

Notwithstanding the impressive chemistry that has been explored with hard carbon nucleophiles, soft carbon nucleophiles, such as enolates, do not react as readily with nitrones and pose an additional challenge. Typically, these Mannich-type reactions are promoted by Lewis acids (similar to Scheme 1.9).[43d] However, it was shown that if nitrones such as **24**, are transformed into their corresponding *N*-acyloxyiminium ions (**25**), their reactivity is greatly enhanced and can rapidly undergo nucleophilic attack to produce adducts of type **26** (Table 1.1).[54] The *N*-

acyloxyiminium species formed *in situ* is compatible with a range of less reactive nucleophiles and can even be used in diastereoselective reactions with chiral boron enolates (**34**) and chiral titanium enolates (**36**). This method was also applied to the asymmetric synthesis of indolizidine alkaloids.[54b] In 2002, Murahashi and co-workers found the first enantioselective addition of silyl ketene acetal **28** to nitrones (**38**) catalyzed by a chiral titanium complex (prepared from Ti(O-*i*-Pr)$_4$, (*S*)-BINOL, and *tert*-butylcatechol) that yields optically active β-amino acids (**39**) (see Scheme 1.10).[55]

Scheme 1.10. Enantioselective reaction with a silyl ketene acetal (**28**) catalyzed by a titanium complex.

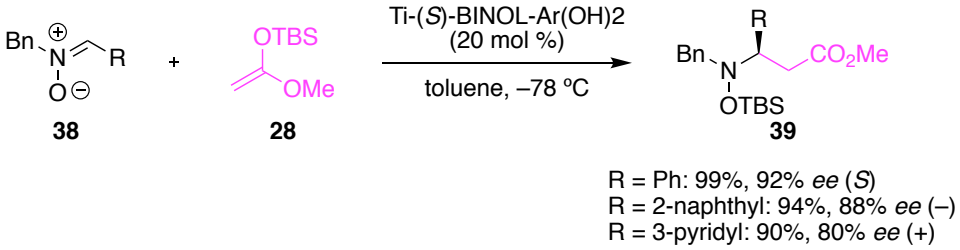

1.2.2 Pictet–Spengler Reactions

While standard nucleophilic addition reactions to nitrones have been well studied, a lesser explored application of nitrones as electrophiles is in the Pictet–Spengler reaction. Although the Pictet–Spengler reaction[56] is one of the most important methods for the synthesis of indole alkaloid scaffolds, only a limited number of nitrone-based Pictet–Spengler reactions have been reported.[57] The idea to use nitrones was originally inspired by the 1984 isolation of a new class of marine alkaloids, the eudistomins (**40**), which possessed an unprecedented oxathiazepine ring (highlighted in yellow) and a 2-oxytetrahydro-β-carboline moiety (colored in red) in addition to potent biological activities (Scheme 1.11a).[58] Cava and co-workers quickly published the first example of a nitrone-based Pictet–Spengler reaction in 1985, where *N*-hydroxytryptamine (**41**) was condensed with a series of aldehydes with ease to build nitrones (**42**) that were subsequently

cyclized to 2-hydroxytetrahydro-β-carbolines (**43**) under acidic conditions (Scheme 1.11b).[38b] A one-pot protocol facilitated by excess TFA in CH_2Cl_2 at room temperature or reflux, depending on the aldehyde, was disclosed soon after.[57e]

Scheme 1.11. (a) The eudistomin natural products isolated in 1984 with potent antiviral properties; (b) the first nitrone-based Pictet–Spengler reaction.

(a)

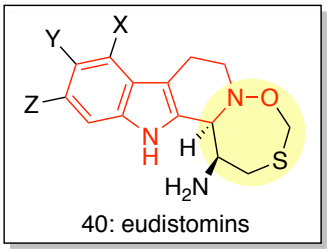

40: eudistomins

eudistomins	X	Y	Z
L	H	Br	H
K	H	H	Br
C	H	OH	Br
E	Br	OH	H

(b)

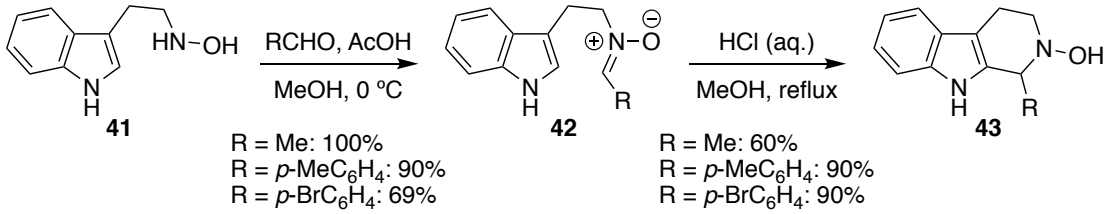

R = Me: 100%
R = *p*-MeC_6H_4: 90%
R = *p*-BrC_6H_4: 69%

R = Me: 60%
R = *p*-MeC_6H_4: 90%
R = *p*-BrC_6H_4: 90%

During the next few years, Pictet–Spengler reactions with *N*-hydroxytryptamine and *N*-hydroxytryptophan attracted the attention of numerous other academic groups as well. Of note, the reactions with *N*-hydroxytryptophans provided rapid access to collections of optically active 1-substituted tetrahydro-β-carbolines.[57a,b,d] Yet, more impressive was the work from Nakagawa and co-workers that demonstrated the first reagent-controlled enantioselective Pictet–Spengler reaction.[57h] As seen in Table 1.2, by using diisopinocampheylchloroborane (Ipc_2BCl) as a chiral Lewis acid catalyst, the Pictet–Spengler reaction of aldonitrones **42** delivered the corresponding 2-hydroxy-tetrahydro-β-carbolines (**43**) with high enantioselectivity (up to 90% *ee*). The largest disadvantages of this method were that (1) stoichiometric chiral promoter was required, and (2) no enantioselectivity was observed in the reaction of the nitrone with an electron-withdrawing nitro group on the benzene ring (entry 3). To address the latter concern, they later employed Brønsted

acid-assisted Lewis acids (BLAs) to swiftly access compounds of type **43**.[57i] In particular, the enantioselectivity of the reaction with the aldonitrone containing an electron-withdrawing nitro substituent was improved to a more acceptable 74% *ee*.

Table 1.2. Chiral Lewis acid-mediate Pictet–Spengler reaction of aldonitrones.

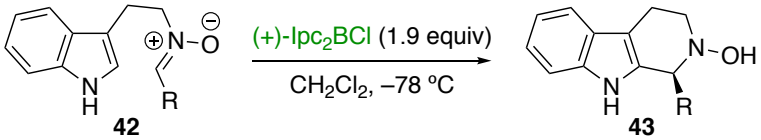

Entry	R	Yield (%)	*ee* (%)
1	Ph	92	75
2	4-$MeOC_6H_4$	65	90
3	4-$NO_2C_6H_4$	81	*rac*
4	1-naphthyl	94	86
5	Me	91	43
6	*i*-Bu	75	35

Overall, these examples highlight the current state-of-the-art chemistry available and what general challenges still exist for reactions where nitrones are electrophiles. Notably, all of the methods discussed above applied aldonitrones and not their less reactive ketonitrone counterparts. There are far fewer examples of asymmetric methodologies utilizing ketonitrones, emphasizing the considerable difficulty they pose in comparison to aldonitrones. The information presented here about Mannich-type and Pictet–Spengler reactions of nitrones is especially significant to provide context for our developed methodologies in the next three chapters.

1.3 References

[1] Pfeiffer, P. *Annalen* **1916**, *411*, 72.

[2] (a) Smith, L. I. *Chem. Rev.* **1938**, *38*, 193; (b) Hamer, J.; Macaluso, A. *Chem. Rev.* **1964**, *64*, 473; (c) Revuelta, J.; Cicchi, S.; Goti, A.; Brandi, A. *Synthesis* **2007**, *2007*, 485; (d) Brandi, A.; Cardona, F.; Cicchi, S.; Cordero, F. M.; Goti, A. *Chem. - Eur. J.* **2009**, *15*, 7808; (e) Murahashi, S.-I.; Imada, Y. *Chem. Rev*. **2019**, *119*, 4684.

[3] Matassini, C.; Cardona, F. *Chimia* **2017**, *71*, 558.

[4] Goti, A.; Cicchi, S.; Fedi, V.; Nannelli, L.; Brandi, A. *J. Org. Chem.* **1997**, *62*, 3119.

[5] Cicchi, S.; Marradi, M.; Goti, A.; Brandi, A. *Tetrahedron Lett.* **2001**, *42*, 6503.

[6] Cicchi, S.; Corsi, M.; Goti, A. *J. Org. Chem.* **1999**, *64*, 7243.

[7] Merino, P.; Delso, I.; Tejero, T.; Cardona, F.; Goti, A. *Synlett* **2007**, *2007*, 2651.

[8] Nguyen, D.-V.; Prakash, P.; Gravel, E.; Doris, E. *RSC Adv.* **2016**, *6*, 89238.

[9] (a) Matassini, C.; Parmeggiani, C.; Cardona, F.; Goti, A. *Org. Lett.* **2015**, *17*, 4082; (b) Parmeggiani, C.; Matassini, C.; Cardona, F.; Goti, A. **2017**, *49*, 2890.

[10] Murahashi, S.-I.; Mitsui, H.; Watanabe, T.; Zenki, S.-i. *Tetrahedron Lett*. **1983**, *24*, 1049.

[11] (a) D'Adamio, G.; Parmeggiani, C.; Goti, A.; Cardona, F. *Eur. J. Org. Chem*. **2015**, *2015*, 6541; (b) Yudha S, S.; Kusuma, I.; Asao, N. *Tetrahedron* **2015**, *71*, 6459; (c) Prakash, P.; Gravel, E.; Nguyen, D.-V.; Namboothiri, I. N. N.; Doris, E. *ChemCatChem* **2017**, *9*, 2091.

[12] (a) Cardona, F.; Gorini, L.; Goti, A. *Lett. Org. Chem.* **2006**, *3*, 118; (b) Goti, A.; De Sarlo, F.; Romani, M. *Tetrahedron Lett*.**1994**, *35*, 6571.

[13] Goti, A.; Nannelli, L. *Tetrahedron Lett.* **1996**, *33*, 6025.

[14] (a) Mitsui, H.; Zenki, S.; Shiota, T.; Murahashi, S.-I. *J. Chem. Soc., Chem. Commun.* **1984**, 874; (b) Murahashi, S.-I.; Mitsui, H.; Shiota, T.; Tsuda, T.; Watanabe, S. *J. Org. Chem.* **1990**, *55*, 1736; (c) Murahashi, S.-I.; Shiota, T.; Imada, Y. *Org. Synth.* **1992**, *70*, 265.

[15] Marcantoni, E.; Petrini, M.; Polimanti, O. *Tetrahedron Lett.* **1995**, *36*, 3561.

[16] Murahashi, S.-I.; Shiota, T. *Tetrahedron Lett.* **1987**, *28*, 2383.

[17] (a) Yamazaki, S. *Bull. Chem. Soc., Jpn.* **1997**, *70*, 877; (b) Goti, A.; Nannelli, L. *Tetrahedron Lett.* **1996**, *37*, 6025; (c) Murray, R. W.; Iyanar, K.; Chen, J.; Wearing, J. T. *J. Org. Chem.* **1996**, *61*, 8099; (d) Goti, A.; Cardona, F.; Soldaini, G. *Org. Synth.* **2005**, *81*, 204.

[18] Zonta, C.; Cazzola, E.; Mba, M.; Licini, G. *Adv. Synth. Catal*. **2008**, *350*, 2503.

[19] Colladon, M.; Scarso, A.; Strukul, G. *Green Chem*. **2008**, *10*, 793.

[20] (a) Forcato, M.; Nugent, W. A.; Licini, G. *Tetrahedron Lett.* **2003**, *44*, 49; (b) Forcato, M.; Mba, M.; Nugent, W. A.; Licini, G. *Eur. J. Org. Chem*. **2010**, *2010*, 740.

[21] (a) Joseph, R.; Sudalai, A.; Ravindranathan, T. *Synlett* **1995**, *1995*, 1177; (b) Sakaue, S.; Sakata, Y.; Nishiyama, Y.; Ishii, Y. *Chem. Lett*. **1992**, *21*, 289; (c) Choudary, B. M.; Reddy, C. V.; Prakash, B. V.; Bharathi, B.; Kantam, M. L. *J. Mol. Catal. A: Chem.* **2004**, *217*, 81; (d) Abrantes, M.; Gonçalves, I. S.; Pillinger, M.; Vurchio, C.; Cordero, F. M.; Brandi, A. *Tetrahedron Lett.* **2011**, *52*, 7079.

[22] Gella, C.; Ferrer, È.; Alibeś, R.; Busque, F.; de March, P.; Figueredo, M.; Font, J. *J. Org. Chem.* **2009**, *74*, 6365.

[23] Murray, R. W.; Singh, M. *J. Org. Chem*. **1990**, *55*, 2954.

[24] (a) Zajac, W. W., Jr.; Walters, T. R.; Darcy, M. G. *J. Org. Chem.* **1988**, *53*, 5856; (b) Brandi, A.; Cicchi, S.; Paschetta, V.; Pardo, D. G.; Cossy, J. *Tetrahedron Lett*. **2002**, *43*, 9357.

[25] (a) Looper, R. E.; Williams, R. M. *Angew. Chem. Int. Ed.* **2004**, *43*, 2930; (b) Tokuyama, H.; Kuboyama, T.; Fukuyama, T. *Org. Synth.* **2003**, *80*, 207.
[26] (a) Imada, Y.; Iida, H.; Ono, S.; Murahashi, S.-I. *J. Am. Chem. Soc.* **2003**, *125*, 2868; (b) Imada, Y.; Iida, H.; Ono, S.; Masui, Y.; Murahashi, S.-I. *Chem. - Asian J.* **2006**, *1*, 136; (c) Iida, H.; Imada, Y.; Murahashi, S.-I. **2015**, *13*, 7599.
[27] Colonna, S.; Pironti, V.; Carrea, G.; Pasta, P.; Zambianchi, F. *Tetrahedron* **2004**, *60*, 569.
[28] Murahashi, S.-I.; Imada, Y.; Ohtake, H. *J. Org. Chem.* **1994**, *59*, 6170.
[29] (a) Ohtake, H.; Imada, Y.; Murahashi, S.-I. *Bull. Chem. Soc. Jpn*. **1999**, *72*, 2737; (b) Murahashi, S.-I.; Ohtake, H.; Imada, Y. *Tetrahedron Lett.* **1998**, *39*, 2765.
[30] Davis, F. A.; Sheppard, A. C. *Tetrahedron*, **1989**, *45*, 5703.
[31] Boyd, D. R.; Coulter, P. B.; McGuckin, M. R.; Sharma, N. D.; Jennings, W. B.; Wilson, V. E. *J. Chem. Soc., Perkin Trans. 1* **1990**, 301.
[32] Christensen, D.; Jørgensen, K. A. *J. Org. Chem*. **1989**, *54*, 126.
[33] Soldaini, G.; Cardona, F.; Goti, A. *Org. Lett.* **2007**, *9*, 473.
[34] Cardona, F.; Bonanni, M.; Soldaini, G.; Goti, A. *ChemSusChem* **2008**, *1*, 327.
[35] Katahara, S.; Kobayashi, S.; Fujita, K.; Matsumoto, T.; Sato, T.; Chida, N. *J. Am. Chem. Soc.* **2016**, *138*, 5246.
[36] (a) LeBel, N. A.; Spurlock, L. A. *J. Org. Chem*. **1964**, *29*, 1337; (b) Tufariello, J. J.; Mullen, G. B.; Tegeler, J. J.; Trybulski, E. J.; Wong, S. C.; Ali, S. A. *J. Am. Chem. Soc*. **1979**, *101*, 2435; (c) Morozov, D. A.; Kirilyuk, I. A.; Komarov, D. A.; Goti, A.; Bagryanskaya, I. Y.; Kuratieva, N. V.; Grigor'ev, I. A. *J. Org. Chem.* **2012**, *77*, 10688; (d) deMarch, P.; Figueredo, M.; Font, J.; Milań, S.; Alvarez-Larena, A.; Piniella, J. F.; Molins, E. *Tetrahedron* **1997**, *53*, 2979.
[37] Merino, P.; Lanaspa, A.; Merchan, F. L.; Tejero, T. *Tetrahedron: Asymmetry* **1997**, *8*, 2381.
[38] (a) Exner, O. Collect. *Czech. Chem. Commun.* **1951**, *16*, 258; (b) S.-Y. Han, M. V. Lakshmikantham, M. P. Cava, *Heterocycles* **1985**, *23*, 1671.
[39] Pfeiffer, J. Y.; Beauchemin, A. M. *J. Org. Chem.* **2009**, *74*, 8381.
[40] Colacino, E.; Nun, P.; Colacino, F. M.; Martinez, J.; Lamaty, F. *Tetrahedron* **2008**, *64*, 5569.
[41] Andrade, M. M.; Barros, M. T.; Pinto, R. C. *Tetrahedron* **2008**, *64*, 10521.
[42] Bonnett, R.; Clark, V. M.; Giddey, A.; Todd, A. *J. Chem. Soc.* **1959**, 2087.
[43] (a) Merino, P.; Franco, S.; Merchan, F. L.; Tejero, T. *Synlett* **2000**, 442; (b) Lombardo, M.; Trombini, C. *Synthesis* **2000**, *2000*, 759; (c) Merino, *C. R. Chim.* **2005**, *8*, 775; (d) Merino, P.; Tejero, T. *Synlett* **2011**, *22*, 1965.
[44] (a) Huisgen, R. *Angew. Chem.* **1963**, *75*, 604; (b) Frederickson, M. *Tetrahedron* **1997**, *53*, 403; (c) Gothelf, K. V.; Jørgensen, K. A. *Chem. Rev.* **1998**, *98*, 863; (d) Stanley, L. M.; Sibi, M. P. *Chem. Rev.* **2008**, *108*, 2887; (e) Hashimoto, T.; Maruoka, K. *Chem. Rev.* **2015**, *115*, 5366; (f) Brandi, A.; Cardona, F.; Cicchi, S.; Cordero, F. M.; Goti, A. *Org. React.* **2017**, *94*, 1; (g) Breugst, M.; Reissig, H.-U. *Angew. Chem. Int. Ed.* **2020**, *59*, 12293.
[45] (a) Cardona, F.; Goti, A. *Angew. Chem. Int. Ed.* **2005**, *44*, 7832; (b) Yang, J. *Synlett* **2012**, *23*, 2293.
[46] (a) Kinugasa, M.; Hashimoto, S. *J. Chem. Soc., Chem. Commun.* **1972**, 466; (b) Marco-Contelles, J. *Angew. Chem. Int. Ed.* **2004**, *43*, 2198.
[47] Young, I. S.; Kerr, M. A. *Angew. Chem. Int. Ed.* **2003**, *42*, 3023.
[48] Stevens, A. C.; Palmer, C.; Pagenkopf, B. L. *Org. Lett.* **2011**, *13*, 1528.

[49] (a) Masson, G.; Cividino, P.; Py, S.; Vallée, Y. *Angew. Chem. Int. Ed*. **2003**, *42*, 2265; (b) Riber, D.; Skrydstrup, T. *Org. Lett.* **2003**, *5*, 229; (c) Cividino, P.; Py, S.; Delair, P.; Greene, A. E. *J. Org. Chem.* **2007**, *72*, 485.

[50] Angeli, A.; Alessandri, L.; Aiazzi-Mancini, M. *Atti Reale Accad. Lincei (Rome)* **1911**, *20*, 546; *Chem. Abstr.* **1911**, *5*, 3403.

[51] (a) Ukaji, Y.; Kenmoku, Y.; Inomata, K. *Tetrahedron: Asymm.* **1996**, *7*, 53; (b) Ukaji, Y.; Shimizu, Y.; Kenmoku, Y.; Ahmed, A.; Inomata, K. *Bull. Chem. Soc. Jpn.* **2000**, *73*, 447; (c) Ukaji, Y.; Inomata, K. *Synlett* **2003**, 1075.

[52] (a) Merchán, F. L.; Merino, P.; Rojo, I.; Tejero, T.; Dondoni, A. *Tetrahedron: Asymm*. **1996**, *7*, 667; (b) Ukaji, Y.; Inomata, K. *Chem. Rec.* **2010**, *10*, 173.

[53] (a) Murahashi, S.-I.; Sun, J.; Tsuda, T. *Tetrahedron Lett.* **1993**, *34*, 2645; (b) Murahashi, S.-I.; Sun, J.; Kurosawa, H.; Imada, Y. *Heterocycles* **2000**, *52*, 557.

[54] (a) Heine, H. W.; Zibuck, R.; VandenHeuvel, W. J. A. *J. Am. Chem. Soc.* **1982**, *104*, 3691; (b) Kawakami, T.; Ohtake, H.; Arakawa, H.; Okachi, T.; Imada Y.; Murahashi, S.-I. *Org. Lett.* **1999**, *1*, 107; (c) Kawakami, T.; Ohtake, H.; Arakawa, H.; Okachi, T.; Imada, Y.; Murahashi, S.-I. *Chem. Lett.* **1999**, 795; (d) Kawakami, T.; Ohtake, H.; Awakawa, H.; Okachi, T.; Imada, Y.; Murahashi, S.-I. *Bull. Chem. Soc. Jpn.* **2000**, *73*, 2423.

[55] (a) Murahashi, S.-I.; Imada, Y.; Kawakami, T.; Harada, K.; Yonemushi, Y.; Tomita, N. *J. Am. Chem. Soc.* **2002**, *124*, 2888; (b) Merino, P.; Franco, S.; Jimenez, P.; Tejero, T.; Chiacchio, M. A. *Lett. Org. Chem.* **2005**, *2*, 302.

[56] (a) Pictet, A.; Spengler, T. *Ber. Dtsch. Chem. Ges.* **1911**, *44*, 2030; (b) Tatsui, G. *Yakugaku Zasshi* **1928**, *48*, 453.

[57] For selected racemic versions, see: (a) Plate, R.; Van Hout, R. H. M.; Behm, H.; Ottenheijm, H. C. J. *J. Org. Chem.* **1987**, *52*, 555; (b) Sandrin, J.; Hollinshead, S. P.; Cook, J. M. *J. Org. Chem.* **1989**, *54*, 5636; (c) Still, I. W. J.; Strautmanis, J. R. *Can. J. Chem.* **1990**, *68*, 1408; (d) Hermkens, P. H. H.; van Maarseveen, J. H.; Cobben, P. L. H. M.; Ottenheijm, H. C. J.; Kruse, C. G.; Scheeren, H. W. *Tetrahedron* **1990**, *46*, 833; (e) Hino, T.; Hasegawa, A.; Liu, J.-J.; Nakagawa M. *Chem. Pharm. Bull.* **1990**, *38*, 59; (f) Liu, J.; Nakagawa, M.; Ogata, K.; Hino, T. *Chem. Pharm. Bull.* **1991**, *39*, 1672; (g) Tsuji, R.; Yamanaka, M.; Nishida, A.; Nakagawa, M. *Chem. Lett.* **2002**, 428. For enantioselective versions, see: (h) Kawate, T.; Yamada, H.; Soe, T.; Nakagawa, M. *Tetrahedron: Asymmetry* **1996**, *7*, 1249; (i) Kawate, T.; Yamada, H.; Matsumizu, M.; Nishida, A.; Nakagawa, M. *Synlett* **1997**, 1761; (j) Yamada, H.; Kawate, T.; Matsumizu, M.; Nishida, A.; Yamaguchi, K.; Nakagawa, M. *J. Org. Chem.* **1998**, *63*, 6348. For a review, see: (k) Hino, T.; Nakagawa, M. *Heterocycles* **1998**, *49*, 499.

[58] Rinehart, K. L. Jr .; Kobayashi, J.; Harbour, G. C.; Hughes, R. G. Jr.; Mizsak, S. A.; Scahill, T. A. *J. Am. Chem. Soc*. **1984**, *106*, 1524.

CHAPTER 2

MANNICH-TYPE REACTIONS OF CYCLIC NITRONES: EFFECTIVE METHODS FOR THE ENANTIOSELECTIVE SYNTHESIS OF PIPERIDINE-CONTAINING ALKALOIDS

2.1 Introduction

Although piperidine heterocycles are a prevalent moiety found in numerous natural products and therapeutic drugs, equally common is their possession of 2- or 2,6-substitution patterning that includes a β-carbonyl and/or alcohol functionality (Figure 2.1, colored in red).[1] Molecules **1**-**7** are representative examples containing this scaffold that were isolated from a diverse array of plants and insects, many of which also exhibit potent pharmacological activities.[2] Biosynthetically, these side-chains are believed to arise via enzyme-catalyzed Mannich-type reaction of carbonyl-derived nucleophiles with piperidine-derived iminium intermediates.[2f,3] Despite this, only a limited number of approaches exist for their synthesis in the laboratory setting.

Figure 2.1. Selected piperidine-containing natural products.

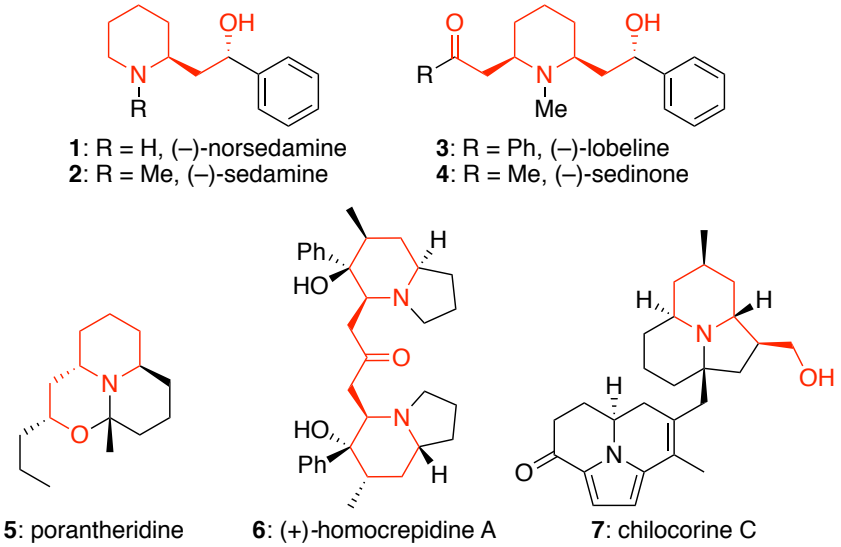

1: R = H, (–)-norsedamine
2: R = Me, (–)-sedamine

3: R = Ph, (–)-lobeline
4: R = Me, (–)-sedinone

5: porantheridine

6: (+)-homocrepidine A

7: chilocorine C

Scheme 2.1 provides two examples of synthetic methods that can proceed with good enantiocontrol. The first is a biomimetic approach from the Bella group, which used L-proline to direct Mannich-type reactions between imines **8** and varied ketones **9** to produce β-aminoketones of type **10**. However, only one example was described where $R_3 \neq H$ and some substrates required stoichiometric L-proline to promote the desired reaction.[4] Second, Kanai and co-workers employed

a chiral copper(I)-conjugated Brønsted base pair to catalyze a one-pot ring-opening/aldol addition/dehydration cascade, followed by an enantioselective intramolecular aza-Michael reaction[5] starting from cyclic hemiaminals **11** and methyl ketones **12**.[6] While both procedures possess significant power, these methods only work effectively if the intermediates have appropriate stability, noting that the free amines cannot be made without partial racemization. Additionally, the preparation of some starting materials can be step-intensive, particularly for more complex piperidines and related azacycles.

Scheme 2.1. Key precedent for enantioselective functionalizations to access the desired azacycles.

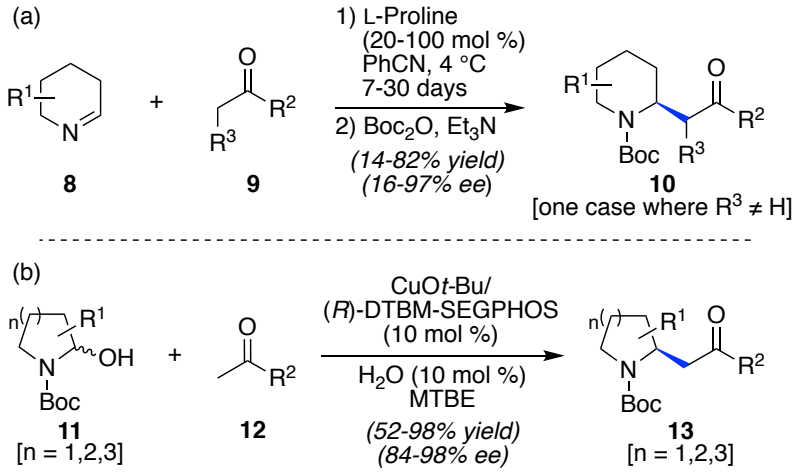

Hence, we wondered whether a method could be established utilizing cyclic nitrones as effective iminium surrogates since such species are swiftly prepared by oxidizing their corresponding secondary amines[7] or hydroxylamines,[8] reasonably stable compounds that exist as the more reactive *E*-isomers,[9] and well documented to accept a variety of nucleophiles.[10] Nonetheless, as shown in Chapter 1, only metal enolates and silyl ketene acetals were used in previously developed asymmetric Mannich-type additions to nitrones. Thus, a method that could directly add ketones would be very advantageous, especially in a catalytic, enantioselective format. Herein, we show that nitrones can be deployed as efficient electrophiles in two distinct Mannich-

type reactions that construct β-*N*-hydroxy-aminoketones in good to high yields. The first exploits asymmetric enamine catalysis to promote the reaction of cyclic, 6-membered nitrones with an array of methyl ketones to form 2-substituted piperidines in high enantioselectivity (up to 98% *ee*). The second, a variation on the well-known Robinson-Schöpf reaction, is a racemic decarboxylative Mannich-type reaction between cyclic or acyclic nitrones and an assortment of β-ketoacids. These procedures can be applied to rapidly generate 2-substituted and 2,6-disubstituted piperidine natural products and other analogous nitrogen-containing compounds of interest, as demonstrated by our implementation of both in the total syntheses of (–)-lobeline (**3**) and (–)-sedinone (**4**).

2.2 Discovery and Exploration of the Asymmetric Mannich-type Reaction of Cyclic Nitrones and Methyl Ketones

Scheme 2.2. Preliminary discovery of the enantioselective Mannich-type reaction between cyclic nitrone (**14**) and acetone (**15**, a) or acetophenone (**19**, b).

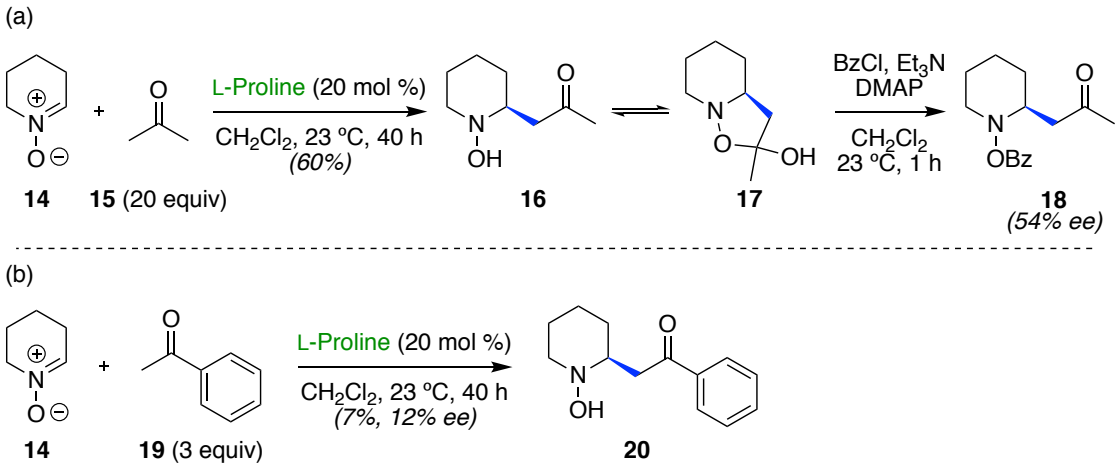

As shown in Scheme 2.2, we began our investigations by exploring whether the simple piperidine-derived nitrone **14** (see Experimental Section for synthesis) could react with acetone (**15**) under similar catalysis conditions reported by the Bella group with L-proline as the promoter.[4] Gratifyingly, the desired β-*N*-hydroxy-aminoketone (**16**), which exists in equilibrium with the cyclic isoxazolidine (**17**), was formed in a 60% yield. The enantioselectivity was determined to be

a modest 54% *ee* after derivatization of the product to the UV-active *O*-benzoyl-hydroxylamine **18**. With this exciting result, we next tested the more challenging, and arguably more useful from the standpoint of complex molecule synthesis (see Figure 1.1), reaction with acetophenone (**19**). Unfortunately, this reaction proceeded with only a 7% yield and 12% *ee*. Consequently, in a pursuit of more synthetically promising scaffolds, all further optimizations were executed with ketone **19** as the model substrate. These preliminary findings were conducted by Dr. Vladislav Lisnyak prior to my joining the project.

Figure 2.2. Activation mechanism of nitrones with thioureas.

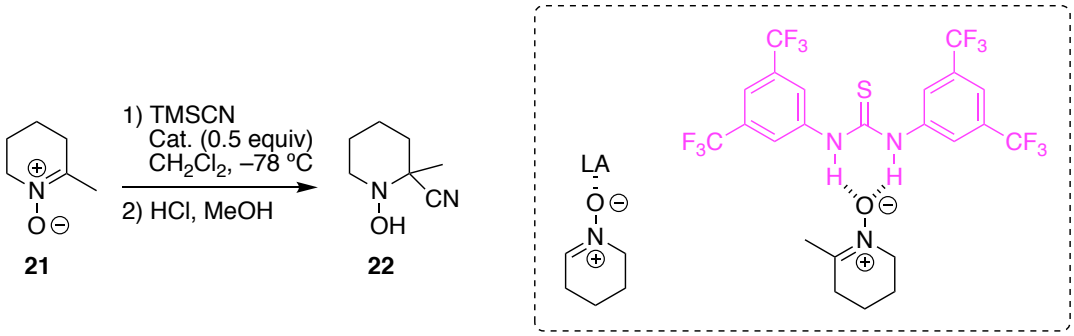

Cat.	–	**23**	**24**	**25**	**26**
Time (min)	300	180	90	45	15
Conv. (%)	79	83	77	81	81

Moving forward, we quickly found that chiral primary amine catalysts such as **29** and **30** (see Table 2.1) could dramatically enhance the enantioselectivity of **20** to 80-86% *ee*, albeit with no substantial yield improvement. Based upon these results, we proposed that the primary/secondary amine was activating the nucleophile by means of enamine catalysis[11] and the carboxylic acid/protonated amine was supplying electrophile activation via hydrogen bonding. This also explains why the MacMillan TiPSY catalyst (**38**), which cannot form the enamine, and the Hayashi-Jørgensen catalyst (**39**), which does not have a hydrogen bond donor, resulted in no

reaction. Inspired by reports from Schreiner[12] and Takemoto[13] (Figure 2.2) showing that thiourea-based hydrogen bonding catalysts[14] can increase the rate of both [3+2] cycloadditions and nucleophilic additions to nitrones, we decided to probe thiourea-based bifunctional organocatalysis.[15] Bifunctional primary amine-catalysis was especially appealing to us since it provides two readily tunable positions, the backbone and linker, that can be explored to improve the outcome of the reaction (Figure 2.3). Pleasingly, thiourea **31**, with an achiral backbone, provided a further increase in enantioselectivity (90% *ee*), but still with no improvement in yield (26%). Interestingly, replacing the thiourea with a squaramide (**34**)[16] performed worse (20% yield, 65% *ee*). Ultimately, Jacobsen catalyst **35**,[17] containing a chiral backbone, resulted in a significant increase in both parameters to 45% yield and 88% *ee*. We then completed further screening of the catalyst loading, additive, solvent, temperature, and time, as detailed in Table 2.2. The best results were obtained when the loading of **35** and benzoic acid additive were increased to 20 mol % and 40 mol %, respectively, in CH_2Cl_2 at 23 ºC for 40 hours (entry 16, 84% yield, 90% *ee*).

Figure 2.3. Catalyst design rational using bifunctional primary amine-thioureas.

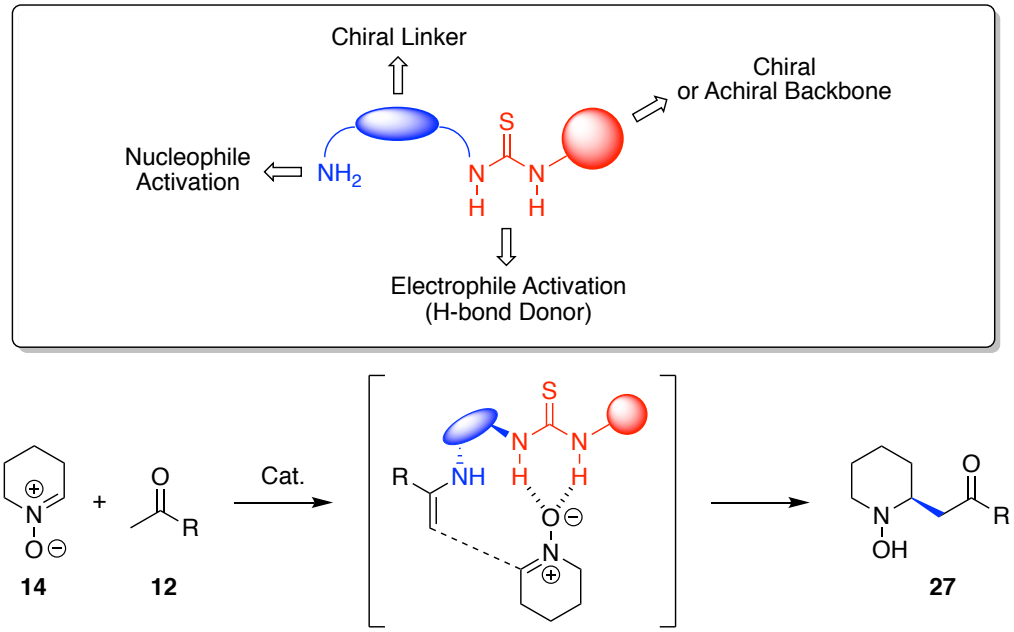

Table 2.1. Exploration of varied catalysts to achieve enantioselective addition of acetophenone (**19**) to nitrone **14**.

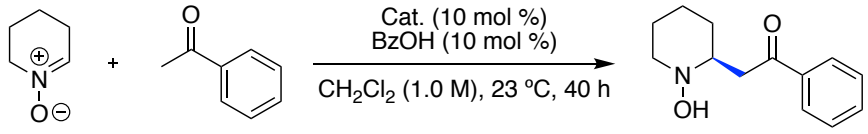

14 **19** **20**

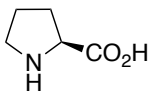

28[a]
7%, 12% *ee*

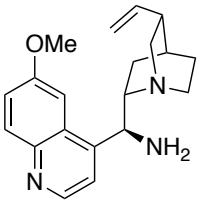

29
10%, –86% *ee*

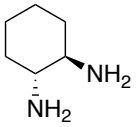

30
25%, 80% *ee*

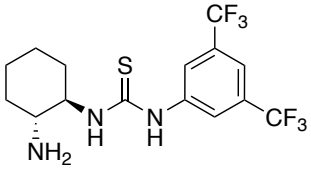

31
26%, 90% *ee*

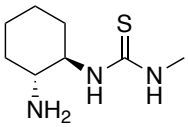

32
53%, 86% *ee*

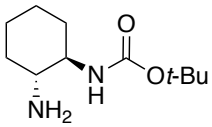

33
31%, 87% *ee*

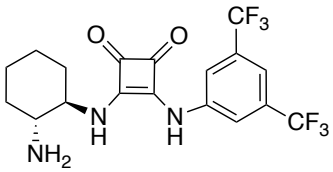

34
20%, 65% *ee*

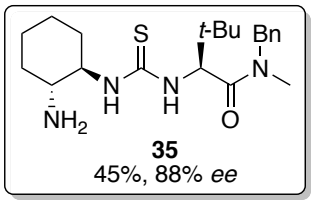

35
45%, 88% *ee*

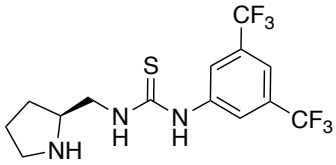

36
<10%

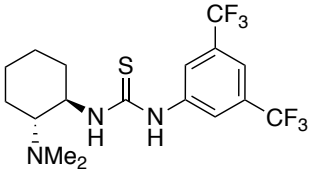

37
<5%[a]

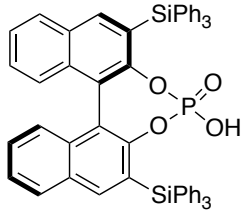

38
NR[a]

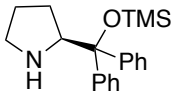

39
NR[a]

[a] No BzOH was used.

Table 2.2. Optimization of the reaction conditions.

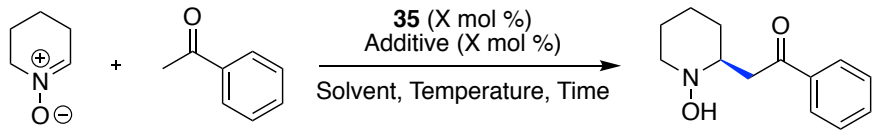

14 **19** **20**

Entry	**35** (X mol %)	Additive (X mol %)	Solvent (M)	Temperature (°C)	Time (h)	Yield (%)	*ee* (%)
1	10	BzOH (10 mol %)	CH_2Cl_2 (1.0)	23	48	45	88
2	10	BzOH (10 mol %)	DCE (1.0)	23	48	46	87
3	10	BzOH (10 mol %)	$PhCH_3$ (1.0)	23	48	41	86
4	10	BzOH (10 mol %)	PhCN (1.0)	23	48	36	76
5	10	—	CH_2Cl_2 (1.0)	23	96	24	75
6	10	BzOH (20 mol %)	CH_2Cl_2 (1.0)	23	40	48	90
7	10	BzOH (20 mol %) H_2O (100 mol %)	CH_2Cl_2 (1.0)	23	40	13	89
8	10	AcOH (20 mol %)	CH_2Cl_2 (1.0)	23	40	37	90
9	10	*p*-$O_2NC_6H_4CO_2H$ (20 mol %)	CH_2Cl_2 (1.0)	23	40	43	85
10	10	BzOH (20 mol %)	CH_2Cl_2 (1.0)	40	40	44	66
11	10	BzOH (20 mol %)	CH_2Cl_2 (1.0)	10	40	34	92
12	10	BzOH (20 mol %)	CH_2Cl_2 (1.0)	0	40	18	96
13	10	BzOH (20 mol %)	CH_2Cl_2 (0.5)	23	40	37	87
14	10	BzOH (20 mol %)	CH_2Cl_2 (2.0)	23	40	36	83
15	5	BzOH (10 mol %)	CH_2Cl_2 (1.0)	23	40	39	87
16	**20**	**BzOH (40 mol %)**	**CH_2Cl_2 (1.0)**	**23**	**40**	**84**	**90**

As presented in the remainder of Table 2.3, use of these optimized conditions with a range of 6-membered cyclic nitrones bearing varied alkyl and ether substituents at the 2-, 3-, and 4-positions afforded products **42-45** in good yields (48-84%) and enantioselectivity (88-98% *ee*). Of particular note, a "heterocyclic" nitrone that is prone to polymerization[18] also reacted successfully to produce **46**. However, 5-membered nitrones suffered from poor yields (<20 %) because of the relatively slower reaction rate, which is consistent with the same observation for [3+2]

cycloadditions that is attributed to greater eclipsing strain introduced in the transition state.[9b] When the same conditions were applied to a 7-membered nitrone, only a small amount of desired product was detected along with decomposition, likely due to oligomerization of the nitrone in the presence of acid (BzOH).[19]

Table 2.3. Exploration of nitrone scope using **19** under optimized conditions.[a]

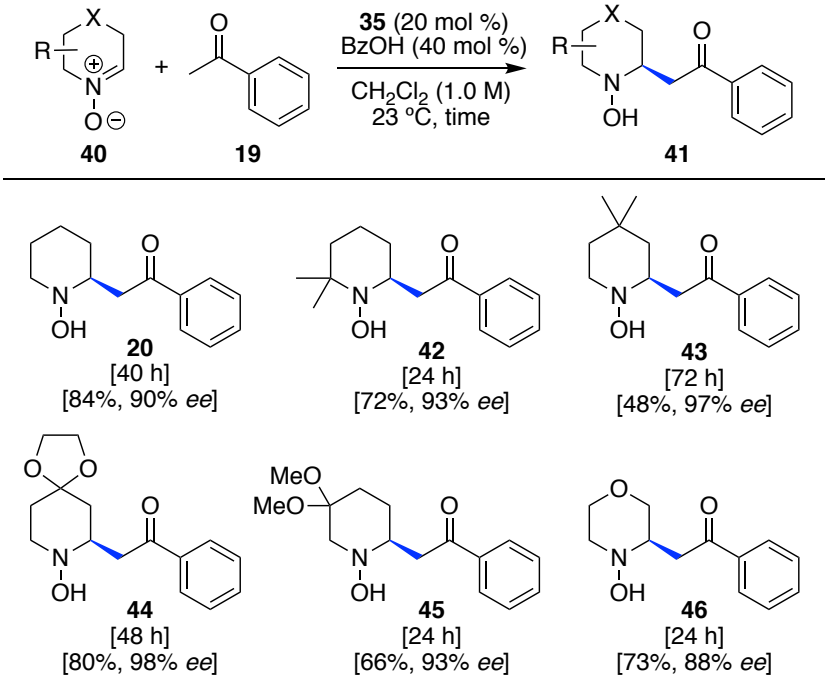

[a] Reactions were performed with **40** (0.5 mmol) and **19** (1.5 mmol) in air.

Next, different electron-rich and -deficient acetophenones were evaluated with nitrone **14** to afford **47**-**52** in moderate to good yields (54-70%) and high enantioselectivity (86-93% *ee*), as denoted in Table 2.4. Importantly, reactions with electron-deficient acetophenones required shorter reaction times to prevent racemization of the products, likely through retro-aza-Michael/aza-Michael pathways. Alkyl methyl ketones were also highly effective (51-90% yield, 94-96% *ee*) under these conditions, though additional substitution at the ketone α-position did decrease yield in some cases (**56** and **57**). Furthermore, our reaction delivers excellent regiocontrol using a range of unique substituents, including fluorine and ether groups. In fact, the formation of **60** is in

contrast to the preferential product generated under enamine catalysis,[17b,20] highlighting an element of complementarity. At this stage, the optical rotation, and hence absolute configuration of **16**, was confirmed after reductive cleavage of the N–O bond.

Table 2.4. Exploration of substrate scope with nitrone **14** using varied methyl ketones of type **12** under the optimized reaction conditions.[a]

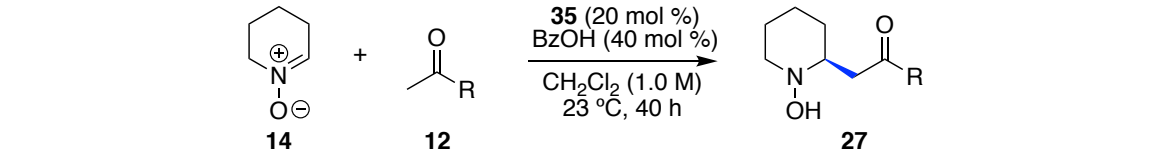

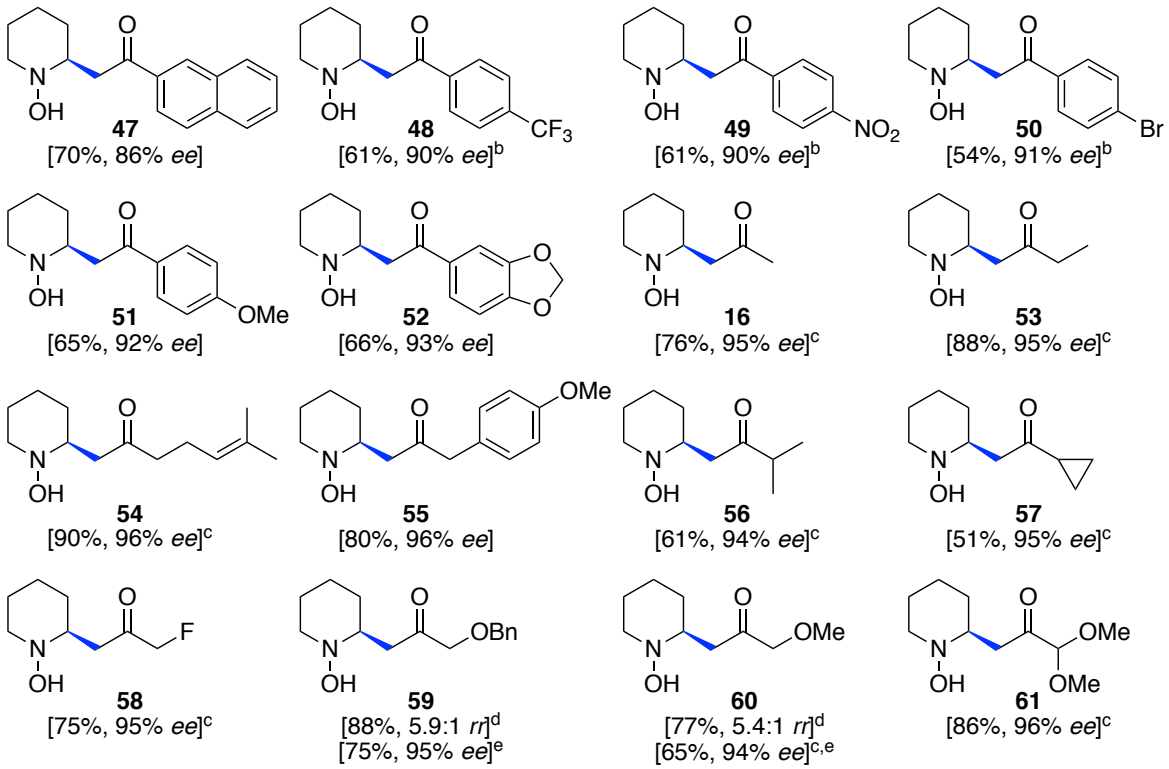

[a] Reactions were performed with **14** (0.5 mmol) and **12** (1.5 mmol) in air; [b] 16 h reaction time; [c] *ee* was determined after *O*-benzoylation; [d] combined yield; [e] major regioisomer.

Notably, all of these reactions could be run open to air, making them experimentally very easy to perform. Also critical, although the oxidation state of the products is higher than that found in most piperidine-containing targets, the hydroxylamine moiety serves as protection against *in situ* racemization.[21] For example, with **20**, only 3% *ee* was lost following 20 hours of standing in

MeOH at 23 ºC. All other products tested via HPLC analysis (**16**, **20**, **47**, **51**, and **52**) were configurationally stable after several months of storage neat at –20ºC, except for those bearing electron-withdrawing substituents on the aromatic ring (**48**-**50**). Moreover, unlike with variants that form amines and normally require a further Boc-protection step in order to be purified and prevent racemization,[4] all of our products can be purified directly by column chromatography. If desired, the N–O bond can be easily cleaved with Zn/AcOH to provide the corresponding free amine, as tested with compounds **16** and **20** (see Experimental Section).

Table 2.5. Limitations of the developed asymmetric method.[a]

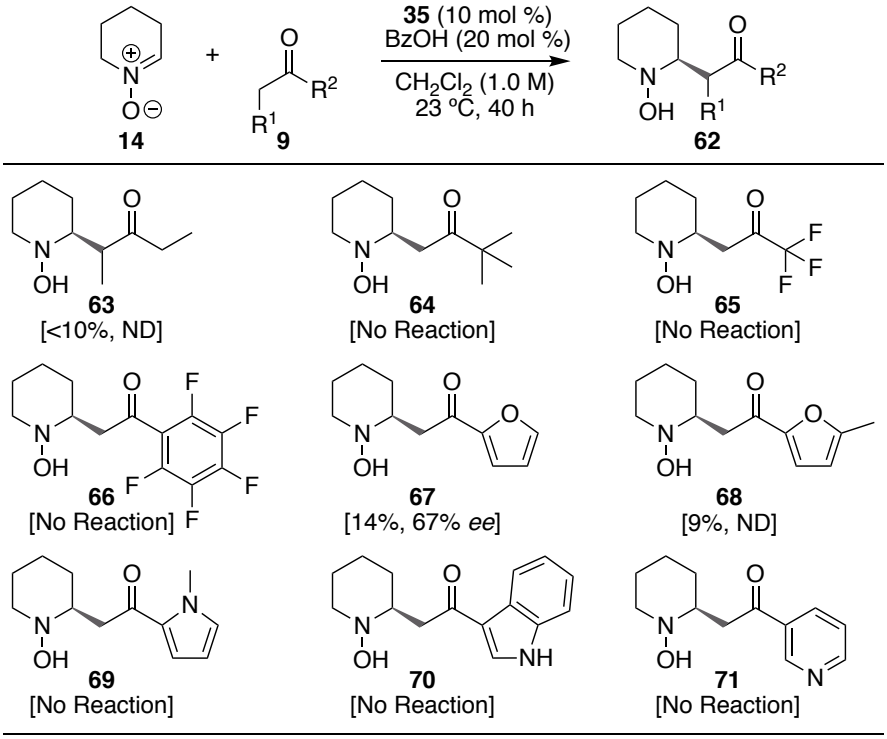

[a] Reactions were performed with **14** (0.5 mmol) and **9** (1.5 mmol) in air.

Nevertheless, there were some limitations to our developed asymmetric method. As indicated earlier, only substituted 6-membered cyclic nitrones are competent under the optimized reaction conditions. However, we were also restricted to methyl ketones, as demonstrated by the poor yield of **63** when 3-pentanone was used as the ketone precursor (Table 2.5). When R^2 was

too sterically bulky (**64**), the enamine could not form, therefore preventing any reaction from taking place. Yet, we also encountered issues when R^2 was extremely electron-withdrawing (**65** and **66**). We believe in these cases that the ketone was rapidly attacked by the primary amine catalyst, but may get stuck at the hemiaminal, imine, or enamine and thus no reaction with the nitrone was detected. Finally, methyl ketones with heterocyclic substituents either performed very poorly or did not react at all (**67-71**). This may be explained by their π-excessive character preventing imine formation, ability to disrupt the required hydrogen bonding activation of the nitrone, and/or neutralization of the BzOH additive important for the enamine catalytic cycle.

2.3 Development of the Racemic Robinson-Schöpf Reaction of Nitrones and β-Ketoacids

Due to the limitations found in the asymmetric reaction above, we thought that it would be beneficial to create an alternative procedure to access compounds of these types, even of only in a racemic format. To achieve this goal, we started by exploring whether nitrones could be applied as an imine surrogate in the well-established Robinson-Schöpf reaction, which involves a decarboxylative Mannich-type reaction between cyclic imines and β-ketoacids.[22] Given that this imine variant is known to be slow, low-yielding, and pH-dependent with side reactions often observed,[22,23] we anticipated that a more broadly effective protocol could be of value. Pleasingly, we found that **72** and **73** could readily merge, simply upon stirring in CH_2Cl_2 at 23 ºC for 16 hours (Table 2.6). This result was exciting since similar reactions usually require the addition of a catalyst or promoter.[24] Though some of the products could be isolated in comparable yields after only 2 hours (***rac*-16** and ***rac*-20**), to achieve full consumption of the starting material and ease reaction set-up, we proceeded with a 16 hour stir time for all future substrates explored.

Table 2.6. Exploration of substrate scope with various nitrones (**72**) and β-ketoacids (**73**).[a]

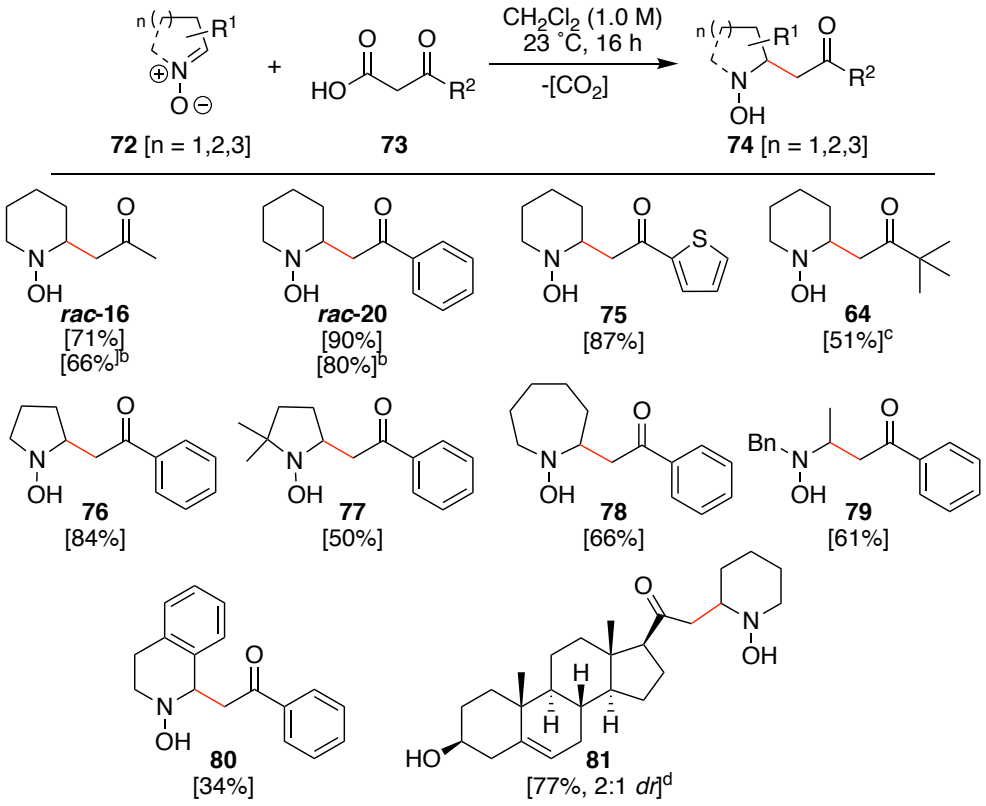

[a] Reactions were performed with **72** (0.50 mmol) and **73** (0.76 mmol) in air; [b] 2 h reaction time; [c] performed in MeOH; [d] 1.5 equiv of nitrone.

Table 2.6 provides the products synthesized (***rac*-16**, ***rac*-20**, **64**, and **75-81**), where no further optimization was performed from our initial result, given the generally smooth and high yielding reaction outcomes (50–90%). The one exception was **80** (34%) that had a conjugated nitrone precursor with low reactivity. Products **64** and **75** are of particular significance given challenges observed for adding heterocycle- and hindered alkyl-substituted β-ketoacids into imines.[25] Of note, 5-membered and 7-membered nitrones that were ineffective in our asymmetric method performed well under these decarboxylative conditions. In addition, a linear nitrone, which tend to be less reactive than their cyclic counterparts,[9] could be used to form **79** in good yield (61%). Finally, the success of a pregnenolone-derived β-ketoacid to form **81** (77% yield, *dr* = 2:1) highlights the ability to use the reaction for late-stage functionalization. For some compounds (**64**,

76, **78**, and **80**), we obtained their *O*-benzoylated adducts for structure confirmation due to the complicating equilibrium between the acyclic β-*N*-hydroxy-aminoketone and cyclic isoxazolidine forms in $CDCl_3$ (see Experimental Section).[26]

2.4 Total Syntheses of (–)-Lobeline and (–)-Sedinone

Finally, we sought to explore the power of these methods to accomplish the total syntheses of (–)-lobeline (**3**) and (–)-sedinone (**4**). While the former target has been prepared numerous times,[27] the most efficient syntheses from Boehringer Ingelheim, Birman, and Stoltz at 2, 5 and 12 steps, respectively, all took advantage of the target's inherent symmetry (Scheme 2.3). The shortest of these, the Boehringer Ingelheim synthesis, accessed key precursor lobelanine (**85**) in 1 step from 3-oxo-3-phenylpropionic acid, glutaric dialdehyde, and methylamine hydrochloride with a citrate buffer before performing an asymmetric hydrogenation to prepare (–)-lobeline (**3**) on industrial scale. Birman and co-workers utilized this same 1-step procedure to make **85**, followed by reduction with $NaBH_4$ to generate lobelanidine (**82**), which could then undergo an enantioselective monoacylation that led to formation of **84** (2 steps from **3**). Lastly, the Stoltz group also synthesized lobelanidine (**82**) as their key intermediate, albeit in 8 steps, and employed an oxidative kinetic resolution method that was developed in their group to afford **86** (3 steps from **3**). By contrast, non-symmetric (–)-sedinone (**4**) has been synthesized twice, as a racemate in 9 steps from commercial materials and in optically active form as a partial synthesis from (–)-norsedamine (**1**).[28] Our approach sought the first unified solution capable of accessing both targets and other analogs, given the known therapeutic value of **3** as a potent antagonist at nicotinic acetylcholine receptors and potential for other biological applications.[2f,29]

Scheme 2.3. Previous total syntheses of (–)-lobeline (**3**) via desymmetrization.

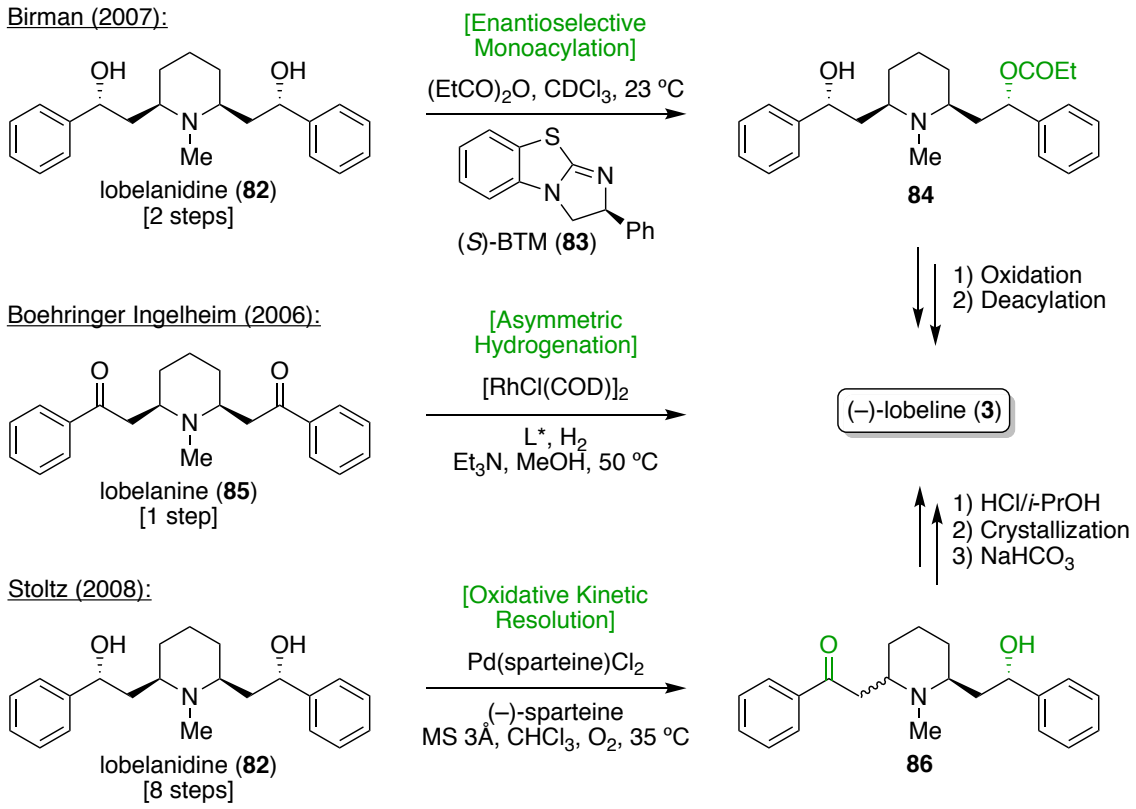

As delineated in Scheme 2.4, these efforts commenced with application of our enantioselective protocol for the preparation of **20**. When this reaction was conducted on gram scale (previously only on 50 mg), we saw a slight decrease in yield (84% to 70%), but pleasingly the enantioselectivity did not change (90% *ee*). Next, a *syn*-reduction of **20** was achieved using $Zn(BH_4)_2$[30] to deliver the desired alcohol with a 9:1 *dr* about the newly established chiral center. Subsequent silylation of the alcohol with TBSOTf and *i*-Pr_2NEt afforded **87** in 67% yield over two steps without significant change in the enantiomeric excess (89% *ee*). To our delight, we were able to grow crystals of **87** suitable for X-ray crystallographic analysis, which confirmed the absolute (*S*,*S*)-configuration of this compound and all the other products in Tables 2.1-2.4 by analogy.

Scheme 2.4. Total syntheses of (–)-lobeline (**3**) and (–)-sedinone (**4**).

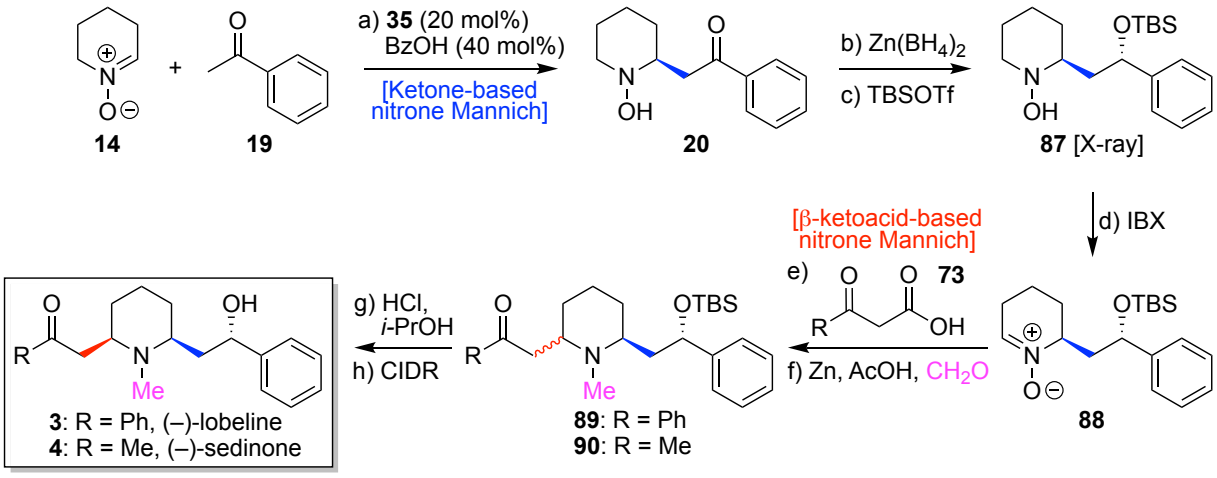

[a] Reagents and conditions: a) **19** (3.0 equiv), **35** (20 mol %), BzOH (40 mol %), CH_2Cl_2, 23 °C, 48 h, 70%, 90% *ee*; b) $Zn(BH_4)_2$ (1.2 equiv), THF, –78→0 °C, 4 h, 9:1 *dr*; c) TBSOTf (1.1 equiv), *i*-Pr_2NEt (2.0 equiv), CH_2Cl_2, 0→23 °C, 0.5 h, 67% over 2 steps, 89% *ee*; d) IBX (1.1 equiv), CH_2Cl_2, –20 °C, 4 h, 99%, 4:1 *rr*; e) **73** (1.5 equiv), CH_2Cl_2, 0→23 °C, 22 h; f) Zn (10 equiv), CH_2O (6.0 equiv), AcOH, 23 °C, 4 h, 75-76% over 2 steps, ≈1:1 *dr* (*cis*:*trans*) (**89**), 1:5.4 *dr* (**90**); g) HCl (conc., 1.3 equiv), *i*-PrOH, 60 °C, 12 h; h) **3**: CIDR, MeOH, 4 °C, 2 weeks, 90% over 2 steps; **4**: MeOH, 23 °C, 12 h, then recrystallization (hexanes/EtOAc), 23→–20 °C, 73% over 2 steps.

With the key chiral center set, we envisioned that we could incorporate our β-ketoacid-based nitrone Mannich-type reaction to build the other halves of the molecules. Accordingly, we next performed a regioselective oxidation of hydroxylamine **87** with IBX[8d] to generate a 4:1 *rr* of aldonitrone **88** and its corresponding ketonitrone (not shown). In comparison, application of more common oxidizing agents, such as HgO[31] or MnO_2,[8c] provided little or no regiocontrol. Then, the two requisite β-ketoacids (**73**, R = Ph or Me) were separately added to **88**, resulting in disubstituted hydroxylamines that predominantly had a *trans*-2,6-arrangement on the piperidine ring (≈ 4:1 *dr* for both). Subsequent reductive cleavage of the N–O bonds produced the desired secondary amines, though these products were prone to equilibration, likely via retro-aza-Michael/aza-Michael pathways (Scheme 2.5),[27a,b,32] to ultimately favor the 2,6-*cis*-isomers.[33] Unfortunately, all attempts to *N*-alkylate these *cis*-isomers (**93**) were unsuccessful, but we noticed that the undesired *trans*-isomers could participate in the proposed reductive amination with ease. Based on these results and literature precedent that the *trans*-isomers can be converted into *cis*-isomers at a later stage,[27e]

we established a one-pot protocol combining these two operations to minimize isomerization by deploying Zn/AcOH in the presence of aqueous formaldehyde.[34] This operation afforded *N*-methylamines **89** and **90** in 75% and 76% yield, respectively, with some equilibration still observed. The *dr* of **89** was batch dependent (≈ 1:1), while **90** was less prone to epimerization with a *dr* = 1:5.4 favoring the *trans*-isomer. To complete the skeleton of the natural products, we effected an acidic silyl deprotection to obtain the desired β-aminoalcohol intermediates (i.e. **3** and **4**) with the same *dr* as the starting materials (**89** and **90**).

Scheme 2.5. Proposed retro-aza-Michael/aza-Michael pathways.

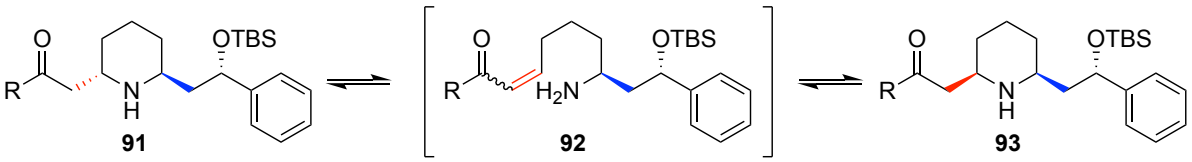

Our goal now was to convert these *dr* mixtures into the desired *cis*-isomers. Encouraged by recent work using crystallization-induced dynamic resolution (CIDR),[35] we attempted to recrystallize their free bases. Pleasingly, slow evaporation of **3** in MeOH at 4 ºC for several weeks exclusively led to *cis*-disposed (–)-lobeline (**3**) in 90% yield over the final 2 steps. Nonetheless, this technique did not work for **4**, presumably due to its greater configurational stability. Ultimately, we found that three rounds of equilibration in MeOH (to 1:1 *dr*) followed by recrystallization in hexanes/EtOAc afforded the *cis*-isomer of (–)-sedinone (**4**) in 73% yield over 2 steps. These total syntheses were performed by my talented collaborator Dr. Vladislav Lisnyak.

2.5 Conclusion

In conclusion, we have developed two distinct methods for the construction of β-*N*-hydroxy-aminoketones via Mannich-type additions of β-ketoacids or methyl ketones to nitrones. These approaches both have diverse substrate scope, with the latter able to afford the desired

products in up to 98% *ee* by employing a chiral bifunctional primary amine-catalyst. Due to the oxidation state of the products, purification is facile and racemization is slow or not observed. Finally, the combination of these protocols, coupled with other unique operations, has enabled the 8-step total syntheses of (–)-lobeline (**3**) and (–)-sedinone (**4**).

(Some contents of this chapter were published in Lisnyak, V. G.; Lynch-Colameta, T.; Snyder, S. A. *Angew. Chem. Int. Ed.* **2018**, *57*, 15162. DOI: 10.1002/anie.201809799. Additional details on the synthetic work conducted by Vladislav Lisnyak can be found in his thesis.)

2.6 Experimental Section

General Procedures. All reactions were carried out under an argon atmosphere with dry solvents under anhydrous conditions, unless otherwise noted. Dry tetrahydrofuran (THF), diethyl ether (Et_2O), and dichloromethane (CH_2Cl_2) were obtained by passing commercially available pre-dried, oxygen-free formulations through activated alumina columns. Yields refer to chromatographically and spectroscopically (^1H and ^{13}C NMR) homogeneous materials, unless otherwise stated. Reagents were purchased at the highest commercial quality and used without further purification, unless otherwise stated. Reactions were magnetically stirred and monitored by thin-layer chromatography (TLC) carried out on 0.25 mm E. Merck silica gel plates (60F-254) using UV light as visualizing agent, and an aqueous solution of $KMnO_4$ and $NaHCO_3$ and heat as a developing agent. SiliCycle silica gel (60, academic grade, particle size 0.040–0.063 mm) was used for flash column chromatography. Preparative thin-layer chromatography separations were carried out on 0.50 mm E. Merck silica gel plates (60F-254). NMR spectra were recorded on Bruker 400 and 500 MHz instruments and calibrated using residual solvent as an internal reference (^1H, δ 7.26 ppm; ^{13}C, δ 77.16 ppm for $CDCl_3$; ^{13}C, δ 49.00 ppm for CD_3OD). The following abbreviations were used to explain the multiplicities: s = singlet, d = doublet, t = triplet, q = quartet, br = broad, m = multiplet. IR spectra were recorded on a Nicolet iS5 FT-IR spectrometer using neat thin film technique. High-resolution mass spectra (HRMS) were recorded on Agilent 6244 TOF-MS using ESI (Electrospray Ionization) at the University of Chicago Mass Spectroscopy Core Facility. Chiral high-performance liquid chromatography (HPLC) analysis was performed using a Shimadzu Prominence analytical chromatograph with commercial ChiralPak columns (OD-H, OJ-H, and IA). The X-ray diffraction data were measured on a Bruker D8 VENTURE diffractometer at the University of Chicago X-ray Laboratory.

Preparation of Nitrones. Modified literature protocols were employed as follows.[7a,36]

Scheme 2.6. Method A for nitrone formation.

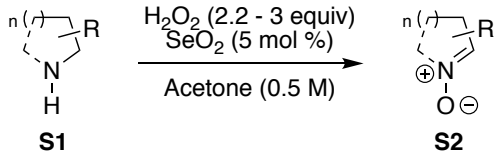

Method A. To a mixture of secondary amine **S1** (1.0 equiv) and SeO_2 (5 mol%) in acetone (0.5 M) was added dropwise an aqueous 30% (w/w) H_2O_2 solution (2.2-3.0 equiv) over 10 min at 0 ºC under an argon atmosphere. The resultant mixture was stirred at 0 ºC for 1 h, and then warmed to 23 ºC for 3 h. Upon completion, the acetone was removed under reduced pressure. The remaining aqueous layer was extracted with CH_2Cl_2 (3 × 60 mL/g of starting secondary amine). The combined organic layers were then dried ($MgSO_4$), filtered, and concentrated. The resultant crude product was purified by flash column chromatography (silica gel, CH_2Cl_2/MeOH). The corresponding nitrone **S2** was stored as a 1.0 M solution in CH_2Cl_2 at –20 ºC to prevent dimerization.

Scheme 2.7. Method B for nitrone formation.

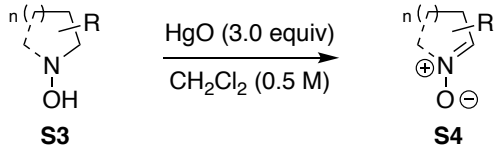

Method B. To a solution of corresponding hydroxylamine **S3** (1.0 equiv) in CH_2Cl_2 (0.5 M) was added yellow HgO (3.0 equiv) in one portion at 23 ºC under an argon atmosphere. The reaction contents were stirred for 1 h and then anhydrous $MgSO_4$ was added. The resulting grey heterogeneous mixture was filtered through a pad of Celite with a layer of $MgSO_4$ on top, washed with CH_2Cl_2, and concentrated to afford the corresponding nitrone **S4** that was used without further

purification. The nitrone **S4** was stored as a 1.0 M solution in CH_2Cl_2 at –20 ºC to prevent dimerization.

Figure 2.4. Nitrones explored in this research.

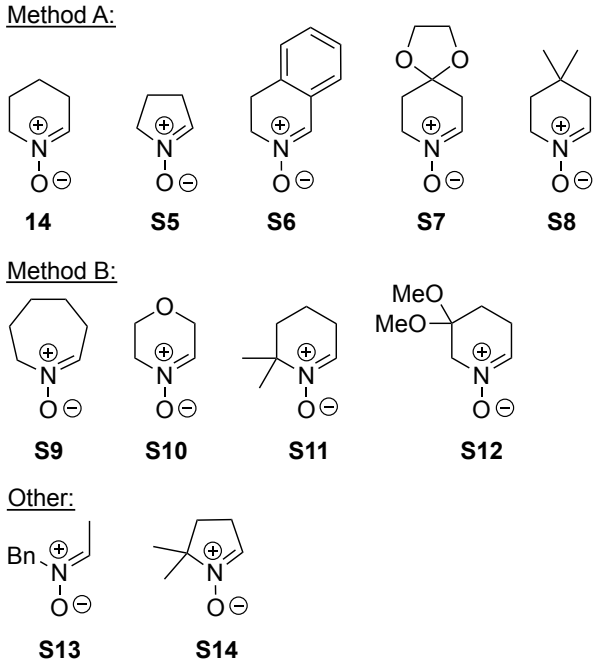

Nitrones **14**,[7a] **S5**,[7a] **S6**,[7a] **S13**,[37] and **S14**[38] were prepared according to the literature procedures. All spectroscopic data matched that reported in the denoted references.

Nitrones **S9** and **S10** were prepared from corresponding hydroxylamines **S3**[39] on a 0.5 mmol scale using a further modified **Method B** to avoid polymerization[18,19]: upon completion, the reaction was filtered through a frit containing $MgSO_4$; the filter cake was washed with CH_2Cl_2 and the excess CH_2Cl_2 was concentrated (bath set to less than 25 ºC) to afford a 1.0 M solution of **S9** or **S10** in CH_2Cl_2 (quantitative conversion assumed) that was used immediately after preparation.

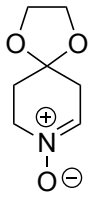

S7

1,4-dioxa-8-azaspiro[4.5]dec-7-ene 8-oxide (S7): Prepared using **Method A** described above, starting from 4,4-ethylenedioxy-piperidine (0.50 g, 3.49 mmol) using 2.2 equiv of H_2O_2 (0.78 mL), yielding **S7** (237 mg, 43%) as a pale-yellow oil. **S7**: R_f = 0.56 (silica gel, CH_2Cl_2/MeOH = 10/1); IR (film) ν_{max} 3380, 2893, 1620, 1441, 1372, 1191, 1077, 1018, 954, 875, 728 cm^{-1}; ^1H NMR (500 MHz, $CDCl_3$) δ 7.00 (t, *J* = 4.0 Hz, 1 H), 4.22–3.81 (m, 6 H), 2.68–2.52 (m, 2 H), 2.08 (t, *J* = 6.4 Hz, 2 H); ^{13}C NMR (125 MHz, $CDCl_3$) δ 133.8, 103.4, 65.0, 57.5, 36.1, 32.0. HRMS (ESI) calcd for $C_7H_{12}NO_3^+$ [M + H^+] 158.0812, found 158.0816.

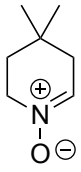

S8

4,4-dimethyl-2,3,4,5-tetrahydropyridine 1-oxide (S8): Prepared using **Method A** described above, starting from 4,4-dimethylpiperidine[40] (0.15 g, 1.33 mmol) using 3.0 equiv of H_2O_2 (0.32 mL), yielding **S8** (87 mg, 53%) as a clear oil. **S8**: R_f = 0.51 (silica gel, CH_2Cl_2/MeOH = 10/1); IR (film) ν_{max} 3387, 2956, 2871, 1620, 1454, 1369, 1236, 1167, 1059, 817, 696 cm^{-1}; ^1H NMR (500 MHz, $CDCl_3$) δ 7.15–7.04 (m, 1 H), 3.81 (t, *J* = 6.1 Hz, 2 H), 2.28–2.14 (m, 2 H), 1.74 (t, *J* = 6.2 Hz, 2 H), 1.06 (s, 6 H); ^{13}C NMR (125 MHz, $CDCl_3$) δ 136.1, 55.4, 39.5, 35.6, 27.8, 26.6; HRMS (ESI) calcd for $C_7H_{14}NO^+$ [M + H^+] 128.1070, found 128.1072.

Scheme 2.8. Preparation of nitrone **S11**.

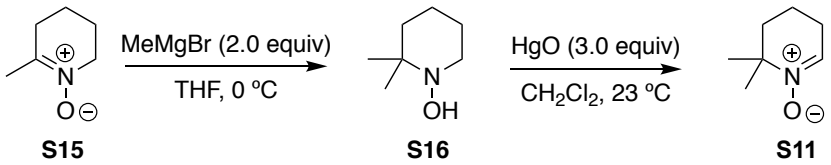

2,2-dimethyl-2,3,4,5-tetrahydropyridine 1-oxide (S11): To a cooled (0 ºC) solution of **S15**[7a] (0.10 g, 0.88 mmol, 1.0 equiv) in THF (2 mL) was added MeMgBr (1.77 mL, 1 M in THF, 2.0 equiv) dropwise. The resulting mixture was stirred for 2 h at 0 ºC then quenched with saturated aqueous NH_4Cl (3 mL). The solution was warmed to 23 ºC, concentrated and the aqueous phase

was extracted with EtOAc (3 × 5 mL). The combined organic layers were then dried ($MgSO_4$), filtered, and concentrated. The resultant crude hydroxylamine **S16** was purified by flash column chromatography (silica gel, hexanes/EtOAc = 1/1). The subsequent oxidation was performed according to **Method B** to afford nitrone **S11** (420 mg, 88%) as a white solid. **S11**: R_f = 0.52 (silica gel, CH_2Cl_2/MeOH = 10/1); IR (film) ν_{max} 3247, 2940, 2874, 1661, 1590, 1460, 1363, 1175, 971, 816 cm^{-1}; ^1H NMR (500 MHz, $CDCl_3$) δ 6.95 (t, *J* = 4.1 Hz, 1 H), 2.31 (td, *J* = 6.3, 4.3 Hz, 2 H), 1.85–1.77 (m, 2 H), 1.71–1.60 (m, 2 H), 1.40 (s, 6 H); ^{13}C NMR (125 MHz, $CDCl_3$) δ 135.5, 66.1, 36.9, 26.8, 26.4, 15.2; HRMS (ESI) calcd for $C_7H_{14}NO^+$ [M + H^+] 128.1070, found 128.1075.

Scheme 2.9. Preparation of nitrone **S12**.

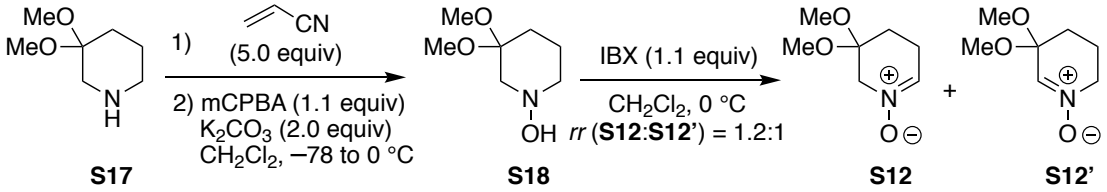

3,3-dimethoxy-2,3,4,5-tetrahydropyridine 1-oxide (S12): A modified literature protocol was employed as follows.[41] To 3,3-dimethoxypiperidine[42] (**S17**, 1.00 g, 6.89 mmol, 1.0 equiv) was added acrylonitrile (2.25 mL, 34.40 mmol, 5.0 equiv) at 23 ºC and the resultant mixture was stirred for 10 h. Then, the excess acrylonitrile was carefully removed under reduced pressure (bath set to less than 30 ºC). The crude tertiary amine was dissolved in CH_2Cl_2 and cooled to –78 ºC. K_2CO_3 (1.90 g, 13.78 mmol, 2.0 equiv) was added in one portion followed by addition of *m*-CPBA (1.82 g, 72%, 7.58 mmol, 1.1 equiv) in two equal portions over 10 min. The resulting solution was stirred at –78 ºC for 1 h and then slowly warmed to 0 ºC over 2 h. The precipitate was filtered, washed with CH_2Cl_2, and the filtrate was concentrated. The crude hydroxylamine was purified by flash column chromatography (silica gel, hexanes/EtOAc = 1/1) to afford **S18**[41b] (0.60 g, 55% over two

steps) as a white solid and immediately subjected to the next step. Hydroxylamine **S18** (0.16 g, 1.00 mmol, 1.0 equiv) was dissolved in CH_2Cl_2 (2 mL, 0.5 M) and cooled to 0 ºC. Then IBX (0.28 g, 1.00 mmol, 1.0 equiv) was added in one portion and the mixture was stirred for 3 h at 0 ºC. Upon completion, the solution was quickly filtered through Celite, washed with cold CH_2Cl_2, and concentrated to afford a mixture of **S12** and **S12'** (1.2:1 according to the crude NMR). The desired nitrone **S12** was separated by flash chromatography (silica gel, CH_2Cl_2/MeOH = 20/1) to afford **S12** (55 mg, 31%) as a clear oil. **S12**: R_f = 0.30 (silica gel, CH_2Cl_2/MeOH = 15/1); IR (film) ν_{max} 3234, 2950, 2833, 1440, 1266, 1114, 1054, 885, 750 cm^{-1}; ^1H NMR (500 MHz, $CDCl_3$) δ 7.18–7.10 (m, 1 H), 3.90–3.81 (m, 2 H), 3.26 (s, 6 H), 2.55–2.32 (m, 2 H), 1.91 (t, J = 6.5 Hz, 2 H); ^{13}C NMR (125 MHz, $CDCl_3$) δ 135.7, 97.4, 62.9, 48.4, 24.9, 22.6; HRMS (ESI) calcd for $C_7H_{14}NO_3^+$ [M + H^+] 160.0968, found 160.0973. ***Note***: Upon the isolation on silica gel the ratio changes to 1:2 (**S12**/**S12'**).

Preparation of β-ketoacids.

Scheme 2.10. Synthesis of β-ketoacid **S20**.

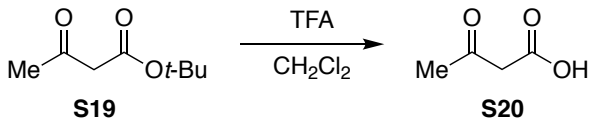

S19 **S20**

To β-ketoester **S19**[43] in CH_2Cl_2 (3.0 M) at 0° C was added trifluoroacetic acid (4 equiv), and the solution was stirred for about 5 min. The reaction mixture was then allowed to warm to room temperature and stirred for 1 hour. Upon completion, the reaction mixture was directly concentrated (bath set to less than 30 ºC) and dried under vacuum give the desired β-ketoacid **S20** (yield up to 90%) that was used without further purification.

Scheme 2.11. Synthesis of β-ketoacids **S24**-**S26**.

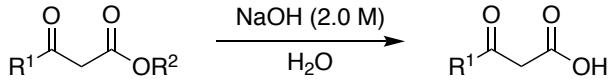

S21: R^1 = Ph, R^2 = Et
S22: R^1 = *t*-Bu, R^2 = Me
S23: R^1 = 2-thiophenyl, R^2 = Me

S24: R^1 = Ph
S25: R^1 = *t*-Bu
S26: R^1 = 2-thiophenyl

β-ketoester **S21**, **S22**, or **S23**[44] (26.0 mmol, 1.0 equiv) and aqueous NaOH (2.0 M, 26 mL) are stirred for 12 h at 23 ºC open to air. Upon completion, the reaction mixture was then diluted with Et_2O (20 mL) and the two phases were separated. The aqueous phase was washed with Et_2O (2 × 20 mL), and then cooled to 0 ºC before being acidified with aqueous HCl (3.0 M) to pH 1-2. If a precipitate was observed, the β-ketoacid (**S24**) was filtered, washed with H_2O, dried under vacuum, and used without further purification (yields up to 90%). Otherwise, the reaction contents were extracted with Et_2O (3 × 50 mL), and the combined organic extracts were dried ($MgSO_4$), filtered, and concentrated (bath set to less than 30 ºC) to give the desired β-ketoacids **S25** and **S26** (yields up to 90%) that were used without further purification.

Scheme 2.12. Synthesis of β-ketoacid **S28**.

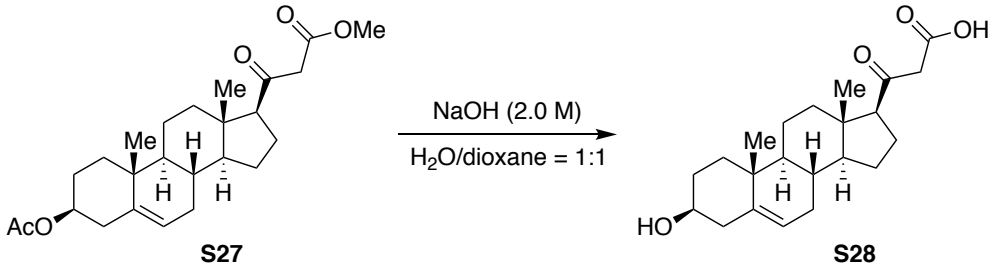

S27 **S28**

3-((3*S*, 8*S*, 9*S*, 10*R*, 13*S*, 14*S*, 17*S*)-3-hydroxy-10, 13-dimethyl-2, 3, 4, 7, 8, 9, 10, 11, 12, 13, 14, 15, 16, 17-tetradecahydro-1*H*-cyclopenta[a]phenanthren-17-yl)-3-oxopropanoic acid (S28): Prepared from **S27**[45] (0.51 g, 1.20 mmol) according to the general procedure using 1,4-dioxane as a co-solvent (H_2O/dioxane = 1/1).

General Procedure for Enantioselective Mannich-type Reactions between Nitrones 40 and Acetophenone 19.

To a vial containing **35** (39.1 mg, 0.10 mmol, 0.2 equiv), BzOH (24.4 mg, 0.20 mmol, 0.4 equiv), and acetophenone **19** (181.4 mg, 1.51 mmol, 3.0 equiv) at 23 ºC under ambient atmosphere was added a solution of nitrone **40** (0.50 mmol, 1.0 equiv) in CH_2Cl_2 (0.50 mL). The reaction mixture was then stirred for 24–72 h. Upon completion, the contents were quenched with saturated aqueous $NaHCO_3$ (2 mL) and extracted with CH_2Cl_2 (3 × 2 mL). The combined organic extracts were then dried ($MgSO_4$), filtered, and concentrated. The resultant crude material was purified by flash column chromatography (silica gel, hexane/EtOAc) to yield **41**.

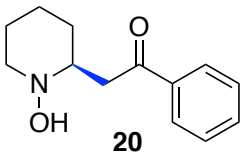

20

(*S*)-2-(1-hydroxypiperidin-2-yl)-1-phenylethan-1-one (20): Prepared using the general procedure described above with **14** ultimately yielding **20** (93 mg, 84% yield, 90% *ee*) as a pale-yellow oil. **20**: R_f = 0.45 (silica gel, EtOAc); $[\alpha]_D^{25}$ = –31.2º (*c* = 1.00, $CHCl_3$); IR (film) ν_{max} 3159, 2937, 2856, 1683, 1597, 1448, 1285, 1205, 973, 752, 691 cm^{-1}; acyclic ^1H NMR (500 MHz, $CDCl_3$) δ 7.96 (d, *J* = 7.6 Hz, 2 H), 7.53 (t, *J* = 7.2 Hz, 1 H), 7.42 (t, *J* = 7.5 Hz, 2 H), 7.19–6.76 (br s, 1 H, exchangeable), 3.74 (dd, *J* = 15.4, 3.9 Hz, 1 H), 3.32 (d, *J* = 9.7 Hz, 1 H), 3.00–3.09 (m, 1 H), 2.84 (dd, *J* = 15.5, 7.4 Hz, 1 H), 2.57 (t, *J* = 10.8 Hz, 1 H), 1.90 (d, *J* = 11.9 Hz, 1 H), 1.73 (d, *J* = 12.1 Hz, 1 H), 1.64–1.53 (m, 2 H), 1.42–1.16 (m, 2 H); ^{13}C NMR (100 MHz, $CDCl_3$) δ 199.7, 137.4, 133.1, 128.7, 128.4, 64.7, 60.0, 43.6, 32.2, 25.9, 23.6; HRMS (ESI) calcd for $C_{13}H_{18}NO_2^+$ [M + H^+] 220.1332, found 220.1332.

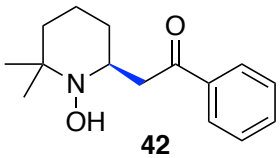

42

(*S*)-2-(1-hydroxy-6,6-dimethylpiperidin-2-yl)-1-phenylethan-1-one (42): Prepared using the general procedure described above with **S11** ultimately yielding **42** (88 mg, 72% yield, 93% *ee*) as a yellow oil. **42**: R_f = 0.75 (silica gel, EtOAc); $[\alpha]_D^{25}$ = –12.1° (*c* = 1.00, $CHCl_3$); IR (film) ν_{max} 3398, 2935, 2869, 1684, 1598, 1449, 1390, 1287, 1211, 1002, 752, 722, 690 cm^{-1}; cyclic:acyclic= 4:1 ^1H NMR (500 MHz, $CDCl_3$) δ 7.97 (d, *J* = 7.5 Hz, 1.66 H), 7.67–7.58 (m, 0.34 H), 7.58–7.50 (m, 0.83 H), 7.50–7.41 (m, 1.66 H), 7.40–7.29 (m, 0.51 H), 4.69–4.26 (m, 0.75 H), 3.80–3.26 (m, 1.75 H), 3.04–2.90 (m, 0.20 H), 2.90–2.60 (m, 0.75 H), 2.60–2.48 (m, 0.25 H), 1.91–1.81 (m, 1.30 H), 1.55–1.43 (m, 3 H), 1.38–1.22 (m, 2 H), 1.18 (s, 3 H), 1.09 (s, 3 H); ^{13}C NMR (100 MHz, $CDCl_3$) δ 200.2, 137.5, 133.0, 130.0, 128.7, 128.4, 127.1, 125.7, 91.7, 59.7, 57.9, 44.5, 39.1, 37.6, 33.1, 32.6, 30.1, 27.4, 19.9, 16.5, 15.0. HRMS (ESI) calcd for $C_{15}H_{22}NO_2^+$ [M + H^+] 248.1645, found 248.1643.

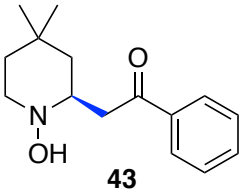

43

(*S*)-2-(1-hydroxy-4,4-dimethylpiperidin-2-yl)-1-phenylethan-1-one (43): Prepared using the general procedure described above with **S8** ultimately yielding **43** (59 mg, 48% yield, 97% *ee*) as a yellow oil. **43**: R_f = 0.44 (silica gel, EtOAc); $[\alpha]_D^{25}$ = –30.7° (*c* = 1.00, $CHCl_3$); IR (film) ν_{max} 2952, 2924, 1684, 1448, 1288, 1207, 1001, 754, 691 cm^{-1}; acyclic ^1H NMR (500 MHz, $CDCl_3$) δ 7.95 (d, *J* = 7.6 Hz, 2 H), 7.58–7.48 (m, 1 H), 7.48–7.34 (m, 2 H), 3.68 (dd, *J* = 15.7, 3.8 Hz, 1 H), 3.42–3.22 (m, 1 H), 3.22–3.00 (m, 1 H), 2.97–2.70 (m, 2 H), 1.71–1.48 (m, 2 H), 1.42–1.20 (m, 2 H), 1.01 (s, 3 H), 0.90 (d, *J* = 11.8 Hz, 3 H); ^{13}C NMR (125 MHz, $CDCl_3$) δ 199.7, 137.5, 133.1, 128.7, 128.3, 60.5, 55.7, 45.3, 43.6, 38.6, 32.1, 29.3, 24.4; HRMS (ESI) calcd for $C_{15}H_{22}NO_2^+$ [M + H^+] 248.1645, found 248.1649.

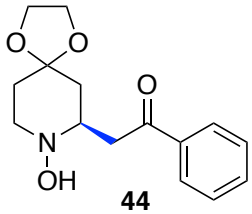

44

(*R*)-2-(8-hydroxy-1,4-dioxa-8-azaspiro[4.5]decan-7-yl)-1-phenylethan-1-one (44): Prepared using the general procedure described above with **S7** ultimately yielding **44** (110 mg, 80% yield, 98% *ee*) as a pale-yellow oil. **44**: R_f = 0.50 (silica gel, EtOAc); $[\alpha]_D^{25}$ = –13.3° (*c* = 1.00, $CHCl_3$); IR (film) ν_{max} 3061, 2960, 2881, 1684, 1448, 1289, 1146, 1055, 929, 753, 691 cm^{-1}; acyclic ^1H NMR (500 MHz, $CDCl_3$) δ 7.95 (d, *J* = 7.5 Hz, 2 H), 7.65–7.50 (m, 1 H), 7.50–7.30 (m, 2 H), 6.56–6.07 (br s, 1 H, exchangeable), 4.04–3.79 (m, 4 H), 3.75–3.54 (m, 1 H), 3.49–3.20 (m, 2 H), 3.20–2.99 (m, 1 H), 2.99–2.70 (m, 1 H), 2.27–1.33 (m, 4 H); ^{13}C NMR (125 MHz, $CDCl_3$) δ 199.2, 137.3, 133.2, 128.8, 128.4, 106.2, 64.6, 64.5, 61.8, 56.3, 43.1, 39.9, 34.4; HRMS (ESI) calcd for $C_{15}H_{20}NO_4^+$ [M + H^+] 278.1389, found 278.1388.

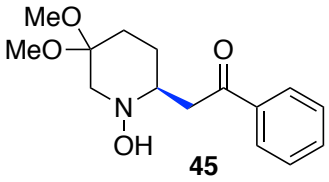

45

(*S*)-2-(1-hydroxy-5,5-dimethoxypiperidin-2-yl)-1-phenylethan-1-one (45): Prepared using the general procedure described above with **S12** ultimately yielding **45** (92 mg, 66% yield, 93% *ee*) as a yellow oil. **45**: R_f = 0.64 (silica gel, EtOAc); $[\alpha]_D^{25}$ = –23.1° (*c* = 1.00, $CHCl_3$); IR (film) ν_{max} 3309, 2958, 2831, 1682, 1597, 1448, 1205, 1054, 890, 752, 691 cm^{-1}; acyclic ^1H NMR (500 MHz, $CDCl_3$) δ 7.98 (d, *J* = 7.5 Hz, 2 H), 7.60–7.50 (m, 1 H), 7.50–7.39 (m, 2 H), 3.85 (d, *J* = 14.3 Hz, 1 H), 3.68–3.45 (m, 1 H), 3.21 (s, 3 H), 3.17 (s, 3 H), 3.11–2.99 (m, 1 H), 2.98–2.81 (m, 1 H), 2.70–2.44 (m, 1 H), 2.08–1.77 (m, 2 H), 1.55–1.23 (m, 2 H); ^{13}C NMR (125 MHz, $CDCl_3$) δ 199.2, 137.3, 133.2, 128.7, 128.3, 99.3, 63.9, 63.4, 48.2, 48.0, 42.6, 30.1, 27.2; HRMS (ESI) calcd for $C_{15}H_{22}NO_4^+$ [M + H^+] 280.1544, found 280.1543.

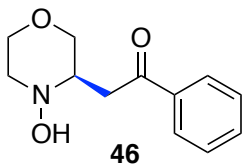

46

(*R*)-2-(4-hydroxymorpholin-3-yl)-1-phenylethan-1-one (46): Prepared using the general procedure described above with **S10** ultimately yielding **46** (80 mg, 73% yield, 88% *ee*) as a yellow oil. **46**: R_f = 0.55 (silica gel, EtOAc);

$[\alpha]_D^{25}$ = –31.2º (*c* = 1.00, $CHCl_3$); IR (film) ν_{max} 3350, 2857, 1681, 1449, 1280, 1108, 1003, 753, 692 cm^{-1}; acyclic ^1H NMR (500 MHz, $CDCl_3$) δ 7.95 (d, *J* = 6.3 Hz, 2 H), 7.70–7.51 (m, 1 H), 7.51–7.36 (m, 2 H), 6.63–6.10 (br s, 1 H, exchangeable), 4.16–3.72 (m, 2 H), 3.72–3.42 (m, 2 H), 3.37–3.02 (m, 3 H), 2.97–2.67 (m, 2 H); ^{13}C NMR (125 MHz, $CDCl_3$) δ 198.7, 137.0, 133.4, 128.8, 128.4, 70.6, 66.7, 63.6, 58.9, 39.1; HRMS (ESI) calcd for $C_{12}H_{16}NO_3^+$ [M + H^+] 222.1125, found 222.1124.

General Procedure for Enantioselective Mannich-type Reactions between Nitrone 14 and Methyl Ketones 12.

To a vial containing **35** (39.1 mg, 0.10 mmol, 0.2 equiv), BzOH (24.4 mg, 0.20 mmol, 0.4 equiv), and the corresponding methyl ketone **12** (1.51 mmol, 3.0 equiv) at 23 ºC under an ambient atmosphere was added a solution of nitrone **14** (49.6 mg, 0.50 mmol, 1.0 equiv) in CH_2Cl_2 (0.50 mL). The reaction mixture was then stirred for 40 h (except **48**-**50**, which were stirred for only 16 h). Upon completion, the contents were quenched with saturated aqueous $NaHCO_3$ (2 mL) and extracted with CH_2Cl_2 (3 × 2 mL). The combined organic extracts were then dried ($MgSO_4$), filtered, and concentrated. The resultant crude material was purified by flash column chromatography (silica gel, hexane/EtOAc) to yield **27**.

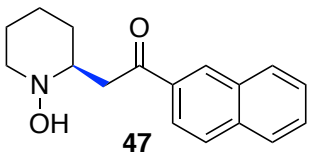

47

(*S*)-2-(1-hydroxypiperidin-2-yl)-1-(naphthalen-2-yl)ethan-1-one (47): Prepared using the general procedure described above yielding **47** (95 mg, 70% yield, 86% *ee*) as a yellow oil. **47**: R_f = 0.44 (silica gel, EtOAc); $[\alpha]_D^{25}$ = –34.1º (*c* = 1.00, $CHCl_3$); IR (film) ν_{max} 3164, 2936, 2856, 1678, 1627, 1468,

1353, 1292, 1184, 1123, 861, 820, 748 cm^{-1}; acyclic ^1H NMR (500 MHz, $CDCl_3$) δ 8.48 (s, 1 H), 8.03 (d, *J* = 8.6 Hz, 1 H), 7.90–7.80 (m, 3 H), 7.60–7.45 (m, 2 H), 6.86–6.36 (br s, 1 H, exchangeable), 3.87 (dd, *J* = 15.2, 3.7 Hz, 1 H), 3.36 (d, *J* = 9.6 Hz, 1 H), 3.17–3.09 (m, 1 H), 2.98 (dd, *J* = 15.3, 7.0 Hz, 1 H), 2.59 (t, *J* = 10.9 Hz, 1 H), 1.94 (d, *J* = 12.9 Hz, 1 H), 1.79–1.71 (m, 1 H), 1.66–1.58 (m, 2 H), 1.44–1.23 (m, 2 H); ^{13}C NMR (100 MHz, $CDCl_3$) δ 199.6, 135.6, 134.6, 132.6, 130.0, 129.7, 128.5, 128.4, 127.7, 126.7, 124.0, 64.8, 60.0, 43.7, 32.3, 25.9, 23.6; HRMS (ESI) calcd for $C_{17}H_{20}NO_2^+$ [M + H^+] 270.1489, found 270.1493.

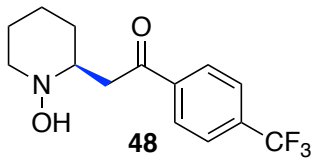

48

(*S*)-2-(1-hydroxypiperidin-2-yl)-1-(4-(trifluoromethyl)phenyl) ethan-1-one (48): Prepared using the general procedure described above yielding **48** (89 mg, 61% yield, 90% *ee*) as a white solid. **48**: R_f = 0.55 (silica gel, EtOAc); $[\alpha]_D^{25}$ = –13.0º (*c* = 1.00, $CHCl_3$); IR (film) ν_{max} 3159, 2941, 2858, 1691, 1410, 1326, 1167, 1129, 1067, 1013, 848, 750 cm^{-1}; acyclic:cyclic = 3:1 ^1H NMR (500 MHz, $CDCl_3$) δ 8.07 (d, *J* = 7.2 Hz, 1.5 H), 7.82–7.74 (m, 0.5 H), 7.73–7.67 (m, 1.5 H), 7.66–7.55 (m, 0.5 H), 6.97–6.52 (br s, 1 H, exchangeable), 3.76–3.64 (m, 0.75 H), 3.62–3.50 (m, 0.25 H), 3.51–3.38 (m, 0.25 H), 3.34–3.25 (m, 0.75 H), 3.12–3.03 (m, 0.75 H), 3.00–2.89 (m, 0.25 H), 2.88–2.77 (m, 0.75 H), 2.69–2.60 (m, 0.25 H), 2.59–2.49 (m, 0.75 H), 2.42–2.23 (m, 0.25 H), 1.96–1.78 (m, 1 H), 1.77–1.53 (m, 3 H), 1.42–1.23 (m, 2 H); ^{13}C NMR (100 MHz, $CDCl_3$) δ 198.7, 147.3, 140.1, 134.3 (q, *J* = 33.3 Hz), 128.7, 126.2, 125.8, 125.3, 122.4, 119.7, 102.6, 68.2, 64.7, 60.0, 55.0, 52.2, 44.0, 43.5, 32.4, 29.8, 28.7, 25.8, 24.6, 23.6, 22.0; HRMS (ESI) calcd for $C_{14}H_{17}F_3NO_2^+$ [M + H^+] 288.1206, found 288.1212.

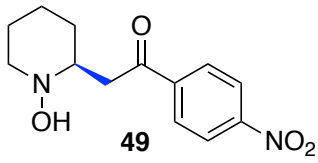

49

(*S*)-2-(1-hydroxypiperidin-2-yl)-1-(4-nitrophenyl)ethan-1-one (49): Prepared using the general procedure described above yielding **49** (81 mg, 61% yield, 90% *ee*) as a yellow solid. **49**: R_f = 0.50 (silica gel,

EtOAc); $[\alpha]_D^{25}$ = +1.7º (*c* = 1.00, $CHCl_3$); IR (film) ν_{max} 3110, 2940, 2856, 1691, 1604, 1524, 1347, 1200, 1106, 1012, 856, 746, 703 cm^{-1}; acyclic:cyclic = 1:1, ^1H NMR (500 MHz, $CDCl_3$) δ 8.34–8.25 (m, 1 H), 8.24–8.17 (m, 1 H), 8.17–8.06 (m, 1 H), 7.90–7.72 (m, 1 H), 7.09–6.66 (br s, 1 H, exchangeable), 3.85–3.65 (m, 0.5 H), 3.65–3.35 (m, 0.5 H), 3.33–3.23 (m, 0.5 H), 3.22–3.13 (m, 0.25 H), 3.13–3.03 (m, *J* = 31.0 Hz, 0.5 H), 3.03–2.92 (m, 0.25 H), 2.91–2.75 (m, 0.5 H), 2.75–2.44 (m, 1.5 H), 2.41–2.32 (m, 0.25 H), 1.95–1.84 (m, 1.25 H), 1.81–1.51 (m, 3 H), 1.46–1.35 (m, 1 H), 1.34–1.22 (m, 1 H); ^{13}C NMR (100 MHz, $CDCl_3$) δ 198.1, 150.3, 142.0, 129.4, 126.9, 123.9, 123.5, 102.4, 68.2, 64.7, 59.9, 55.0, 52.3, 44.2, 32.3, 28.7, 25.6, 24.7, 24.6, 23.5; HRMS (ESI) calcd for $C_{13}H_{17}N_2O_4^+$ [M + H^+] 265.1183, found 265.1188.

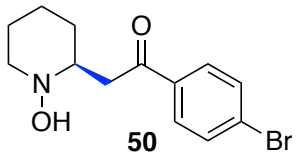

50

(*S*)-1-(4-bromophenyl)-2-(1-hydroxypiperidin-2-yl)ethan-1-one (50): Prepared using the general procedure described above yielding **50** (81 mg, 54% yield, 91% *ee*) as a pale-yellow solid. **50**: R_f = 0.45 (silica gel, EtOAc); $[\alpha]_D^{25}$ = –25.8º (*c* = 1.00, $CHCl_3$); IR (film) ν_{max} 3159, 2937, 2856, 1684, 1585, 1396, 1288, 1203, 1071, 1007, 841, 752 cm^{-1}; acyclic ^1H NMR (500 MHz, $CDCl_3$) δ 7.83 (d, *J* = 14.9 Hz, 2 H), 7.58 (d, *J* = 15.3 Hz, 2 H), 6.56–5.67 (br s, 1 H, exchangeable), 3.65 (dd, *J* = 16.0, 10.2 Hz, 1 H), 3.35–3.27 (m, 1 H), 3.07–2.97 (m, 1 H), 2.78 (dd, *J* = 15.3, 6.4 Hz, 1 H), 2.59–2.51 (m, 1 H), 1.90–1.84 (m, 1 H), 1.76–1.70 (m, 1 H), 1.65–1.57 (m, 2 H), 1.37–1.24 (m, 2 H); ^{13}C NMR (100 MHz, $CDCl_3$) δ 198.6, 136.0, 132.0, 129.9, 128.3, 64.7, 60.0, 43.6, 32.2, 25.8, 23.6; HRMS (ESI) calcd for $C_{13}H_{17}BrNO_2^+$ [M + H^+] 298.0437, found 298.0437.

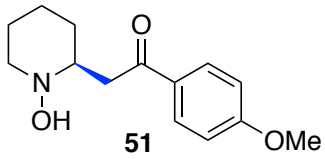

51

(*S*)-2-(1-hydroxypiperidin-2-yl)-1-(4-methoxyphenyl)ethan-1-one (51): Prepared using the general procedure described above yielding **51** (82 mg, 65% yield, 92% *ee*) as a pale-yellow oil. **51**: R_f = 0.38 (silica gel, EtOAc); $[\alpha]_D^{25}$ = –32.7º (*c* = 1.00, $CHCl_3$); IR (film) ν_{max} 3176, 2936, 2855, 1673, 1601, 1511,

1258, 1172, 1030, 843, 749 cm^{-1}; acyclic ^1H NMR (500 MHz, $CDCl_3$) δ 7.96 (d, *J* = 8.7 Hz, 2 H), 6.90 (d, *J* = 8.7 Hz, 2 H), 3.85 (s, 3 H), 3.68 (dd, *J* = 15.1, 3.6 Hz, 1 H), 3.34 (d, *J* = 9.1 Hz, 1 H), 3.06–2.97 (m, 1 H), 2.79 (dd, *J* = 15.1, 7.4 Hz, 1 H), 2.56 (t, *J* = 10.4 Hz, 1 H), 1.91–1.85 (m, 1 H), 1.77–1.69 (m, 1 H), 1.64–1.55 (m, 2 H), 1.37–1.21 (m, 2 H); ^{13}C NMR (100 MHz, $CDCl_3$) δ 198.3, 163.6, 130.7, 130.5, 113.9, 65.0, 60.0, 55.6, 43.2, 32.3, 26.0, 23.7; HRMS (ESI) calcd for $C_{14}H_{20}NO_3^+$ [M + H^+] 250.1438, found 250.1439.

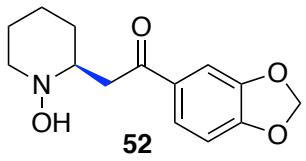

52

(*S*)-1-(benzo[d][1,3]dioxol-5-yl)-2-(1-hydroxypiperidin-2-yl)ethan-1-one (52): Prepared using the general procedure described above yielding **52** (88 mg, 66% yield, 93% *ee*) as a clear oil. **52**: R_f = 0.46 (silica gel, EtOAc); $[\alpha]_D^{25}$ = –26.9º (*c* = 1.00, $CHCl_3$); IR (film) ν_{max} 3188, 2936, 2857, 1673, 1604, 1503, 1443, 1354, 1249, 1112, 1038, 933, 809, 736 cm^{-1}; acyclic ^1H NMR (500 MHz, $CDCl_3$) δ 7.58 (d, *J* = 8.1 Hz, 1 H), 7.45 (s, 1 H), 6.81 (d, *J* = 8.1 Hz, 1 H), 6.41–6.22 (br s, 1 H, exchangeable), 6.03 (s, 2 H), 3.62 (dd, *J* = 15.2, 4.2 Hz, 1 H), 3.33 (d, *J* = 9.6 Hz, 1 H), 3.06–2.96 (m, 1 H), 2.75 (dd, *J* = 15.2, 7.2 Hz, 1 H), 2.55 (t, *J* = 10.5 Hz, 1 H), 1.87 (d, *J* = 12.3 Hz, 1 H), 1.73 (d, *J* = 12.2 Hz, 1 H), 1.60 (t, *J* = 13.1 Hz, 2 H), 1.35–1.22 (m, 2 H); ^{13}C NMR (100 MHz, $CDCl_3$) δ 197.8, 151.8, 148.3, 132.2, 124.7, 108.2, 108.0, 101.9, 64.9, 60.0, 43.4, 32.3, 25.9, 23.7; HRMS (ESI) calcd for $C_{14}H_{18}NO_4^+$ [M + H^+] 264.1230, found 264.1242.

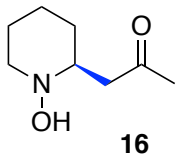

16

(*S*)-1-(1-hydroxypiperidin-2-yl)propan-2-one (16): Prepared using the general procedure described above yielding **16** (60 mg, 76% yield, 95% *ee*) as a pale-yellow oil. **16**: R_f = 0.36 (silica gel, EtOAc); $[\alpha]_D^{25}$ = +8.3º (*c* = 1.00, $CHCl_3$); IR (film) ν_{max} 3158, 2937, 2856, 1713, 1443, 1358, 1226, 1165, 1063, 862, 774 cm^{-1}; acyclic:cyclic = 1:1 ^1H NMR (500 MHz, $CDCl_3$) δ 7.89–7.33 (br s, 0.5 H, exchangeable), 6.16–5.55 (br s, 0.5 H, exchangeable), 3.44–3.33 (m, 0.5 H), 3.31–3.26 (m, 0.5 H), 3.06–2.96 (m, 0.5 H), 2.95–2.86 (m,

0.5 H), 2.59–2.28 (m, 2.5 H), 2.18 (s, 1.5 H), 2.08–1.95 (m, 0.5 H), 1.94–1.52 (m, 4.5 H), 1.45 (s, 1.5 H), 1.34–1.16 (m, 1.5 H); ^{13}C NMR (100 MHz, $CDCl_3$) δ 208.3, 102.4, 68.1, 64.1, 60.0, 54.8, 49.4, 49.2, 32.2, 30.5, 28.9, 26.7, 25.7, 24.6, 23.6; HRMS (ESI) calcd for $C_8H_{16}NO_2^+$ [M + H^+] 158.1176, found 158.1173.

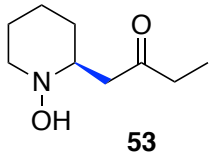

53

(*S*)-1-(1-hydroxypiperidin-2-yl)butan-2-one (53): Prepared using the general procedure described above yielding **53** (76 mg, 88% yield, 95% *ee*) as a clear oil. **53**: R_f = 0.40 (silica gel, EtOAc); $[\alpha]_D^{25}$ = +10.0º (*c* = 1.00, $CHCl_3$); IR (film) ν_{max} 3159, 2937, 2857, 1712, 1444, 1377, 1215, 1113, 952, 897, 767 cm^{-1}; acyclic:cyclic = 1:1 ^{1}H NMR (500 MHz, $CDCl_3$) δ 7.56–7.33 (br s, 0.5 H, exchangeable), 5.69–5.35 (br s, 0.5 H, exchangeable), 3.45–3.35 (m, 0.5 H), 3.31–3.23 (m, 0.5 H), 3.00 (dd, *J* = 15.5, 5.1 Hz, 0.5 H), 2.95–2.87 (m, 0.5 H), 2.55–2.37 (m, 2.5 H), 2.36–2.23 (m, 1 H), 1.99–1.84 (m, 1 H), 1.83–1.66 (m, 3 H), 1.65–1.52 (m, 1.5 H), 1.50–1.37 (m, 0.5 H), 1.32–1.17 (m, 1.5 H), 1.04 (t, *J* = 7.2 Hz, 1.5 H), 0.98 (t, *J* = 7.2 Hz, 1.5 H); ^{13}C NMR (100 MHz, $CDCl_3$) δ 210.8, 104.4, 68.1, 64.2, 60.0, 54.8, 47.8, 47.2, 36.4, 32.2, 29.0, 25.7, 24.6, 23.7, 8.6, 7.9; HRMS (ESI) calcd for $C_9H_{18}NO_2^+$ [M + H^+] 172.1332, found 172.1334.

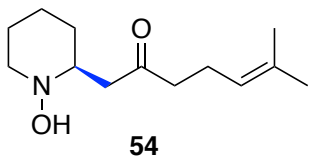

54

(*S*)-1-(1-hydroxypiperidin-2-yl)-6-methylhept-5-en-2-one (54): Prepared using the general procedure described above yielding **54** (102 mg, 90% yield, 96% *ee*) as a clear oil. **54**: R_f = 0.53 (silica gel, EtOAc); $[\alpha]_D^{25}$ = +2.9º (*c* = 1.00, $CHCl_3$); IR (film) ν_{max} 3163, 2936, 2857, 1713, 1444, 1377, 1277, 1110, 985, 861, 778 cm^{-1}; acyclic:cyclic = 1.5:1 ^{1}H NMR (500 MHz, $CDCl_3$) δ 7.23–6.94 (br s, 0.6 H, exchangeable), 5.73–5.34 (br s, 0.4 H, exchangeable), 5.19–5.09 (m, 0.4 H), 5.09–5.00 (m, 0.6 H), 3.44–3.23 (m, 1 H), 3.11–2.80 (m, 1 H), 2.62–2.32 (m, 3 H), 2.32–2.01 (m, 3 H), 2.00–1.71 (m, 3 H), 1.68–1.51 (m, 8 H), 1.50–1.14 (m, 2 H); ^{13}C NMR (100 MHz, $CDCl_3$) δ 210.0, 132.7, 132.0,

124.1, 123.0, 103.9, 68.0, 64.0, 59.9, 54.8, 48.2, 47.9, 43.3, 39.6, 32.3, 28.9, 25.8, 25.7, 24.6, 23.6, 23.0, 22.6, 17.8; HRMS (ESI) calcd for $C_{13}H_{24}NO_2^+$ [M + H^+] 226.1802, found 226.1803.

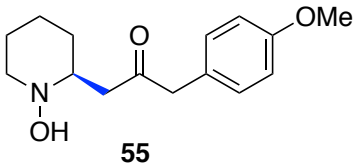

55

(*S*)-1-(1-hydroxypiperidin-2-yl)-3-(4-methoxyphenyl)propan-2-one (55): Prepared using the general procedure described above yielding **55** (106 mg, 80% yield, 96% *ee*) as a clear oil. **55**: R_f = 0.51 (silica gel, EtOAc); $[\alpha]_D^{25}$ = +16.0º (*c* = 1.00, $CHCl_3$); IR (film) ν_{max} 3148, 2937, 2836, 1710, 1611, 1513, 1442, 1301, 1248, 1178, 1036, 825 cm^{-1}; acyclic:cyclic = 1:1.7 ^1H NMR (500 MHz, $CDCl_3$) δ 7.24 (d, *J* = 8.2 Hz, 1.2 H), 7.11 (d, *J* = 7.8 Hz, 0.8 H), 6.92–6.77 (m, 2 H), 6.77–6.62 (br s, 1 H, exchangeable), 3.84–3.74 (m, 3 H), 3.74–3.60 (m, 0.8 H), 3.48–3.35 (m, 0.6 H), 3.33–3.22 (m, 0.4 H), 3.05–2.85 (m, 2 H), 2.55–2.44 (m, 0.4 H), 2.44–2.31 (m, 1.3 H), 1.96–1.79 (m, 1 H), 1.79–1.68 (m, 2 H), 1.67–1.51 (m, 2 H), 1.38–1.17 (m, 2 H), 1.17–1.04 (m, 0.5 H); ^{13}C NMR (100 MHz, $CDCl_3$) δ 207.9, 158.7, 158.6, 132.0, 130.7, 128.3, 126.5, 114.2, 114.0, 113.9, 113.5, 103.6, 68.0, 64.1, 60.0, 55.4, 54.8, 49.6, 47.2, 46.9, 44.3, 32.2, 28.8, 26.9, 25.7, 24.6, 23.6; HRMS (ESI) calcd for $C_{15}H_{22}NO_3^+$ [M + H^+] 264.1594, found 264.1593.

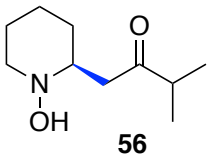

56

(*S*)-1-(1-hydroxypiperidin-2-yl)-3-methylbutan-2-one (56): Prepared using the general procedure described above yielding **56** (57 mg, 61% yield, 94% *ee*) as a clear oil. **56**: R_f = 0.49 (silica gel, EtOAc); $[\alpha]_D^{25}$ = +21.1º (*c* = 1.00, $CHCl_3$); IR (film) ν_{max} 3163, 2938, 2858, 1710, 1468, 1382, 1268, 1149, 1107, 1031, 955, 759 cm^{-1}; acyclic:cyclic = 1:1 ^1H NMR (500 MHz, $CDCl_3$) δ 7.18–6.83 (br s, 0.5 H, exchangeable), 5.23–4.54 (br s, 0.5 H, exchangeable), 3.43–3.35 (m, 0.5 H), 3.32–3.25 (m, 0.5 H), 3.07 (dd, *J* = 16.1, 4.7 Hz, 0.5 H), 2.93–2.86 (m, 0.5 H), 2.71–2.62 (m, 0.5 H), 2.54–2.35 (m, 2 H), 2.27–2.17 (m, 0.5 H), 1.91–1.84 (m, 1 H), 1.81–1.75 (m, 1 H), 1.74–1.67 (m, 1 H), 1.65–1.56 (m, 1.5 H), 1.47–1.37 (m, 0.5 H), 1.29–1.17 (m, 1.5 H), 1.11–1.05 (m, 3.5 H), 1.02–0.94 (m, 3 H); ^{13}C NMR (100 MHz,

$CDCl_3$) δ 214.0, 106.0, 68.2, 64.0, 60.0, 54.8, 45.6, 45.5, 41.1, 35.9, 32.2, 29.1, 25.8, 24.7, 23.7, 23.6, 18.3, 17.8, 17.3; HRMS (ESI) calcd for $C_{10}H_{20}NO_2^+$ [M + H^+] 186.1489, found 186.1492.

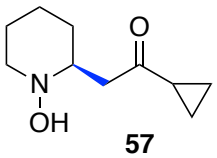

57

(*S*)-1-cyclopropyl-2-(1-hydroxypiperidin-2-yl)ethan-1-one (57): Prepared using the general procedure described above yielding **57** (47 mg, 51% yield, 95% *ee*) as a clear oil. **57**: R_f = 0.36 (silica gel, EtOAc); $[\alpha]_D^{25}$ = –31.1º (*c* = 1.00, $CHCl_3$); IR (film) ν_{max} 3183, 2037, 2857, 1695, 1444, 1389, 1276, 1065, 903, 822, 764 cm^{-1}; acyclic ^1H NMR (500 MHz, $CDCl_3$) δ 7.14–6.53 (br s, 1 H, exchangeable), 3.30 (d, *J* = 9.9 Hz, 1 H), 3.18 (dd, *J* = 15.5, 4.8 Hz, 1 H), 2.97–2.87 (m, 1 H), 2.59–2.44 (m, 2 H), 1.97 (td, *J* = 7.7, 4.0 Hz, 1 H), 1.86–1.77 (m, 1 H), 1.75–1.68 (m, 1 H), 1.65–1.54 (m, 2 H), 1.31–1.21 (m, 2 H), 1.06–0.98 (m, 2 H), 0.90–0.83 (m, 2 H); ^{13}C NMR (100 MHz, $CDCl_3$) δ 210.5, 64.3, 59.9, 48.8, 32.3, 25.9, 23.7, 21.1, 11.2, 11.0; HRMS (ESI) calcd for $C_{10}H_{18}NO_2^+$ [M + H^+] 184.1332, found 184.1335.

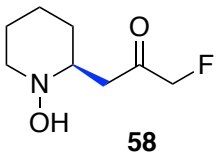

58

(*S*)-1-fluoro-3-(1-hydroxypiperidin-2-yl)propan-2-one (58): Prepared using the general procedure described above yielding **58** (66 mg, 75% yield, 95% *ee*) as a clear oil. **58**: R_f = 0.54 (silica gel, EtOAc); $[\alpha]_D^{25}$ = +75.5º (*c* = 1.00, $CHCl_3$); IR (film) ν_{max} 3399, 3139, 2941, 2857, 1728, 1445, 1282, 1152, 1109, 1047, 861, 779 cm^{-1}; cyclic, *dr* (cyclic) = 7:1, major dr: ^1H NMR (500 MHz, $CDCl_3$) δ 4.89–4.56 (br s, 1 H, exchangeable), 4.32 (d, *J* = 47.1 Hz, 2 H), 3.52–3.35 (m, 1 H), 2.62–2.45 (m, 2 H), 2.44–2.29 (m, 1 H), 2.14–1.97 (m, 1 H), 1.96–1.86 (m, 1 H), 1.85–1.62 (m, 3 H), 1.55–1.41 (m, 1 H), 1.31–1.19 (m, 1 H); ^{13}C NMR (100 MHz, $CDCl_3$) δ 101.3 (d, *J* = 13.7 Hz), 83.7 (d, *J* = 176.0 Hz), 68.2, 55.0, 44.9, 28.8, 24.6, 23.6; HRMS (ESI) calcd for $C_8H_{15}FNO_2^+$ [M + H^+] 176.1081, found 176.1084.

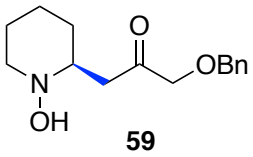

59

(*S*)-1-(benzyloxy)-3-(1-hydroxypiperidin-2-yl)propan-2-one (59): Prepared using the general procedure described above yielding **59** (99 mg major regioisomer, 75% yield, 95% *ee*; 117 mg combined, 5.9:1 *rr*, 88% yield). **59**: IR (film) ν_{max} 3400, 2940, 2857, 1722, 1453, 1260, 1104, 850, 738, 698 cm^{-1}; ^1H NMR (500 MHz, $CDCl_3$) δ 7.40–7.27 (m, 5 H), 4.68–4.58 (m, 2 H), 4.15–4.07 (m, 0.3 H), 3.56–3.52 (m, 1.5 H), 3.49–3.43 (m, 0.9 H), 2.63–2.56 (m, 0.3 H), 2.53–2.44 (m, 0.9 H), 2.42–2.34 (m, 0.8 H), 2.34–2.25 (m, 0.8 H), 2.19–2.12 (m, 0.2 H), 2.06–1.96 (m, 0.7 H), 1.91–1.83 (m, 1 H), 1.81–1.75 (m, 0.9 H), 1.74–1.66 (m, 1.9 H), 1.62–1.53 (m, 0.5 H), 1.52–1.40 (m, .9 H), 1.29–1.14 (m, 1.2 H); HRMS (CI) calcd for $C_{15}H_{22}NO_3^+$ [M + H^+] 264.1594, found 264.1600.

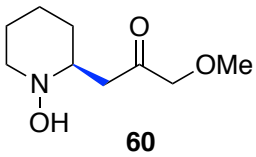

60

(*S*)-1-(1-hydroxypiperidin-2-yl)-3-methoxypropan-2-one (60): Prepared using the general procedure described above yielding **60** (61 mg major regioisomer, 65% yield, 94% *ee*; 73 mg combined 5.4:1 *rr*, 77% yield) as a yellow oil. **60**: R_f = 0.29 (silica gel, EtOAc); $[\alpha]_D^{25}$ = +59.2º (*c* = 1.00, $CHCl_3$); IR (film) ν_{max} 3401, 3148, 2938, 2857, 1722, 1445, 1261, 1120, 1049, 980, 861, 780 cm^{-1}; cyclic, *dr* (cyclic) = 2.7:1 ^1H NMR (500 MHz, $CDCl_3$) δ 4.09–3.99 (m, 0.3 H), 3.61–3.34 (m, 6 H), 2.66–2.52 (m, 0.3 H), 2.51–2.42 (m, 0.7 H), 2.42–2.32 (m, 0.8 H), 2.32–2.25 (m, 0.7 H), 2.20–2.07 (m, 0.2 H), 2.06–1.94 (m, 0.6 H), 1.96–1.83 (m, 1 H), 1.82–1.55 (m, 3 H), 1.53–1.42 (m, 0.9 H), 1.40–1.15 (m, 1.5 H); ^{13}C NMR (100 MHz, $CDCl_3$) δ 102.1, 101.8, 76.5, 76.3, 68.0, 65.6, 59.8, 59.7, 55.8, 55.2, 45.2, 43.8, 29.0, 28.9, 24.9, 24.6, 23.7; HRMS (ESI) calcd for $C_9H_{18}NO_3^+$ [M + H^+] 188.1281, found 188.1282.

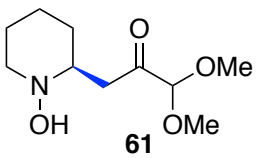

61

(*S*)-3-(1-hydroxypiperidin-2-yl)-1,1-dimethoxypropan-2-one (61): Prepared using the general procedure described above yielding **61** (94 mg, 86% yield, 96% *ee*) as a clear oil. **61**: R_f = 0.32 (silica gel, EtOAc); $[\alpha]_D^{25}$ =

+65.1º (*c* = 1.00, $CHCl_3$); IR (film) ν_{max} 3417, 3149, 2938, 2833, 1729, 1446, 1351, 1262, 1152, 1086, 988, 862 cm^{-1}; cyclic, *dr*(cyclic) = 2:1 ^1H NMR (500 MHz, $CDCl_3$) δ 4.31 (s, 0.33 H), 4.26 (s, 0.67 H), 3.81 (br s, 0.33 H, exchangeable), 3.66 (br s, 0.67 H, exchangeable), 3.58 (s, 1 H), 3.53 (s, 2 H), 3.50 (s, 2 H), 3.45 (s, 1 H), 2.64–2.41 (m, 2 H), 2.35–2.23 (m, 0.67 H), 2.20–2.08 (m, 0.33 H), 2.07–1.91 (m, 1 H), 1.91–1.56 (m, 4 H), 1.56–1.30 (m, 1.67 H), 1.30–1.09 (m, 1.33 H); ^{13}C NMR (100 MHz, $CDCl_3$) δ 105.9, 105.3, 103.0, 102.6, 68.0, 65.6, 57.7, 56.8, 56.6, 56.0, 55.5, 55.4, 43.8, 42.6, 29.0, 24.9, 24.7, 23.7, 23.7; HRMS (ESI) calcd for $C_{10}H_{20}NO_4^+$ [M + H^+] 218.1387, found 218.1389.

General Procedure for Decarboxylative Mannich-type Reactions between Nitrones 72 and β-ketoacids 73.

To a vial containing β-ketoacid **73** (0.76 mmol, 1.5 equiv) at 23 ºC under an ambient atmosphere was added a solution of nitrone **72** (0.50 mmol, 1.0 equiv) in CH_2Cl_2 (0.5 mL). The reaction mixture was then stirred for 16 h. Upon completion, the contents were quenched with saturated aqueous $NaHCO_3$ (2 mL) and extracted with CH_2Cl_2 (3 × 2 mL). The combined organic extracts were then dried ($MgSO_4$), filtered, and concentrated. The resultant crude material was purified by flash column chromatography (silica gel, hexane/EtOAc) to yield **74**.

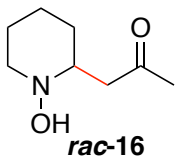

***rac*-16**

(±)-1-(1-hydroxypiperidin-2-yl)propan-2-one (*rac*-16): Prepared using the general procedure described above with **14** and **S20** ultimately yielding ***rac*-16** (16 h: 56 mg, 71% yield; 2 h: 52 mg, 66% yield) as a pale-yellow oil. ***rac*-16**: See above.

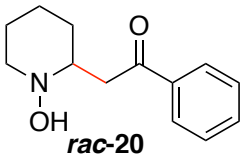

***rac*-20**

(±)-2-(1-hydroxypiperidin-2-yl)-1-phenylethan-1-one (*rac*-20): Prepared using the general procedure described above with **14** and **S24** ultimately yielding ***rac*-20** (16 h: 100 mg, 90% yield; 2 h: 88 mg, 80% yield) as a pale-yellow oil. ***rac*-20**: See above.

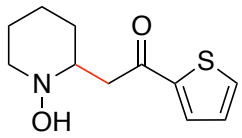

75

(±)-2-(1-hydroxypiperidin-2-yl)-1-(thiophen-2-yl)ethan-1-one (75): Prepared using the general procedure described above with **14** and **S25** ultimately yielding **75** (99 mg, 87% yield) as a yellow oil. **75**: R_f = 0.49 (silica gel, EtOAc); IR (film) ν_{max} 3102, 2937, 2856, 1656, 1518, 1415, 1355, 1291, 1235, 1059, 859, 730 cm^{-1}; acyclic ^1H NMR (500 MHz, $CDCl_3$) δ 7.75 (d, *J* = 3.2 Hz, 1 H), 7.62 (d, *J* = 4.8 Hz, 1 H), 7.18–7.05 (m, 1 H), 6.60–6.07 (br s, 1 H, exchangeable), 3.59 (dd, *J* = 14.9, 4.0 Hz, 1 H), 3.34 (d, *J* = 8.5 Hz, 1 H), 3.09–2.99 (m, 1 H), 2.81 (dd, *J* = 14.9, 7.1 Hz, 1 H), 2.57 (t, *J* = 10.8 Hz, 1 H), 1.95–1.82 (m, 1 H), 1.80–1.67 (m, 1 H), 1.67–1.51 (m, 2 H), 1.42–1.20 (m, 2 H); ^{13}C NMR (100 MHz, $CDCl_3$) δ 192.3, 144.9, 133.8, 132.3, 128.2, 64.9, 59.9, 44.3, 32.2, 25.9, 23.6; HRMS (ESI) calcd for $C_{11}H_{16}NO_2S^+$ [M + H^+] 226.0896, found 226.0899.

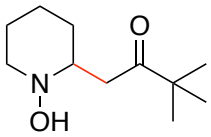

64

(±)-1-(1-hydroxypiperidin-2-yl)-3,3-dimethylbutan-2-one (64): Prepared using the general procedure described above (except using MeOH as the solvent) with **14** and **S26** ultimately yielding **64** (51 mg, 51% yield) as a white solid. **64**: R_f = 0.59 (silica gel, EtOAc); IR (film) ν_{max} 3166, 2939, 2860, 1704, 1479, 1363, 1271, 1149, 1102, 963, 898, 747 cm^{-1}; acyclic:cyclic = 1:1 ^1H NMR (500 MHz, $CDCl_3$) δ 6.43–5.96 (br s, 0.5 H, exchangeable), 4.35–3.95 (br s, 0.5 H, exchangeable), 3.42–3.35 (m, 0.5 H), 3.34–3.28 (m, 0.5 H), 3.20–3.12 (m, 0.5 H), 2.96–2.85 (m, 0.5 H), 2.62–2.42 (m, 2 H), 2.25–2.13 (m, 0.5 H), 1.91–1.82 (m, 0.5 H), 1.82–1.63 (m, 3 H), 1.63–1.54 (m, 1 H), 1.48–1.37 (m, 0.5 H), 1.33–1.16 (m, 1.5 H), 1.13 (s, 5 H), 1.01 (s, 4 H); ^{13}C NMR (100 MHz, $CDCl_3$) δ 215.1, 107.4, 68.3, 63.9, 60.0, 54.9,

45.0, 44.5, 41.1, 37.3, 31.9, 29.2, 26.4, 26.0, 25.2, 24.7, 23.8, 23.7; HRMS (ESI) calcd for $C_{11}H_{22}NO_2^+$ [M + H^+] 200.1645, found 200.1648. See **S37** for ^1H and ^{13}C NMR data of the *O*-benzoylated adduct.

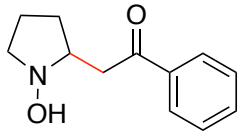

76

(±)-2-(1-hydroxypyrrolidin-2-yl)-1-phenylethan-1-one (76): Prepared using the general procedure described above with **S5** and **S24** ultimately yielding **76** (86 mg, 84% yield) as a yellow oil. **76**: R_f = 0.40 (silica gel, EtOAc); IR (film) ν_{max} 3213, 2963, 1681, 1598, 1450, 1259, 1065, 1025, 754, 710 cm^{-1}; acyclic ^1H NMR (500 MHz, $CDCl_3$) δ 8.02–7.87 (m, 2 H), 7.62–7.48 (m, 1 H), 7.48–7.33 (m, 2 H), 3.64–3.45 (m, 1 H), 3.44–3.18 (m, 2 H), 3.12–2.94 (m, 1 H), 2.92–2.76 (m, 1 H), 2.27–2.05 (m, 1 H), 1.89–1.68 (m, 2 H), 1.55–1.31 (m, 1 H); ^{13}C NMR (125 MHz, $CDCl_3$) δ 199.4, 137.2, 133.2, 128.7, 128.3, 65.1, 57.6, 42.6, 27.9, 20.1; HRMS (ESI) calcd for $C_{12}H_{16}NO_2^+$ [M + H^+] 206.1176, found 206.1174. See **S38** for ^1H and ^{13}C NMR data of the *O*-benzoylated adduct.

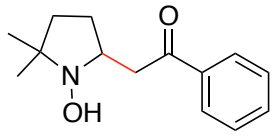

77

(±)-2-(1-hydroxy-5,5-dimethylpyrrolidin-2-yl)-1-phenylethan-1-one (77): Prepared using the general procedure described above with **S14** and **S24** ultimately yielding **77** (59 mg, 50% yield) as a yellow oil. **77**: R_f = 0.50 (silica gel, hexane/EtOAc = 1/1); IR (film) ν_{max} 3175, 2968, 2874, 1682, 1597, 1449, 1210, 1002, 755, 691 cm^{-1}; acyclic:cyclic = 4:1 ^1H NMR (500 MHz, $CDCl_3$) δ 7.92 (d, *J* = 7.5 Hz, 1.6 H), 7.69–7.60 (m, 0.4 H), 7.57–7.48 (m, 0.8 H), 7.47–7.28 (m, 2.2 H), 6.61–5.97 (br s, 1 H, exchangeable), 4.22–3.97 (m, 0.2 H), 3.75–3.41 (m, 1.4 H), 3.10 (dd, *J* = 17.0, 9.6 Hz, 0.8 H), 3.02–2.94 (m, 0.2 H), 2.49–2.28 (m, 0.2 H), 2.13 (dd, *J* = 12.1, 9.2 Hz, 1.2 H), 1.69–1.55 (m, 2 H), 1.41–1.32 (m, 1.4 H), 1.22 (s, 2.4 H), 1.08 (s, 3.2 H); ^{13}C NMR (100 MHz, $CDCl_3$) δ 200.2, 137.5, 133.0, 128.7, 128.4, 59.7, 57.9, 44.5, 39.1, 33.1, 30.1, 27.6, 19.9, 15.0; HRMS (ESI) calcd for $C_{14}H_{20}NO_2^+$ [M + H^+] 234.1489, found 234.1491.

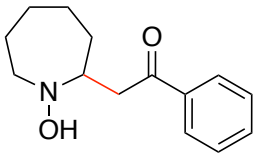

78

(±)-2-(1-hydroxyazepan-2-yl)-1-phenylethan-1-one (78): Prepared using the general procedure described above with **S9** and **S24** ultimately yielding **78** (78 mg, 66% yield) as a yellow oil. **78**: R_f = 0.68 (silica gel, EtOAc); IR (film) ν_{max} 3061, 2932, 2857, 1683, 1598, 1450, 1246, 1063, 710 cm^{-1}; acyclic:cyclic = 1:3.4 ^1H NMR (500 MHz, $CDCl_3$) δ 8.07–7.80 (m, 0.5 H), 7.78–7.59 (m, 1.5 H), 7.58–7.08 (m, 3 H), 6.18–4.85 (br s, 1 H, exchangeable), 3.84–3.38 (m, 1.5 H), 3.31–2.84 (m, 1.5 H), 2.84–2.52 (m, 1.2 H), 2.51–2.34 (m, 0.4 H), 2.26–2.02 (m, 0.4 H), 2.01–1.34 (m, 8 H); ^{13}C NMR (100 MHz, MeOD) δ 143.7, 142.0, 132.9, 127.7, 125.6, 103.9, 65.9, 60.8, 57.8, 52.0, 29.6, 29.1, 26.9, 26.2, 25.0, 24.4, 24.3; HRMS (ESI) calcd for $C_{14}H_{20}NO_2^+$ [M + H^+] 234.1489, found 234.1490. See **S39** for ^1H and ^{13}C NMR data of the *O*-benzoylated adduct.

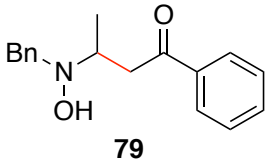

79

(±)-3-(benzyl(hydroxy)amino)-1-phenylbutan-1-one (79): Prepared using the general procedure described above with **S13** and **S24** ultimately yielding **79** (82 mg, 61% yield) as a yellow oil. **79**: R_f = 0.42 (silica gel, hexanes/EtOAc = 4/1); IR (film) ν_{max} 3168, 2974, 2875, 1681, 1587, 1449, 1370, 1287, 1210, 1003, 738, 697 cm^{-1}; acyclic:cyclic = 2:1, *dr*(acyclic) = 2:1 ^1H NMR (500 MHz, $CDCl_3$) δ 7.98 (d, *J* = 7.5 Hz, 1.2 H), 7.67–7.53 (m, 1.4 H), 7.52–7.42 (m, 2 H), 7.41–7.20 (m, 5.4 H), 6.40–6.01 (br s, 1 H, exchangeable), 4.35–4.12 (m, 0.5 H), 3.93 (dd, *J* = 13.4, 9.0 Hz, 0.9 H), 3.76 (d, *J* = 13.0 Hz, 0.7 H), 3.59 (dq, *J* = 12.9, 6.4 Hz, 0.8 H), 3.46 (dd, *J* = 15.9, 4.9 Hz, 0.6 H), 2.96 (dd, *J* = 15.9, 8.0 Hz, 0.9 H), 2.73 (dd, *J* = 12.4, 5.8 Hz, 0.1 H), 2.56 (dd, *J* = 13.3, 7.5 Hz, 0.2 H), 2.27–2.12 (m, 0.1 H), 2.08–1.96 (m, 0.2 H), 1.24 (d, *J* = 6.4 Hz, 1.8 H), 1.16 (d, *J* = 6.1 Hz, 0.4 H), 1.11 (d, *J* = 6.1 Hz, 0.8 H); ^{13}C NMR (100 MHz, $CDCl_3$) δ 199.7, 143.1, 137.7, 137.5, 137.2, 136.1, 133.0, 130.0, 129.8, 129.3, 128.3, 128.3, 128.2, 128.1, 127.9, 127.5, 127.8, 127.4, 127.3, 125.7, 125.6,

104.7, 102.6, 61.8, 61.3, 60.5, 60.0, 58.2, 53.1, 51.9, 42.2, 16.3, 15.1; HRMS (ESI) calcd for $C_{17}H_{20}NO_2^+$ [M + H$^+$] 270.1489, found 270.1489.

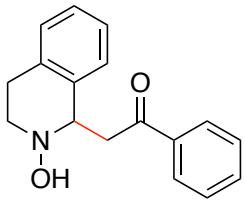

80

(±)-2-(2-hydroxy-1,2,3,4-tetrahydroisoquinolin-1-yl)-1-phenylethan-1-one (80): Prepared using the general procedure described above with **S6** and **S24** ultimately yielding **80** (46 mg, 34% yield) as a yellow oil. **80**: R_f = 0.50 (silica gel, hexane/EtOAc, 1/1); IR (film) ν_{max} 3062, 2929, 2848, 1684, 1597, 1493, 1448, 1354, 1276, 1209, 1002, 912, 748, 690 cm^{-1}; acyclic:cyclic = 1.5:1 ^{1}H NMR (500 MHz, $CDCl_3$) δ 8.16–7.81 (m, 1 H), 7.74–6.93 (m, 8 H), 6.93–6.66 (br s, 1 H, exchangeable), 5.16–4.96 (m, 0.4 H), 4.96–4.73 (m, 0.6 H), 3.95–3.63 (m, 0.6 H), 3.53–2.80 (m, 5 H), 2.65–2.35 (m, 0.4 H); ^{13}C NMR (100 MHz, $CDCl_3$) δ 199.1, 136.9, 133.7, 133.6, 133.2, 128.6, 128.5, 128.5, 127.4, 127.2, 126.9, 126.7, 126.0, 125.9, 125.7, 104.8, 63.4, 61.9, 52.2, 51.9, 51.7, 50.2, 49.8, 44.1, 28.6, 27.0; HRMS (ESI) calcd for $C_{17}H_{18}NO_2^+$ [M + H$^+$] 268.1332, found 268.1332. See **S40** for ^{1}H and ^{13}C NMR data of the *O*-benzoylated adduct.

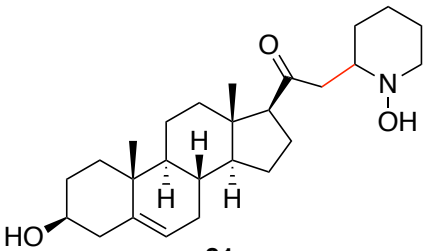

81

(±)-1-((3*S*, 8*S*, 9*S*, 10*R*, 13*S*, 14*S*, 17*S*)-3-hydroxy-10,13-dimethyl-2, 3, 4, 7, 8, 9, 10, 11, 12, 13, 14, 15, 16, 17-tetradecahydro-1*H*-cyclopenta[a]phenanthren-17-yl)-2-(1-hydroxypiperidin-2-yl)ethan-1-one (81): Prepared using the general procedure described above with **14** (1.5 equiv) and **S28** (1.0 equiv) ultimately yielding **81** (161 mg, 77% yield, 2:1 *dr*) as a white solid. **81**: R_f = 0.16 (silica gel, hexanes/EtOAc = 1/1); $[\alpha]_D^{25}$ = –19.7° (*c* = 1.00, $CHCl_3$); IR (film) ν_{max} 3307, 2936, 2849, 1701, 1450, 1377, 1266, 1110, 1058, 954, 737 cm^{-1}; acyclic, *dr*(acyclic) = 2:1 ^{1}H NMR (500 MHz, $CDCl_3$) δ 7.18–6.86 (br s, 1 H, exchangeable), 5.33 (s, 1 H), 3.63–3.42 (m, 1 H), 3.41–3.20 (m, 1 H), 3.14–2.98 (m, 1 H), 2.97–2.83 (m, 1 H), 2.70–2.58 (m, 1 H), 2.58–2.46 (m, 1 H), 2.41–2.10 (m, 4 H), 2.08–1.93 (m, 2 H),

1.96–1.78 (m, 3 H), 1.79–1.35 (m, 11 H), 1.35–1.05 (m, 5 H), 0.98 (s, 3 H), 0.96–0.88 (m, 1 H), 0.63 (s, 2 H, major), 0.62 (s, 1 H, minor); ^{13}C NMR (125 MHz, $CDCl_3$) δ 210.8 (major), 210.5 (minor), 141.0, 121.4, 71.6, 64.4 (minor), 64.2 (major), 63.5 (minor), 63.2 (major), 60.1 (major), 60.0 (minor), 57.2 (minor), 57.2 (major), 50.3 (major), 50.2 (minor), 49.5 (major), 49.2 (minor), 44.4 (minor), 44.3 (major), 42.4, 39.2, 39.0, 37.5, 36.6, 32.3, 32.0, 31.9, 25.9, 25.5, 24.6, 23.7, 23.1, 23.1, 21.3, 19.5, 13.6 (minor), 13.4 (major); HRMS (ESI) calcd for $C_{26}H_{42}NO_3^+$ [M + H^+] 416.3158, found 416.3162.

General Procedure for Benzoylation of Hydroxylamines.

To a solution of hydroxylamine **27** or **74** (1.0 equiv) in CH_2Cl_2 (0.1 M) at 0 ºC were sequentially added 4-DMAP (0.2 equiv), Et_3N (4.0 equiv), and BzCl (2.0 equiv). The mixture was then warmed to 23 ºC and stirred at this temperature for 2 h. Upon completion (monitored by TLC), the contents were quenched with saturated aqueous $NaHCO_3$ (5 mL) and extracted with CH_2Cl_2 (3 × 5 mL). The combined organic layers were then dried ($MgSO_4$), filtered, and concentrated. The resultant crude product was purified by flash column chromatography (silica gel, hexane/EtOAc, 20/1→1/1) with yields up to 80%. The products **S29**-**S40** were then used to determine enantiopurity by HPLC.

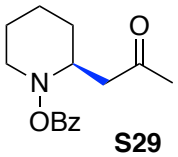

S29

(*S*)-2-(2-oxopropyl)piperidin-1-yl benzoate (S29): ^{1}H NMR (500 MHz, $CDCl_3$) δ 7.96 (d, *J* = 7.4 Hz, 2 H), 7.64–7.49 (m, 1 H), 7.48–7.34 (m, 2 H), 3.65–3.50 (m, 1 H), 3.49–3.33 (m, 1 H), 2.87 (dd, *J* = 17.1, 5.0 Hz, 1 H), 2.74 (t, *J* = 9.5 Hz, 1 H), 2.44 (dd, *J* = 17.1, 6.4 Hz, 1 H), 2.01 (s, 3 H), 1.92–1.62 (m, 4 H), 1.61–1.47 (m, 1 H), 1.44–

1.28 (m, 1 H); ^{13}C NMR (100 MHz, $CDCl_3$) δ 207.3, 165.0, 133.3, 129.6, 129.1, 128.6, 62.7, 58.0, 48.1, 32.1, 31.2, 25.5, 23.6.

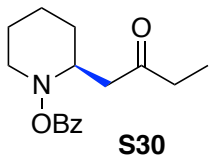

S30

(*S*)-2-(2-oxobutyl)piperidin-1-yl benzoate (S30): ^{1}H NMR (500 MHz, $CDCl_3$) δ 7.95 (d, *J* = 7.2 Hz, 2 H), 7.63–7.49 (m, 1 H), 7.49–7.35 (m, 2 H), 3.58–3.51 (m, 1 H), 3.50–3.36 (m, 1 H), 2.84 (dd, *J* = 16.9, 5.3 Hz, 1 H), 2.75 (t, *J* = 9.9 Hz, 1 H), 2.40 (dd, *J* = 16.9, 5.6 Hz, 1 H), 2.36–2.27 (m, 1 H), 2.27–2.16 (m, 1 H), 1.89–1.64 (m, 4 H), 1.60–1.46 (m, 1 H), 1.43–1.29 (m, 1 H), 0.85 (t, *J* = 6.7 Hz, 3 H); ^{13}C NMR (100 MHz, $CDCl_3$) δ 209.8, 165.0, 133.3, 129.6, 129.1, 128.6, 62.6, 58.0, 47.0, 37.2, 32.2, 25.5, 23.6, 7.5.

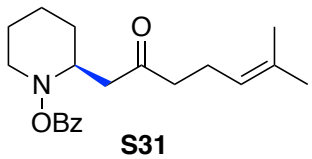

S31

(*S*)-2-(6-methyl-2-oxohept-5-en-1-yl)piperidin-1-yl benzoate (S31): ^{1}H NMR (500 MHz, $CDCl_3$) δ 7.97 (d, *J* = 7.0 Hz, 2 H), 7.66–7.50 (m, 1 H), 7.49–7.33 (m, 2 H), 5.03–4.78 (m, 1 H), 3.67–3.53 (m, 1 H), 3.53–3.37 (m, 1 H), 2.84 (dd, *J* = 17.1, 5.0 Hz, 1 H), 2.75 (t, *J* = 9.7 Hz, 1 H), 2.41 (dd, *J* = 17.0, 5.7 Hz, 1 H), 2.36–2.28 (m, 1 H), 2.28–2.18 (m, 1 H), 2.18–2.09 (m, 1 H), 2.07–1.97 (m, 1 H), 1.94–1.64 (m, 4 H), 1.58 (s, 3 H), 1.56-1.50 (m, 1 H), 1.48 (s, 3 H), 1.42–1.30 (m, 1 H); ^{13}C NMR (100 MHz, $CDCl_3$) δ 209.2, 165.0, 133.3, 132.8, 129.6, 129.1, 128.6, 122.6, 62.6, 58.1, 47.4, 44.1, 32.2, 25.7, 25.5, 23.6, 22.3, 17.7.

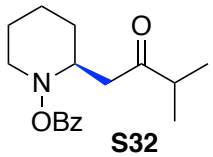

S32

(*S*)-2-(3-methyl-2-oxobutyl)piperidin-1-yl benzoate (S32): ^{1}H NMR (500 MHz, $CDCl_3$) δ 7.97 (d, *J* = 7.0 Hz, 2 H), 7.64–7.50 (m, 1 H), 7.49–7.35 (m, 2 H), 3.63–3.51 (m, 1 H), 3.50–3.37 (m, 1 H), 2.89 (dd, *J* = 17.4, 4.5 Hz, 1 H), 2.76 (t, *J* = 9.8 Hz, 1 H), 2.50 (dd, *J* = 17.4, 6.9 Hz, 1 H), 2.48–2.34 (m, 1 H), 1.94–1.61 (m, 4 H), 1.60–1.44 (m, 1 H), 1.36 (d, *J* = 12.7 Hz, 1 H), 1.00 (d, *J* = 6.8 Hz, 3 H), 0.88 (d, *J* = 6.2 Hz, 3 H); ^{13}C NMR (100 MHz, $CDCl_3$) δ 212.9, 165.1, 133.3, 129.7, 129.2, 128.6, 62.4, 58.1, 45.0, 41.6, 32.2, 25.6, 23.6, 18.2, 17.7.

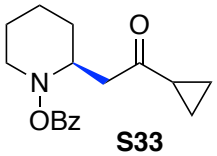

S33

(*S*)-2-(2-cyclopropyl-2-oxoethyl)piperidin-1-yl benzoate (S33): ^{1}H NMR (500 MHz, $CDCl_3$) δ 7.98 (d, *J* = 7.2 Hz, 2 H), 7.63–7.50 (m, 1 H), 7.50–7.36 (m, 2 H), 3.67–3.51 (m, 1 H), 3.50–3.34 (m, 1 H), 2.99 (dd, *J* = 16.8, 4.5 Hz, 1 H), 2.87–2.65 (m, 1 H), 2.55 (dd, *J* = 16.7, 5.9 Hz, 1 H), 1.91–1.62 (m, 5 H), 1.62–1.49 (m, 1 H), 1.45–1.23 (m, 1 H), 0.97–0.70 (m, 3 H), 0.68–0.52 (m, 1 H); ^{13}C NMR (100 MHz, $CDCl_3$) δ 209.2, 165.1, 133.2, 129.7, 129.2, 128.5, 62.7, 58.1, 47.6, 32.2, 25.5, 23.6, 21.6, 11.1, 10.6.

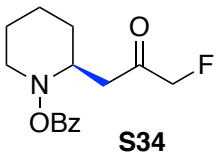

S34

(*S*)-2-(3-fluoro-2-oxopropyl)piperidin-1-yl benzoate (S34): ^{1}H NMR (500 MHz, $CDCl_3$) δ 7.96 (d, *J* = 6.4 Hz, 2 H), 7.63–7.53 (m, 1 H), 7.50–7.39 (m, 2 H), 4.64 (d, *J* = 47.6 Hz, 2 H), 3.65–3.57 (m, 1 H), 3.57–3.42 (m, 1 H), 3.02–2.90 (m, 1 H), 2.86–2.68 (m, 1 H), 2.51 (ddd, *J* = 17.1, 6.0, 2.2 Hz, 1 H), 1.95–1.77 (m, 3 H), 1.76–1.68 (m, 1 H), 1.65–1.54 (m, 1 H), 1.44–1.30 (m, 1 H); ^{13}C NMR (100 MHz, $CDCl_3$) δ 205.0 (d, *J* = 18.9 Hz), 164.9, 133.4, 129.6, 129.0, 128.7, 85.0 (d, *J* = 186.0 Hz), 62.1, 58.0, 42.9, 32.2, 25.4, 23.6.

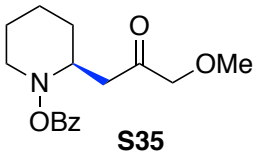

S35

(*S*)-2-(3-methoxy-2-oxopropyl)piperidin-1-yl benzoate (S35): ^{1}H NMR (500 MHz, $CDCl_3$) δ 7.97 (d, *J* = 7.0 Hz, 2 H), 7.65–7.51 (m, 1 H), 7.50–7.36 (m, 2 H), 3.94–3.75 (m, 2 H), 3.62–3.55 (m, 1 H), 3.53–3.44 (m, 1 H), 3.17 (s, 3 H), 2.88 (dd, *J* = 16.8, 5.5 Hz, 1 H), 2.75 (t, *J* = 9.8 Hz, 1 H), 2.40 (dd, *J* = 16.6, 4.8 Hz, 1 H), 1.96–1.76 (m, 3 H), 1.75–1.65 (m, 1 H), 1.63–1.53 (m, 1 H), 1.46–1.30 (m, 1 H); ^{13}C NMR (100 MHz, $CDCl_3$) δ 206.7, 164.9, 133.3, 129.6, 129.1, 128.6, 78.0, 62.4, 59.2, 58.0, 43.5, 32.2, 25.5, 23.6.

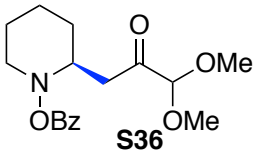

S36

(*S*)-2-(3,3-dimethoxy-2-oxopropyl)piperidin-1-yl benzoate (S36). ^{1}H NMR (500 MHz, $CDCl_3$) δ 7.90 (d, *J* = 7.3 Hz, 2 H), 7.61–7.44 (m, 1 H), 7.44–7.30 (m, 2 H), 4.18 (s, 1 H), 3.51 (d, *J* = 9.8 Hz, 1 H), 3.45–3.31 (m,

1 H), 3.18 (s, 3 H), 3.11 (s, 3 H), 2.99 (dd, J = 17.6, 5.2 Hz, 1 H), 2.86–2.55 (m, 1 H), 2.53–2.35 (m, 1 H), 1.87–1.48 (m, 5 H), 1.41–1.19 (m, 1 H); ^{13}C NMR (100 MHz, $CDCl_3$) δ 204.0, 164.9, 133.2, 129.6, 129.3, 128.5, 104.1, 62.3, 58.0, 54.9, 54.7, 42.3, 32.3, 25.5, 23.6.

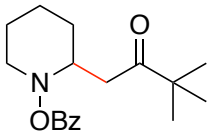

S37

(±)-2-(3,3-dimethyl-2-oxobutyl)piperidin-1-yl benzoate (S37): ^{1}H NMR (500 MHz, $CDCl_3$) δ 7.99 (d, J = 7.4 Hz, 2 H), 7.64–7.45 (m, 1 H), 7.49–7.37 (m, 2 H), 3.67–3.53 (m, 1 H), 3.53–3.40 (m, 1 H), 2.90 (dd, J = 17.7, 4.1 Hz, 1 H), 2.83–2.70 (m, 1 H), 2.62 (dd, J = 17.7, 7.4 Hz, 1 H), 1.96–1.74 (m, 3 H), 1.68 (d, J = 12.1 Hz, 1 H), 1.51 (d, J = 12.8 Hz, 1 H), 1.38 (d, J = 13.0 Hz, 1 H), 1.01 (s, 9 H); ^{13}C NMR (100 MHz, $CDCl_3$) δ 214.2, 165.0, 133.2, 129.6, 129.2, 128.5, 62.3, 58.1, 44.4, 41.3, 32.0, 26.2, 25.6, 23.6.

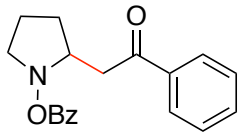

S38

(±)-2-(2-oxo-2-phenylethyl)pyrrolidin-1-yl benzoate (S38): ^{1}H NMR (500 MHz, $CDCl_3$) δ 8.10–7.79 (m, 4 H), 7.59–7.46 (m, 2 H), 7.46–7.28 (m, 4 H), 3.84 (ddd, J = 17.0, 8.8, 4.2 Hz, 1 H), 3.72–3.62 (m, 1 H), 3.62–3.52 (m, 1 H), 3.13 (dd, J = 16.9, 8.8 Hz, 1 H), 3.08–2.93 (m, 1 H), 2.35 (dt, J = 20.5, 7.6 Hz, 1 H), 1.99 (dt, J = 14.1, 8.4 Hz, 2 H), 1.64–1.50 (m, 2 H); ^{13}C NMR (125 MHz, $CDCl_3$) δ 198.5, 165.5, 136.9, 133.3, 133.2, 129.5, 129.2, 128.7, 128.5, 128.2, 64.5, 56.2, 42.5, 27.7, 20.6.

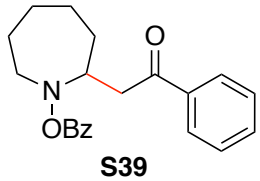

S39

(±)-2-(2-oxo-2-phenylethyl)azepan-1-yl benzoate (S39): ^{1}H NMR (500 MHz, $CDCl_3$) δ 7.96 (d, J = 7.3 Hz, 2 H), 7.88 (d, J = 7.3 Hz, 2 H), 7.59–7.43 (m, 2 H), 7.43–7.31 (m, 4 H), 4.06–3.77 (m, 1 H), 3.55–3.41 (m, 1 H), 3.41–3.31 (m, 2 H), 3.14 (dd, J = 17.0, 8.8 Hz, 1 H), 2.00–1.64 (m, 7 H), 1.64–1.49 (m, 1 H); ^{13}C NMR (125 MHz, $CDCl_3$) δ 198.8, 165.2, 137.0, 133.1, 129.4, 129.4, 128.6, 128.4, 128.2, 64.2, 57.8, 44.3, 30.5, 27.4, 25.9, 24.3.

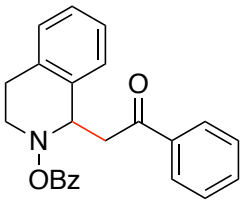

S40

(±)-1-(2-oxo-2-phenylethyl)-3,4-dihydroisoquinolin-2(1H)-yl benzoate (S40): ^{1}H NMR (500 MHz, $CDCl_3$) δ 7.93 (d, *J* = 7.3 Hz, 2 H), 7.84 (d, *J* = 7.3 Hz, 2 H), 7.50 (dd, *J* = 11.3, 7.3 Hz, 2 H), 7.42–7.37 (m, 2 H), 7.37–7.31 (m, 2 H), 7.22–7.05 (m, 4 H), 5.50–5.06 (m, 1 H), 3.78 (dd, *J* = 17.3, 5.0 Hz, 1 H), 3.75–3.66 (m, 1 H), 3.57–3.45 (m, 1 H), 3.40 (dd, *J* = 17.2, 5.8 Hz, 1 H), 3.24–3.12 (m, 1 H), 3.05 (dt, *J* = 16.7, 5.4 Hz, 1 H); ^{13}C NMR (100 MHz, $CDCl_3$) δ 197.8, 164.9, 136.8, 136.5, 133.4, 133.2, 133.2, 129.6, 129.0, 128.7, 128.6, 128.4, 128.4, 127.0, 126.8, 126.7, 61.6, 51.2, 44.8, 26.7.

Reductive Cleavage of 16 and 20.

Scheme 2.13. Reductive cleavage of **16**.

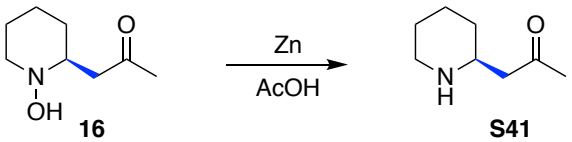

16 **S41**

(+)-Pelletierine (S41). To a solution of freshly prepared ***rac*-16** (33.1 mg, 0.21 mmol) in AcOH (1 mL) at 23 °C was added Zn powder (137.0 mg, 2.10 mmol, 10 equiv). The resulting mixture was stirred vigorously for 2-3 h at 23 ºC to avoid Zn clumping. Upon completion, the reaction contents were filtered through a pad of Celite, washed with MeOH, and concentrated to dryness. To the resulting solid was sequentially added saturated aqueous $NaHCO_3$ (2 mL) and aqueous NH_3 (2 mL, 30 wt. %). The resulting mixture was then diluted with EtOAc (10 mL) and transferred to a separatory funnel. The organic layer was separated and the aqueous phase was extracted with EtOAc (3 × 10 mL). The combined organic extracts were washed with saturated aqueous $NaHCO_3$

(2 × 4 mL), brine (4 mL), dried ($MgSO_4$), filtered, and concentrated to afford pure ***rac*-S41** (26.0 mg, 90%) as a yellow oil. ^1H and ^{13}C NMR data matched that reported by Chiou and co-workers.[46]

The same procedure repeated for the ***ent*-16** (18.0 mg, 0.11 mmol, 88% *ee*) prepared with **31** afforded ***ent*-S41** (12.0 mg, 74%) with $[\alpha]_D^{25} = -14.0°$ ($c = 0.25$, $CHCl_3$) [lit. $[\alpha]_D^{20} = -22°$ ($c = 0.9$, $CHCl_3$)][47]

Scheme 2.14. Reductive cleavage of **20**.

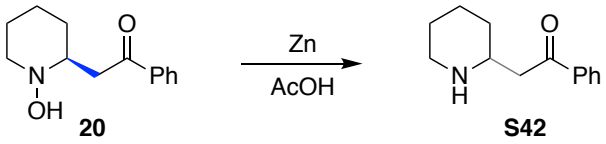

20 **S42**

Norsedaminone (S42). Prepared on the same scale as **S41** by analogy starting with freshly prepared **20** (45 mg, 0.21 mmol, 88% *ee*) to afford **S42** (42 mg, 98%) as a yellow oil. ^1H and ^{13}C NMR data matched that reported by Scarpi and co-workers.[48] ***Note***: **S42** racemizes upon standing.

Total Synthesis of (–)-Lobeline and (–)-Sedinone.

Scheme 2.15. Gram-scale preparation of **20**.

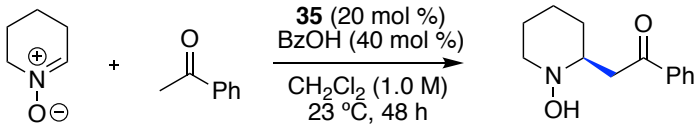

14 **19** **20**

Compound 20. To a flask containing **35** (0.78 g, 2.0 mmol, 0.2 equiv), BzOH (0.49 g, 4.0 mmol, 0.4 equiv), and methyl ketone **19** (3.50 mL, 30.3 mmol, 3.0 equiv) at 23 ºC under an ambient atmosphere was added a solution of nitrone **14** (1.00 g, 10.1 mmol, 1.0 equiv) in CH_2Cl_2 (10 mL). The reaction mixture was then stirred for 48 h at 23 ºC. Upon completion, the contents were quenched with saturated aqueous $NaHCO_3$ (40 mL) and extracted with CH_2Cl_2 (3 × 40 mL). The

combined organic extracts were then dried ($MgSO_4$), filtered, and concentrated. The resultant crude material was purified by flash column chromatography (silica gel, hexanes/EtOAc = 2/1) to yield **20** (1.55 g, 70%, 90% *ee*).

Scheme 2.16. Reduction and subsequent silyl protection of **20**.

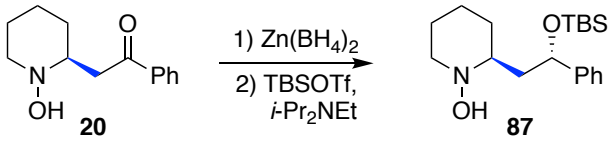

Compound 87. To a solution of **20** (0.62 g, 2.83 mmol, 1.0 equiv) in THF (20 mL) at –78 ºC under an argon atmosphere was added $Zn(BH_4)_2$ (6.50 mL, 0.52 M solution in THF, 3.39 mmol, 1.2 equiv) dropwise over 5 min. The resulting solution was stirred for 1 h at –78 ºC and then slowly warmed to 0 ºC over the course of 2 h. After stirring at 0 ºC for an additional 1 h, the reaction was quenched by careful addition of saturated aqueous NH_4Cl (20 mL), keeping the internal temperature at less than 5 ºC. The mixture was then warmed to 23 ºC, the organic layer was separated, and the aqueous layer was extracted with EtOAc (3 × 30 mL). The combined organic layers were dried ($MgSO_4$), filtered, and concentrated. Pressing forward without any additional purification, this crude intermediate was dissolved in CH_2Cl_2 (20 mL), *i*-Pr_2NEt (0.99 mL, 5.66 mmol, 2.0 equiv) was added at 0 ºC followed by dropwise addition of TBSOTf (0.72 mL, 3.11 mmol, 1.1 equiv). The resultant mixture was stirred at 0 ºC for 30 min. Upon completion, the mixture was warmed to 23 ºC, diluted with CH_2Cl_2 (40 mL), and successively washed with saturated aqueous $NaHCO_3$ (10 mL), saturated aqueous NH_4Cl (10 mL), and brine (20 mL). The organic phase was then dried ($MgSO_4$), filtered, and concentrated. The resultant crude material was dissolved in MeOH and refluxed for 2 h. The MeOH was then evaporated and the resultant residue was purified by flash column chromatography (silica gel, hexanes/EtOAc, 10/1→2/1) to afford **87** (0.64 g, 67% over 2

steps, 89% *ee*) as a white solid. **87**: R_f = 0.35 (silica gel, EtOAc); $[\alpha]_D^{25}$ = –23.3º (*c* = 1.00, $CHCl_3$); IR (film) ν_{max} 3186, 2931, 2857, 1472, 1361, 1256, 1092, 836, 775, 700 cm^{-1}; ^1H NMR (500 MHz, $CDCl_3$) δ 7.45–7.25 (m, 4 H), 7.25–7.15 (m, 1 H), 6.38–5.65 (br s, 1 H, exchangeable), 4.76 (dd, *J* = 8.8, 3.8 Hz, 1 H), 3.27 (d, *J* = 10.3 Hz, 1 H), 2.95–2.64 (m, 0.5 H), 2.64–2.28 (m, 2.5 H), 1.98–1.78 (m, 1 H), 1.76–1.40 (m, 4 H), 1.36–1.04 (m, 2 H), 0.87 (s, 9 H), 0.01 (s, 3 H), -0.23 (s, 3 H); ^{13}C NMR (125 MHz, $CDCl_3$) δ 145.7, 128.1, 127.0, 126.3, 125.9, 72.9, 64.5, 59.9, 44.3, 31.4, 25.9, 25.8, 23.7, 18.2, –4.4, –4.9; HRMS (ESI) calcd for $C_{19}H_{34}NO_2Si^+$ [M + H^+] 336.2353, found 336.2352.

Scheme 2.17. Oxidation of **87**.

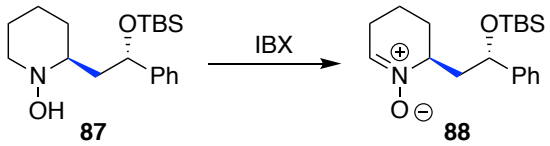

Compound 61. To a solution of **87** (0.60 g, 1.80 mmol, 1.0 equiv) in CH_2Cl_2 (5 mL) at –20 ºC under an argon atmosphere was added IBX (0.55 g, 1.98 mmol, 1.1 equiv) in a single portion. The resultant reaction mixture was stirred vigorously at –20 ºC for 4 h. Upon completion, anhydrous $MgSO_4$ (0.25 g) was added to the reaction solution and the contents were stirred for 30 minutes. The reaction contents were then quickly filtered through a pad of Celite while still cold and concentrated directly to afford **88** (0.59 g, 99%, *rr* of aldonitrone:ketonitrone = 4:1) as a colorless oil, which was used in the next step without any further purification. **88**: $[\alpha]_D^{25}$ = –44.0º (*c* = 1.00, $CHCl_3$); IR (film) ν_{max} 2953, 2856, 1472, 1361, 1257, 1200, 1064, 836, 756, 701 cm^{-1}; ^1H NMR (500 MHz, $CDCl_3$) δ 7.43–7.34 (m, 2 H), 7.33–7.27 (m, 2 H), 7.25–7.21 (m, 1 H), 7.09 (t, *J* = 3.9 Hz, 0.6 H), 5.50 (dd, *J* = 8.5, 4.9 Hz, 0.2 H), 4.93 (dd, *J* = 8.4, 4.7 Hz, 0.8 H), 3.93–3.70 (m, 1 H), 2.94–2.82 (m, 0.8 H), 2.82–2.77 (m, 0.2 H), 2.68–2.61 (m, 0.2 H), 2.52–2.45 (m, 0.2 H), 2.40–

2.36 (m, 1.4 H), 2.04–1.83 (m, 2.6 H), 1.83–1.76 (m, 1 H), 1.76–1.68 (m, 0.8 H), 1.68–1.58 (m, 1.2 H), 0.93–0.80 (m, 9 H), 0.02 (s, 3 H), -0.16 (s, 0.6 H), -0.17–-0.26 (m, 2.4 H); ^{13}C NMR (125 MHz, $CDCl_3$) δ 146.6, 145.2, 144.2, 136.1, 128.3, 128.2, 127.5, 127.2, 126.4, 125.6, 72.7, 69.9, 64.3, 58.3, 44.6, 43.0, 31.3, 27.2, 25.9, 25.7, 23.1, 18.8, 18.2, 15.0, –4.5, –4.8, –5.0; HRMS (ESI) calcd for $C_{19}H_{32}NO_2Si^+$ [M + H^+] 334.2197, found 334.2200.

Scheme 2.18. Addition of β-ketoacid **S24**.

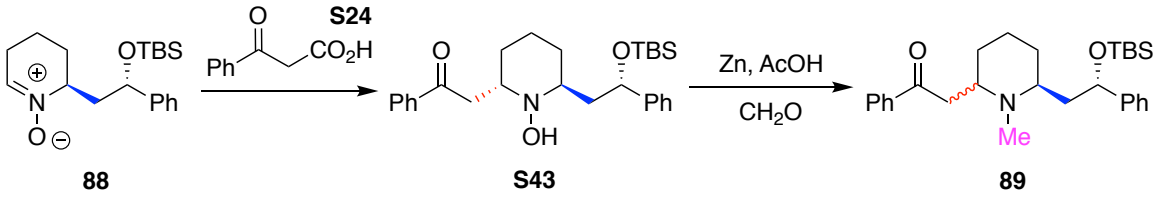

Compound 62. To a solution of **88** (0.27 g, 0.81 mmol, 1 equiv) in CH_2Cl_2 (1 mL) at 0 ºC was added β-ketoacid **S24** (0.20 g, 1.22 mmol, 1.5 equiv) in a single portion under an ambient atmosphere. The resulting mixture was stirred at 0 ºC for 20 h and then for 2 h at 23 ºC. Upon completion, the reaction contents were diluted with CH_2Cl_2 (10 mL), quenched with saturated aqueous $NaHCO_3$ (10 mL), and transferred to a separatory funnel. The organic layer was separated and the aqueous phase was extracted with CH_2Cl_2 (3 × 10 mL). The combined organic layers were washed with saturated aqueous $NaHCO_3$ (2 × 10 mL), brine (10 mL), dried ($MgSO_4$), filtered, and concentrated. The resultant residue was purified via flash column chromatography (silica gel, hexanes/EtOAc, 10/1→2/1) to afford intermediate **S43**. Pushing forward, to a solution of intermediate **S43** in AcOH (8 mL) at 23 °C was sequentially added CH_2O (0.36 mL, 37 wt. % in H_2O, 4.86 mmol, 6.0 equiv,) and Zn powder (0.56 g, 8.10 mmol, 10 equiv) at 23 ºC. The resulting mixture was stirred vigorously for 4 h at 23 ºC to avoid Zn clumping. Upon completion, the reaction contents were filtered through a pad of Celite, washed with MeOH, and concentrated to

dryness. To the resulting solid was sequentially added saturated aqueous $NaHCO_3$ (10 mL) and aqueous NH_3 (10 mL, 30 wt. %). The resulting mixture was diluted with EtOAc (50 mL) and transferred to a separatory funnel. The organic layer was separated and the aqueous phase was extracted with EtOAc (3 × 50 mL). The combined organic extracts were washed with saturated aqueous $NaHCO_3$ (2 × 20 mL), brine (20 mL), dried ($MgSO_4$), filtered, and concentrated to afford **89** (0.27 g, 76%, *cis*:*trans* = 1.3:1) as a pale-yellow oil, which was used without any further purification. **89**: R_f = 0.52 (silica gel, CH_2Cl_2/MeOH = 10:1); $[\alpha]_D^{25}$ = –20.1º (*c* = 1.00, $CHCl_3$); ^{1}H NMR (500 MHz, $CDCl_3$) δ 7.98 (d, *J* = 7.3 Hz, 1.2 H), 7.95 (d, *J* = 7.3 Hz, 0.8 H), 7.62–7.52 (m, 1 H), 7.52–7.42 (m, 2 H), 7.34–7.16 (m, 5 H), 4.65 (dd, *J* = 11.2, 5.5 Hz, 1 H), 3.43–3.32 (m, 0.4 H), 3.25 (td, *J* = 15.7, 5.0 Hz, 1 H), 3.18–3.09 (m, 0.6 H), 3.03–2.85 (m, 1.4 H), 2.55–2.39 (m, 0.6 H), 2.34 (s, 1.2 H), 2.22 (s, 1.8 H), 2.12–1.96 (m, 1 H), 1.75–1.32 (m, 7 H), 0.89 (s, 3.6 H), 0.86 (s, 5.4 H), 0.02 (s, 1.2 H), –0.00 (s, 1.8 H), –0.21 (s, 1.8 H), –0.22 (s, 1.2 H); ^{13}C NMR (100 MHz, $CDCl_3$) δ 199.6, 199.5, 146.0, 145.9, 137.5, 137.4, 137.4, 133.1, 128.8, 128.8, 128.3, 128.2, 128.2, 128.1, 127.1, 127.0, 126.2, 126.1, 77.5, 77.2, 76.9, 72.8, 72.4, 60.1, 59.8, 59.7, 54.8, 54.8, 45.9, 44.7, 40.8, 40.5, 38.8, 31.8, 28.4, 27.3, 26.9, 26.4, 26.0, 24.5, 19.7, 18.3, 6.1, 2.6, 2.6, 1.6, 1.6, –4.3, –4.4, –4.8, –4.9; HRMS (ESI) calcd for $C_{28}H_{42}NO_2Si^+$ [M + H^+] 452.2980, found 452.2973. ***Note***: the ratio *cis*:*trans* is in equilibrium in solution and can vary.

Scheme 2.19. Addition of β-ketoacid **S20**.

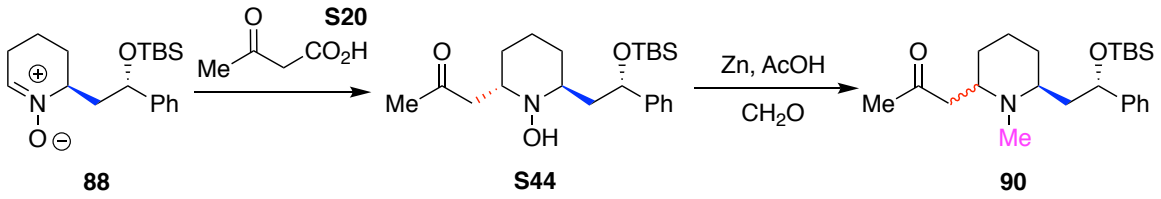

Compound 90. Prepared on the same scale as **89** by analogy with **S20**. The intermediate **S44** was isolated via column chromatography (silica gel, hexanes/EtOAc, 5/1→1/1). Compound **90** (0.23 g, 75%, *cis*:*trans* = 1:5.4) was isolated as a pale-yellow oil, which was used without any further purification. **90**: R_f = 0.35 (silica gel, CH_2Cl_2/MeOH = 10:1); $[\alpha]_D^{25}$ = –38.1° (*c* = 1.00, $CHCl_3$); IR (film) ν_{max} 2929, 2856, 1714, 1472, 1360, 1251, 1084, 1006, 836, 775, 700 cm^{-1}; ^1H NMR (500 MHz, $CDCl_3$) δ 7.33–7.27 (m, 4 H), 7.25–7.19 (m, 1 H), 4.63 (dd, *J* = 9.0, 4.1 Hz, 1 H), 3.19–3.11 (m, 0.8 H), 3.00–2.93 (m, 0.1 H), 2.92–2.76 (m, 1 H), 2.68 (dd, *J* = 15.9, 5.5 Hz, 1 H), 2.58–2.48 (m, 0.1 H), 2.39 (dd, *J* = 15.9, 6.8 Hz, 1 H), 2.27 (s, 2.7 H), 2.21–2.11 (m, 3.3 H), 2.02–1.93 (m, 1 H), 1.68–1.22 (m, 7 H), 0.93–0.81 (m, 9 H), 0.00 (s, 3 H), –0.15—0.29 (m, 3 H); ^{13}C NMR (125 MHz, $CDCl_3$) δ 208.0, 145.9, 145.8, 128.2, 128.1, 127.1, 127.1, 126.2, 126.1, 77.4, 77.2, 76.9, 72.8, 72.6, 59.5, 54.8, 54.1, 49.5, 46.3, 45.9, 40.6, 38.3, 31.1, 30.7, 30.4, 27.9, 26.7, 26.2, 25.9, 24.5, 19.7, 18.2, 6.1, 2.6, 2.6, 1.6, 1.6, –4.4, –4.4, –4.9, –5.0; HRMS (ESI) calcd for $C_{23}H_{40}NO_2Si^+$ [M + H^+] 390.2823, found 390.2824. ***Note***: the ratio *cis*:*trans* is in equilibrium in solution and can vary.

Scheme 2.20. Synthesis of (–)-lobeline (**3**).

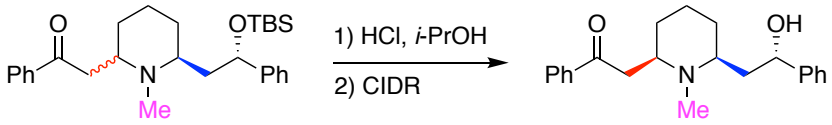

89 **3**

(–)-Lobeline (3): To a solution of **89** (0.25 g, 0.55 mmol, 1.0 equiv) in *i*-PrOH (6 mL) was added concentrated HCl (0.06 mL, 0.70 mmol, 1.3 equiv). The resulting mixture was stirred at 60 ºC for 12 h. Upon completion, the mixture was cooled to 23 ºC and concentrated. The resulting solid was washed with Et_2O (4 × 6 mL, removed by decantation) and dried under high vacuum. Then saturated aqueous $NaHCO_3$ (6 mL) was added, followed by EtOAc (10 mL), and the resulting mixture was transferred to a separatory funnel. The organic layer was separated and the aqueous phase was extracted with EtOAc (3 × 10 mL). The combined organic extracts were washed with saturated aqueous $NaHCO_3$ (10 mL), brine (10 mL), dried ($MgSO_4$), filtered, and concentrated to afford **3** (0.18 g, 95%, *cis*:*trans* = 1:1) as a yellow oil. Crude **3** was then dissolved in MeOH (1 mL) and the solvent was left to slowly evaporate in a vial with a loosened cap for 2 weeks at 4 ºC to yield yellow crystals. The crystals were washed with cold (0 ºC) hexanes (3 × 0.5 mL) and dried under high vacuum to afford (–)-lobeline (**3**), (0.17 g, 90% over two steps) as a pale-yellow solid exclusively as the *cis*-isomer. **3**: R_f = 0.20 (silica gel, CH_2Cl_2/MeOH = 10:1); $[\alpha]_D^{25}$ = –31.0º (*c* = 1.00, $CHCl_3$) [lit. $[\alpha]_D^{21}$ = –38.2º (*c* = 1.986, $CHCl_3$)];[49] IR (film) ν_{max} 3085, 2936, 1687, 1450, 1302, 1214, 1062, 1002, 951 cm^{-1}; ^1H NMR (500 MHz, $CDCl_3$) δ 8.00–7.94 (m, 2 H), 7.61–7.52 (m, 1 H), 7.52–7.41 (m, 2 H), 7.41–7.34 (m, 2 H), 7.34–7.28 (m, 2 H), 7.27–7.19 (m, 1 H), 6.70–6.36 (br s, 1 H, exchangeable), 4.95 (dd, *J* = 10.7, 2.9 Hz, 1 H), 3.63–3.52 (m, 1 H), 3.26–3.15 (m, 2 H), 3.02 (dd, *J* = 16.0, 8.5 Hz, 1 H), 2.35 (s, 3 H), 1.99–1.88 (m, 1 H), 1.86–1.76 (m, 1 H), 1.70–1.40 (m, 5 H), 1.23–1.10 (m, 1 H); ^{13}C NMR (125 MHz, $CDCl_3$) δ 198.3, 145.2, 137.2, 133.2,

128.8, 128.3, 128.2, 127.0, 125.6, 75.8, 64.6, 59.1, 43.9, 40.6, 27.4, 24.9, 23.5, 23.4; HRMS (ESI) calcd for $C_{22}H_{28}NO_2^+$ [M + H$^+$] 338.2115, found 338.2113.

Scheme 2.21. Synthesis of (–)-sedinone (**4**).

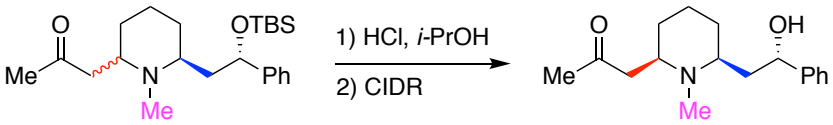

90 **4**

(–)-Sedinone (4). To a solution of **90** (0.20 g, 0.51 mmol, 1.0 equiv) in *i*-PrOH (6 mL) was added concentrated HCl (0.06 mL, 0.70 mmol, 1.4 equiv). The resulting mixture was stirred at 60 ºC for 12 h. Upon completion, the mixture was cooled to 23 ºC and concentrated. The resulting solid was washed with Et_2O (4 × 6 mL, removed by decantation) and dried under high vacuum. Then saturated aqueous $NaHCO_3$ (6 mL) was added, followed by EtOAc (10 mL), and the resulting mixture was transferred to a separatory funnel. The organic layer was separated and the aqueous phase was extracted with EtOAc (3 × 10 mL). The combined organic extracts were washed with saturated aqueous $NaHCO_3$ (10 mL), brine (10 mL), dried ($MgSO_4$), filtered, and concentrated to afford mostly *epi*-sedinone (*epi*-**4** 0.13 g, 93%, *cis*:*trans* = 1:5.4) as a yellow oil. *epi*-**4**: ^{1}H NMR (500 MHz, $CDCl_3$) δ 7.44–7.28 (m, 4 H), 7.27–7.20 (m, 1 H), 7.06–6.52 (br s, 1 H, exchangeable), 4.90 (dd, *J* = 10.7, 2.1 Hz, 1 H), 3.71–3.58 (m, 0.85 H), 3.45–3.35 (m, 0.15 H), 3.25–3.16 (m, 1 H), 2.74–2.51 (m, 2 H), 2.48 (s, 3 H), 2.21 (s, 3 H), 1.88–1.68 (m, 1 H), 1.67–1.17 (m, 7 H); ^{13}C NMR (125 MHz, $CDCl_3$) δ 206.9, 206.8, 145.4, 145.1, 128.3, 127.1, 125.6, 125.6, 77.5, 77.2, 76.8, 76.0, 76.0, 64.7, 61.0, 58.8, 51.1, 49.1, 48.1, 40.4, 38.9, 35.7, 32.4, 30.3, 30.3, 29.8, 26.9, 24.9, 23.5, 23.3, 23.2, 23.1, 20.6. The crude *epi*-**4** was then dissolved in MeOH (1 mL) and left for 12 h at 23 ºC. At this stage, the ratio determined by ^{1}H NMR analysis revealed a 1:1 mixture of

diastereomers. The mixture was then concentrated and hexanes (4 mL) was added to the residue, yielding a cloudy yellow solution, which was made transparent by the dropwise addition of EtOAc (~0.8 mL) with stirring. The solution was then placed in the freezer at –20 ºC for 16 h. The precipitated crystals were collected by filtration, washed with cold (–20 ºC) hexanes, and dried under high vacuum. The filtrate was evaporated and the procedure was repeated two additional times, starting from equilibration in MeOH at 23 ºC, followed by crystallization at –20 ºC using scaled amounts of solvents. Combining all the crystal fractions afforded (–)-sedinone (**4**, 0.10 g, 73% over two steps) as a white solid predominantly as the *cis* isomer (*dr* > 97:3 after 1 h in $CDCl_3$, slowly epimerizes). The hydrochloride salt of **4** was obtained by dissolving **4** in Et_2O and adding HCl (2.0 equiv, 1.0 M in Et_2O), followed by filtration and drying. **4**: R_f = 0.18 (silica gel, CH_2Cl_2/MeOH = 10:1); $[\alpha]_D^{25}$ = –67.8º (*c* = 1.10, MeOH) (hydrochloride) [lit. $[\alpha]_D^{20}$ = –79.4º (*c* = 1.0, MeOH)];[50] IR (film) ν_{max} 3150, 2932, 2858, 1711, 1451, 1359, 1060, 836, 760, 701 cm^{-1}; ^1H NMR (500 MHz, $CDCl_3$) δ 7.42–7.35 (m, 2 H), 7.35–7.29 (m, 2 H), 7.25–7.18 (m, 1 H), 6.73–6.28 (br s, 1 H, exchangeable), 4.95 (dd, *J* = 10.8, 2.9 Hz, 1 H), 3.48–3.34 (m, 1 H), 3.28–3.16 (m, 1 H), 2.65 (dd, *J* = 16.0, 6.1 Hz, 1 H), 2.49 (dd, *J* = 15.7, 8.3 Hz, 1 H), 2.27 (s, 3 H), 2.18 (s, 3 H), 1.91 (dt, *J* = 14.8, 11.1 Hz, 1 H), 1.85–1.77 (m, 1 H), 1.69–1.43 (m, 4 H), 1.37–1.30 (m, 1 H), 1.20–1.10 (m, 1 H); ^{13}C NMR (100 MHz, $CDCl_3$) δ 206.9, 145.1, 128.4, 127.1, 125.6, 76.1, 64.7, 58.8, 49.1, 40.4, 30.3, 26.9, 24.9, 23.3, 23.2; HRMS (ESI) calcd for $C_{17}H_{26}NO_2^+$ [M + H^+] 276.1958, found 276.1957.

Table 2.7. NMR comparison of **3**.

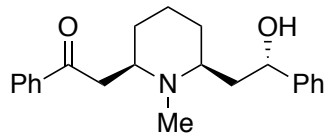

(–)-lobeline (**3**)

reported ^{1}H δ (ppm)[27e]	**synthetic ^{1}H δ (ppm)**	**reported ^{13}C δ (ppm)[27e]**	**synthetic ^{13}C δ (ppm)**
8.01-7.97 (comp. m, 2H)	8.00–7.94 (m, 2 H),	198.3	198.3
7.64–7.22 (comp m, 8 H)	7.61–7.19 (m, 8 H)	145.2	145.2
4.97 (dd, *J* = 10.8, 2.9 Hz, 1H)	4.95 (dd, *J* = 10.7, 2.9 Hz, 1 H)	137.1	137.2
3.65-3.59 (m, 1H)	3.63–3.52 (m, 1 H)	133.3	133.2
3.26 (dd, J = 16.0, 5.0 Hz, 2H)	3.26–3.15 (m, 2 H),	128.8	128.8
3.00 (dd, *J* = 16.0, 8.5 Hz, 1H)	3.02 (dd, *J* = 16.0, 8.5 Hz, 1 H),	128.3	128.3
2.38 (s, 3H),	2.35 (s, 3 H),	128.2	128.2
2.06-1.46 (comp. m, 7H),	1.99–1.40 (m, 7H)	127.1	127.0
1.29-1.18 (m, 1H)	1.23–1.10 (m, 1 H)	125.6	125.6
		75.8	75.8
		64.6	64.6
		59.1	59.1
		43.8	43.9
		40.5	40.6
		27.4	27.4
		24.8	24.9
		23.5	23.5
		23.4	23.4

Table 2.8. NMR comparison of **4**.

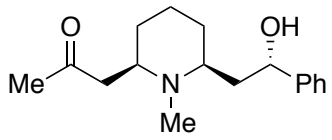

(–)-sedinone (**4**)

reported ^{1}H δ (ppm)[51]	**synthetic ^{1}H δ (ppm)**	**reported ^{13}C δ (ppm)[52]**	**synthetic ^{13}C δ (ppm)**
7.4–7.2 (m, 5H)	7.42–7.18 (m, 5 H)	206.6	206.9
4.95 (dd, 1H)	4.95 (dd, *J* = 10.8, 2.9 Hz, 1 H)	75.8	76.1
3.4 (m, 1H)	3.48–3.34 (m, 1 H)	64.5	64.7
3.2 (m, 1H)	3.28–3.16 (m, 1 H)	58.9	58.8
2.65 (dd, 1H)	2.65 (dd, *J* = 16.0, 6.1 Hz, 1 H)	49.0	49.1
2.5 (dd, 1H)	2.49 (dd, *J* = 15.7, 8.3 Hz, 1 H)	40.5	40.4
2.3 (s, 3H)	2.27 (s, 3 H)	30.1	30.3
2.2 (s, 3H)	2.18 (s, 3 H)	27.1	26.9
2.0-1.1 (9H)	1.95-1.10 (8H)	24.8	24.9
		23.4	23.3
		23.4	23.2

2.7 References

[1] (a) "Pyridine and piperidine alkaloids: an update": Schneider, M. J. in *Alkaloids: chemical and biochemical perspectives Vol. 10* (Ed.: Pelletier, S. W.), Pergamon, Oxford, **1996**, *10*, pp. 155 – 299; (b) Michael, J. P. *Nat. Prod. Rep.* **2008**, *25*, 139; c) O'Hagan, D. *Nat. Prod. Rep.* **2000**, *17*, 435; d) Vitaku, E.; Smith, D. T.; Njardarson, J. T. *J. Med. Chem.* **2014**, *57*, 10257.

[2] (a) Marion, L.; Lavigne, R.; Lemay, L. *Can. J. Chem*. **1951**, *29*, 347; (b) Franck, B. *Chem. Ber.* **1959**, *92*, 1001; (c) Denne, W. A.; Johns, S. R.; Lamberton, J. A.; Mathieson, A. M.; Snares, H. *Tetrahedron Lett.* **1972**, *13*, 1767; (d) Colau, B.; Hootelé, C. *Can. J. Chem.* **1983**, *61*, 470; (e) Huang, Q.; Attygale, A. B.; Meinwald, J.; Houck, M. A.; Eisner, T. *J. Nat. Prod.* **1998**, *61*, 598; (f) Felpin, F.-X.; Lebreton, J. *Tetrahedron* **2004**, *60*, 10127; (g) Hu, Y.; Zhang, C.; Zhao, X.; Wang, Y.; Feng, D.; Zhang, M.; Xie, H. *J. Nat. Prod.* **2016**, *79*, 252; (h) V. G. Lisnyak, S. A. Snyder. *J. Am. Chem. Soc*. **2020**, *142*, 12027.

[3] (a) Gupta, R. N.; Spenser, I. D. *Can. J. Chem.* **1967**, *45*, 1275; (b) Hemscheidt, T.; Spenser, I. D. *J. Am. Chem. Soc.* **1990**, *112*, 6360; (c) Bunsupa, S.; Yamazaki, M.; Saito, K. *Front. Plant Sci.* **2012**, *3*, 239.

[4] Monaco, M. R.; Renzi, P.; Schietroma, D. M. S.; Bella, M. *Org. Lett.* **2011**, *13*, 4546.

[5] For selected examples of intramolecular aza-Michael reactions, see: (a) Carlson, E. C.; Rathbone, L. K.; Yang, H.; Collett, N. D.; Carter, R. G. *J. Org. Chem.* **2008**, *73*, 5155; (b) Fustero, S.; del Pozo, C.; Mulet, C.; Lazaro, R.; Sánchez-Roselló, M. *Chem. Eur. J.* **2011**, *17*, 14267; (c) He, W.; Hu, J.; Wang, P.; Chen, L.; Ji, K.; Yang, S.; Li, Y.; Xie, Z.; Xie, W. *Angew. Chem. Int. Ed.* **2018**, *57*, 3806; *Angew. Chem.* **2018**, *130*, 3868; (d) Roy, T. K.; Parhi, B.; Ghorai, P. *Angew. Chem. Int. Ed.* **2018**, *57*, 9397; *Angew. Chem.* **2018**, *130*, 9541.

[6] Shi, S.-L.; Wei, X.-F.; Shimizu, Y.; Kanai, M. *J. Am. Chem. Soc.* **2012**, *134*, 17019.

[7] (a) Murahashi, S.-I.; Shiota, T. *Tetrahedron Lett.* **1987**, *28*, 2383; (b) Murahashi, S.-I.; Mitsui, H.; Shiota, T.; Tsuda, T.; Watanabe, S. *J. Org. Chem*. **1990**, *55*, 1736; (c) Goti, A.; Nannelli, L. *Tetrahedron Lett.* **1996**, *37*, 6025.

[8] (a) Goti, A.; De Sarlo, F.; Romani, M. *Tetrahedron Lett.* **1994**, *35*, 6571; (b) Cicchi, S.; Goti, A.; Brandi, A. *J. Org. Chem.* **1995**, *60*, 4743; (c) Cicchi, S.; Marradi, M.; Goti, A.; Brandi, A. *Tetrahedron Lett.* **2001**, *42*, 6503; (d) Matassini, C.; Parmeggiani, C.; Cardona, F.; Goti, A. *Org. Lett.* **2015**, *17*, 4082.

[9] (a) Huisgen, R.; Seidl, H.; Brüning, I. *Chem. Ber.* **1969**, *102*, 1102; (b) Ali, Sk. A.; Khan, J. H.; Wazeer, M. I. M.; Perzanowski, H. P. *Tetrahedron* **1989**, *45*, 5979.

[10] See Chapter 1. For reviews, see: (a) Lombardo, M.; Trombini, C. *Synthesis* **2000**, *6*, 759; (b) Merino, P.; Tejero, T. *Synlett* **2011**, *14*, 1965. For recent examples, see: (c) Postikova, S.; Tite, T.; Levacher, V.; Briére, J.-F. *Adv. Synth. Catal.* **2013**, *355*, 2513; (d) Juste-Navarro, V.; Prieto, L.; Delso, I.; Manzano, R.; Tejero, T.; Reyes, E.; Vicario, J. L.; Merino, P. *Adv. Synth. Catal.* **2017**, *359*, 4122.

[11] For recent reviews, see: (a) Mukherjee, S.; Yang, J. W.; Hoffmann, S.; List, B. *Chem. Rev*. **2007**, *107*, 5471; (b) Bertelsen, S.; Jørgensen, K. A. *Chem. Soc. Rev.* **2009**, *38*, 2178.

[12] Wittkopp, A.; Schreiner, P. R. *Chem. Eur. J.* **2003**, *9*, 407.

[13] Okino, T.; Hoashi, Y.; Takemoto, Y. *Tetrahedron Lett.* **2003**, *44*, 2817.

[14] For selected, recent reviews, see: (a) Doyle, A. G.; Jacobsen, E. N. *Chem. Rev*. **2007**, *107*, 5713; (b) Tsogoeva, S. B. *Org. Biomol. Chem.* **2013**, *11*, 7051.

[15] (a) Mei, K.; Jin, M.; Zhang, S.; Li, P.; Liu, W.; Chen, X.; Xue, F.; Duan, W.; Wang, W. *Org. Lett.* **2009**, *11*, 2864; (b) Zhang, X.-J.; Liu, S.-P.; Lao, J.-H.; Du, G.-J.; Yan, M.; Chan, A. S. C. *Tetrahedron: Asymmetry* **2009**, *20*, 1451; (c) Uehara, H.; Barbas, C. F. *Angew. Chem. Int. Ed.* **2009**, *48*, 9848; *Angew. Chem.* **2009**, *121*, 10032.
[16] Konishi, H.; Lam, T. Y.; Malerich, J. P.; Rawal, V. H. *Org. Lett.* **2010**, *12*, 2028.
[17] (a) Wenzel, A. G.; Jacobsen, E. N. *J. Am. Chem. Soc*. **2002**, *124*, 12964; (b) Huang, H.; Jacobsen, E. N. *J. Am. Chem. Soc.* **2006**, *128*, 7170; (c) Puglisi, A.; Raimondi, L.; Benaglia, M.; Bonsignore, M.; Rossi, S. *Tetrahedron Lett.* **2009**, *50*, 4340.
[18] (a) Elsworth, J. F.; Lamchen, M. *J. Chem. Soc. C* **1968**, 2423; (b) Ali, Sk. A.; Almuallem, H. A. *Tetrahedron* **1992**, *48*, 5273.
[19] Imada, Y.; Okita, C.; Maeda, H.; Kishimoto, M.; Sugano, Y.; Kaneshiro, H.; Nishida, Y.; Kawamorita, S.; Komiya, N.; Naota, T. *Eur. J. Org. Chem*. **2014**, 5670.
[20] (a) Cheng, L.; Han, X.; Huang, H.; Wong, M. W.; Lu, Y. *Chem. Commun.* **2007**, 4143; (b) Ayats, C.; Hensler, A. H.; Dibello, E.; Pericás, M. A. *ACS Catal.* **2014**, *4*, 3027.
[21] (a) Galinovsky, F.; Bianchetti, G.; Weiser, R. *Monatsh. Chem.* **1953**, *84*, 1221; (b) Schöpf, C.; Kauffmann, T.; Berth, P.; Bundschuh, W.; Dummer, G.; Fett, H.; Habermehl, G.; Wieters, E.; Wüst, W. *Justus Liebigs Ann. Chem.* **1957**, *608*, 88; (c) Chen, L.-J.; Hou, D.-R. *Tetrahedron: Asymmetry* **2008**, *19*, 715.
[22] Schöpf, C.; Braun, F.; Burkhardt, K.; Dummer, G.; Müller, H. *Justus Liebigs Ann. Chem.* **1959**, *626*, 123.
[23] (a) Wisse, J. H.; De Klonia, H.; Visser, B. J. *Recl. Trav. Chim. Pays-Bas* **1964**, *83*, 1265; (b) Cragg, J. E.; Herbert, R. B.; Jackson, F. B.; Moody, C. J.; Nicolson, I. T. *J. Chem. Soc. Perkin Trans. 1* **1982**, 2477; (c) Devijver, C.; Macours, P.; Braekman, J.-C.; Daloze, D.; Pasteels, J. M. *Tetrahedron* **1995**, *51*, 10913.
[24] (a) Zhong, F.; Jiang, C.; Yao, W.; Xu, L.-W.; Lu, Y. *Tetrahedron Lett.* **2013**, *54*, 4333; (b) Jia C.-M.; Zhang, H.-X.; Nie, J.; Ma, J.-A. *J. Org. Chem.* **2016**, *81*, 8561; (c) Liu, Y.-J.; Li, J.-S; Nie, J.; Ma, J.-A. *Org. Lett.* **2018**, *20*, 3643. (d) Böhm; M.; Proksch, K.; Mahrwald, R. *Eur. J. Org. Chem.* **2013**, 1046.
[25] (a) Grisar, J. M.; Claxton, G. P.; Stewart, K. T. *Synthesis* **1974**, 284; (b) Grisar, J. M.; Claxton, G. P.; Stewart, K. T.; MacKenzie, R. D.; Kariya, T. *J. Med. Chem.* **1976**, *19*, 1195.
[26] Pesciaioli, F.; DeVincentiis, F.; Galzerano, P.; Bencivenni, G.; Bartoli, G.; Mazzanti, A.; Melchiorre, P. *Angew. Chem. Int. Ed.* **2008**, *47*, 8703; *Angew. Chem*. **2008**, *120*, 8831.
[27] (a) Compère, D.; Marazano, C.; Das, B. C. *J. Org. Chem.* **1999**, *64*, 4528; (b) Felpin, F.-X.; Lebreton, J. *J. Org. Chem*. **2002**, *67*, 9192; (c) Klingler, F.-D.; Sobotta, R. U.S. Patent 2006014791, **2006**; (d) Birman, V.; Jiang, H.; Li, X. *Org. Lett*. **2007**, *9*, 3237; (e) Krishnan, S.; Bagdanoff, J. T.; Ebner, D. C.; Ramtohul, Y. K.; Tambar, U. K.; Stoltz, B. M. *J. Am. Chem. Soc*. **2008**, *130*, 13745; (f) Zheng, G.; Crooks, P. A. *Org. Prep. Proced. Int.* **2015**, *47*, 317.
[28] Driessens, F.; Hootelé, C. *Can. J. Chem.* **1991**, *69*, 211.
[29] (a) Dwoskin, L. P.; Crooks, P. A. *Biochem. Pharmacol*. **2002**, *63*, 89; (b) Zheng, G.; Dwoskin, L. P.; Deacuic, A. G.; Norrholm, S. D.; Crooks, P. A. *J. Med. Chem.* **2005**, *48*, 5551.
[30] Pilli, R. A.; Dias, L. C. *Synth. Commun*. **1991**, *21*, 2213.
[31] Gössinger, E. *Tetrahedron Lett.* **1980**, *21*, 2229; (b) Ali, S. A. *Tetrahedron Lett.* **1993**, *34*, 5325. Any attempt to reproduce the result reported by Ali for his substrates 14 b, 15 b did not succeed in our hands. Instead, we observed a 1:1 mixture of regioisomers.

[32] Zheng, G.; Dwoskin, L. P.; Crooks, P. A. *J. Org. Chem*. **2004**, *69*, 8514.
[33] Ryan, J.; Šiaučiulis, M.; Gomm, A.; Maciá, B.; OReilly, E.; Caprio, V. *J. Am. Chem. Soc*. **2016**, *138*, 15798.
[34] da Silva, R. A.; Estevam, I. H. S.; Bieber, L. W. *Tetrahedron Lett.* **2007**, *48*, 7680.
[35] Amara, Z.; Bernadat, G.; Venot, P.-E.; Retailleau, P.; Troufflard, C.; Drège, E.; Le Bideau, F.; Joseph, D. *Org. Biomol. Chem.* **2014**, *12*, 9797.
[36] Padwa, A.; Bullock, W. H.; Norman, B. H.; Perumattam, J. *J. Org. Chem.* **1991**, *56*, 4252.
[37] Aschwanden, P.; Kvaerno, L.; Geisser, R. W.; Kleinbeck, F.; Carreira, E. M. *Org. Lett.* **2005**, *7*, 5741.
[38] Haire, D. L.; Hilborn, J. W.; Janzen, E. G. *J. Org. Chem.* **1986**, *51*, 4298.
[39] Svejstrup, T. D.; Ruffoni, A.; Juliá, F.; Aubert, V. M.; Leonori, D. *Angew. Chem.* **2017**, *129*, 15144.
[40] Mimura, M.; Hayashida, M.; Nomiyama, K.; Ikegami, S.; Iida, Y.; Tamura, M.; Hiyama, Y.; Ohishi, Y. *Chemical and Pharmaceutical Bulletin*. **1993**, *41*, 1971.
[41] a) Henry, N.; O'Neil, I. A. *Tetrahedron Lett.* **2007**, *48*, 1691; b) Ibebeke-Bomangwa, W.; Hootelé, C. *Tetrahedron* **1987**, *43*, 935.
[42] Depré, D.; Vermeulen, W. A. A.; Lang, Y.; Dubois, J.; Vandevivere, J.; Vandermeersch, J.; Huang, L.; Robiette,R. *Org. Lett.* **2017**, *19*, 1414.
[43] Taotao, L.; Danishefsky, S. NEREUS PHARMACEUTICALS, INC. US2009/234137, **2009**, A1.
[44] Xu, X. Chen, H.; He, J.; Xu, H. *Chin. J. Chem*. **2017**, *35*, 1665.
[45] Allan, K. M.; Hong, B. D.; Stoltz, B. M. *Org. Biomol. Chem.* **2009**, *7*, 4960.
[46] Chiou, W.-H.; Chen, G.-T.; Kaoa, C.-L.; Gao, Y.-K. *Org. Biomol. Chem.* **2012**, *10*, 2518.
[47] Louis, C.; Mill, S.; Mancuso, V.; Hootelé, C. *Can. J. Chem.* **1994**, *72*, 1347.
[48] Scarpi, D.; Begliomini, S.; Prandi, C.; Oppedisano, A.; Deagostino, A.; Gómez-Bengoa, E.; Fiser, B.; Occhiato, E. G. *Eur. J. Org. Chem.* **2015**, *2015*, 3251.
[49] Ebnother, A. *Helv. Chim. Acta.* **1958**, *41*, 386.
[50] Franck, B. *Chem. Ber.* **1958**, *91*, 2803.
[51] Stevens, J. F.; Hart, H. ‘T.; Hendriks, H.; Malingré, T. M. *Phytochemistry* **1992**, *31*, 3917.
[52] Colau, B.; Hootelé, C. *Tetrahedron* **1984**, *40*, 2171.

2.8 NMR Spectra

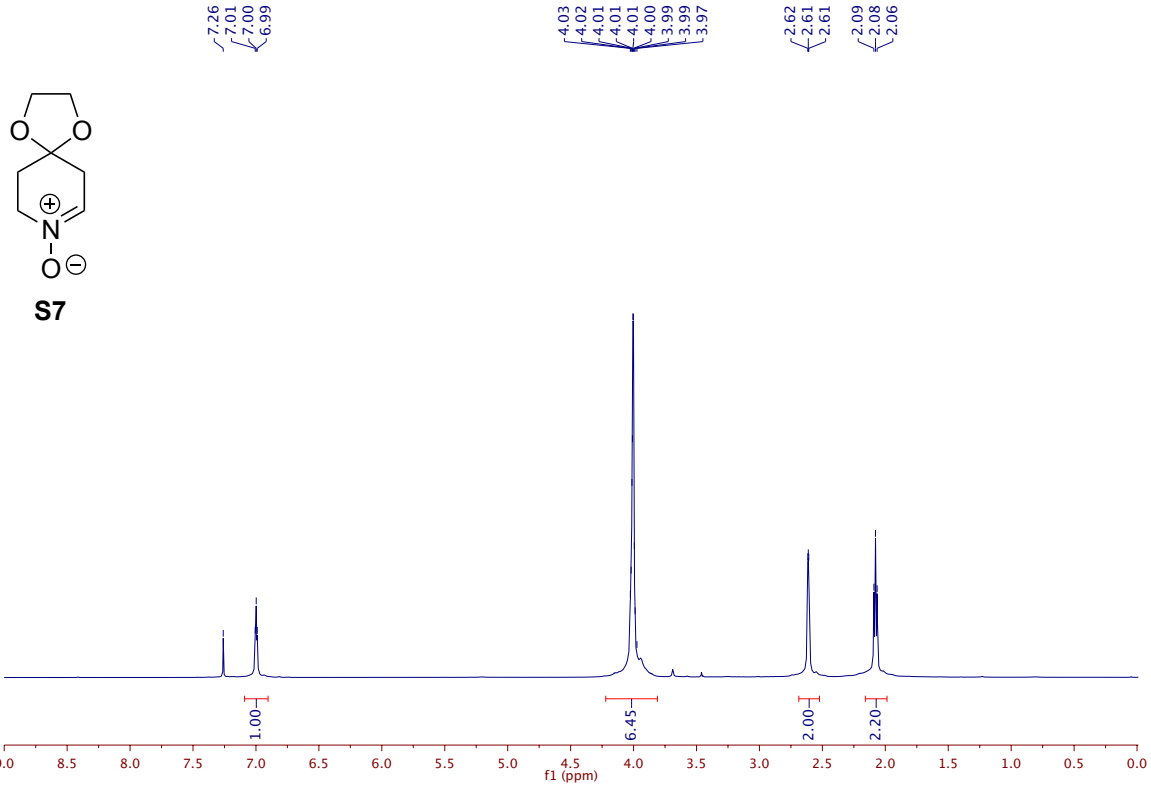

S7

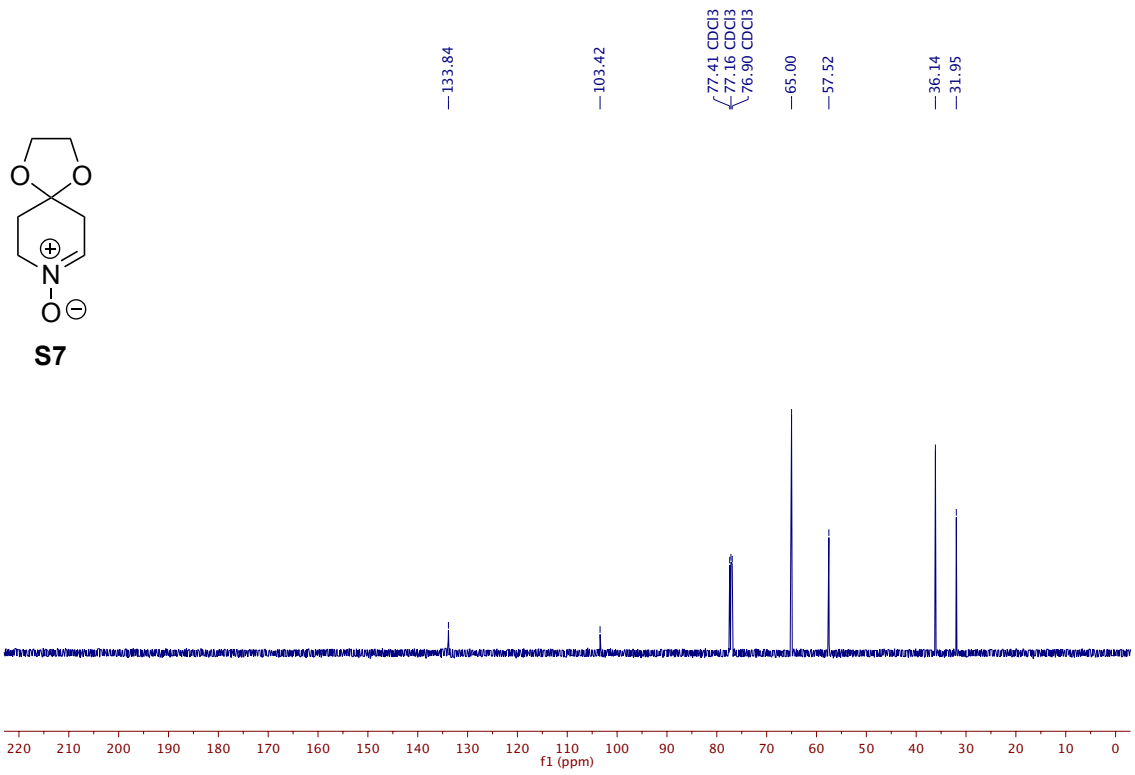

S7

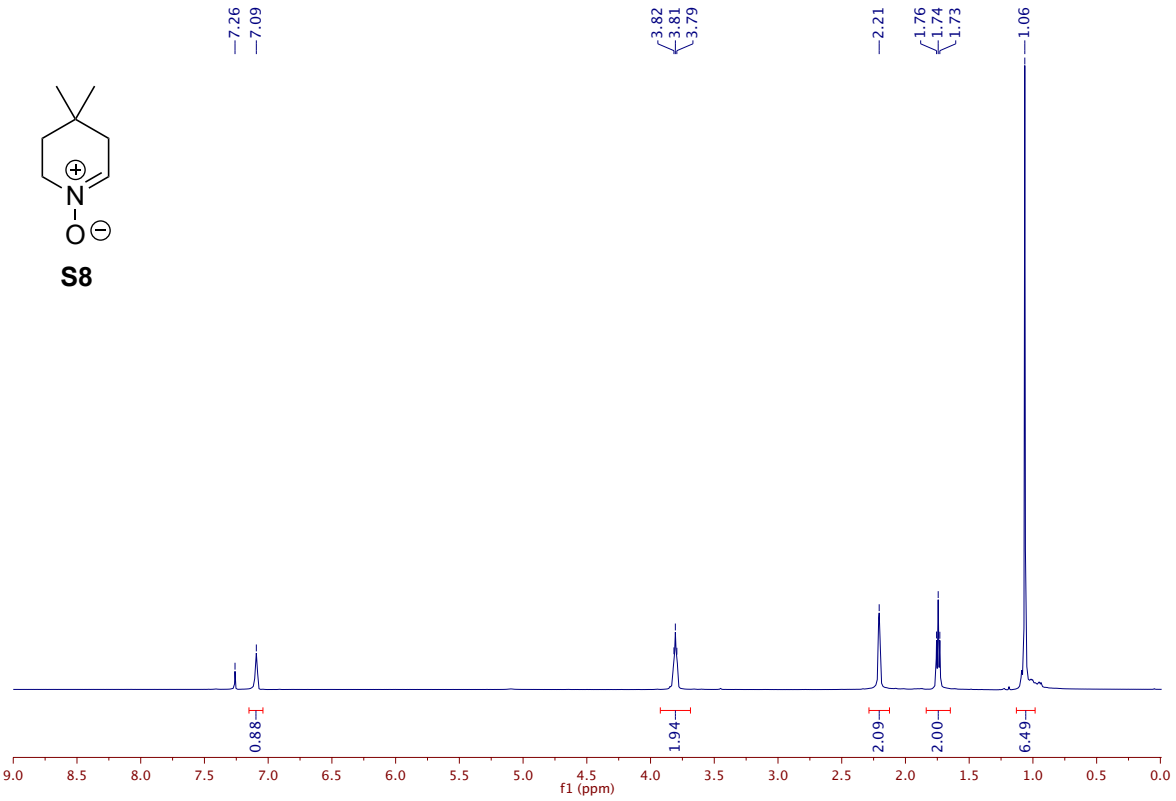
7.26
7.09
3.82
3.81
3.79
2.21
1.76
1.74
1.73
1.06
0.88
1.94
2.09
2.00
6.49
f1 (ppm)

S8

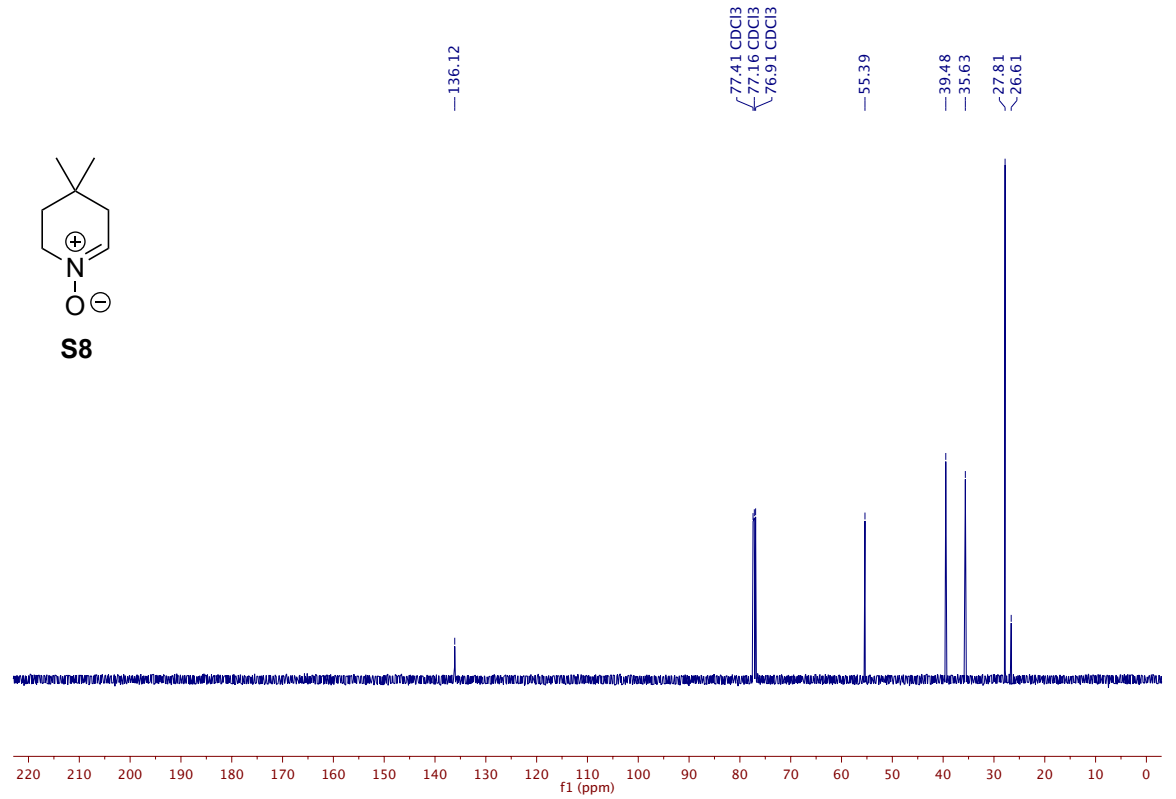
136.12
77.41 CDCl3
77.16 CDCl3
76.91 CDCl3
55.39
39.48
35.63
27.81
26.61
f1 (ppm)

S8

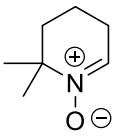

S17

7.26
6.96
6.95
6.94
2.32
2.31
2.31
2.30
2.30
2.29
1.82
1.81
1.81
1.80
1.80
1.68
1.67
1.66
1.66
1.66
1.65
1.65
1.63
1.40
0.71
2.00
1.96
2.00
6.02
f1 (ppm)

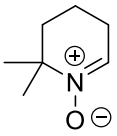

S17

135.48
77.41 CDCl3
77.16 CDCl3
76.90 CDCl3
66.06
36.89
26.81
26.36
15.23
f1 (ppm)

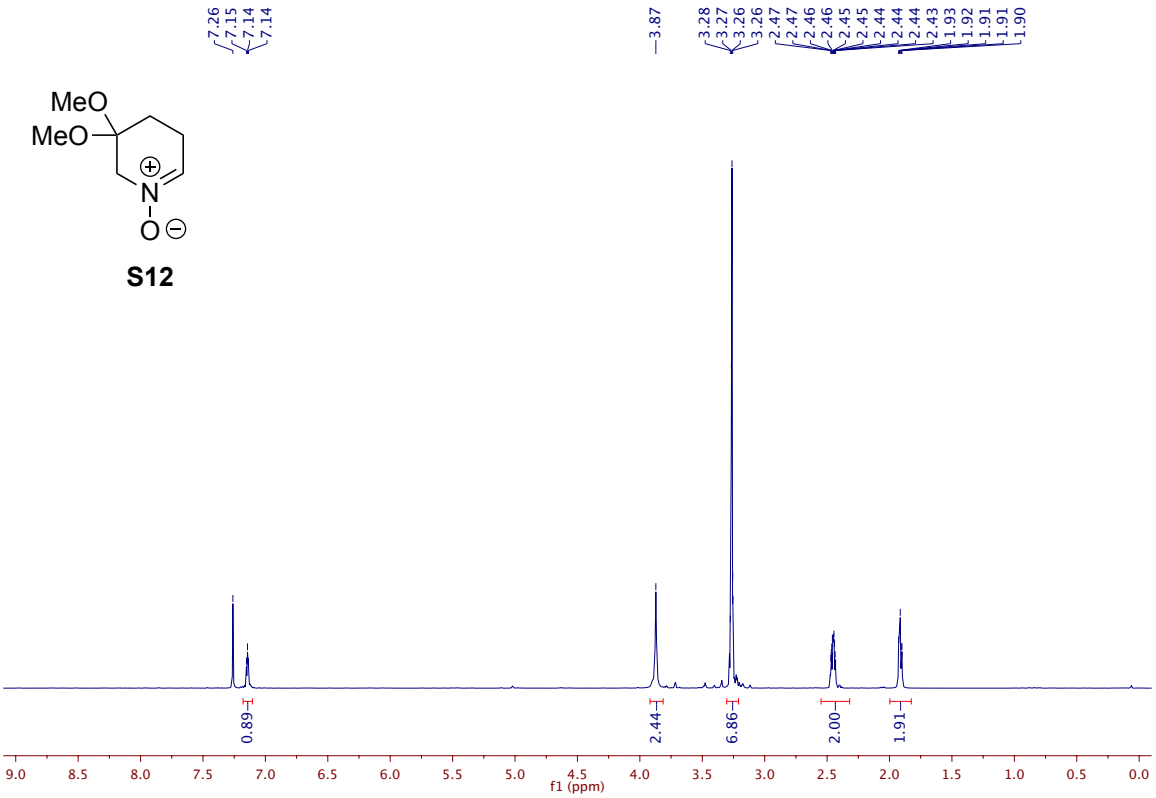
7.26
7.15
7.14
7.14
3.87
3.28
3.27
3.26
3.26
2.47
2.47
2.46
2.46
2.45
2.45
2.44
2.44
2.44
2.43
1.93
1.92
1.91
1.91
1.90
MeO
MeO
N
O
0.89
2.44
6.86
2.00
1.91
9.0
8.5
8.0
7.5
7.0
6.5
6.0
5.5
5.0
4.5
4.0
3.5
3.0
2.5
2.0
1.5
1.0
0.5
0.0
f1 (ppm)

S12

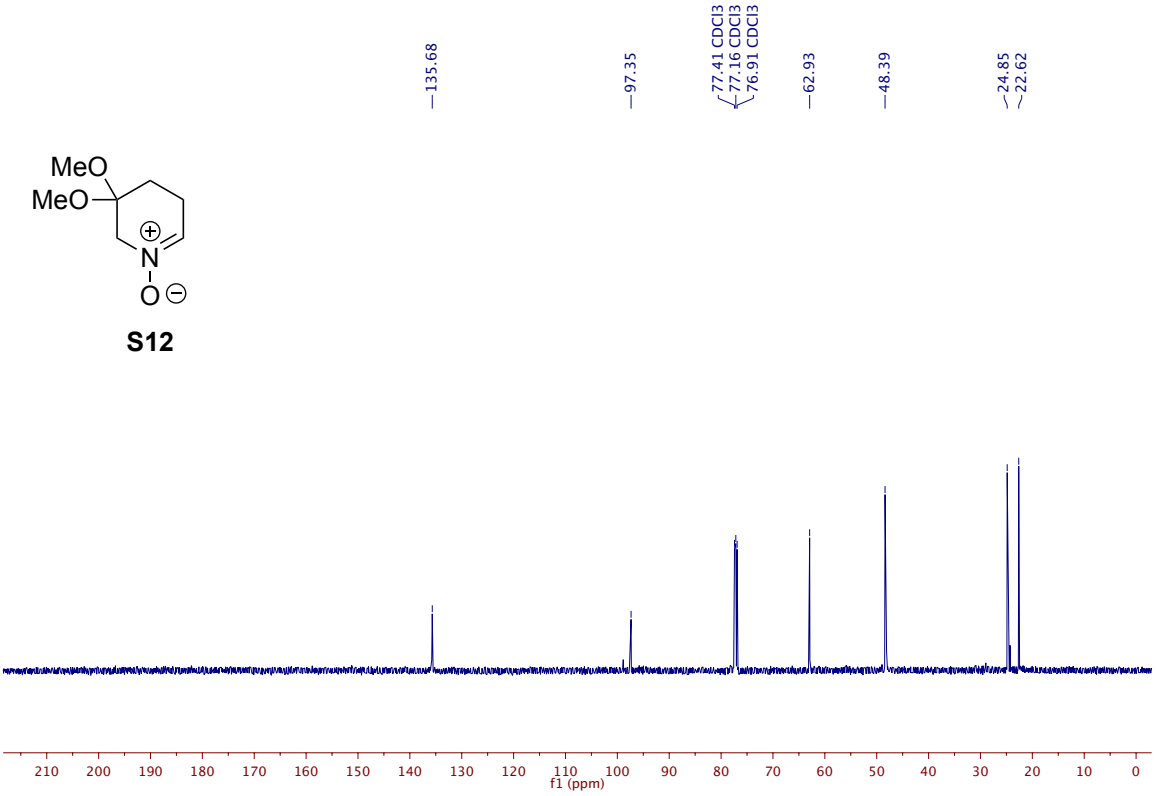
135.68
97.35
77.41 CDCl3
77.16 CDCl3
76.91 CDCl3
62.93
48.39
24.85
22.62
MeO
MeO
N
O
210
200
190
180
170
160
150
140
130
120
110
100
90
80
70
60
50
40
30
20
10
0
f1 (ppm)

S12

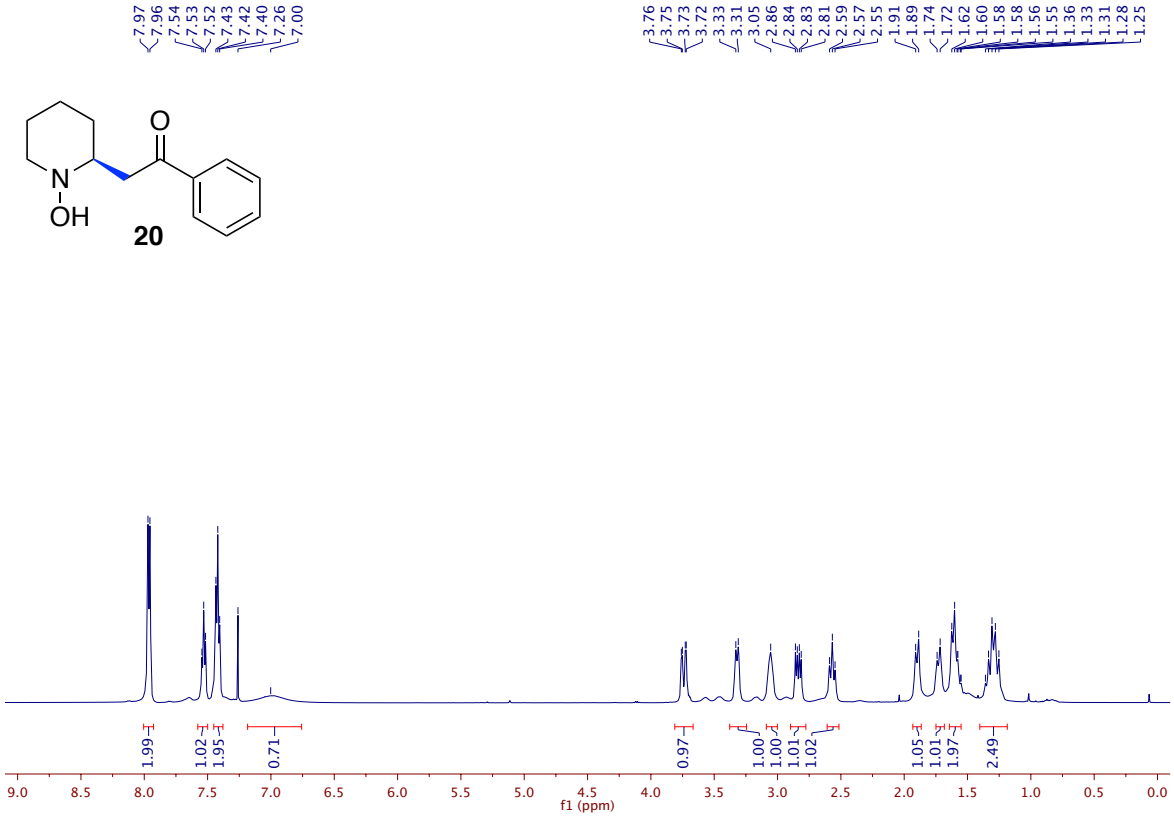
7.97
7.96
7.54
7.53
7.52
7.43
7.42
7.40
7.26
7.00
3.76
3.75
3.73
3.72
3.33
3.31
3.05
2.86
2.84
2.83
2.81
2.59
2.57
2.55
1.91
1.89
1.74
1.72
1.62
1.60
1.58
1.58
1.56
1.55
1.36
1.33
1.31
1.28
1.25
O
N
OH
20
1.99
1.02
1.95
0.71
0.97
1.00
1.00
1.01
1.02
1.05
1.01
1.97
2.49
9.0
8.5
8.0
7.5
7.0
6.5
6.0
5.5
5.0
4.5
4.0
3.5
3.0
2.5
2.0
1.5
1.0
0.5
0.0
f1 (ppm)

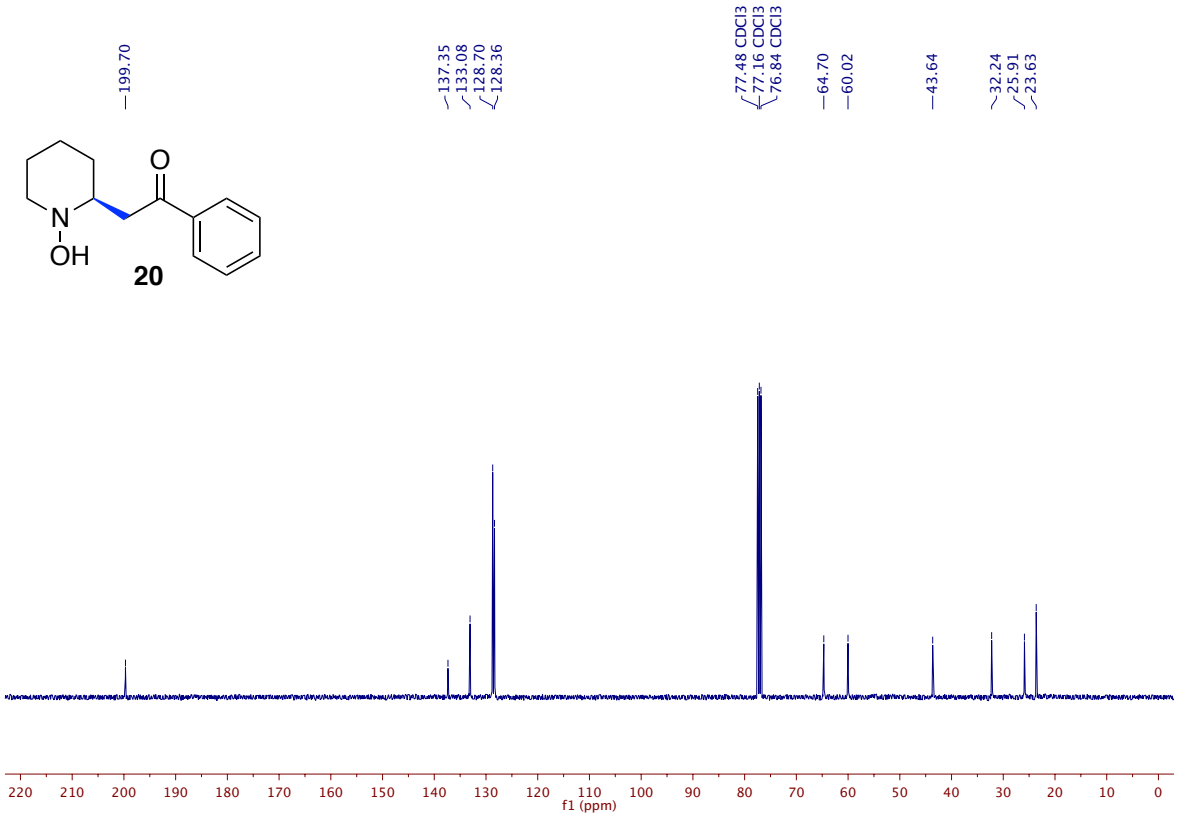
199.70
137.35
133.08
128.70
128.36
77.48 CDCl3
77.16 CDCl3
76.84 CDCl3
64.70
60.02
43.64
32.24
25.91
23.63
O
N
OH
20
220
210
200
190
180
170
160
150
140
130
120
110
100
90
80
70
60
50
40
30
20
10
0
f1 (ppm)

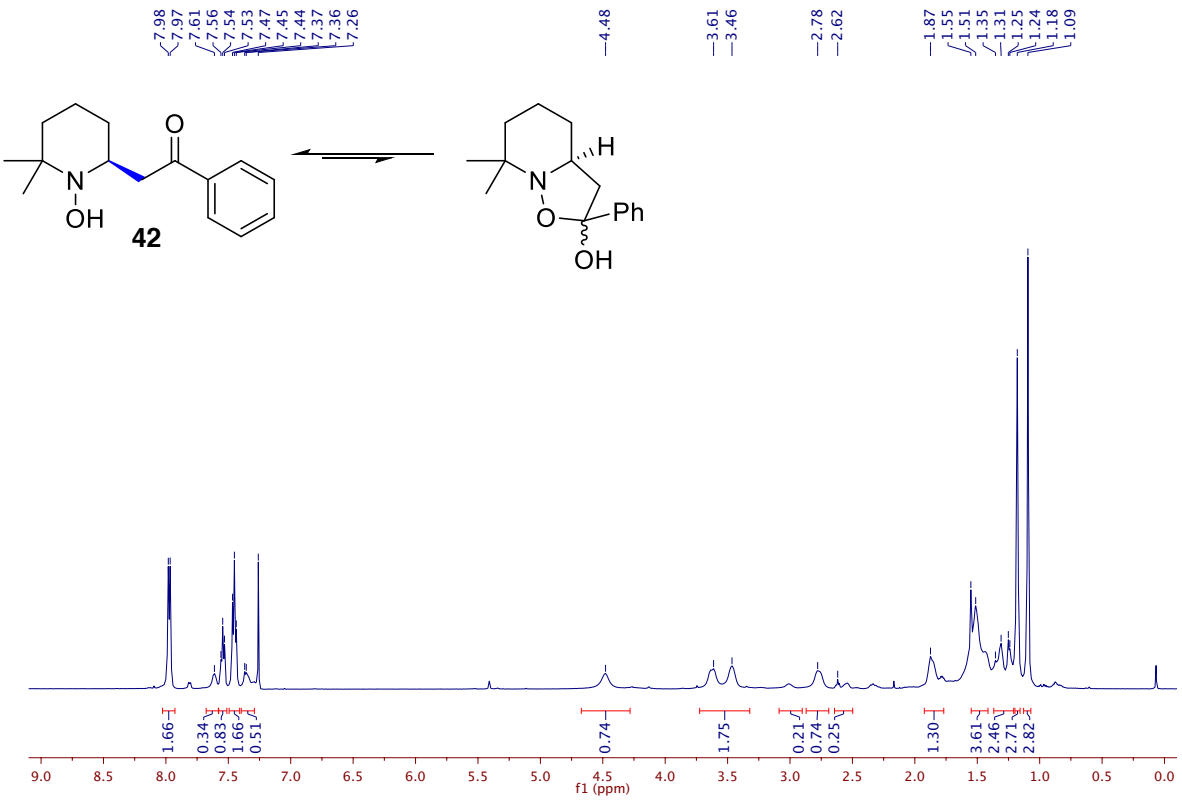
7.98
7.97
7.61
7.56
7.54
7.53
7.47
7.45
7.44
7.37
7.36
7.26
4.48
3.61
3.46
2.78
2.62
1.87
1.55
1.51
1.35
1.31
1.25
1.24
1.18
1.09
O
N
OH
42
H
N
O
Ph
OH
1.66
0.34
0.83
1.66
0.51
0.74
1.75
0.21
0.74
0.25
1.30
3.61
2.46
2.71
2.82
9.0
8.5
8.0
7.5
7.0
6.5
6.0
5.5
5.0
4.5
4.0
3.5
3.0
2.5
2.0
1.5
1.0
0.5
0.0
f1 (ppm)

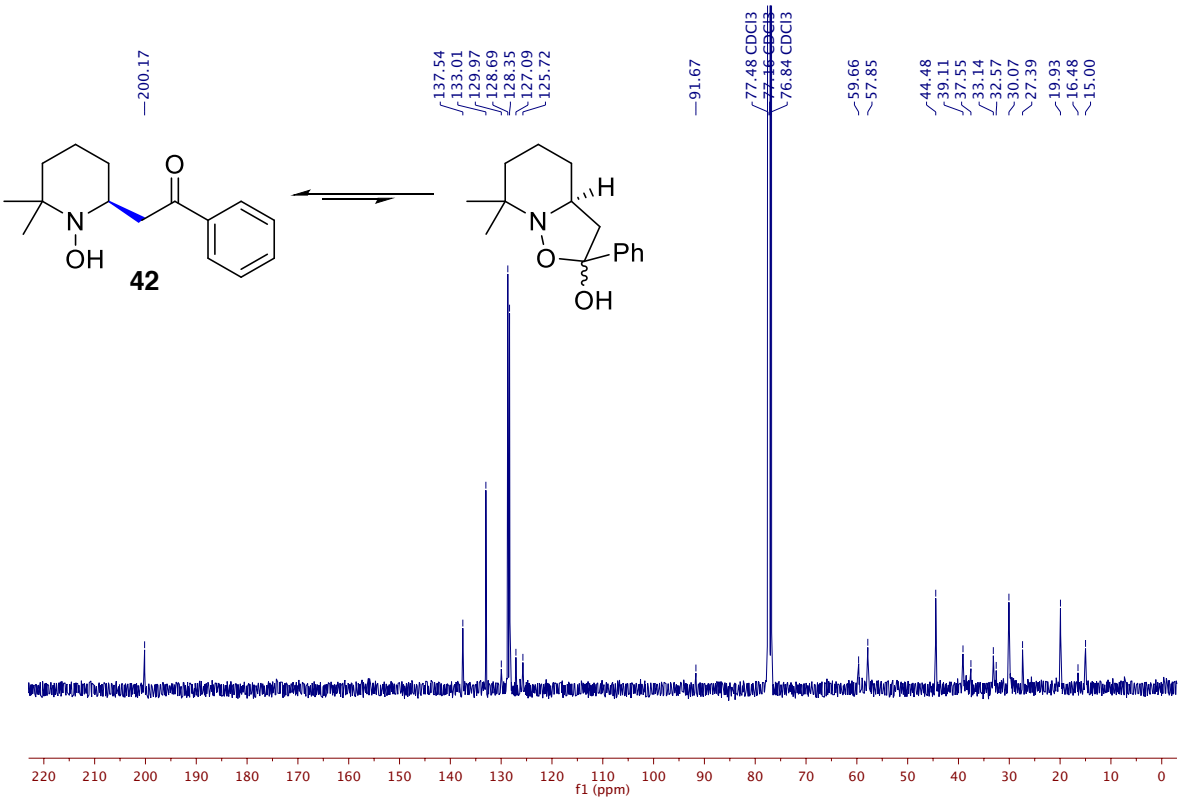
200.17
137.54
133.01
129.97
128.69
128.35
127.09
125.72
91.67
77.48 CDCl3
77.16 CDCl3
76.84 CDCl3
59.66
57.85
44.48
39.11
37.55
33.14
32.57
30.07
27.39
19.93
16.48
15.00
O
N
OH
42
H
N
O
Ph
OH
220
210
200
190
180
170
160
150
140
130
120
110
100
90
80
70
60
50
40
30
20
10
0
f1 (ppm)

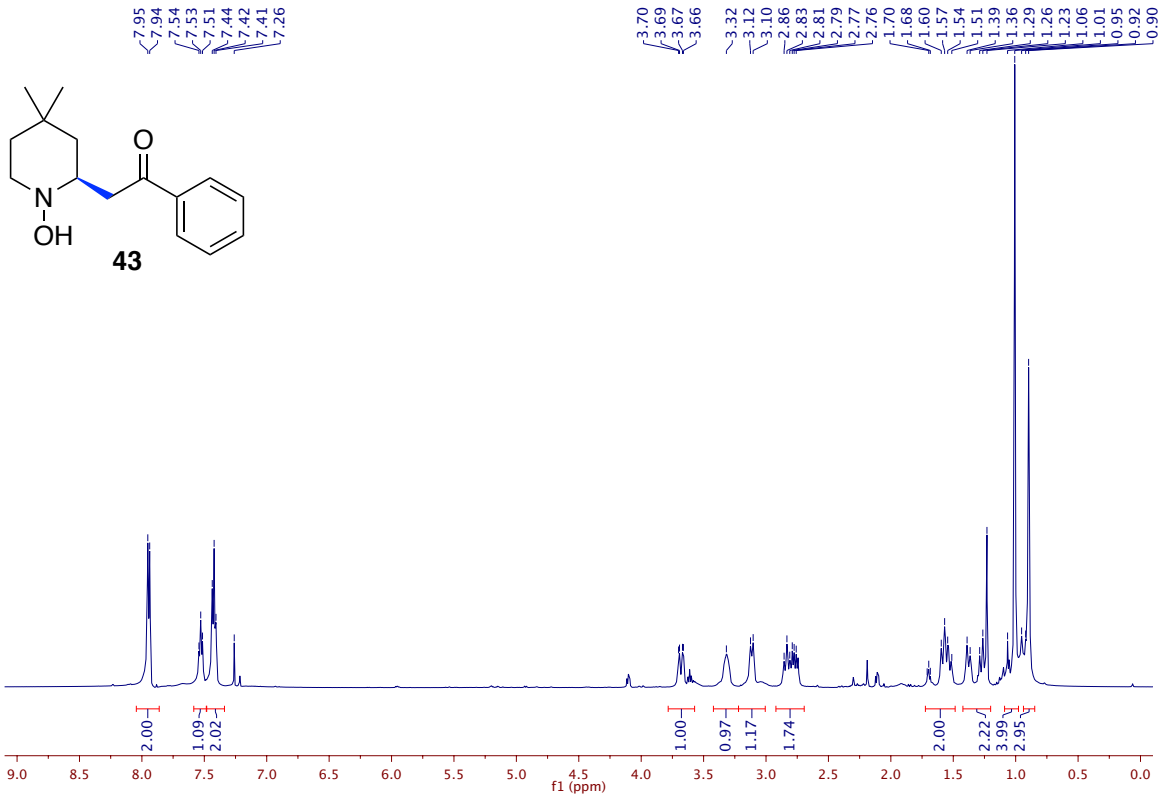
7.95
7.94
7.54
7.53
7.51
7.44
7.42
7.41
7.26
3.70
3.69
3.67
3.66
3.32
3.12
3.10
2.86
2.83
2.81
2.79
2.77
2.76
1.70
1.68
1.60
1.57
1.54
1.51
1.39
1.36
1.29
1.26
1.23
1.06
1.01
0.95
0.92
0.90
O
N
OH
43
2.00
1.09
2.02
1.00
0.97
1.17
1.74
2.00
2.22
3.99
2.95
9.0
8.5
8.0
7.5
7.0
6.5
6.0
5.5
5.0
4.5
4.0
3.5
3.0
2.5
2.0
1.5
1.0
0.5
0.0
f1 (ppm)

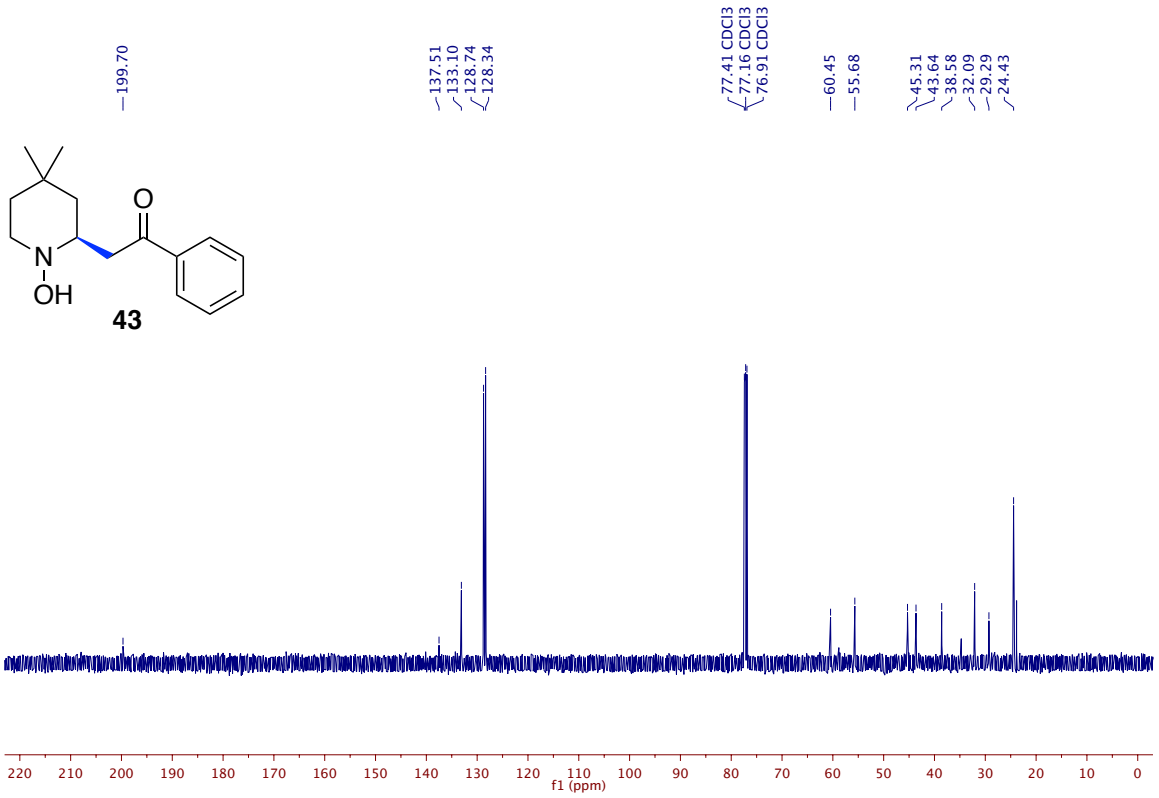
199.70
137.51
133.10
128.74
128.34
77.41 CDCl3
77.16 CDCl3
76.91 CDCl3
60.45
55.68
45.31
43.64
38.58
32.09
29.29
24.43
O
N
OH
43
220
210
200
190
180
170
160
150
140
130
120
110
100
90
80
70
60
50
40
30
20
10
0
f1 (ppm)

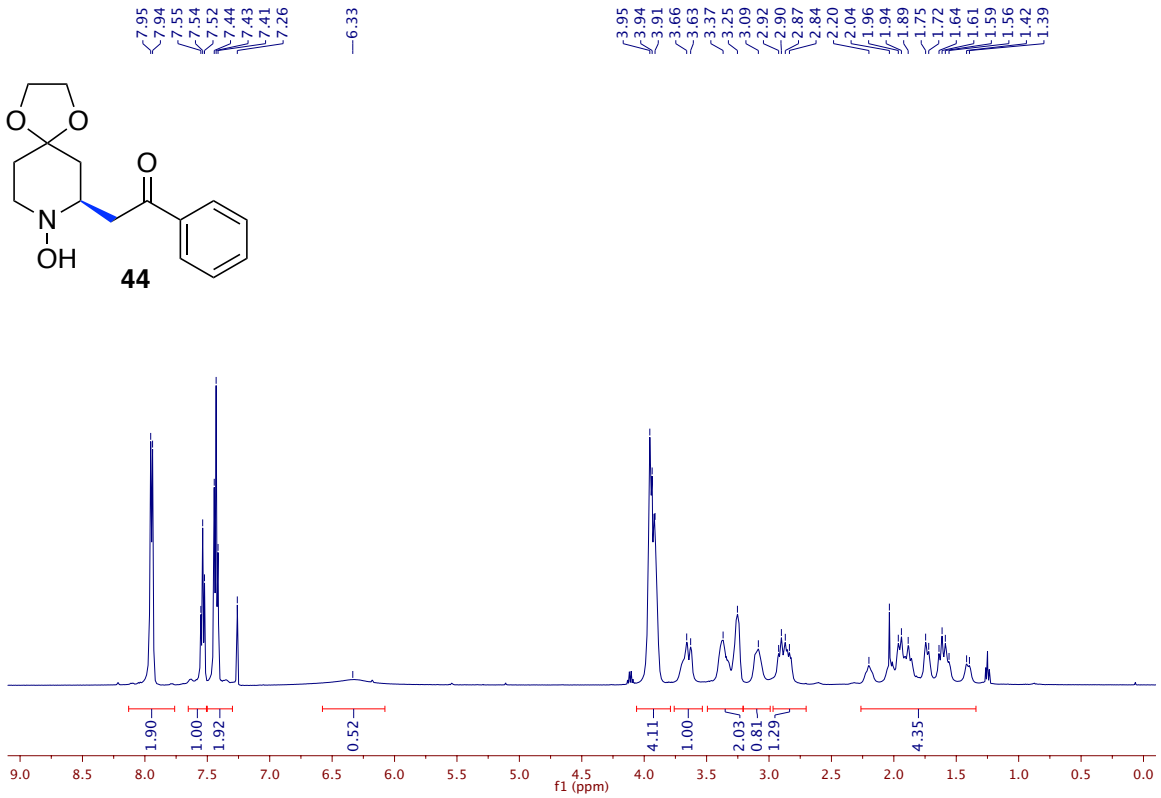
7.95
7.94
7.55
7.54
7.52
7.44
7.43
7.41
7.26
6.33
3.95
3.94
3.91
3.66
3.63
3.37
3.25
3.09
2.92
2.90
2.87
2.84
2.20
2.04
1.96
1.94
1.89
1.75
1.72
1.64
1.61
1.59
1.56
1.42
1.39
O
O
O
N
OH
44
1.90
1.00
1.92
0.52
4.11
1.00
2.03
0.81
1.29
4.35
9.0
8.5
8.0
7.5
7.0
6.5
6.0
5.5
5.0
4.5
4.0
3.5
3.0
2.5
2.0
1.5
1.0
0.5
0.0
f1 (ppm)

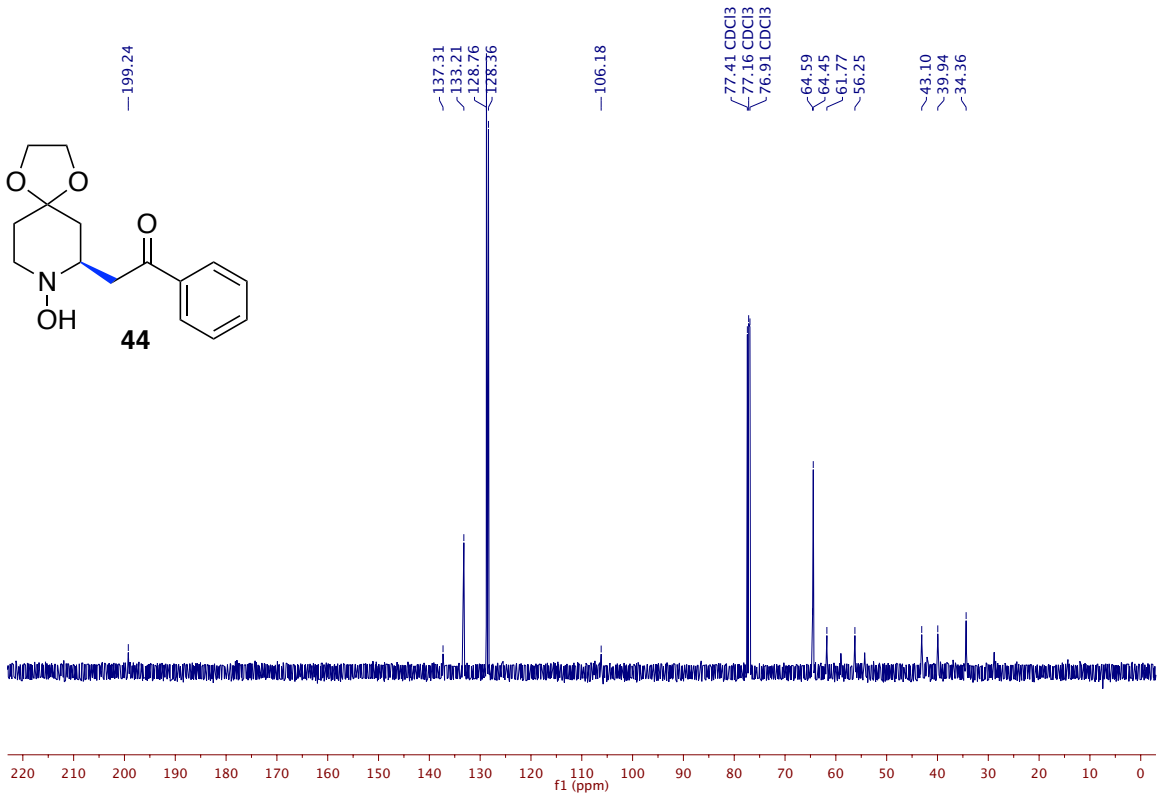
199.24
137.31
133.21
128.76
128.36
106.18
77.41 CDCl3
77.16 CDCl3
76.91 CDCl3
64.59
64.45
61.77
56.25
43.10
39.94
34.36
O
O
O
N
OH
44
220
210
200
190
180
170
160
150
140
130
120
110
100
90
80
70
60
50
40
30
20
10
0
f1 (ppm)

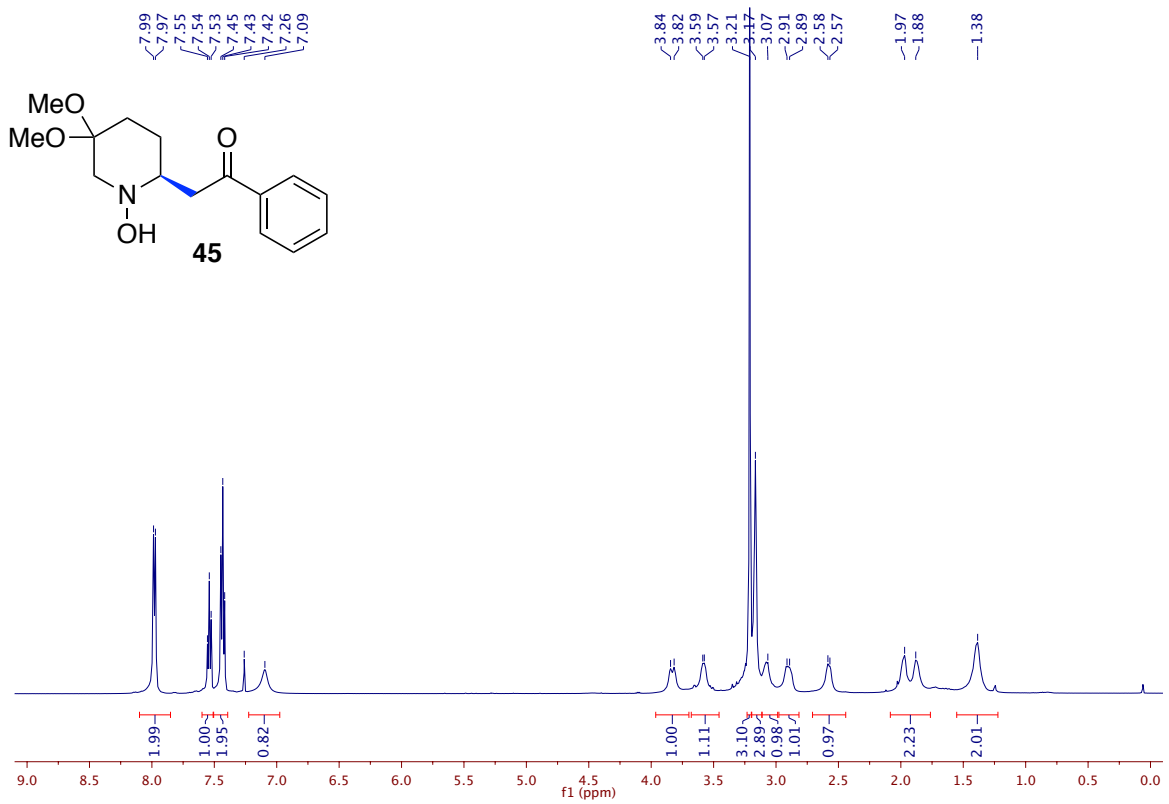
7.99
7.97
7.55
7.54
7.53
7.45
7.43
7.42
7.26
7.09
3.84
3.82
3.59
3.57
3.21
3.17
3.07
2.91
2.89
2.58
2.57
1.97
1.88
1.38
MeO
MeO
O
N
OH
45
1.99
1.00
1.95
0.82
1.00
1.11
3.10
2.89
0.98
1.01
0.97
2.23
2.01
f1 (ppm)

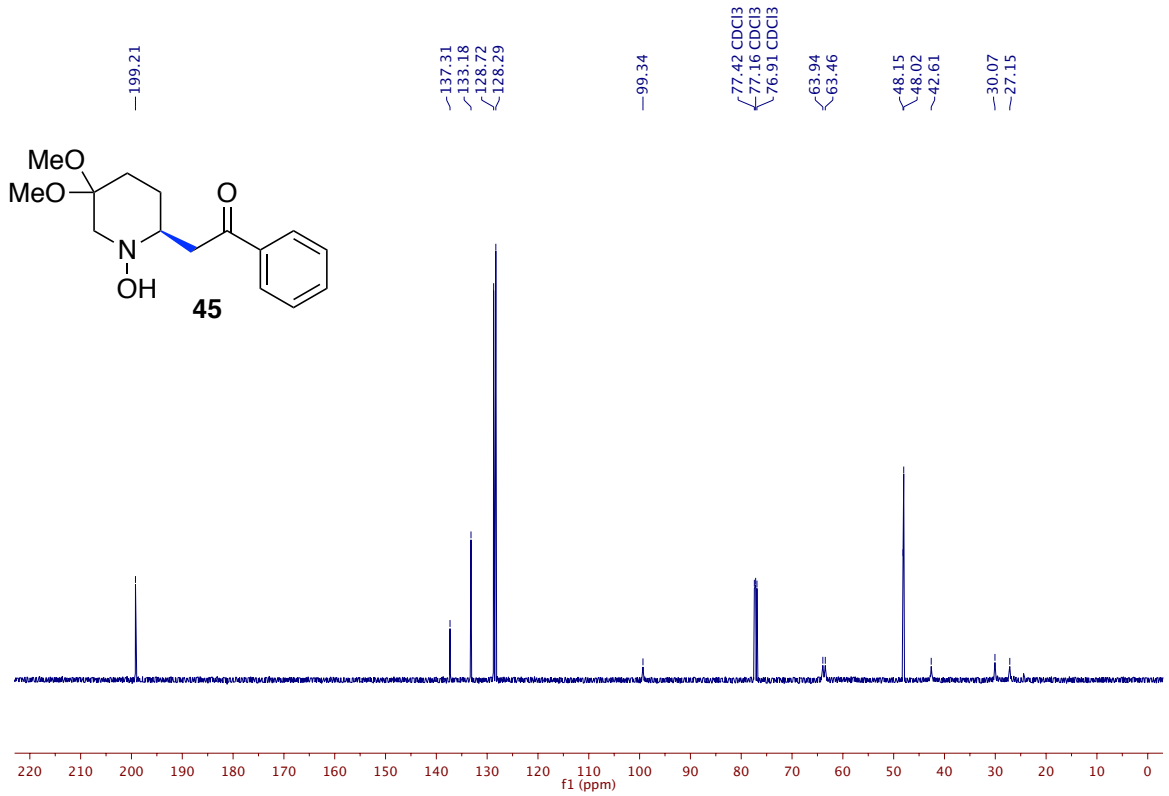
199.21
137.31
133.18
128.72
128.29
99.34
77.42 CDCl3
77.16 CDCl3
76.91 CDCl3
63.94
63.46
48.15
48.02
42.61
30.07
27.15
MeO
MeO
O
N
OH
45
f1 (ppm)

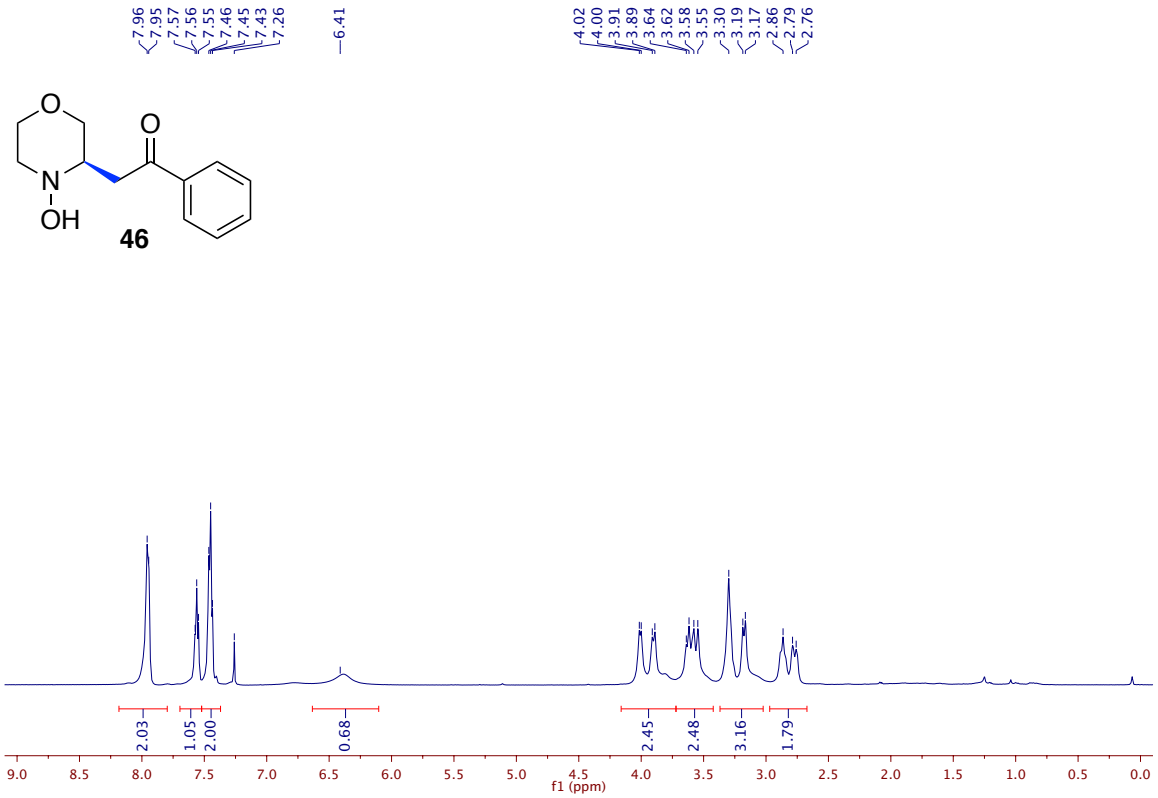
7.96
7.95
7.57
7.56
7.55
7.46
7.45
7.43
7.26
6.41
4.02
4.00
3.91
3.89
3.64
3.62
3.58
3.55
3.30
3.19
3.17
2.86
2.79
2.76
O
O
N
OH
46
2.03
1.05
2.00
0.68
2.45
2.48
3.16
1.79
9.0
8.5
8.0
7.5
7.0
6.5
6.0
5.5
5.0
4.5
4.0
3.5
3.0
2.5
2.0
1.5
1.0
0.5
0.0
f1 (ppm)

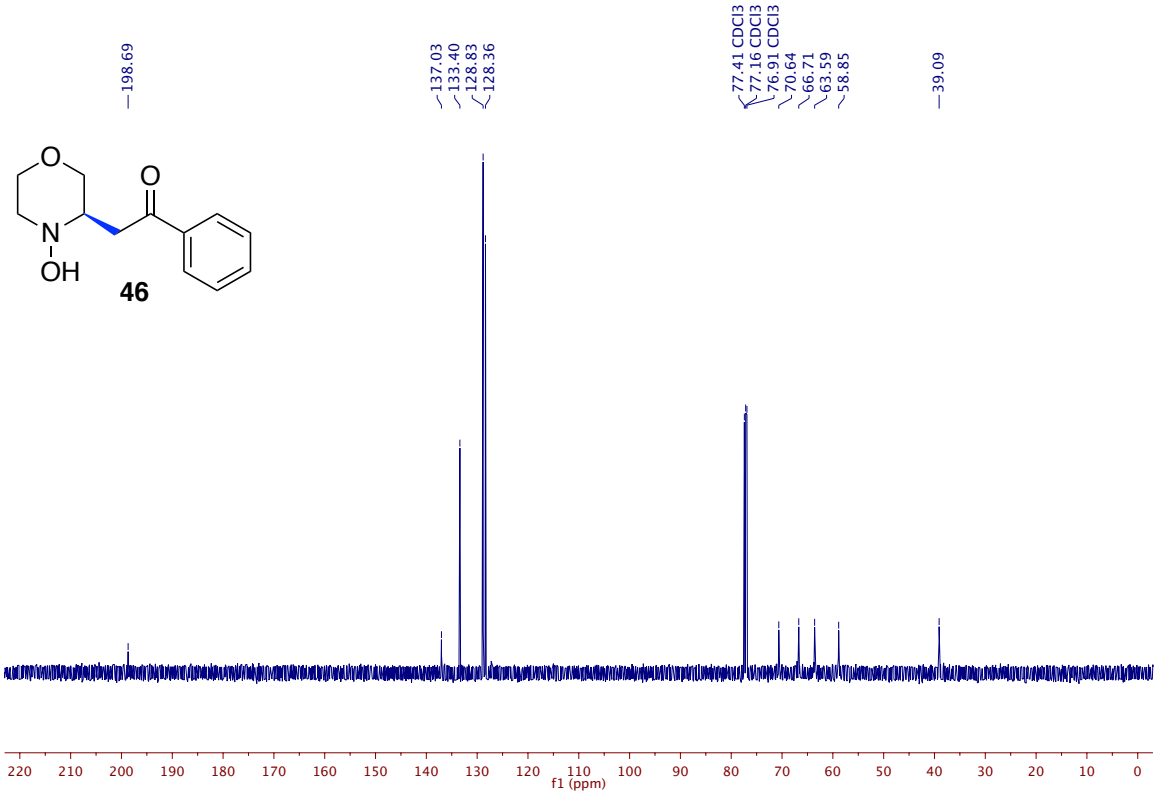
198.69
137.03
133.40
128.83
128.36
77.41 CDCl3
77.16 CDCl3
76.91 CDCl3
70.64
66.71
63.59
58.85
39.09
O
O
N
OH
46
220
210
200
190
180
170
160
150
140
130
120
110
100
90
80
70
60
50
40
30
20
10
0
f1 (ppm)


8.48
8.04
8.02
7.89
7.87
7.85
7.83
7.81
7.57
7.56
7.54
7.50
7.49
7.47
7.26
3.89
3.88
3.86
3.85
3.37
3.14
3.00
2.98
2.97
2.95
2.61
2.59
2.57
1.95
1.93
1.75
1.73
1.65
1.62
1.42
1.40
1.37
1.35
1.33
1.30
1.29
1.28
1.27
O
N
OH

47

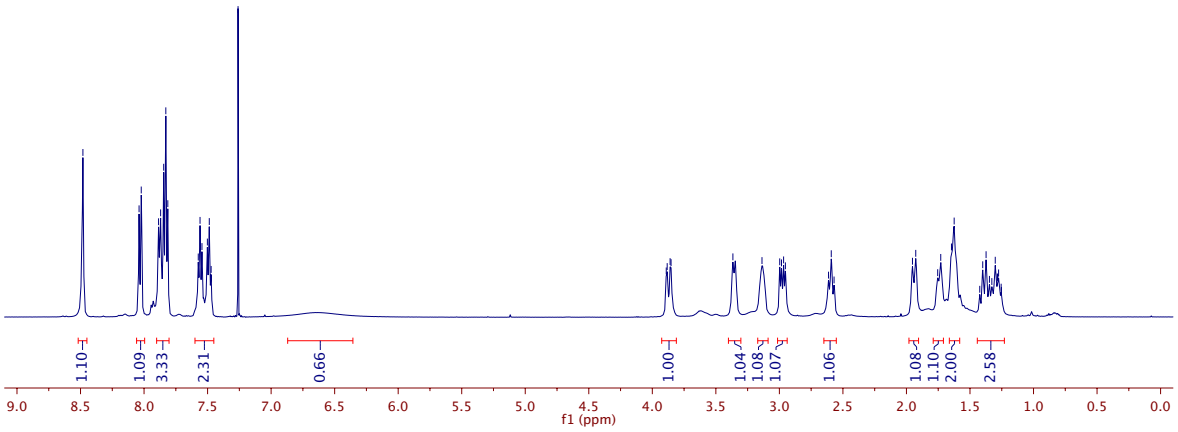
1.10
1.09
3.33
2.31
0.66
1.00
1.04
1.08
1.07
1.06
1.08
1.10
2.00
2.58
9.0
8.5
8.0
7.5
7.0
6.5
6.0
5.5
5.0
4.5
4.0
3.5
3.0
2.5
2.0
1.5
1.0
0.5
0.0
f1 (ppm)

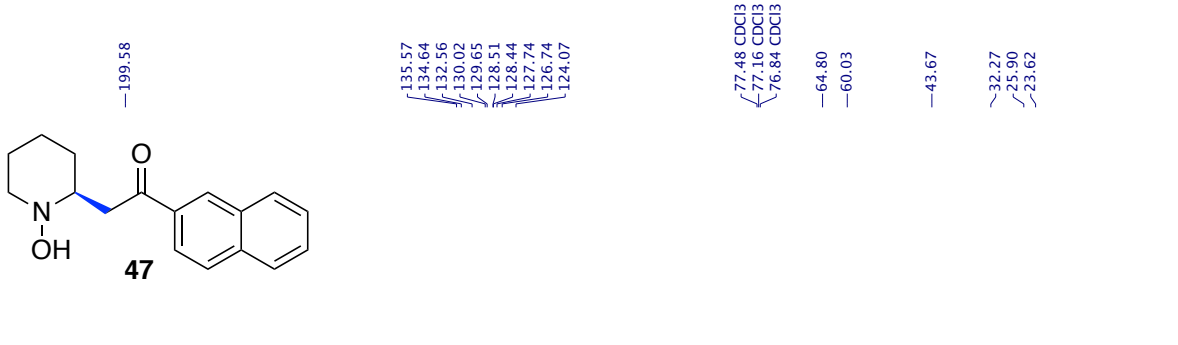
199.58
135.57
134.64
132.56
130.02
129.65
128.51
128.44
127.74
126.74
124.07
77.48 CDCl3
77.16 CDCl3
76.84 CDCl3
64.80
60.03
43.67
32.27
25.90
23.62
O
N
OH

47

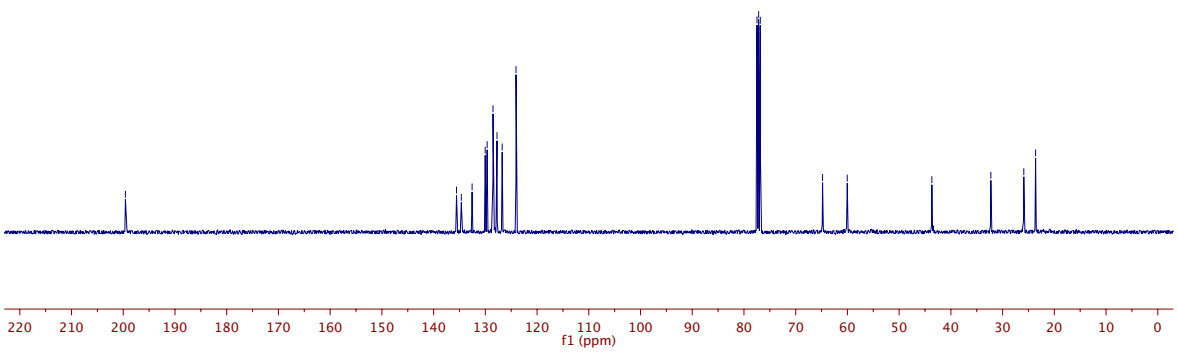
220
210
200
190
180
170
160
150
140
130
120
110
100
90
80
70
60
50
40
30
20
10
0
f1 (ppm)

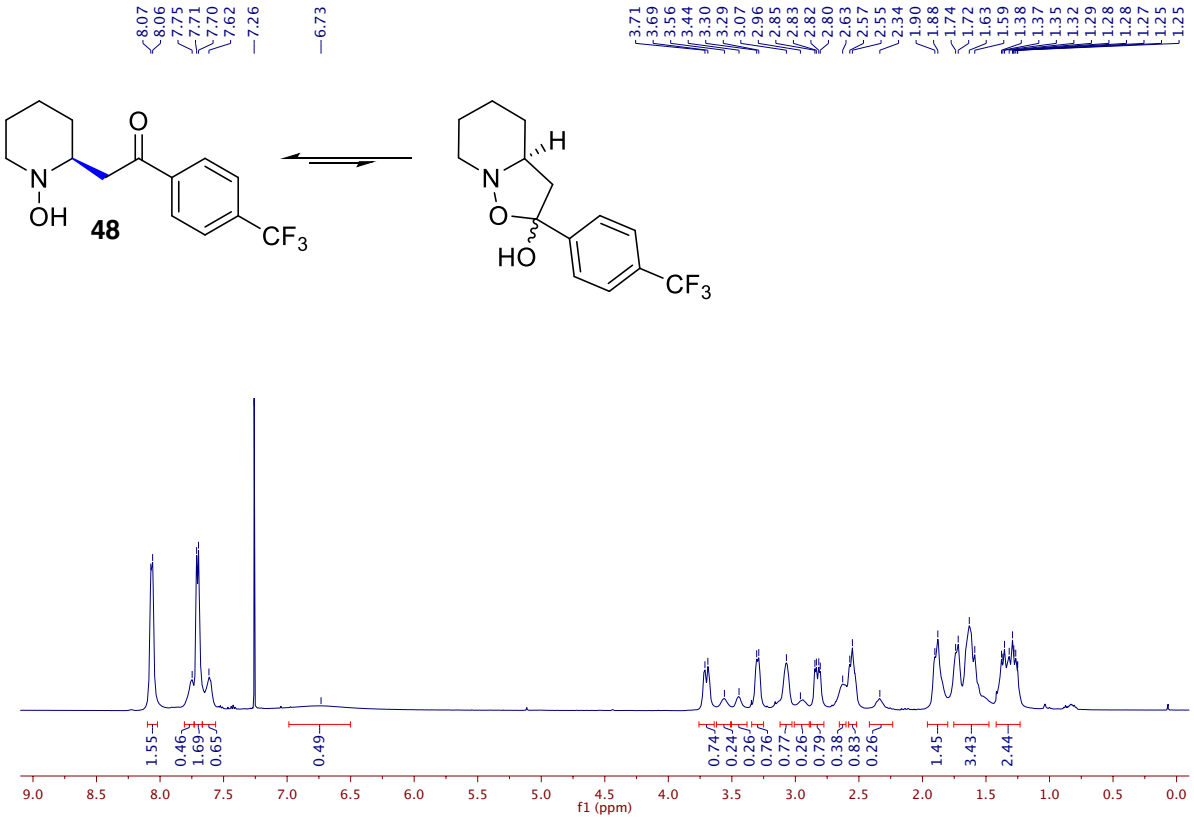
8.07
8.06
7.75
7.71
7.70
7.62
7.26
6.73
3.71
3.69
3.56
3.44
3.30
3.29
3.07
2.96
2.85
2.83
2.82
2.80
2.63
2.57
2.55
2.34
1.90
1.88
1.74
1.72
1.63
1.59
1.38
1.37
1.35
1.32
1.29
1.28
1.28
1.27
1.25
1.25
O
N
OH
48
CF3
H
N
O
HO
CF3
1.55
0.46
1.69
0.65
0.49
0.74
0.24
0.26
0.76
0.77
0.26
0.79
0.38
0.83
0.26
1.45
3.43
2.44
9.0
8.5
8.0
7.5
7.0
6.5
6.0
5.5
5.0
4.5
4.0
3.5
3.0
2.5
2.0
1.5
1.0
0.5
0.0
f1 (ppm)

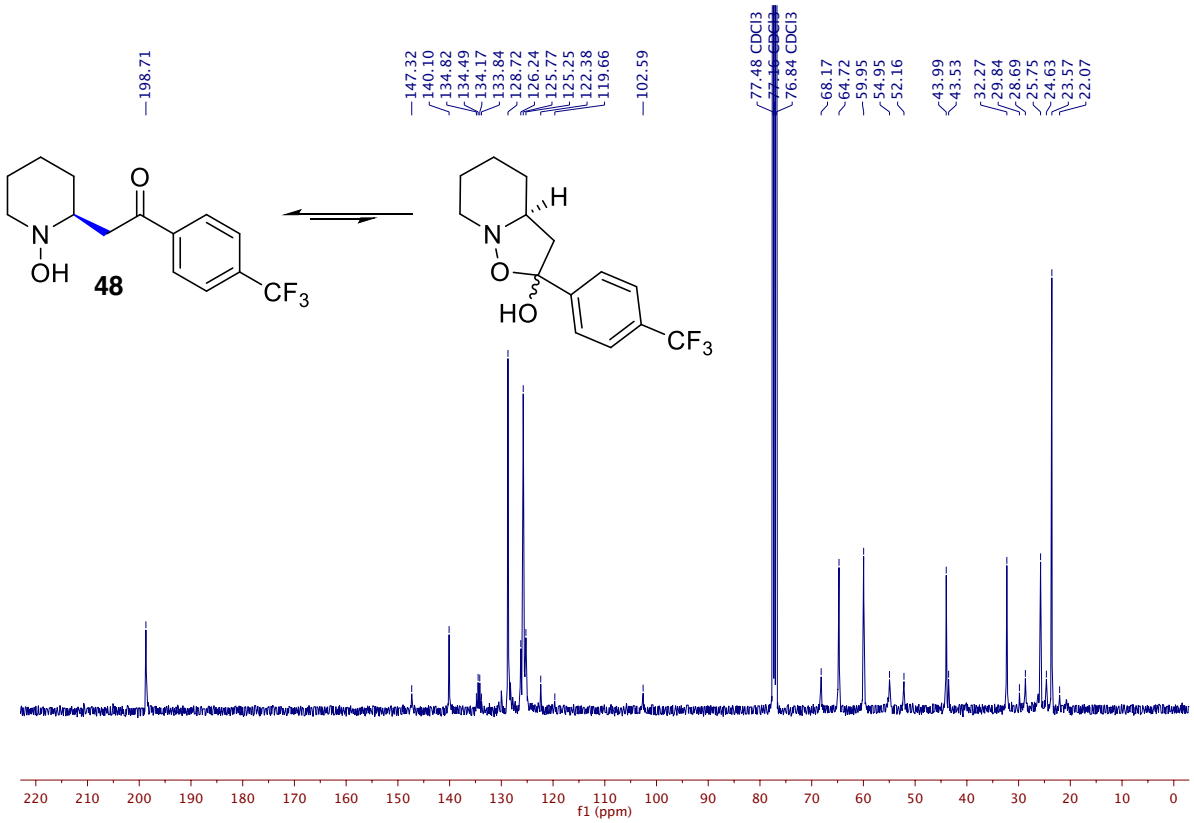
198.71
147.32
140.10
134.82
134.49
134.17
133.84
128.72
126.24
125.77
125.25
122.38
119.66
102.59
77.48 CDCl3
77.16 CDCl3
76.84 CDCl3
68.17
64.72
59.95
54.95
52.16
43.99
43.53
32.27
29.84
28.69
25.75
24.63
23.57
22.07
O
N
OH
48
CF3
H
N
O
HO
CF3
220
210
200
190
180
170
160
150
140
130
120
110
100
90
80
70
60
50
40
30
20
10
0
f1 (ppm)

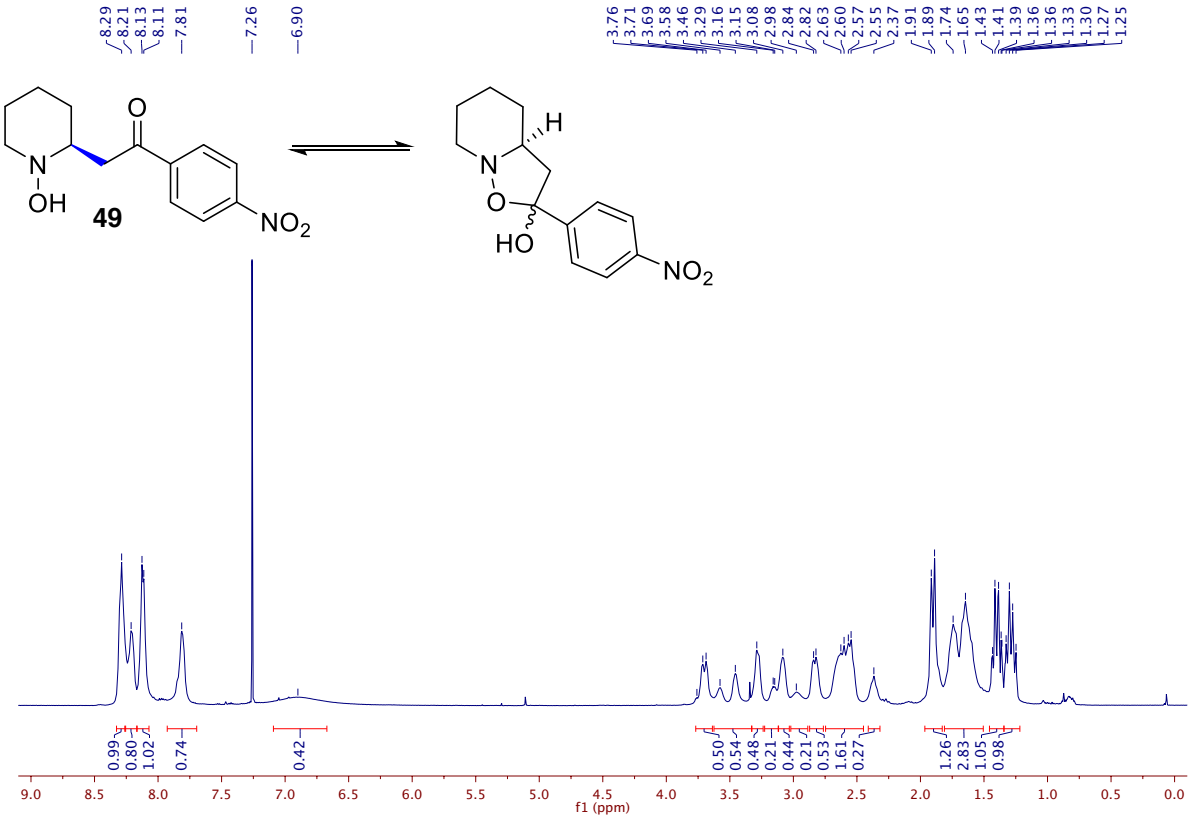
8.29
8.21
8.13
8.11
7.81
7.26
6.90
3.76
3.71
3.69
3.58
3.46
3.29
3.16
3.15
3.08
2.98
2.84
2.82
2.63
2.60
2.57
2.55
2.37
1.91
1.89
1.74
1.65
1.43
1.41
1.39
1.36
1.36
1.33
1.30
1.27
1.25
O
N
OH
49
NO2
H
N
O
HO
NO2
0.99
0.80
1.02
0.74
0.42
0.50
0.54
0.48
0.21
0.44
0.21
0.53
1.61
0.27
1.26
2.83
1.05
0.98
9.0
8.5
8.0
7.5
7.0
6.5
6.0
5.5
5.0
4.5
4.0
3.5
3.0
2.5
2.0
1.5
1.0
0.5
0.0
f1 (ppm)

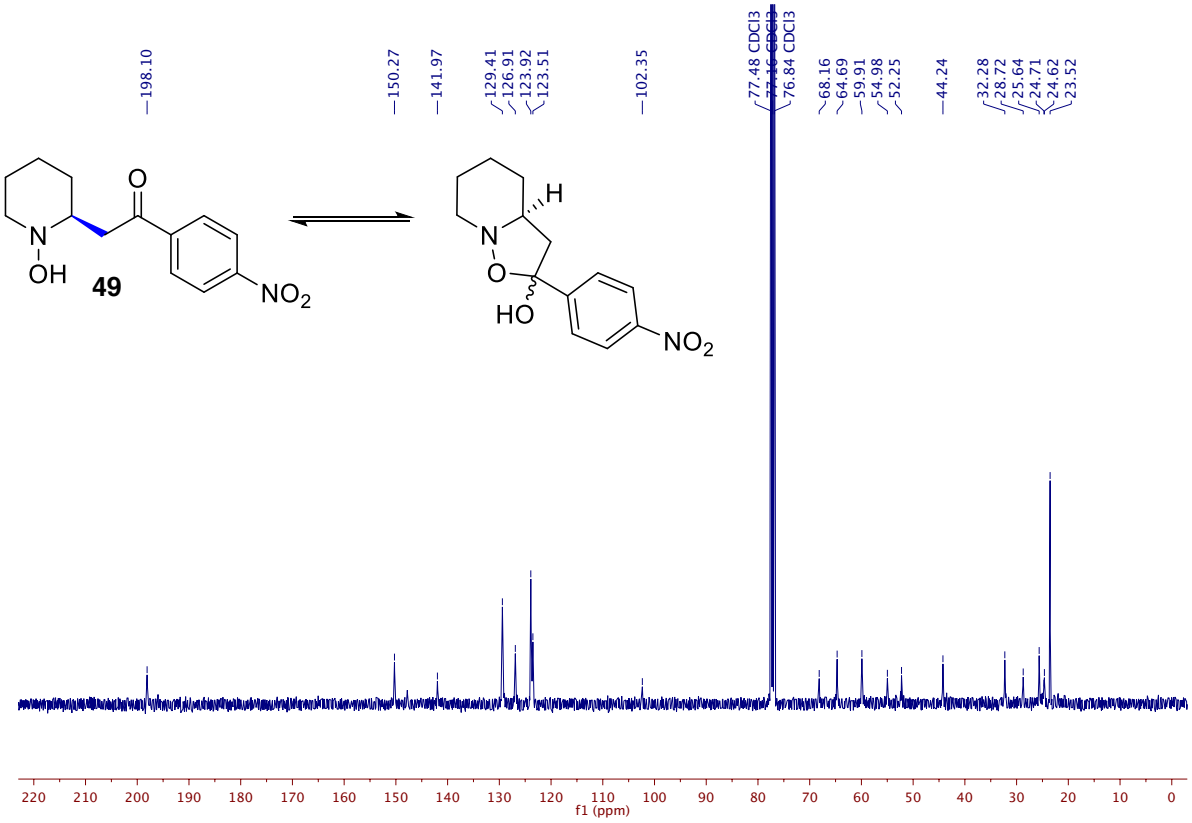
198.10
150.27
141.97
129.41
126.91
123.92
123.51
102.35
77.48 CDCl3
77.16 CDCl3
76.84 CDCl3
68.16
64.69
59.91
54.98
52.25
44.24
32.28
28.72
25.64
24.71
24.62
23.52
O
N
OH
49
NO2
H
N
O
HO
NO2
220
210
200
190
180
170
160
150
140
130
120
110
100
90
80
70
60
50
40
30
20
10
0
f1 (ppm)

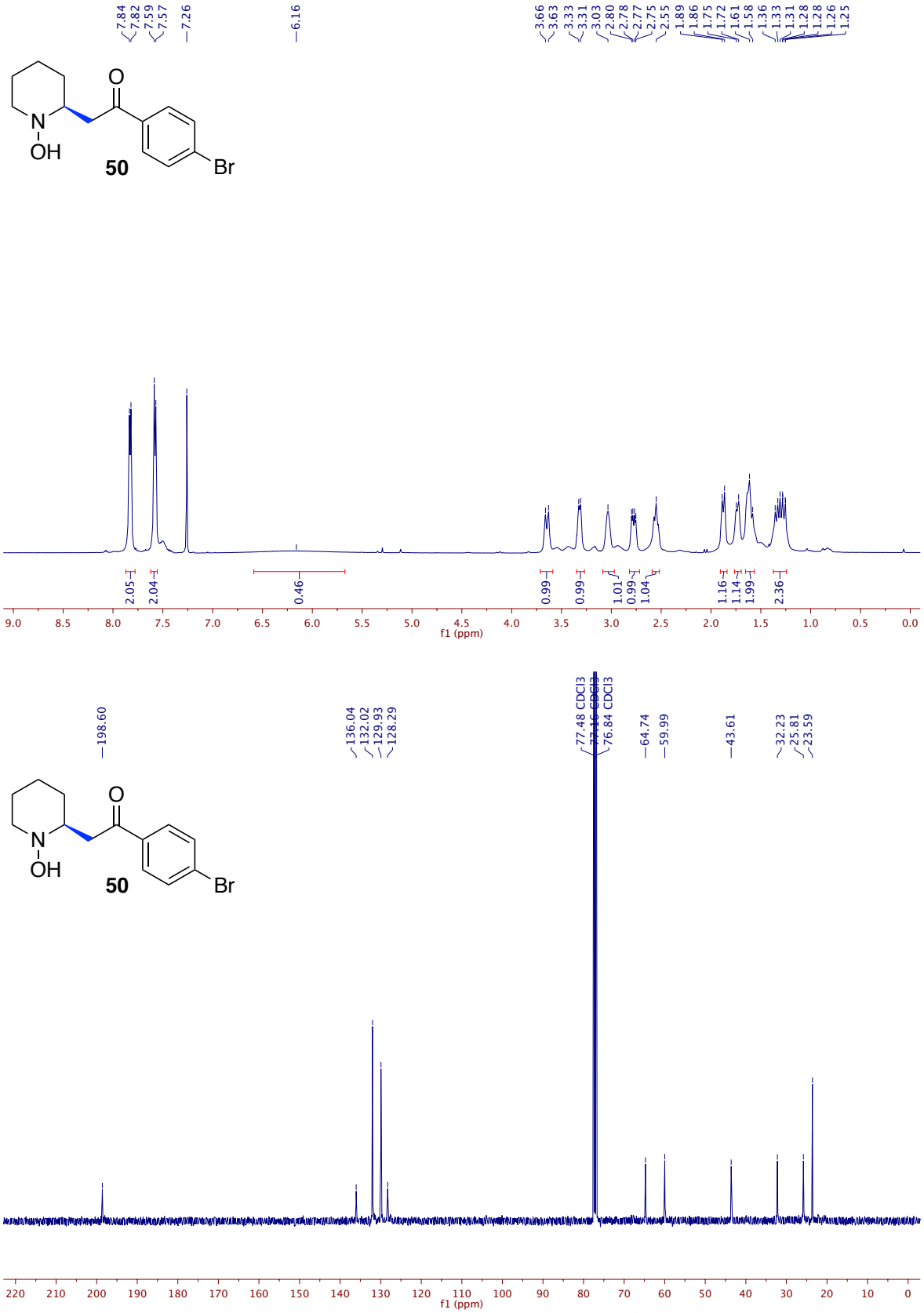
7.84
7.82
7.59
7.57
7.26
6.16
3.66
3.63
3.33
3.31
3.03
2.80
2.78
2.77
2.75
2.55
1.89
1.86
1.75
1.72
1.61
1.58
1.36
1.33
1.31
1.28
1.28
1.26
1.25
O
N
OH
Br
50
2.05
2.04
0.46
0.99
0.99
1.01
0.99
1.04
1.16
1.14
1.99
2.36
f1 (ppm)
198.60
136.04
132.02
129.93
128.29
77.48 CDCl3
77.16 CDCl3
76.84 CDCl3
64.74
59.99
43.61
32.23
25.81
23.59
f1 (ppm)

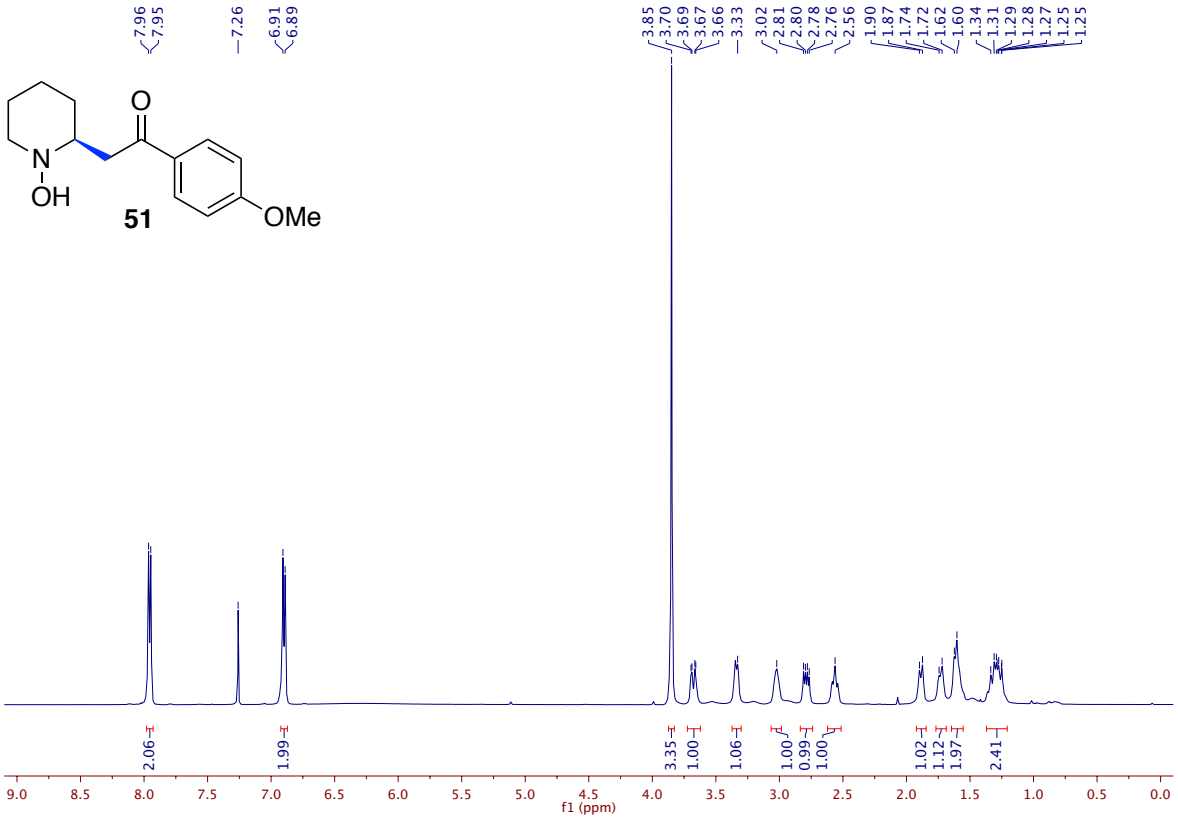
7.96
7.95
7.26
6.91
6.89
3.85
3.70
3.69
3.67
3.66
3.33
3.02
2.81
2.80
2.78
2.76
2.56
1.90
1.87
1.74
1.72
1.62
1.60
1.34
1.31
1.29
1.28
1.27
1.25
1.25
O
N
OH
51
OMe
2.06
1.99
3.35
1.00
1.06
1.00
0.99
1.00
1.02
1.12
1.97
2.41
f1 (ppm)

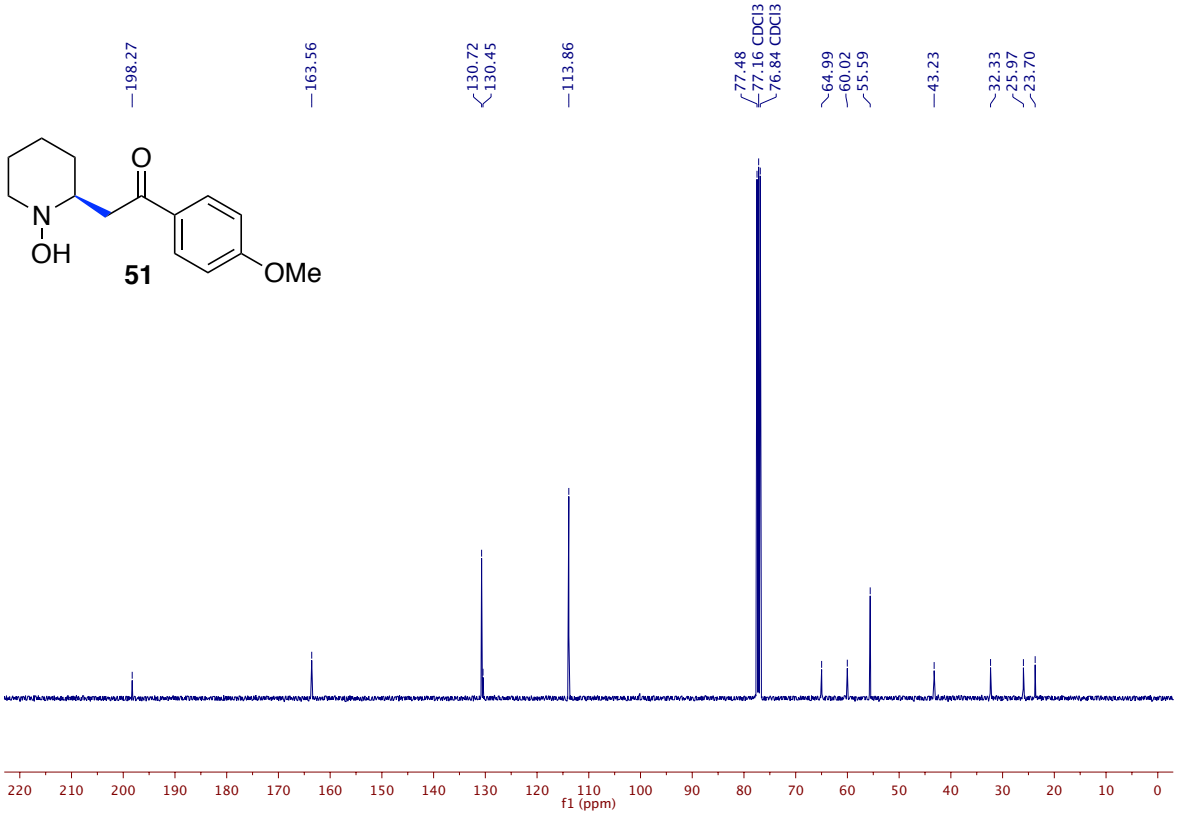
198.27
163.56
130.72
130.45
113.86
77.48
77.16 CDCl3
76.84 CDCl3
64.99
60.02
55.59
43.23
32.33
25.97
23.70
O
N
OH
51
OMe
f1 (ppm)

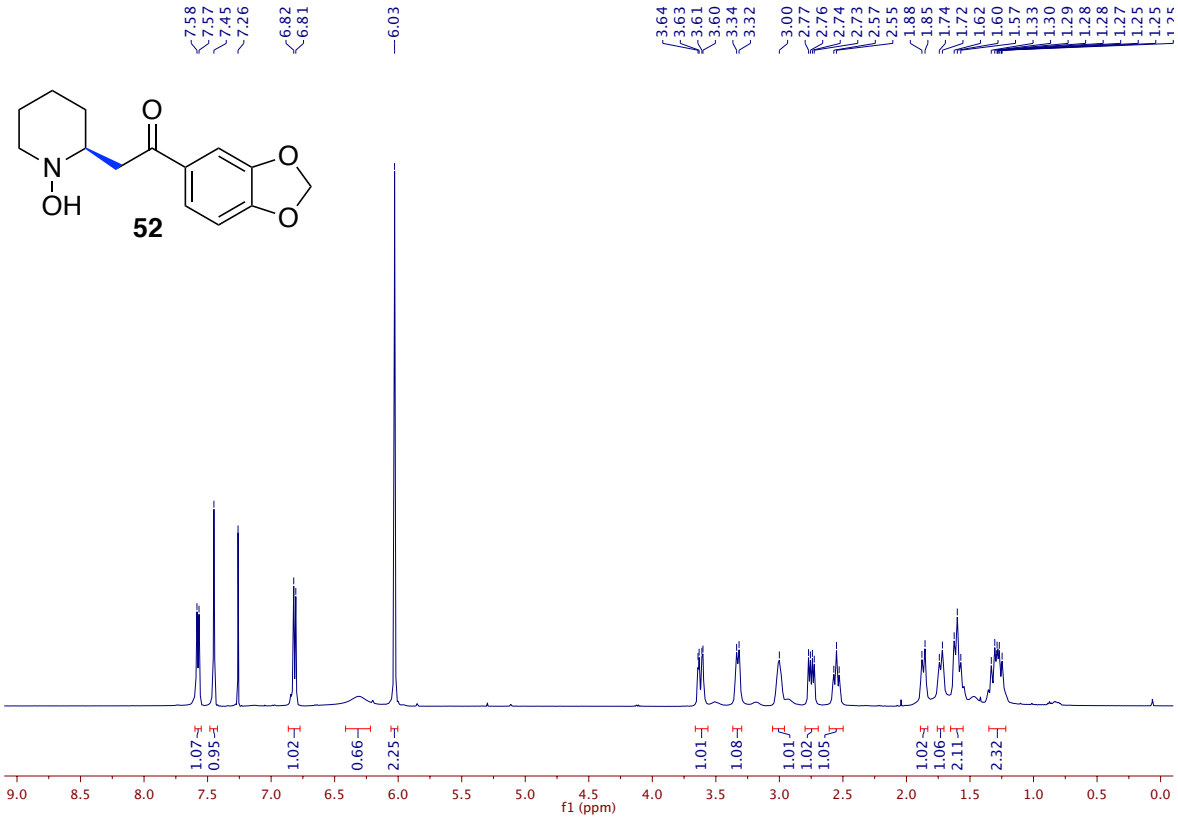
7.58
7.57
7.45
7.26
6.82
6.81
6.03
3.64
3.63
3.61
3.60
3.34
3.32
3.00
2.77
2.76
2.74
2.73
2.57
2.55
1.88
1.85
1.74
1.72
1.62
1.60
1.57
1.33
1.30
1.29
1.28
1.28
1.27
1.25
1.25
O
N
OH
O
O
52
1.07
0.95
1.02
0.66
2.25
1.01
1.08
1.01
1.02
1.05
1.02
1.06
2.11
2.32
9.0 8.5 8.0 7.5 7.0 6.5 6.0 5.5 5.0 4.5 4.0 3.5 3.0 2.5 2.0 1.5 1.0 0.5 0.0
f1 (ppm)

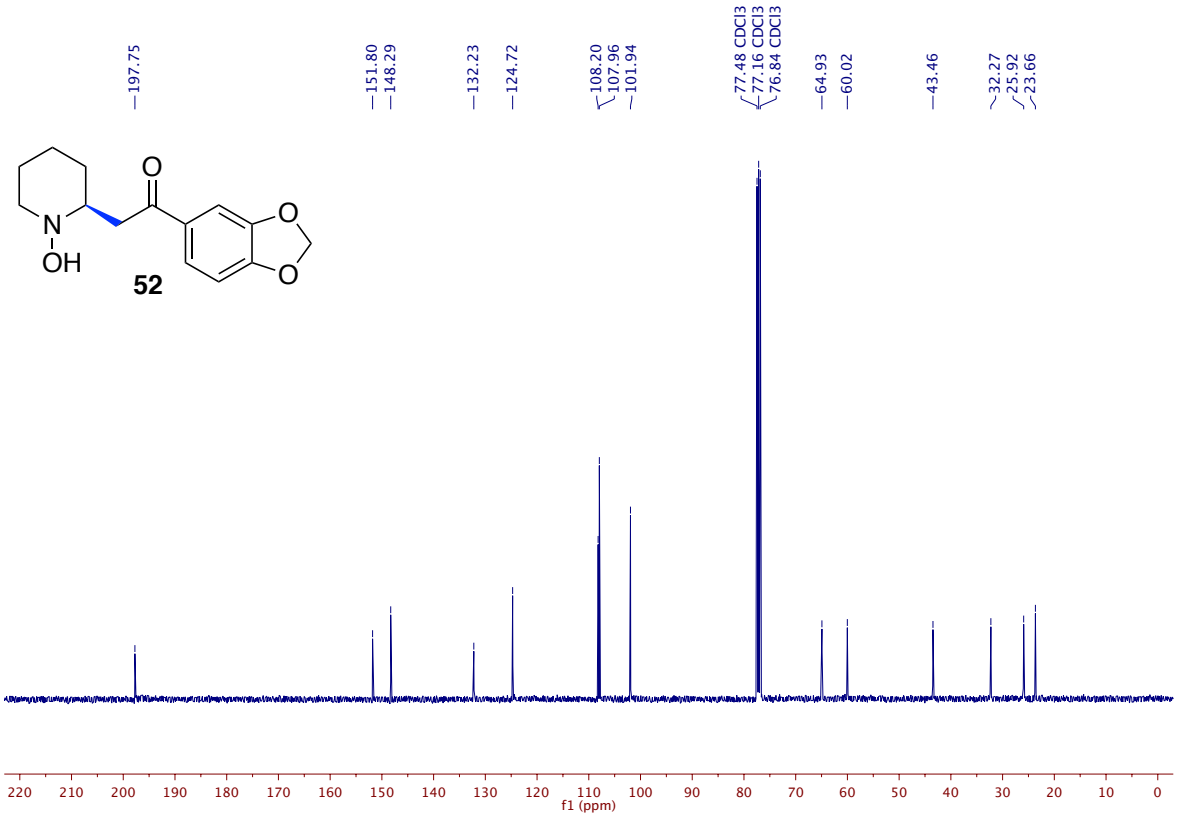
197.75
151.80
148.29
132.23
124.72
108.20
107.96
101.94
77.48 CDCl3
77.16 CDCl3
76.84 CDCl3
64.93
60.02
43.46
32.27
25.92
23.66
O
N
OH
O
O
52
220 210 200 190 180 170 160 150 140 130 120 110 100 90 80 70 60 50 40 30 20 10 0
f1 (ppm)

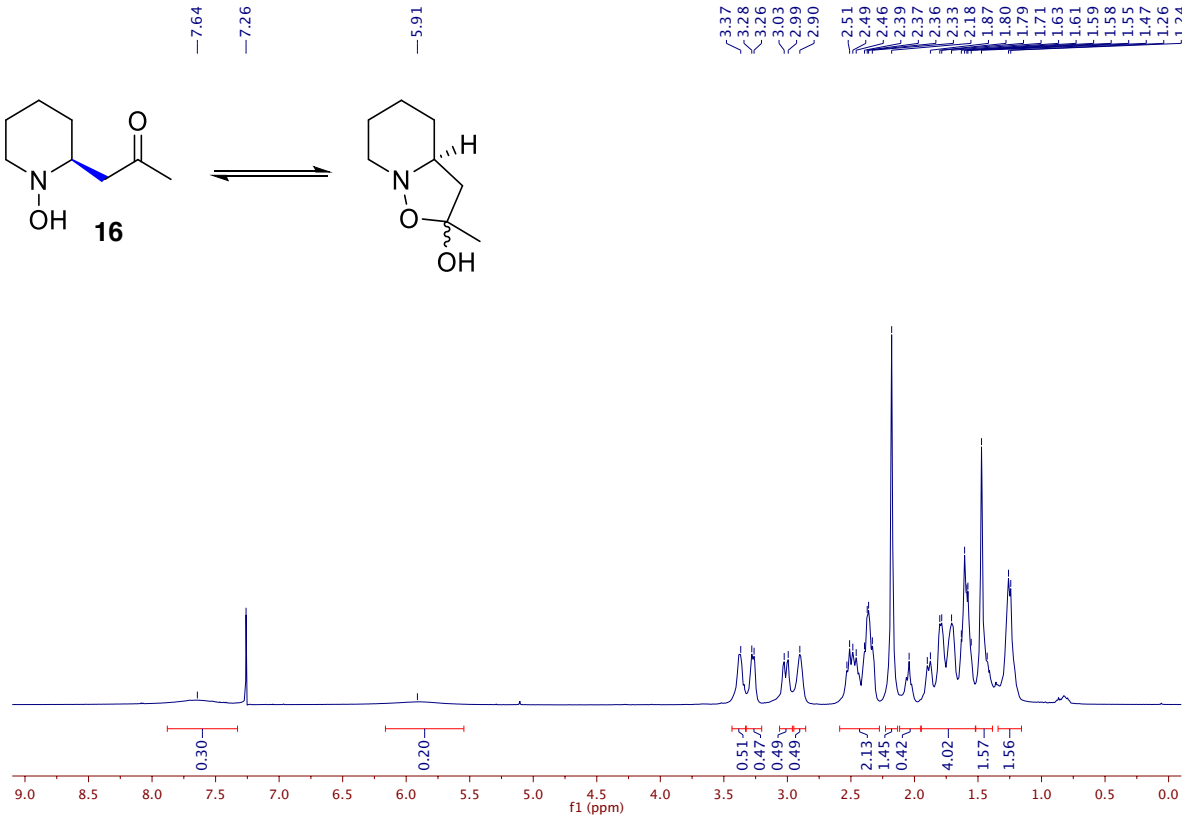
7.64
7.26
5.91
3.37
3.28
3.26
3.03
2.99
2.90
2.51
2.49
2.46
2.39
2.37
2.36
2.33
2.18
1.87
1.80
1.79
1.71
1.63
1.61
1.59
1.58
1.55
1.47
1.26
O
N
OH
16
H
N
O
OH
0.30
0.20
0.51
0.47
0.49
0.49
2.13
1.45
0.42
4.02
1.57
1.56
9.0
8.5
8.0
7.5
7.0
6.5
6.0
5.5
5.0
4.5
4.0
3.5
3.0
2.5
2.0
1.5
1.0
0.5
0.0
f1 (ppm)

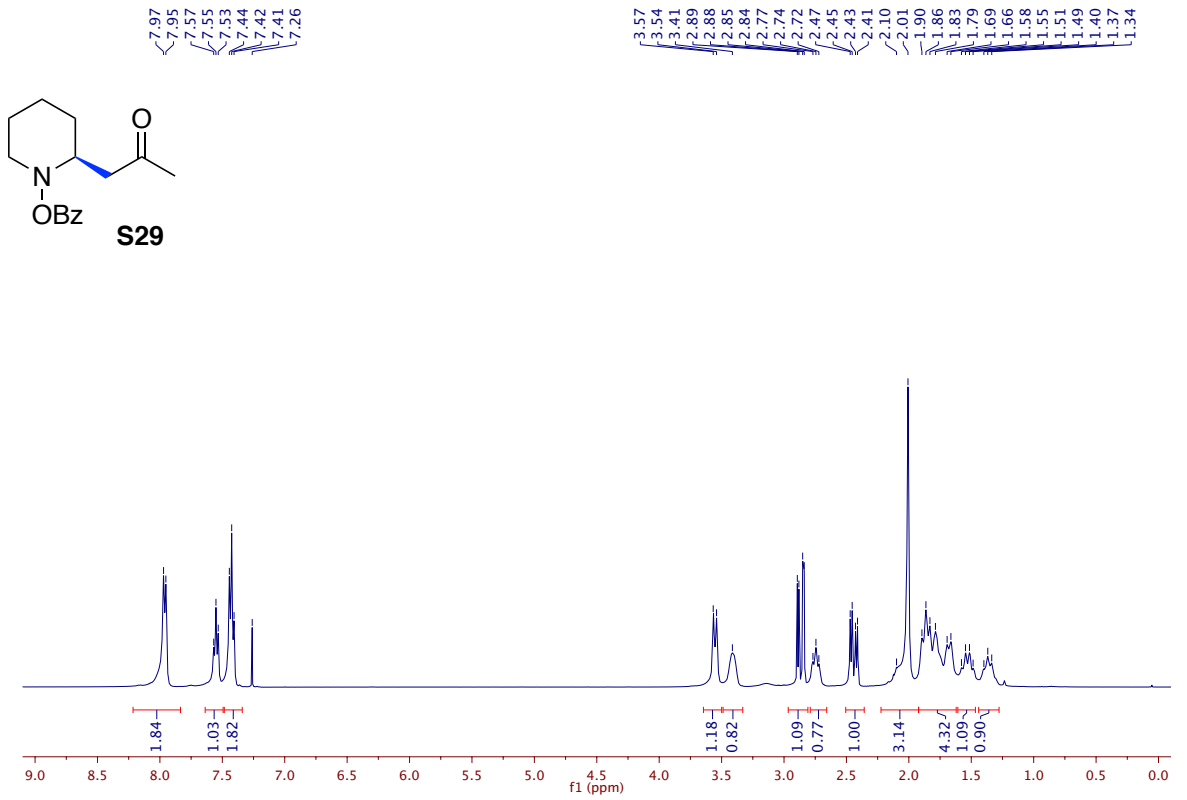
7.97
7.95
7.57
7.55
7.53
7.44
7.42
7.41
7.26
3.57
3.54
3.41
2.89
2.88
2.85
2.84
2.77
2.74
2.72
2.47
2.45
2.43
2.41
2.10
2.01
1.90
1.86
1.83
1.79
1.69
1.66
1.58
1.55
1.51
1.49
1.40
1.37
1.34
O
N
OBz
S29
1.84
1.03
1.82
1.18
0.82
1.09
0.77
1.00
3.14
4.32
1.09
0.90
9.0
8.5
8.0
7.5
7.0
6.5
6.0
5.5
5.0
4.5
4.0
3.5
3.0
2.5
2.0
1.5
1.0
0.5
0.0
f1 (ppm)

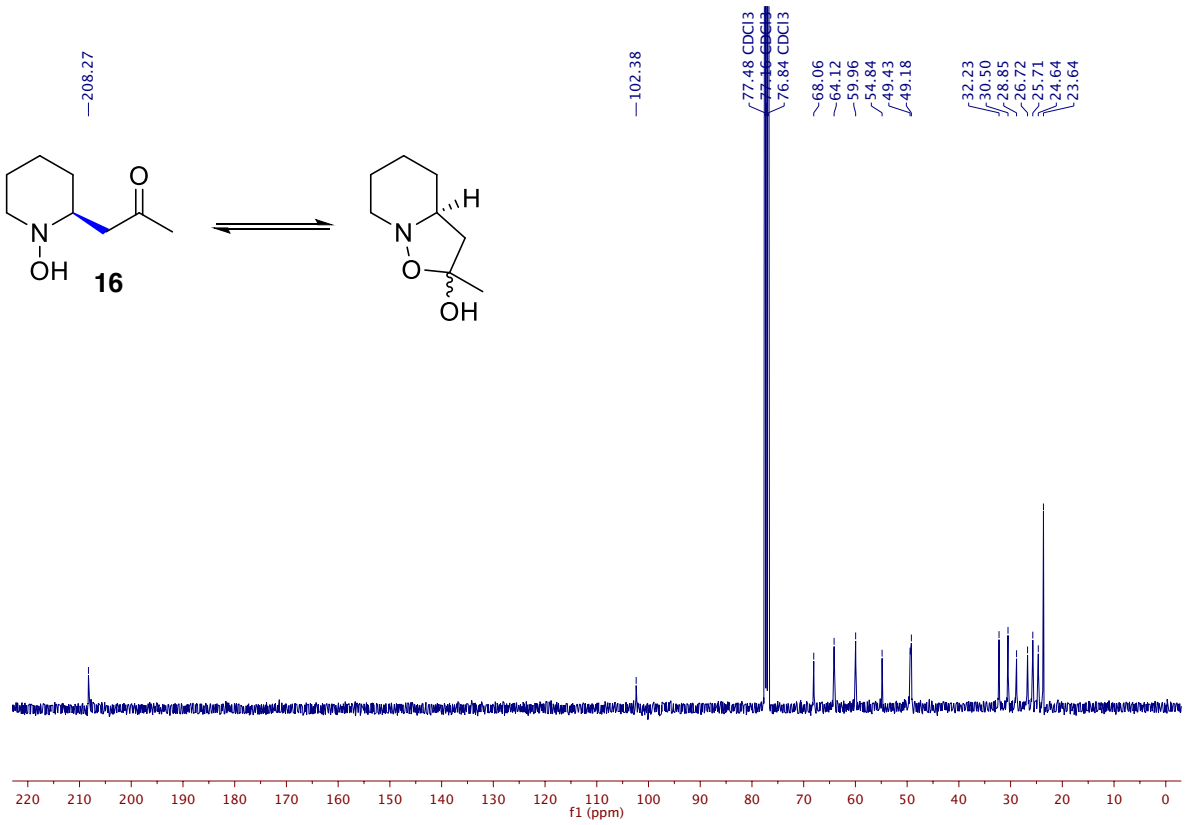
208.27
102.38
77.48 CDCl3
77.16 CDCl3
76.84 CDCl3
68.06
64.12
59.96
54.84
49.43
49.18
32.23
30.50
28.85
26.72
25.71
24.64
23.64
O
N
OH
16
H
N
O
OH
220 210 200 190 180 170 160 150 140 130 120 110 100 90 80 70 60 50 40 30 20 10 0
f1 (ppm)

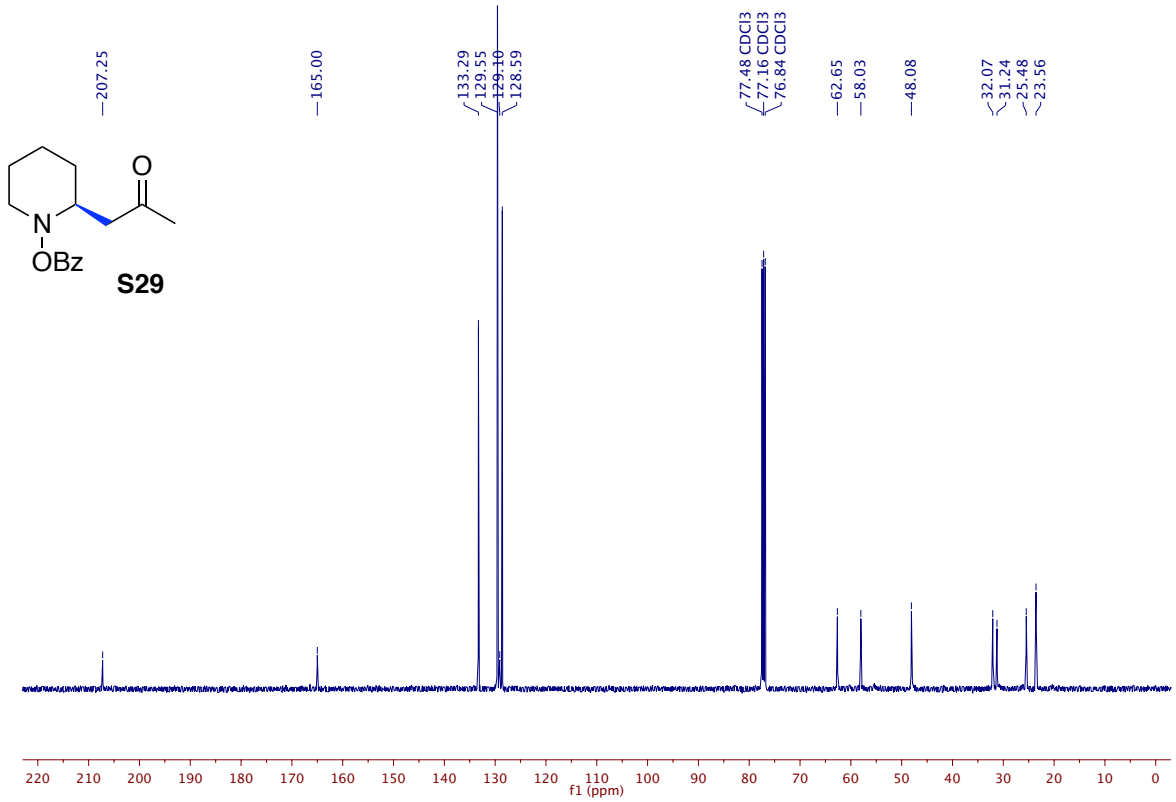
207.25
165.00
133.29
129.55
129.10
128.59
77.48 CDCl3
77.16 CDCl3
76.84 CDCl3
62.65
58.03
48.08
32.07
31.24
25.48
23.56
O
N
OBz
S29
220 210 200 190 180 170 160 150 140 130 120 110 100 90 80 70 60 50 40 30 20 10 0
f1 (ppm)

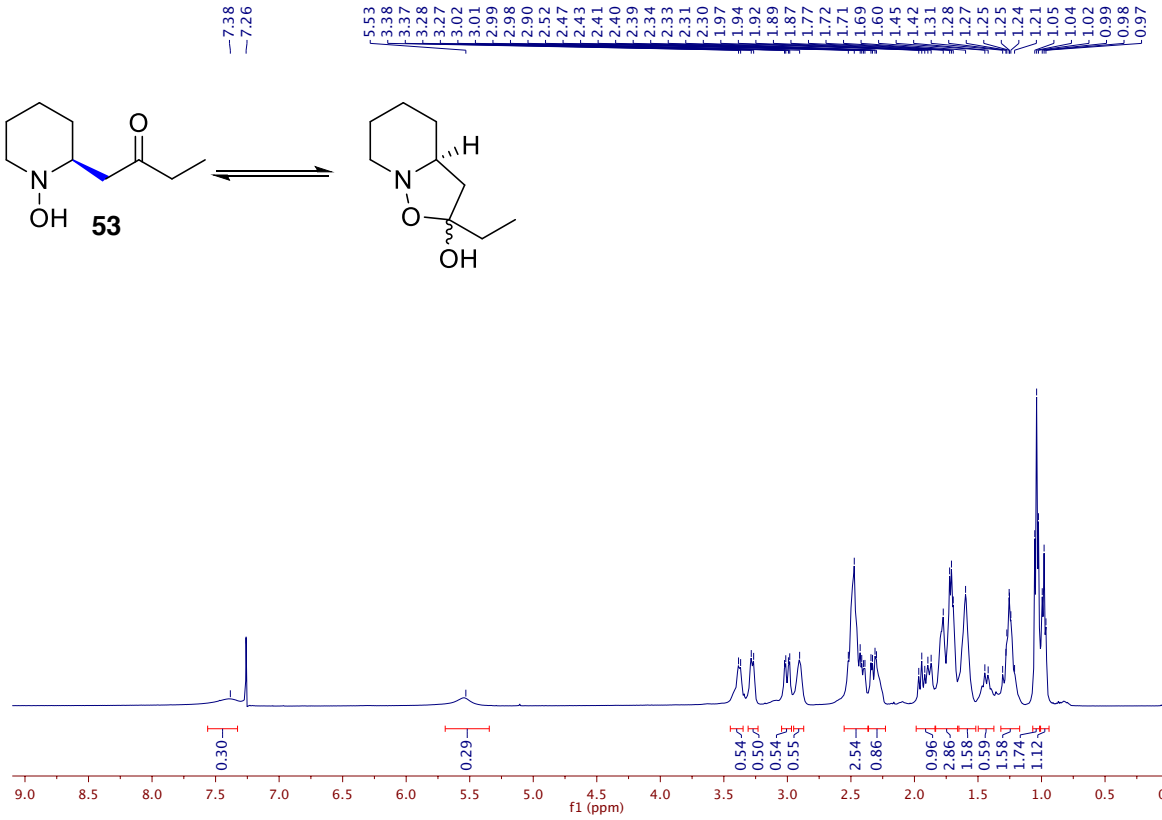
7.38
7.26
5.53
3.38
3.37
3.28
3.27
3.02
3.01
2.99
2.98
2.90
2.52
2.47
2.43
2.41
2.40
2.39
2.34
2.33
2.31
2.30
1.97
1.94
1.92
1.89
1.87
1.77
1.72
1.71
1.69
1.60
1.45
1.42
1.31
1.28
1.27
1.25
1.25
1.24
1.21
1.05
1.04
1.02
0.99
0.98
0.97
O
N
OH
53
H
N
O
OH
0.30
0.29
0.54
0.50
0.54
0.55
2.54
0.86
0.96
2.86
1.58
0.59
1.58
1.74
1.12
9.0
8.5
8.0
7.5
7.0
6.5
6.0
5.5
5.0
4.5
4.0
3.5
3.0
2.5
2.0
1.5
1.0
0.5
0.0
f1 (ppm)

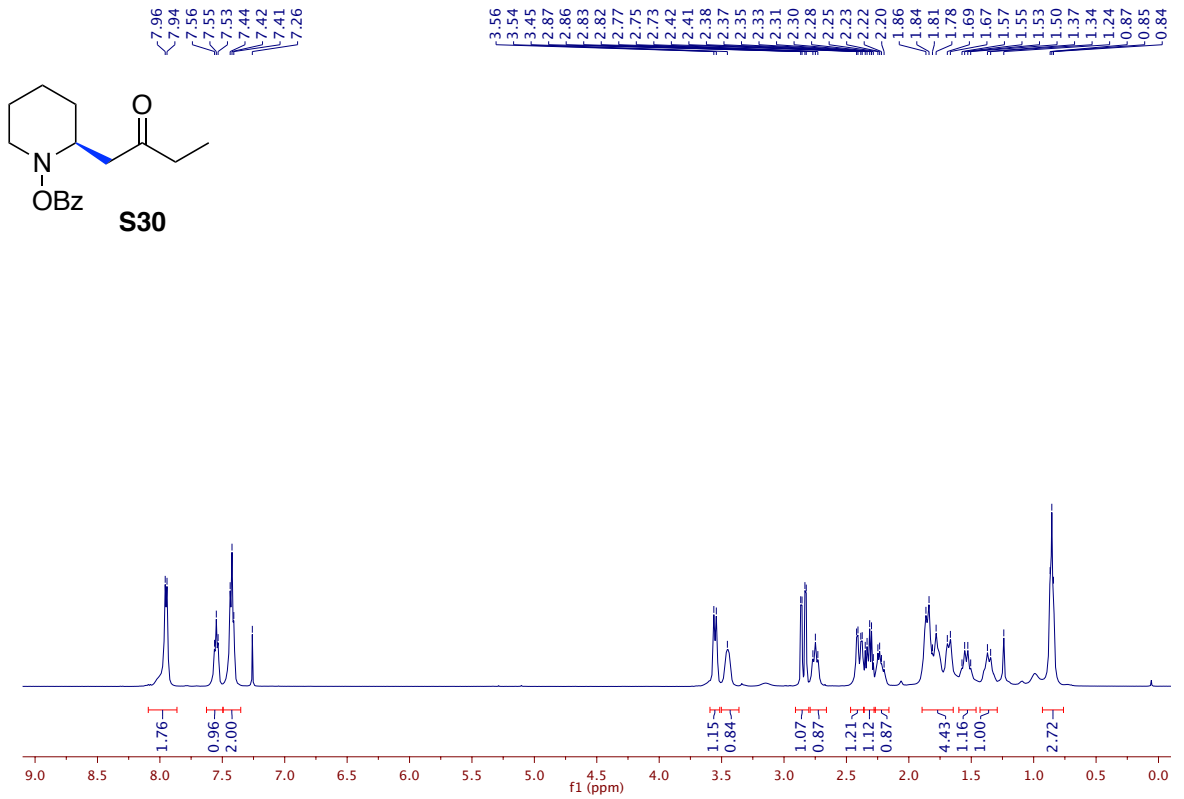
7.96
7.94
7.56
7.55
7.53
7.44
7.42
7.41
7.26
3.56
3.54
3.45
2.87
2.86
2.83
2.82
2.77
2.75
2.73
2.42
2.41
2.38
2.37
2.35
2.33
2.31
2.30
2.28
2.25
2.23
2.22
2.20
1.86
1.84
1.81
1.78
1.69
1.67
1.57
1.55
1.53
1.50
1.37
1.34
1.24
0.87
0.85
0.84
O
N
OBz
S30
1.76
0.96
2.00
1.15
0.84
1.07
0.87
1.21
1.12
0.87
4.43
1.16
1.00
2.72
9.0
8.5
8.0
7.5
7.0
6.5
6.0
5.5
5.0
4.5
4.0
3.5
3.0
2.5
2.0
1.5
1.0
0.5
0.0
f1 (ppm)

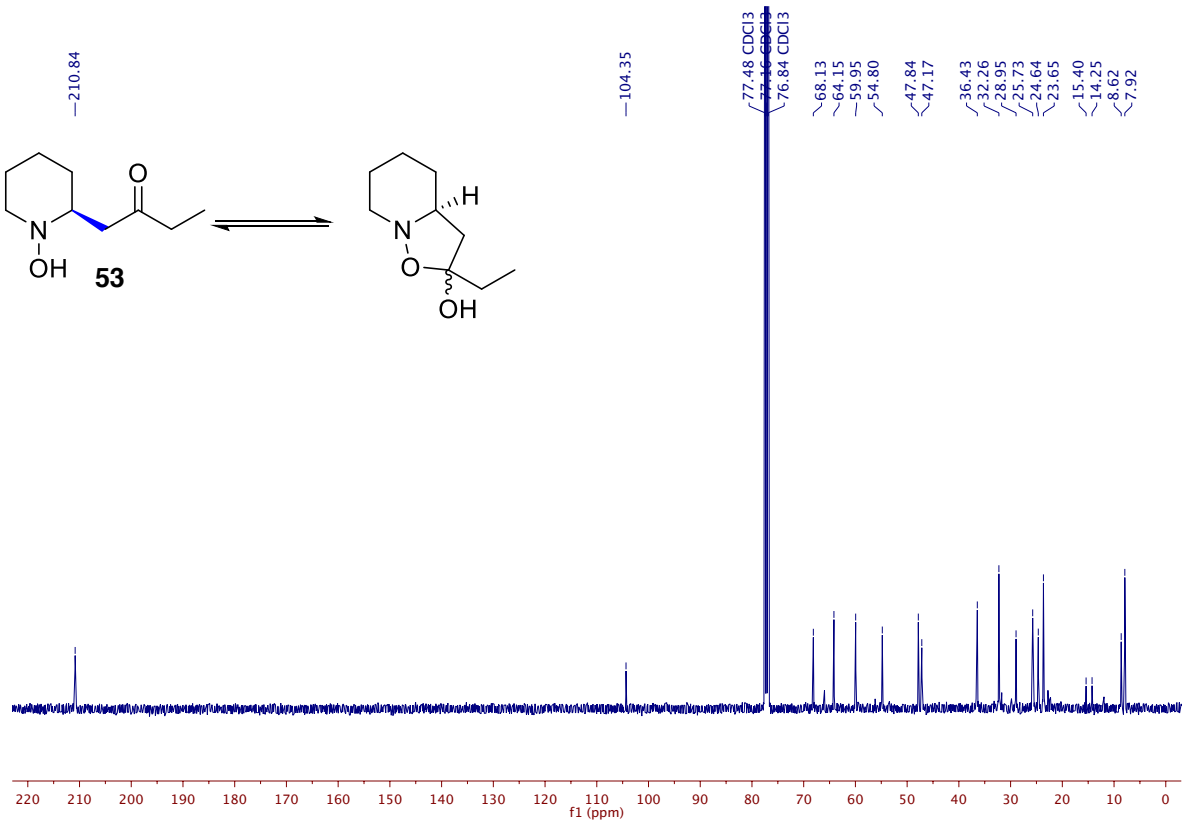
210.84
104.35
77.48 CDCl3
77.16 CDCl3
76.84 CDCl3
68.13
64.15
59.95
54.80
47.84
47.17
36.43
32.26
28.95
25.73
24.64
23.65
15.40
14.25
8.62
7.92
O
N
OH
53
H
N
O
OH
f1 (ppm)

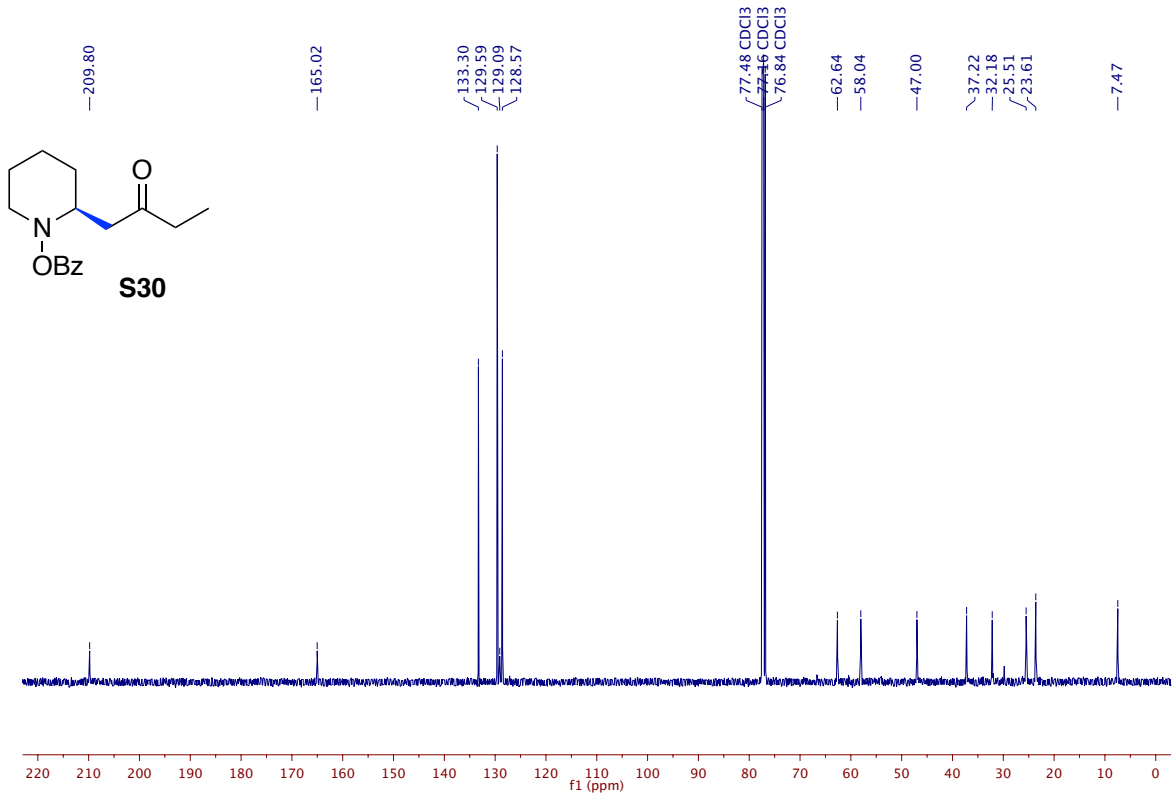
209.80
165.02
133.30
129.59
129.09
128.57
77.48 CDCl3
77.16 CDCl3
76.84 CDCl3
62.64
58.04
47.00
37.22
32.18
25.51
23.61
7.47
O
N
OBz
S30
f1 (ppm)

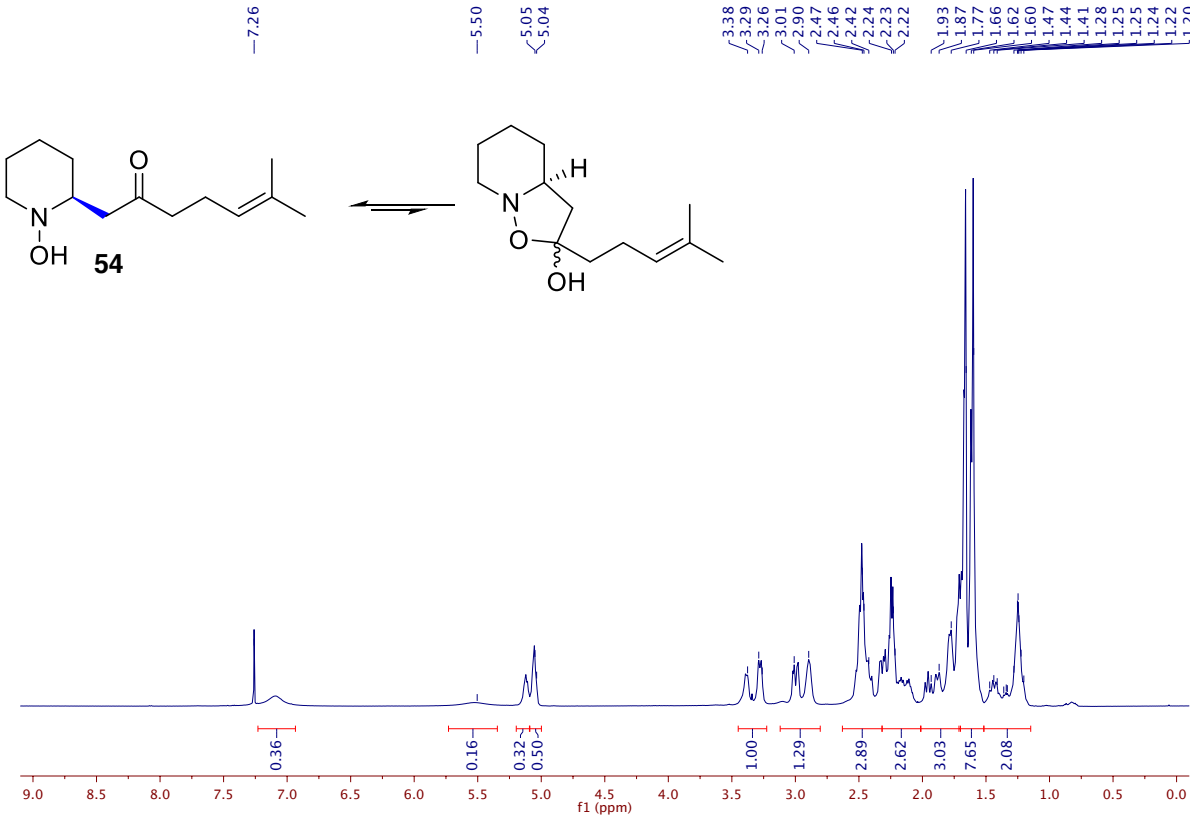
7.26
5.50
5.05
5.04
3.38
3.29
3.26
3.01
2.90
2.47
2.46
2.42
2.24
2.23
2.22
1.93
1.87
1.77
1.66
1.62
1.60
1.47
1.44
1.41
1.28
1.25
1.25
1.24
1.22
O
N
OH
54
H
N
O
OH
0.36
0.16
0.32
0.50
1.00
1.29
2.89
2.62
3.03
7.65
2.08
9.0
8.5
8.0
7.5
7.0
6.5
6.0
5.5
5.0
4.5
4.0
3.5
3.0
2.5
2.0
1.5
1.0
0.5
0.0
f1 (ppm)

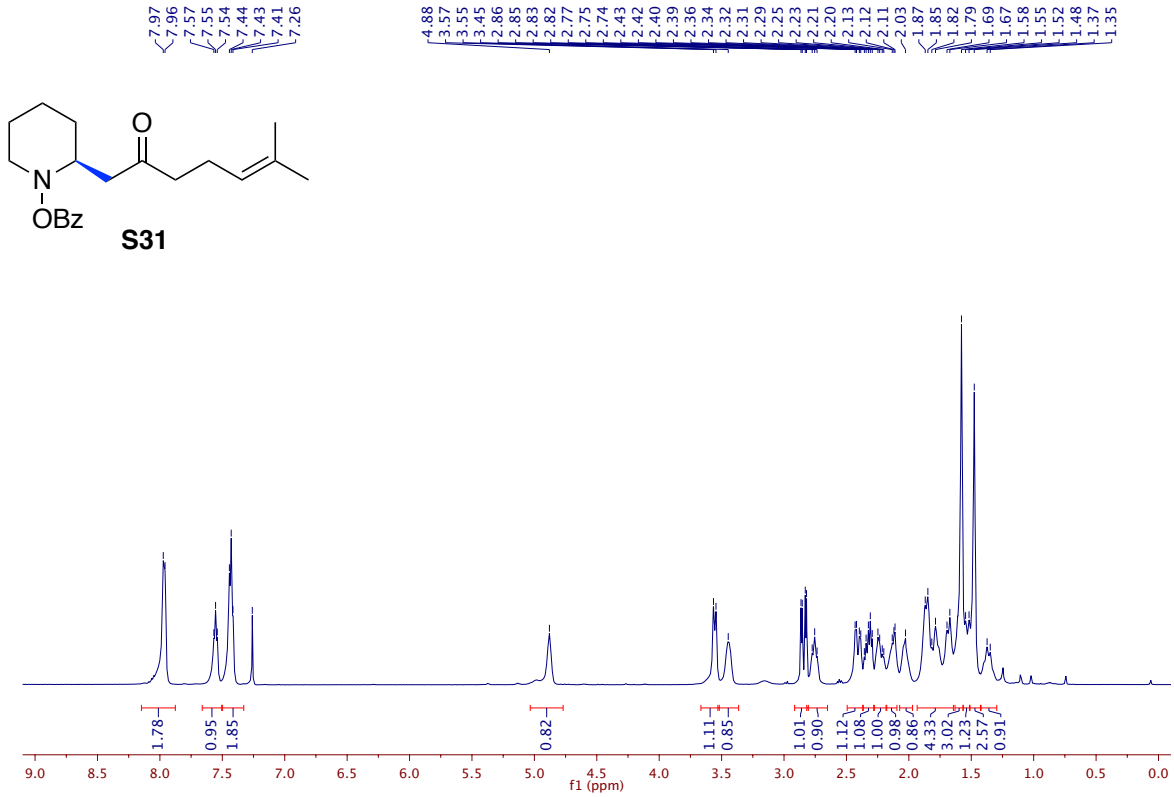
7.97
7.96
7.57
7.55
7.54
7.44
7.43
7.41
7.26
4.88
3.57
3.55
3.45
2.86
2.85
2.83
2.82
2.77
2.75
2.74
2.43
2.42
2.40
2.39
2.36
2.34
2.32
2.31
2.29
2.25
2.23
2.21
2.20
2.13
2.12
2.11
2.03
1.87
1.85
1.82
1.79
1.69
1.67
1.58
1.55
1.52
1.48
1.37
1.35
O
N
OBz
S31
1.78
0.95
1.85
0.82
1.11
0.85
1.01
0.90
1.12
1.08
1.00
0.98
0.86
4.33
3.02
1.23
2.57
0.91
9.0
8.5
8.0
7.5
7.0
6.5
6.0
5.5
5.0
4.5
4.0
3.5
3.0
2.5
2.0
1.5
1.0
0.5
0.0
f1 (ppm)

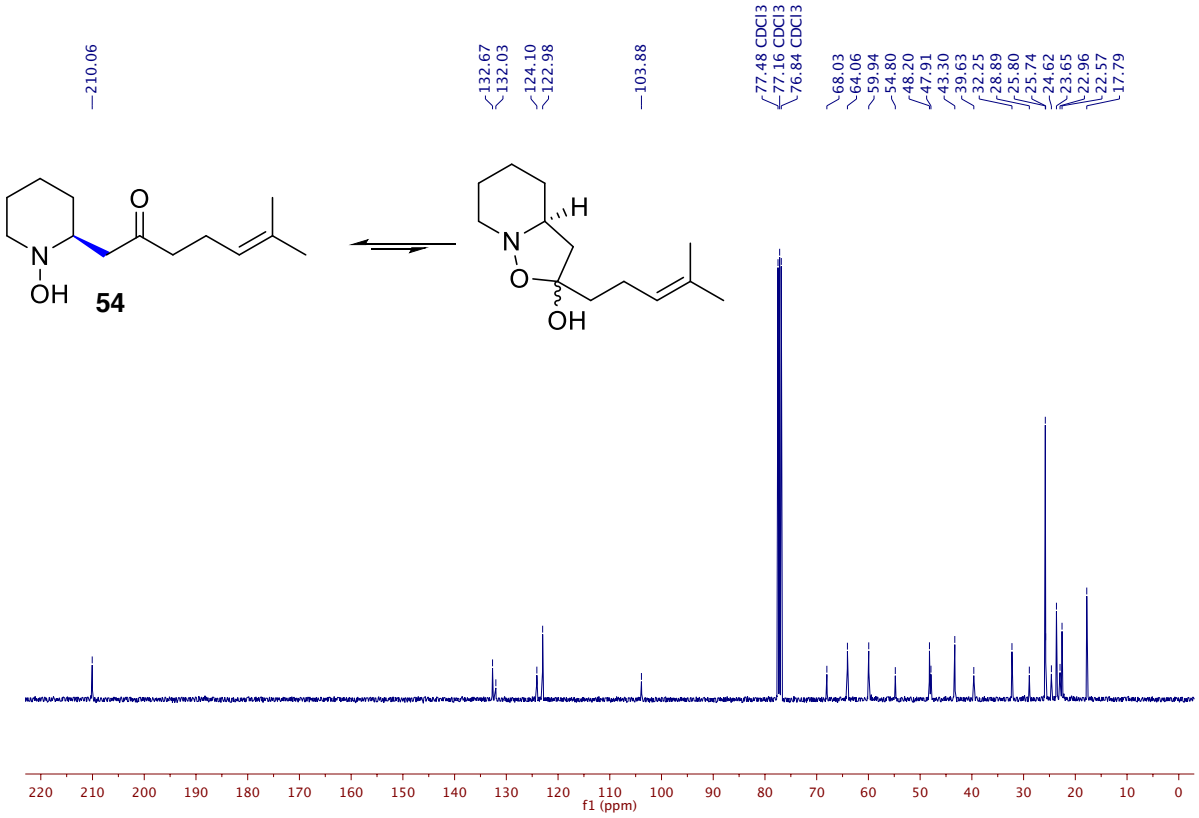
210.06
132.67
132.03
124.10
122.98
103.88
77.48 CDCl3
77.16 CDCl3
76.84 CDCl3
68.03
64.06
59.94
54.80
48.20
47.91
43.30
39.63
32.25
28.89
25.80
25.74
24.62
23.65
22.96
22.57
17.79
O
N
OH
54
H
N
O
OH
220 210 200 190 180 170 160 150 140 130 120 110 100 90 80 70 60 50 40 30 20 10 0
f1 (ppm)

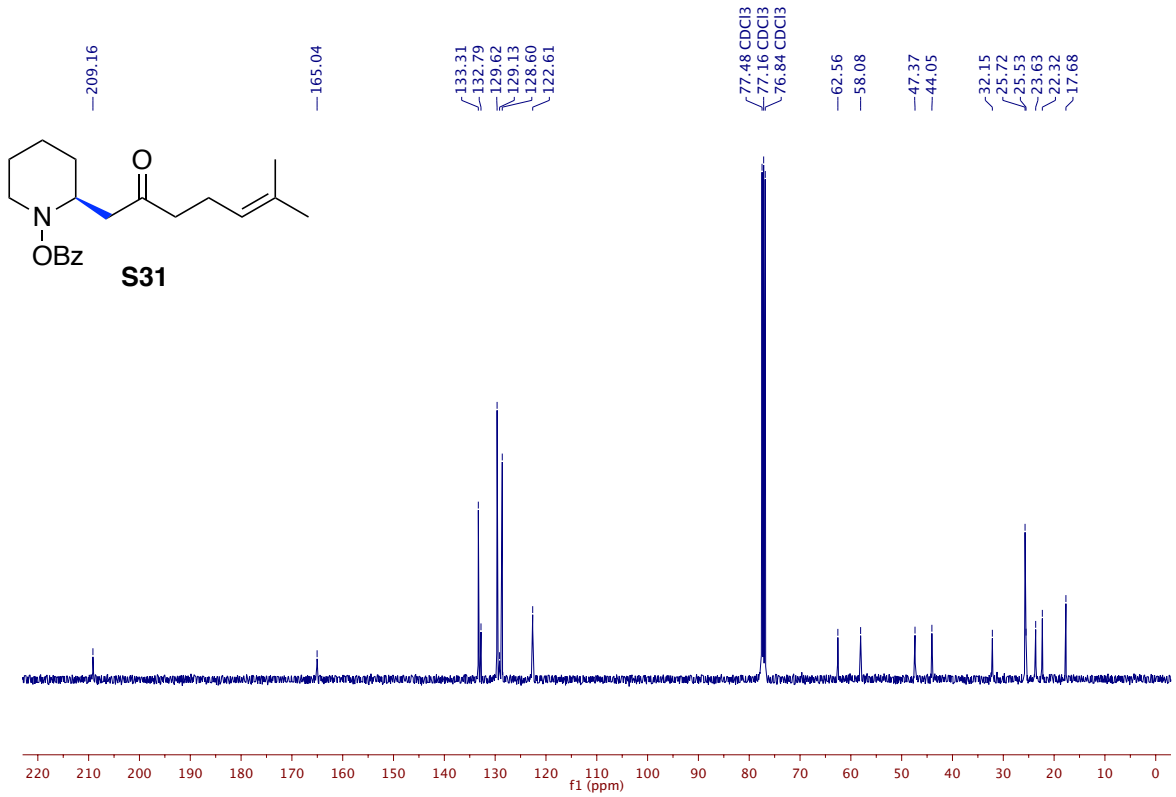
209.16
165.04
133.31
132.79
129.62
129.13
128.60
122.61
77.48 CDCl3
77.16 CDCl3
76.84 CDCl3
62.56
58.08
47.37
44.05
32.15
25.72
25.53
23.63
22.32
17.68
O
N
OBz
S31
220 210 200 190 180 170 160 150 140 130 120 110 100 90 80 70 60 50 40 30 20 10 0
f1 (ppm)

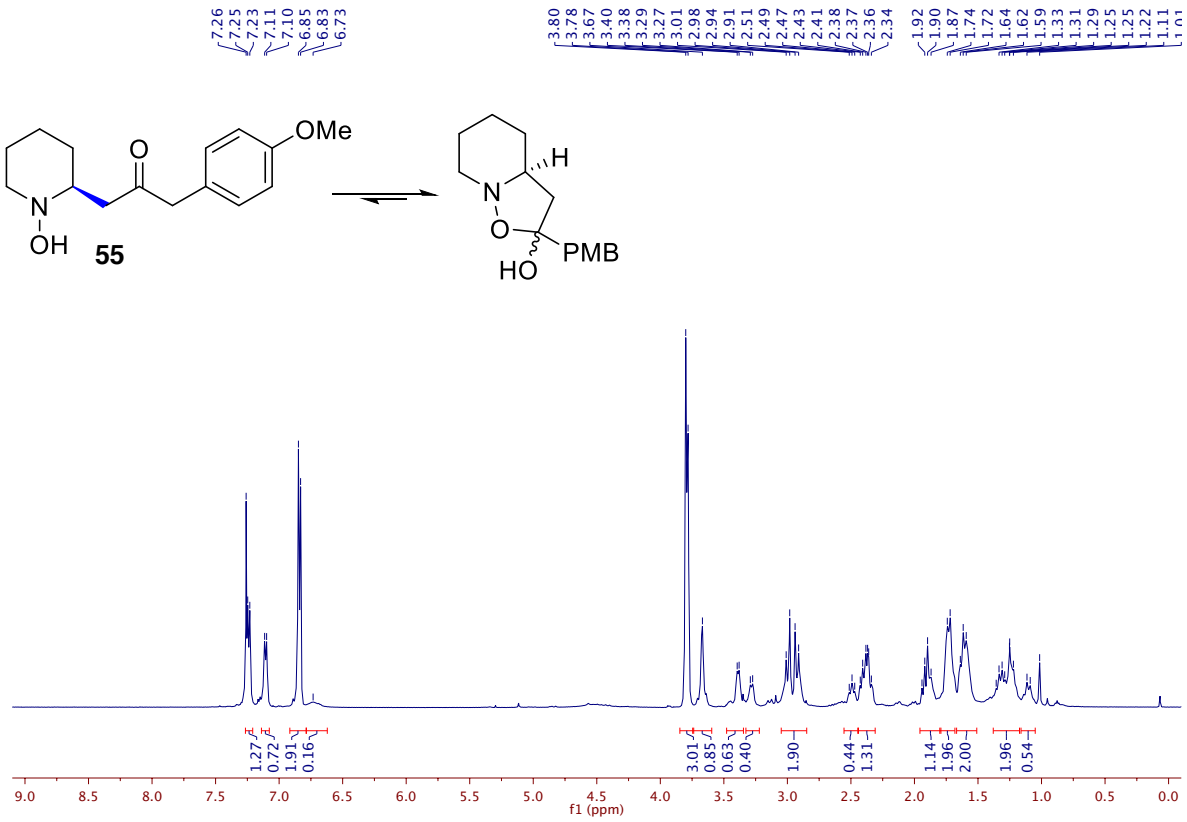
OMe
O
N
OH
55
H
N
O
HO
PMB
f1 (ppm)

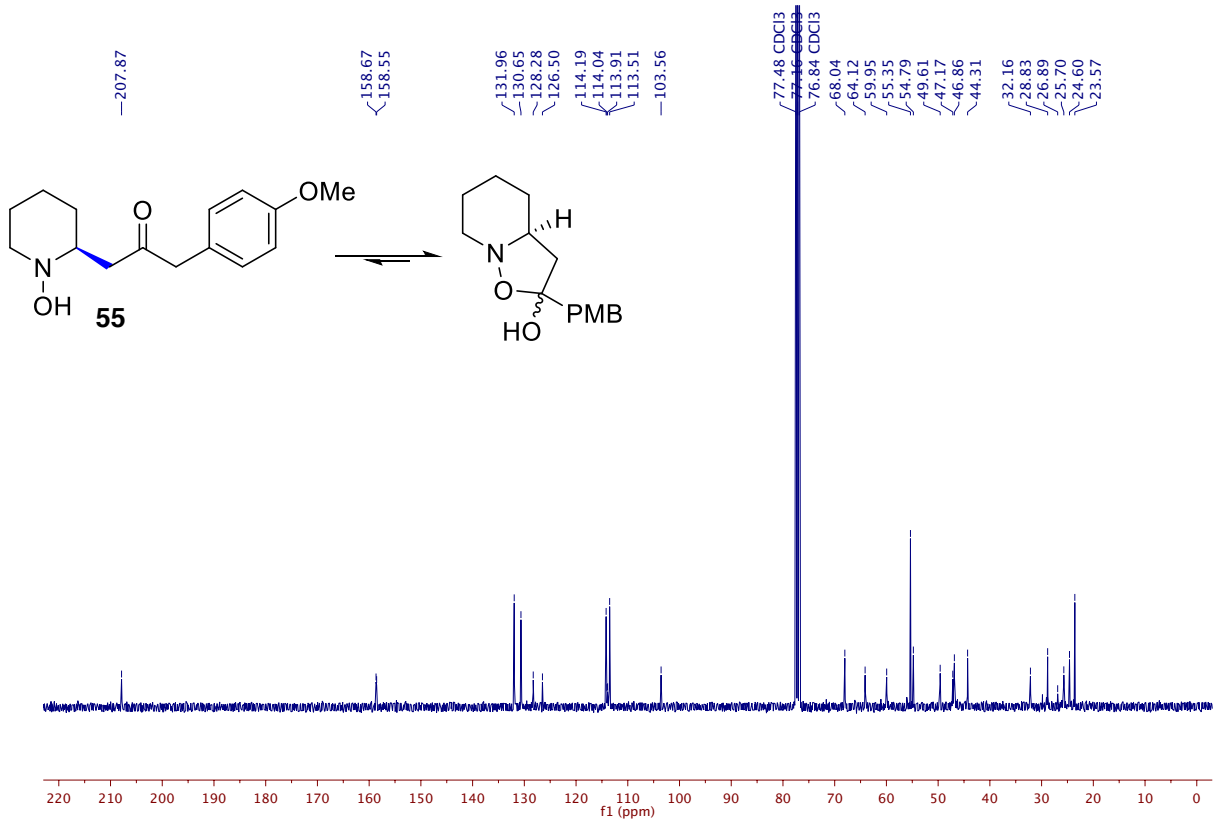
OMe
O
N
OH
55
H
N
O
HO
PMB
f1 (ppm)

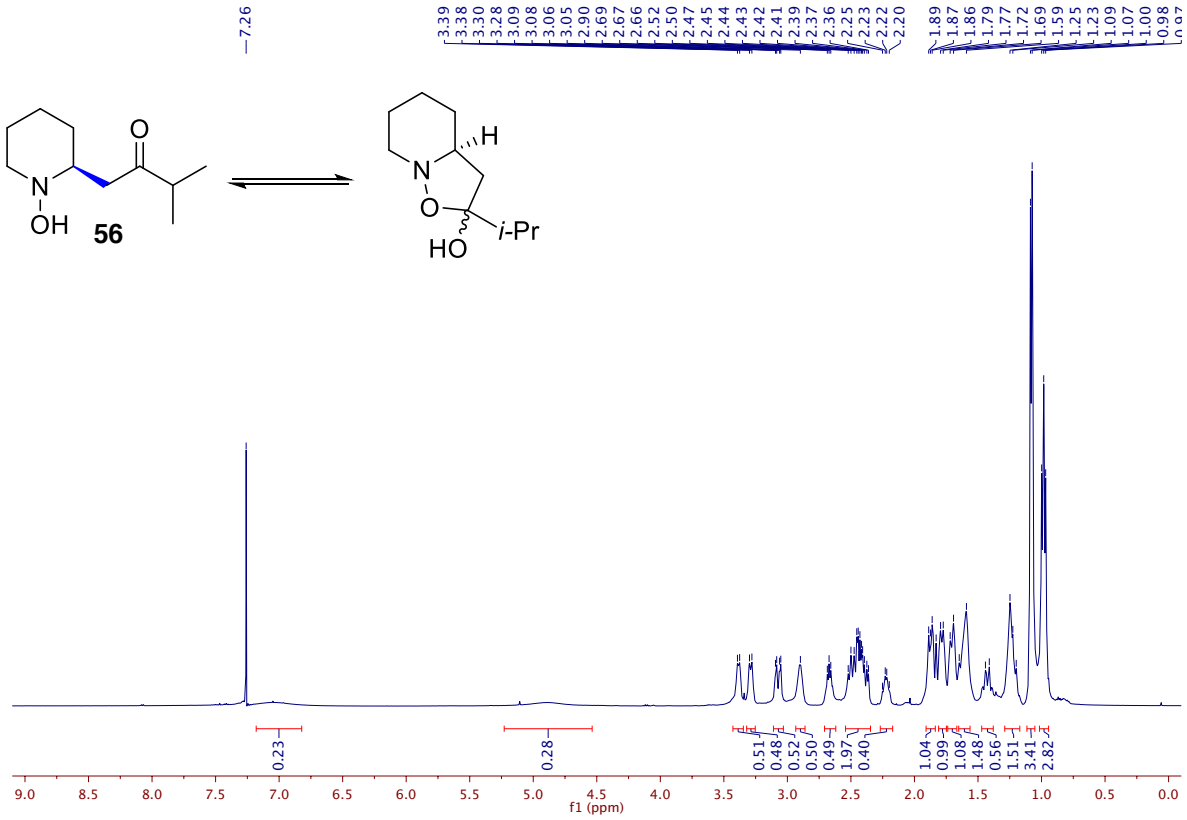
7.26
3.39
3.38
3.30
3.28
3.09
3.08
3.06
3.05
2.90
2.69
2.67
2.66
2.52
2.50
2.47
2.45
2.44
2.43
2.42
2.41
2.39
2.37
2.36
2.25
2.23
2.22
2.20
1.89
1.87
1.86
1.79
1.77
1.72
1.69
1.59
1.25
1.23
1.09
1.07
1.00
0.98
O
N
OH
56
H
N
O
HO
i-Pr
0.23
0.28
0.51
0.48
0.52
0.50
0.49
1.97
0.40
1.04
0.99
1.08
1.48
0.56
1.51
3.41
2.82
9.0
8.5
8.0
7.5
7.0
6.5
6.0
5.5
5.0
4.5
4.0
3.5
3.0
2.5
2.0
1.5
1.0
0.5
0.0
f1 (ppm)

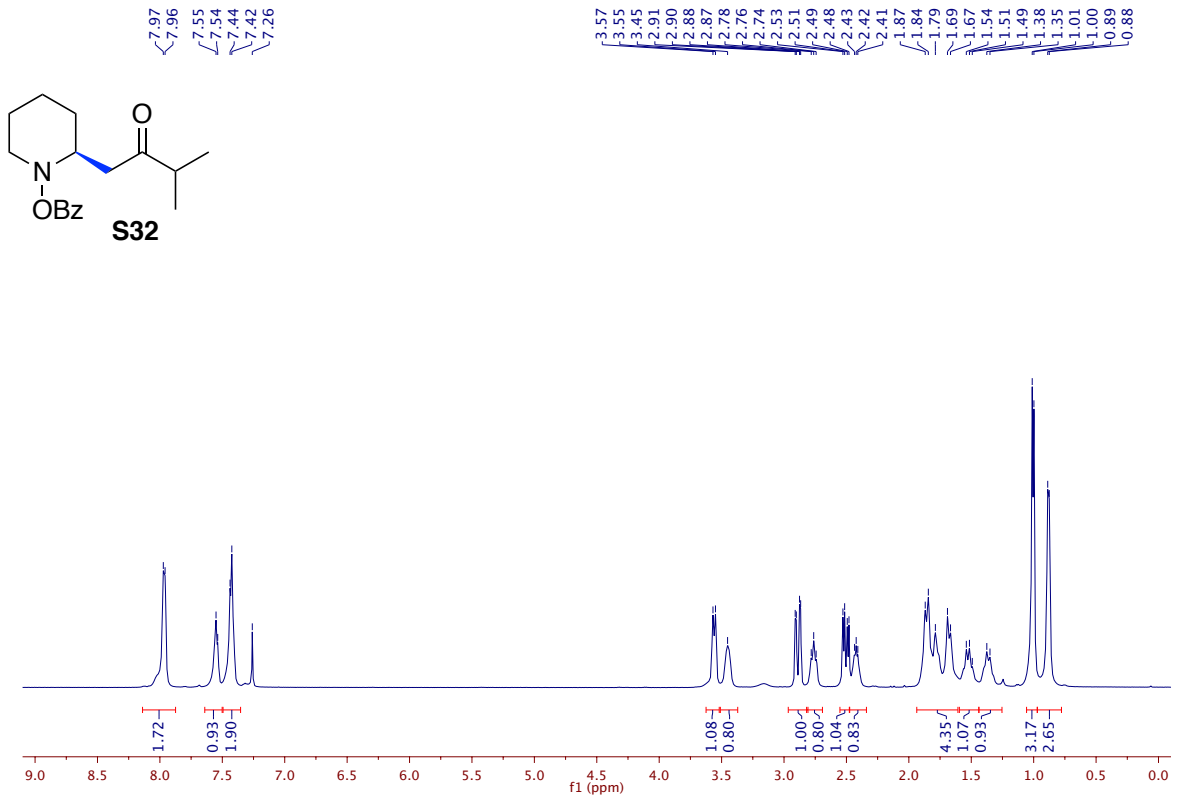
7.97
7.96
7.55
7.54
7.44
7.42
7.26
3.57
3.55
3.45
2.91
2.90
2.88
2.87
2.78
2.76
2.74
2.53
2.51
2.49
2.48
2.43
2.42
2.41
1.87
1.84
1.79
1.69
1.67
1.54
1.51
1.49
1.38
1.35
1.01
1.00
0.89
0.88
O
N
OBz
S32
1.72
0.93
1.90
1.08
0.80
1.00
0.80
1.04
0.83
4.35
1.07
0.93
3.17
2.65
9.0
8.5
8.0
7.5
7.0
6.5
6.0
5.5
5.0
4.5
4.0
3.5
3.0
2.5
2.0
1.5
1.0
0.5
0.0
f1 (ppm)

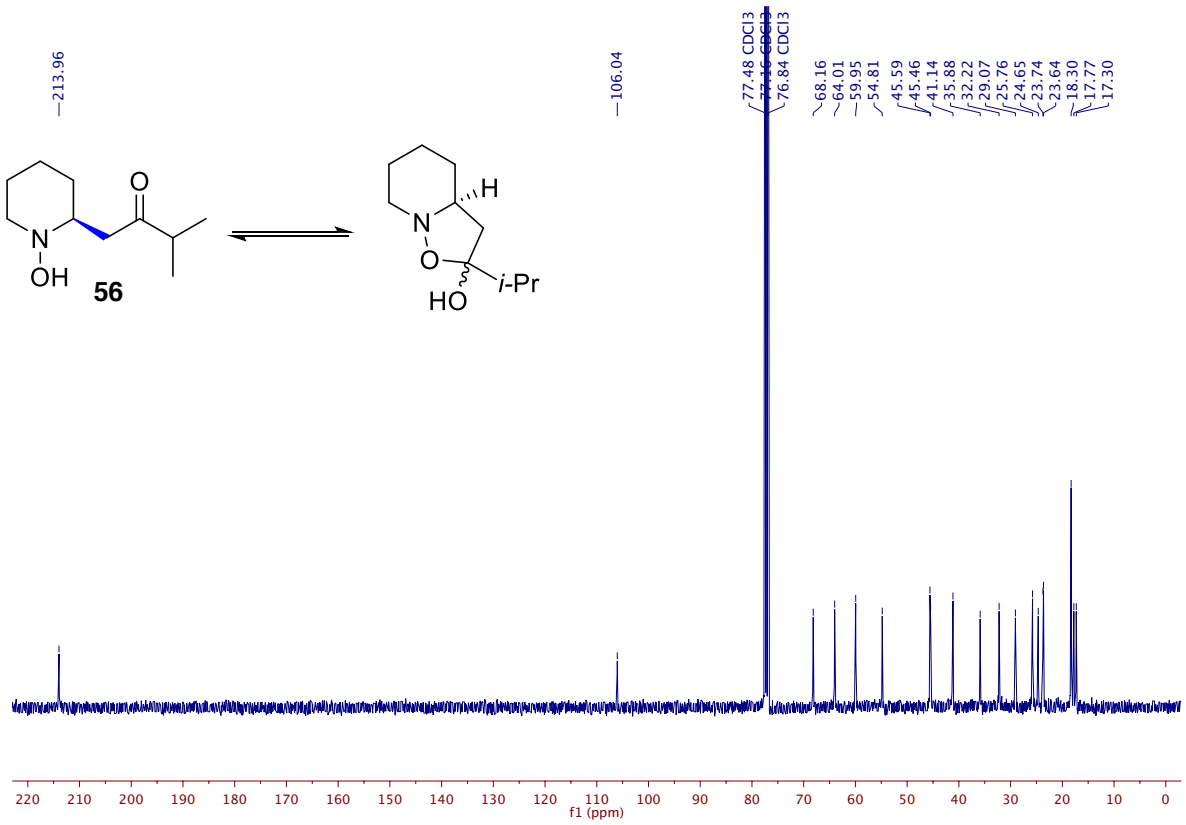
213.96
106.04
77.48 CDCl3
77.16 CDCl3
76.84 CDCl3
68.16
64.01
59.95
54.81
45.59
45.46
41.14
35.88
32.22
29.07
25.76
24.65
23.74
23.64
18.30
17.77
17.30
O
N
OH
56
H
N
O
HO
i-Pr
220 210 200 190 180 170 160 150 140 130 120 110 100 90 80 70 60 50 40 30 20 10 0
f1 (ppm)

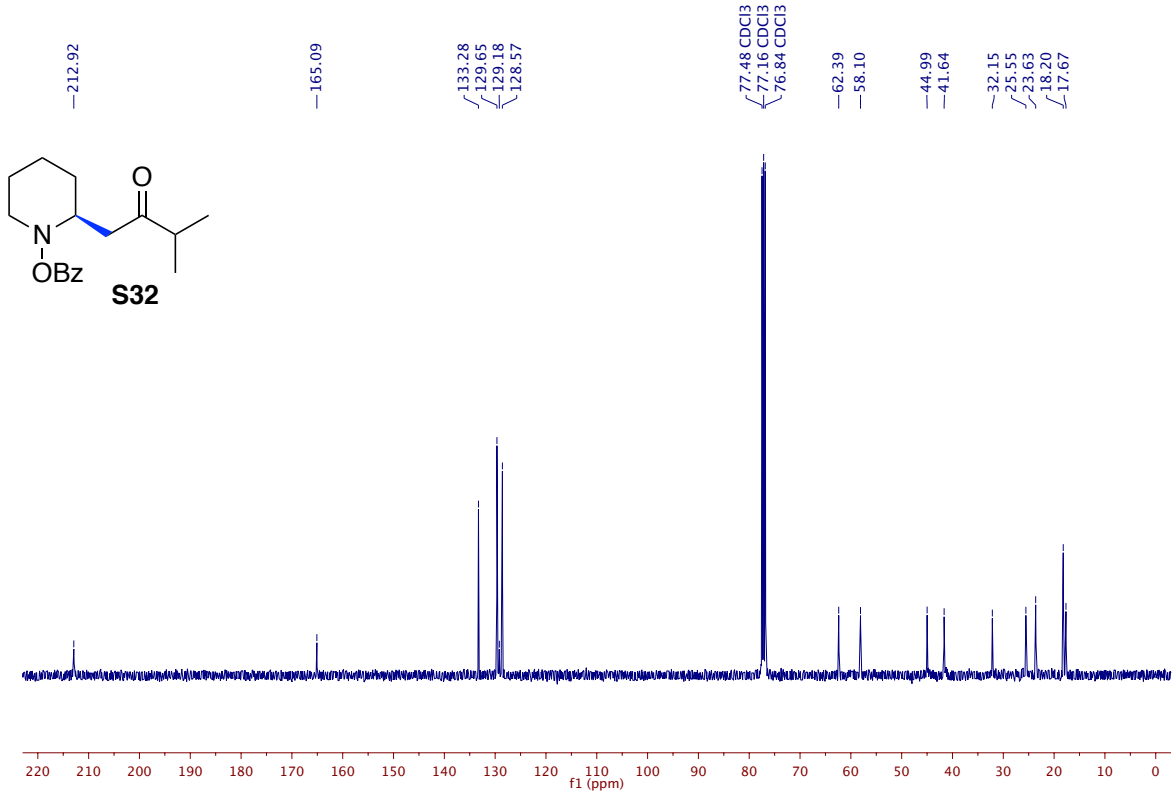
212.92
165.09
133.28
129.65
129.18
128.57
77.48 CDCl3
77.16 CDCl3
76.84 CDCl3
62.39
58.10
44.99
41.64
32.15
25.55
23.63
18.20
17.67
O
N
OBz
S32
220 210 200 190 180 170 160 150 140 130 120 110 100 90 80 70 60 50 40 30 20 10 0
f1 (ppm)

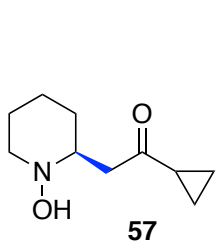
O
N
OH

57

7.26
3.31
3.29
3.20
3.19
3.17
3.16
2.92
2.55
2.53
2.50
2.49
2.47
2.46
2.00
1.99
1.98
1.97
1.95
1.82
1.80
1.73
1.71
1.61
1.56
1.28
1.27
1.25
1.03
1.02
1.01
0.88
0.87
0.86
0.86
0.57
1.00
1.04
1.03
2.01
1.01
1.02
1.06
2.08
2.06
2.17
2.25
9.0
8.5
8.0
7.5
7.0
6.5
6.0
5.5
5.0
4.5
4.0
3.5
3.0
2.5
2.0
1.5
1.0
0.5
0.0
f1 (ppm)


7.99
7.98
7.57
7.56
7.54
7.45
7.43
7.42
7.26
3.57
3.55
3.44
3.02
3.01
2.98
2.97
2.79
2.77
2.75
2.58
2.56
2.54
2.53
1.90
1.88
1.86
1.83
1.79
1.70
1.68
1.58
1.55
1.37
0.92
0.85
0.78
0.77
0.62

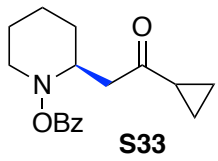
O
N
OBz

S33

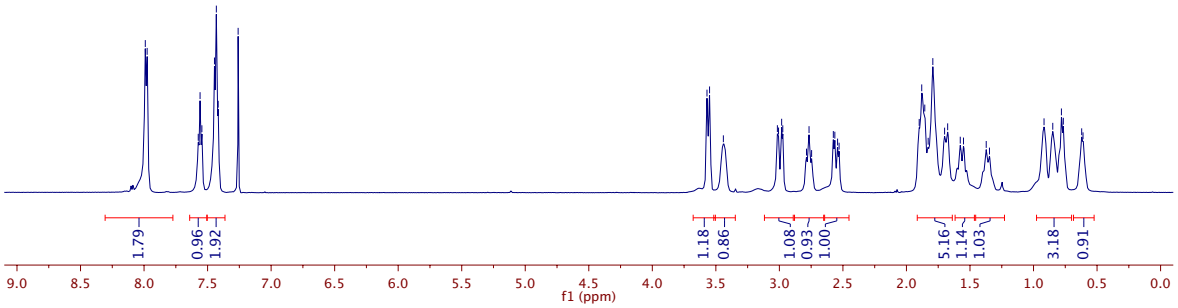
1.79
0.96
1.92
1.18
0.86
1.08
0.93
1.00
5.16
1.14
1.03
3.18
0.91
9.0
8.5
8.0
7.5
7.0
6.5
6.0
5.5
5.0
4.5
4.0
3.5
3.0
2.5
2.0
1.5
1.0
0.5
0.0
f1 (ppm)

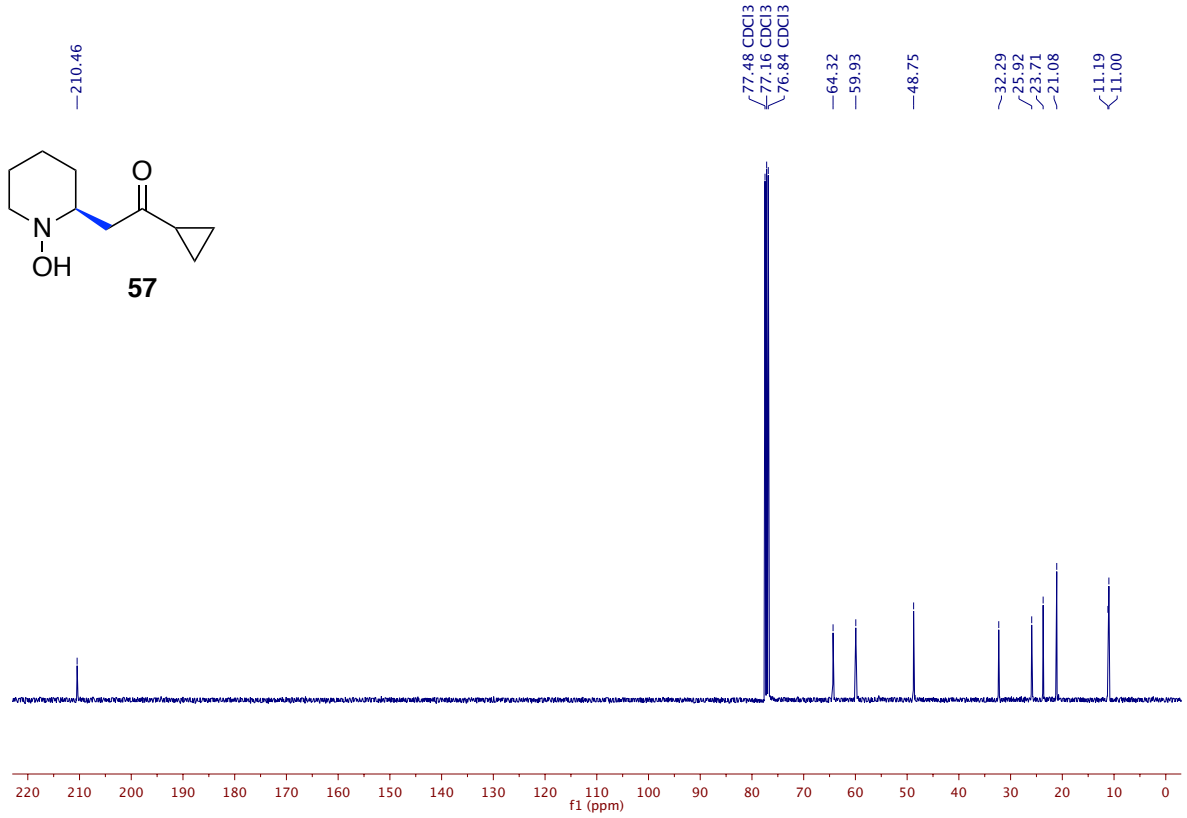
210.46
77.48 CDCl3
77.16 CDCl3
76.84 CDCl3
64.32
59.93
48.75
32.29
25.92
23.71
21.08
11.19
11.00
O
N
OH
57
220 210 200 190 180 170 160 150 140 130 120 110 100 90 80 70 60 50 40 30 20 10 0
f1 (ppm)

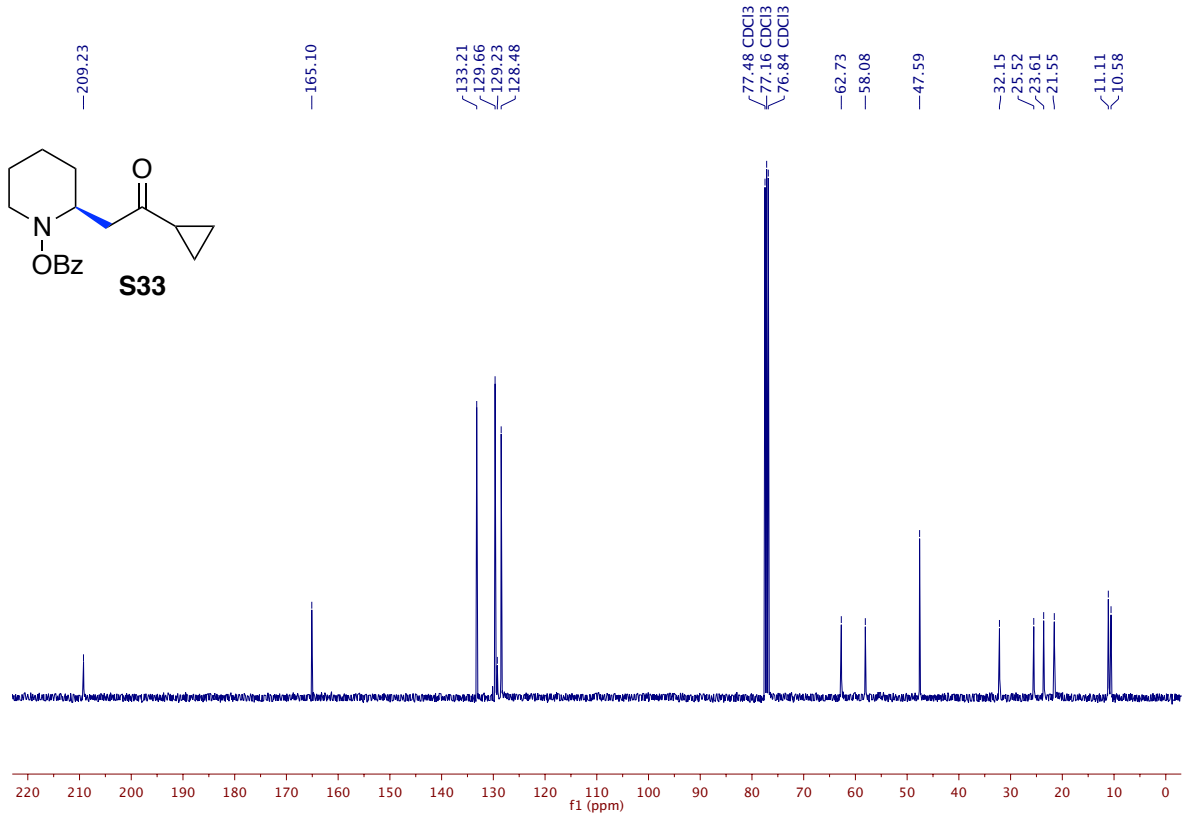
209.23
165.10
133.21
129.66
129.23
128.48
77.48 CDCl3
77.16 CDCl3
76.84 CDCl3
62.73
58.08
47.59
32.15
25.52
23.61
21.55
11.11
10.58
O
N
OBz
S33
220 210 200 190 180 170 160 150 140 130 120 110 100 90 80 70 60 50 40 30 20 10 0
f1 (ppm)

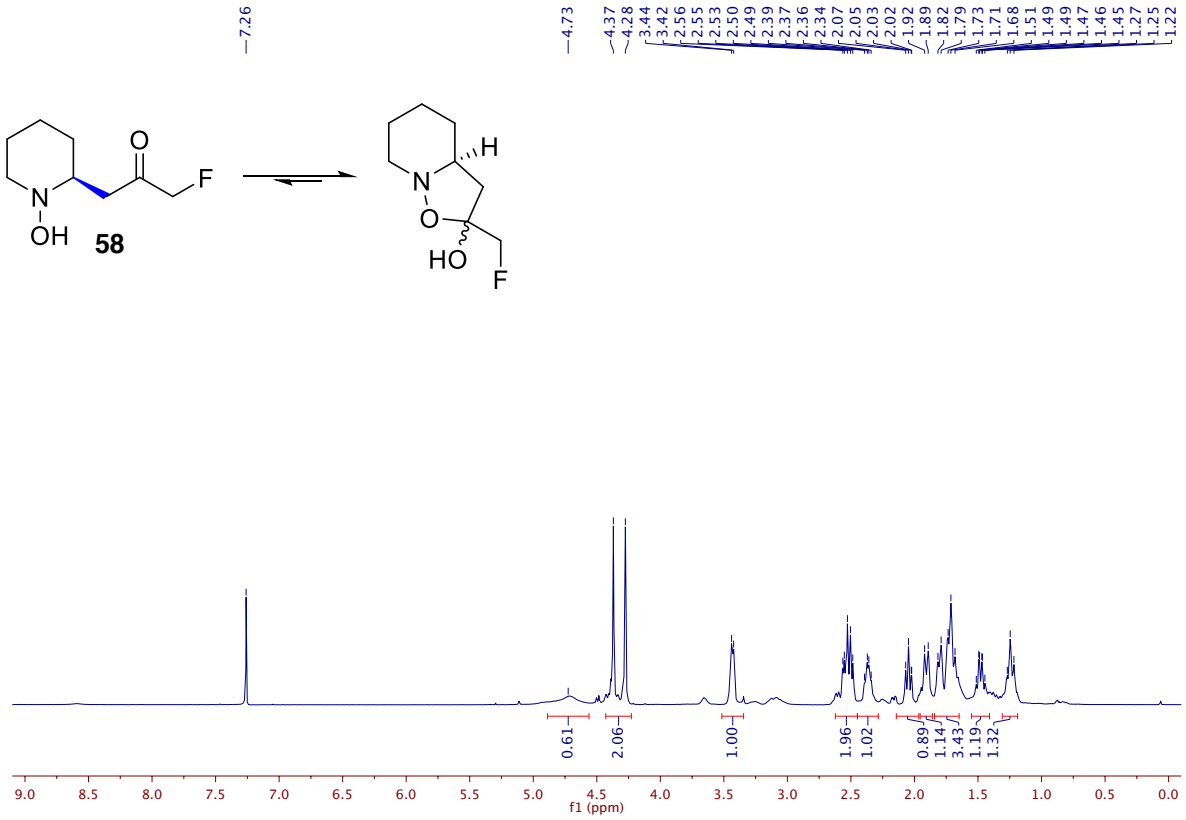
7.26
4.73
4.37
4.28
3.44
3.42
3.42
2.56
2.55
2.53
2.50
2.49
2.39
2.37
2.36
2.34
2.07
2.05
2.03
2.02
1.92
1.89
1.82
1.79
1.73
1.71
1.68
1.51
1.49
1.49
1.47
1.46
1.45
1.27
1.25
1.22
O
F
N
OH
58
H
N
O
HO
F
0.61
2.06
1.00
1.96
1.02
0.89
1.14
3.43
1.19
1.32
9.0
8.5
8.0
7.5
7.0
6.5
6.0
5.5
5.0
4.5
4.0
3.5
3.0
2.5
2.0
1.5
1.0
0.5
0.0
f1 (ppm)

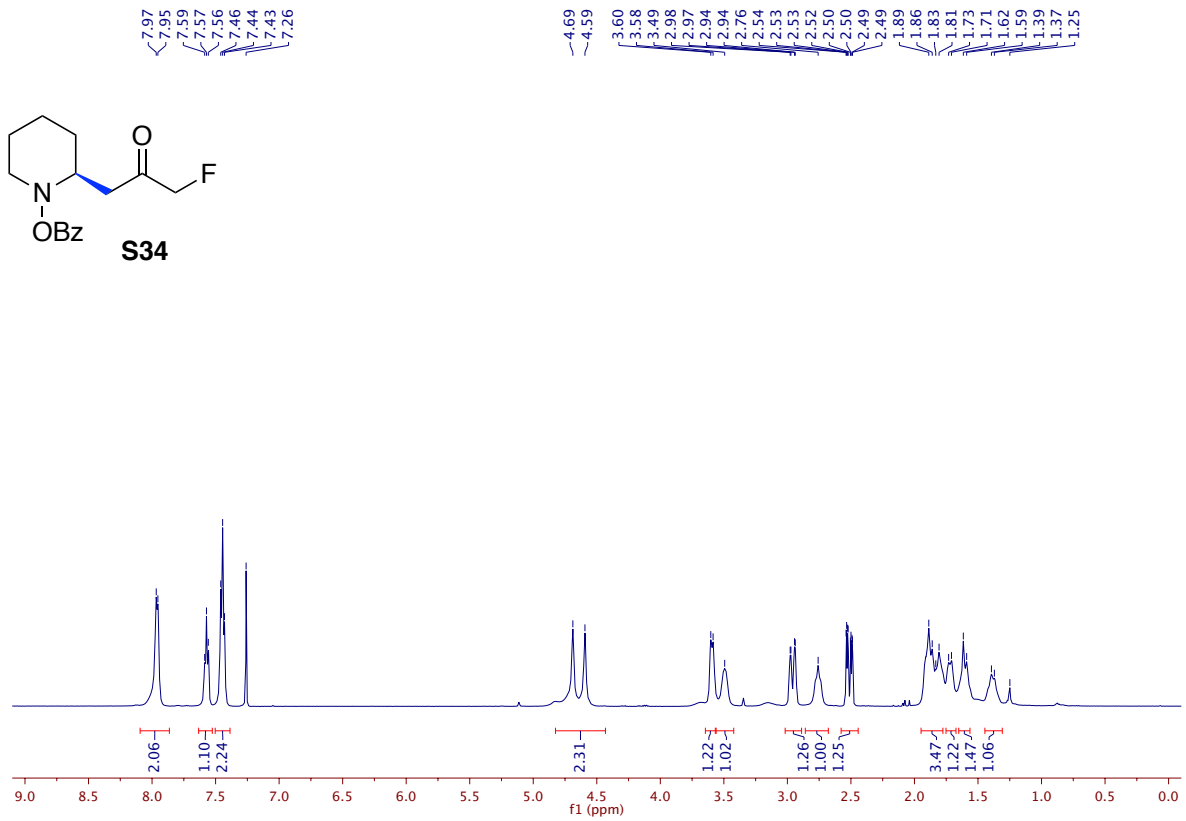
7.97
7.95
7.59
7.57
7.56
7.46
7.44
7.43
7.26
4.69
4.59
3.60
3.58
3.49
2.98
2.97
2.94
2.94
2.76
2.54
2.53
2.53
2.52
2.50
2.50
2.49
2.49
1.89
1.86
1.83
1.81
1.73
1.71
1.62
1.59
1.39
1.37
1.25
O
F
N
OBz
S34
2.06
1.10
2.24
2.31
1.22
1.02
1.26
1.00
1.25
3.47
1.22
1.47
1.06
9.0
8.5
8.0
7.5
7.0
6.5
6.0
5.5
5.0
4.5
4.0
3.5
3.0
2.5
2.0
1.5
1.0
0.5
0.0
f1 (ppm)

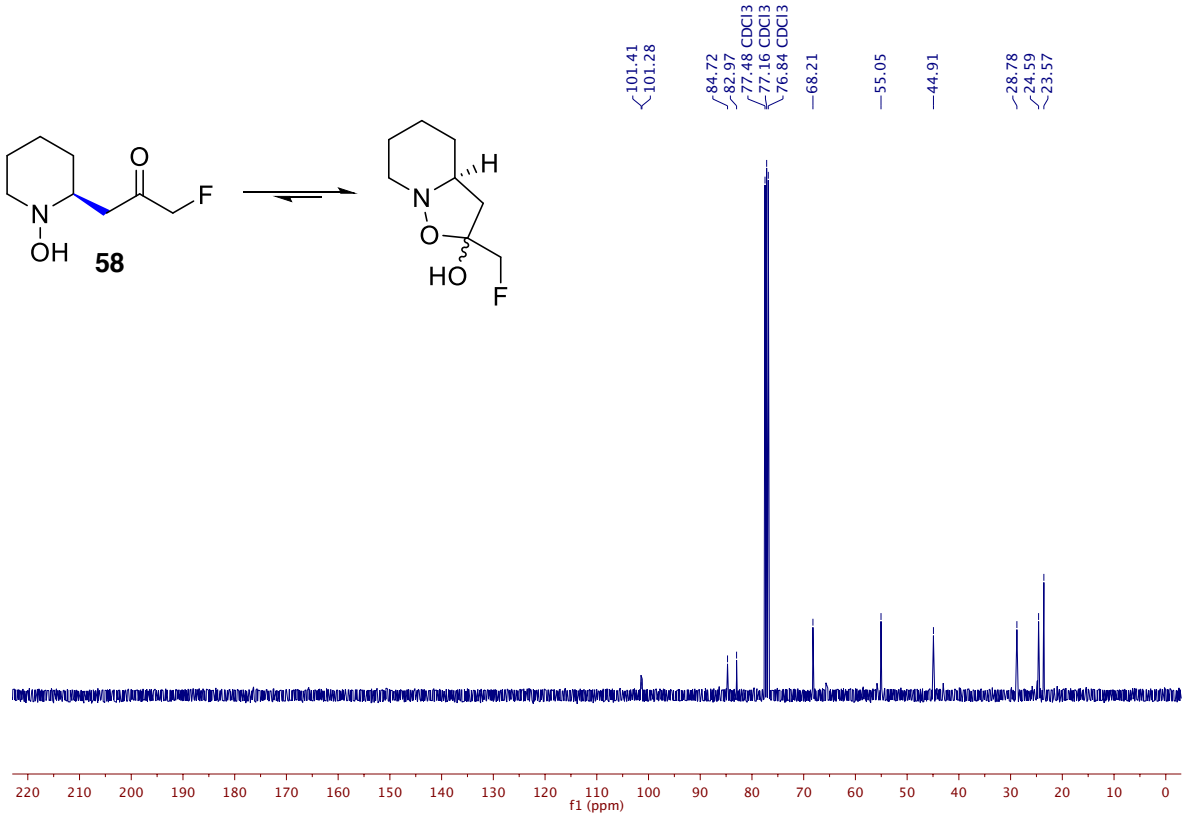
101.41
101.28
84.72
82.97
77.48 CDCl3
77.16 CDCl3
76.84 CDCl3
68.21
55.05
44.91
28.78
24.59
23.57
O
F
N
OH
58
H
N
O
HO
F
220 210 200 190 180 170 160 150 140 130 120 110 100 90 80 70 60 50 40 30 20 10 0
f1 (ppm)

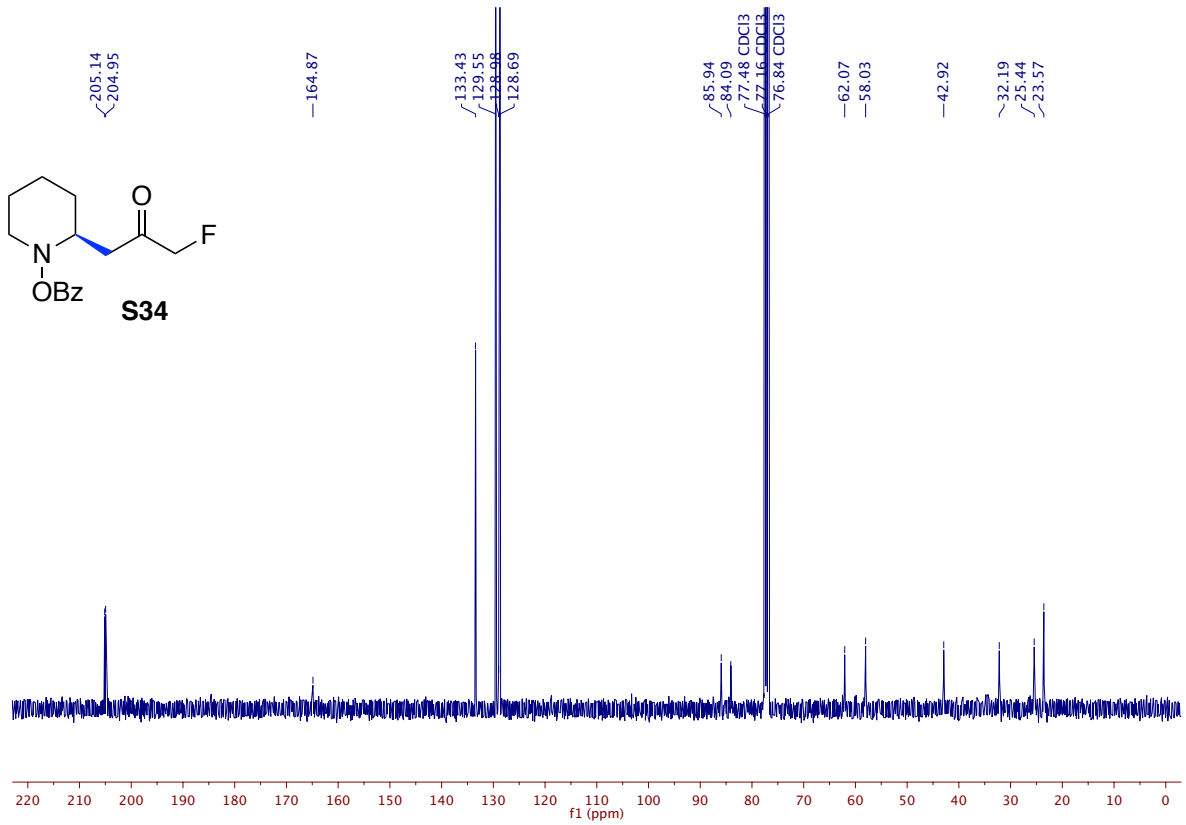
205.14
204.95
164.87
133.43
129.55
128.98
128.69
85.94
84.09
77.48 CDCl3
77.16 CDCl3
76.84 CDCl3
62.07
58.03
42.92
32.19
25.44
23.57
O
F
N
OBz
S34
220 210 200 190 180 170 160 150 140 130 120 110 100 90 80 70 60 50 40 30 20 10 0
f1 (ppm)

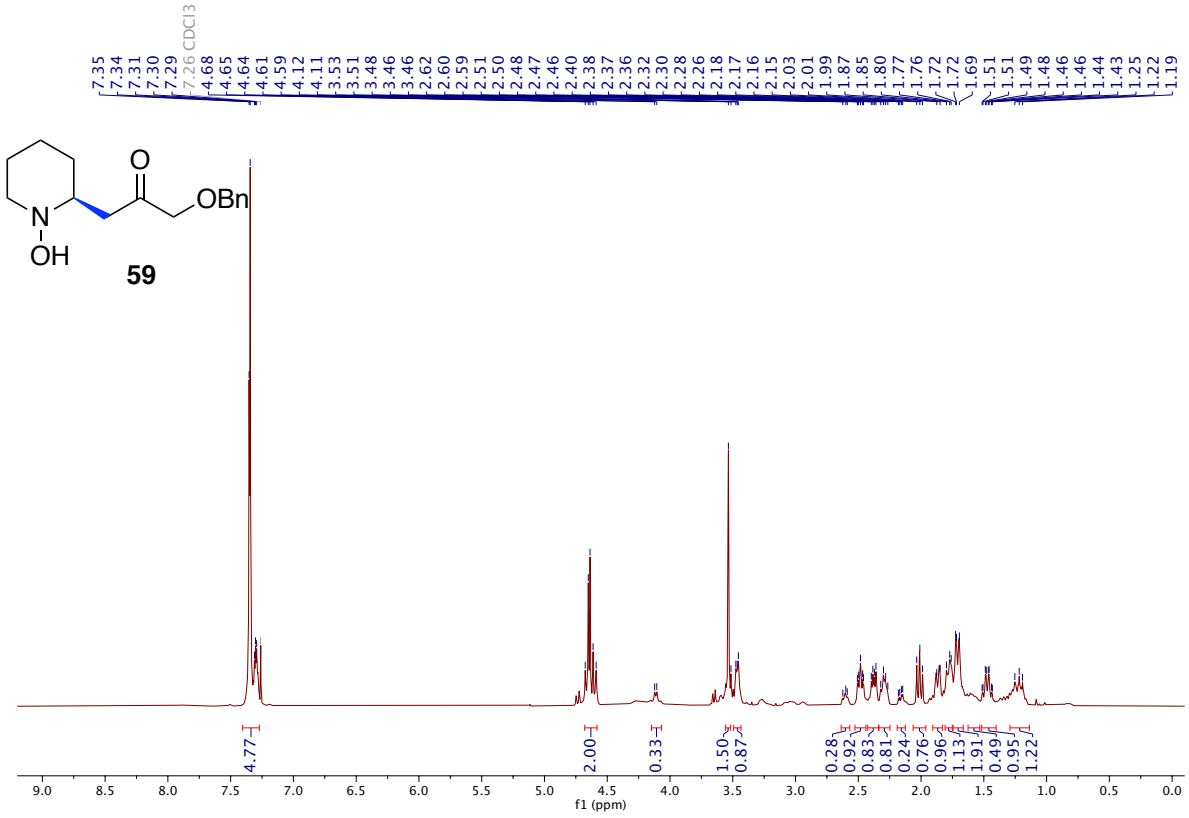
7.35
7.34
7.31
7.30
7.29
7.26 CDCl3
4.68
4.65
4.64
4.61
4.59
4.12
4.11
3.53
3.51
3.48
3.46
3.46
2.62
2.60
2.59
2.51
2.50
2.48
2.47
2.46
2.40
2.38
2.37
2.36
2.32
2.30
2.28
2.26
2.18
2.17
2.16
2.15
2.03
2.01
1.99
1.87
1.85
1.80
1.77
1.76
1.72
1.72
1.69
1.51
1.51
1.49
1.48
1.46
1.46
1.44
1.43
1.25
1.22
1.19
O
OBn
N
OH
59
4.77
2.00
0.33
1.50
0.87
0.28
0.92
0.83
0.81
0.24
0.76
0.96
1.13
1.91
0.49
0.95
1.22
9.0
8.5
8.0
7.5
7.0
6.5
6.0
5.5
5.0
4.5
4.0
3.5
3.0
2.5
2.0
1.5
1.0
0.5
0.0
f1 (ppm)

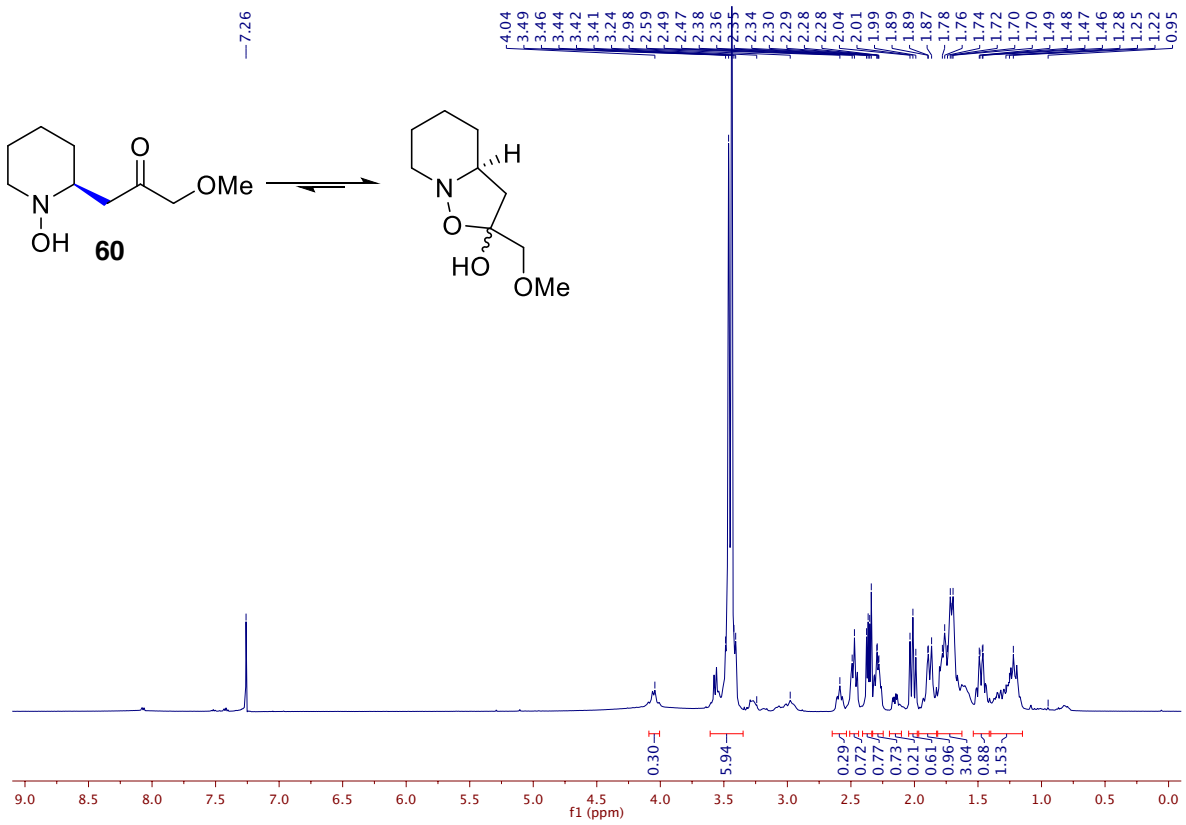
7.26
4.04
3.49
3.46
3.44
3.42
3.41
3.24
2.98
2.59
2.49
2.47
2.38
2.36
2.35
2.34
2.30
2.29
2.28
2.28
2.04
2.01
1.99
1.89
1.89
1.87
1.78
1.76
1.74
1.72
1.70
1.70
1.49
1.48
1.47
1.46
1.28
1.25
1.22
0.95
O
OMe
N
OH
60
H
N
O
HO
OMe
0.30
5.94
0.29
0.72
0.77
0.73
0.21
0.61
0.96
3.04
0.88
1.53
9.0
8.5
8.0
7.5
7.0
6.5
6.0
5.5
5.0
4.5
4.0
3.5
3.0
2.5
2.0
1.5
1.0
0.5
0.0
f1 (ppm)

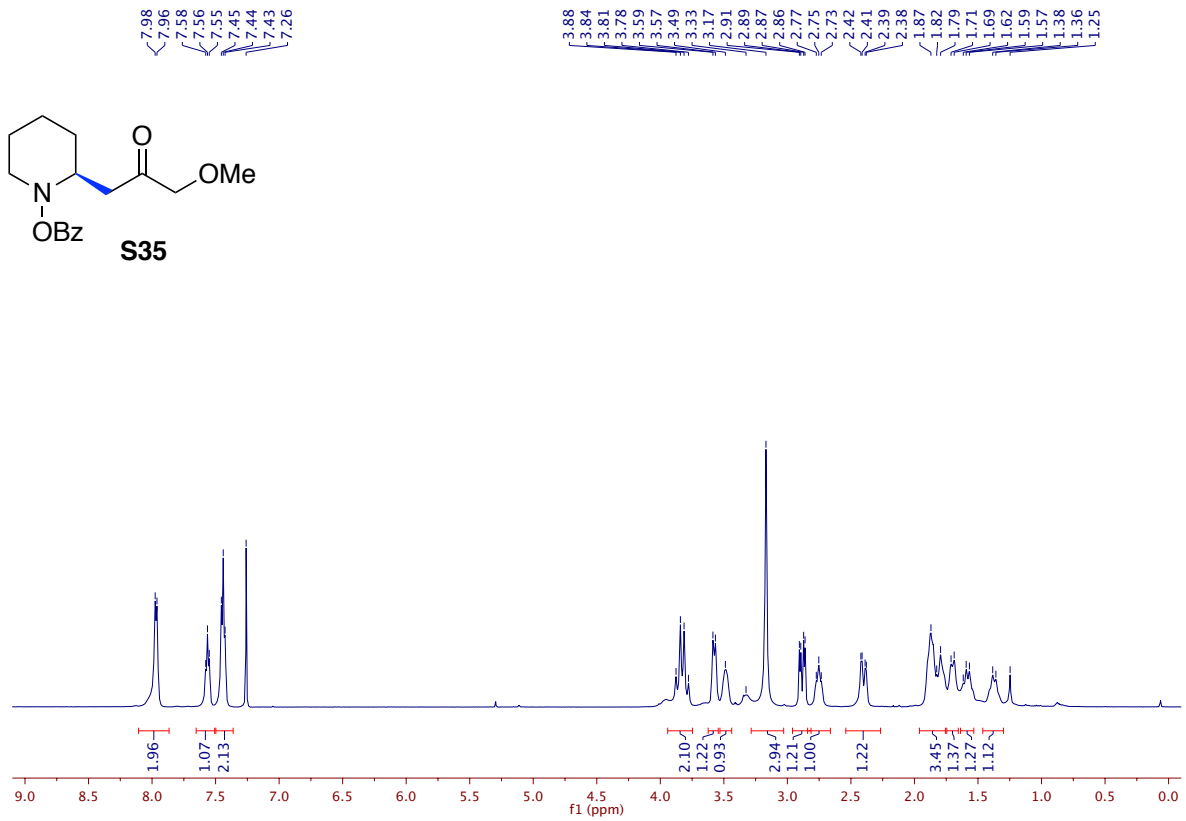
7.98
7.96
7.58
7.56
7.55
7.45
7.44
7.43
7.26
3.88
3.84
3.81
3.78
3.59
3.57
3.49
3.33
3.17
2.91
2.89
2.87
2.86
2.77
2.75
2.73
2.42
2.41
2.39
2.38
1.87
1.82
1.79
1.71
1.69
1.62
1.59
1.57
1.38
1.36
1.25
O
OMe
N
OBz
S35
1.96
1.07
2.13
2.10
1.22
0.93
2.94
1.21
1.00
1.22
3.45
1.37
1.27
1.12
9.0
8.5
8.0
7.5
7.0
6.5
6.0
5.5
5.0
4.5
4.0
3.5
3.0
2.5
2.0
1.5
1.0
0.5
0.0
f1 (ppm)

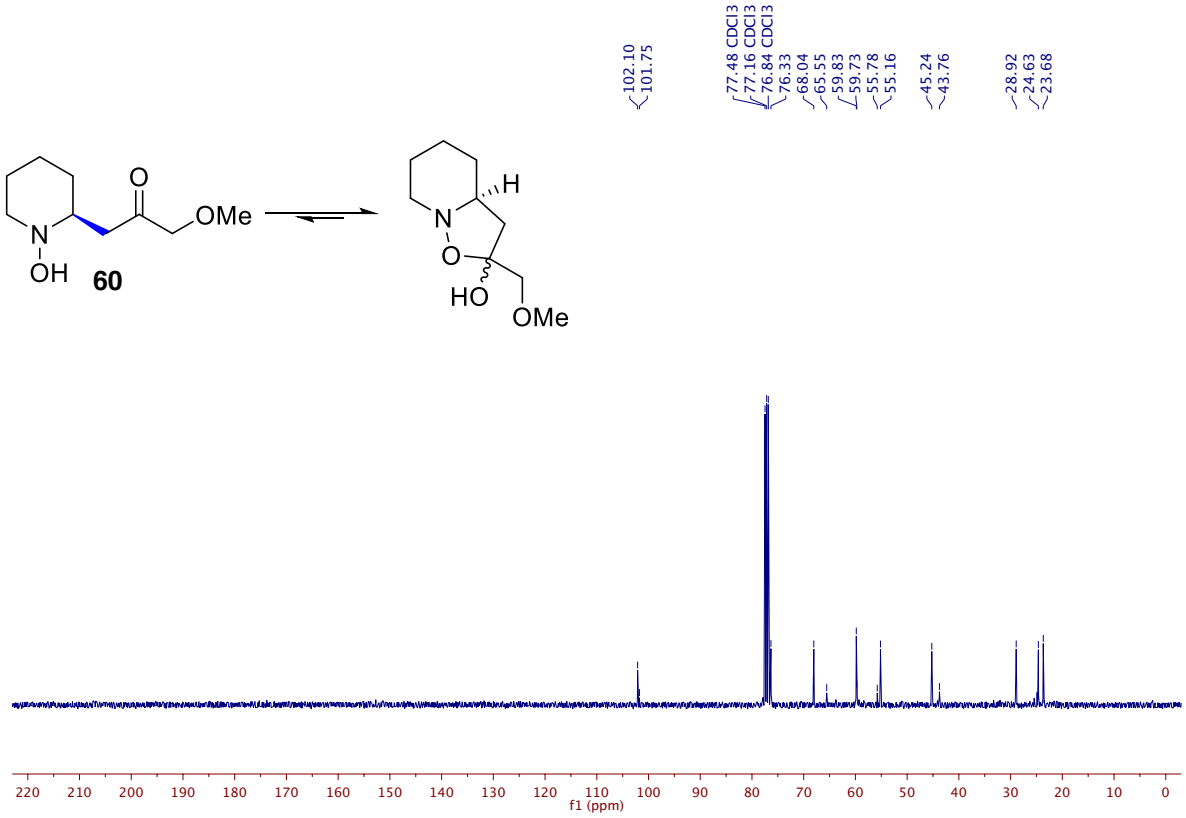
102.10
101.75
77.48 CDCl3
77.16 CDCl3
76.84 CDCl3
76.33
68.04
65.55
59.83
59.73
55.78
55.16
45.24
43.76
28.92
24.63
23.68
O
OMe
N
OH
60
H
N
O
HO
OMe
220 210 200 190 180 170 160 150 140 130 120 110 100 90 80 70 60 50 40 30 20 10 0
f1 (ppm)

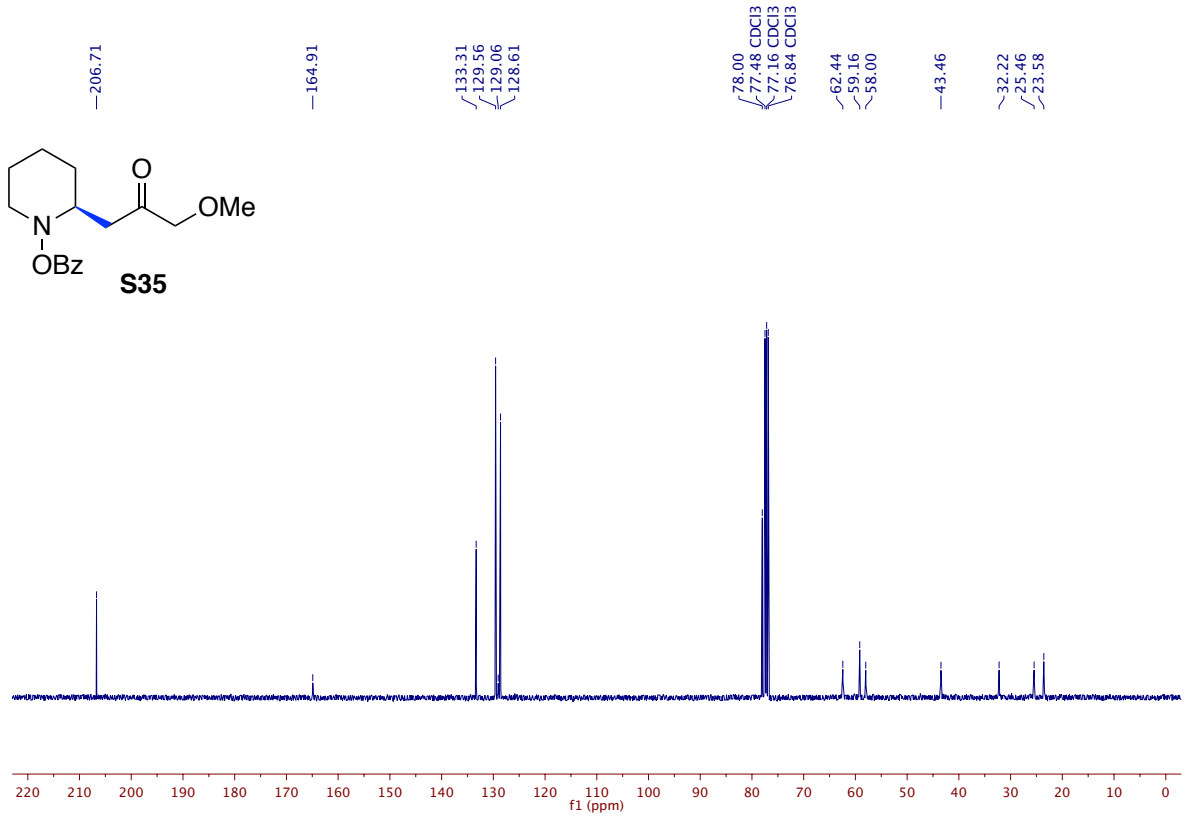
206.71
164.91
133.31
129.56
129.06
128.61
78.00
77.48 CDCl3
77.16 CDCl3
76.84 CDCl3
62.44
59.16
58.00
43.46
32.22
25.46
23.58
O
OMe
N
OBz
S35
220 210 200 190 180 170 160 150 140 130 120 110 100 90 80 70 60 50 40 30 20 10 0
f1 (ppm)

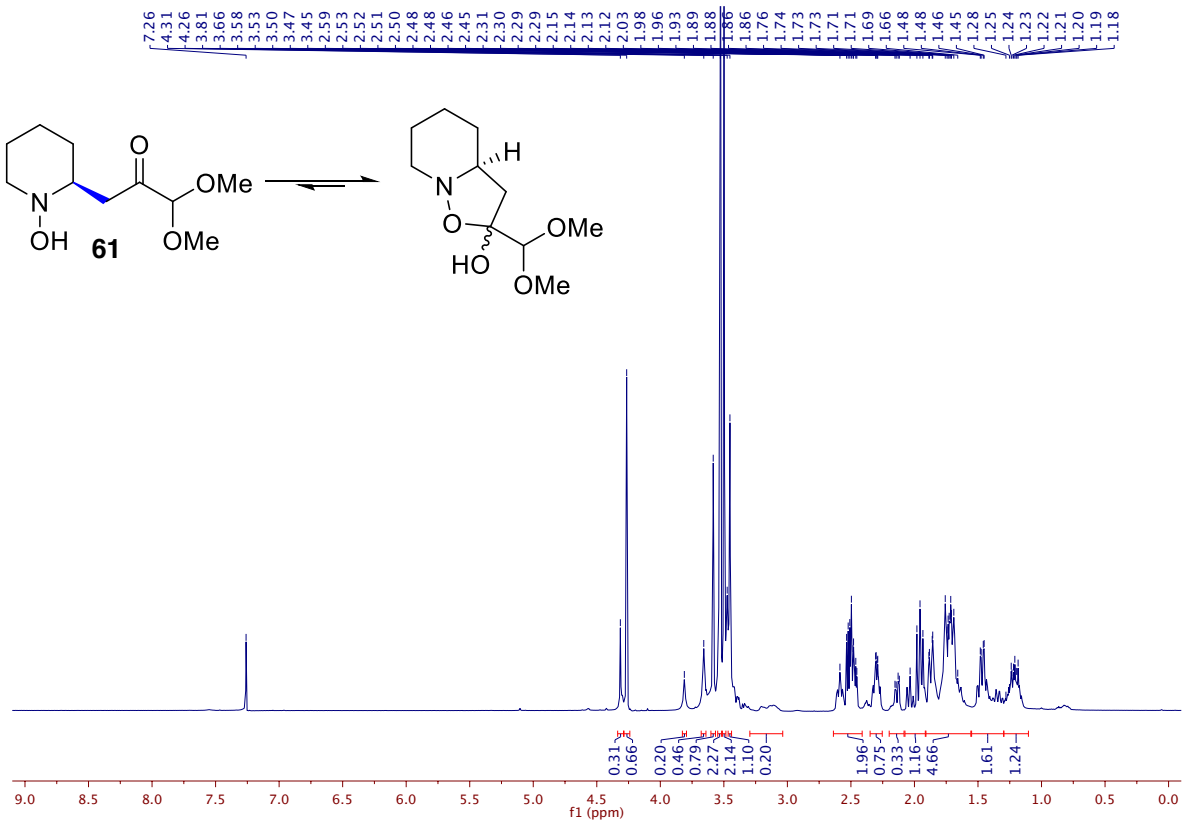
61
OMe
OMe
OH
N
O
H
HO
OMe
OMe
f1 (ppm)

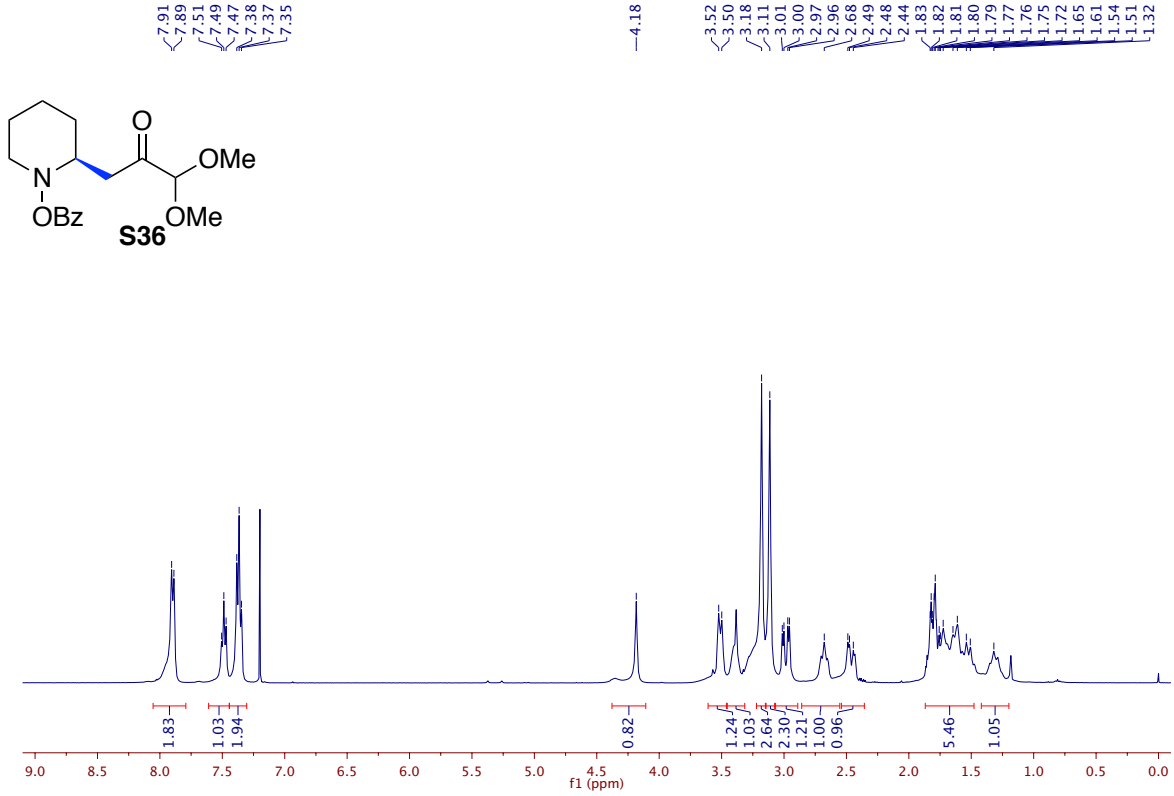
S36
OMe
OMe
OBz
N
O
f1 (ppm)

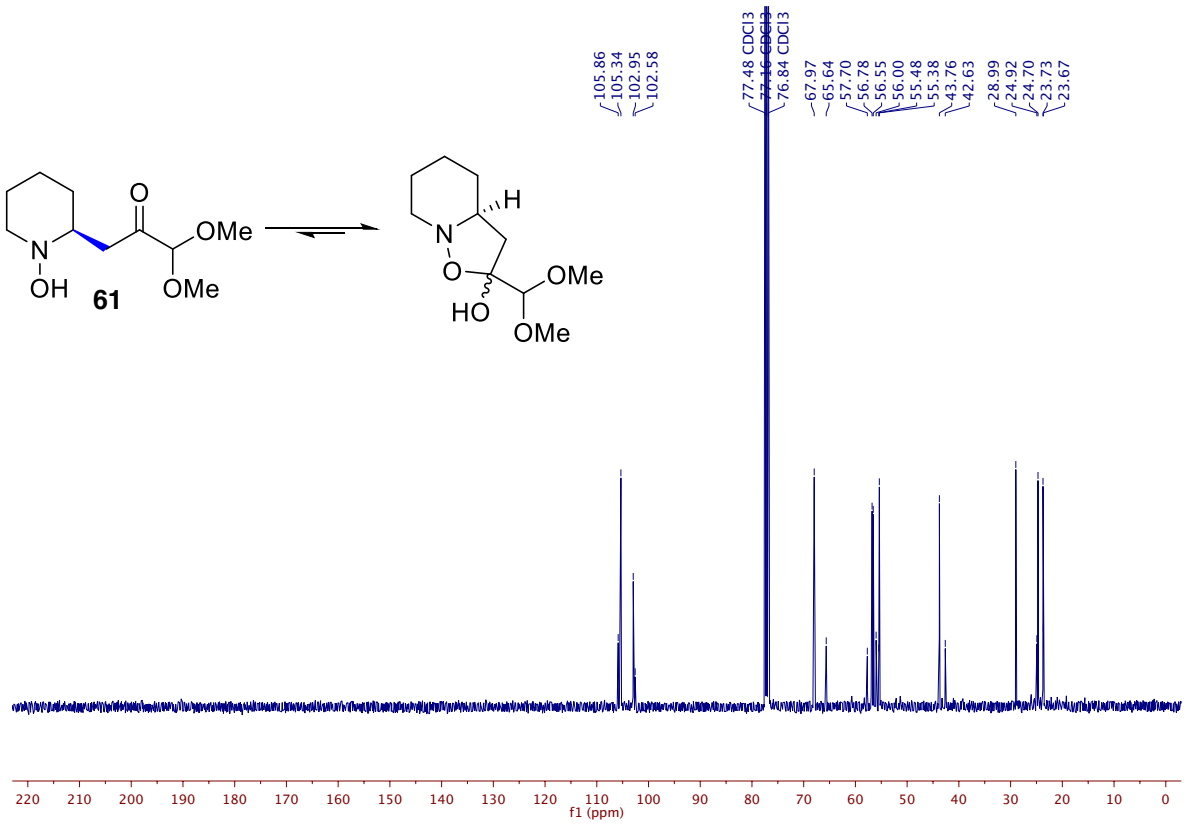
105.86
105.34
102.95
102.58
77.48 CDCl3
77.16 CDCl3
76.84 CDCl3
67.97
65.64
57.70
56.78
56.55
56.00
55.48
55.38
43.76
42.63
28.99
24.92
24.70
23.73
23.67
O
OMe
N
OH
OMe
61
H
N
O
HO
OMe
OMe
220 210 200 190 180 170 160 150 140 130 120 110 100 90 80 70 60 50 40 30 20 10 0
f1 (ppm)

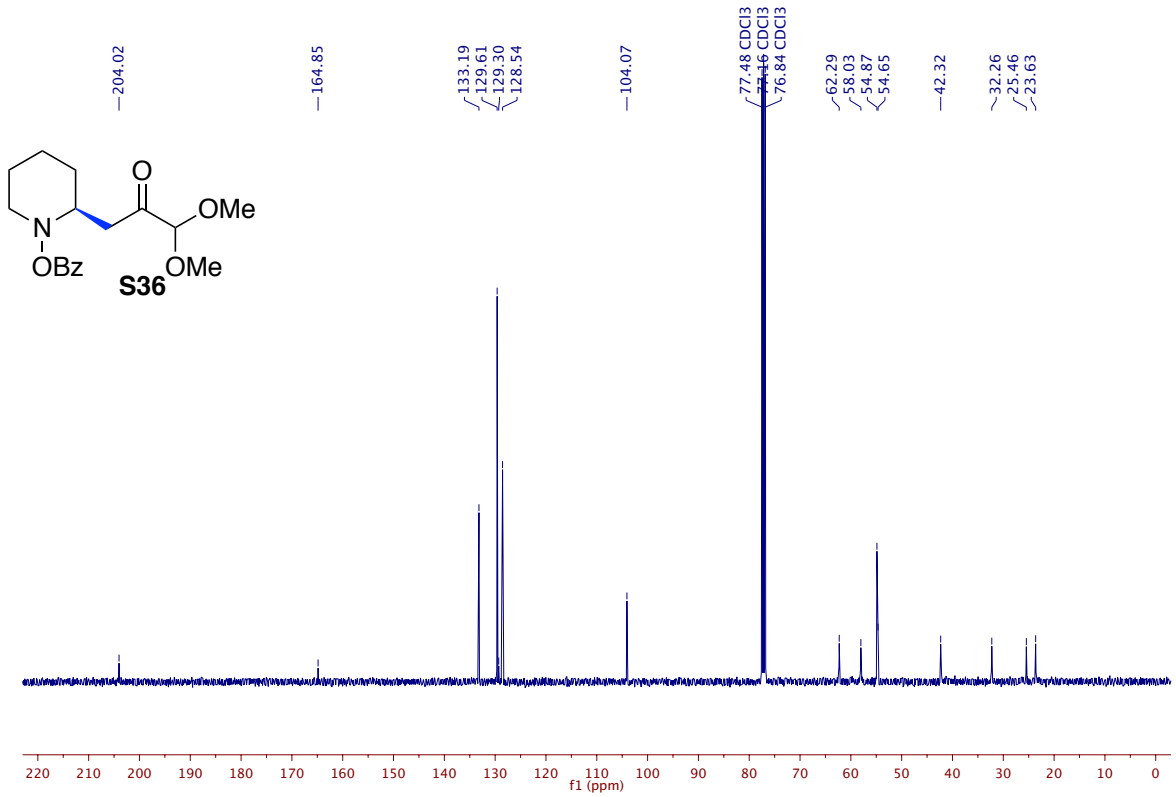
204.02
164.85
133.19
129.61
129.30
128.54
104.07
77.48 CDCl3
77.16 CDCl3
76.84 CDCl3
62.29
58.03
54.87
54.65
42.32
32.26
25.46
23.63
O
OMe
N
OBz
OMe
S36
220 210 200 190 180 170 160 150 140 130 120 110 100 90 80 70 60 50 40 30 20 10 0
f1 (ppm)

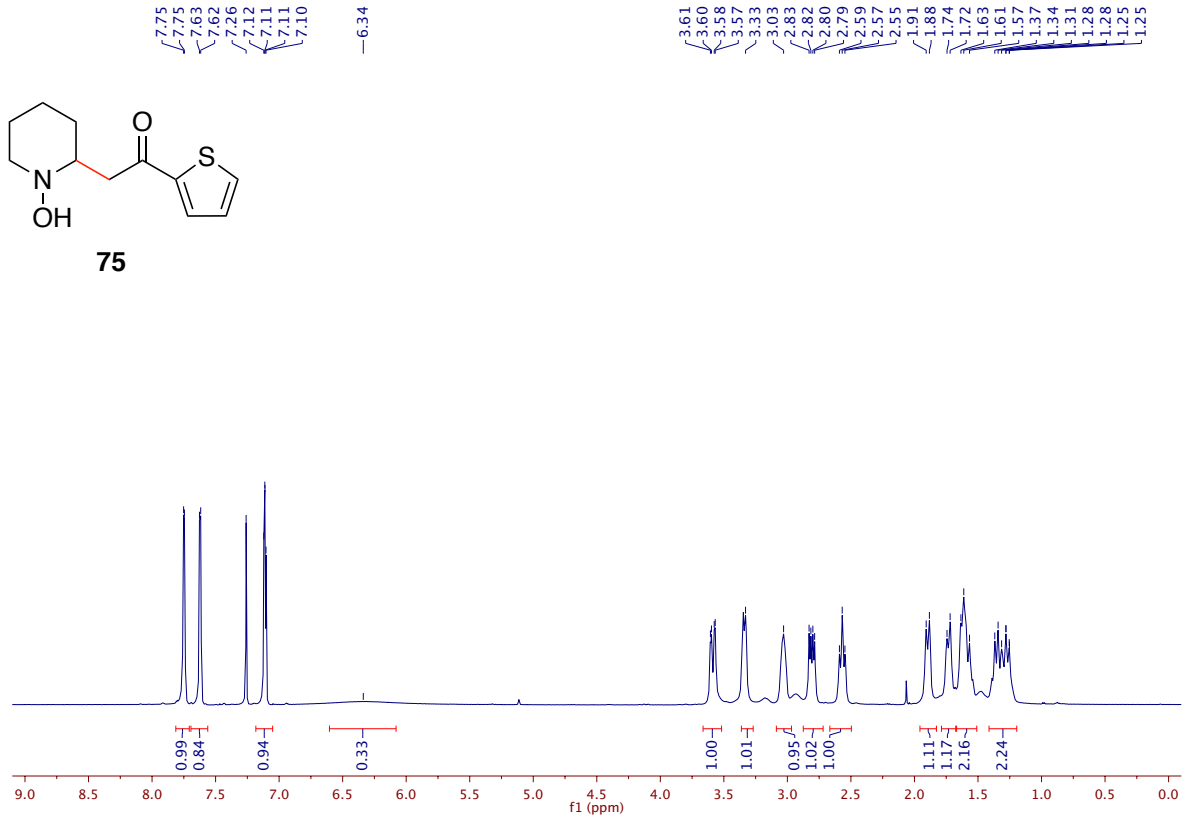
7.75
7.75
7.63
7.62
7.26
7.12
7.11
7.11
7.10
6.34
3.61
3.60
3.58
3.57
3.33
3.03
2.83
2.82
2.80
2.79
2.59
2.57
2.55
1.91
1.88
1.74
1.72
1.63
1.61
1.57
1.37
1.34
1.31
1.28
1.28
1.25
1.25
O
S
N
OH
75
0.99
0.84
0.94
0.33
1.00
1.01
0.95
1.02
1.00
1.11
1.17
2.16
2.24
9.0
8.5
8.0
7.5
7.0
6.5
6.0
5.5
5.0
4.5
4.0
3.5
3.0
2.5
2.0
1.5
1.0
0.5
0.0
f1 (ppm)

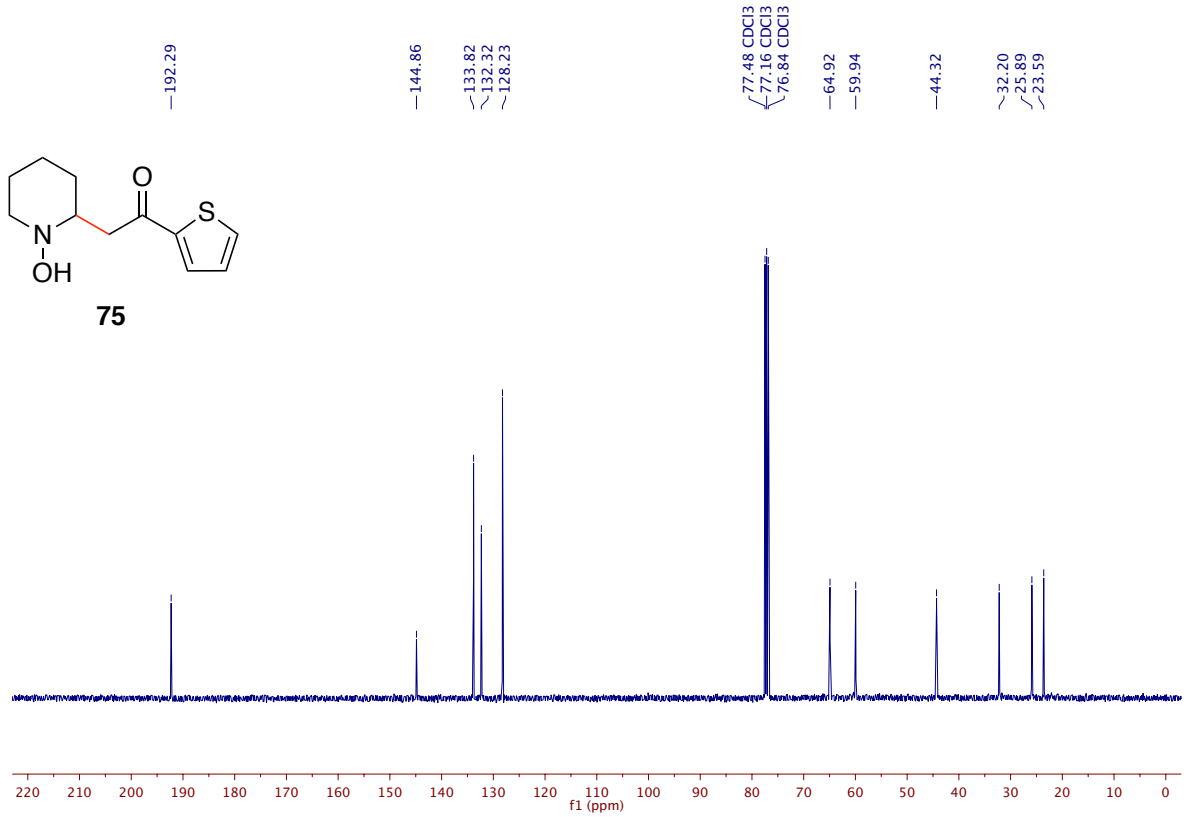
192.29
144.86
133.82
132.32
128.23
77.48 CDCl3
77.16 CDCl3
76.84 CDCl3
64.92
59.94
44.32
32.20
25.89
23.59
O
S
N
OH
75
220
210
200
190
180
170
160
150
140
130
120
110
100
90
80
70
60
50
40
30
20
10
0
f1 (ppm)

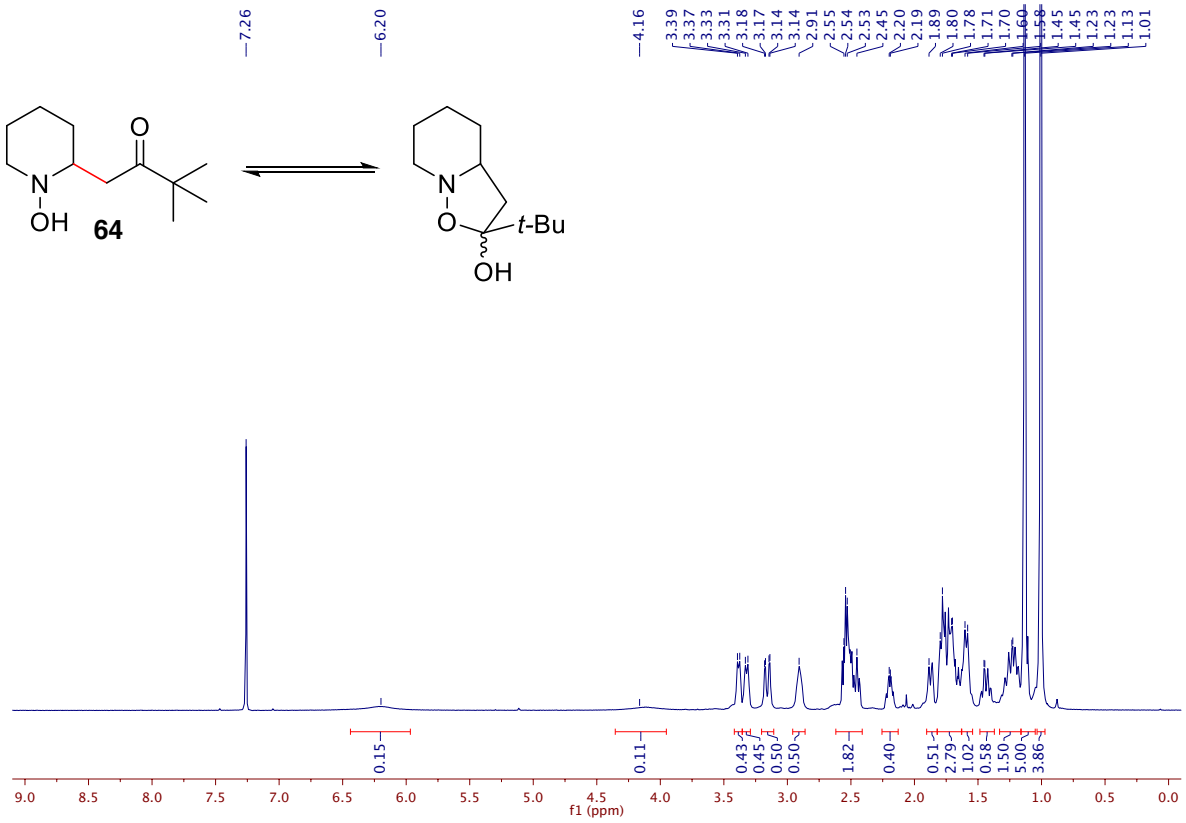
7.26
6.20
4.16
3.39
3.37
3.33
3.31
3.18
3.17
3.14
3.14
2.91
2.55
2.54
2.53
2.45
2.20
2.19
1.89
1.80
1.78
1.71
1.70
1.60
1.58
1.45
1.45
1.23
1.23
1.13
1.01
O
N
OH
64
N
O
t-Bu
OH
0.15
0.11
0.43
0.45
0.50
0.50
1.82
0.40
0.51
2.79
1.02
0.58
1.50
5.00
3.86
9.0 8.5 8.0 7.5 7.0 6.5 6.0 5.5 5.0 4.5 4.0 3.5 3.0 2.5 2.0 1.5 1.0 0.5 0.0
f1 (ppm)

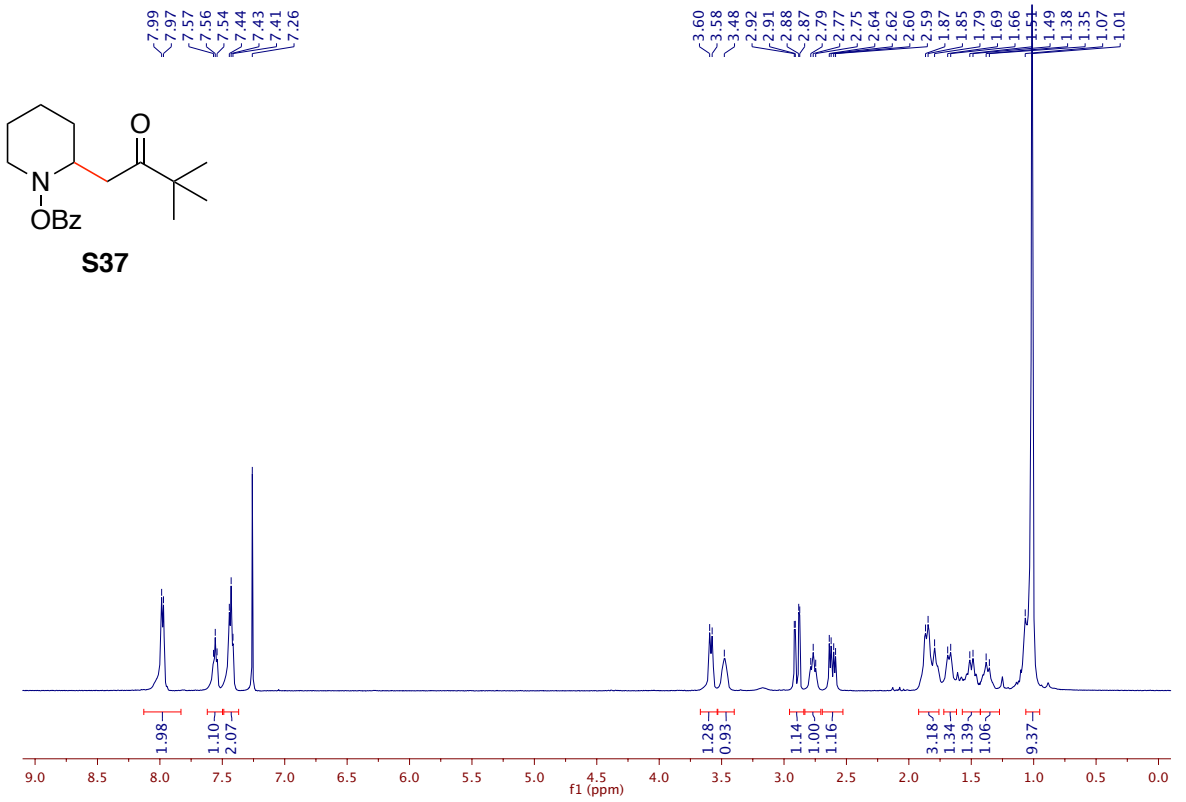
7.99
7.97
7.57
7.56
7.54
7.44
7.43
7.41
7.26
3.60
3.58
3.48
2.92
2.91
2.88
2.87
2.79
2.77
2.75
2.64
2.62
2.60
2.59
1.87
1.85
1.79
1.69
1.66
1.51
1.49
1.38
1.35
1.07
1.01
O
N
OBz
S37
1.98
1.10
2.07
1.28
0.93
1.14
1.00
1.16
3.18
1.34
1.39
1.06
9.37
9.0 8.5 8.0 7.5 7.0 6.5 6.0 5.5 5.0 4.5 4.0 3.5 3.0 2.5 2.0 1.5 1.0 0.5 0.0
f1 (ppm)

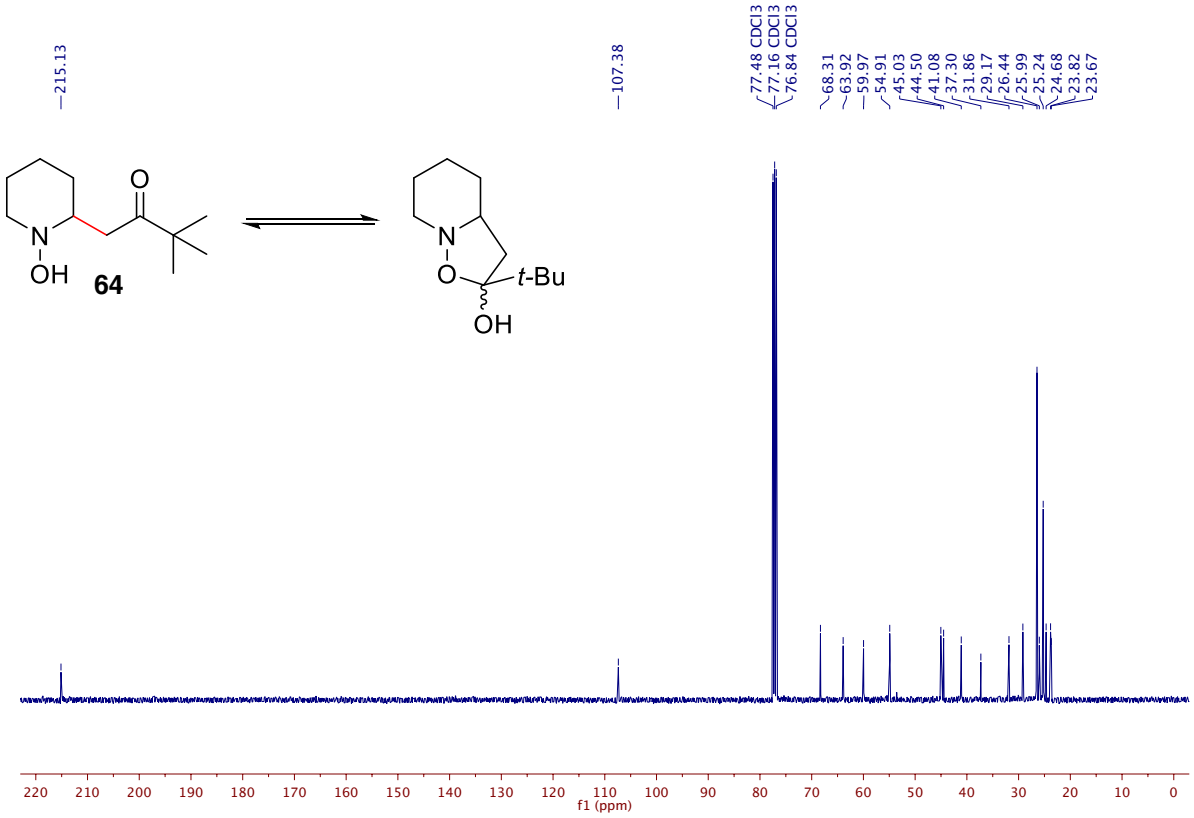
215.13
107.38
77.48 CDCl3
77.16 CDCl3
76.84 CDCl3
68.31
63.92
59.97
54.91
45.03
44.50
41.08
37.30
31.86
29.17
26.44
25.99
25.24
24.68
23.82
23.67
O
N
OH
64
N
O
t-Bu
OH
220 210 200 190 180 170 160 150 140 130 120 110 100 90 80 70 60 50 40 30 20 10 0
f1 (ppm)

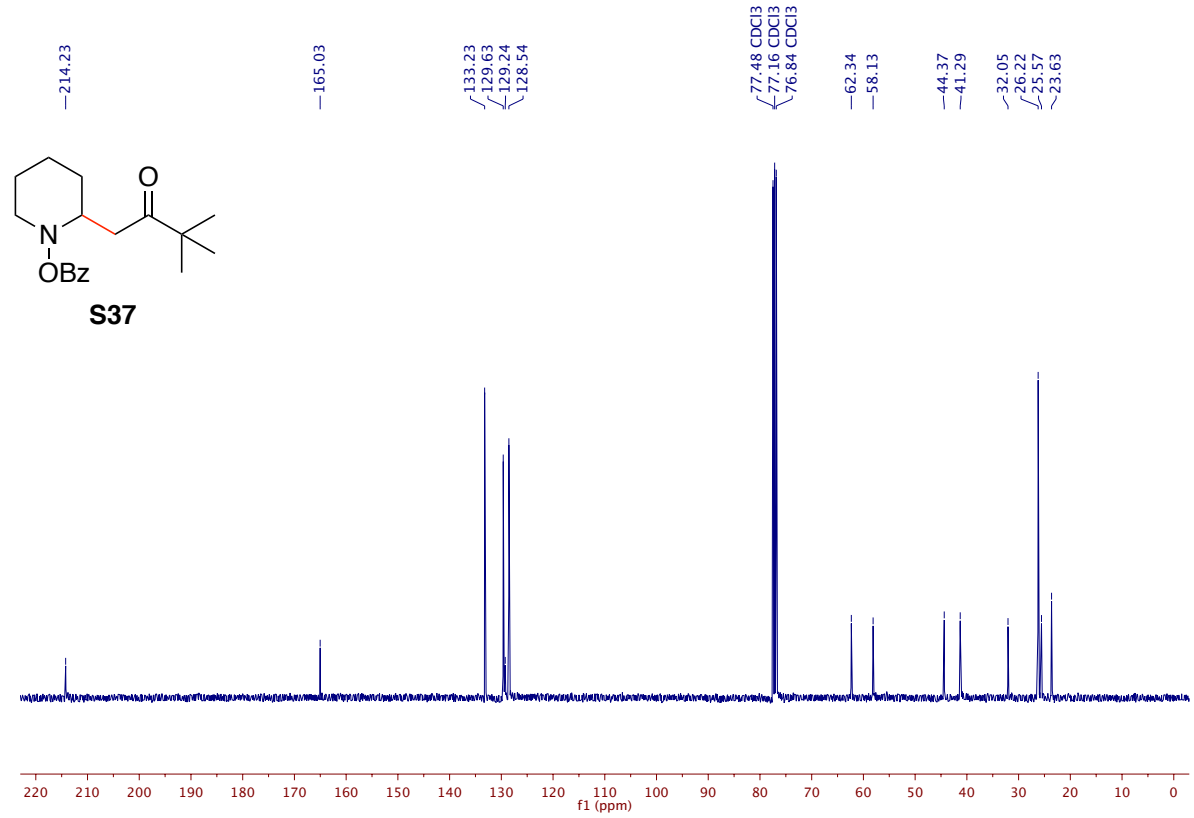
214.23
165.03
133.23
129.63
129.24
128.54
77.48 CDCl3
77.16 CDCl3
76.84 CDCl3
62.34
58.13
44.37
41.29
32.05
26.22
25.57
23.63
O
N
OBz
S37
220 210 200 190 180 170 160 150 140 130 120 110 100 90 80 70 60 50 40 30 20 10 0
f1 (ppm)

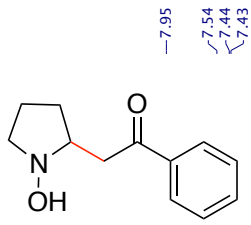
O
N
OH

76

7.95
7.54
7.44
7.43
7.26
3.56
3.53
3.37
3.29
3.02
3.01
2.85
2.83
2.17
2.07
1.84
1.83
1.82
1.82
1.45
1.96
1.13
2.31
1.00
2.11
1.23
1.18
1.30
2.42
1.20
f1 (ppm)

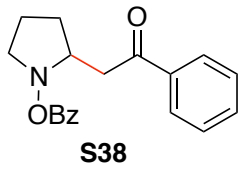
O
N
OBz

S38

7.94
7.93
7.92
7.91
7.90
7.55
7.53
7.51
7.50
7.48
7.41
7.40
7.38
7.37
7.26
3.87
3.86
3.85
3.84
3.83
3.82
3.81
3.81
3.69
3.67
3.66
3.65
3.64
3.61
3.60
3.57
3.16
3.14
3.13
3.11
3.03
3.02
2.39
2.37
2.36
2.35
2.33
2.32
2.02
2.00
1.99
1.97
1.96
1.78
1.62
1.60
1.58
1.58
1.56
1.54
4.00
2.05
3.64
1.00
1.05
0.96
1.04
1.03
1.09
2.07
1.15
f1 (ppm)

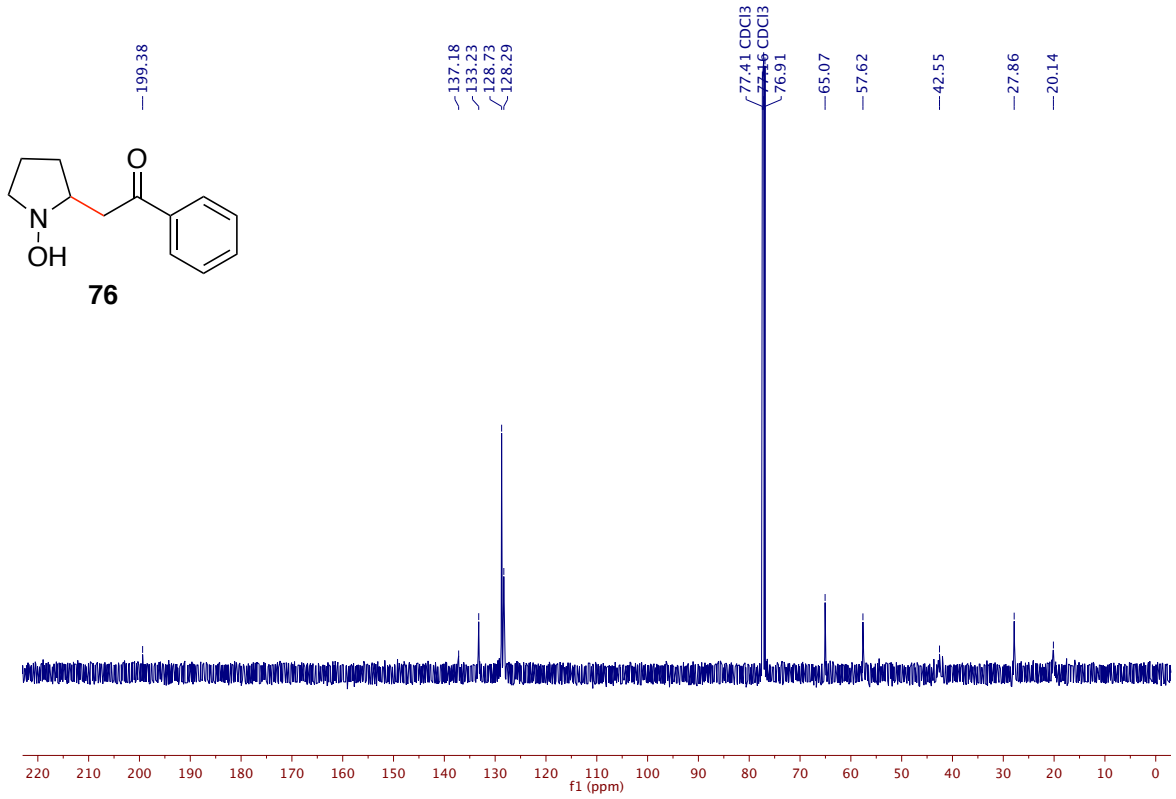
199.38
137.18
133.23
128.73
128.29
77.41 CDCl3
77.16 CDCl3
76.91
65.07
57.62
42.55
27.86
20.14
O
N
OH
76
f1 (ppm)

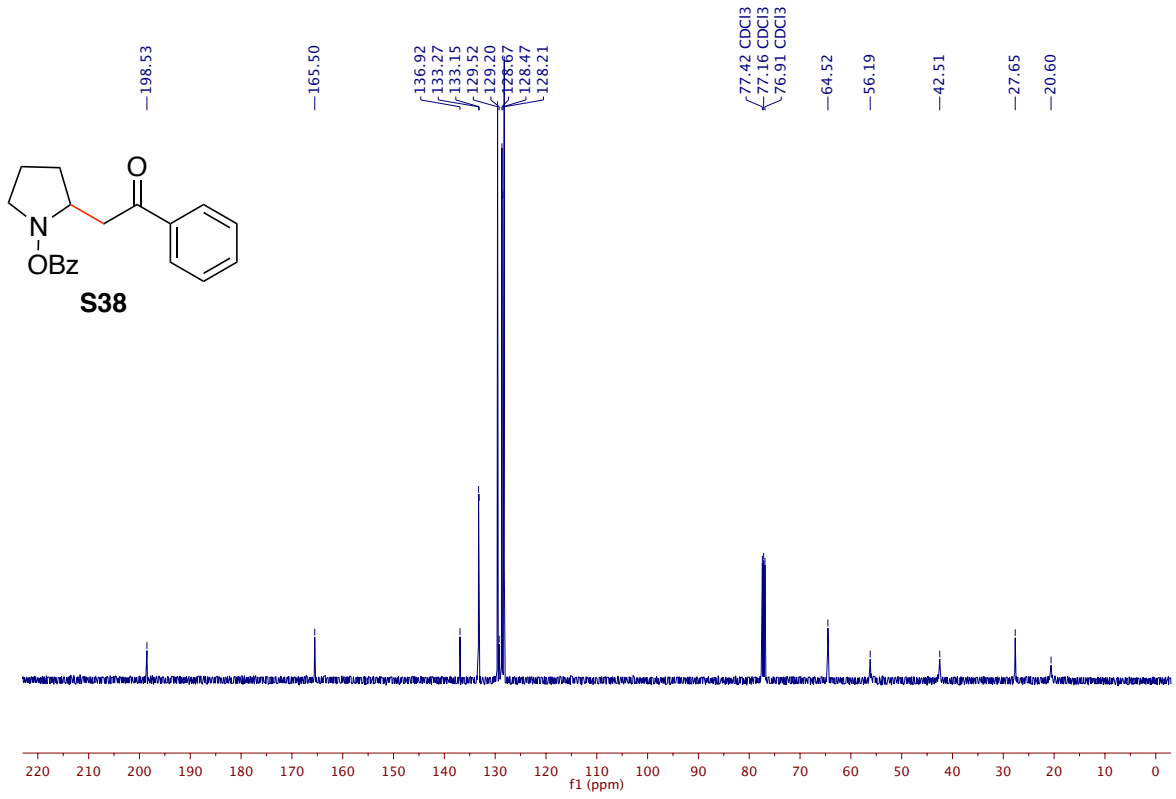
198.53
165.50
136.92
133.27
133.15
129.52
129.20
128.67
128.47
128.21
77.42 CDCl3
77.16 CDCl3
76.91 CDCl3
64.52
56.19
42.51
27.65
20.60
O
N
OBz
S38
f1 (ppm)

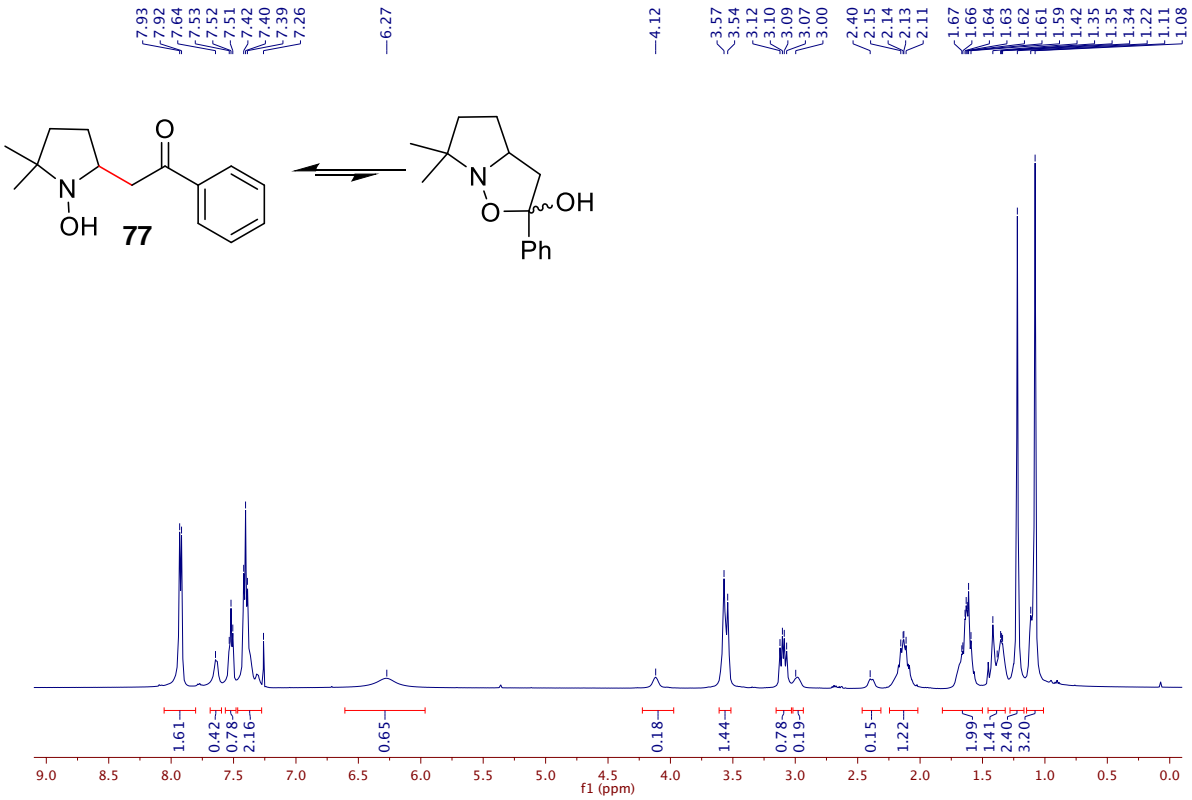
7.93
7.92
7.64
7.53
7.52
7.51
7.42
7.40
7.39
7.26
6.27
4.12
3.57
3.54
3.12
3.10
3.09
3.07
3.00
2.40
2.15
2.14
2.13
2.11
1.67
1.66
1.64
1.63
1.62
1.61
1.59
1.42
1.35
1.35
1.34
1.22
1.11
1.08
O
N
OH
77
N
O
OH
Ph
1.61
0.42
0.78
2.16
0.65
0.18
1.44
0.78
0.19
0.15
1.22
1.99
1.41
2.40
3.20
f1 (ppm)

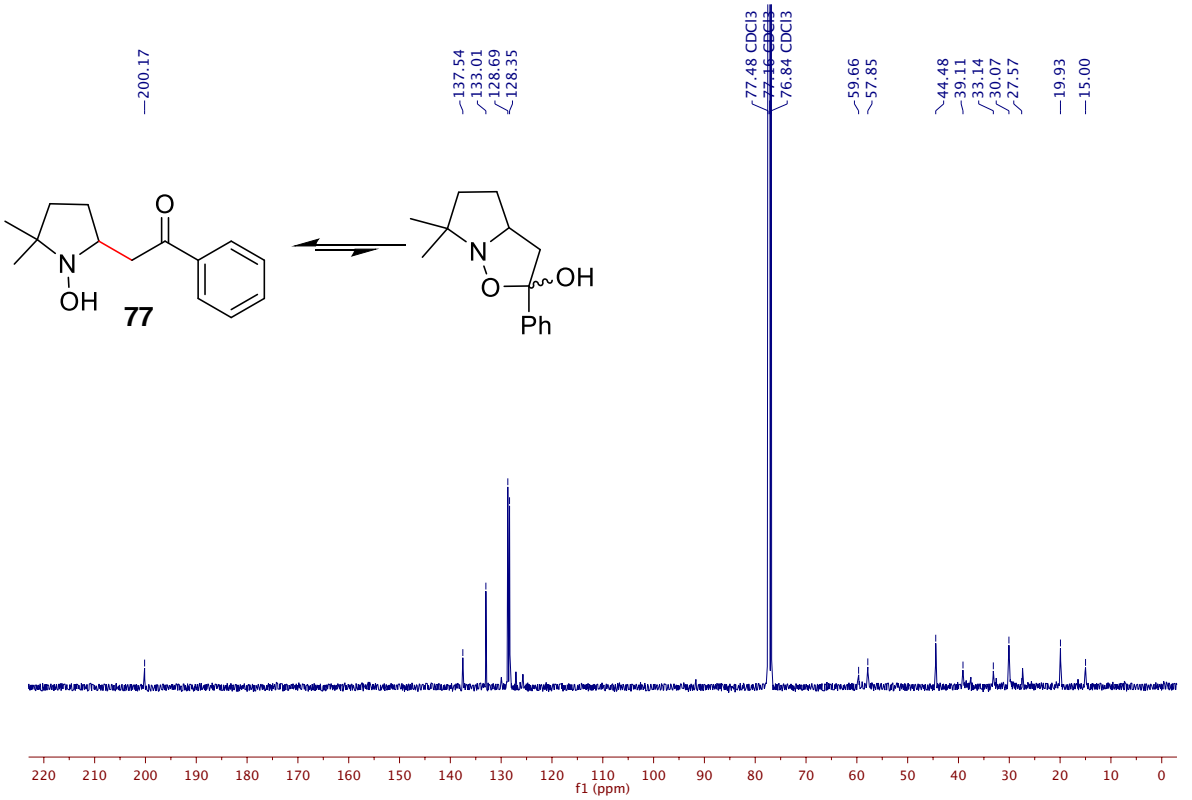
200.17
137.54
133.01
128.69
128.35
77.48 CDCl3
77.16 CDCl3
76.84 CDCl3
59.66
57.85
44.48
39.11
33.14
30.07
27.57
19.93
15.00
O
N
OH
77
N
O
OH
Ph
f1 (ppm)

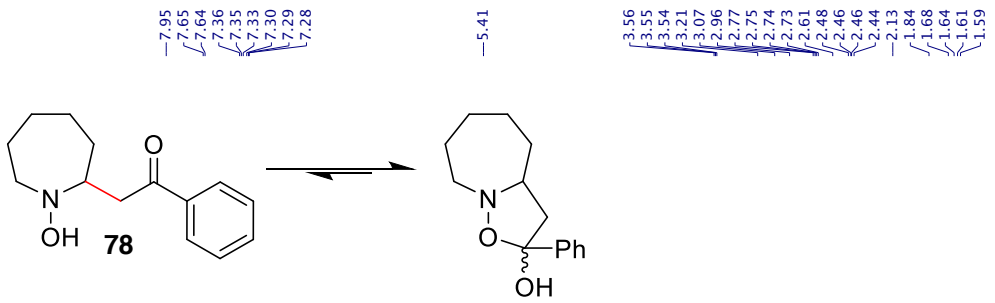
7.95
7.65
7.64
7.36
7.35
7.33
7.30
7.29
7.28
5.41
3.56
3.55
3.54
3.21
3.07
2.96
2.77
2.75
2.74
2.73
2.61
2.48
2.46
2.46
2.44
2.13
1.84
1.68
1.64
1.61
1.59
O
N
OH
78
N
O
Ph
OH

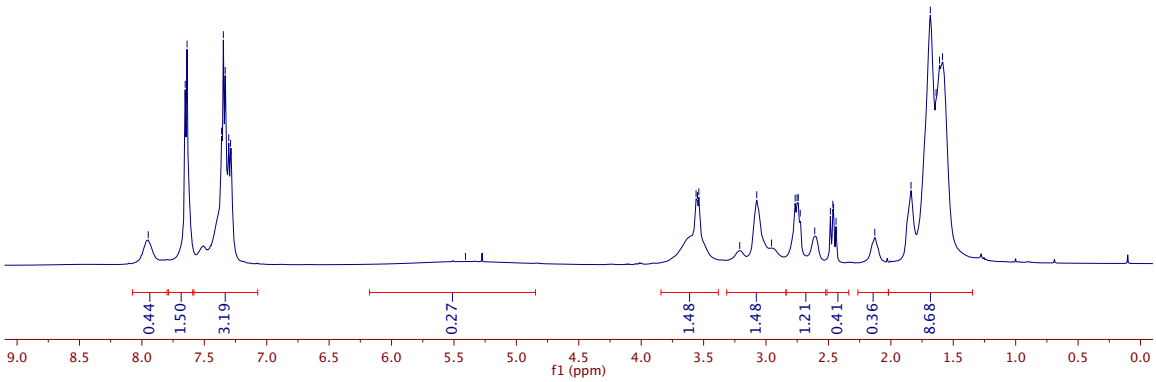
0.44
1.50
3.19
0.27
1.48
1.48
1.21
0.41
0.36
8.68
9.0
8.5
8.0
7.5
7.0
6.5
6.0
5.5
5.0
4.5
4.0
3.5
3.0
2.5
2.0
1.5
1.0
0.5
0.0
f1 (ppm)

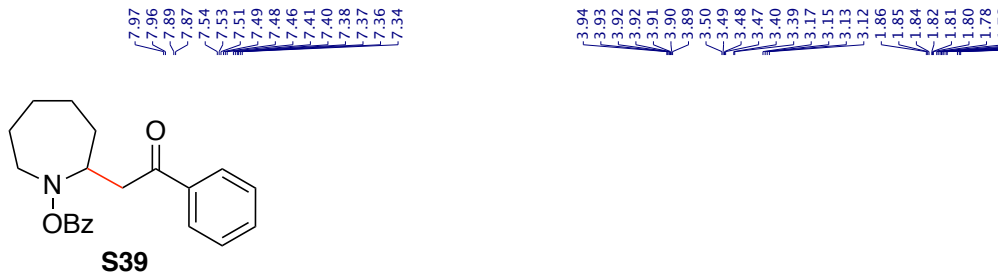
7.97
7.96
7.89
7.87
7.54
7.53
7.51
7.49
7.48
7.46
7.41
7.40
7.38
7.37
7.36
7.34
3.94
3.93
3.92
3.92
3.91
3.90
3.89
3.50
3.49
3.48
3.47
3.40
3.39
3.17
3.15
3.13
3.12
1.86
1.85
1.84
1.82
1.81
1.80
1.78
1.76
1.75
1.74
1.73
1.72
1.70
1.69
1.61
1.60
1.59
O
N
OBz
S39

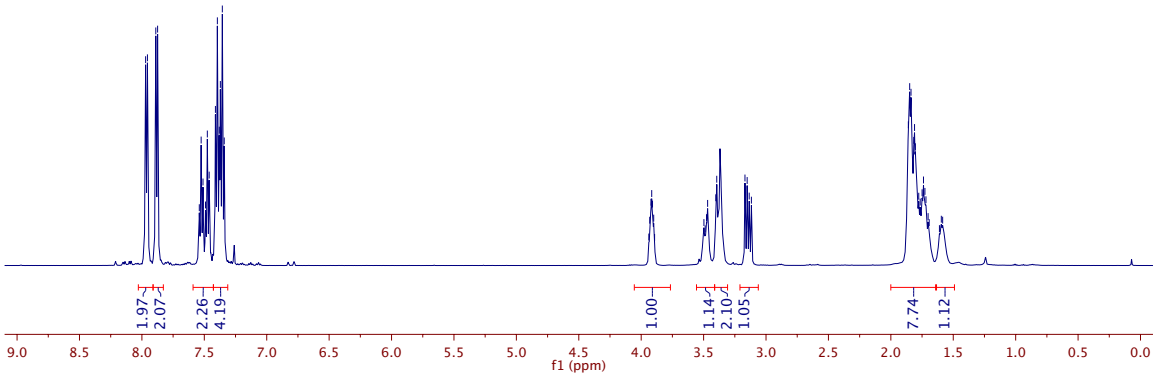
1.97
2.07
2.26
4.19
1.00
1.14
2.10
1.05
7.74
1.12
9.0
8.5
8.0
7.5
7.0
6.5
6.0
5.5
5.0
4.5
4.0
3.5
3.0
2.5
2.0
1.5
1.0
0.5
0.0
f1 (ppm)

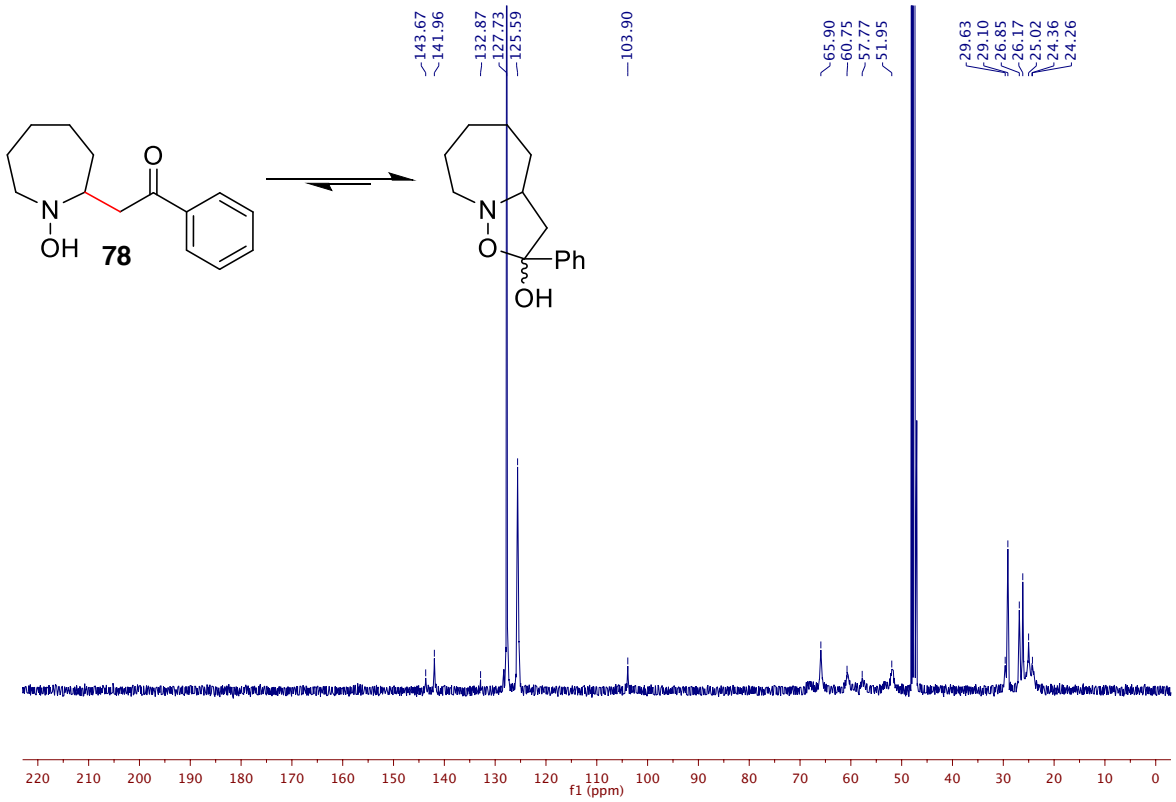
143.67
141.96
132.87
127.73
125.59
103.90
65.90
60.75
57.77
51.95
29.63
29.10
26.85
26.17
25.02
24.36
24.26
O
N
OH
78
N
O
Ph
OH
220 210 200 190 180 170 160 150 140 130 120 110 100 90 80 70 60 50 40 30 20 10 0
f1 (ppm)

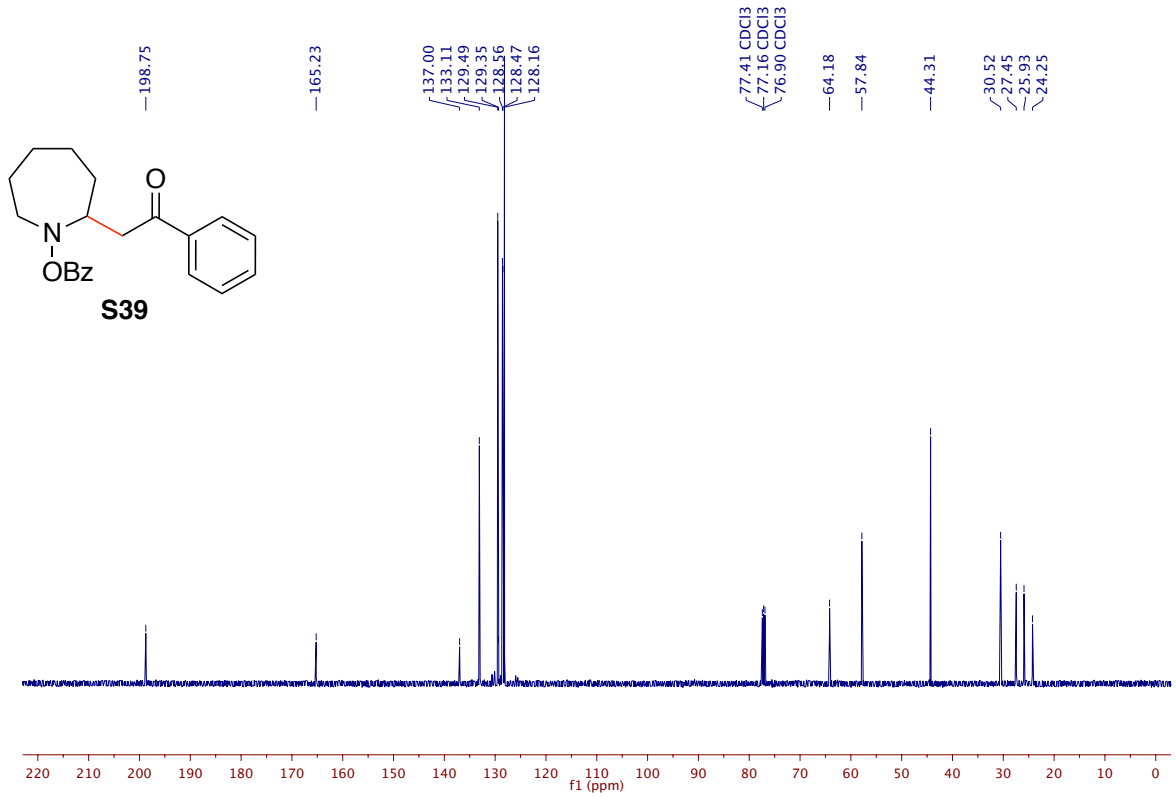
198.75
165.23
137.00
133.11
129.49
129.35
128.56
128.47
128.16
77.41 CDCl3
77.16 CDCl3
76.90 CDCl3
64.18
57.84
44.31
30.52
27.45
25.93
24.25
O
N
OBz
S39
220 210 200 190 180 170 160 150 140 130 120 110 100 90 80 70 60 50 40 30 20 10 0
f1 (ppm)

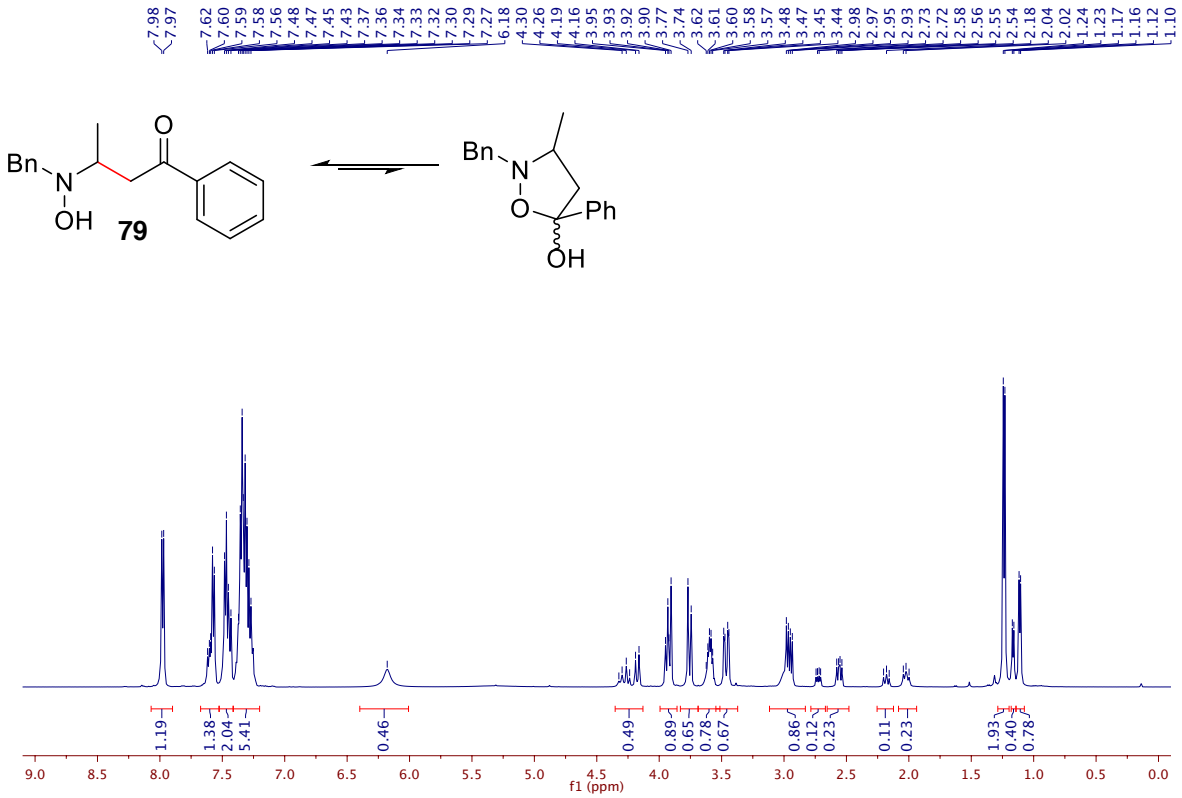
7.98
7.97
7.62
7.60
7.59
7.58
7.56
7.48
7.47
7.45
7.43
7.37
7.36
7.34
7.33
7.32
7.30
7.29
7.27
6.18
4.30
4.26
4.19
4.16
3.95
3.93
3.92
3.90
3.77
3.74
3.62
3.61
3.60
3.58
3.57
3.48
3.47
3.45
3.44
2.98
2.97
2.95
2.93
2.73
2.72
2.58
2.56
2.55
2.54
2.18
2.04
2.02
1.24
1.23
1.17
1.16
1.12
1.10
Bn
N
OH
O
79
Bn
N
O
Ph
OH
1.19
1.38
2.04
5.41
0.46
0.49
0.89
0.65
0.78
0.67
0.86
0.12
0.23
0.11
0.23
1.93
0.40
0.78
9.0
8.5
8.0
7.5
7.0
6.5
6.0
5.5
5.0
4.5
4.0
3.5
3.0
2.5
2.0
1.5
1.0
0.5
0.0
f1 (ppm)

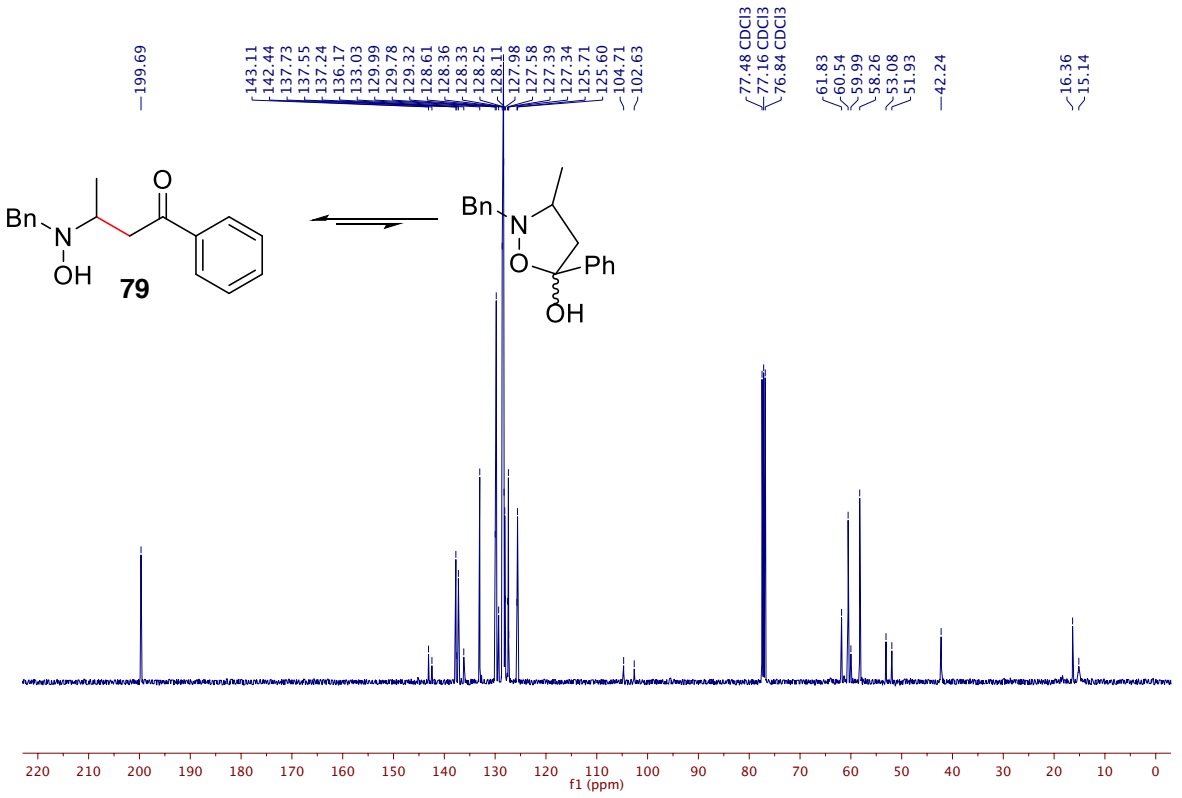
199.69
143.11
142.44
137.73
137.55
137.24
136.17
133.03
129.99
129.78
129.32
128.61
128.36
128.33
128.25
128.11
127.98
127.58
127.39
127.34
125.71
125.60
104.71
102.63
77.48 CDCl3
77.16 CDCl3
76.84 CDCl3
61.83
60.54
59.99
58.26
53.08
51.93
42.24
16.36
15.14
Bn
N
OH
O
79
Bn
N
O
Ph
OH
220
210
200
190
180
170
160
150
140
130
120
110
100
90
80
70
60
50
40
30
20
10
0
f1 (ppm)


7.98
7.67
7.66
7.55
7.48
7.44
7.39
7.38
7.36
7.34
7.33
7.27
7.26
7.16
7.12
7.10
7.08
7.00
6.99
6.86
5.09
4.86
4.85
3.83
3.76
3.74
3.41
3.40
3.31
3.29
3.19
3.02
2.99
2.93
2.91
2.50

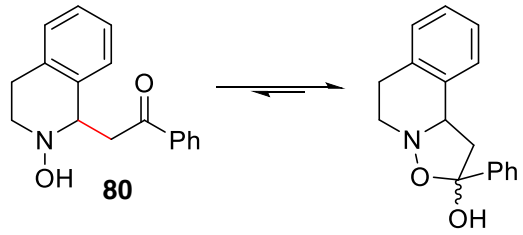
O
Ph
N
OH
80
N
O
Ph
OH

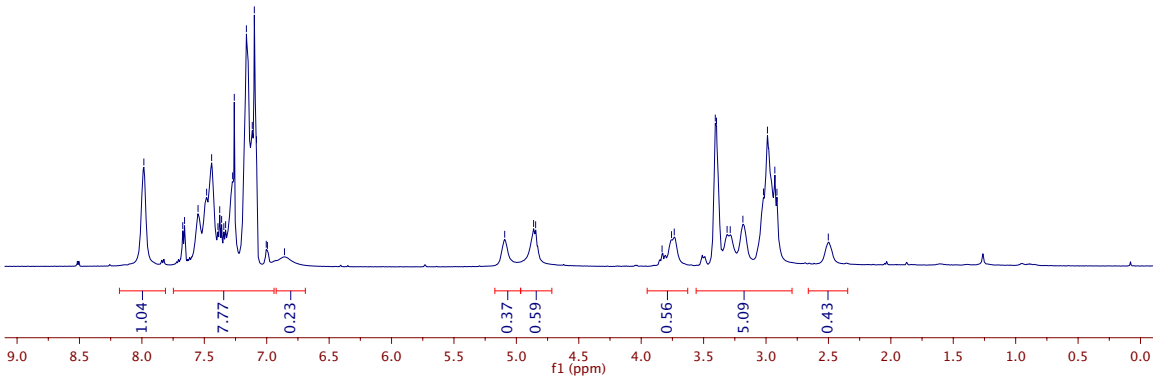
1.04
7.77
0.23
0.37
0.59
0.56
5.09
0.43
9.0
8.5
8.0
7.5
7.0
6.5
6.0
5.5
5.0
4.5
4.0
3.5
3.0
2.5
2.0
1.5
1.0
0.5
0.0
f1 (ppm)


7.94
7.92
7.85
7.83
7.51
7.50
7.49
7.40
7.39
7.37
7.36
7.34
7.33
7.26
7.20
7.19
7.18
7.17
7.15
7.12
7.11
5.30
3.81
3.80
3.77
3.76
3.74
3.73
3.72
3.53
3.52
3.50
3.49
3.48
3.43
3.42
3.39
3.22
3.21
3.19
3.18
3.16
3.08
3.07
3.06
3.05
3.04
3.03

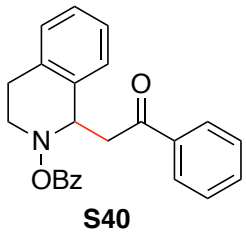
O
N
OBz
S40

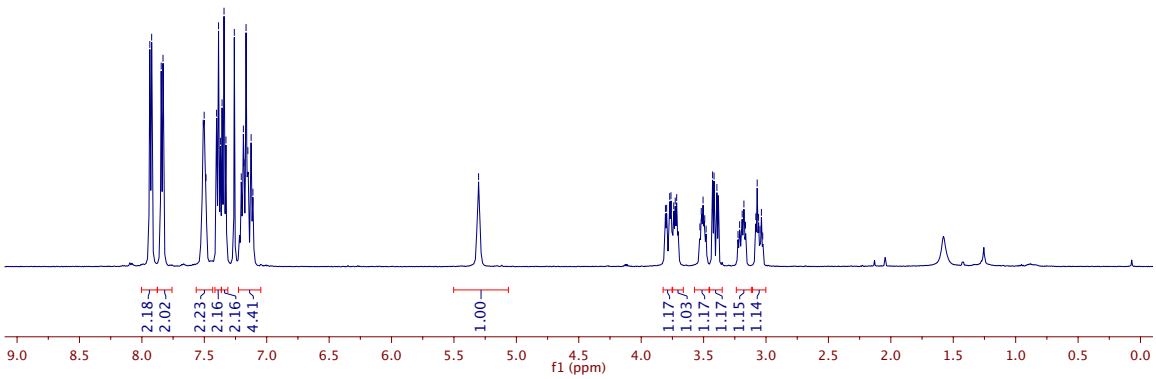
2.18
2.02
2.23
2.16
2.16
4.41
1.00
1.17
1.03
1.17
1.17
1.15
1.14
9.0
8.5
8.0
7.5
7.0
6.5
6.0
5.5
5.0
4.5
4.0
3.5
3.0
2.5
2.0
1.5
1.0
0.5
0.0
f1 (ppm)

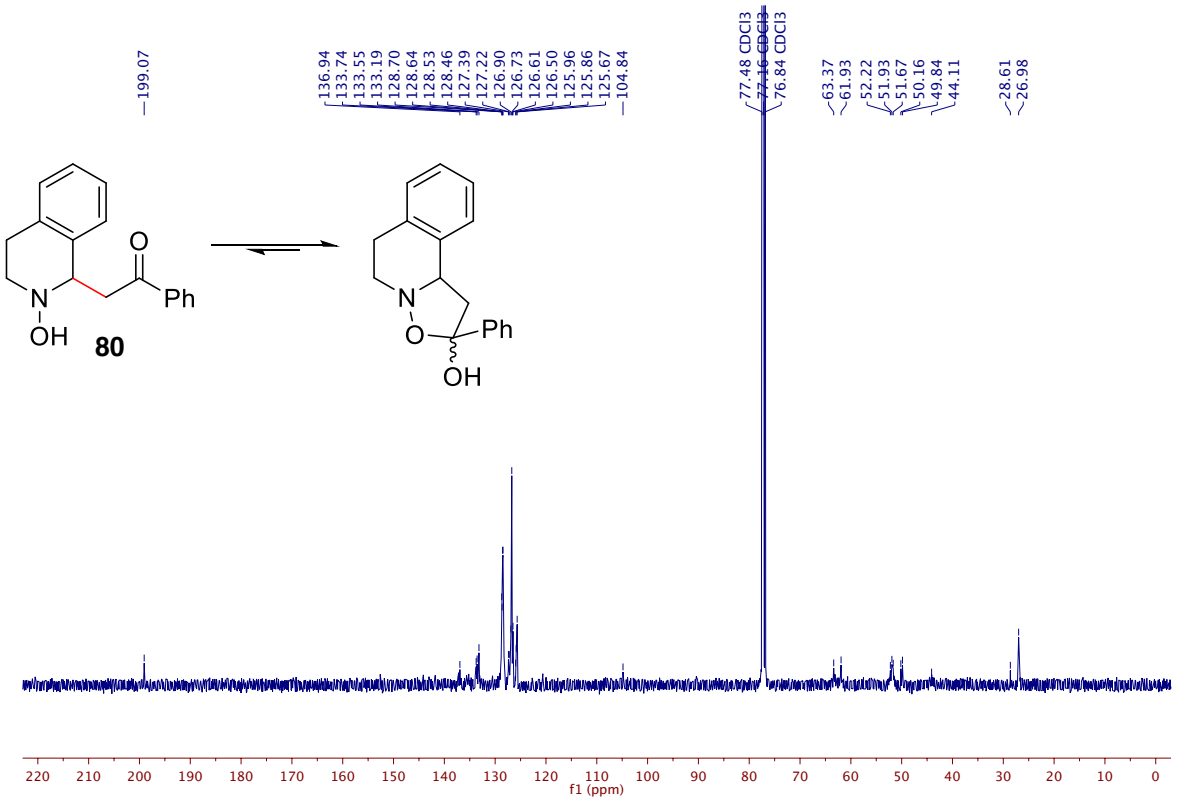
199.07
136.94
133.74
133.55
133.19
128.70
128.64
128.53
128.46
127.39
127.22
126.90
126.73
126.61
126.50
125.96
125.86
125.67
104.84
77.48 CDCl3
77.16 CDCl3
76.84 CDCl3
63.37
61.93
52.22
51.93
51.67
50.16
49.84
44.11
28.61
26.98
O
Ph
N
OH
80
N
O
Ph
OH
220 210 200 190 180 170 160 150 140 130 120 110 100 90 80 70 60 50 40 30 20 10 0
f1 (ppm)

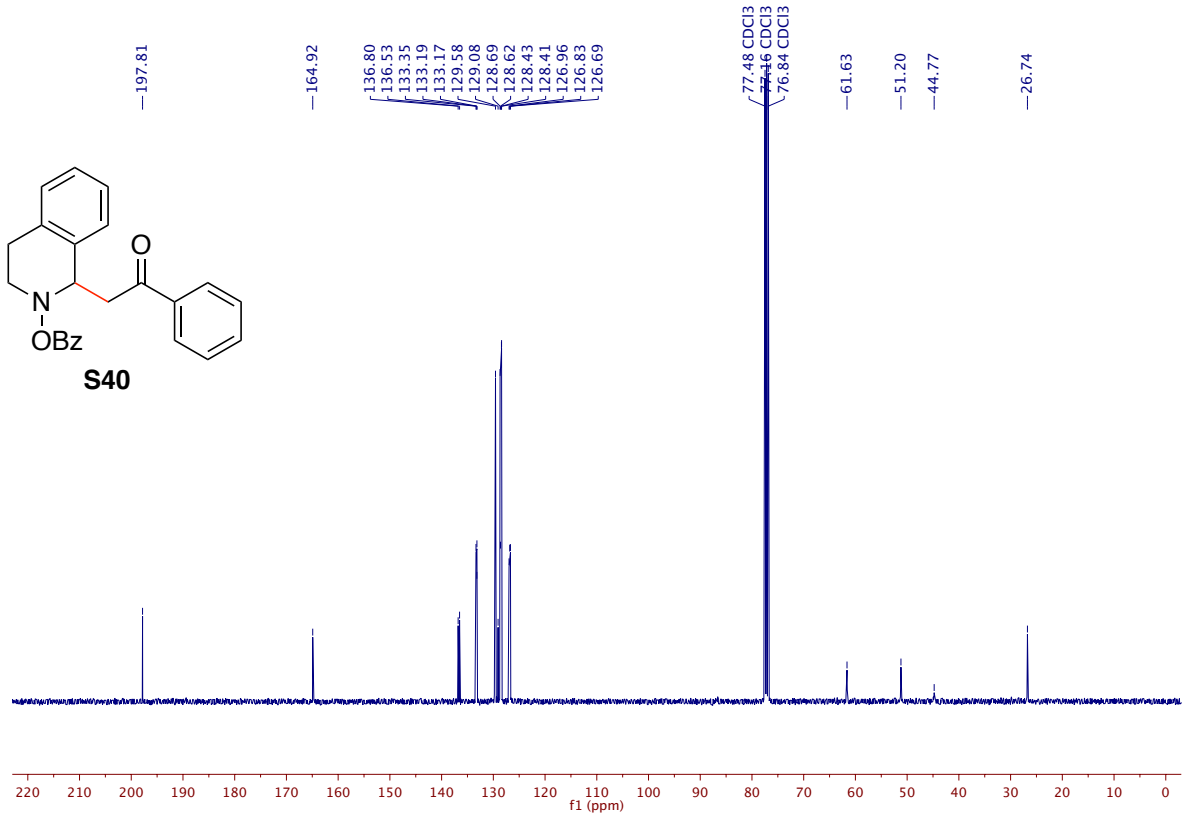
197.81
164.92
136.80
136.53
133.35
133.19
133.17
129.58
129.08
128.69
128.62
128.43
128.41
126.96
126.83
126.69
77.48 CDCl3
77.16 CDCl3
76.84 CDCl3
61.63
51.20
44.77
26.74
O
N
OBz
S40
220 210 200 190 180 170 160 150 140 130 120 110 100 90 80 70 60 50 40 30 20 10 0
f1 (ppm)

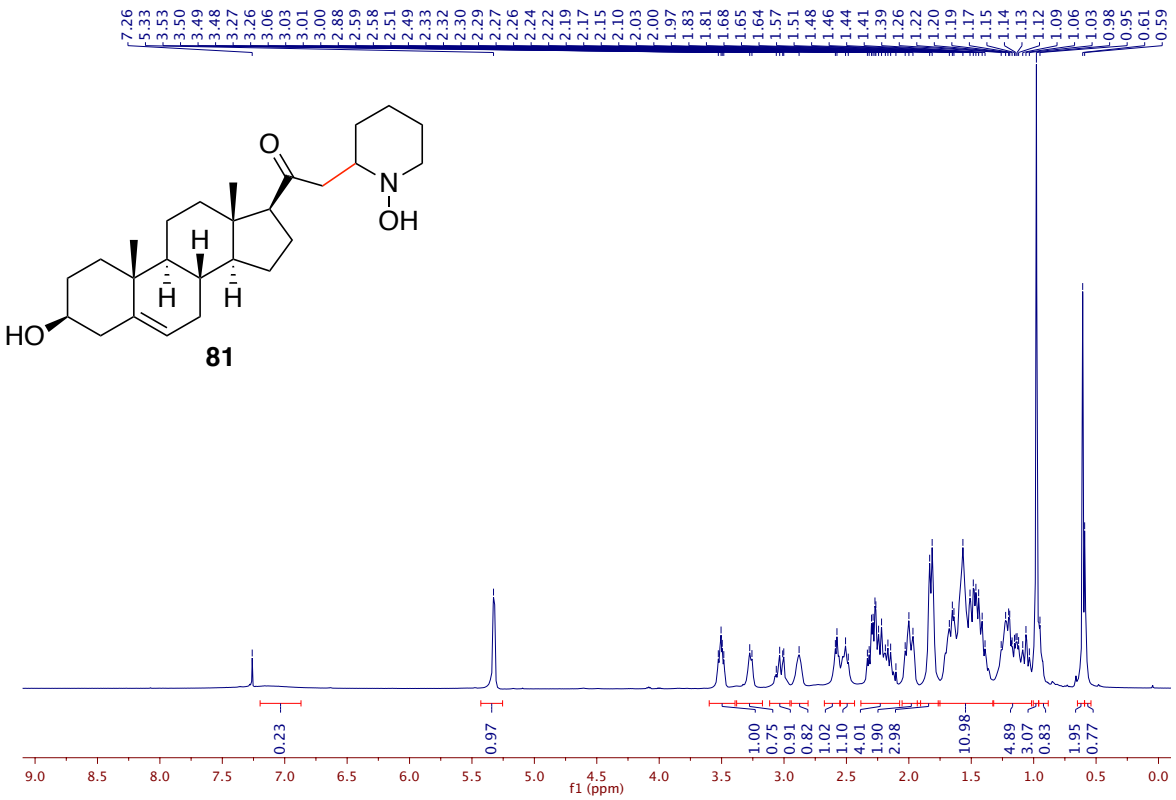
7.26
5.33
3.53
3.50
3.49
3.48
3.27
3.26
3.06
3.03
3.01
3.00
2.88
2.59
2.58
2.51
2.49
2.33
2.32
2.30
2.29
2.27
2.26
2.24
2.22
2.19
2.17
2.15
2.10
2.03
2.00
1.97
1.83
1.81
1.68
1.65
1.64
1.57
1.51
1.48
1.46
1.44
1.41
1.39
1.26
1.22
1.20
1.19
1.17
1.15
1.14
1.13
1.12
1.09
1.06
1.03
0.98
0.95
0.61
0.59
O
N
OH
H
H
H
HO
81
0.23
0.97
1.00
0.75
0.91
0.82
1.02
1.10
4.01
1.90
2.98
10.98
4.89
3.07
0.83
1.95
0.77
9.0
8.5
8.0
7.5
7.0
6.5
6.0
5.5
5.0
4.5
4.0
3.5
3.0
2.5
2.0
1.5
1.0
0.5
0.0
f1 (ppm)

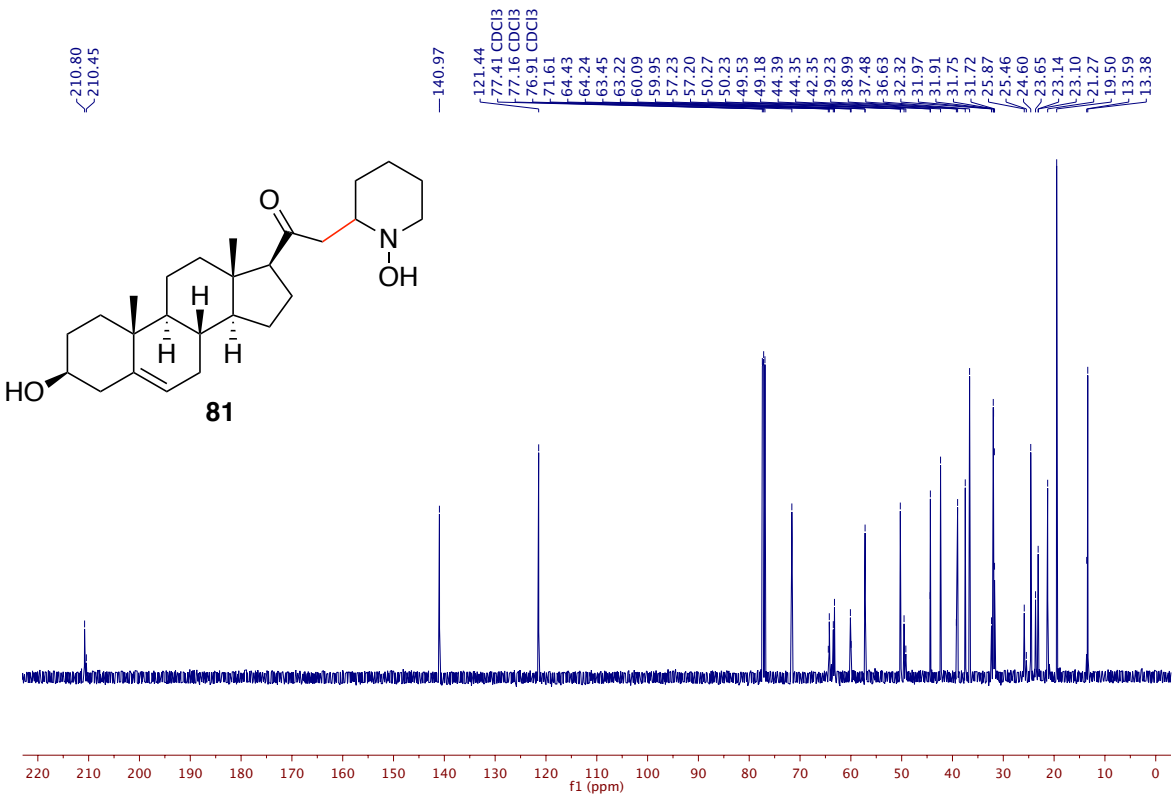
210.80
210.45
140.97
121.44
77.41 CDCl3
77.16 CDCl3
76.91 CDCl3
71.61
64.43
64.24
63.45
63.22
60.09
59.95
57.23
57.20
50.27
50.23
49.53
49.18
44.39
44.35
42.35
39.23
38.99
37.48
36.63
32.32
31.97
31.91
31.75
31.72
25.87
25.46
24.60
23.65
23.14
23.10
21.27
19.50
13.59
13.38
O
N
OH
H
H
H
HO
81
220
210
200
190
180
170
160
150
140
130
120
110
100
90
80
70
60
50
40
30
20
10
0
f1 (ppm)

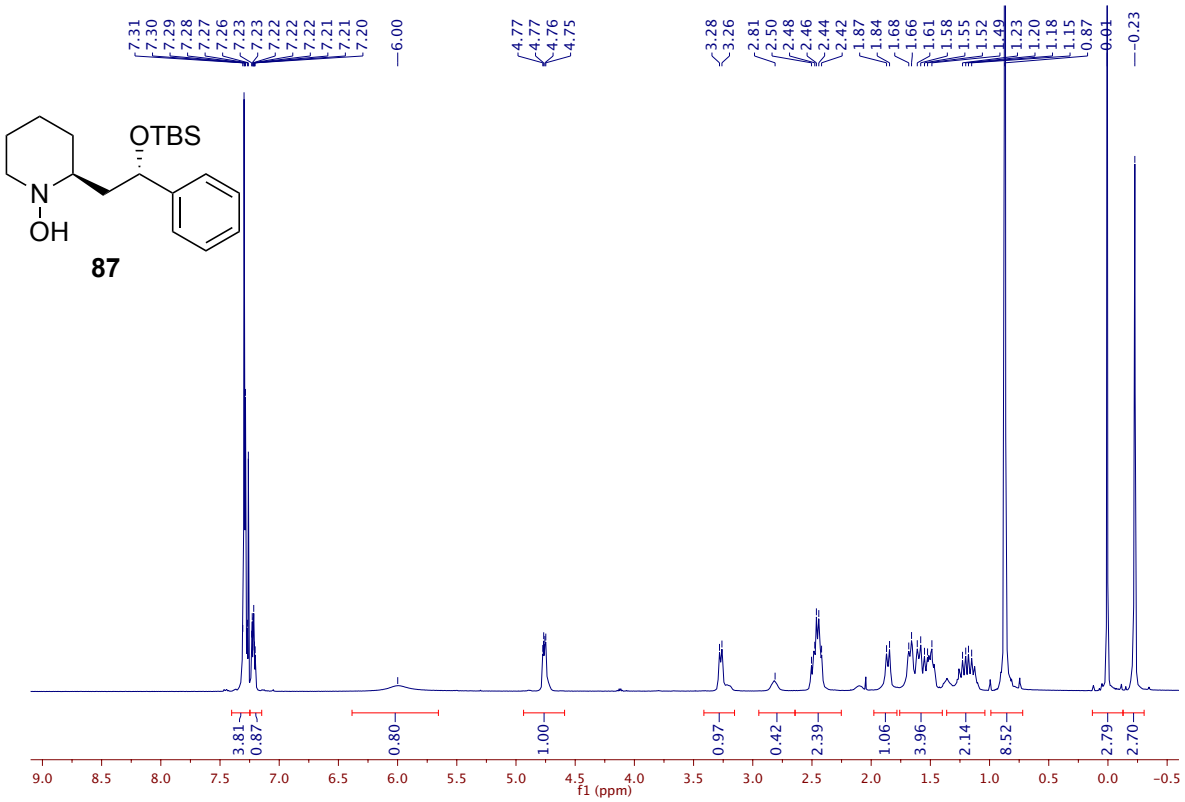
OTBS
N
OH
87
f1 (ppm)

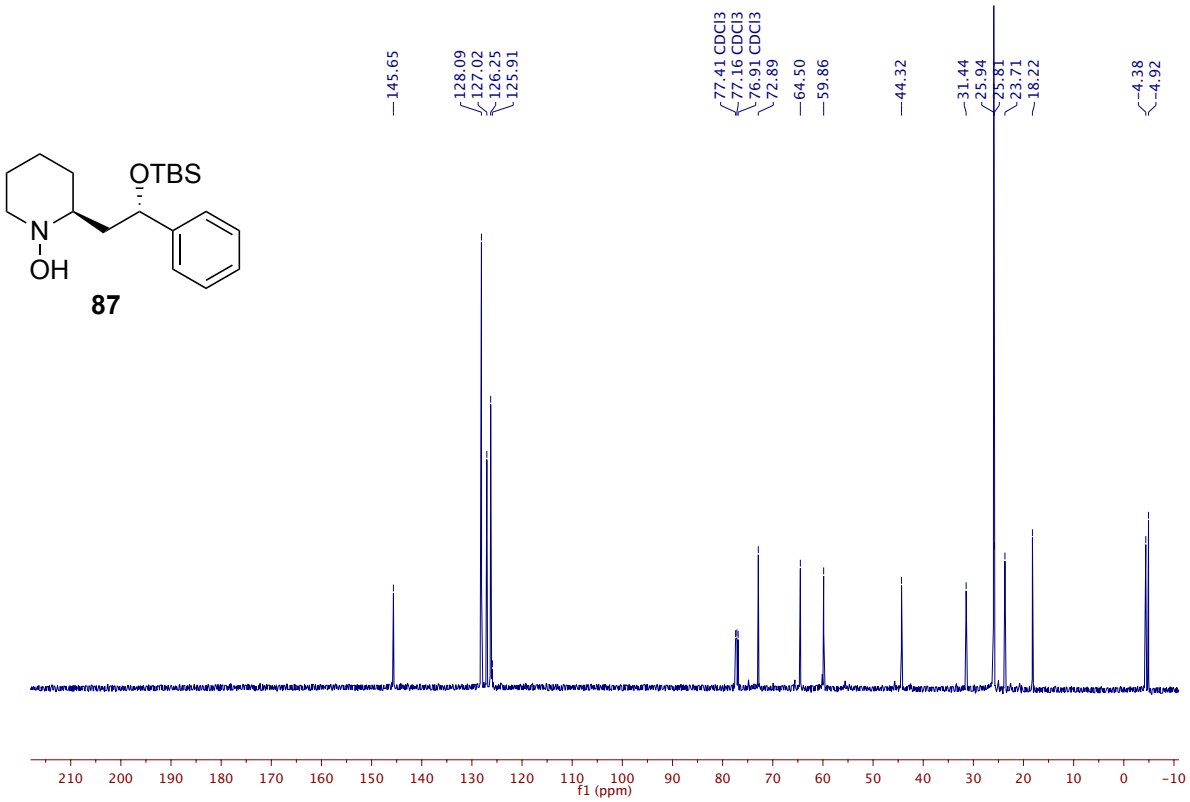
OTBS
N
OH
87
f1 (ppm)

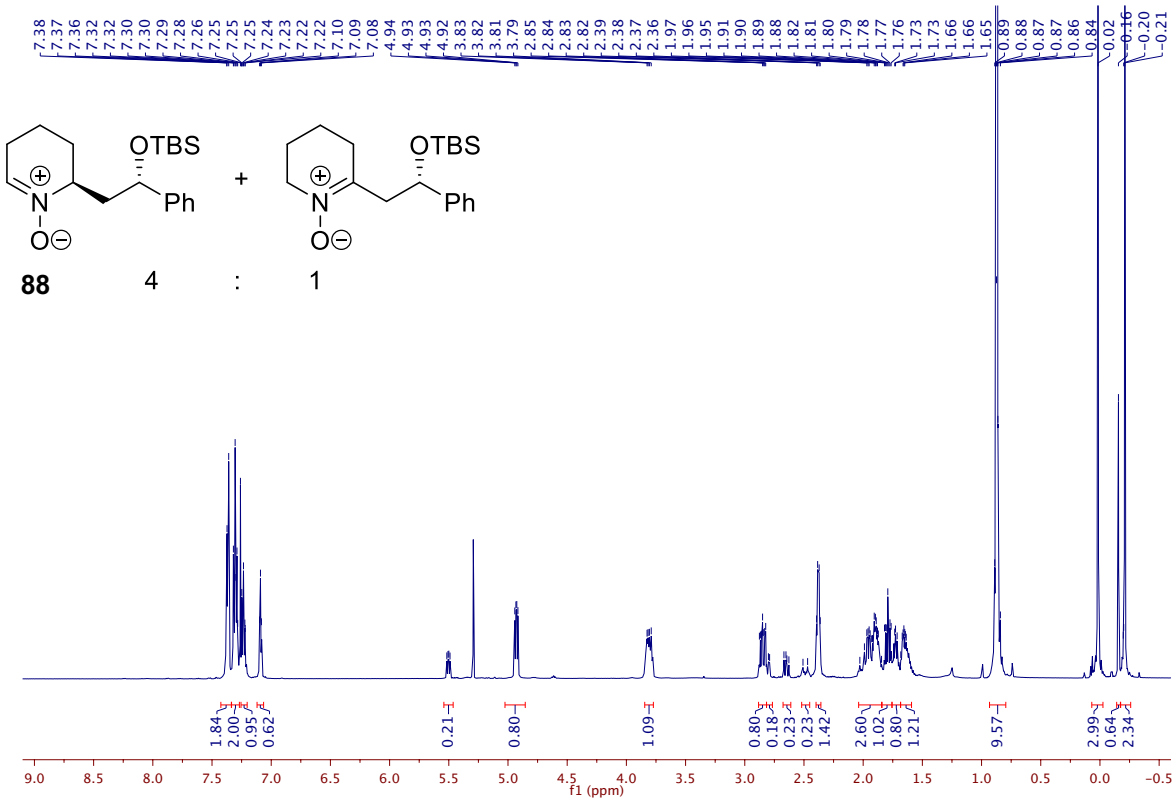
OTBS
Ph
+
OTBS
Ph
88
4
:
1
f1 (ppm)

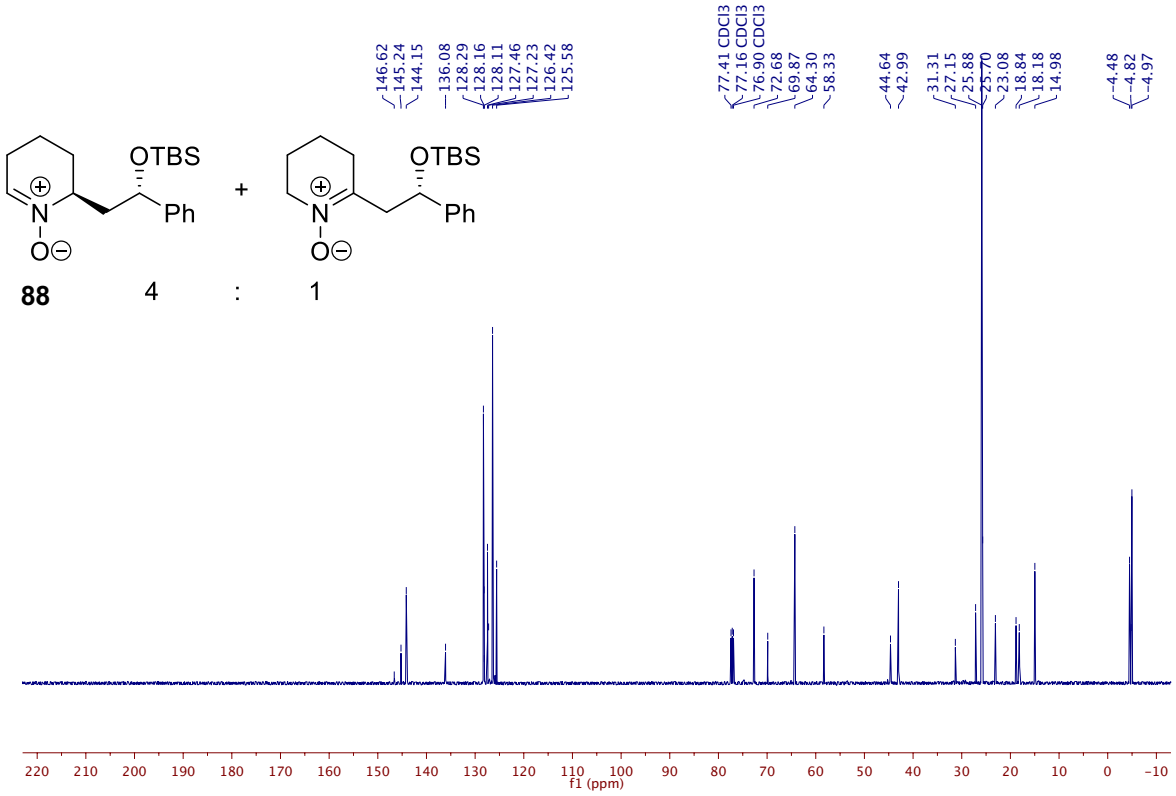
OTBS
Ph
+
OTBS
Ph
88
4
:
1
f1 (ppm)

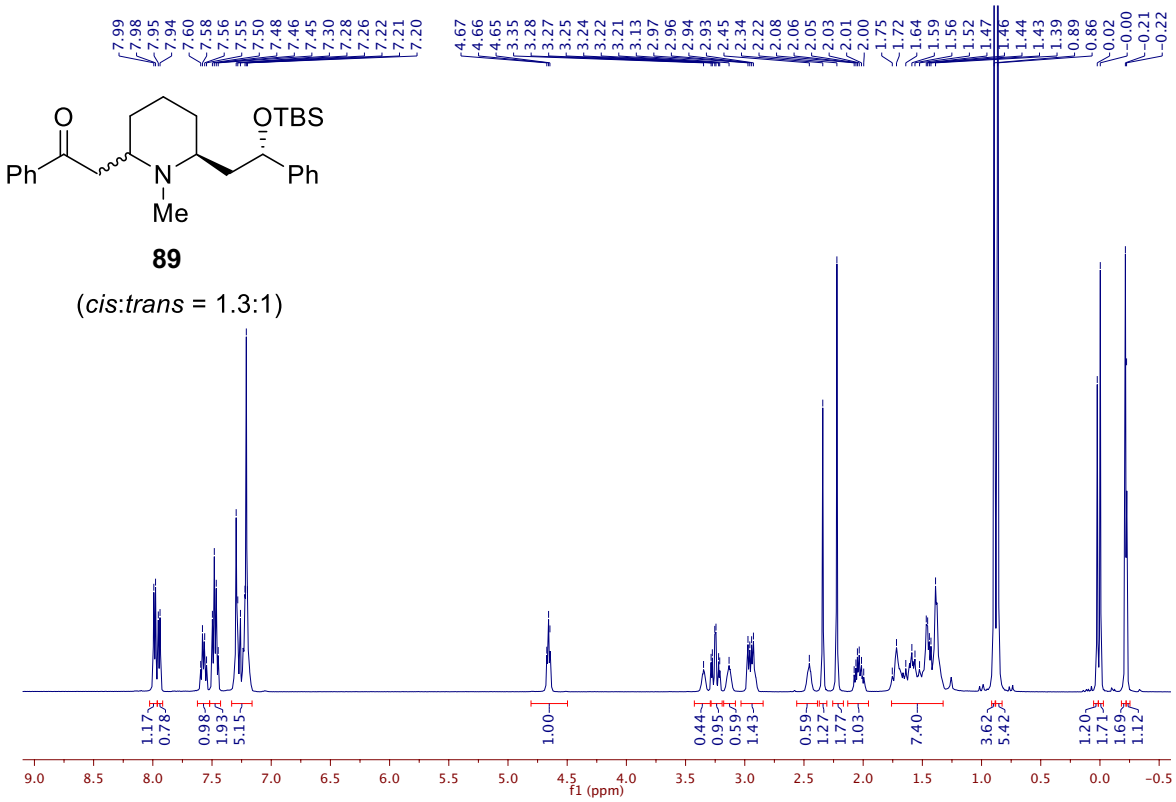

89

(*cis*:*trans* = 1.3:1)

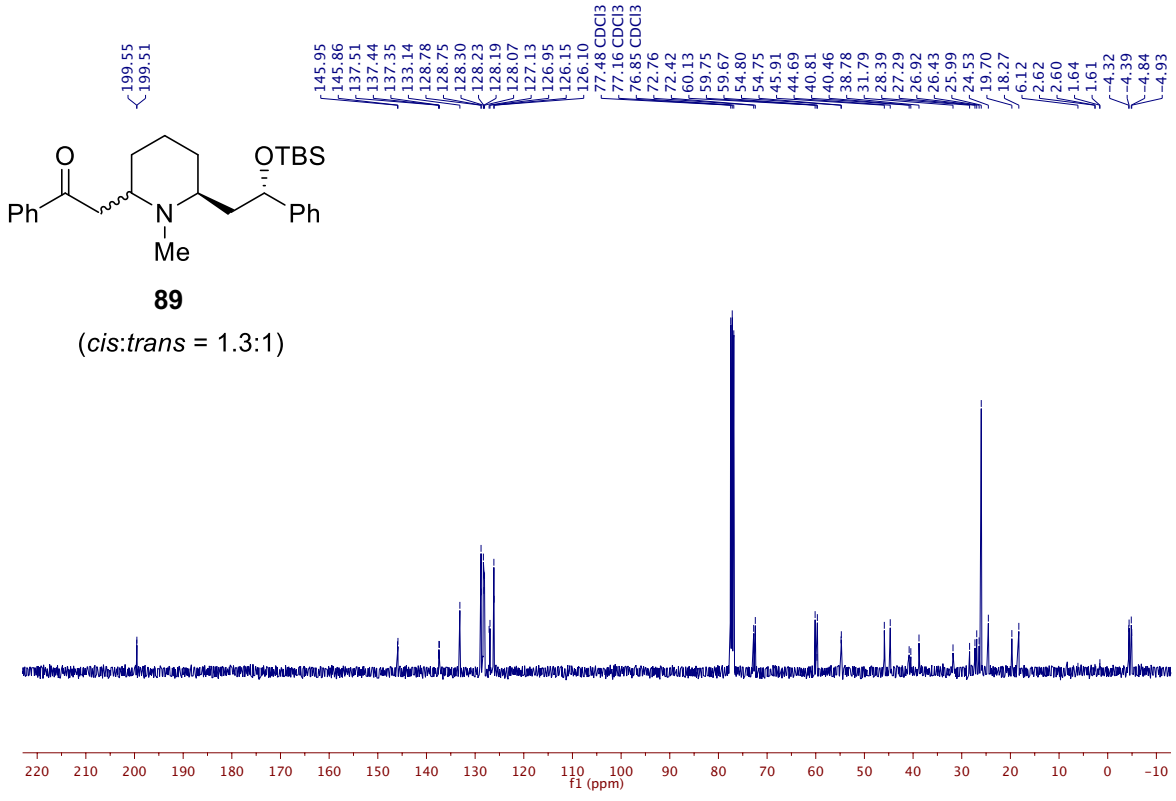

89

(*cis*:*trans* = 1.3:1)

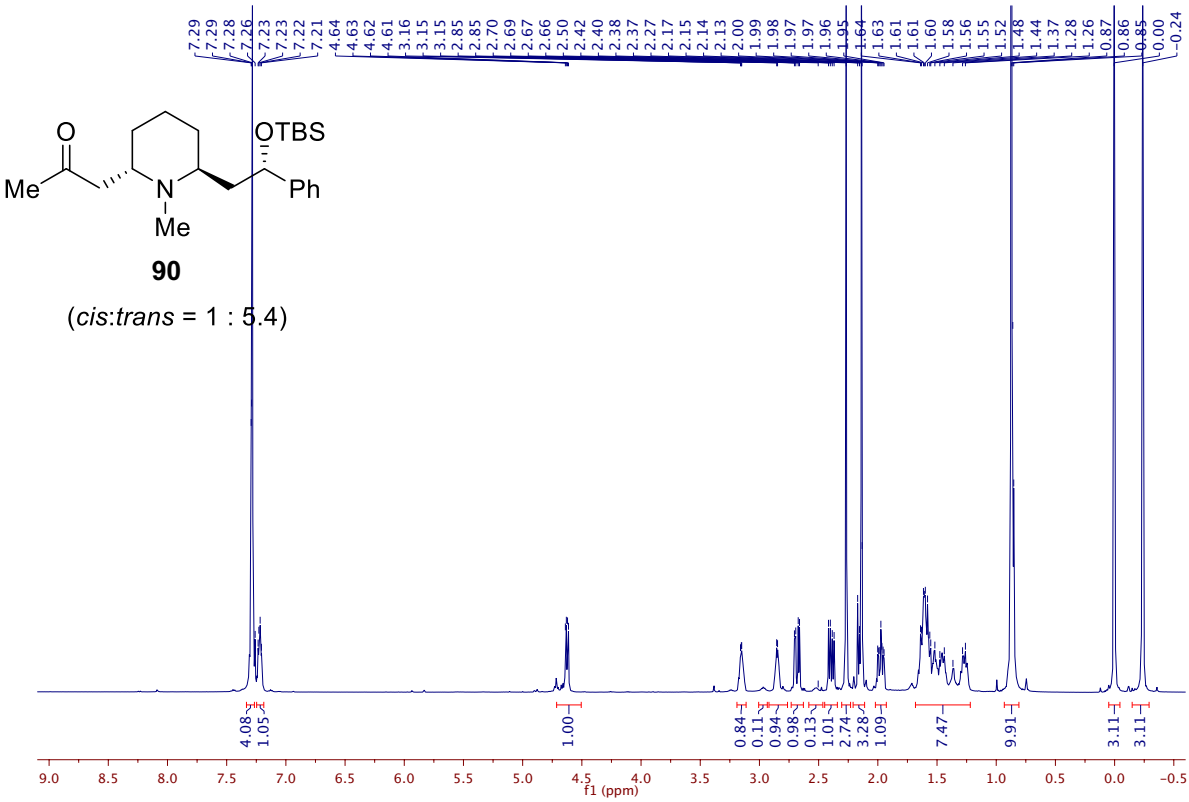

90

(*cis*:*trans* = 1 : 5.4)

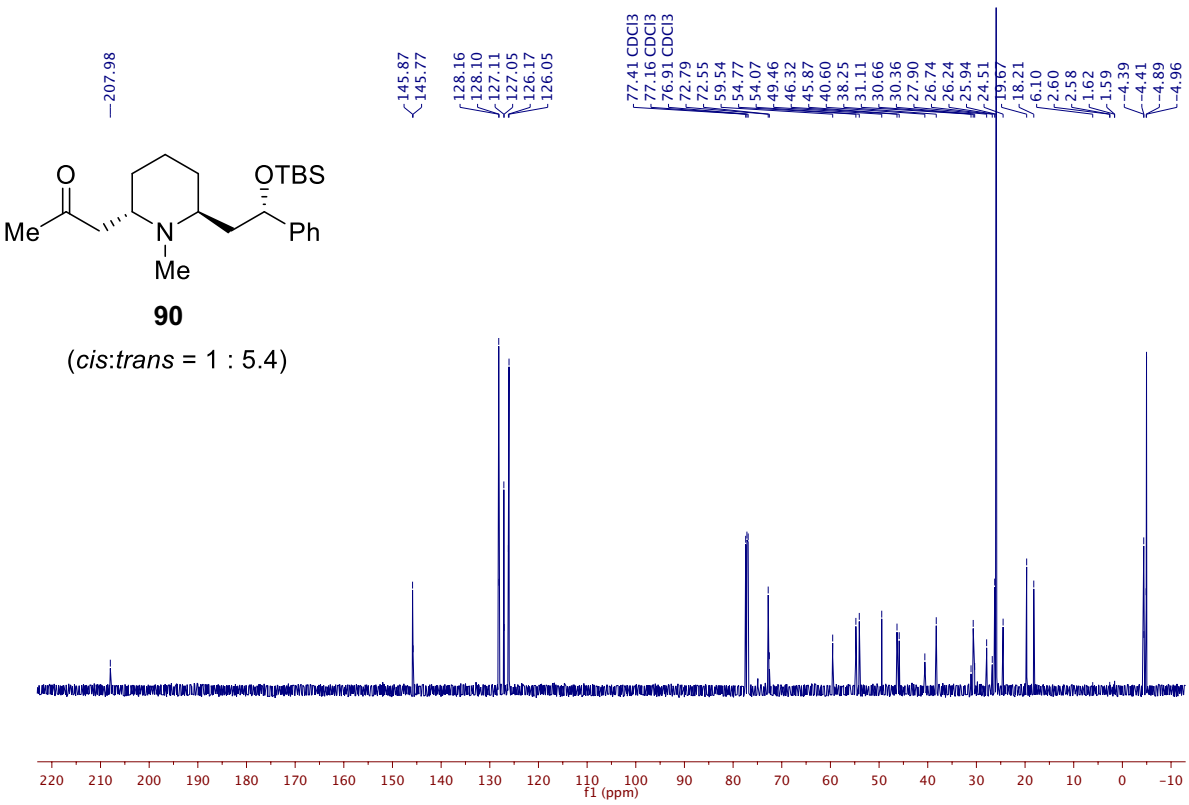

90

(*cis*:*trans* = 1 : 5.4)

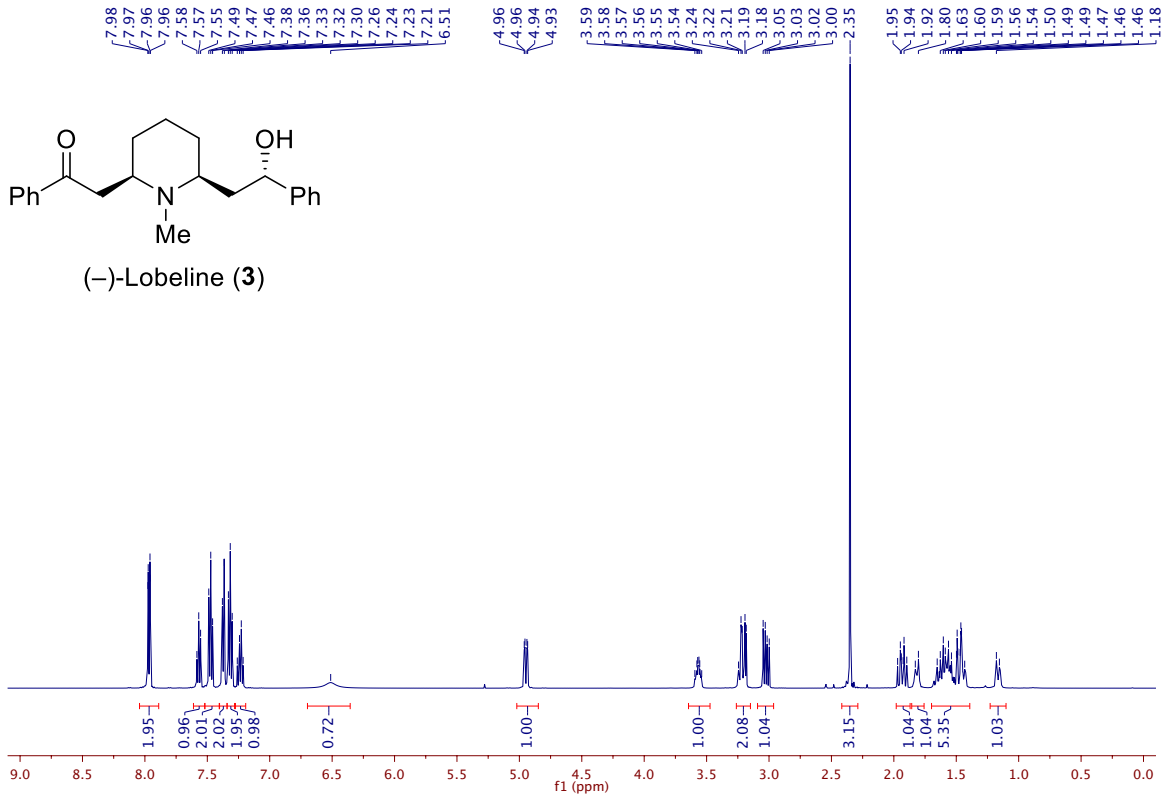
7.98
7.97
7.96
7.96
7.58
7.57
7.55
7.49
7.47
7.46
7.38
7.36
7.33
7.32
7.30
7.26
7.24
7.23
7.21
6.51
4.96
4.96
4.94
4.93
3.59
3.58
3.57
3.56
3.55
3.54
3.24
3.22
3.21
3.19
3.18
3.05
3.03
3.02
3.00
2.35
1.95
1.94
1.92
1.80
1.63
1.60
1.59
1.56
1.54
1.50
1.49
1.49
1.47
1.46
1.46
1.18
O
OH
Ph
N
Ph
Me
(–)-Lobeline (3)
1.95
0.96
2.01
2.02
1.95
0.98
0.72
1.00
1.00
2.08
1.04
3.15
1.04
1.04
5.35
1.03
9.0
8.5
8.0
7.5
7.0
6.5
6.0
5.5
5.0
4.5
4.0
3.5
3.0
2.5
2.0
1.5
1.0
0.5
0.0
f1 (ppm)

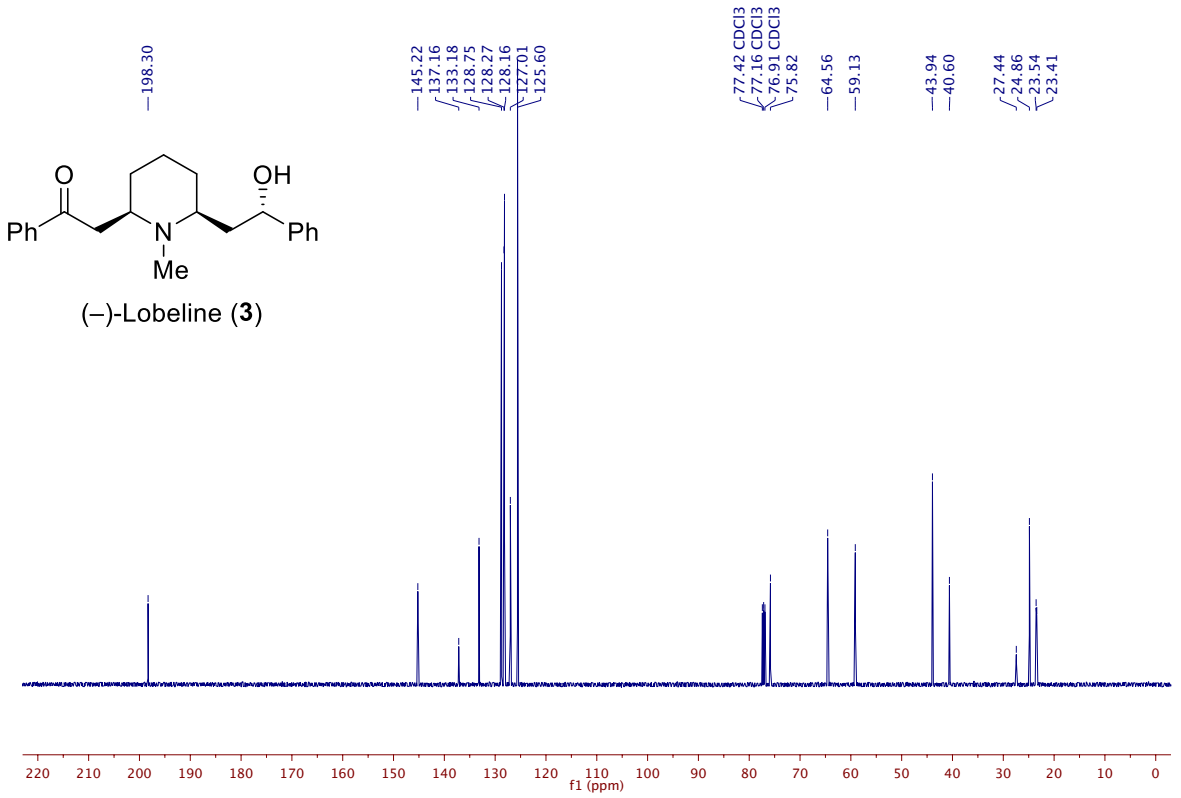
198.30
145.22
137.16
133.18
128.75
128.27
128.16
127.01
125.60
77.42 CDCl3
77.16 CDCl3
76.91 CDCl3
75.82
64.56
59.13
43.94
40.60
27.44
24.86
23.54
23.41
O
OH
Ph
N
Ph
Me
(–)-Lobeline (3)
220
210
200
190
180
170
160
150
140
130
120
110
100
90
80
70
60
50
40
30
20
10
0
f1 (ppm)

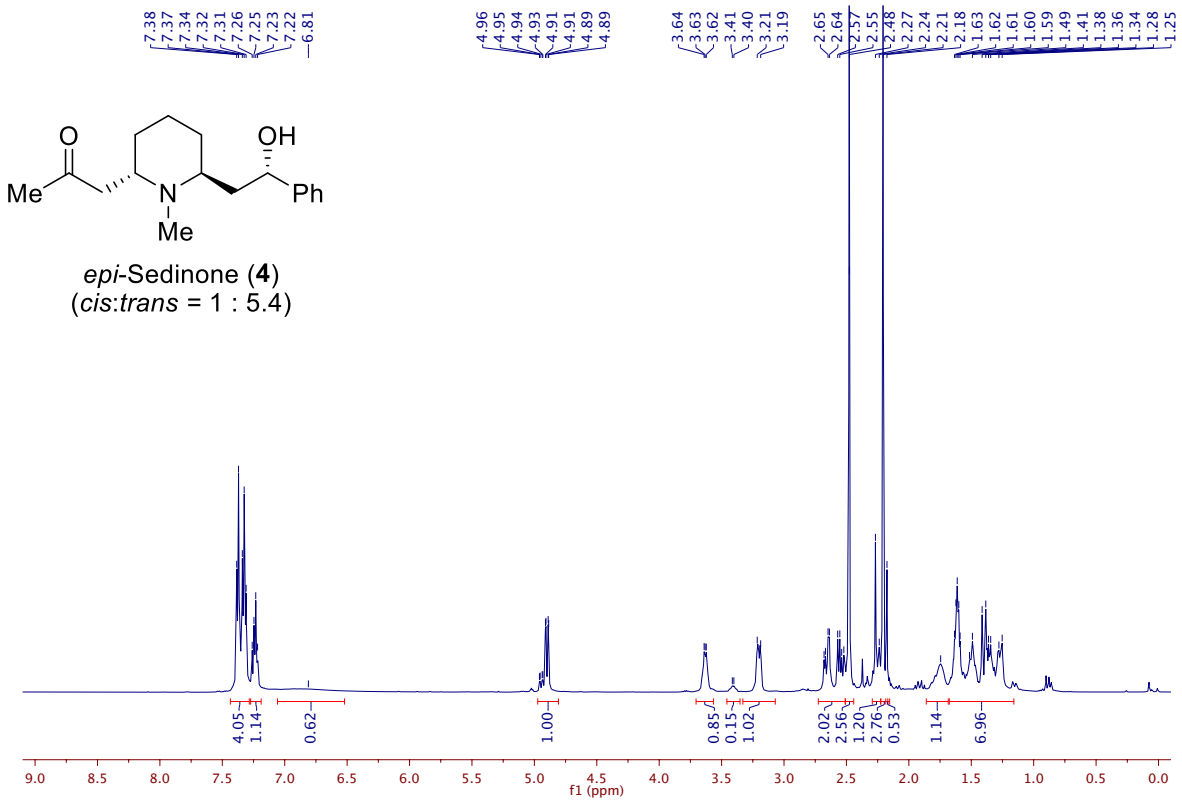

epi-Sedinone (**4**)
(*cis*:*trans* = 1 : 5.4)

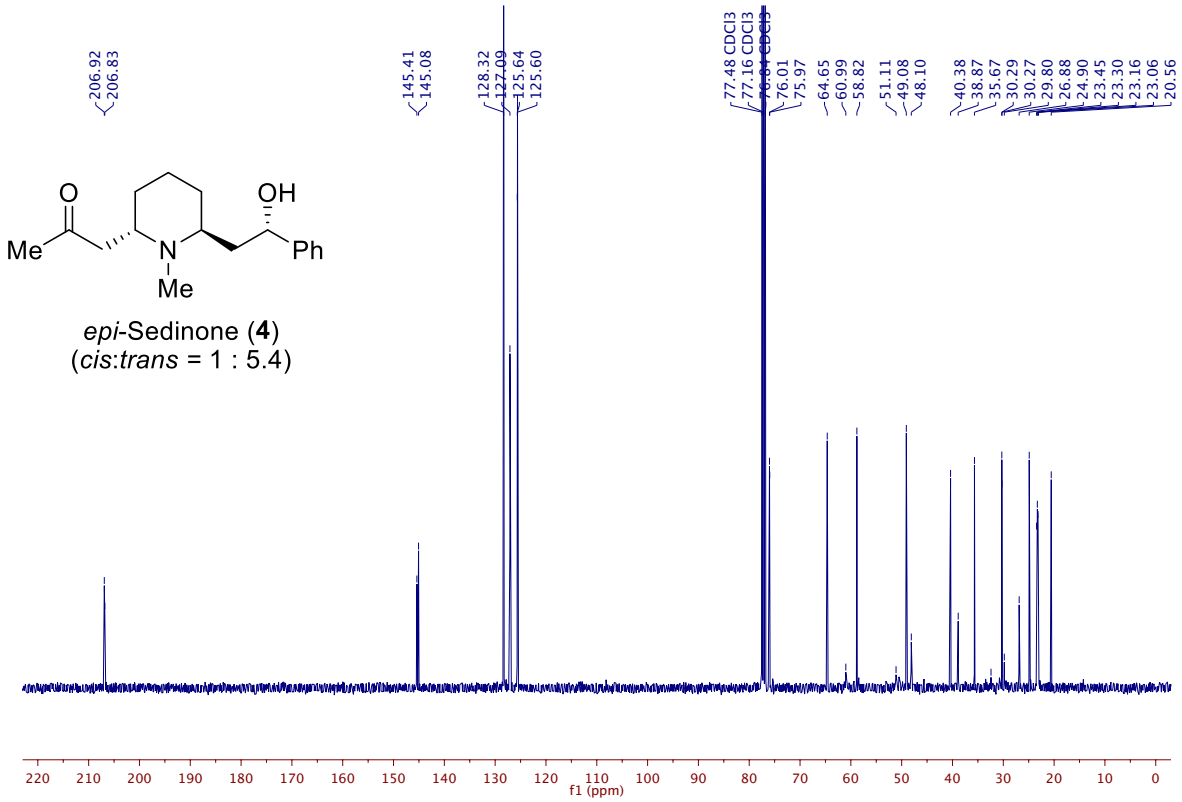

epi-Sedinone (**4**)
(*cis*:*trans* = 1 : 5.4)

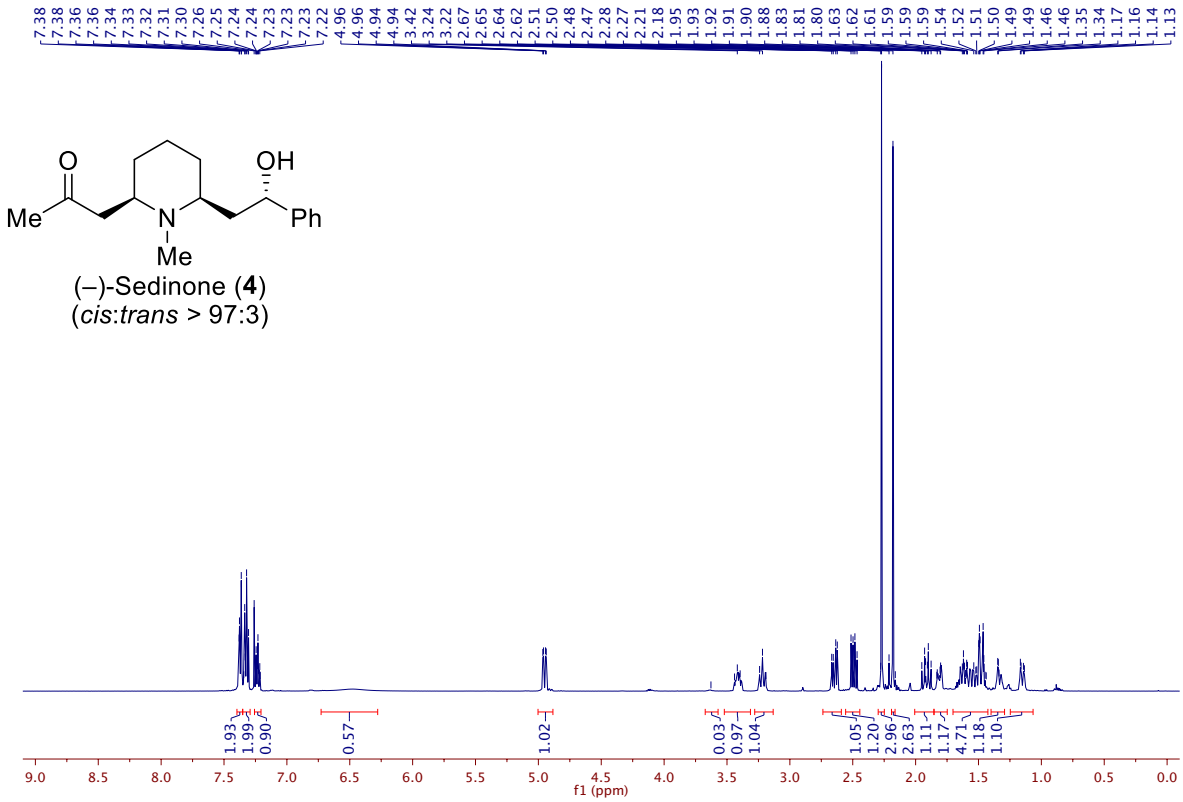

(–)-Sedinone (**4**)
(*cis*:*trans* > 97:3)

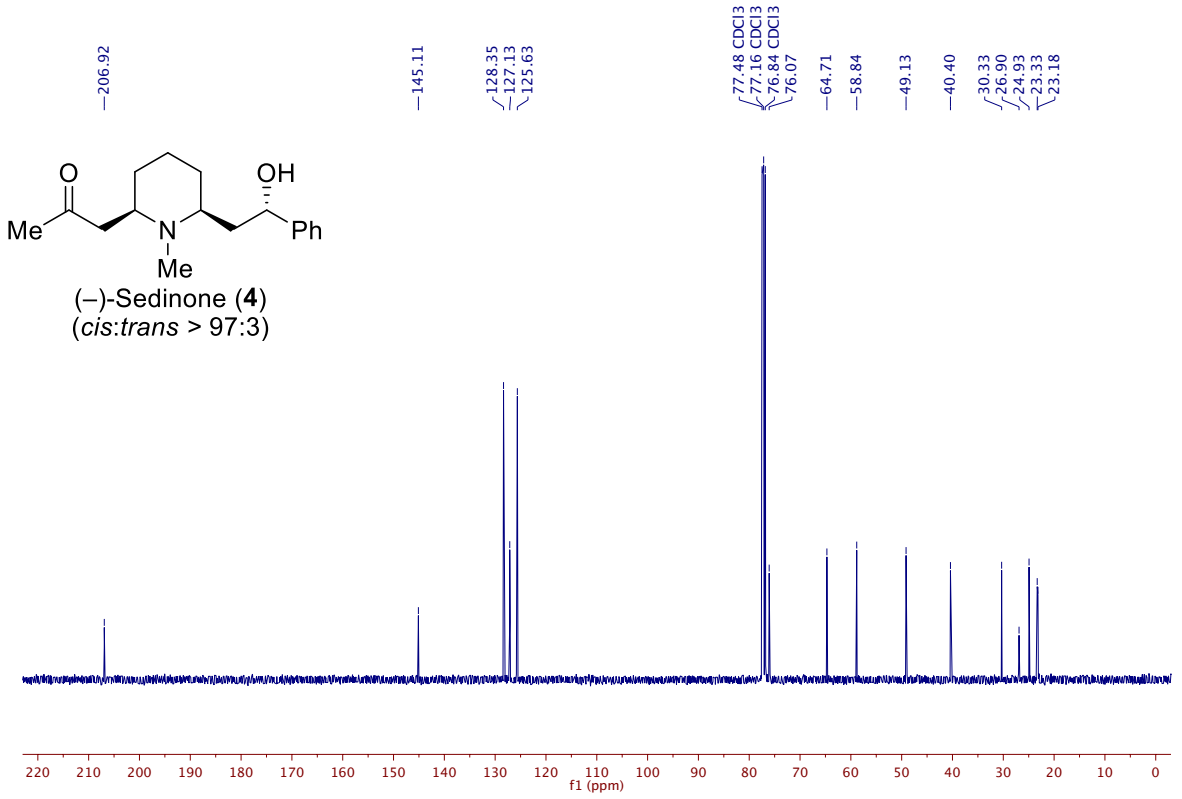

(–)-Sedinone (**4**)
(*cis*:*trans* > 97:3)

2.9 HPLC Traces

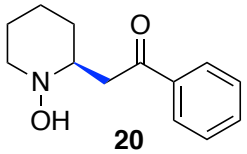

20

Conditions: HPLC (ChiralPak OD-H, 98:2 hexanes/*i*-PrOH, 1 mL/min, 254 nm)

Racemic Sample:

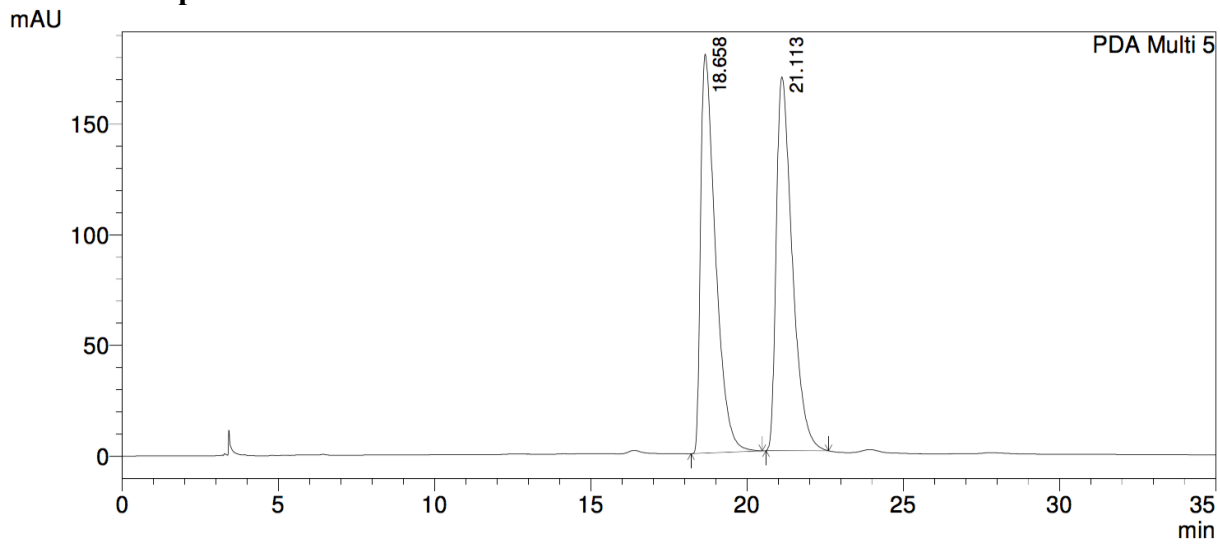

Peak#	Ret. Time	Area	Height	Area %	Height %
1	18.658	5952142	180281	49.728	51.632
2	21.113	6017315	168884	50.272	48.368
Total		11969457	349165	100.000	100.000

Enantioenriched Sample:

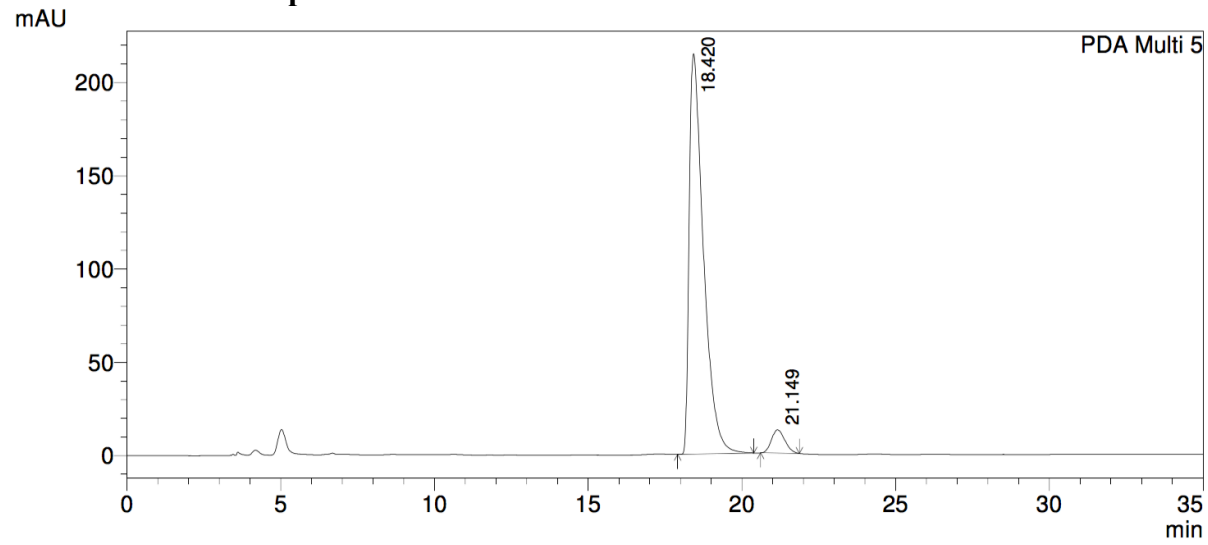

Peak#	Ret. Time	Area	Height	Area %	Height %
1	18.420	6924486	214602	94.789	94.506
2	21.149	380680	12476	5.211	5.494
Total		7305165	227077	100.000	100.000

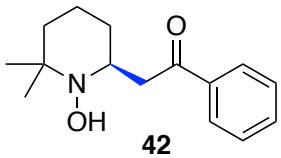

42

Conditions: HPLC (ChiralPak IA, 98:2 hexanes/*i*-PrOH, 1 mL/min, 220 nm)

Racemic Sample:

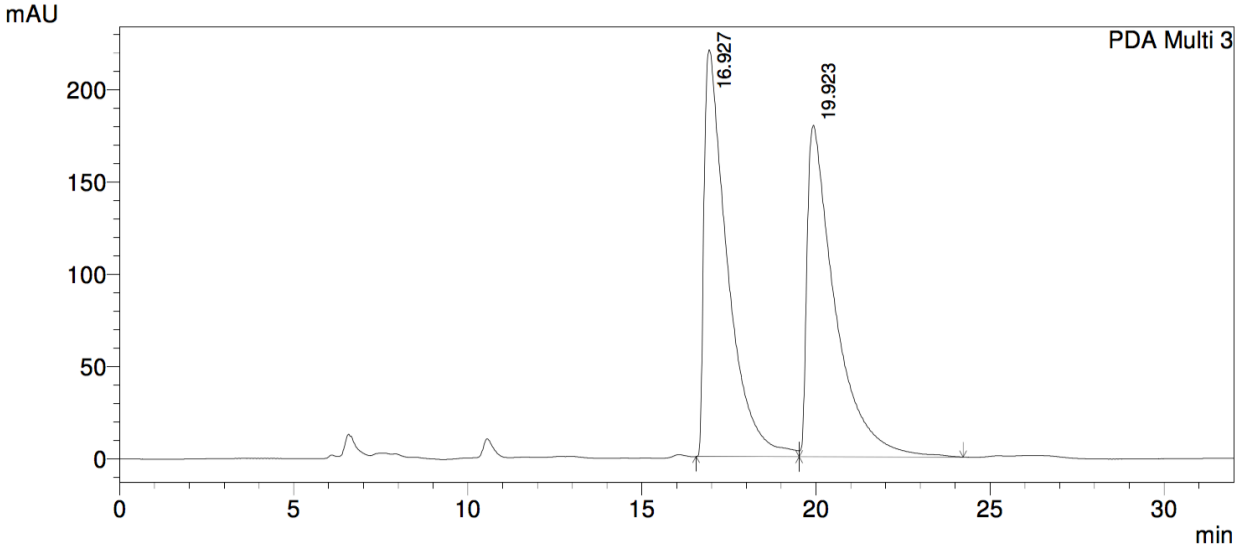

Peak#	Ret. Time	Area	Height	Area %	Height %
1	16.927	10303750	220564	50.692	55.097
2	19.923	10022590	179757	49.308	44.903
Total		20326340	400321	100.000	100.000

Enantioenriched Sample:

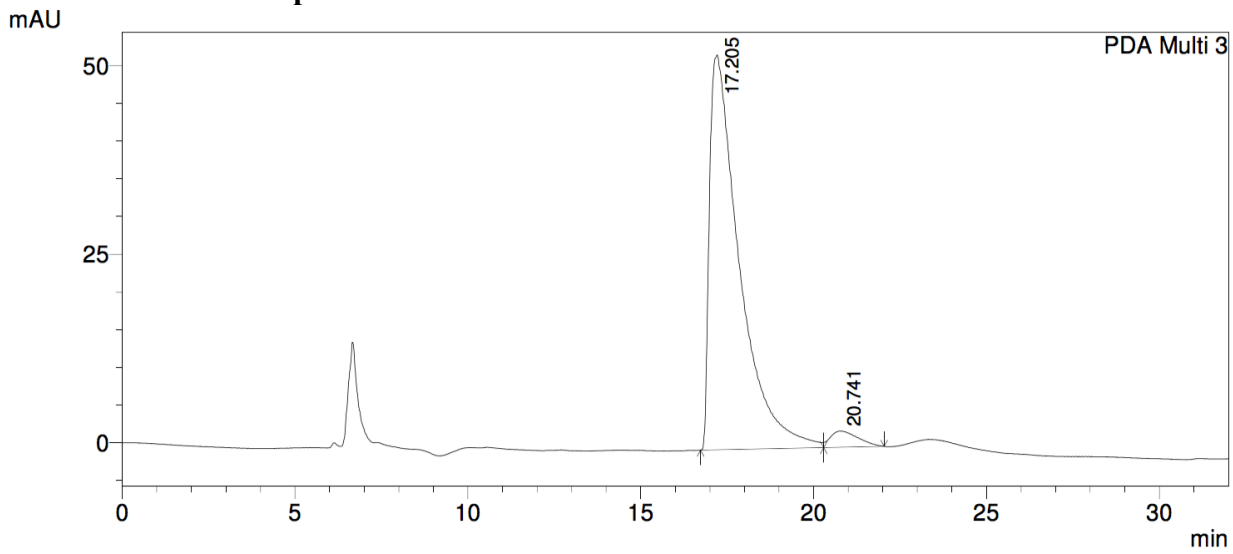

Peak#	Ret. Time	Area	Height	Area %	Height %
1	17.205	3139360	52311	96.361	96.055
2	20.741	118539	2149	3.639	3.945
Total		3257899	54460	100.000	100.000

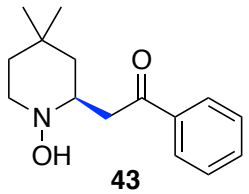

43

Conditions: HPLC (ChiralPak IA, 98:2 hexanes/*i*-PrOH, 1 mL/min, 254 nm)

Racemic sample:

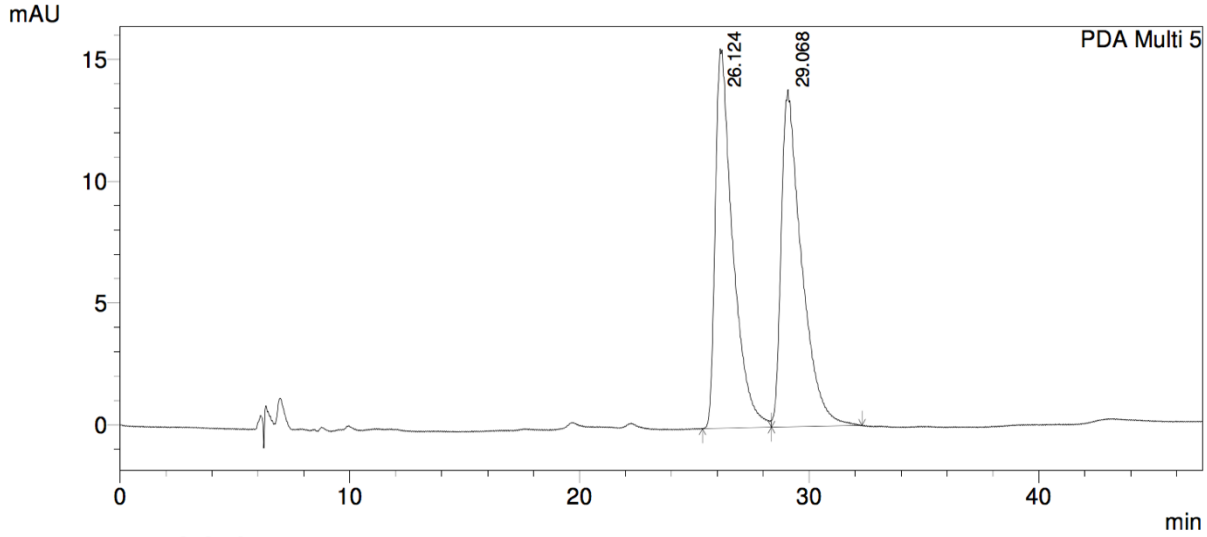

Peak#	Ret. Time	Area	Height	Area %	Height %
1	26.124	828397	15584	49.303	52.954
2	29.068	851823	13846	50.697	47.046
Total		1680220	29430	100.000	100.000

Enantioenriched Sample:

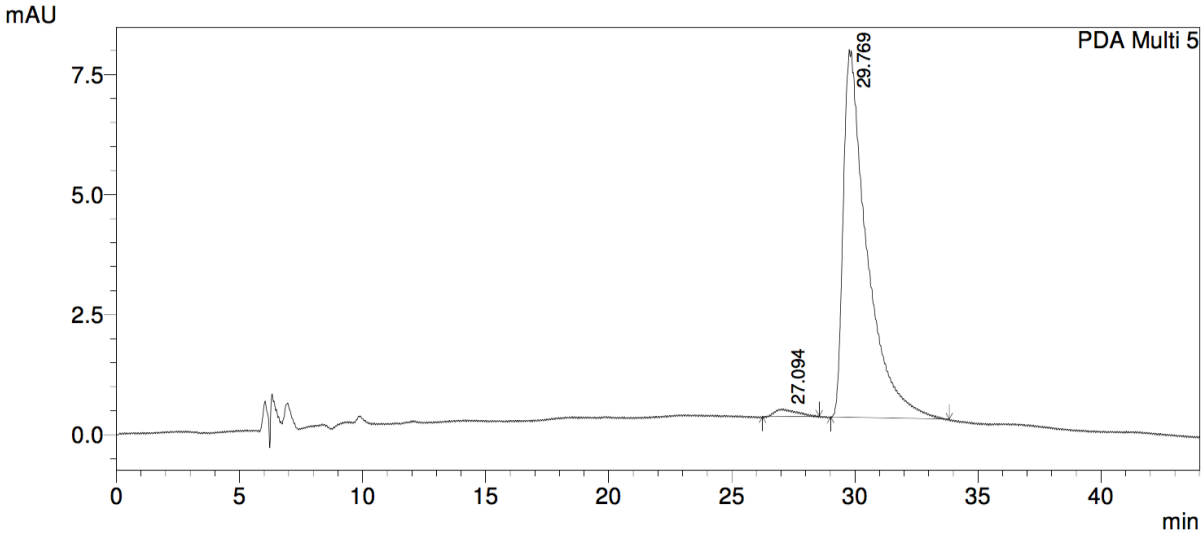

Peak#	Ret. Time	Area	Height	Area %	Height %
1	27.094	8901	160	1.714	2.050
2	29.769	510388	7649	98.286	97.950
Total		519289	7809	100.000	100.000

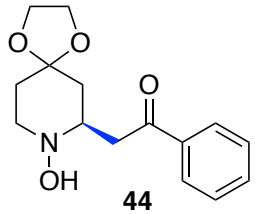

44

Conditions: HPLC (ChiralPak OD-H, 95:5 hexanes/*i*-PrOH, 1 mL/min, 254 nm)

Racemic Sample:

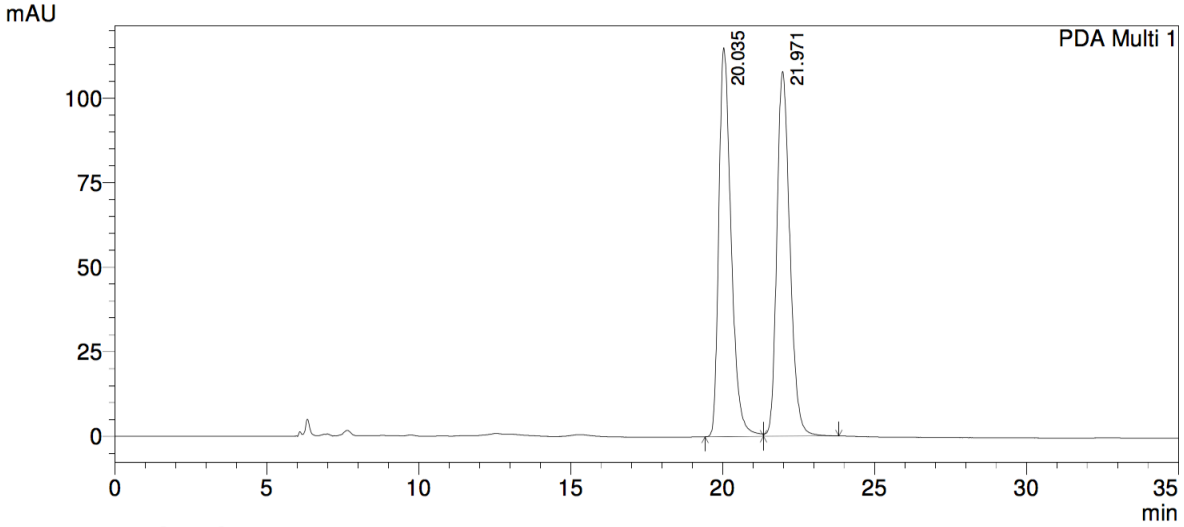

Peak#	Ret. Time	Area	Height	Area %	Height %
1	20.035	3239277	114984	50.092	51.596
2	21.971	3227422	107872	49.908	48.404
Total		6466699	222856	100.000	100.000

Enantioenriched Sample:

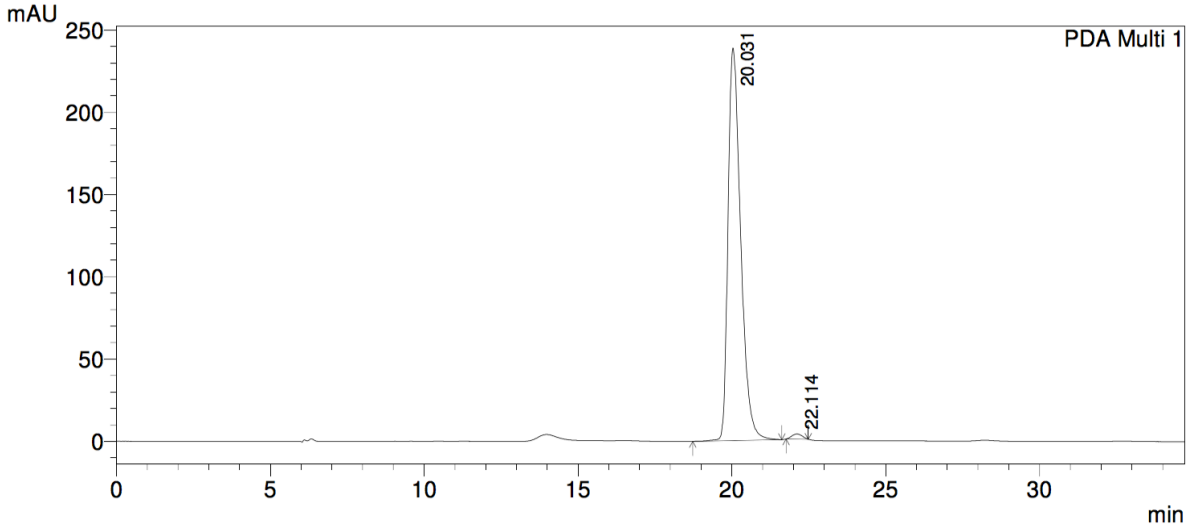

Peak#	Ret. Time	Area	Height	Area %	Height %
1	20.031	6830704	238510	98.927	98.689
2	22.114	74057	3169	1.073	1.311
Total		6904761	241679	100.000	100.000

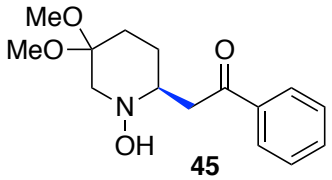

45

Conditions: HPLC (ChiralPak OD-H, 90:10 hexanes/*i*-PrOH, 1 mL/min, 254 nm)

Racemic Sample:

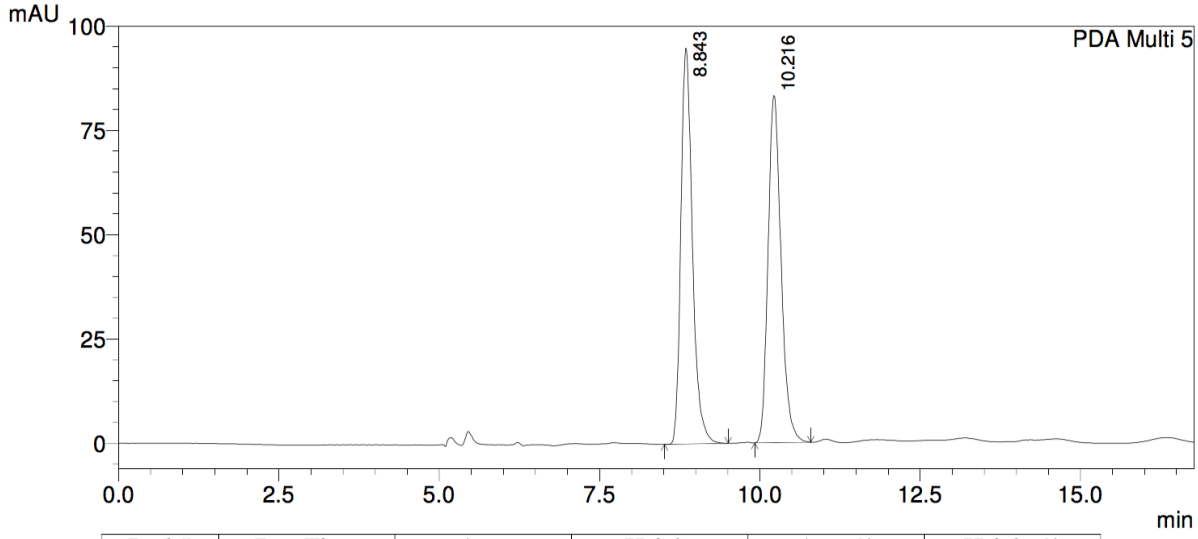

Peak#	Ret. Time	Area	Height	Area %	Height %
1	8.843	1188162	94811	50.277	53.269
2	10.216	1175064	83176	49.723	46.731
Total		2363226	177987	100.000	100.000

Enantioenriched Sample:

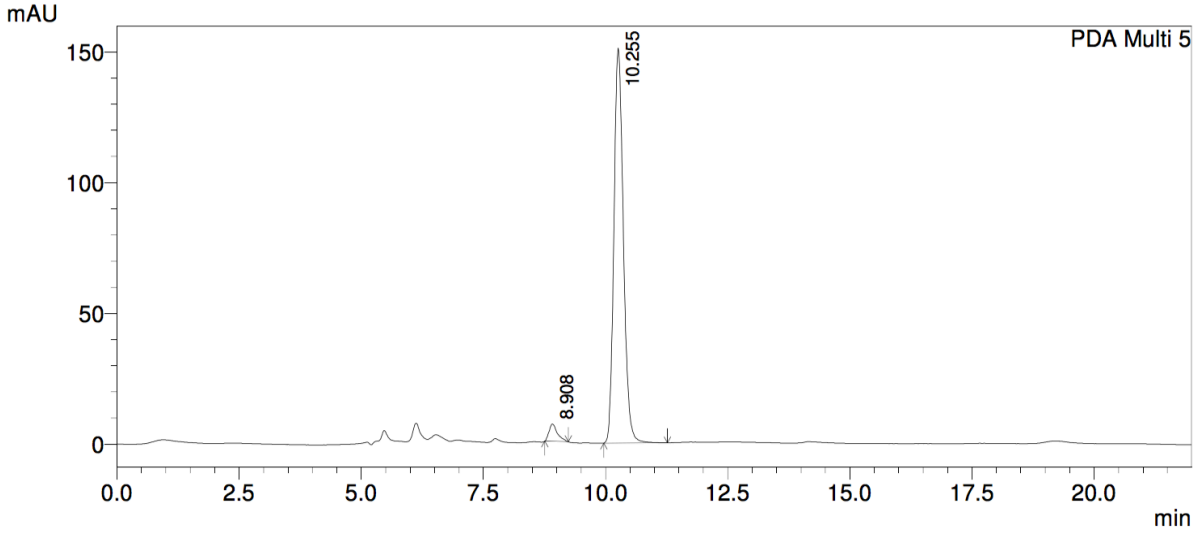

Peak#	Ret. Time	Area	Height	Area %	Height %
1	8.908	79241	6632	3.748	4.209
2	10.255	2034966	150928	96.252	95.791
Total		2114207	157560	100.000	100.000

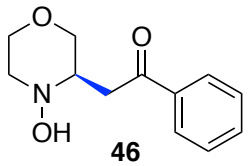

46

Conditions: HPLC (ChiralPak OD-H, 90:10 hexanes/*i*-PrOH, 1 mL/min, 254 nm)

Racemic Sample:

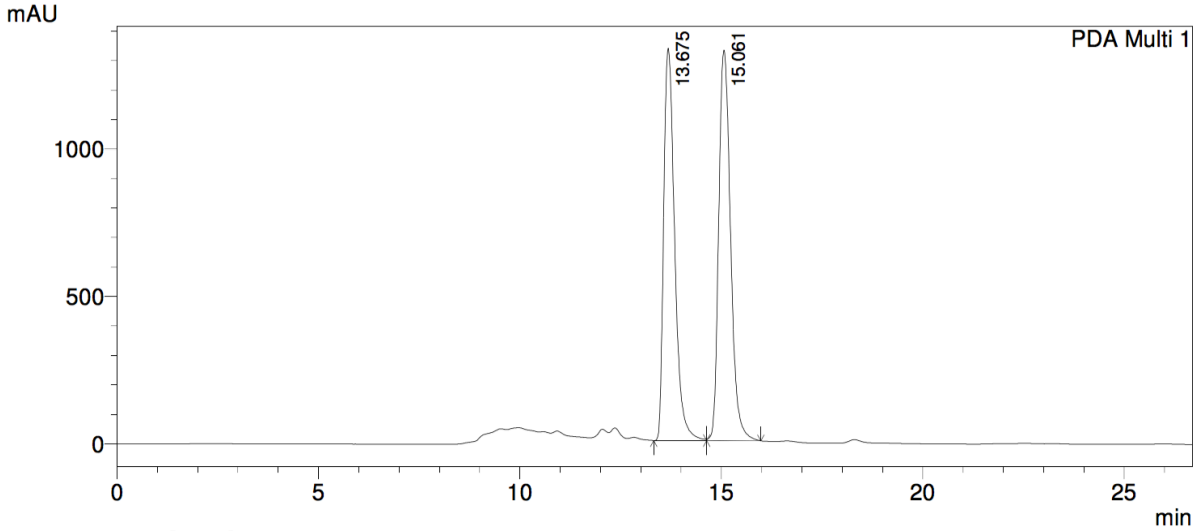

Peak#	Ret. Time	Area	Height	Area %	Height %
1	13.675	25172210	1330370	48.214	50.106
2	15.061	27037356	1324764	51.786	49.894
Total		52209565	2655134	100.000	100.000

Enantioenriched Sample: HPLC (ChiralPak OD-H, 90:10 hexanes/*i*-PrOH, 1 mL/min, 254 nm), 88% *ee*

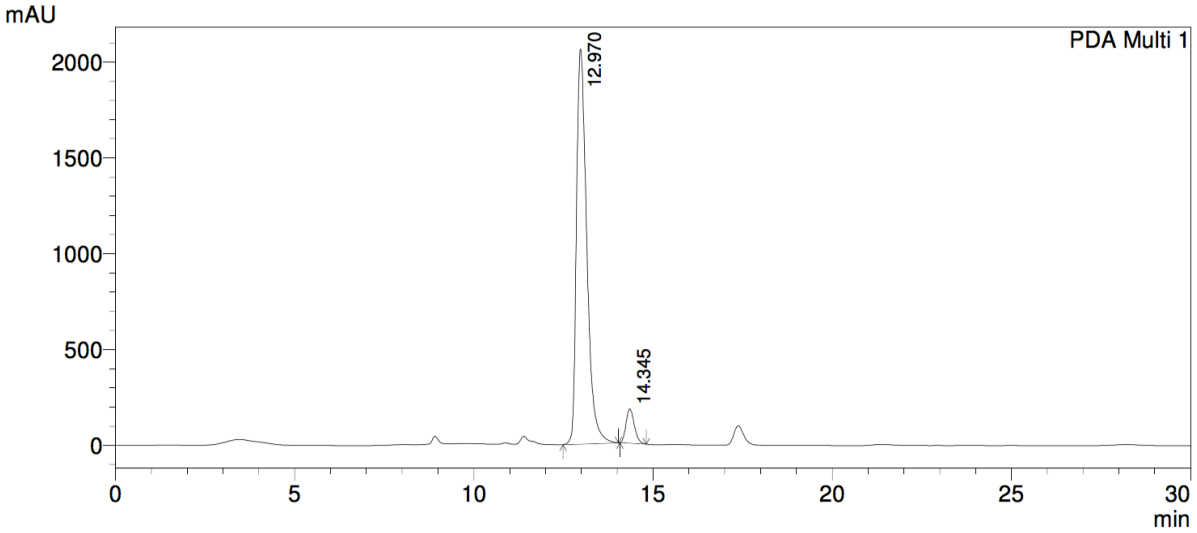

Peak#	Ret. Time	Area	Height	Area %	Height %
1	12.970	41180227	2060380	93.945	92.272
2	14.345	2654071	172559	6.055	7.728
Total		43834298	2232939	100.000	100.000

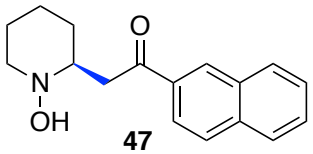

47

Conditions: HPLC (ChiralPak OD-H, 98:2 hexanes/*i*-PrOH, 1 mL/min, 215 nm)

Racemic Sample:

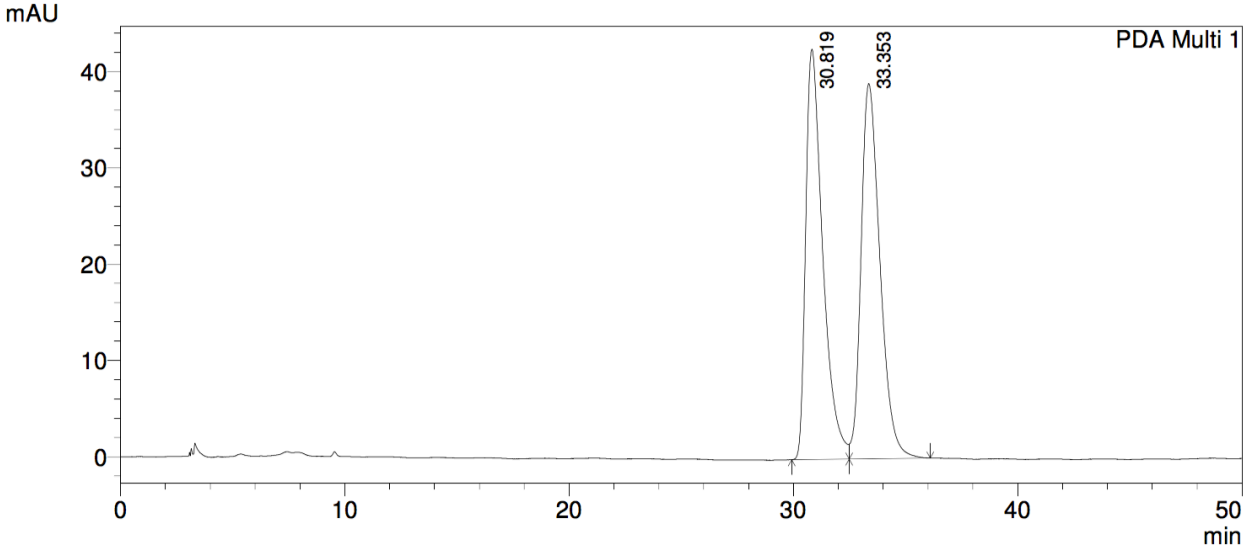

Peak#	Ret. Time	Area	Height	Area %	Height %
1	30.819	2250074	42598	49.531	52.235
2	33.353	2292709	38953	50.469	47.765
Total		4542784	81552	100.000	100.000

Enantioenriched Sample:

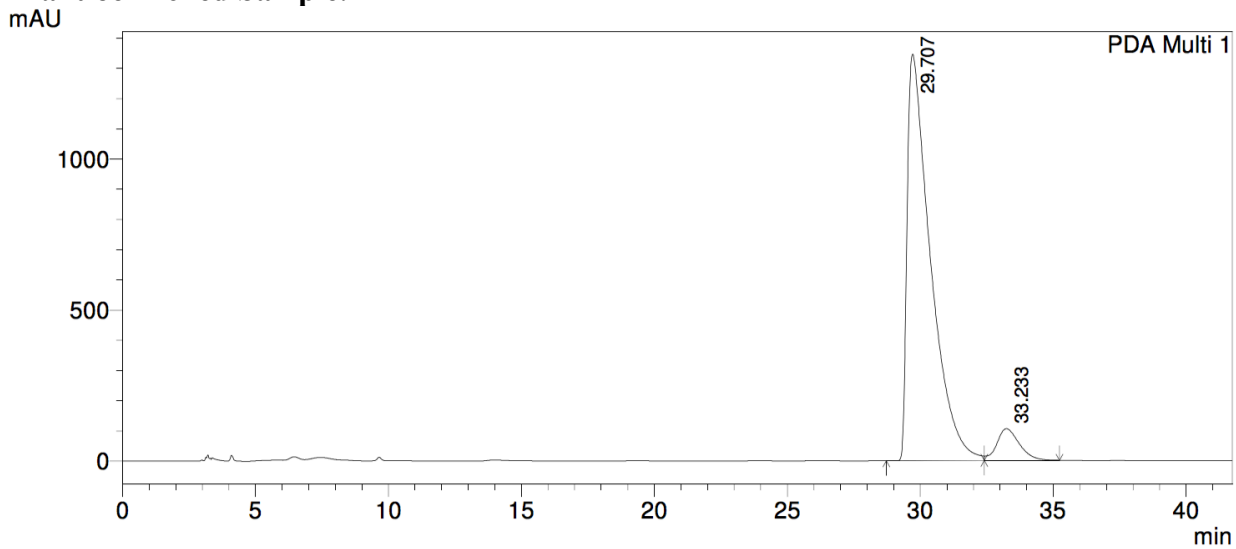

Peak#	Ret. Time	Area	Height	Area %	Height %
1	29.707	81738609	1345707	92.960	92.748
2	33.233	6190618	105226	7.040	7.252
Total		87929228	1450933	100.000	100.000

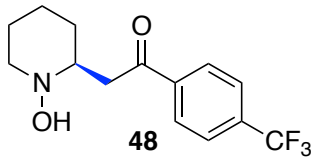

48

Conditions: HPLC (ChiralPak OD-H, 95:5 hexanes/*i*-PrOH, 1 mL/min, 215 nm)

Racemic Sample:

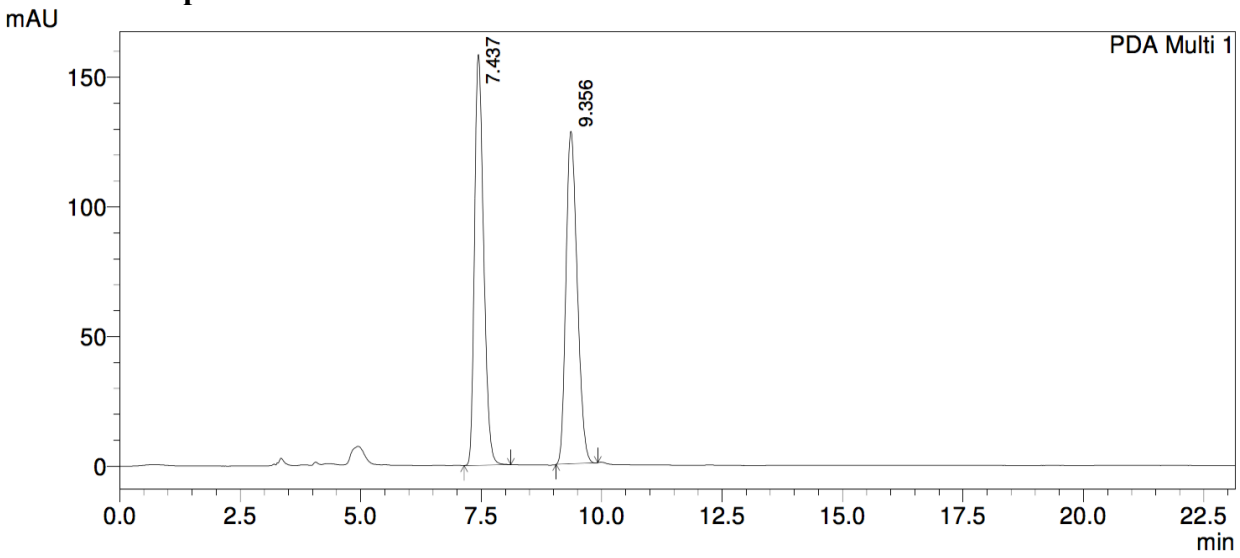

Peak#	Ret. Time	Area	Height	Area %	Height %
1	7.437	2081735	158410	49.963	55.259
2	9.356	2084781	128259	50.037	44.741
Total		4166517	286669	100.000	100.000

Enantioenriched Sample:

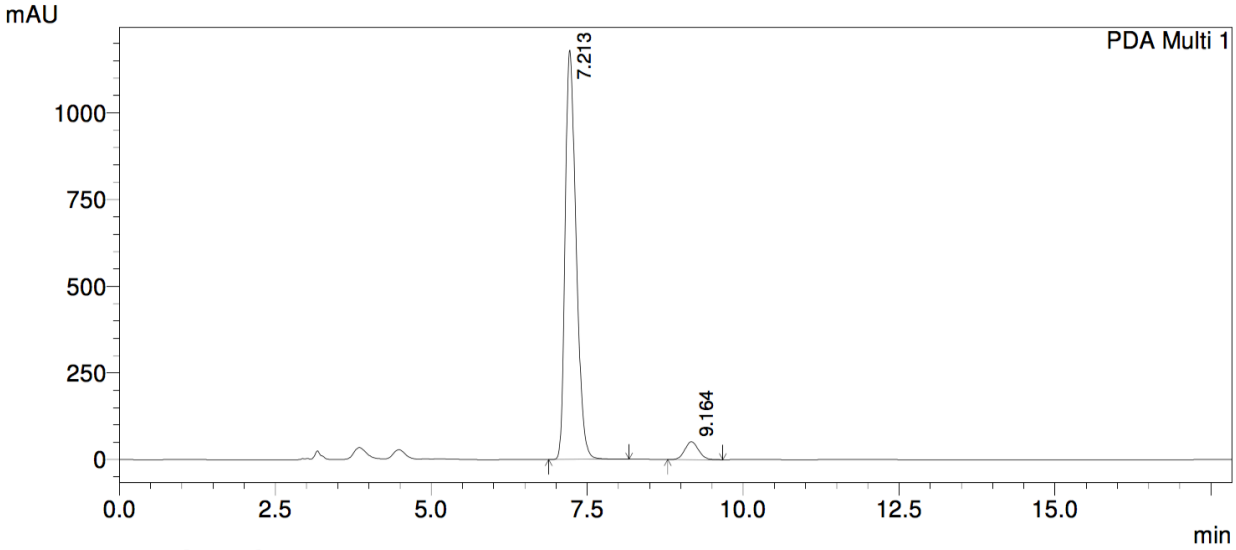

Peak#	Ret. Time	Area	Height	Area %	Height %
1	7.213	14451879	1180494	94.854	95.840
2	9.164	784004	51241	5.146	4.160
Total		15235883	1231735	100.000	100.000

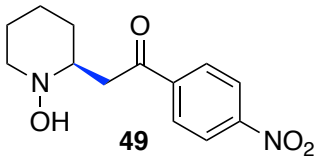

49

Conditions: HPLC (ChiralPak OD-H, 95:5 hexanes/*i*-PrOH, 1 mL/min, 254 nm)

Racemic Sample:

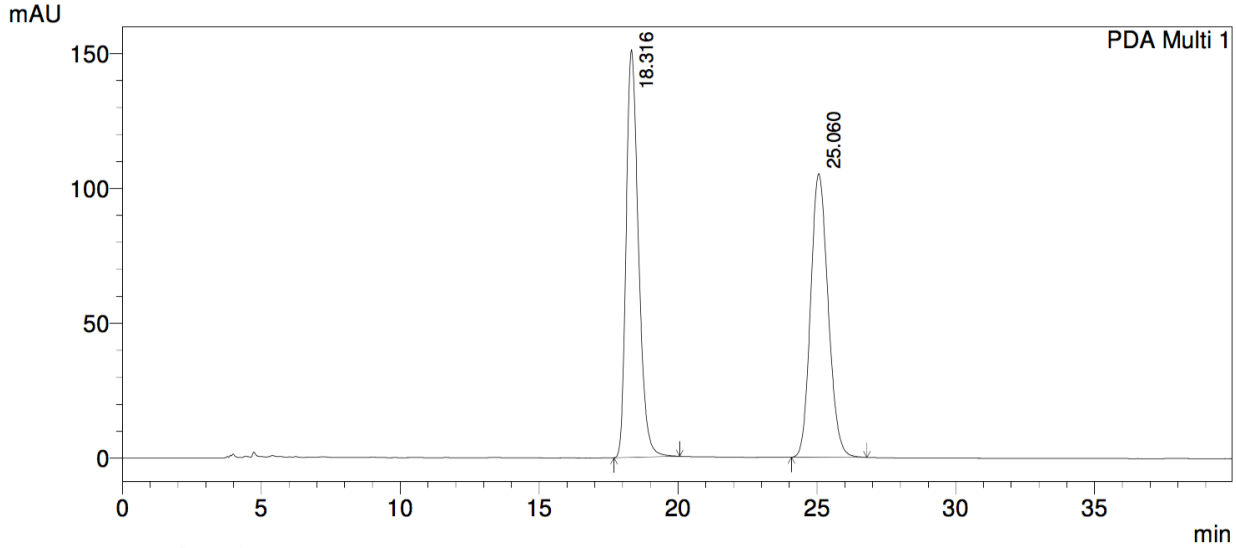

Peak#	Ret. Time	Area	Height	Area %	Height %
1	18.316	4652315	151199	50.280	58.973
2	25.060	4600463	105186	49.720	41.027
Total		9252777	256386	100.000	100.000

Enantioenriched Sample:

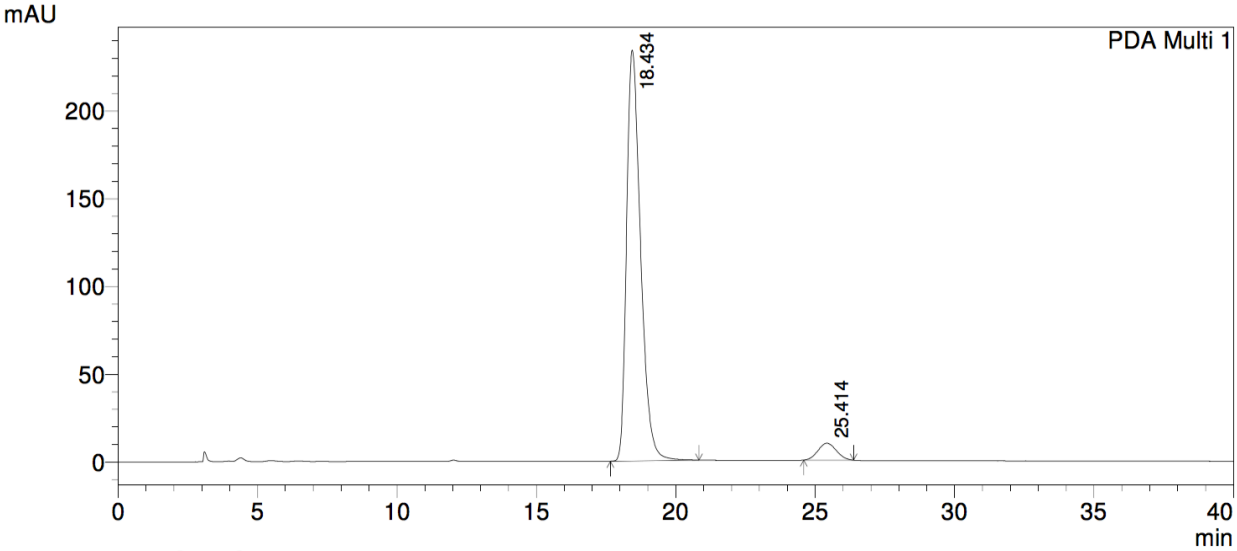

Peak#	Ret. Time	Area	Height	Area %	Height %
1	18.434	8178740	234085	94.878	96.042
2	25.414	441538	9647	5.122	3.958
Total		8620277	243731	100.000	100.000

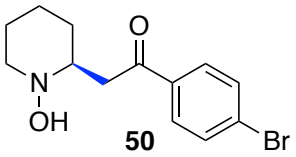

50

Conditions: HPLC (ChiralPak OD-H, 95:5 hexanes/*i*-PrOH, 1 mL/min, 254 nm)

Racemic Sample:

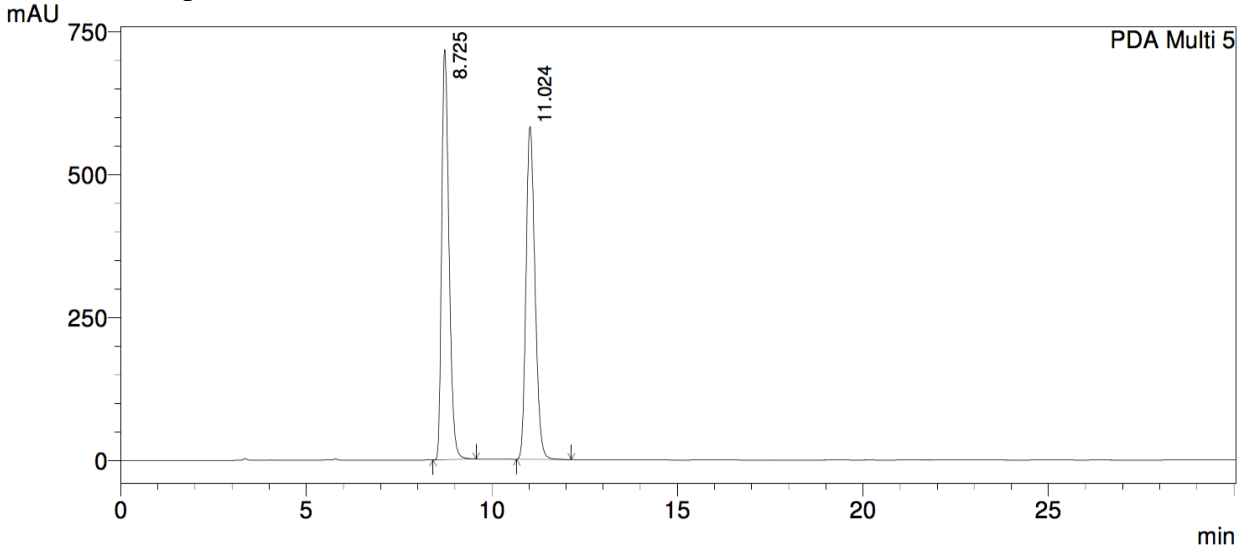

Peak#	Ret. Time	Area	Height	Area %	Height %
1	8.725	9843686	717248	50.045	55.182
2	11.024	9825795	582539	49.955	44.818
Total		19669482	1299788	100.000	100.000

Enantioenriched Sample:

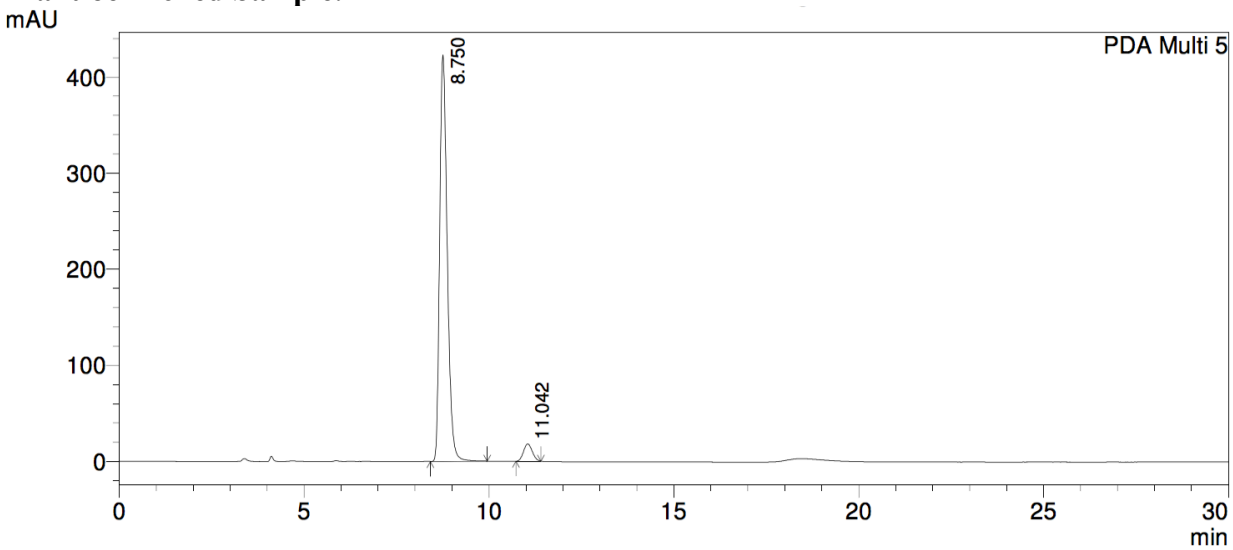

Peak#	Ret. Time	Area	Height	Area %	Height %
1	8.750	6018177	422756	95.313	95.920
2	11.042	295931	17984	4.687	4.080
Total		6314108	440740	100.000	100.000

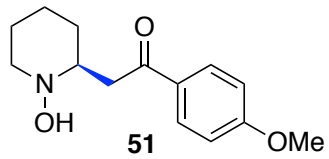

51

Conditions: HPLC (ChiralPak OD-H, 95:5 hexanes/*i*-PrOH, 1 mL/min, 254 nm)

Racemic Sample:

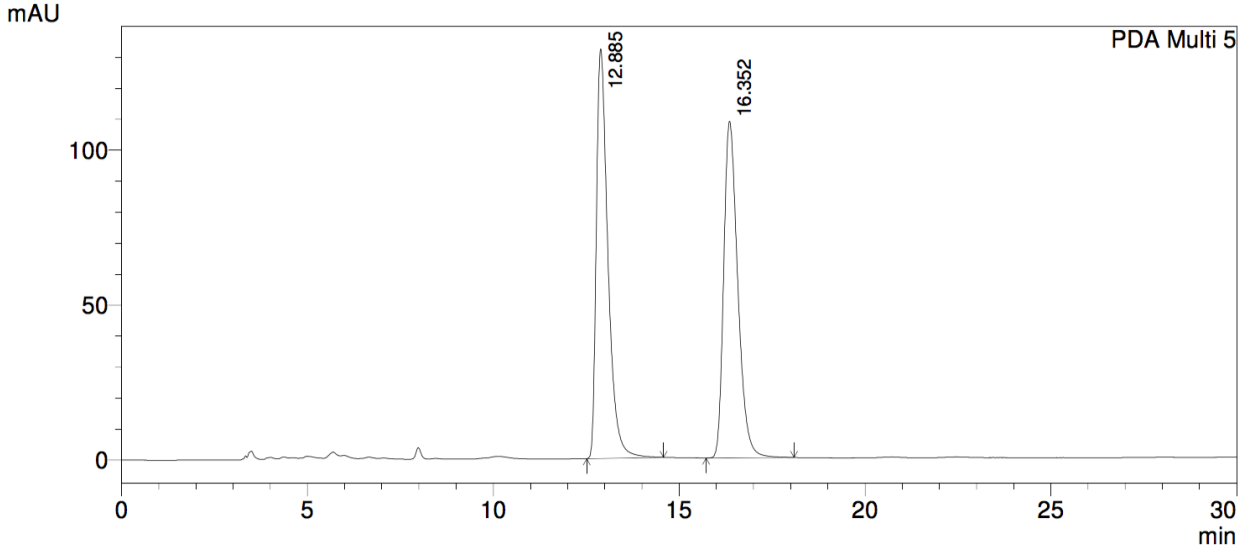

Peak#	Ret. Time	Area	Height	Area %	Height %
1	12.885	2861416	132034	50.060	54.879
2	16.352	2854565	108558	49.940	45.121
Total		5715981	240592	100.000	100.000

Enantioenriched:

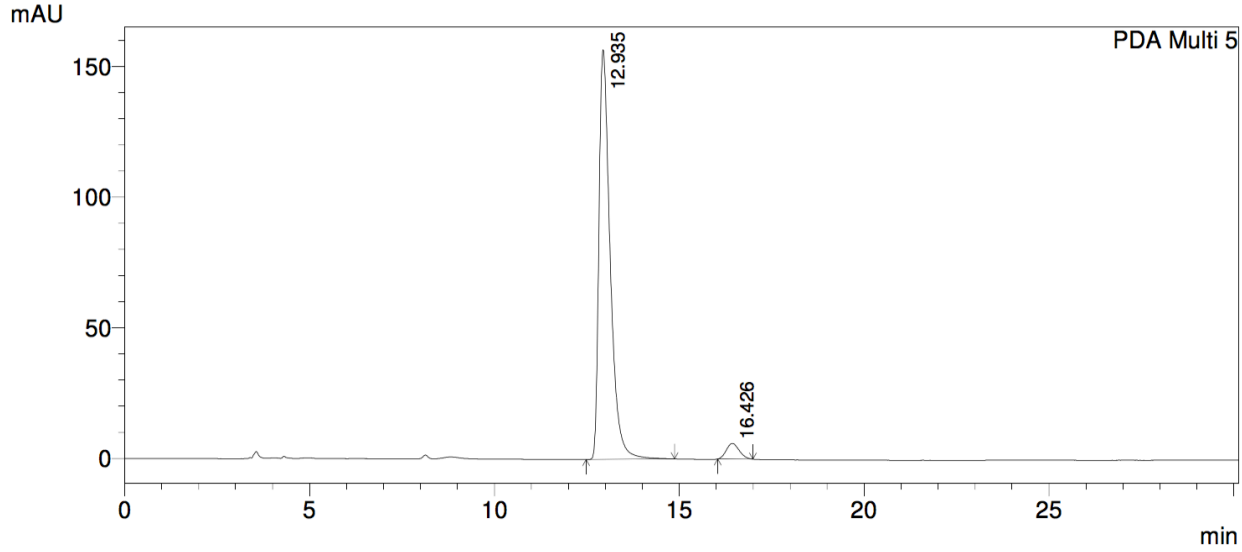

Peak#	Ret. Time	Area	Height	Area %	Height %
1	12.935	3311341	156673	95.802	96.327
2	16.426	145112	5974	4.198	3.673
Total		3456452	162648	100.000	100.000

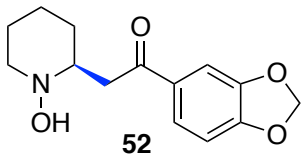

52

Conditions: HPLC (ChiralPak OD-H, 95:5 hexanes/*i*-PrOH, 1 mL/min, 254 nm)

Racemic Sample:

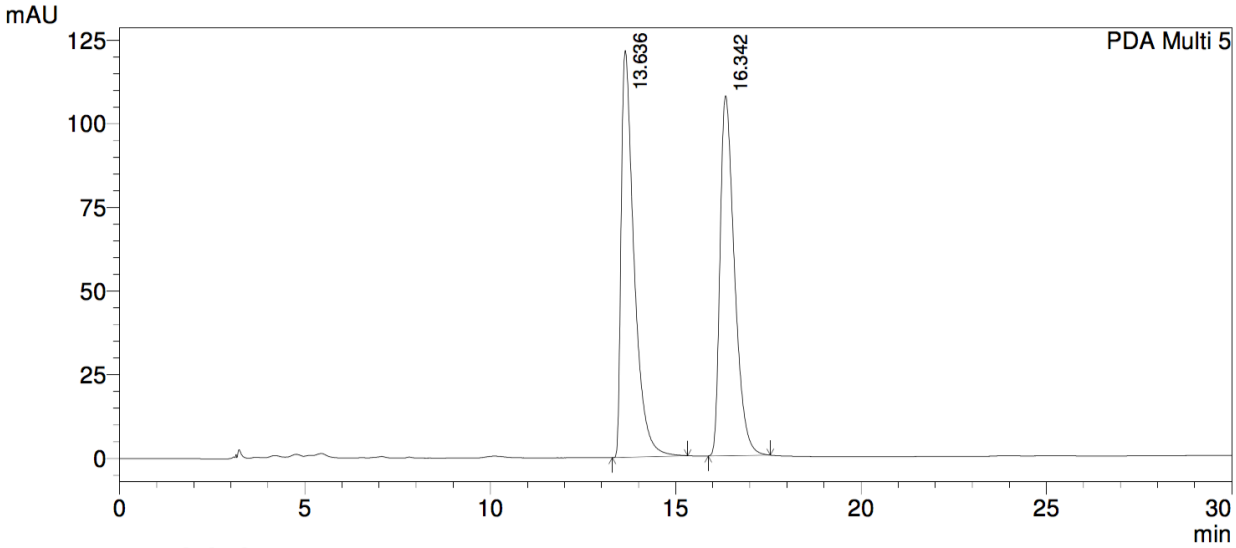

Peak#	Ret. Time	Area	Height	Area %	Height %
1	13.636	2935315	121498	50.221	53.059
2	16.342	2909505	107488	49.779	46.941
Total		5844820	228986	100.000	100.000

Enantioenriched Sample:

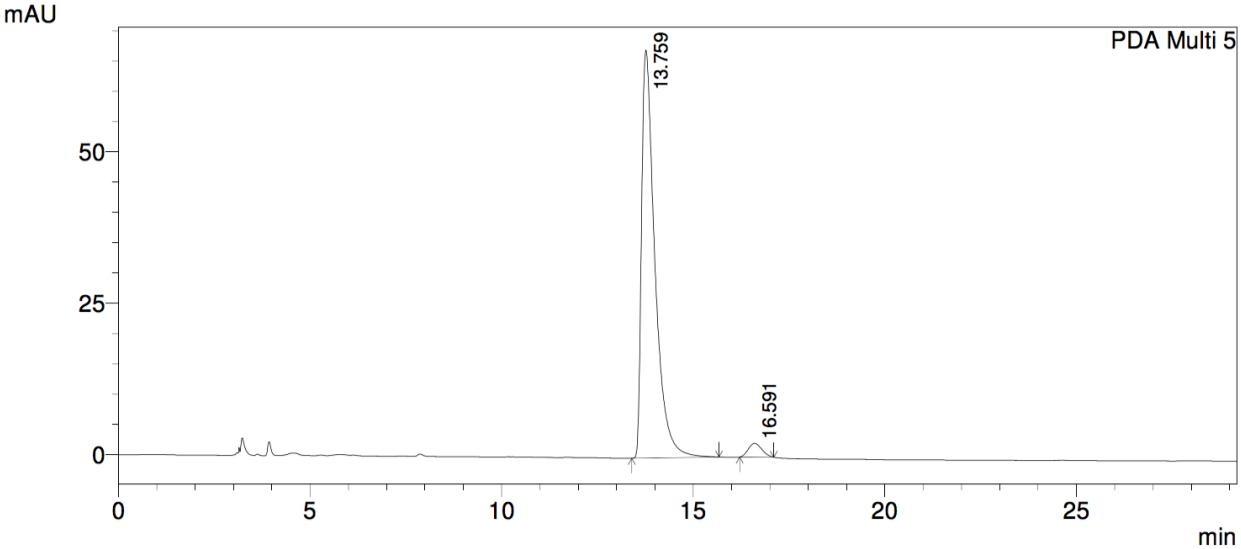

Peak#	Ret. Time	Area	Height	Area %	Height %
1	13.759	1628948	67370	96.702	96.754
2	16.591	55553	2260	3.298	3.246
Total		1684501	69630	100.000	100.000

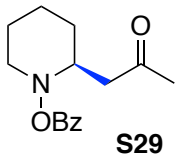

S29

Conditions: HPLC (ChiralPak OD-H, 99:1 hexanes/*i*-PrOH, 1 mL/min, 254 nm)

Racemic Sample:

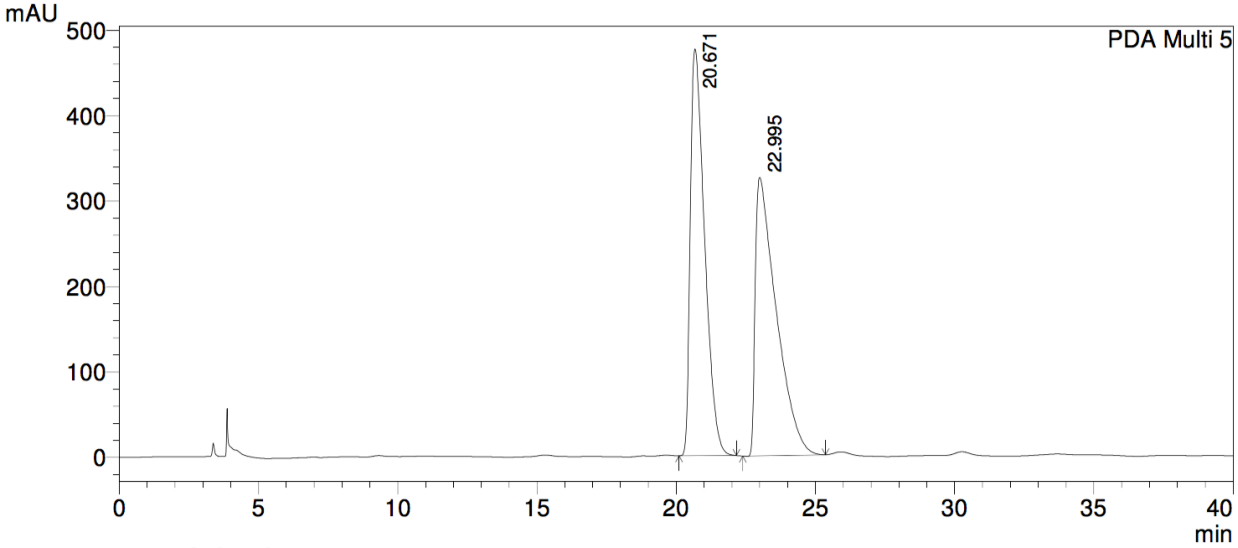

Peak#	Ret. Time	Area	Height	Area %	Height %
1	20.671	17011683	475861	49.881	59.360
2	22.995	17093005	325796	50.119	40.640
Total		34104688	801658	100.000	100.000

Enantioenriched Sample:

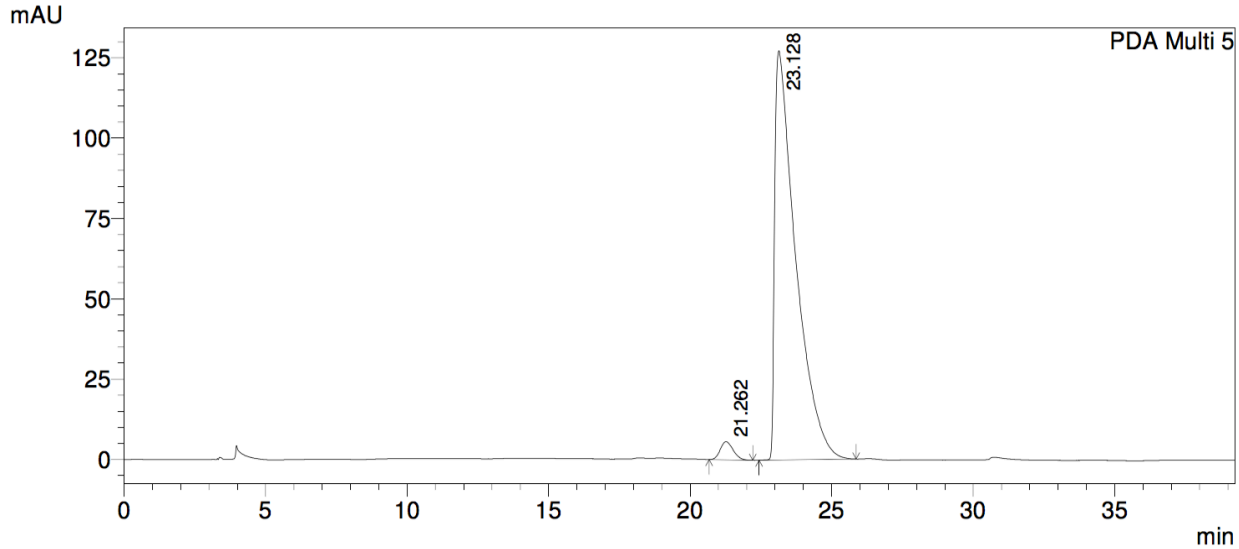

Peak#	Ret. Time	Area	Height	Area %	Height %
1	21.262	179442	5651	2.660	4.248
2	23.128	6566841	127379	97.340	95.752
Total		6746282	133030	100.000	100.000

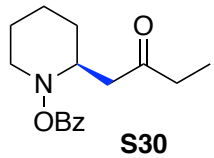

S30

Conditions: HPLC (ChiralPak OD-H, 99:1 hexanes/*i*-PrOH, 1 mL/min, 254 nm)

Racemic Sample:

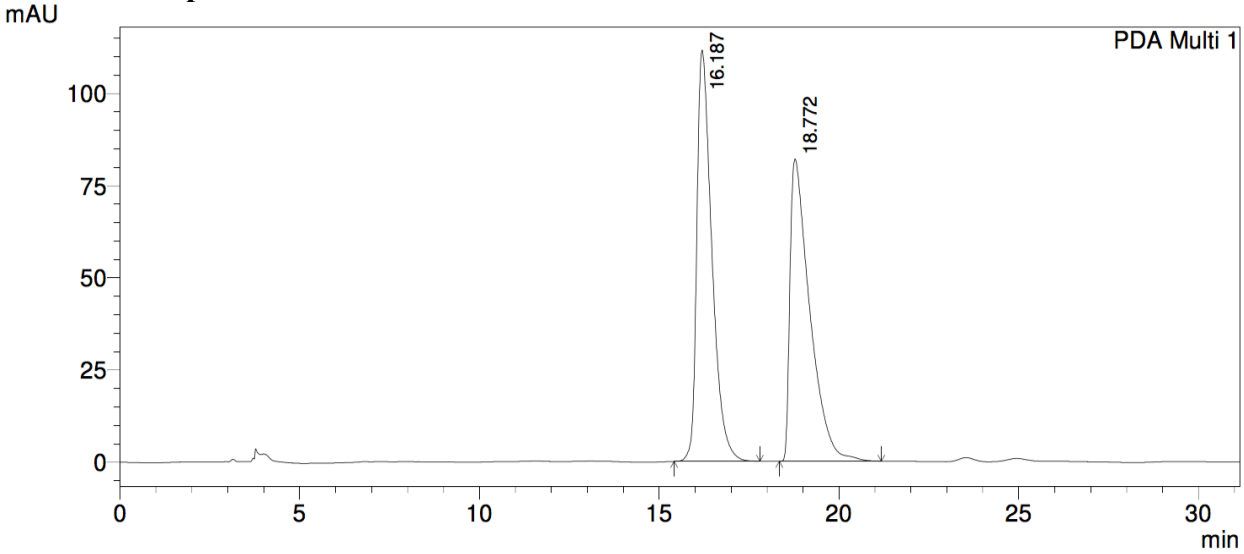

Peak#	Ret. Time	Area	Height	Area %	Height %
1	16.187	3251227	111520	50.858	57.629
2	18.772	3141579	81994	49.142	42.371
Total		6392806	193514	100.000	100.000

Enantioenriched Sample:

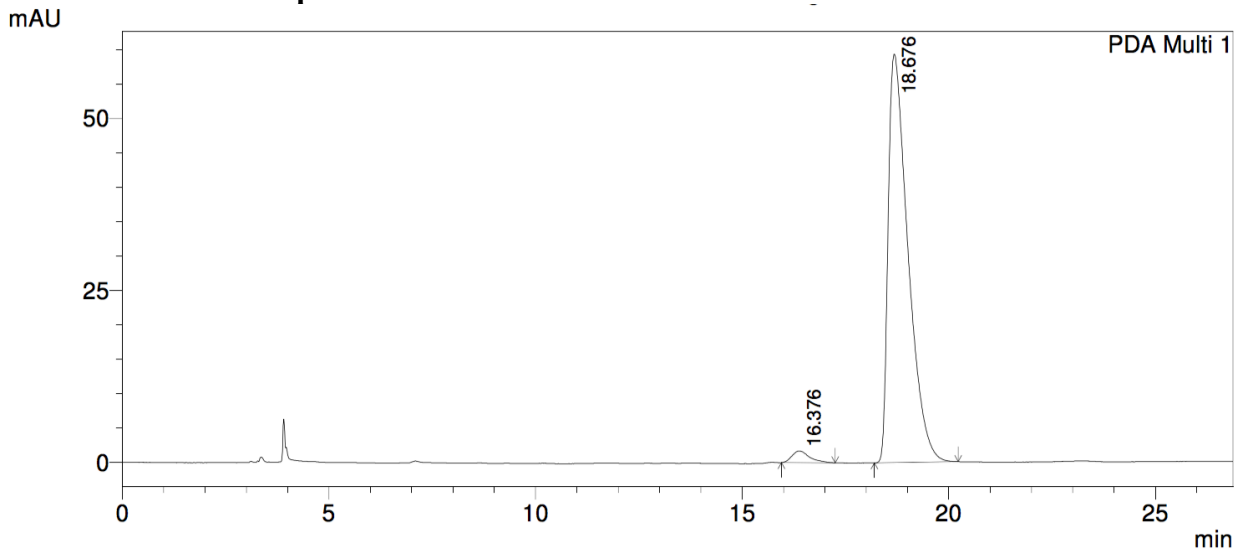

Peak#	Ret. Time	Area	Height	Area %	Height %
1	16.376	50691	1710	2.496	2.798
2	18.676	1980395	59377	97.504	97.202
Total		2031086	61087	100.000	100.000

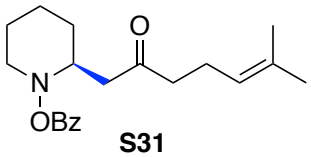

S31

Conditions: HPLC (ChiralPak OD-H, 99:1 hexanes/*i*-PrOH, 1 mL/min, 254 nm)

Racemic Sample:

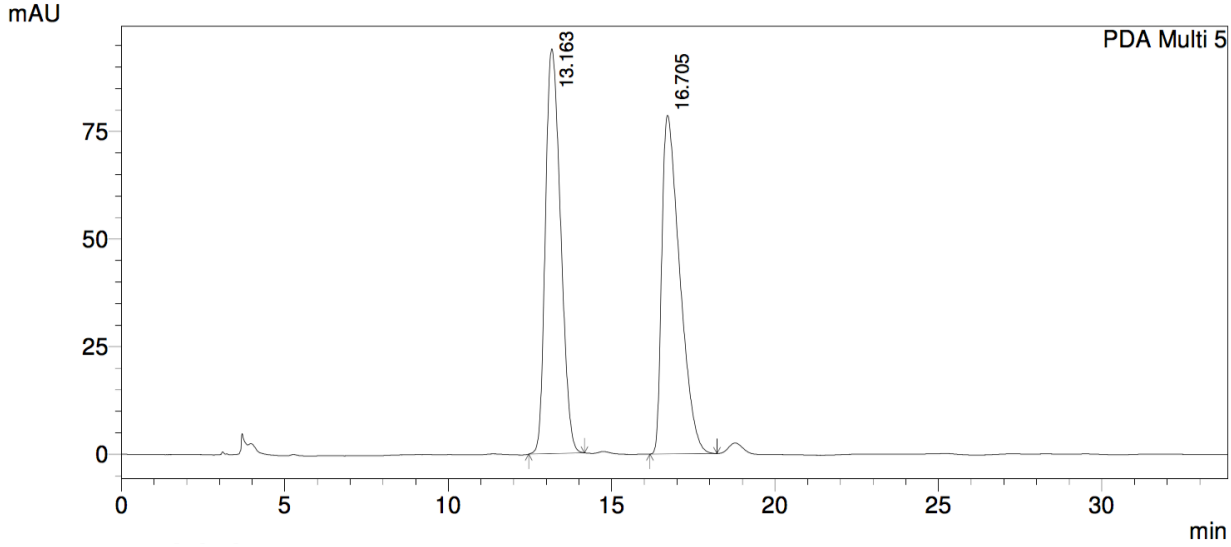

Peak#	Ret. Time	Area	Height	Area %	Height %
1	13.163	3041718	94044	50.216	54.455
2	16.705	3015522	78655	49.784	45.545
Total		6057241	172699	100.000	100.000

Enantioenriched Sample:

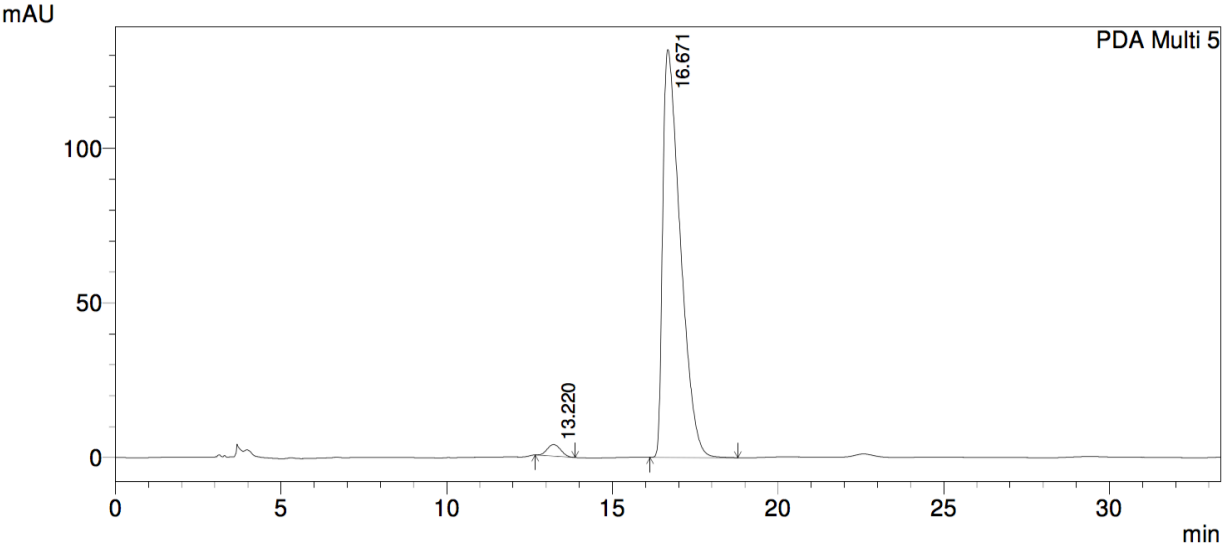

Peak#	Ret. Time	Area	Height	Area %	Height %
1	13.220	105139	3709	2.116	2.737
2	16.671	4864102	131796	97.884	97.263
Total		4969241	135505	100.000	100.000

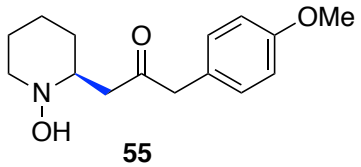

55

Conditions: HPLC (ChiralPak OD-H, 97:3 hexanes/*i*-PrOH, 1 mL/min, 254 nm)

Racemic Sample:

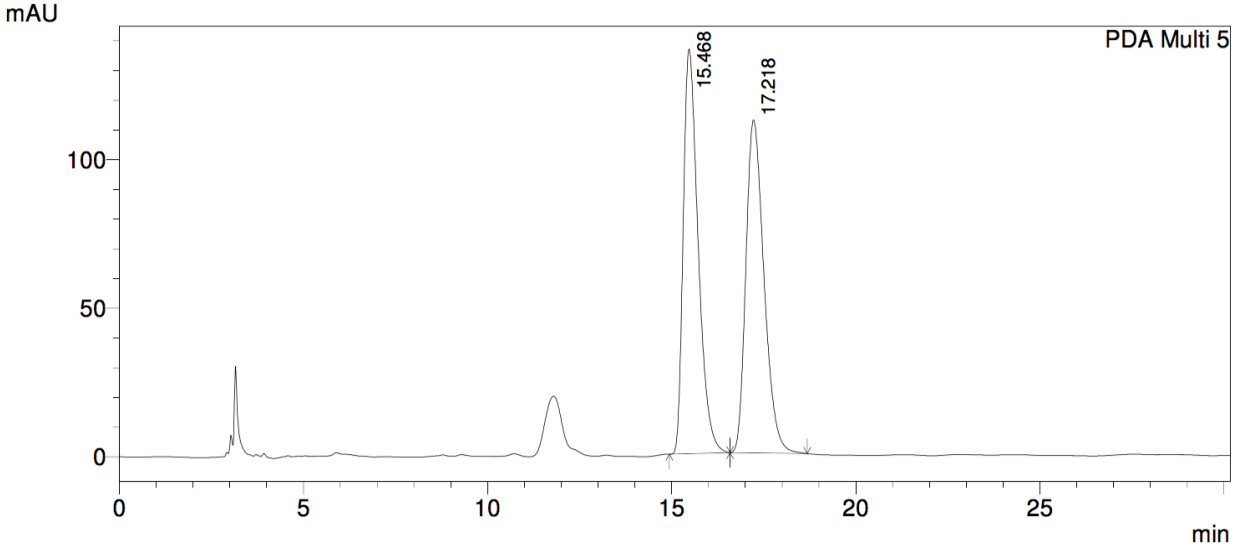

Peak#	Ret. Time	Area	Height	Area %	Height %
1	15.468	3831520	136172	50.019	54.869
2	17.218	3828672	112004	49.981	45.131
Total		7660191	248176	100.000	100.000

Enantioenriched Sample:

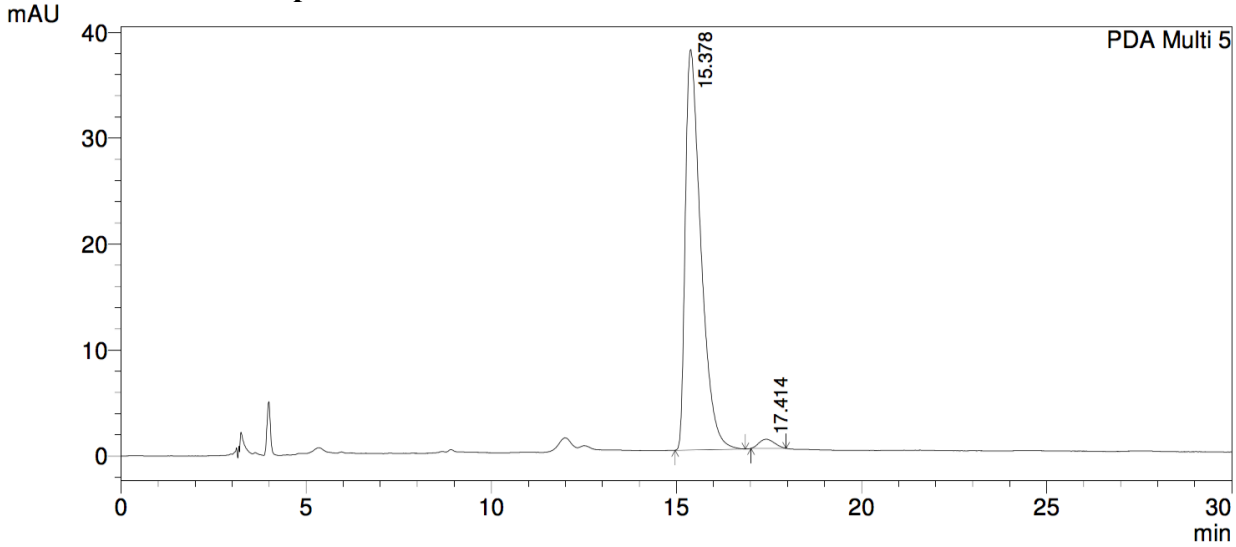

Peak#	Ret. Time	Area	Height	Area %	Height %
1	15.378	1104567	37797	97.784	97.761
2	17.414	25031	866	2.216	2.239
Total		1129598	38663	100.000	100.000

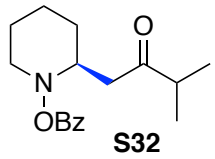

S32

Conditions: HPLC (ChiralPak OD-H, 95:5 hexanes/*i*-PrOH, 1 mL/min, 215 nm)

Racemic Sample:

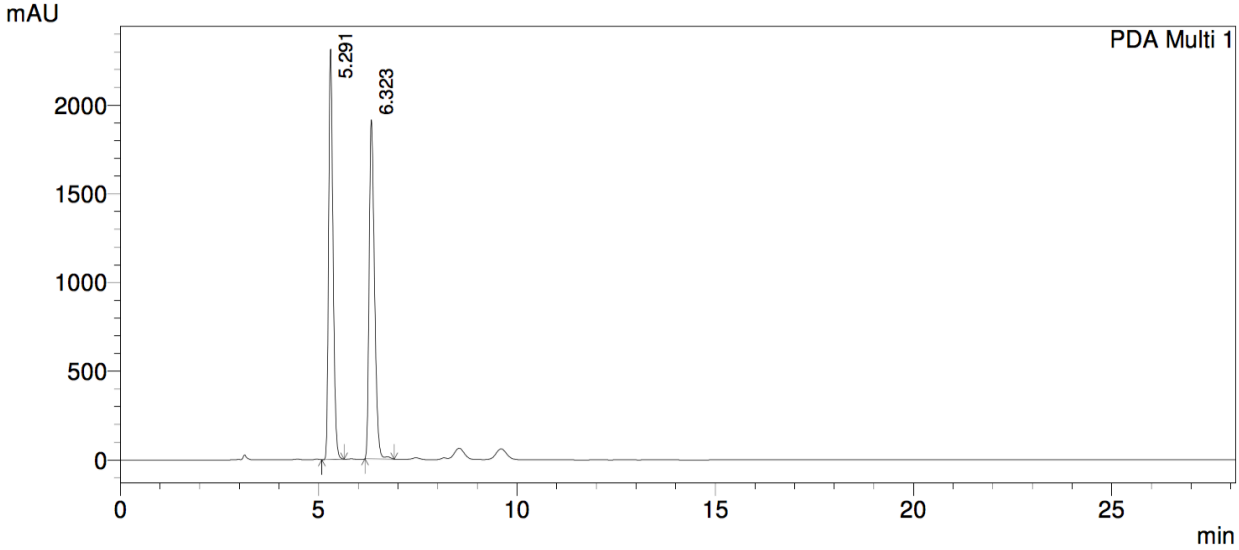

Peak#	Ret. Time	Area	Height	Area %	Height %
1	5.291	17833478	2309022	49.887	54.735
2	6.323	17914616	1909519	50.113	45.265
Total		35748094	4218541	100.000	100.000

Enantioenriched Sample:

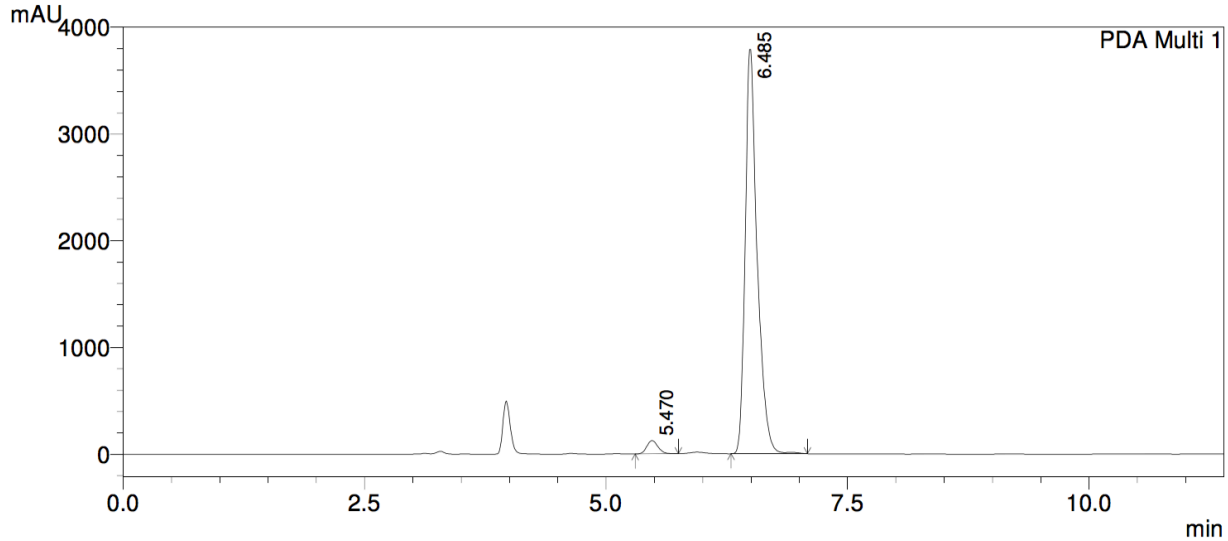

Peak#	Ret. Time	Area	Height	Area %	Height %
1	5.470	992071	124271	2.939	3.176
2	6.485	32757928	3788035	97.061	96.824
Total		33749998	3912306	100.000	100.000

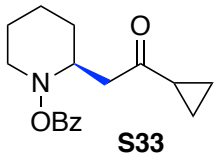

S33

Conditions: HPLC (ChiralPak OD-H, 95:5 hexanes/*i*-PrOH, 1 mL/min, 254 nm)

Racemic Sample:

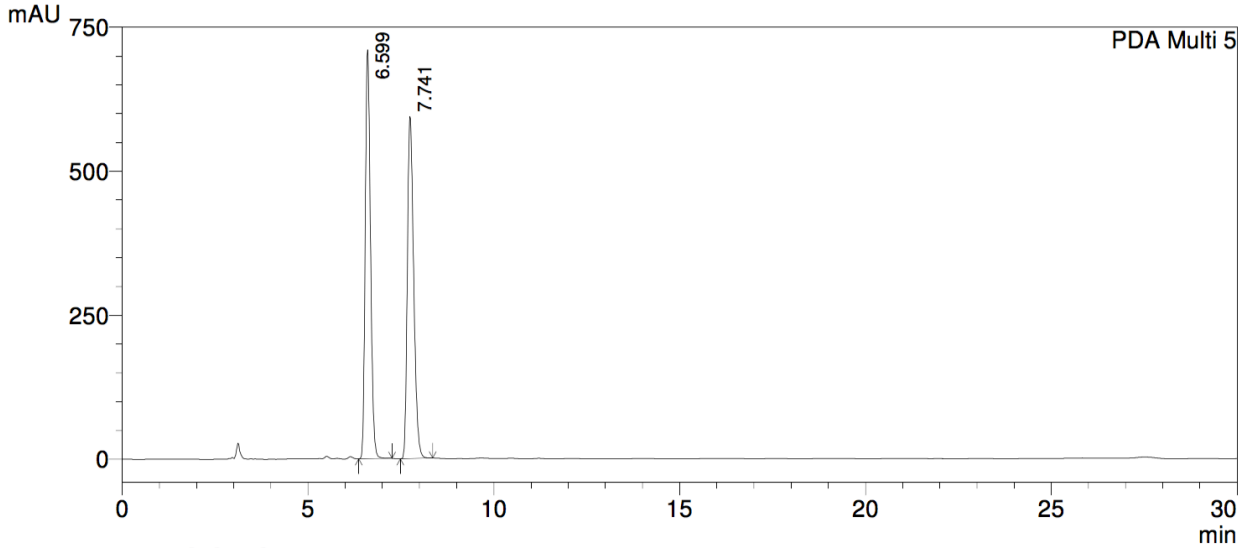

Peak#	Ret. Time	Area	Height	Area %	Height %
1	6.599	6968760	709596	49.860	54.436
2	7.741	7007796	593945	50.140	45.564
Total		13976556	1303541	100.000	100.000

Enantioenriched Sample:

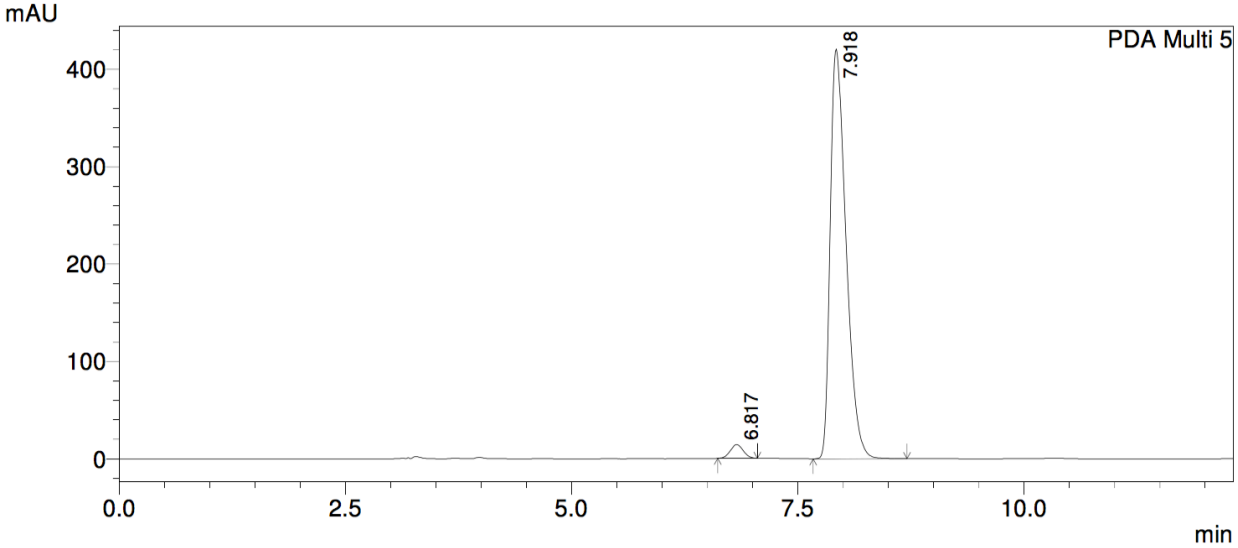

Peak#	Ret. Time	Area	Height	Area %	Height %
1	6.817	142258	14233	2.708	3.272
2	7.918	5111098	420770	97.292	96.728
Total		5253356	435003	100.000	100.000

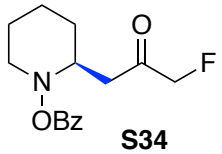

S34

Conditions: HPLC (ChiralPak OD-H, 97:3 hexanes/*i*-PrOH, 1 mL/min, 254 nm)

Racemic Sample:

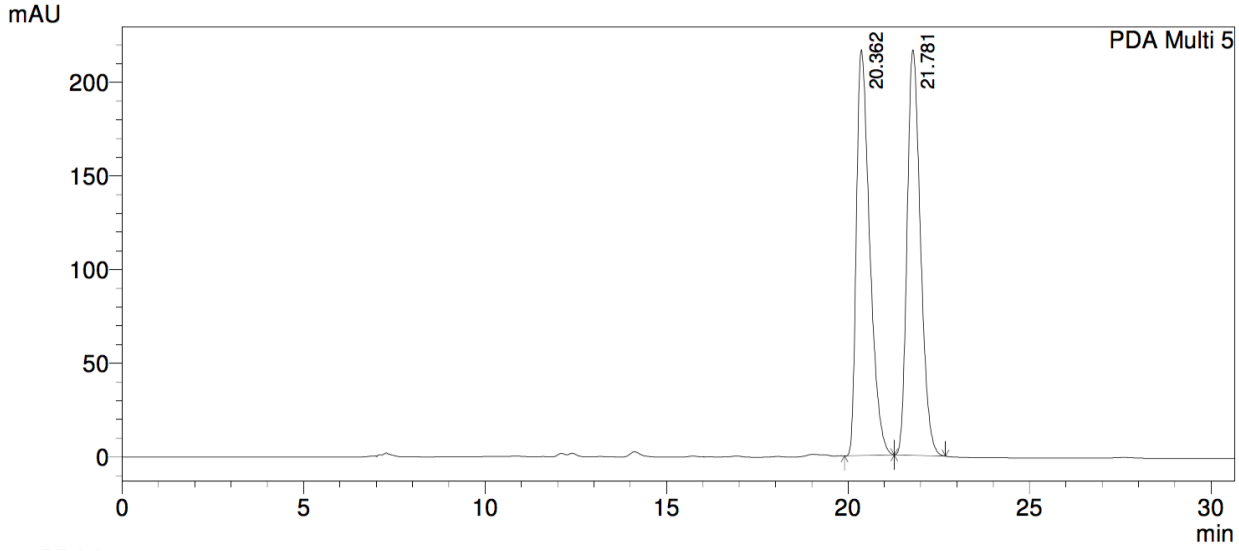

Peak#	Ret. Time	Area	Height	Area %	Height %
1	20.362	5527800	216631	49.927	50.023
2	21.781	5543998	216433	50.073	49.977
Total		11071798	433064	100.000	100.000

Enantioenriched Sample:

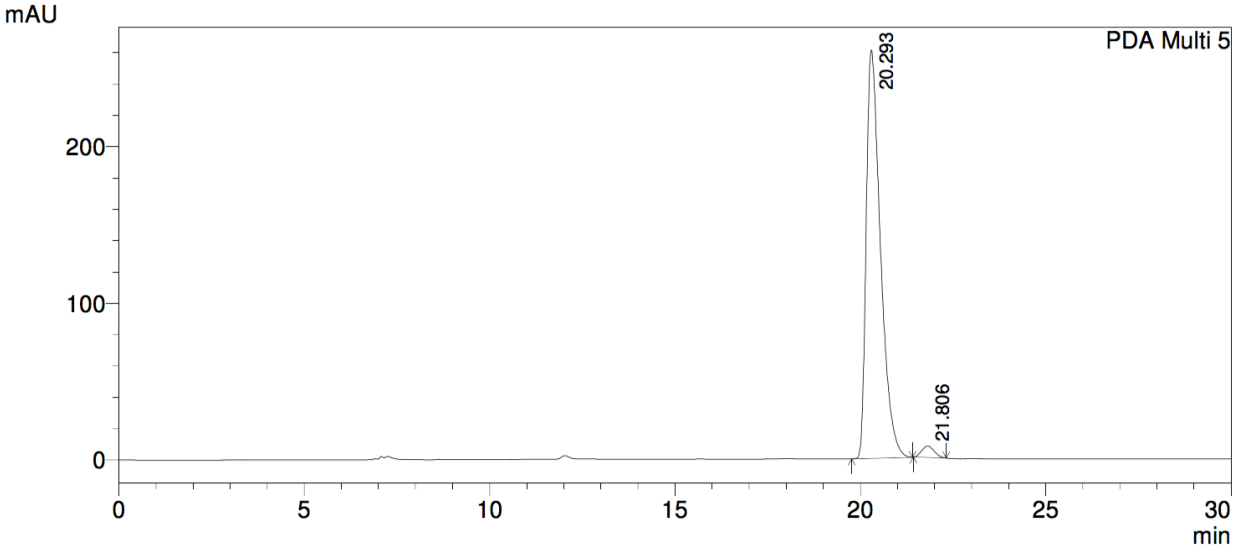

Peak#	Ret. Time	Area	Height	Area %	Height %
1	20.293	6969940	260619	97.547	97.271
2	21.806	175260	7313	2.453	2.729
Total		7145200	267932	100.000	100.000

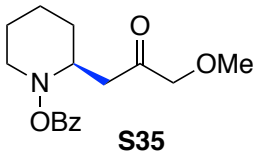

S35

Conditions: HPLC (ChiralPak OD-H, 99:1 hexanes/*i*-PrOH, 1 mL/min, 230 nm)

Racemic Sample:

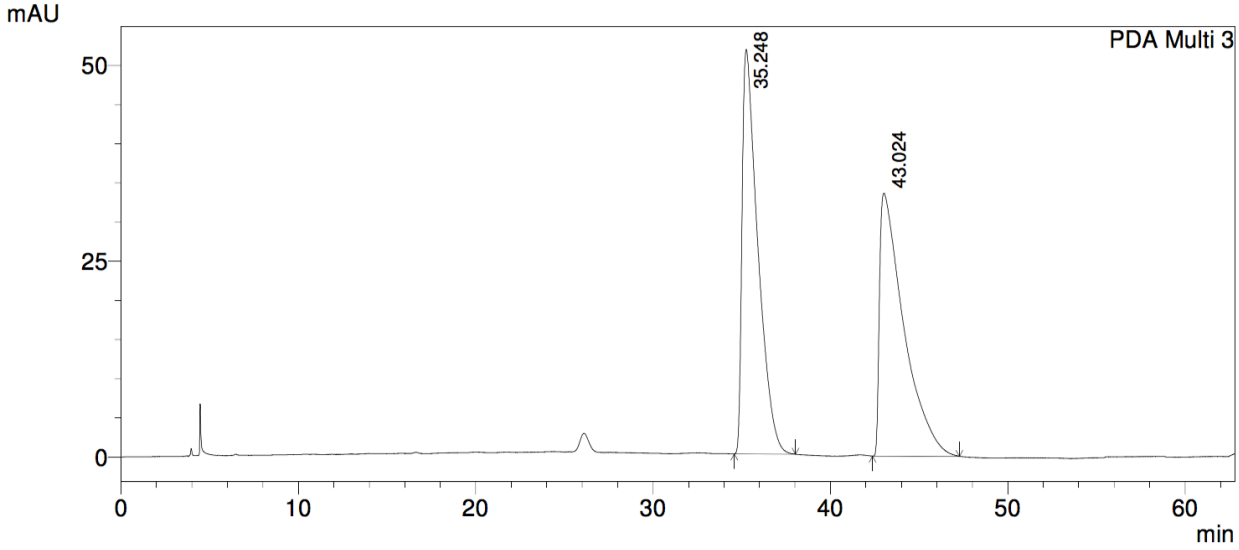

Peak#	Ret. Time	Area	Height	Area %	Height %
1	35.248	3198848	51696	50.115	60.631
2	43.024	3184114	33568	49.885	39.369
Total		6382962	85264	100.000	100.000

Enantioenriched Sample:

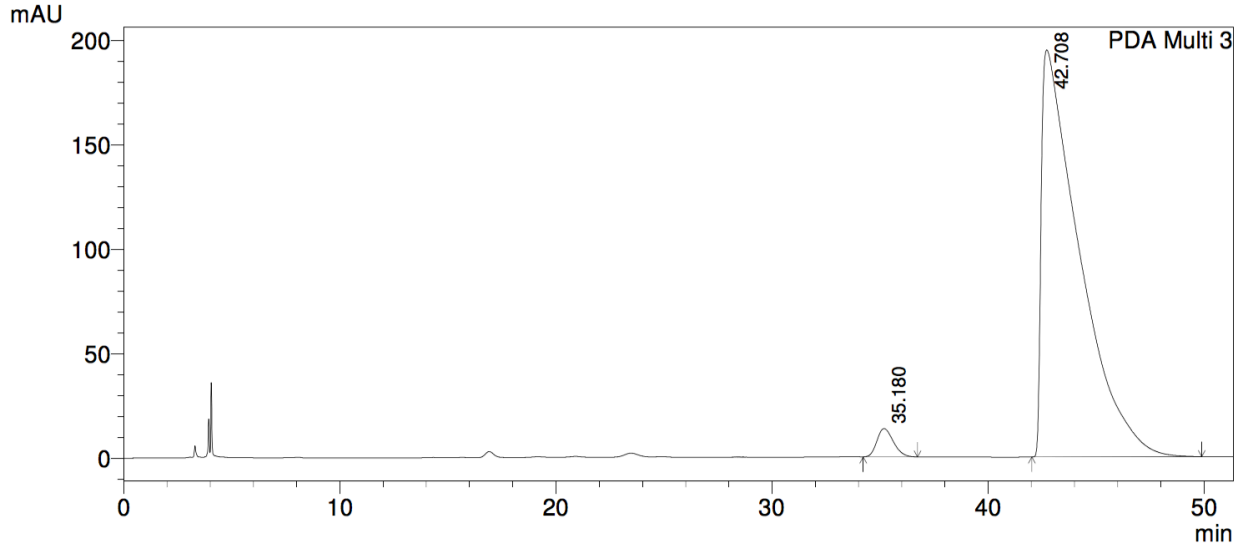

Peak#	Ret. Time	Area	Height	Area %	Height %
1	35.180	717200	13554	2.920	6.501
2	42.708	23844062	194925	97.080	93.499
Total		24561263	208479	100.000	100.000

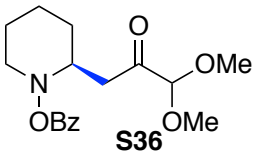

S36

Conditions: HPLC (ChiralPak OJ-H, 95:5 hexanes/*i*-PrOH, 1 mL/min, 254 nm)

Racemic Sample:

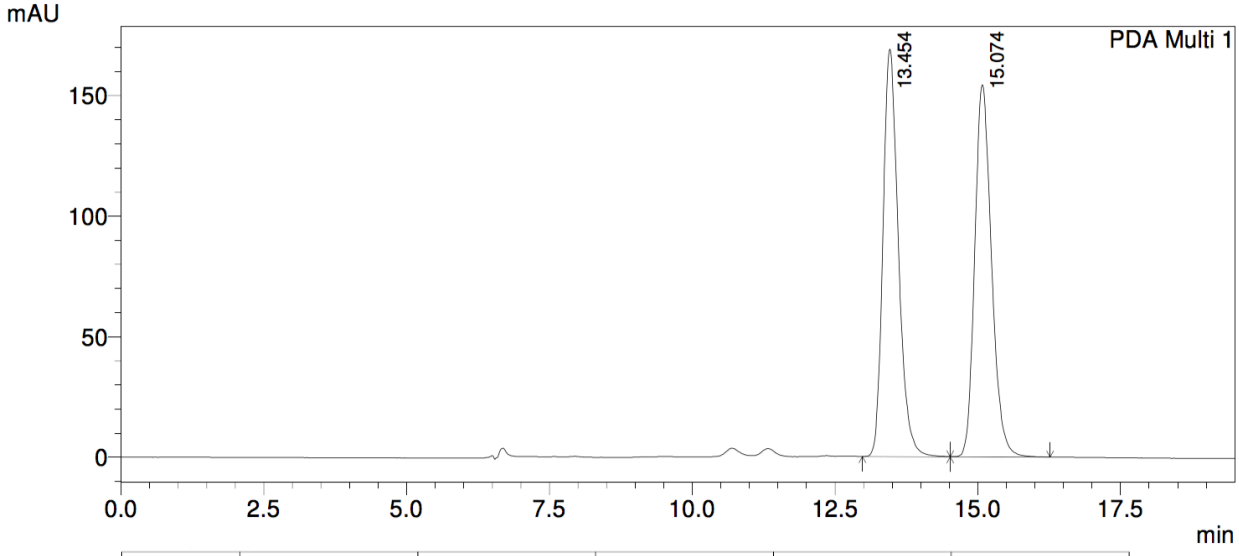

Peak#	Ret. Time	Area	Height	Area %	Height %
1	13.454	3174035	168993	50.107	52.266
2	15.074	3160533	154337	49.893	47.734
Total		6334568	323331	100.000	100.000

Enantioenriched Sample:

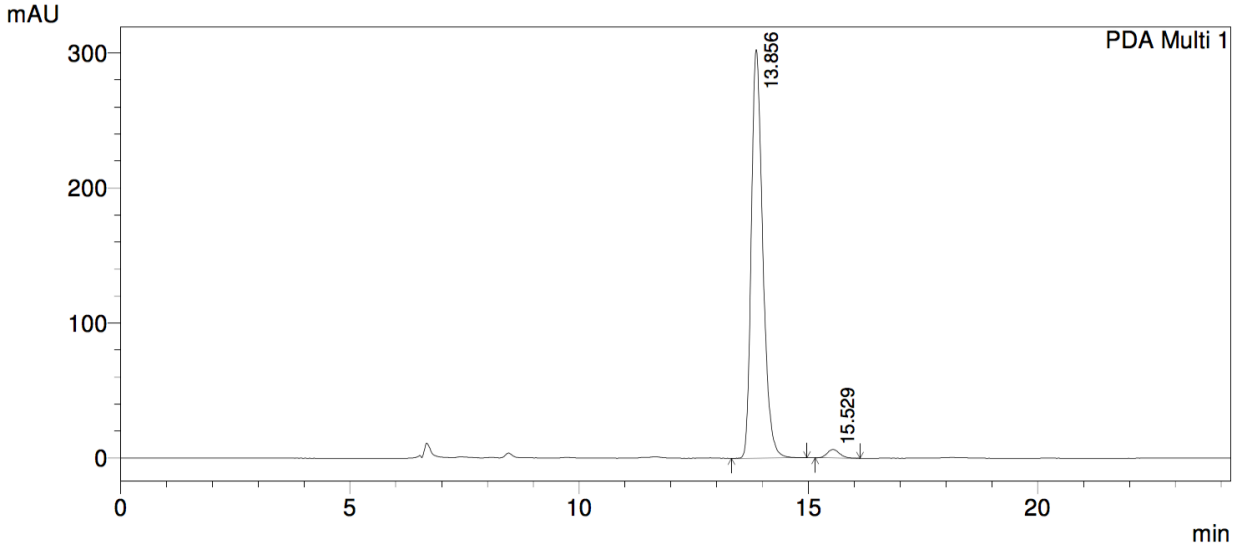

Peak#	Ret. Time	Area	Height	Area %	Height %
1	13.856	5250265	302329	97.814	97.974
2	15.529	117347	6252	2.186	2.026
Total		5367612	308582	100.000	100.000

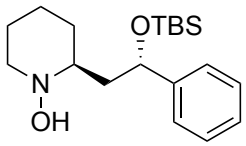

87

Conditions: HPLC (ChiralPak OD-H, 98:2 hexanes/*i*-PrOH, 1 mL/min, 215 nm)

Racemic Sample:

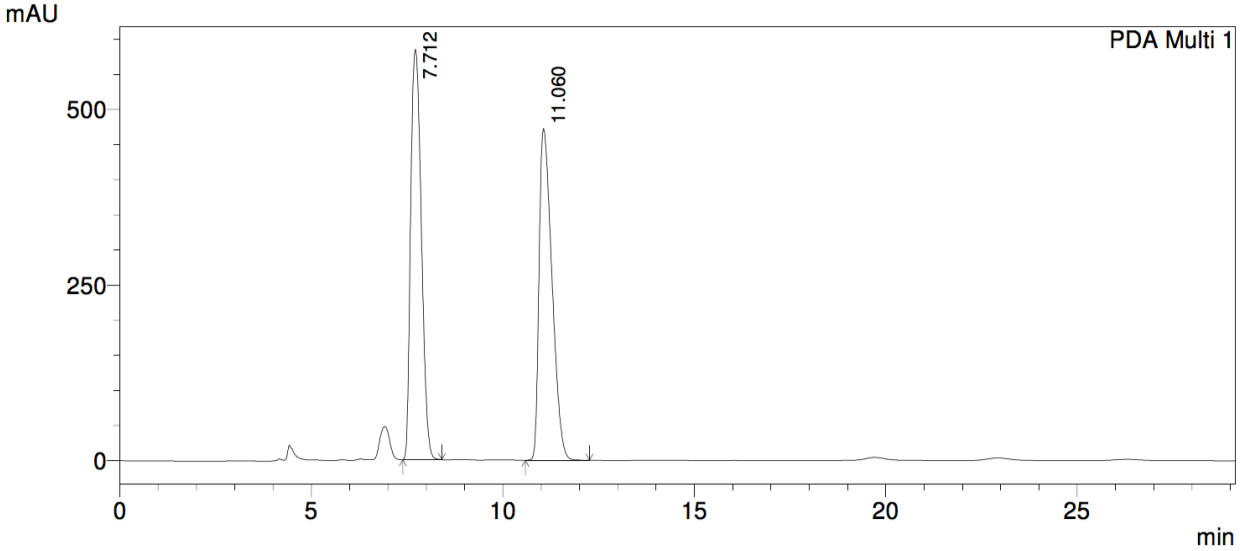

Peak#	Ret. Time	Area	Height	Area %	Height %
1	7.712	11318560	583744	50.732	55.289
2	11.060	10991802	472069	49.268	44.711
Total		22310363	1055812	100.000	100.000

Enantioenriched Sample:

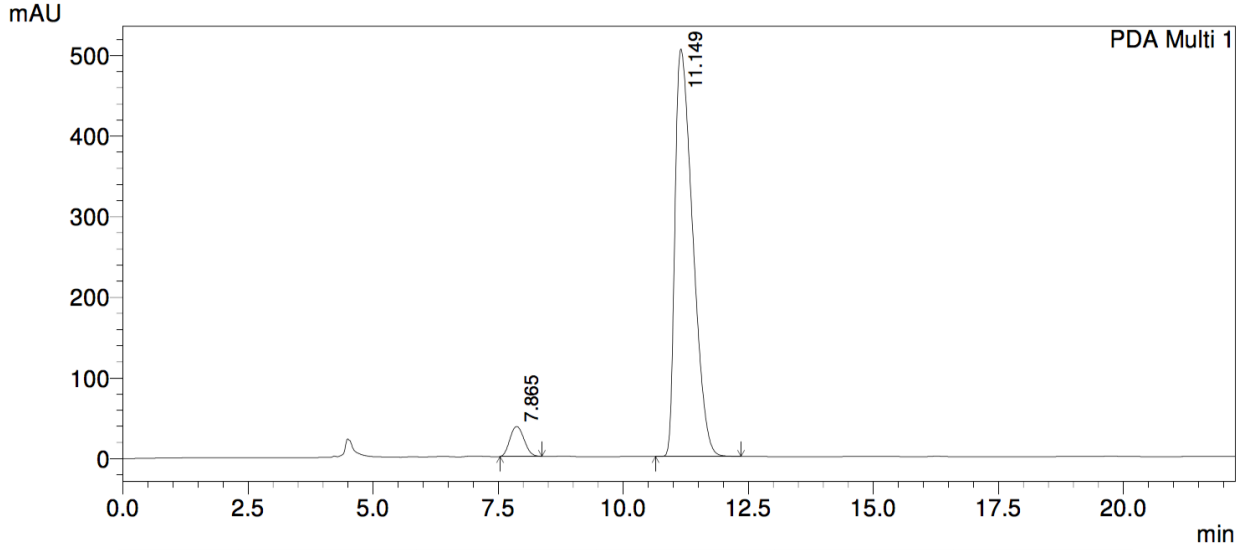

Peak#	Ret. Time	Area	Height	Area %	Height %
1	7.865	732079	37076	5.538	6.835
2	11.149	12486313	505366	94.462	93.165
Total		13218392	542442	100.000	100.000

2.10 X-Ray Crystallography Data

General information: The diffraction data were measured at 100 K on a Bruker D8 VENTURE diffractometer equipped with a microfocus Mo-target X-ray tube (λ = 0.71073 Å) and microfocus Cu-target X-ray tube (λ = 1.54178 Å) and PHOTON 100 CMOS detector. Data were collected using ϕ and ω scans to survey a hemisphere of reciprocal space. Data reduction and integration were performed with the Bruker APEX3 software package (Bruker AXS, version 2017.3-0, 2018). Data were scaled and corrected for absorption effects using the multi-scan procedure as implemented in SADABS (Bruker AXS, version 2014/5, Krause, Herbst-Irmer, Sheldrick & Stalke, *J. Appl. Cryst.* **2015**, *48*, 3-10). The structure was solved by SHELXT (Version 2018/2: Sheldrick, G. M. *Acta Crystallogr*. **2015**, ***A71***, 3-8) and refined by a full-matrix least-squares procedure using OLEX2 (O. V. Dolomanov, L. J. Bourhis, R. J. Gildea, J. A. K. Howard and H. Puschmann. J. Appl. Crystallogr. **2009**, *42*, 339-341) (XL refinement program version 2018/3, *Sheldrick, G. M. Acta Crystallogr.* **2015**, *C71*, 3-8). Crystallographic data and details of the data collection and structure refinement are listed below for Mo radiation and for Cu radiation.

Specific details for structure refinement: All atoms were refined with anisotropic thermal parameters. Hydrogen atoms were included in idealized positions for structure factor calculations except those bound to oxygen atoms O1 and O3. These hydrogen atoms were located in the difference Fourier map and allowed to be refined freely. All structures are drawn with thermal ellipsoids at 50% probability (Mo-radiation).

Figure 2.5. ORTEP representation of **87**.

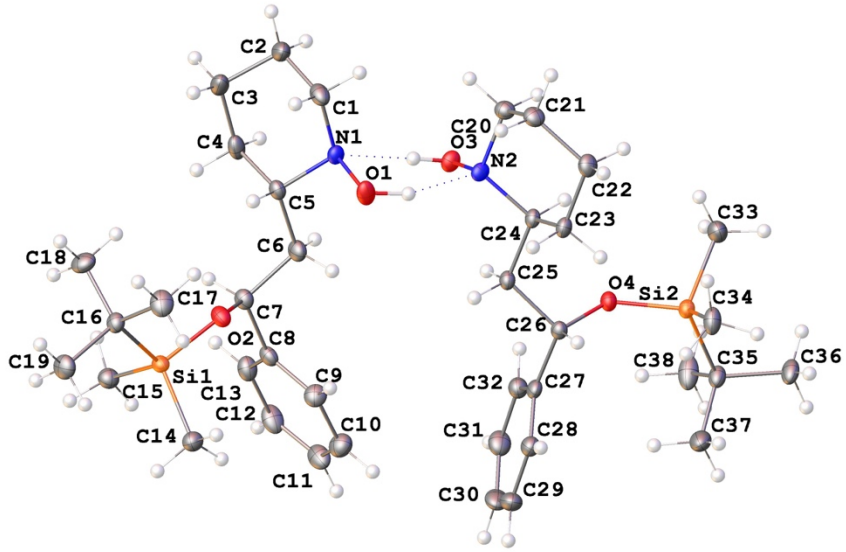

Crystal data and structure refinement for data collected with Mo X-ray tube (λ = 0.71073 Å).

Identification code	0584_lisnyak
Empirical formula	$C_{19}H_{33}NO_2Si$
Formula weight	335.55
Temperature/K	100(2)
Crystal system	monoclinic
Space group	$P2_1$
a/Å	17.1344(10)
b/Å	6.5231(4)
c/Å	18.2696(11)
α/°	90
β/°	100.047(2)
γ/°	90
Volume/Å^3	2010.7(2)
Z	4
ρ_{calc}g/cm^3	1.108
μ/mm^{-1}	0.126
F(000)	736.0
Crystal size/mm^3	0.36 × 0.32 × 0.24
Radiation	MoKα (λ = 0.71073)
2Θ range for data collection/°	4.528 to 55.996
Index ranges	$-22 \le h \le 22$, $-7 \le k \le 8$, $-23 \le l \le 23$
Reflections collected	62733
Independent reflections	8335 [R_{int} = 0.0487, R_{sigma} = 0.0486]
Data/restraints/parameters	8335/1/433
Goodness-of-fit on F^2	1.028
Final R indexes [I>=2σ (I)]	R_1 = 0.0368, wR_2 = 0.0686
Final R indexes [all data]	R_1 = 0.0585, wR_2 = 0.0742
Largest diff. peak/hole / e Å^{-3}	0.33/-0.21
Flack parameter	0.02(3)

Crystal data and structure refinement for data collected with Cu-target X-ray tube (λ = 1.54178 Å).

Identification code	0608_lisnyak
Empirical formula	$C_{19}H_{33}NO_2Si$
Formula weight	335.55
Temperature/K	100(2)
Crystal system	monoclinic
Space group	$P2_1$
a/Å	17.1453(12)
b/Å	6.5277(6)
c/Å	18.2721(14)
α/°	90
β/°	100.099(5)
γ/°	90
Volume/Å^3	2013.3(3)
Z	4
ρ_{calc}g/cm^3	1.107
μ/mm^{-1}	1.089
F(000)	736.0
Crystal size/mm^3	0.32 × 0.14 × 0.12
Radiation	CuKα (λ = 1.54178)
2Θ range for data collection/°	4.912 to 150.626
Index ranges	$-21 \le h \le 21$, $-7 \le k \le 6$, $-22 \le l \le 22$
Reflections collected	22270
Independent reflections	7436 [R_{int} = 0.1597, R_{sigma} = 0.1702]
Data/restraints/parameters	7436/1/427
Goodness-of-fit on F^2	0.986
Final R indexes [I>=2σ (I)]	R_1 = 0.0847, wR_2 = 0.1921
Final R indexes [all data]	R_1 = 0.1523, wR_2 = 0.2339
Largest diff. peak/hole / e Å^{-3}	0.75/-0.48
Flack parameter	0.05(5)

$R_{int} = \Sigma \mid F_o^2 - \langle F_o^2 \rangle \mid / \Sigma \mid F_o^2 \mid$

$R1 = \Sigma \mid \mid F_o \mid - \mid F_c \mid \mid / \Sigma \mid F_o \mid$

$wR2 = [\Sigma [w (F_o^2 - F_c^2)^2] / \Sigma [w (F_o^2)^2]]^{1/2}$

Goodness-of-fit = $[\Sigma [w (F_o^2 - F_c^2)^2] / (n-p)]^{1/2}$

n: number of independent reflections; p: number of refined parameters

CHAPTER 3

SYNTHESIS OF AZA-QUATERNARY CENTERS VIA PICTET–SPENGLER REACTIONS OF KETONITRONES

3.1 Introduction

The tetrahydro-β-carboline core is a privileged scaffold found in many natural products, folk medicines, and pharmaceuticals.[1] Due to the diverse biological activities and complex structures of these and other related indole-containing compounds, there has been substantial investigation into the synthesis of the β-carboline skeleton. The most prominent example, the Pictet–Spengler reaction, [2,3] is one of the most widely used methods for the construction of tetrahydro-β-carbolines, especially as a result of recent advancements in asymmetric methods promoted by organocatalysis.[4] Although less common, because of the sterically demanding nature and lower reactivity of the requisite ketimine starting material, the 1,1-disubstituted-β-carboline framework is found in a significant array of alkaloids, drug candidates, and useful building blocks as exemplified by **1**-**5** in Figure 3.1.[5] However, effective methods to racemically or enantioselectively access such aza-quaternary centers via Pictet–Spengler reactions are quite rare.[4b,6,7]

Figure 3.1. Selected structures of natural products and drugs containing a shared β-carboline framework (colored in blue) with an aza-quaternary center (highlighted in green).

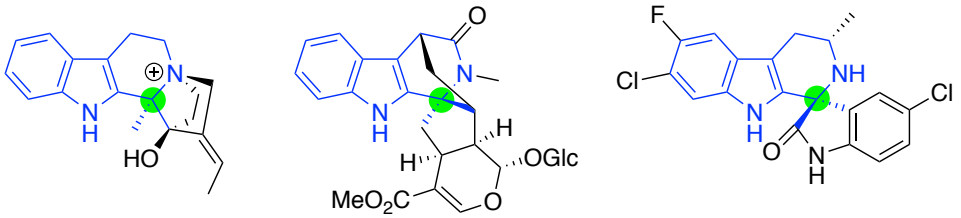

1: (–)-subincanadine B **2**: ophiorrhine A **3**: cipargamin (NITD609)

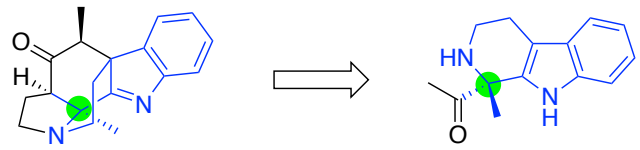

4: (+)-arborisidine **5**

The Pictet–Spengler reaction was first discovered in 1911 by the reaction's namesakes Amé Pictet and Theodor Spengler, yet, it was 17 years before Tatsui found that tryptamine (**8**) could be employed as the amine component to produce 1-methyl-2,3,4-tetrahydro-β-carboline **9** (Scheme 3.1).[2] Since this breakthrough, the Pictet–Spengler reaction has become one of the most commonly utilized methods in the synthesis of indole alkaloid compounds. Despite its widespread use, it was not until 2004 that the first catalytic, enantioselective Pictet–Spengler reaction was reported by the Jacobsen group (Scheme 3.2).[4a] By reacting tryptamine derivatives (**10**) with various aldehydes and subsequent addition of AcCl, they generated *N*-acyliminium ions to enhance the low reactivity of the corresponding imines. This, in combination with a chiral thiourea hydrogen bonding catalyst (**12**), successfully promoted the desired cyclization to **11** in an asymmetric fashion. Soon after, List and co-workers demonstrated that geminally disubstituted tryptamines **13** (relying on the Thorpe–Ingold effect) and aldehydes could be treated with chiral phosphoric acids (**15**) to form tetrahydro-β-carbolines (**14**) in high enantioselectivity.[4f] While both precedents are innovative in their own right, with many other exemplary works published since, the synthesis of 1,1-disubstituted-tetrahydro-β-carbolines through Pictet–Spengler reactions remains a challenge today.

Scheme 3.1. Discovery of the Pictet–Spengler reaction.

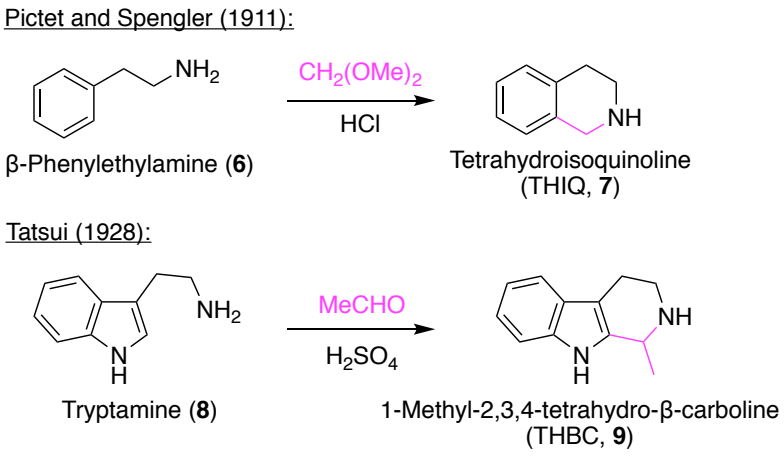

Scheme 3.2. Foundational precedents for asymmetric Pictet–Spengler chemistry with organocatalysts: (a) Jacobsen's work with thioureas; (b) List's procedure utilizing phosphoric acids.

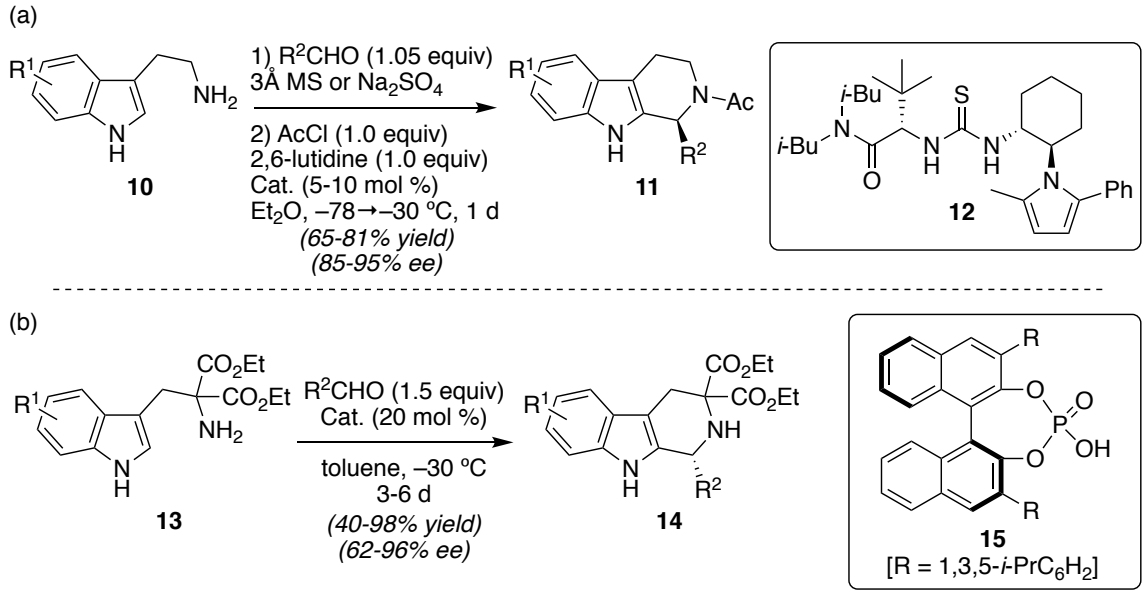

Indeed, in our own recent total synthesis of (+)-**4**, although the racemic variant worked well, we could not directly form the lone chiral center of **5** as a single enantiomer from achiral starting materials via a Pictet–Spengler reaction.[5h] Instead, as seen in Scheme 3.3, we performed a diastereoselective Pictet–Spengler reaction with D-tryptophan methyl ester (**16**), followed by an eloquent decyanation protocol to afford the desired aza-quaternary center (**5**). In a recent synthesis of the same target by Zhu and co-workers, extensive investigations ultimately achieved an enantioselective synthesis of **20** (in 86% *ee*) through the identification of a highly specific squaramide catalyst, despite requiring prolonged reaction times (12 days).[5i] Nonetheless, this precisely exemplifies that if developed, methods such as this can lead to improvements of already highly efficient syntheses, with the Zhu route providing **4** in almost half the step-count of our own synthesis. To further illustrate the difficulty of this task, there is only one other example of an asymmetric procedure involving non-spirocyclic 1,2-dicarbonyls, which used α-ketoamide-derived ketimines and stoichiometric, chiral chlorosilanes to promote the reaction.[6k]

Scheme 3.3. Previous approaches using Pictet–Spengler reactions to access key intermediates in the total syntheses of arborisidine (**4**): (a) Snyder and co-workers; (b) Zhu and co-workers.

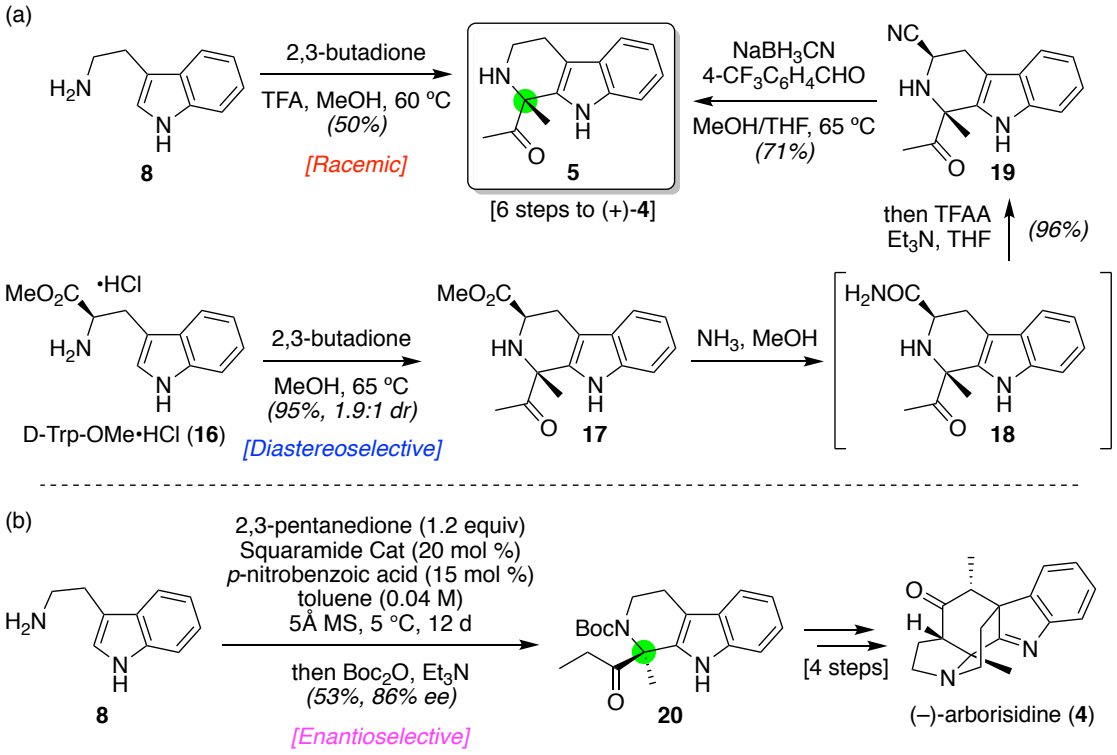

Inspired by this challenge and our recent work using nitrones in Mannich-type reactions (Chapter 2),[7] we thought it would be highly desirable to establish a robust method applying nitrones to make tetrahydro-β-carbolines bearing aza-quaternary centers. Though a limited number of nitrone-based Pictet–Spengler reactions have been published (see Chapter 1 for more details),[8] the conditions employed in these examples usually require strong acids and/or high temperatures to transform aldonitrones like **21** to cyclized products **22** (Scheme 3.4).[8f] Further studies also disclosed the ability to provide reagent-based enantiocontrol for this type of reaction, albeit the need for superstoichiometric quantities of the reagent.[8i-k] Furthermore, to the best of our knowledge, just one case of a successful reaction with a ketonitrone, in which acetone was used to generate that species, was reported in a racemic format.[8d] This lack of examples may reflect that ketonitrones are generally less reactive than their aldonitrone counterparts. Nevertheless, it has been shown in separate studies that *N*-acyloxyiminium ions (**24**), formed by the reaction of nitrones

(**23**) with acyl halides, have greatly enhanced reactivity and can undergo reactions with a wide range of nucleophiles to form materials of type **25**.[9] We anticipated that such a mode of activation might enable Pictet–Spengler chemistry to proceed when it otherwise would not (i.e. with electronically or sterically unfavored ketonitrones).

Scheme 3.4. Inspiration for our unique approach to access the desired framework.

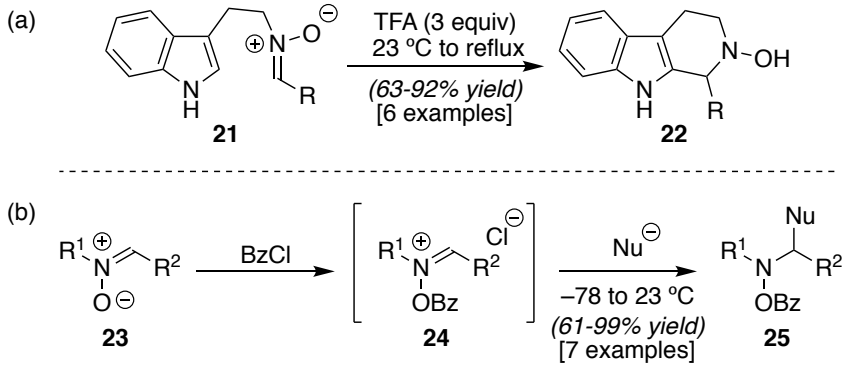

Herein we present a distinct approach for the synthesis of tetrahydro-β-carbolines with aza-quaternary centers through Pictet-Spengler reactions of ketonitrones, taking advantage of the amplified reactivity of their *N*-acyloxyiminium analogues. This process has been demonstrated, in both racemic and asymmetric formats, to provide rapid and high-yielding access to variety of such 1,1-disubstituted materials, many of which are novel compounds that have never been synthesized by Pictet–Spengler or other reactions. Finally, as illustrated by some concluding transformations, the resultant N–O bond in the products can be used to generate compounds that would otherwise be more challenging to obtain from materials fashioned through a traditional imine-based Pictet–Spengler approach.

3.2 Establishment of the Racemic Pictet–Spengler Reaction of Ketonitrones

Our studies began with efforts to affect a racemic version of the process, exploiting *N*-hydroxytryptamine **29** as our key precursor to synthesize a library of ketonitrones. To prepare this

compound, we initially attempted to use the same synthetic approach as Nakagawa and co-workers (Scheme 3.5).[8f] This 3-step procedure included: 1) the condensation of 3-indolecarboxaldehyde (**26**) with nitromethane in the presence of ammonium acetate, 2) subsequent reduction of the alkene using sodium borohydride to **28**, and finally 3) a partial reduction of the nitro group with Zn dust and aqueous NH_4Cl or aluminium amalgam to give the desired *N*-hydroxytryptamine (**29**). Though Nakagawa reported a modest 46-55% yield for the last step, in our hands this reaction was quite messy and even lower yielding. Hence, we designed a new, simple synthetic route to the vital *N*-hydroxytryptamine (**29**). Our 2-step procedure utilized a Mitsunobu reaction[10] between tryptophol (**30**) and *N*,*O*-Di-Boc-hydroxylamine, followed by a facile Boc-deprotection[11] under acidic conditions to afford **29** in a 49% yield overall (Table 3.1). It should be noted that substitution with alternative acids (such as TFA or HCl) produced **29** in lower yields. An alternative protocol involving 3 steps (oxidation to aldehyde, oxime formation, reduction to **29**) was also identified for substituted indoles that were not compatible with our 2-step approach (see Experimental Section).

Scheme 3.5. Previously reported synthesis of *N*-hydroxytryptamine (**29**).

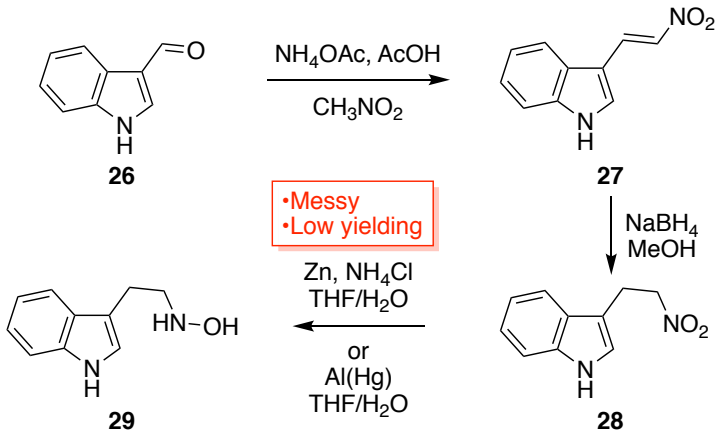

Next, we prepared ketonitrone **32**, which is an easily purifiable, bench-stable solid, as our inaugural substrate via condensation of **29** with acetophenone (**31**) on gram-scale under catalytic acidic conditions (Table 3.1).[8a] We quickly found that if this compound was combined with 1.05

equiv of benzoyl chloride in the presence of 4Å molecular sieves in CH_2Cl_2 at 23 °C, the desired product (**33a**) was obtained in 86% yield after just 30 min, which was unambiguously confirmed by X-ray crystallographic analysis. Of note, the presence of molecular sieves was crucial to prevent deterioration of the yield due the hydrolysis of the *N*-acyloxyiminium species formed *in situ* (Scheme 3.6, see **S46** Experimental Section).[9d,12] Pleasingly, all acyl chlorides screened performed well under the reaction conditions irrespective of their steric bulk or electronic properties (entries 2–5), though ultimately phenylacetyl chloride imparted the highest yield at 95% and was chosen as our activator to explore the scope of the reaction. This compatibility of an assortment of acyl chlorides further demonstrates the synthetic utility of the reaction; for example, it can be used for selective protection/deprotection sequences and rapid structure–activity relationship studies.

Table 3.1. Synthesis of nitrone **32** and screening of acyl chlorides to determine optimized conditions to generate **33**.[a]

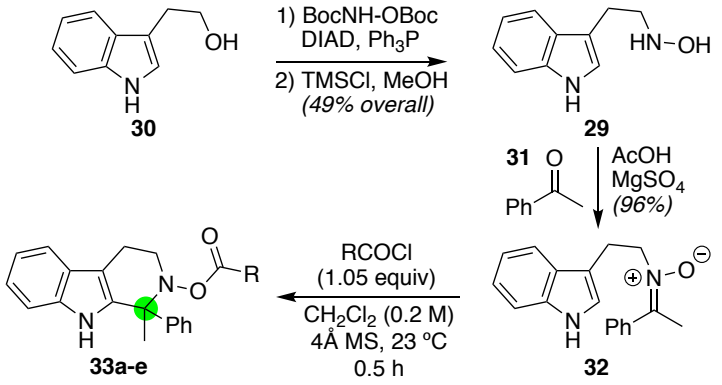

Entry	R	Product	Yield [%]
1	Ph	**33a** [X-ray]	86
2	Me	**33b**	86
3	*t*-Bu	**33c**	88
4	OMe	**33d**	87
5	CH_2Ph	**33e**	95

[a] Final reactions were performed with **32** (0.25 mmol) under argon.

With optimized conditions in hand, we turned our attention to the substrate scope of the reaction, as presented in Table 3.2. A wide variety of ketonitrones could be synthesized and

undergo the established Pictet–Spengler reaction in yields ranging from 71–97% for **40-57** when phenylacetyl chloride was used as the activating species. Some ketonitrones were isolated as inseparable *E*-/*Z*- mixtures (see Experimental Section), but this element did not affect the outcome of these racemic reactions. Both aryl and heteroaryl substituted ketonitrones afforded products (**40-45**) in good yields (83-97%); as expected, precursors with electron-deficient groups produced higher yields. While alkyl substrates (**46-49**) generally worked well, steric hinderance slightly lowered the yield, as indicated by **48** with a moderate 74% yield. Pleasingly, ether-, ester-, and ketone-substituted nitrones were highly effective under these conditions (**50-53**). Although materials leading to spirocyclic adducts **54-57** had high yields (86-85%), we found that substrates with extended ring sizes (**59** and **60**) or an indanone-based system (**58**) resulted in significantly lower yields (<50%). Compounds of this type are known to be challenging in the imine variant of this, and related, reactions.[13] Suspecting that prolonged reaction times may be causing increased decomposition/hydrolysis of the *N*-acyloxyiminium ion, we switched to a more sterically hindered acyl chloride (PivCl) to attempt to slow down the intermolecular decomposition/hydrolysis pathways, while still providing ample activation of the ketonitrone necessary for cyclization to occur (Scheme 3.6). As proposed, the yields for **58-60** were significantly enhanced. Therefore, we recommend to apply PivCl for any ketonitrones that are ineffective with other acyl groups.

Scheme 3.6. Proposed hydrolysis / decomposition pathways.

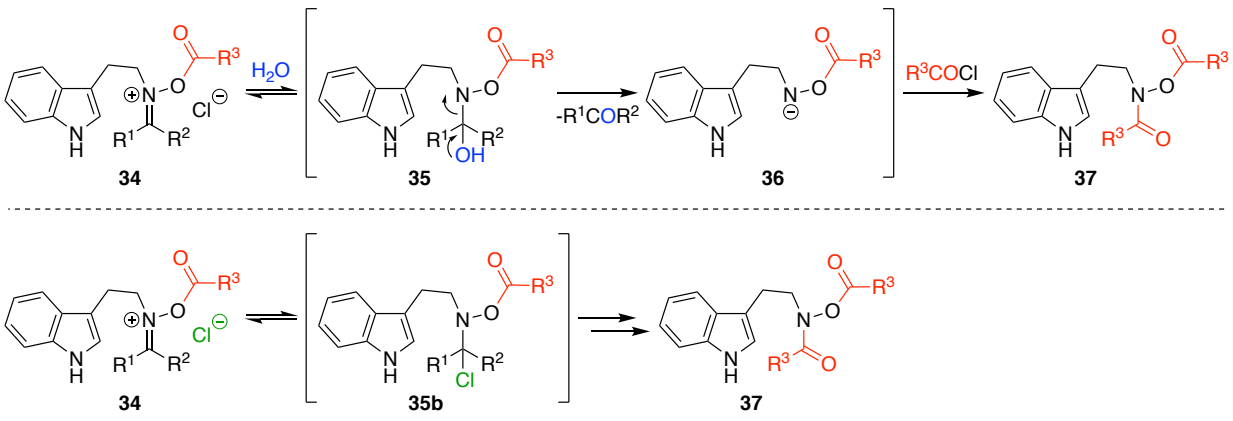

Table 3.2. Exploration of substrate scope with various ketonitrones.[a]

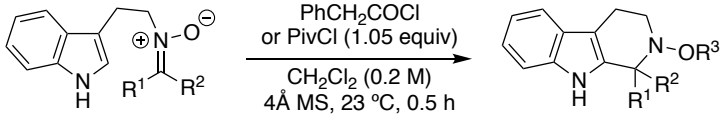

38 **39**

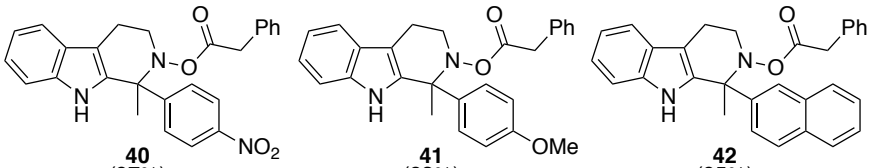

40 (97%)

41 (83%)

42 (95%)

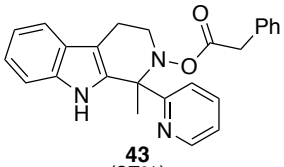

43 (87%)

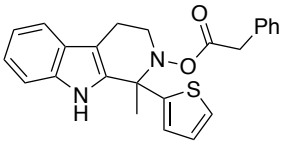

44 (96%)

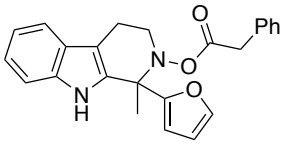

45 (93%)

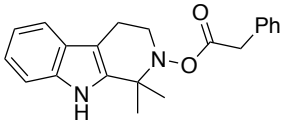

46 (97%)

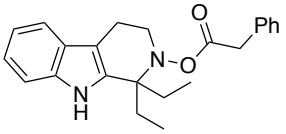

47 (85%)

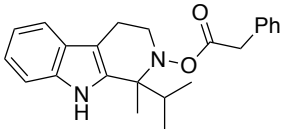

48 (74%)

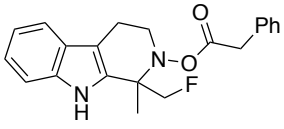

49 (71%)

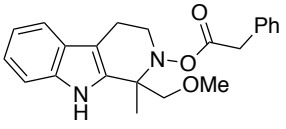

50 (87%)

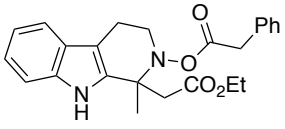

51 (96%)

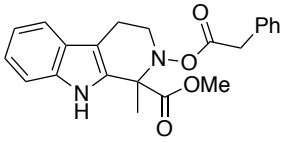

52 (92%)

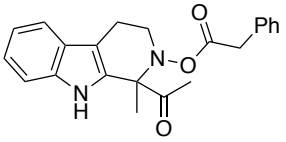

53 (80%)

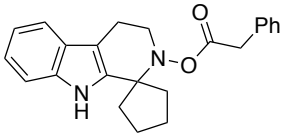

54 (95%)

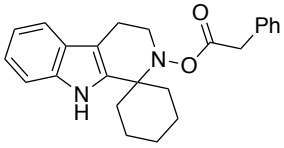

55 (86%)

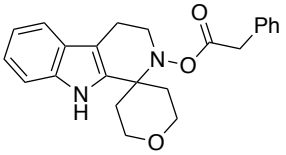

56 (94%)

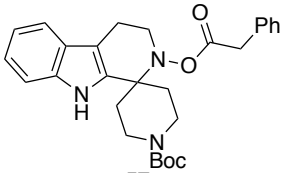

57 (91%)

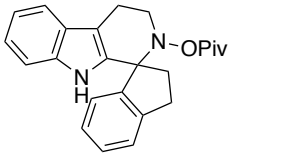

58 (90%) (27% with $PhCH_2COCl$)

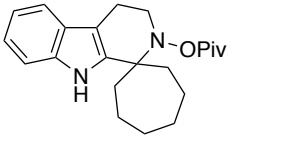

59 (72%) (48% with $PhCH_2COCl$)

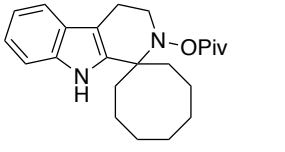

60 (54%) (35% with $PhCH_2COCl$)

[a] Final reactions were performed with **34** (0.25 mmol) under argon.

Notably, the only limitation identified for our racemic method was that we could not condense **29** with ketones that possessed a very sterically encumbered (i.e. if R^1 or R^2 = *t*-Bu) or electron-deficient group (i.e. if R^1 or R^2 = CF_3), even at elevated temperature. However, as long as the ketonitrone could be made, the Pictet–Spengler reaction was always successful.

We next examined the extent to which the electronic properties of the indole core could be modulated. As seen in Table 3.3, and as expected, substrates with electron-donating groups proceeded smoothly to generate **63** and **64** in high yield (92% and 90%, respectively). The compounds with weakly electron-withdrawing bromine substituents (**65** and **66**) also performed well with 83% and 74% yields, respectively. To our delight, indoles with strongly electron-withdrawing groups (**67** and **68**) successfully underwent the cyclization in modest yield (62-65%). These results were surprising due to the very low yields seen in standard, imine-based Pictet–Spengler reactions with electron-withdrawing substituents on the indole core,[14] highlighting how our system utilizing activated nitrones provides enhanced electrophilicity that can broaden scope.

Table 3.3. Continued exploration of substrate scope using substituted indoles.[a]

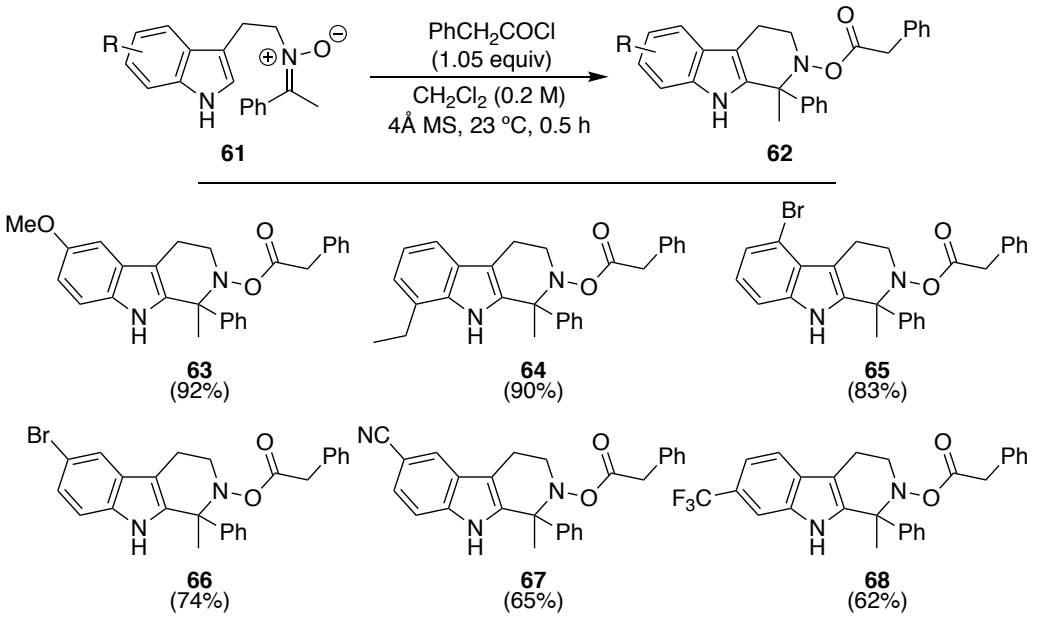

[a] Final reactions were performed with **61** (0.25 mmol) under argon.

Interestingly, when we attempted to construct product **53**, it was found that the HCl formed during the reaction could affect the cyclization of the starting material directly from the ketonitrone without generation of the *N*-acyloxyiminium ion. Further exploration showed that compounds **49**, **52**, and **53** with highly favorable electronics (i.e. highly electrophilic nitrone intermediates) could all be cyclized to their free hydroxylamines (**71**-**73**) by simply reacting the selected ketone with **29** under catalytic acidic conditions at room temperature (Table 3.4). The ease of this reaction was unexpected considering the only ketonitrone-based Pictet–Spengler example in the literature at the time (with acetone as the ketone precursor) required excess TFA and reflux conditions to promote the cyclization.[8d] In general, however, the majority of our substrates were ineffective without the formation of the *N*-acyloxyiminium intermediate, as demonstrated when acetophenone was employed in this procedure (no detection of **69**). I would like to acknowledge that Sarah Greta, my undergraduate colleague, synthesized several starting materials and contributed significantly to the examples in the substrate tables discussed.

Table 3.4. Investigation of direct cyclizations without acyl chloride additive.

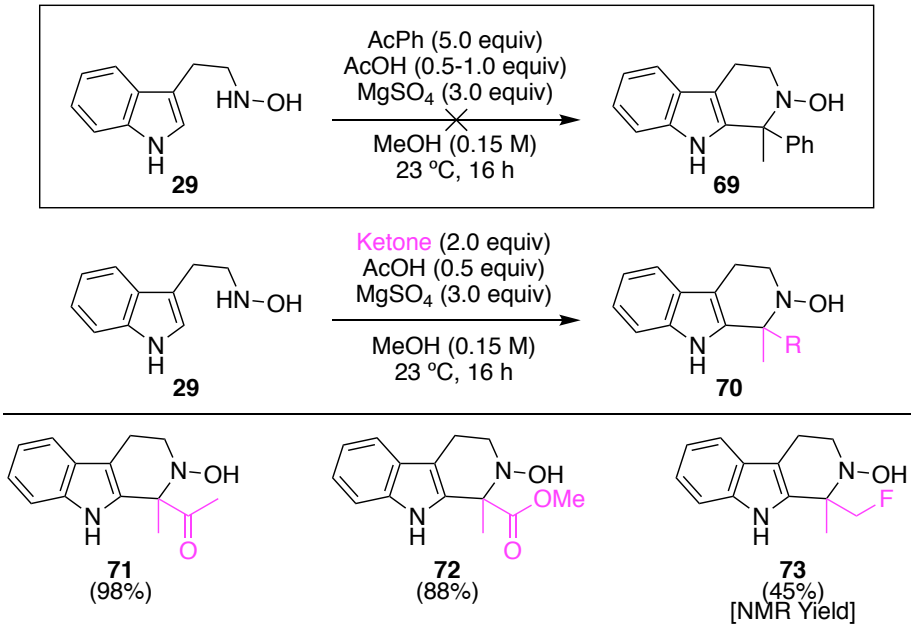

3.3 Optimization and Scope of an Asymmetric Variant of the Reaction

In addition to the racemic method described above, efforts were also placed on establishing an enantioselective variant. Attracted by reports of thioureas having the ability to promote enantioselectivity by inducing the dissociation of chloride counterions and their precedented use in promoting asymmetric Pictet–Spengler reactions, we began our investigation by testing different thiourea catalysts.[4a-e,15] Our first effective hit came when the reaction was run with **32**, benzoyl chloride, 20 mol % loading of a thiourea catalyst (**74**), and 4 Å molecular sieves in CH_2Cl_2 at a concentration of 0.015 M at –78 °C; product ***ent*-33a** was observed in a satisfactory 79% yield and modest 51% *ee* (Table 3.5). Next, a change in solvent to toluene increased the enantioselectivity to 64% *ee*, although with a slight decrease in yield (52%). A screening of additional catalysts was able to further enhance the enantioselectivity to 81% *ee* with catalyst **79**, but could not provide any solution to the low yield of the reaction.

Table 3.5. Selected exploration of varied catalysts to achieve asymmetric cyclization of nitrone **32** using BzCl.[a]

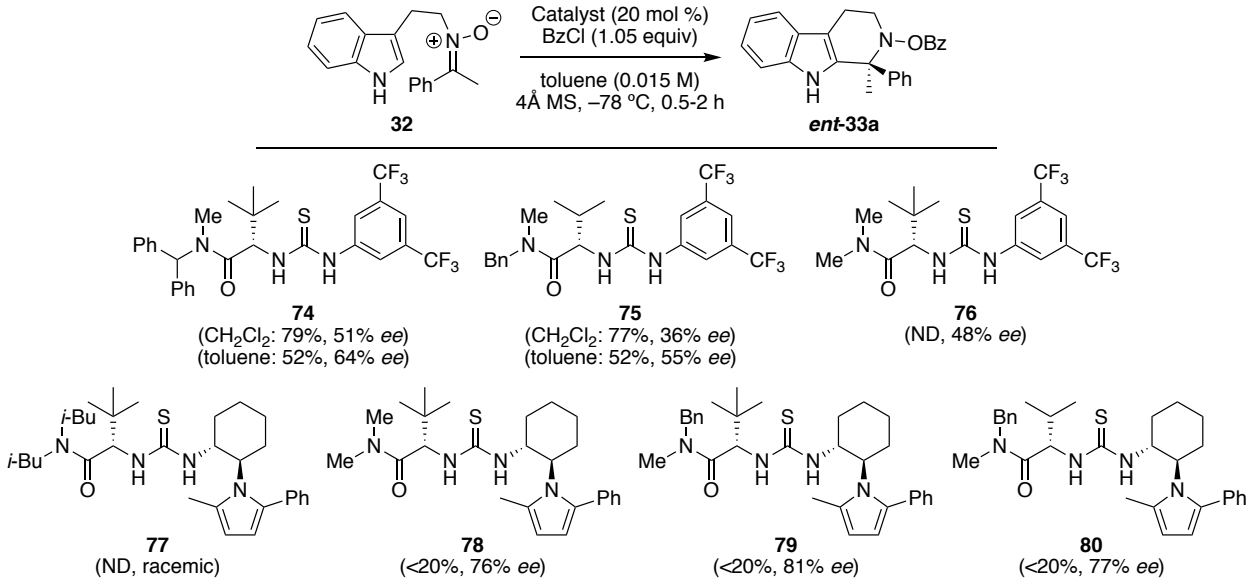

[a] Final reactions were performed with **32** (0.09 mmol) under argon.

When different thiourea catalysts could not provide a solution, we transitioned to adjusting other parameters of the reaction in an effort to boost the yield and enantioselectivity. Though many acyl chlorides were subsequently screened (4-OMeBzCl, 4-ClBzCl, 4-NO_2BzCl, 4-CF_3BzCl, 2-CF_3BzCl, 3,5-CF_3BzCl, AcCl, PivCl, methyl chloroformate, $PhCH_2COCl$, $Ph_2CHCOCl$, 9-anthracenecarbonyl chloride, 1-naphthoyl chloride), none supplied substantial improvements over BzCl. Additionally, the multiple chiral auxiliary-based acyl chlorides tested were not able to induce good diastereoselectivity (~1:1 *dr*). Unexpectedly, Bz_2O was unable to form the desired *N*-acyloxyiminium species, and thus no reaction occurred. All acid (HCl) and base (2,6-lutidine, 2,6-di-*tert*-butylpyridine, pyridine, 4-DMAP, *i*-Pr_2NEt, TMPDA) additives caused detrimental effects to the enantioselectivity of the reaction. Other solvents probed either led to no reaction (Et_2O or hexanes), explained by poor solubility of the ketonitrone, or lower enantioselectivity (MTBE). Finally, chiral phosphoric acids were not successful in promoting the desired cyclization.

After this exhaustive screening of catalysts and other variables under the benzoyl chloride system, we opted to change the activator to benzoyl bromide based on the known effect halide counterions can have on thiourea binding.[15] Furthermore, bromide has been demonstrated to be a better counter anion than chloride to predominately form *N*-acyloxyiminium ions without observation of halide addition to the C=N bond of the species (Scheme 3.6), which we thought may be beneficial to improve yields by slowing decomposition pathways.[9d] We then rescreened our collection of catalysts that were purchased, donated by Merck, or synthesized according to literature procedures,[4a-c,e] with key results shown in Table 3.6. Following this change in activating species, we finally saw retention of good yield in combination with high enantioselectivity for almost all the catalysts tested. There were a few exceptions with low enantioselectivity, such as when the methyl substituent on the amide of the catalyst was replaced with a longer carbon chain

(*i*-Bu, **77**) or the thiourea was substituted with a squaramide (**90**). Also, while Takemoto's bifunctional chiral thioureas **88** and **89** did not perform well, these results showed that reversing enantiomers of the catalyst could provide equal but opposite enantioselectivities (–41% *ee* and 41% *ee*).

Table 3.6. Exploration of varied catalysts to achieve asymmetric cyclization of nitrone **32** using BzBr.[a]

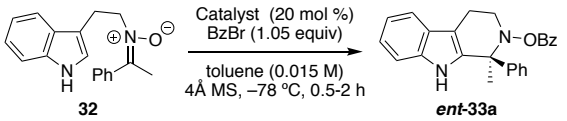

32 → ***ent*-33a**

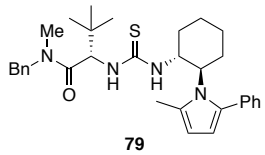 **79** (60%, 80% *ee*)	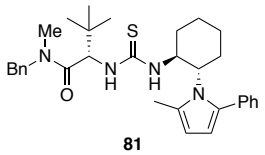 **81** (ND, 40% *ee*)	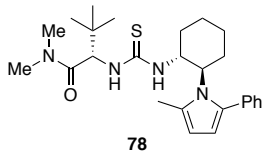 **78** (45%, 79% *ee*)	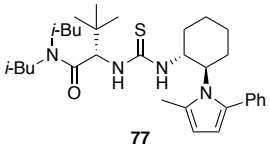 **77** (ND, 15% *ee*)
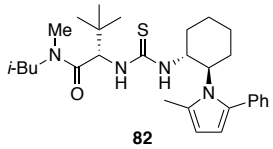 **82** (ND, 69% *ee*)	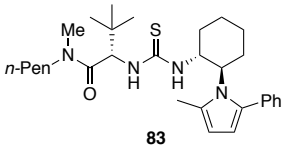 **83** (ND, 70% *ee*)	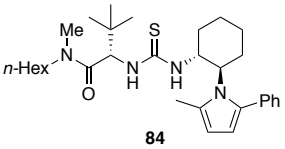 **84** (ND, 70% *ee*)	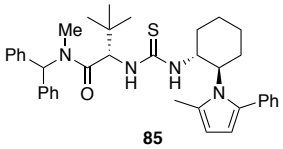 **85** (55%, 87% *ee*)[b,c]
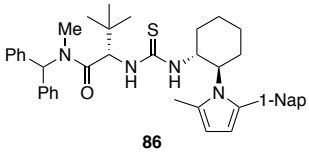 **86** (ND, 81% *ee*)[b]	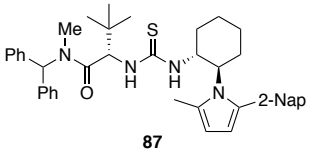 **87** (ND, 85% *ee*)[b,c]	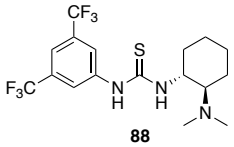 **88** (ND, –41% *ee*)	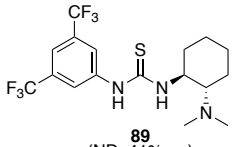 **89** (ND, 41% *ee*)
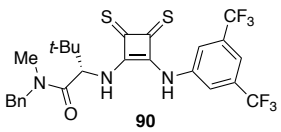 **90** (ND, 21% *ee*)	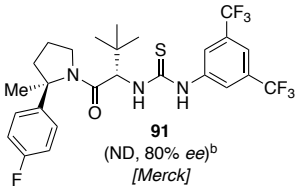 **91** (ND, 80% *ee*)[b] *[Merck]*	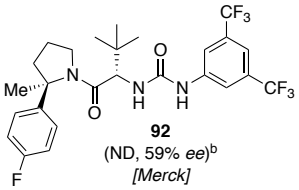 **92** (ND, 59% *ee*)[b] *[Merck]*	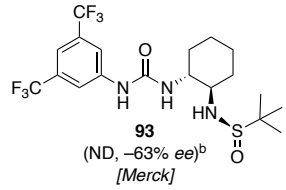 **93** (ND, –63% *ee*)[b] *[Merck]*
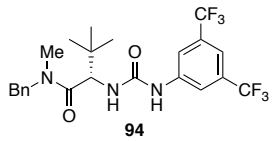 **94** (ND, 73% *ee*)	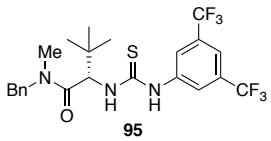 **95** (52%, 79% *ee*)	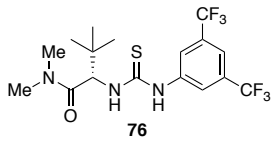 **76** (50%, 80% *ee*)	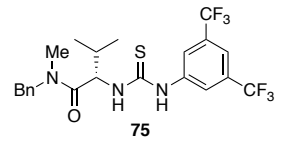 **75** (53%, 82% *ee*)
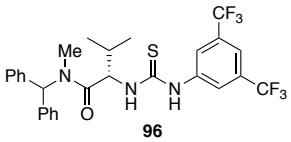 **96** (ND, 83% *ee*)	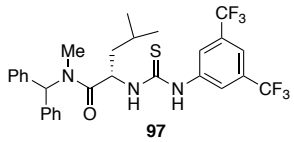 **97** (ND, 79% *ee*)	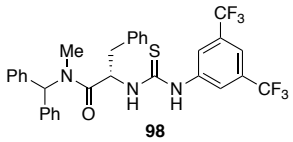 **98** (ND, 68% *ee*)	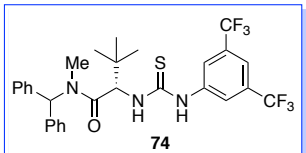 **74** (75%, 83% *ee*)

[a] Final reactions were performed with **32** (0.09 mmol) under argon; [b] Catalyst (10 mol %); [c] very challenging or unsuccesful separation of catalyst and product.

Ultimately, catalyst **74** delivered the best results with a 75% yield and 83% *ee* (boxed in Table 3.6). This result implies that our reaction may not be going through a traditional anion binding mechanism since a switch to bromide under that system would normally lead to a decrease in enantioselectivity.[4b] Hence, we propose that the catalyst instead could be interacting with the carbonyl of the *N*-acyloxyiminium species, as well as the benzene ring of the Bz group. In support of the latter proposal, when AcBr was used as the activating species, the *ee* of the product dropped by ~10%.

Following extensive optimization of catalyst loading, molarity, and temperature, the reaction afforded the best results in combination with ease of reaction set-up when conducted using 10 mol % catalyst loading of thiourea **74** in toluene at –78 °C and a concentration of 0.01 M (Table 3.7, entry 6). However, when the reaction was run on scale (0.25 mmol) the yield and enantioselectivity slightly decreased to 83% and 82% *ee*, respectively (see Table 3.8, ***ent*-33a**).

Table 3.7. Optimization of reaction conditions with thiourea **74**.[a]

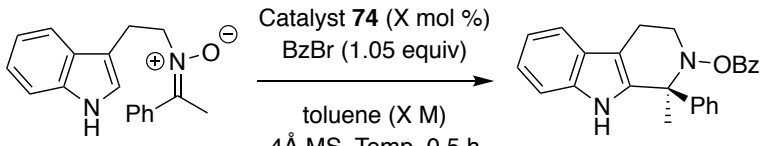

32 ***ent*-33a**

Entry	(X mol %)	M (mol/L)	Temp (ºC)	Yield [%]	*ee* [%]
1	20 mol %	0.015	–78 ºC	75	83
2	5 mol %	0.015	–78 ºC	59	77
3	10 mol %	0.015	–78 ºC	83	83
4	10 mol %	0.02	–78 ºC	83	78
5	10 mol %	0.005	–78 ºC	85	85
6	10 mol %	0.01	–78 ºC	85	84
7	10 mol %	0.01	–93 ºC	90	82

[a] Final reactions were performed with **32** (0.09 mmol) under argon.

As indicated in Table 3.8, ketonitrones possessing a variety of appended benzene rings (***ent*-33a**, **101**-**104**) all performed well in the reaction (75-83% yield, 80-83% *ee*), with no dramatic

differences based upon the electronics of the substituents on the benzene ring or indole core. The absolute configuration of all the products was determined by analogy of the X-ray crystallographic analysis of **102**. This crystallization provided enantioenrichment to afford **102** in near optical purity (99% *ee* by HPLC analysis), which we believe could be applied to enhance the enantiomeric excess of other products as well. These results in terms of enantioselectivities are comparable with Zhu's results for aza-quaternary center generation with only a single compound (Scheme 3.3, **20**, 53% yield, 86% *ee*), yet our method provides much higher yields and significantly faster reaction times. In addition, substrates with a heterocyclic substituent (pyridine **105** or thiophene **106**) also worked well, though with a decrease in enantioselectivity (55% *ee* and 53% *ee*, respectively). All nitrone precursors for Table 3.8 were determined to be the *E*-isomers via NOESY experiments, except for the formation of substrate **106**, which had a *Z*-nitrone precursor. Hence, this product was assigned as the opposite enantiomer. Noting that, unlike as discussed earlier with the racemic variant of the reaction, the ketonitrones must be obtained as single regioisomers to provide the opportunity for enantiocontrol. Since most alkyl-alkyl nitrones were isolated as inseparable *E*-/*Z*-mixtures, we were only able to test one example (**107**) that resulted in a modest enantioselectivity of 62% *ee*. Here, a 7:1 mixture of *E*-/*Z*- nitrone isomers used for the synthesis of **107**. By contrast, when a 1:7 mixture of *E*-/*Z*- nitrone isomers was utilized, a –49% *ee* was obtained, although a yield for this conversion was not reported because we were unable to perform this reaction on scale. Consequently, we were able to show that *E*-/*Z*- isomers gave approximately equal, but opposite, enantioselectivities under the optimized conditions. Disappointingly, the presence of an additional carbonyl group (like in **108**) was unsuited for this asymmetric version of the reaction and led to products with poor enantioselectivity (16% *ee*). This can be attributed to the competing racemic background reaction, which effects this electronically favored substrate more than the

others. Additionally, when the indole core had a strongly electron-withdrawing substituent (-CF_3 or -CN) no desired product could be detected and only the undesired hydrolysis side-products were obtained (not shown).

Table 3.8. Substrate scope for an asymmetric version of the reaction promoted by thiourea **74**.[a]

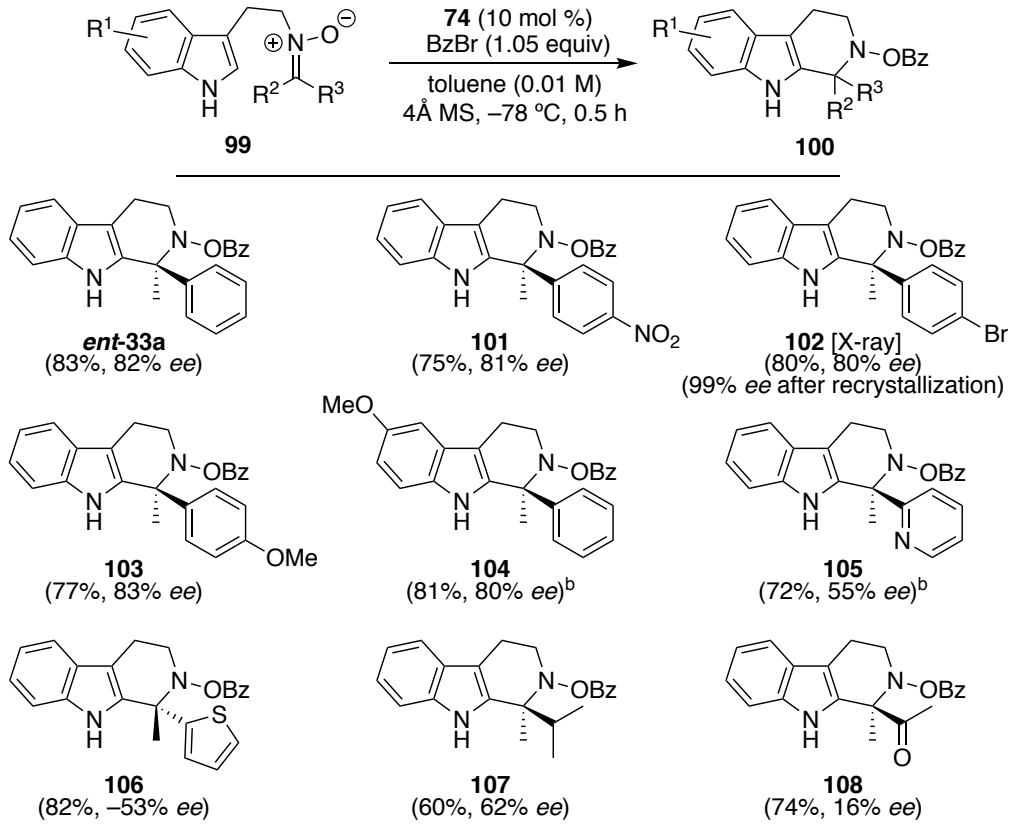

[a] Final reactions were performed with **99** (0.25 mmol) under argon;
[b] performed in toluene:CH_2Cl_2 (4:1).

3.4 Selected Transformations of Pictet–Spengler Products

To further illustrate the value of the developed methodology, supplementary transformations were executed on our original model substrate **33e**, as shown in Scheme 3.7. First, a facile N–O bond cleavage was achieved by treatment of **33e** with Zn powder in AcOH at 60 °C to form **109** in quantitative yield.[7,17] Alternatively, a one-pot procedure could be used to generate **110** by concurrently cleaving the N–O bond and undergoing a reductive amination.[7,18] Next, we

explored the effectiveness of **33e** in electrophilic amination reactions.[19] Though *O*-acyl hydroxylamines are commonly applied in this reaction class, to our knowledge the phenylacetyl group has never been evaluated, and the α-aza-quaternary center was also a concern. Nevertheless, applying Johnson's conditions,[19a] we were able to access the desired tertiary amine **111** via a copper-catalyzed electrophilic amination with a diorganozinc reagent (Ph_2Zn). Strikingly, the use of the phenylacetyl group afforded comparable yields to the commonly utilized benzoyl group with this substrate, 82% and 84%, respectively. It is worth noting that Knochel's conditions[19b] for this event employing an organozinc chloride reagent (PhZnCl) and $CoCl_2$ delivered the electrophilic amination product (**111**), but in lower yield (57%).

Scheme 3.7. Selected transformations of Pictet–Spengler product **33e** to afford additional compounds of value.

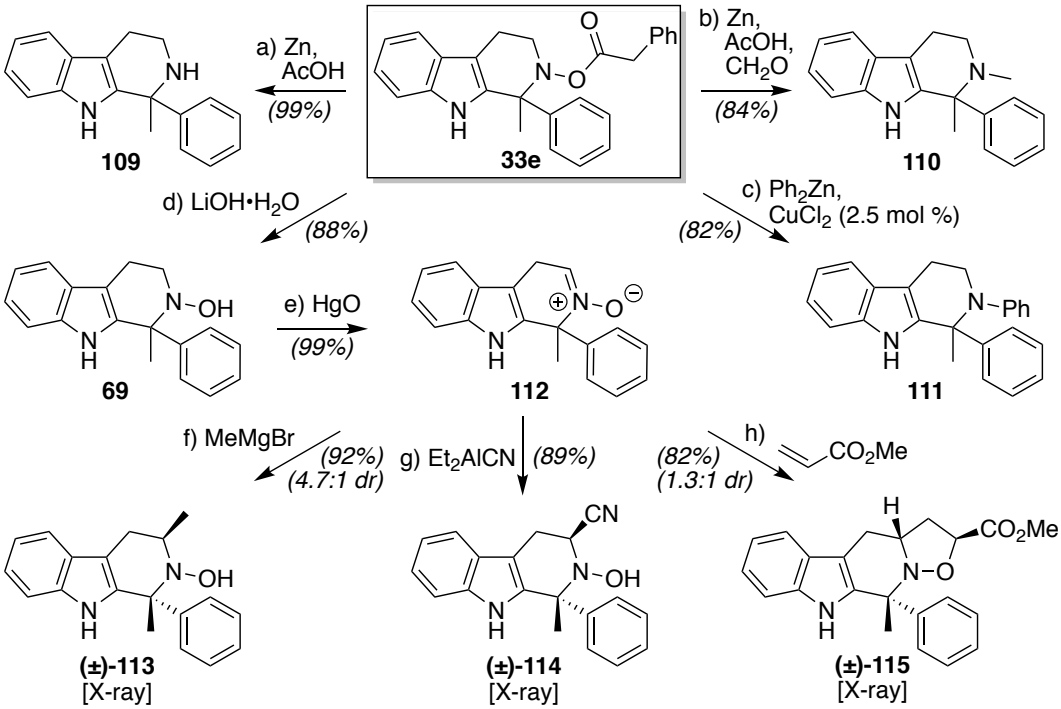

Reagents and conditions: (a) Zn (15 equiv), AcOH, 60 ºC, 3 h, 99%; (b) Zn (15 equiv), CH_2O (6 equiv), AcOH, 60 ºC, 3 h, 84%; (c) Ph_2Zn (1.1 equiv), $CuCl_2$ (2.5 mol %), THF, 23 ºC, 2 h, 82%; (d) $LiOH•H_2O$ (1.1 equiv), MeOH, 23 ºC, 0.5 h, 88%; (e) HgO (3 equiv), CH_2Cl_2:MeOH (10:1), 23 ºC, 0.5 h, sonication, 99%; (f) MeMgBr (10 equiv), THF, –78 to 0 ºC, 1 h, 92%, 4.7:1 *dr*; (g) Et_2AlCN (3 equiv), CH_2Cl_2, 0 ºC 23 ºC, 2 h, 89%; (h) methyl acrylate (10 equiv), CH_2Cl_2, 23 ºC, 2 h, 82%, 1.3:1 *dr*.

After demonstrating the ease of cleavage and reactivity of the N–O bond, selected derivatizations exploiting nitrones were investigated. We began our studies by implementing a facile acetyl deprotection procedure using LiOH•H_2O to release free hydroxylamine **69**,[20] which was quantitatively converted into aldonitrone **112** through the action of HgO and subsequent filtration.[7,21] Noticeably, sonication of the reaction mixture allowed for shortened reaction times, but should be limited in scale to avoid intense heating. This nitrone was used immediately without further purification to prevent decomposition. Unfortunately, the more environmentally friendly procedure employing IBX was not able to successfully oxidize hydroxylamine **69** to aldonitrone **112**. Nonetheless, with **112** in hand, we chose three classic reactions to demonstrate the potential of the aldonitrone.[22] First, a Grignard addition using MeMgBr at low temperature produced **113** in a mixture of 4.7:1 *dr*.[23] While other Grignard reagents and temperatures were probed, these conditions led to the best results. Second, a Strecker-type reaction with Et_2AlCN cleanly effected the conversion of **112** to **114** as a single diastereomer.[24] TMSCN was also tested, but led to a messier and non-reproducible reaction profile. Finally, **112** readily underwent a [3+2] cycloaddition with methyl acrylate to generate **115** with a 1.4:1 *dr*.[25] All of these products (**113-115**) were confirmed by X-ray crystallography as possessing the relative configurations shown. These reactions highlight the benefits of the higher oxidation state of our Pictet–Spengler products through distinct reactions with aldonitrones that would be challenging to implement from conventional amine precursors.

Regrettably, a few transformations that we attempted were unsuccessful. For example, we hoped to employ our previously developed β-ketoacid-based nitrone Mannich reaction[7] (Chapter 2) with aldonitrone **112** to create **116**, but all efforts led to complete decomposition of **112** (Scheme 3.8). We then synthesized the less sterically encumbered, geminally methyl substituted aldonitrone

117 and tried to promote our ketone-based nitrone Mannich reaction, yet once again this reaction resulted in only decomposition of the starting material. Lastly, we envisioned that establishment of a second aza-quaternary center, like in **119**, could provide means to explore unique chemical space. Although we were able to oxidize **113** to the corresponding ketonitrone by deploying HgO (not shown), all subsequent nucleophilic additions led to decomposition of this nitrone. Even when we tried to increase the reactivity of the ketonitrone via formation of the *N*-acyloxyiminium species with BzCl, the reactions were still fruitless.

Scheme 3.8. Unsuccessful transformations of Pictet–Spengler product derivatives.

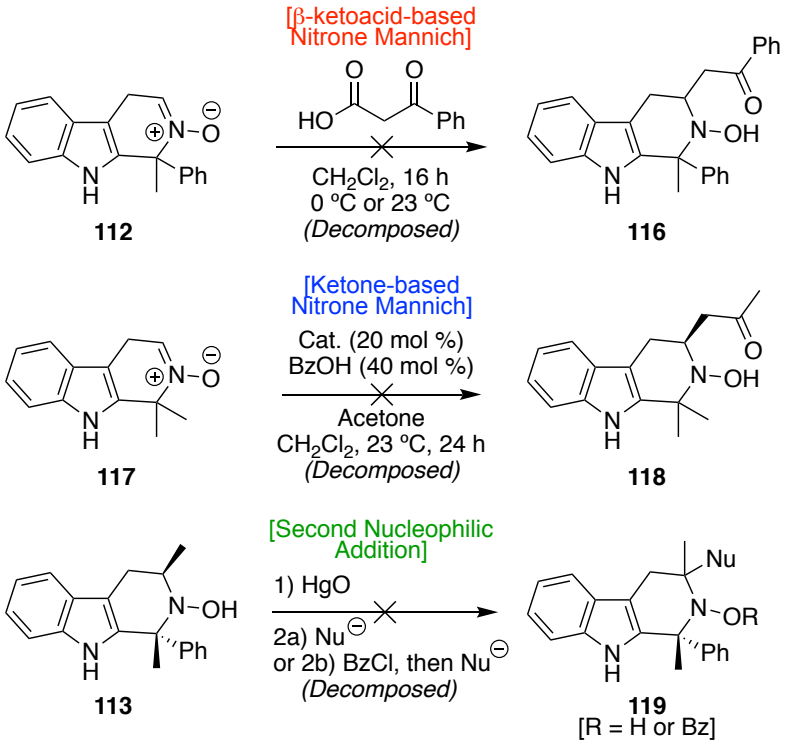

3.5 Mechanistic Understanding

Investigations into the mechanism of Pictet–Spengler-type reactions have been of high interest for several decades. There are two possible reaction mechanisms (Figure 3.2): direct attack of the C2 position of indole to the *N*-acyloxyiminium species (Path A) or attack of the C3 position

of the indole to undergo a stepwise spiroindolization/migration sequence (Path B). Despite that historically there has been experimental evidence supporting the fast and reversible formation of the spiroindolenine (like **121**), it is still unclear if this intermediate ultimately rearranges to the carbonium ion (like **122**).[8g,26] Nonetheless, according to recent computational studies, there is a strong energetic preference for C2 addition over C3 addition.[4b,27] These studies also propose that rearomatization via deprotonation of the carbonium ion intermediate is both the rate- and enantioselective-determining step. Hence, it is challenging to definitively state which pathway our reaction undergoes without kinetic, computational, and/or structure–activity relationship studies, especially since it involves an *N*-acyloxyiminium species that has not been previously explored in this reaction type. Nonetheless, these mechanistic studies are of current interest.

Figure 3.2. Current mechanistic understanding of the developed ketonitrone-based Pictet–Spengler reaction.

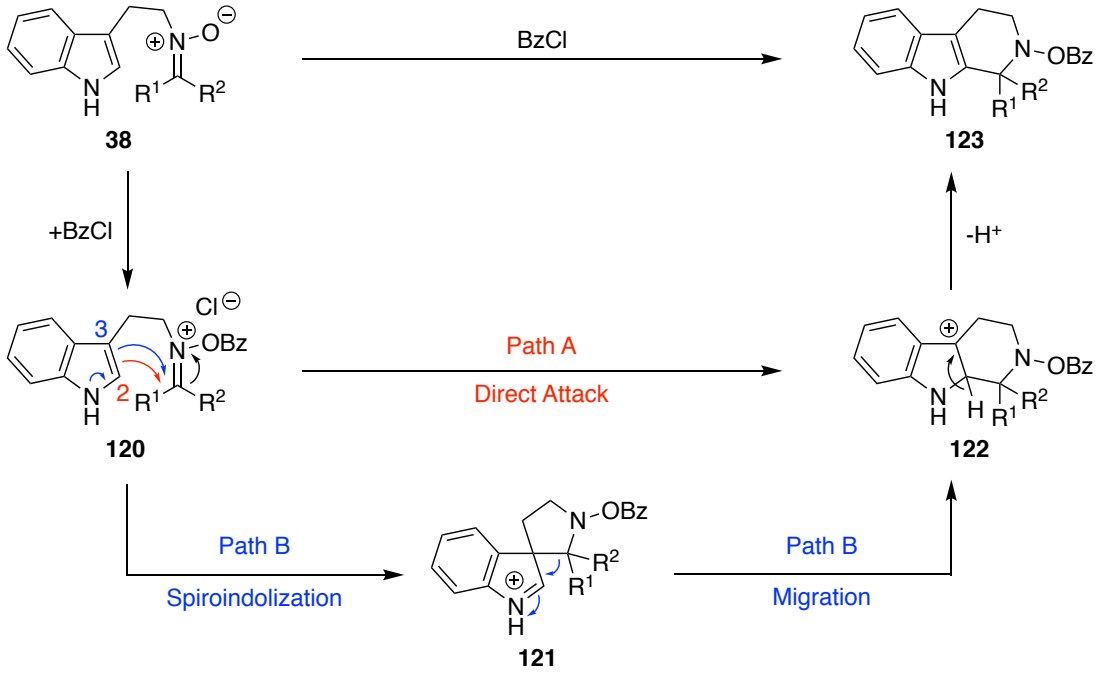

3.6 Conclusion

In conclusion, we have developed a mild, fast, and high-yielding method to generate a variety of tetrahydro-β-carbolines with aza-quaternary centers via Pictet–Spengler reactions of ketonitrones, rendered competent by converting them into *N*-acyloxyiminium ions. As illustrated by >40 examples, this approach allows for diverse substrate scope with high functional group tolerance and good to excellent yields. Moreover, we have established a catalytic, asymmetric variant of the reaction with good enantioselectivity and moderate substrate compatibility. Overall, we believe this method can be utilized in a wide range of synthetic strategies in order to access compounds of interest, such as those highlighted in Figure 3.1. The presentation of various facile and successful transformations of the products support the validity of this idea. My undergraduate colleague, Sarah Greta performed initial explorations of a route for (−)-subincanadine B (**1**), although this work was ultimately abandoned due to the low enantioselectivity of the key Pictet–Spengler product (similar to **108**). Still, we are excited at the possibility to apply our method to the synthesis of other complex molecules. Additionally, we plan to conduct mechanistic studies of the asymmetric reaction to enhance our substrate scope further.

(Some contents of this chapter were published in Lynch-Colameta, T.; Greta, S.; Snyder, S. A. *Chem. Sci.* **2021**, *12*, 6181. DOI: 10.1039/D1SC00882J.)

3.7 Experimental Section

General Procedures. All reactions were carried out under an argon atmosphere with dry solvents under anhydrous conditions, unless otherwise noted. Dry tetrahydrofuran (THF), toluene, acetonitrile (MeCN), and dichloromethane (CH_2Cl_2) were obtained by passing commercially available pre-dried, oxygen-free formulations through activated alumina columns. Yields refer to chromatographically and spectroscopically (^1H and ^{13}C NMR) homogeneous materials, unless otherwise stated. Reagents were purchased at the highest commercial quality and used without further purification, unless otherwise stated. Reactions were magnetically stirred and monitored by thin-layer chromatography (TLC) carried out on 0.25 mm E. Merck silica gel plates (60F-254) using UV light as visualizing agent, and an aqueous solution of ceric ammonium sulfate, ammonium molybdate, and sulfuric acid or aqueous solution of potassium permanganate and sodium bicarbonate and heat as a developing agent. SiliCycle silica gel (60, academic grade, particle size 0.040–0.063 mm) was used for flash column chromatography. Preparative thin-layer chromatography separations were carried out on 0.50 mm E. Merck silica gel plates (60F-254). NMR spectra were recorded on Bruker 400 and 500 MHz instruments and calibrated using residual undeuterated solvent as an internal reference. The following abbreviations were used to explain the multiplicities: s = singlet, d = doublet, t = triplet, q = quartet, br = broad, m = multiplet. IR spectra were recorded on a Nicolet iS5 FT-IR spectrometer using neat thin film technique. High-resolution mass spectra (HRMS) were recorded on Agilent 6244 TOF-MS using ESI (Electrospray Ionization) or CI (Chemical Ionization) at the University of Chicago Mass Spectroscopy Core Facility. Chiral high-performance liquid chromatography (HPLC) analysis was performed using a Shimadzu Prominence analytical chromatograph with commercial ChiralPak columns (OD-H).

The X-ray diffraction data were measured on a Bruker D8 VENTURE diffractometer at the University of Chicago X-ray Laboratory.

Preparation of Hydroxylamines.

Scheme 3.9. Method A to prepare hydroxylamines.

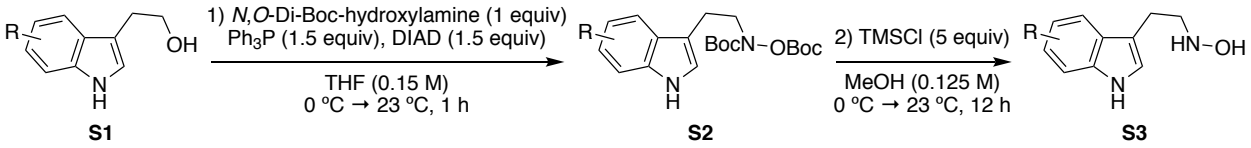

Method A.[10,11] *Step 1:* To a solution of tryptophol **S1** (1.0 equiv), Ph_3P (1.5 equiv), *N*,*O*-Di-Boc-hydroxylamine (1.0 equiv) in THF (0.15 M) at 0 ºC was added DIAD (1.5 equiv) dropwise under an argon atmosphere. The resultant mixture was warmed to 23 ºC and stirred for 1 h. Upon completion, MeOH (10.0 equiv) was added and the reaction was stirred for 15 min. The reaction contents were then concentrated directly and the resultant crude material was purified by flash column chromatography (silica gel, hexanes/EtOAc = 1/0→3/1) to yield **S2**. *Step 2:* Next, to a solution of the newly-formed **S2** (1.0 equiv) in MeOH (0.125 M) at 0 ºC was added TMSCl (5.0 equiv) dropwise under an argon atmosphere. The resultant mixture was slowly warmed to 23 ºC and stirred for 12 h. Upon completion, the reaction contents were concentrated directly and then diluted with CH_2Cl_2:MeOH (9:1). Saturated aqueous Na_2CO_3 was added, the contents were poured into a separatory funnel, and then the product was extracted with CH_2Cl_2 (3 ×). The combined organic extracts were then dried (Na_2SO_4), filtered, and concentrated. The resultant crude material was purified either by flash column chromatography (silica gel, CH_2Cl_2/MeOH = 1/0→9/1) or recrystallization (CH_2Cl_2) to afford **S3**.

Scheme 3.10. Method B to prepare hydroxylamines.

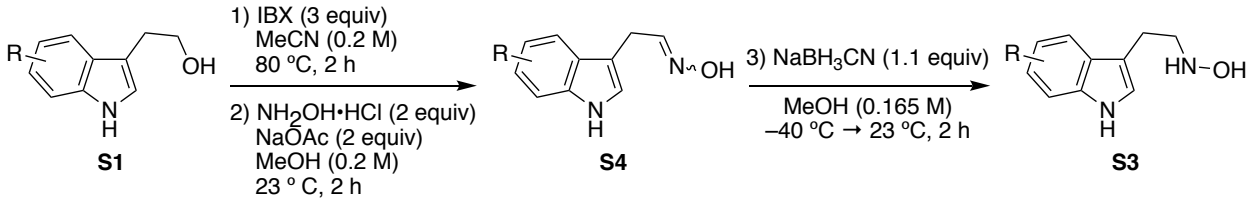

Method B.[28,29] *Step 1:* To a solution of tryptophol **S1** (1.0 equiv) in MeCN (0.2 M) at 23 ºC was added IBX (3.0 equiv) under an argon atmosphere. The resultant mixture was then heated at 80 ºC with stirring for 2 h. Upon completion, the reaction contents were cooled to 23 ºC, filtered through a pad of Celite, and rinsed with MeCN. The reaction contents were then concentrated directly to yield an aldehyde (not shown). This material was carried forward without any further purification. *Step 2:* Next, to a solution of the newly-prepared aldehyde (1.0 equiv) and NaOAc (2.0 equiv) in MeOH (0.2 M) at 23 ° C was added NH_2OH•HCl (2.0 equiv) under an argon atmosphere. The resultant mixture was stirred for 2 h at 23 ºC. Upon completion, the reaction contents were concentrated directly and then diluted with EtOAc. Saturated aqueous $NaHCO_3$ was added, the contents were poured into a separatory funnel, and then the product was extracted with EtOAc (3 ×). The combined organic extracts were then dried (Na_2SO_4), filtered, and concentrated. The resultant crude material was purified by flash column chromatography (silica gel, CH_2Cl_2/MeOH = 1/0→9/1) to yield **S4**. *Step 3:* Finally, to a solution of **S4** (1.0 equiv) and methyl orange (~5 mg) in MeOH (0.2 M) at –40 ºC was concurrently added a solution of $NaBH_3CN$ (1.1 equiv) in MeOH (1.0 M) and 6 M aqueous HCl/MeOH (1/1) dropwise open to air. The resultant mixture was slowly warmed to 23 ºC over 2 h, adding HCl as needed to maintain the color of the reaction solution red (pH < 3.1). Upon completion, the reaction contents were concentrated directly and then diluted with Et_2O. Saturated aqueous NaCl was added and the solution was basified with 6 M aqueous KOH. The contents were then poured into a separatory funnel and then the product was extracted

with EtOAc (3 ×). The combined organic extracts were then dried (Na_2SO_4), filtered, and concentrated. The resultant crude material was purified by flash column chromatography (silica gel, CH_2Cl_2/MeOH = 1/0→9/1) to yield **S3**.

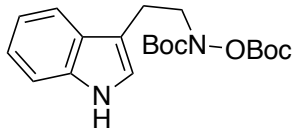

S5

***tert*-butyl (2-(1*H*-indol-3-yl)ethyl)((*tert*-butoxycarbonyl)oxy)carbamate (S5).** Prepared using Method A, Step 1 described above, starting from tryptophol **30** (2.00 g, 12.41 mmol), ultimately yielding **S5** (2.81 g, 60% yield) as a pale-yellow solid. **S5**: R_f = 0.44 (silica gel, hexanes/EtOAc = 4/1); IR (film) ν_{max} 3373, 2980, 1786, 1710, 1597, 1458, 1395, 1370, 1244, 1145, 1099, 743 cm^{-1}; ^1H NMR (500 MHz, $CDCl_3$) δ 8.06 (br s, 1 H, exchangeable), 7.62 (d, *J* = 7.8 Hz, 1 H), 7.36 (d, *J* = 8.1 Hz, 1 H), 7.22–7.15 (m, 1 H), 7.15–7.09 (m, 1 H), 7.06 (d, *J* = 2.1 Hz, 1 H), 3.91 (m, 2 H), 3.09 (t, *J* = 7.6 Hz, 2 H), 1.54 (s, 9 H), 1.38 (s, 9 H); ^{13}C NMR (101 MHz, $CDCl_3$) δ 154.9, 152.5, 136.4, 127.5, 122.5, 122.0, 119.3, 118.7, 112.3, 111.3, 85.0, 82.4, 50.9, 28.1, 27.7, 23.1; HRMS (ESI) calcd for $C_{20}H_{29}N_2O_5^+$ $[M + H]^+$ 377.2071, found 377.2071.

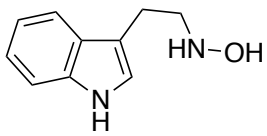

29

***N*-(2-(1*H*-indol-3-yl)ethyl)hydroxylamine (29).** Prepared using Method A, Step 2 described above with **S5** (2.50 g, 6.64 mmol), ultimately yielding **29** (0.950 g, 81% yield) as a white solid. **29**: R_f = 0.36 (silica gel, CH_2Cl_2/MeOH = 9/1); IR (film) ν_{max} 3395, 2926, 1597, 1564, 1455, 1228, 1093, 1024, 857, 808, 742 cm^{-1}; ^1H NMR (500 MHz, DMSO-d_6) δ 10.77 (br s, 1 H, exchangeable), 7.50 (d, *J* = 7.8 Hz, 1 H), 7.32 (d, *J* = 8.1 Hz, 1 H), 7.23 (br s, 1 H, exchangeable), 7.13 (d, *J* = 2.3 Hz, 1 H), 7.08–7.02 (m, 1 H), 7.00–6.92 (m, 1 H), 5.59 (br s, 1 H, exchangeable), 3.01 (t, *J* = 7.5 Hz, 2 H), 2.84 (t, *J* = 7.4 Hz, 2 H); ^{13}C NMR (101 MHz, DMSO-d_6) δ 136.3, 127.4, 122.6, 120.9, 118.3, 118.2, 112.5, 111.4, 54.5, 23.0; HRMS (CI) calcd for $C_{10}H_{13}N_2O^+$ $[M + H]^+$ 177.1022, found 177.1026.

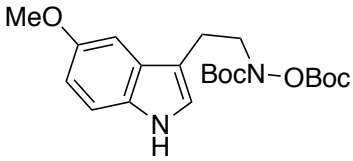

S6

***tert*-butyl ((*tert*-butoxycarbonyl)oxy)(2-(5-methoxy-1*H*-indol-3-yl)ethyl)carbamate (S6).** Prepared using Method A, Step 1 described above, starting from 5-methoxytryptophol (0.900 g, 4.71 mmol), ultimately yielding **S6** (0.950 g, 50% yield) as a yellow solid. **S6**: R_f = 0.30 (silica gel, hexanes/EtOAc = 4/1); IR (film) ν_{max} 3373, 1785, 1597, 1564, 1482, 1448, 1394, 1219, 1145, 1097 cm^{-1}; ^1H NMR (400 MHz, $CDCl_3$) δ 8.09 (br s, 1 H, exchangeable), 7.24 (d, *J* = 8.8 Hz, 1 H), 7.06 (d, *J* = 2.5 Hz, 1 H), 7.01 (d, *J* = 2.5 Hz, 1 H), 6.85 (dd, *J* = 8.8, 2.5 Hz, 1 H), 3.96–3.88 (m, 2 H), 3.87 (s, 3 H), 3.06 (t, *J* = 7.1 Hz, 2 H), 1.54 (s, 9 H), 1.37 (s, 9 H); ^{13}C NMR (101 MHz, $CDCl_3$) δ 154.9, 154.0, 152.5, 131.5, 127.9, 123.2, 112.3, 112.2, 112.0, 100.6, 84.9, 82.3, 56.0, 50.8, 28.1, 27.8, 23.1; HRMS (ESI) calcd for $C_{21}H_{31}N_2O_6^+$ $[M + H]^+$ 407.2177, found 407.2175.

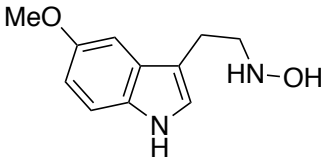

S7

***N*-(2-(5-methoxy-1*H*-indol-3-yl)ethyl)hydroxylamine (S7).** Prepared using Method A, Step 2 described above with **S6** (0.870 g, 2.14 mmol), ultimately yielding **S7** (0.355 g, 80% yield) as a white solid. **S7**: R_f = 0.35 (silica gel, CH_2Cl_2/MeOH = 9/1); IR (film) ν_{max} 3409, 2936, 1597, 1485, 1450, 1295, 1217, 1173, 1069, 1029, 798 cm^{-1}; ^1H NMR (400 MHz, DMSO-d_6) δ 10.62 (br s, 1 H exchangeable), 7.30–7.18 (m, 2 H), 7.09 (d, *J* = 2.4 Hz, 1 H), 6.99 (d, *J* = 2.4 Hz, 1 H), 6.71 (dd, *J* = 8.7, 2.4 Hz, 1 H), 5.60 (br s, 1 H, exchangeable), 3.76 (s, 3 H), 3.02 (t, *J* = 7.4 Hz, 2 H), 2.82 (t, *J* = 7.4 Hz, 2 H); ^{13}C NMR (101 MHz, DMSO-d_6) δ 152.9, 131.4, 127.6, 123.3, 112.2, 112.0, 111.0, 100.1, 55.3, 54.4, 22.9; HRMS (CI) calcd for $C_{11}H_{15}N_2O_2^+$ $[M + H]^+$ 207.1128, found 207.1130.

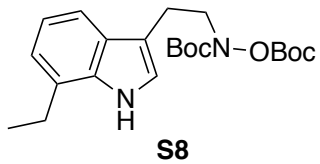

S8

***tert*-butyl ((*tert*-butoxycarbonyl)oxy)(2-(7-ethyl-1*H*-indol-3-yl)ethyl)carbamate (S8).** Prepared using Method A, Step 1 described above, starting from 7-ethyltryptophol (1.00 g, 5.28 mmol), ultimately

yielding **S8** (1.30 g, 61% yield) as a yellow solid. **S8**: R_f = 0.50 (silica gel, hexanes/EtOAc = 4/1); IR (film) ν_{max} 3373, 2978, 1786, 1712, 1597, 1564, 1448, 1395, 1370, 1246, 1151, 1131 cm^{-1}; ^1H NMR (400 MHz, $CDCl_3$) δ 8.14 (br s, 1 H, exchangeable), 7.49 (d, *J* = 7.4 Hz, 1 H), 7.12–7.01 (m, 3 H), 4.00–3.84 (m, 2 H), 3.10 (t, *J* = 7.7 Hz, 2 H), 2.85 (q, *J* = 7.6 Hz, 2 H), 1.55 (s, 9 H), 1.38 (s, 9 H), 1.34 (t, *J* = 7.6 Hz, 3 H); ^{13}C NMR (101 MHz, $CDCl_3$) δ 154.9, 152.5, 135.2, 127.2, 126.7, 122.1, 120.6, 119.7, 116.5, 112.9, 84.9, 82.3, 50.9, 28.1, 27.7, 24.1, 23.2, 14.0; HRMS (CI) calcd for $C_{22}H_{33}N_2O_5^+$ $[M + H]^+$ 405.2384, found 405.2376.

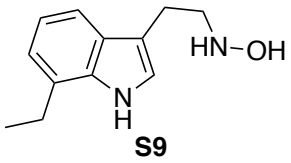

S9

***N*-(2-(7-ethyl-1*H*-indol-3-yl)ethyl)hydroxylamine (S9).** Prepared using Method A, Step 2 described above with **S8** (1.20 g, 2.97 mmol), ultimately yielding **S9** (0.400 g, 66% yield) as a white solid. **S9**: R_f = 0.45 (silica gel, CH_2Cl_2/MeOH = 9/1); IR (film) ν_{max} 3402, 2925, 1597, 1566, 1436, 1411, 1222, 1095, 794, 742 cm^{-1}; ^1H NMR (400 MHz, DMSO-d_6) δ 10.75 (br s, 1 H, exchangeable), 7.35 (dd, *J* = 7.4, 1.6 Hz, 1 H), 7.27 (br s, 1 H, exchangeable), 7.12 (d, *J* = 2.5 Hz, 1 H), 6.95–6.86 (m, 2 H), 5.60 (br s, 1 H, exchangeable), 3.08–2.98 (m, 2 H), 2.89–2.78 (m, 4 H), 1.26 (t, *J* = 7.5 Hz, 3 H); ^{13}C NMR (101 MHz, DMSO-d_6) δ 135.0, 127.2, 126.8, 122.2, 119.6, 118.5, 116.0, 112.8, 54.5, 23.7, 23.1, 14.5; HRMS (CI) calcd for $C_{12}H_{17}N_2O^+$ $[M + H]^+$ 205.1335, found 205.1337.

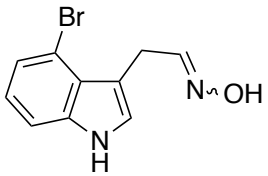

S10

2-(4-bromo-1*H*-indol-3-yl)acetaldehyde oxime (S10). Prepared using Method B, Steps 1 and 2 described above, starting from 4-bromotryptophol (2.10 g, 8.75 mmol), ultimately yielding **S10** (1.26 g, 57% yield over 2 steps, single undetermined stereoisomer) as a pale-yellow solid. **S10**: R_f = 0.38 (silica gel, CH_2Cl_2/MeOH = 9/1); IR (film) ν_{max} 3419, 2924, 1620, 1424, 1334, 1186, 1043, 912, 773, 736 cm^{-1}; ^1H NMR (500 MHz, DMSO-d_6) δ 11.29 (br s, 1 H, exchangeable), 10.93 (br s, 1 H, exchangeable), 7.38 (d, *J* = 8.0 Hz, 1 H), 7.33 (d, *J* = 2.5 Hz, 1 H), 7.17 (d, *J* = 7.5 Hz, 1 H), 6.98 (t, *J* = 7.8 Hz, 1 H), 6.87

(t, J = 4.8 Hz, 1 H), 3.91 (d, J = 4.8 Hz, 2 H); ^{13}C NMR (101 MHz, DMSO-d_6) δ 150.0, 137.8, 125.7, 124.8, 122.7, 122.3, 112.8, 111.4, 110.3, 22.5; HRMS (ESI) calcd for $C_{10}H_{10}BrN_2O^+$ [M + H]$^+$ 252.9971, found 252.9971.

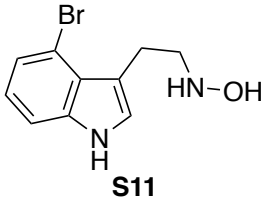

S11

***N*-(2-(4-bromo-1*H*-indol-3-yl)ethyl)hydroxylamine (S11).** Prepared using Method A, Step 3 described above with **S10** (0.360 g, 1.42 mmol), ultimately yielding **S11** (0.314 g, 87% yield) as a white solid. **S11**: R_f = 0.29 (silica gel, CH_2Cl_2/MeOH = 9/1); IR (film) ν_{max} 3272, 1477, 1333, 1183, 1119, 1032, 913, 856, 769, 736 cm^{-1}; ^{1}H NMR (500 MHz, DMSO-d_6) δ 11.18 (br s, 1 H, exchangeable), 7.36 (d, J = 8.1 Hz, 1 H), 7.25 (d, J = 2.4 Hz, 1 H), 7.15 (d, J = 7.6 Hz, 1 H), 6.95 (t, J = 7.8 Hz, 1 H), 5.75 (br s, 1 H, exchangeable), 3.13–3.01 (m, 4 H); ^{13}C NMR (101 MHz, DMSO-d_6) δ 137.8, 125.2, 124.9, 122.5, 121.9, 113.0, 112.9, 111.2, 55.4, 23.8; HRMS (ESI) calcd for $C_{10}H_{12}BrN_2O^+$ [M + H]$^+$ 255.0128, found 255.0124.

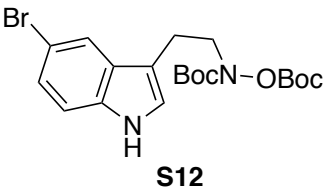

S12

***tert*-butyl (2-(5-bromo-1*H*-indol-3-yl)ethyl)((*tert*-butoxycarbonyl)oxy)carbamate (S12).** Prepared using Method A, Step 1 described above, starting from 5-bromotryptophol (1.10 g, 4.58 mmol), ultimately yielding **S12** (0.506 g, 24% yield) as a pale-yellow solid. **S12**: R_f = 0.53 (silica gel, hexanes/EtOAc = 2/1); IR (film) ν_{max} 3354, 2981, 1785, 1715, 1597, 1456, 1370, 1242, 1147, 1102 cm^{-1}; ^{1}H NMR (500 MHz, $CDCl_3$) δ 8.20 (br s, 1 H, exchangeable), 7.72 (d, J = 1.8 Hz, 1 H), 7.27–7.19 (m, 2 H), 7.05 (d, J = 2.4 Hz, 1 H), 3.94–3.82 (m, 2 H), 3.03 (t, J = 7.3 Hz, 2 H), 1.54 (s, 9 H), 1.36 (s, 9 H); ^{13}C NMR (101 MHz, $CDCl_3$) δ 154.9, 152.4, 135.0, 129.3, 124.9, 123.8, 121.4, 112.8 (2 C), 112.3, 85.1, 82.5, 50.7, 28.1, 27.8, 23.0; HRMS (ESI) calcd for $C_{20}H_{28}BrN_2O_5^+$ [M + H]$^+$ 455.1176, found 455.1177.

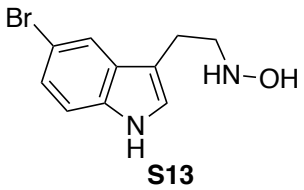

S13

***N*-(2-(5-bromo-1*H*-indol-3-yl)ethyl)hydroxylamine (S13).** Prepared using Method A, Step 2 described above with **S12** (0.410 g, 0.89 mmol), ultimately yielding **S13** (0.172 g, 75% yield) as a white solid. **S13**: R_f = 0.42 (silica gel, CH_2Cl_2/MeOH = 9/1); IR (film) ν_{max} 3425, 2921, 1597, 1564, 1449, 1394, 1220, 1096, 1049, 859, 797, 735 cm^{-1}; ^1H NMR (500 MHz, DMSO-d_6) δ 11.01 (br s, 1 H, exchangeable), 7.67 (d, J = 2.0 Hz, 1 H), 7.30 (d, J = 8.6 Hz, 1 H), 7.24 (br s, 1 H, exchangeable), 7.20 (d, J = 2.4 Hz, 1 H), 7.16 (dd, J = 8.6, 1.9 Hz, 1 H), 5.63 (br s, 1 H, exchangeable), 2.97 (t, J = 7.4 Hz, 2 H), 2.81 (t, J = 7.4 Hz, 2 H); ^{13}C NMR (101 MHz, DMSO-d_6) δ 134.9, 129.2, 124.4, 123.2, 120.6, 113.3, 112.4, 110.8, 54.4, 22.6; HRMS (ESI) calcd for $C_{10}H_{12}BrN_2O^+$ $[M + H]^+$ 255.0128, found 255.0132.

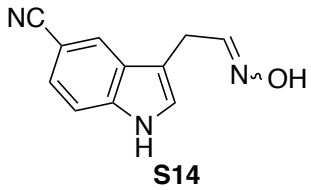

S14

(*E/Z*)-3-(2-(hydroxyimino)ethyl)-1*H*-indole-5-carbonitrile (S14). Prepared using Method B, Steps 1 and 2 described above, starting from 5-carbonitriletryptophol[30] (0.600 g, 3.22 mmol), ultimately yielding **S14** (0.415 g, 64% yield over 2 steps, 1:1 *E:Z*) as a yellow solid. **S14**: R_f = 0.42 (silica gel, CH_2Cl_2/MeOH = 9/1); IR (film) ν_{max} 3363, 2227, 1597, 1564, 1485, 1395, 1219 1100, 858, 799 cm^{-1}; ^1H NMR (500 MHz, DMSO-d_6) δ 11.51 (br s, 2 H, exchangeable), 11.09 (br s, 1 H, exchangeable), 10.53 (br s, 1 H, exchangeable), 8.08–8.01 (m, 2 H), 7.56–7.49 (m, 2 H), 7.49–7.38 (m, 5 H), 6.85 (t, J = 5.4 Hz, 1 H), 3.72 (d, J = 6.3 Hz, 2 H), 3.59 (d, J = 5.5 Hz, 2 H); ^{13}C NMR (101 MHz, DMSO-d_6) δ 148.5, 148.1, 138.1, 138.0, 126.9, 126.9, 126.0, 125.9, 124.3 124.2, 123.9 (2 C), 120.9 (2 C), 112.8 (2 C), 111.0, 111.0, 100.5, 100.5, 25.3, 20.8; HRMS (ESI) calcd for $C_{11}H_{10}N_3O^+$ $[M + H]^+$ 200.0818, found 200.0818.

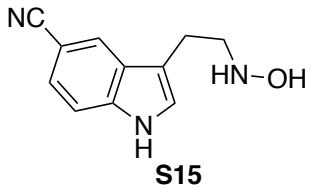

S15

3-(2-(hydroxyamino)ethyl)-1*H*-indole-5-carbonitrile (S15). Prepared using Method A, Step 3 described above with **S14** (0.150 g, 0.74 mmol), ultimately yielding **S15** (0.140 g, 94% yield) as a white solid. **S15**: R_f = 0.27 (silica gel, CH_2Cl_2/MeOH = 9/1); IR (film) ν_{max} 3362, 2924, 2370, 1597, 1563, 1448, 1394, 1219, 1091, 861 cm^{-1}; ^1H NMR (500 MHz, DMSO-d_6) δ 11.40 (br s, 1 H, exchangeable), 8.21–7.92 (m, 1 H), 7.49 (d, J = 8.4 Hz, 1 H), 7.40 (dd, J = 8.4, 1.6 Hz, 1 H), 7.36 (d, J = 2.3 Hz, 1 H), 7.25 (br s, 1 H, exchangeable), 5.65 (br s, 1 H, exchangeable), 3.00 (t, J = 7.2 Hz, 2 H), 2.86 (t, J = 7.2 Hz, 2 H); ^{13}C NMR (101 MHz, DMSO-d_6) δ 137.9, 127.3, 125.4, 124.3, 123.5, 121.0, 114.1, 112.6, 100.2, 54.3, 22.5; HRMS (ESI) calcd for $C_{11}H_{12}N_3O^+$ $[M + H]^+$ 202.0975, found 202.0975.

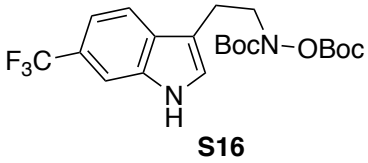

S16

***tert*-butyl ((*tert*-butoxycarbonyl)oxy)(2-(6-(trifluoromethyl)-1*H*-indol-3-yl)ethyl)carbamate (S16).** Prepared using Method A, Step 1 described above, starting from 6-trifluoromethyltryptophol[31] (1.00 g, 4.36 mmol), ultimately yielding **S16** (0.556 g, 29% yield) as a pale-yellow solid. **S16**: R_f = 0.44 (silica gel, hexanes/EtOAc = 4/1); IR (film) ν_{max} 3357, 2982, 1786, 1709, 1597, 1459, 1395, 1337, 1242, 1149, 1107, 1070 cm^{-1}; ^1H NMR (500 MHz, $CDCl_3$) δ 8.37 (br s, 1 H, exchangeable), 7.69 (dd, J = 8.4, 0.8 Hz, 1 H), 7.65 (s, 1 H), 7.35 (dd, J = 8.6, 1.6 Hz, 1 H), 7.20 (d, J = 2.4 Hz, 1 H), 3.99–3.83 (m, 2 H), 3.09 (t, J = 7.3 Hz, 2 H), 1.53 (s, 9 H), 1.34 (s, 9 H); ^{13}C NMR (101 MHz, $CDCl_3$) δ 154.9, 152.4, 135.2, 129.8, 125.4 (q, J = 271.6 Hz) 125.3, 124.2 (q, J = 31.6 Hz), 119.2, 116.1, 112.9, 108.9, 85.2, 82.5, 50.7, 28.1, 27.7, 23.0; HRMS (ESI) calcd for $C_{21}H_{27}F_3N_2NaO_5^+$ $[M + Na]^+$ 467.1764, found 467.1769.

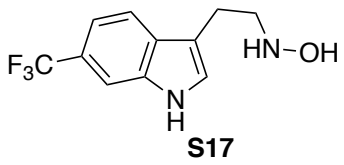

S17

***N*-(2-(6-(trifluoromethyl)-1*H*-indol-3-yl)ethyl)hydroxylamine (S17).** To a solution of **S16** (0.500 g, 1.13 mmol, 1 equiv) in CH_2Cl_2 (2.25 mL) at 23 ºC was added TFA (4.5 mL) and stirred for 2 h under

an argon atmosphere. Then followed Method A, Step 2 work-up and purification procedure described above, ultimately yielding **S17** (0.212 g, 77% yield) as a white solid. **S17**: R_f = 0.41 (silica gel, CH_2Cl_2/MeOH = 9/1); IR (film) ν_{max} 3269, 1597, 1563, 1457, 1337, 1243, 1219, 1162, 1109, 1052, 815 cm^{-1}; ^1H NMR (400 MHz, DMSO-d_6) δ 11.27 (br s, 1 H, exchangeable), 7.74–7.66 (m, 2 H), 7.41 (d, *J* = 2.4 Hz, 1 H), 7.31–7.22 (m, 2 H), 5.64 (br s, 1 H, exchangeable), 3.02 (t, *J* = 7.4 Hz, 2 H), 2.89 (t, *J* = 7.3 Hz, 2 H); ^{13}C NMR (101 MHz, DMSO-d_6) δ 135.0, 129.8, 126.3, 125.6 (q, *J* = 271.2 Hz), 121.3 (q, *J* = 31.0 Hz), 119.2, 114.4, 113.2, 108.7, 54.3, 22.7; HRMS (ESI) calcd for $C_{11}H_{12}F_3N_2O^+$ $[M + H]^+$ 245.0896, found 245.0899.

General Procedure for Preparation of Nitrones.[8a]

To a solution of hydroxylamine **29** (0.100 g, 0.57 mmol, 1.0 equiv) in CH_2Cl_2/MeOH (1/1, 3.8 mL) or MeOH (3.8 mL) at 23 ºC was added the requisite ketone (0.85-2.84 mmol, 1.5-5.0 equiv), AcOH (10 drops, from a syringe fitted with 3" needle), and $MgSO_4$ (0.205 g, 1.70 mmol, 3.0 equiv) under an argon atmosphere. The resultant mixture was stirred for 12 h either at 23 ºC or 50 ºC. Upon completion, the contents were quenched at 23 ºC with saturated aqueous $NaHCO_3$ (5 mL), poured into a separatory funnel, and extracted with CH_2Cl_2 (3 × 5 mL). The combined organic extracts were then dried (Na_2SO_4), filtered, and concentrated. The resultant crude material was purified by flash column chromatography (silica gel, CH_2Cl_2/MeOH = 1/0→9/1) to yield nitrone **32**, **S18**-**S45**. *Note:* The ratio of mixed *E-/Z-* isomers can vary depending on conditions (time, temperature, and equivalents). In addition, the *E-/Z-* ratio for each nitrone was determined by NOESY experiments.

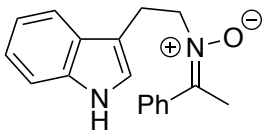

32

(*E*)-*N*-(2-(1*H*-indol-3-yl)ethyl)-1-phenylethan-1-imine oxide (32). Prepared using the general procedure described above with **29** and acetophenone (5.0 equiv) in CH_2Cl_2/MeOH (1/1) at 23 ºC, ultimately yielding **32** (0.152 g, 96% yield) as a white solid. When executed on gram scale with **29** (1.41 g, 8.00 mmol, 1.0 equiv), acetophenone (3.0 equiv), and AcOH (1 equiv) in CH_2Cl_2/MeOH (1/1) at 23 ºC, ultimately yielding **32** (2.13 g, 96% yield) as a white solid. **32**: R_f = 0.62 (silica gel, CH_2Cl_2/MeOH = 9/1); IR (film) ν_{max} 3213, 2922, 1597, 1564, 1446, 1220, 1165, 1071, 763, 744, 700 cm^{-1}; ^1H NMR (500 MHz, $CDCl_3$) δ 8.23 (br s, 1 H, exchangeable), 7.36 (d, *J* = 8.2 Hz, 1 H), 7.29–7.22 (m, 2 H), 7.21–7.13 (m, 3 H), 7.02–6.95 (m, 2 H), 6.74 (m, 2 H), 4.07 (t, *J* = 7.0 Hz, 2 H), 3.37 (t, *J* = 7.1 Hz, 2 H), 2.36 (s, 3 H); 13C NMR (101 MHz, $CDCl_3$) δ 148.5, 136.3, 136.1, 128.9, 128.7, 127.4, 127.2, 122.7, 122.0, 119.3, 118.5, 111.7, 111.3, 60.3, 23.9, 20.8; HRMS (ESI) calcd for $C_{18}H_{19}N_2O^+$ $[M + H]^+$ 279.1492, found 279.1497.

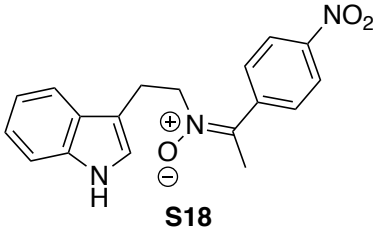

S18

(*E*)-*N*-(2-(1*H*-indol-3-yl)ethyl)-1-(4-nitrophenyl)ethan-1-imine oxide (S18). Prepared using the general procedure described above with **29** and 4′-nitroacetophenone (2.5 equiv) in CH_2Cl_2/MeOH (1/1) at 23 ºC, ultimately yielding **S18** (0.162 g, 88% yield) as a bright yellow solid. **S18**: R_f = 0.43 (silica gel, CH_2Cl_2/MeOH = 9/1); IR (film) ν_{max} 3245, 1598, 1561, 1518, 1400, 1349, 1219, 1069, 857, 744 cm^{-1}; ^1H NMR (400 MHz, $CDCl_3$) δ 8.50 (br s, 1 H, exchangeable), 7.83–7.75 (m, 2 H), 7.42–7.36 (m, 1 H), 7.22–7.14 (m, 2 H), 6.99 (d, *J* = 2.3 Hz, 1 H), 6.95–6.88 (m, 1 H), 6.60–6.53 (m, 2 H), 4.10 (t, *J* = 6.0 Hz, 2 H), 3.33 (t, *J* = 6.1 Hz, 2 H), 2.28 (s, 3 H); ^{13}C NMR (101 MHz, $CDCl_3$) δ 147.3, 146.2, 142.0, 136.3, 128.3, 127.4, 123.6, 122.9, 122.5, 119.7, 118.3, 111.6, 111.4, 60.8, 23.7, 20.5; HRMS (CI) calcd for $C_{18}H_{18}N_3O_3^+$ $[M + H]^+$ 324.1343, found 324.1342.

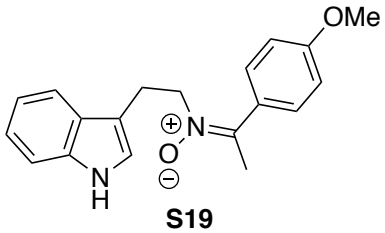

S19

(*E*)-*N*-(2-(1*H*-indol-3-yl)ethyl)-1-(4-methoxyphenyl)ethan-1-imine oxide (S19). Prepared using the general procedure described above with **29** and 4′-methoxyacetophenone (3.5 equiv) in MeOH at 50 ºC, ultimately yielding **S19** (0.155 g, 89% yield) as a gray solid. **S19**: R_f = 0.46 (silica gel, CH_2Cl_2/MeOH = 9/1); IR (film) ν_{max} 3181, 2922, 1607, 1513, 1457, 1289, 1250, 1165, 1071, 1028, 833, 743 cm^{-1}; ^1H NMR (500 MHz, $CDCl_3$) δ 8.19 (br s, 1 H, exchangeable), 7.39–7.33 (m, 1 H), 7.28 (d, *J* = 7.9 Hz, 1 H), 7.21–7.13 (m, 1 H), 7.04–6.97 (m, 2 H), 6.66 (d, *J* = 0.9 Hz, 4 H), 4.08 (t, *J* = 7.0 Hz, 2 H), 3.76 (s, 3 H), 3.36 (t, *J* = 7.0 Hz, 2 H), 2.34 (s, 3 H); ^{13}C NMR (101 MHz, $CDCl_3$) δ 159.8, 148.6, 136.4, 128.6, 128.3, 127.5, 122.8, 121.9, 119.3, 118.6, 114.0, 111.7, 111.3, 60.1, 55.4, 23.9, 20.9; HRMS (ESI) calcd for $C_{19}H_{21}N_2O_2^+$ $[M + H]^+$ 309.1598, found 309.1604.

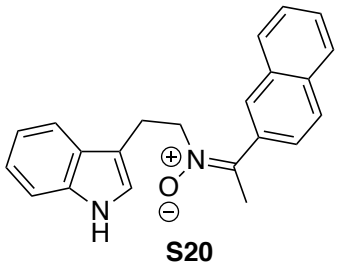

S20

(*E*)-*N*-(2-(1*H*-indol-3-yl)ethyl)-1-(naphthalen-2-yl)ethan-1-imine oxide (S20). Prepared using the general procedure described above with **29** and 2-acetonaphthone (5.0 equiv) in CH_2Cl_2/MeOH (1/1) at 23 ºC, ultimately yielding **S20** (0.160 g, 86% yield) as a pale-yellow solid. **S20**: R_f = 0.51 (silica gel, CH_2Cl_2/MeOH = 9/1); IR (film) ν_{max} 3210, 1597, 1563, 1448, 1389, 1219, 1164, 1065, 858, 744 cm^{-1}; ^1H NMR (500 MHz, $CDCl_3$) δ 8.14 (br s, 1 H, exchangeable), 7.77 (d, *J* = 8.1 Hz, 1 H), 7.66 (d, *J* = 8.5 Hz, 1 H), 7.53–7.47 (m, 1 H), 7.47–7.42 (m, 1 H), 7.42–7.36 (m, 2 H), 7.24 (d, *J* = 7.9 Hz, 1 H), 7.18–7.12 (m, 1 H), 7.01–6.97 (m, 1 H), 6.97–6.94 (m, 1 H), 6.91–6.83 (m, 2 H), 4.13 (t, *J* = 6.7 Hz, 2 H), 3.41 (t, *J* = 6.8 Hz, 2 H), 2.43 (s, 3 H); ^{13}C NMR (101 MHz, $CDCl_3$) δ 148.7, 136.3, 133.3, 132.8, 132.7, 128.6, 128.3, 127.7, 127.5, 127.1, 127.0, 126.8, 124.4, 122.9, 122.1, 119.4, 118.6, 111.7, 111.3, 60.3, 23.7, 21.0; HRMS (CI) calcd for $C_{22}H_{21}N_2O^+$ $[M + H]^+$ 329.1648, found 329.1657.

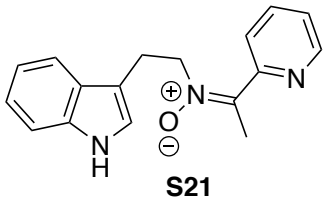

S21

(*E*)-*N*-(2-(1*H*-indol-3-yl)ethyl)-1-(pyridin-2-yl)ethan-1-imine oxide (S21). Prepared using the general procedure described above with **29** and 2-acetylpyridine (3.0 equiv) in CH_2Cl_2/MeOH (1/1) at 23 ºC, ultimately yielding **S21** (0.120 g, 76% yield) as a yellow solid. **S21**: R_f = 0.37 (silica gel, CH_2Cl_2/MeOH = 9/1); IR (film) ν_{max} 3220, 2922, 1586, 1561, 1430, 1264, 1223, 1169, 1102, 1085, 784, 743 cm^{-1}; ^1H NMR (500 MHz, $CDCl_3$) δ 8.60–8.44 (m, 1 H), 8.24 (br s, 1 H, exchangeable), 7.43–7.30 (m, 3 H), 7.17–7.11 (m, 1 H), 7.09 (ddd, *J* = 7.6, 4.8, 1.0 Hz, 1 H), 7.02–6.95 (m, 2 H), 6.67–6.61 (m, 1 H), 4.32 (t, *J* = 7.1 Hz, 2 H), 3.41 (t, *J* = 7.1 Hz, 2 H), 2.40 (s, 3 H); ^{13}C NMR (101 MHz, $CDCl_3$) δ 153.8, 149.2, 146.4, 136.5, 136.3, 127.4, 123.2, 123.1, 122.7, 122.0, 119.3, 118.5, 112.0, 111.3, 61.0, 24.1, 19.4; HRMS (ESI) calcd for $C_{17}H_{18}N_3O^+$ $[M + H]^+$ 280.1444, found 280.1451.

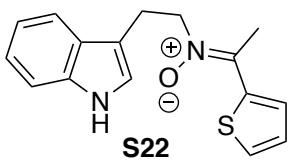

S22

(*Z*)-*N*-(2-(1*H*-indol-3-yl)ethyl)-1-(thiophen-2-yl)ethan-1-imine oxide (S22). Prepared using the general procedure described above with **29** and 2-acetylthiophene (5.0 equiv) in MeOH at 50 ºC, ultimately yielding **S22** (0.136 g, 84% yield) as a yellow solid. **S22**: R_f = 0.55 (silica gel, CH_2Cl_2/MeOH = 9/1); IR (film) ν_{max} 3180, 2921, 1597, 1563, 1456, 1419, 1365, 1337, 1212, 1160, 1101, 744 cm^{-1}; ^1H NMR (500 MHz, $CDCl_3$) δ 8.10 (br s, 1 H, exchangeable), 7.63 (d, *J* = 7.8 Hz, 1 H), 7.48 (d, *J* = 5.1 Hz, 1 H), 7.41–7.33 (m, 2 H), 7.23–7.17 (m, 1 H), 7.16–7.08 (m, 2 H), 6.99 (d, *J* = 2.2 Hz, 1 H), 4.36 (t, *J* = 7.0 Hz, 2 H), 3.48 (t, *J* = 7.0 Hz, 2 H), 2.15 (s, 3 H); ^{13}C NMR (101 MHz, $CDCl_3$) δ 137.6, 136.3, 134.6, 130.2, 129.1, 127.2, 126.0, 122.9, 122.2, 119.7, 118.4, 111.5 (2 C), 59.9, 23.8, 16.4; HRMS (ESI) calcd for $C_{16}H_{17}N_2OS^+$ $[M + H]^+$ 285.1056, found 285.1058.

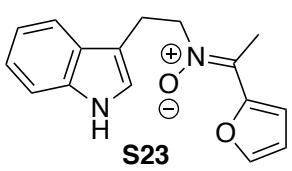

S23

(*Z*)-*N*-(2-(1*H*-indol-3-yl)ethyl)-1-(furan-2-yl)ethan-1-imine oxide (S23). Prepared using the general procedure described above with **29** and 2-acetylfuran (5.0 equiv) in MeOH at 50 ºC, ultimately yielding **S23** (0.126 g, 83% yield) as a yellow solid. **S23**: R_f = 0.47 (silica gel, CH_2Cl_2/MeOH = 9/1); IR (film) ν_{max} 3178, 1597, 1563, 1482, 1449, 1389, 1219, 1153, 1073, 744 cm^{-1}; ^1H NMR (500 MHz, $CDCl_3$) δ 8.16–8.05 (m, 2 H, 1 exchangeable), 7.64 (d, *J* = 7.7 Hz, 1 H), 7.50–7.45 (m, 1 H), 7.40–7.33 (m, 1 H), 7.24–7.17 (m, 1 H), 7.16–7.08 (m, 1 H), 7.04 (d, *J* = 2.3 Hz, 1 H), 6.58 (dd, *J* = 3.5, 1.7 Hz, 1 H), 4.27 (t, *J* = 7.2 Hz, 2 H), 3.45 (t, *J* = 7.2 Hz, 2 H), 2.12 (s, 3 H); ^{13}C NMR (101 MHz, $CDCl_3$) δ 148.0, 143.6, 136.4, 134.4, 127.2, 122.9, 122.1, 119.5, 118.3, 117.0, 112.7, 111.5, 111.4, 60.7, 23.7, 14.7; HRMS (CI) calcd for $C_{16}H_{17}N_2O_2^+$ $[M + H]^+$ 269.1285, found 269.1287.

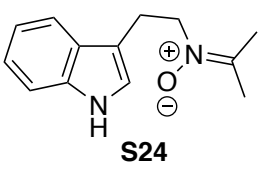

S24

***N*-(2-(1*H*-indol-3-yl)ethyl)propan-2-imine oxide (S24).** Prepared using the general procedure described above with **29** and acetone (50.0 equiv) at 23 ºC, ultimately yielding **S24** (0.112 g, 91% yield) as a white solid. **S24**: R_f = 0.38 (silica gel, CH_2Cl_2/MeOH = 9/1); IR (film) ν_{max} 3182, 2922, 1597, 1564, 1448, 1392, 1218, 1141, 1071, 858, 798, 744 cm^{-1}; ^1H NMR (500 MHz, $CDCl_3$) δ 8.72 (br s, 1 H, exchangeable), 7.61 (d, *J* = 7.9 Hz, 1 H), 7.38 (d, *J* = 8.1 Hz, 1 H), 7.22–7.16 (m, 1 H), 7.14–7.08 (m, 1 H), 7.04 (d, *J* = 2.4 Hz, 1 H), 4.13 (t, *J* = 6.9 Hz, 2 H), 3.39 (t, *J* = 6.9 Hz, 2 H), 2.08 (s, 3 H), 1.66 (s, 3 H); ^{13}C NMR (101 MHz, $CDCl_3$) δ 144.9, 136.3, 127.3, 122.7, 122.1, 119.5, 118.4, 111.8, 111.4, 59.4, 23.4, 20.3, 20.1; HRMS (ESI) calcd for $C_{13}H_{17}N_2O^+$ $[M + H]^+$ 217.1335, found 217.1336.

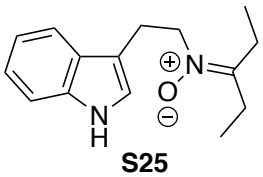

S25

***N*-(2-(1*H*-indol-3-yl)ethyl)pentan-3-imine oxide (S25).** Prepared using the general procedure described above with **29** and 3-pentanone (5.0 equiv) in CH_2Cl_2/MeOH (1/1) at 23 ºC, ultimately yielding **S25** (0.133 g, 96%

yield) as a yellow solid. **S25**: R_f = 0.49 (silica gel, CH_2Cl_2/MeOH = 9/1); IR (film) ν_{max} 3173, 2974, 1597, 1458, 1342, 1234, 1141, 1108, 1072, 743 cm^{-1}; ^1H NMR (500 MHz, $CDCl_3$) δ 8.42 (br s, 1 H, exchangeable), 7.63 (d, *J* = 7.8 Hz, 1 H), 7.41–7.34 (m, 1 H), 7.23–7.16 (m, 1 H), 7.15–7.09 (m, 1 H), 7.06 (d, *J* = 2.2 Hz, 1 H), 4.11 (t, *J* = 7.0 Hz, 2 H), 3.41 (t, *J* = 7.0 Hz, 2 H), 2.54 (q, *J* = 7.5 Hz, 2 H), 2.02 (q, *J* = 7.6 Hz, 2 H), 1.07 (t, *J* = 7.5 Hz, 3 H), 0.81 (t, *J* = 7.6 Hz, 3 H); ^{13}C NMR (101 MHz, $CDCl_3$) δ 154.8, 136.5, 127.2, 123.2, 121.8, 119.2, 118.2, 111.6, 111.1, 59.0, 24.9, 24.2, 23.7, 11.0, 9.3; HRMS (CI) calcd for $C_{15}H_{21}N_2O^+$ $[M + H]^+$ 245.1648, found 245.1660.

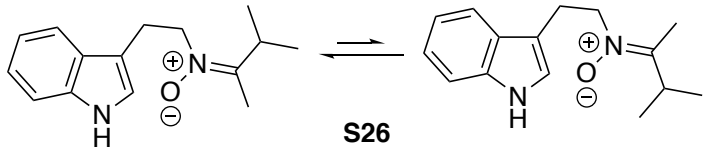

(*E/Z*)-*N*-(2-(1*H*-indol-3-yl)ethyl)-3-methylbutan-2-imine oxide (S26). Prepared using the general procedure described above with **29** and methyl isopropyl ketone (5.0 equiv) in CH_2Cl_2/MeOH (1/1) at 23 ºC, ultimately yielding **S26** (0.130 g, 94% yield, 1.4:1 *E*:*Z*) as a yellow solid. **S26**: R_f = 0.43 (silica gel, CH_2Cl_2/MeOH = 9/1); IR (film) ν_{max} 3178, 1597, 1561, 1449, 1389, 1207, 1095,1074, 858, 744 cm^{-1}; ^1H NMR (500 MHz, $CDCl_3$, 1.4:1 *E*:*Z*) δ 8.53 (br s, 1 H, exchangeable), 7.63 (t, *J* = 7.6 Hz, 1 H), 7.40–7.32 (m, 1 H), 7.22–7.15 (m, 1 H), 7.15–7.09 (m, 1 H), 7.08–7.03 (m, 1 H), 4.19 (t, *J* = 6.8 Hz, 1.1 H), 4.11 (t, *J* = 6.9 Hz, 0.8 H), 3.84–3.74 (m, 0.3 H), 3.43–3.35 (m, 2 H), 2.60–2.48 (m, 0.6 H), 1.94 (s, 1.7 H), 1.48 (s, 1.2 H), 0.93 (d, *J* = 7.0 Hz, 2.5 H), 0.65 (d, *J* = 6.8 Hz, 3.5 H); ^{13}C NMR (101 MHz, $CDCl_3$, 1.4:1 *E*:*Z*) δ 154.5, 153.2, 136.6, 136.5, 127.3, 127.3, 123.2, 123.0, 122.0, 121.9, 119.4, 119.4, 118.3, 118.2, 111.6, 111.6, 111.4, 111.3, 59.8, 58.9, 31.4, 28.4, 23.9, 23.4, 19.3, 18.3, 13.4, 13.1; HRMS (ESI) calcd for $C_{15}H_{21}N_2O^+$ $[M + H]^+$ 245.1648, found 245.1653.

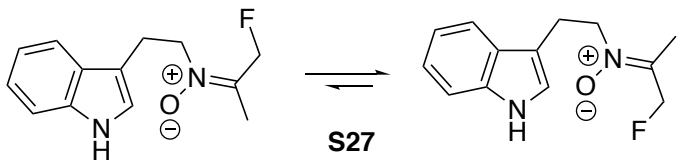

S27

(*E/Z*)-*N*-(2-(1*H*-indol-3-yl)ethyl)-1-fluoropropan-2-imine oxide (S27). Prepared using the general procedure described above with **29** and fluoroacetone (5.0 equiv) in CH_2Cl_2/MeOH (1/1) at 23 ºC, ultimately yielding **S27** (0.060 g, 45% yield, 1:3.6 *E*:*Z*) as a white solid. **S27**: R_f = 0.41 (silica gel, CH_2Cl_2/MeOH = 9/1); IR (film) ν_{max} 3220, 1597, 1562, 1481, 1448, 1389, 1219, 1157, 1030, 708, 745 cm^{-1}; ^1H NMR (500 MHz, $CDCl_3$, 1:3.6 *E*:*Z*) δ 8.11 (br s, 1 H, exchangeable), 7.65–7.57 (m, 1 H), 7.41–7.34 (m, 1 H), 7.24–7.19 (m, 1 H), 7.17–7.11 (m, 1 H), 7.09–7.03 (m, 1 H), 5.26 (d, *J* = 48.5 Hz, 1.5 H), 4.44 (d, *J* = 47.2 Hz, 0.4 H), 4.22 (t, *J* = 7.3 Hz, 0.4 H), 4.11 (t, *J* = 6.7 Hz, 1.6 H), 3.43–3.35 (m, 2 H), 2.09 (d, *J* = 4.2 Hz, 0.6 H), 1.67–1.57 (m, 2.6 H); ^{13}C NMR (101 MHz, $CDCl_3$, 1:3.6 *E*:*Z*) δ 145.29 (d, *J* = 28.3 Hz), 142.24 (d, *J* = 14.6 Hz), 136.4, 136.3, 127.2, 127.1, 122.8, 122.8, 122.5, 122.4, 119.8, 119.7, 118.3, 118.2, 111.6, 111.5, 111.4, 111.4, 80.7 (d, *J* = 169.9 Hz), 79.1 (d, *J* = 168.4 Hz), 61.2, 60.1, 24.1, 23.3, 16.7 (d, *J* = 2.9 Hz), 13.2 (d, *J* = 6.3 Hz); HRMS (CI) calcd for $C_{13}H_{16}FN_2O^+$ $[M + H]^+$ 235.1241, found 235.1242.

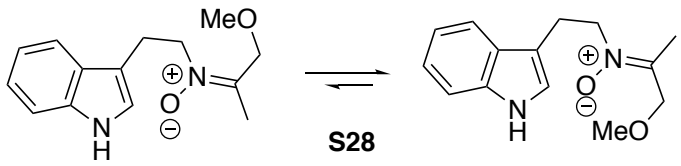

S28

(*E/Z*)-*N*-(2-(1*H*-indol-3-yl)ethyl)-1-methoxypropan-2-imine oxide (S28). Prepared using the general procedure described above with **29** and methoxyacetone (5.0 equiv) in CH_2Cl_2/MeOH (1/1) at 23 ºC, ultimately yielding **S28** (0.118 g, 84% yield, 1:1.9 *E*:*Z*) as a yellow solid. **S28**: R_f = 0.49 (silica gel, CH_2Cl_2/MeOH = 9/1); IR (film) ν_{max} 3220, 2925, 1597, 1562, 1449, 1389, 1198, 1105, 798, 744 cm^{-1}; ^1H NMR (500 MHz, $CDCl_3$, 1:1.9 *E*:*Z*) δ 8.19 (br s, 1 H, exchangeable), 7.63 (d, *J* = 7.9 Hz, 1 H), 7.37 (d, *J* = 8.1 Hz, 1 H), 7.23–7.17 (m, 1 H), 7.16–7.11 (m, 1 H), 7.06 (d, *J* = 2.2 Hz, 1 H), 4.35 (s, 1.3 H), 4.19 (t, *J* = 6.9 Hz, 0.7 H), 4.11 (t, *J* = 6.9 Hz, 1.3 H), 3.61 (s, 0.7 H), 3.43–

3.36 (m, 2 H), 3.28 (s, 1.8 H), 3.04 (s, 0.9 H), 2.09 (s, 1 H), 1.64 (s, 1.8 H); ^{13}C NMR (101 MHz, $CDCl_3$, 1:1.9 *E*:*Z*) δ 147.9, 145.6, 136.4, 136.4, 127.2 (2 C), 123.0, 122.9, 122.1 (2 C), 119.5 (2 C), 118.3, 118.3, 111.6 (2 C), 111.4 (2 C), 70.7, 70.1, 60.2, 60.1, 59.2, 58.3, 23.9, 23.3, 17.1, 13.7; HRMS (ESI) calcd for $C_{14}H_{19}N_2O_2^+$ $[M + H]^+$ 247.1441, found 247.1445.

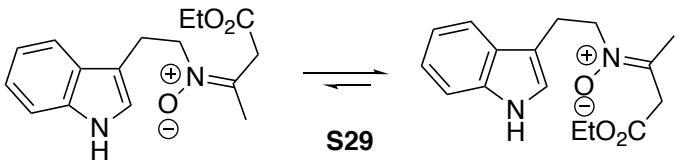

S29

(*E/Z*)-*N*-(2-(1*H*-indol-3-yl)ethyl)-4-ethoxy-4-oxobutan-2-imine oxide (S29). Prepared using the general procedure described above with **29** and ethyl acetoacetate (5.0 equiv) in CH_2Cl_2/MeOH (1/1) at 23 ºC, ultimately yielding **S29** (0.144 g, 88% yield, 1:4.0 *E*:*Z*) as a white solid. **S29**: R_f = 0.46 (silica gel, CH_2Cl_2/MeOH = 9/1); IR (film) ν_{max} 3181, 2980, 1734, 1598, 1458, 1369, 1303, 1158, 1031, 744 cm^{-1}; ^{1}H NMR (500 MHz, $CDCl_3$, 1:4.0 *E*:*Z*) δ 8.34 (br s, 1 H, exchangeable), 7.61 (d, *J* = 7.8 Hz, 1 H), 7.41–7.34 (m, 1 H), 7.23–7.16 (m, 1 H), 7.16–7.04 (m, 2 H), 4.23–4.12 (m, 3.4 H), 4.05 (q, *J* = 7.1 Hz, 0.4 H), 3.50 (s, 1.6 H), 3.43–3.36 (m, 2 H), 2.95 (s, 0.4 H), 2.12 (s, 0.6 H), 1.77 (s, 2.4 H), 1.26 (t, *J* = 7.1 Hz, 2.3 H), 1.19 (t, *J* = 7.1 Hz, 0.6 H); ^{13}C NMR (101 MHz, $CDCl_3$, 1:4.0 *E*:*Z*) δ 168.5, 167.5, 141.4, 140.9, 136.4, 127.2, 123.2, 123.0, 122.1, 122.0, 119.5, 119.4, 118.3, 118.2, 111.6 (2 C), 111.3, 111.2, 61.8, 61.2, 60.3, 59.7, 39.4, 38.9, 23.6, 23.4, 19.4, 19.3, 14.2, 14.1; HRMS (ESI) calcd for $C_{16}H_{21}N_2O_3^+$ $[M + H]^+$ 289.1547, found 289.1556.

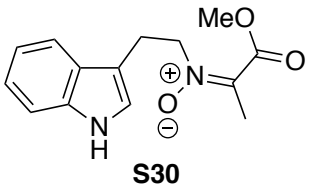

S30

(*E*)-*N*-(2-(1*H*-indol-3-yl)ethyl)-1-methoxy-1-oxopropan-2-imine oxide (S30). Prepared using the general procedure described above with **29** and methyl pyruvate (2.0 equiv) in CH_2Cl_2/MeOH (1/1) at 23 ºC for 2 h, ultimately yielding **S30** (0.146 g, 99% yield) as a pink solid. **S30**: R_f = 0.54 (silica gel, CH_2Cl_2/MeOH = 9/1); IR (film) ν_{max} 3278, 1718, 1597, 1562, 1448, 1389, 1304, 1219, 1194, 1136, 744 cm^{-1}; ^{1}H NMR (500 MHz, $CDCl_3$) δ 8.06 (br s, 1 H, exchangeable), 7.71 (d, *J* = 7.6 Hz, 1 H),

7.39–7.33 (m, 1 H), 7.23–7.18 (m, 1 H), 7.17–7.12 (m, 1 H), 7.06 (d, J = 2.3 Hz, 1 H), 4.78 (t, J = 7.5 Hz, 2 H), 3.55 (s, 3 H), 3.36 (t, J = 7.7 Hz, 2 H), 2.19 (s, 3 H); ^{13}C NMR (101 MHz, $CDCl_3$) δ 162.8, 138.5, 136.3, 127.2, 122.8, 122.2, 119.6, 118.9, 111.6, 111.2, 64.3, 52.5, 25.0, 15.4; HRMS (ESI) calcd for $C_{14}H_{17}N_2O_3^+$ [M + H]$^+$ 261.1234, found 261.1235.

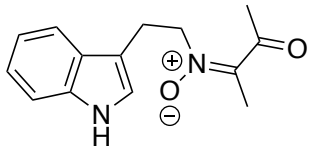

S31

(*E*)-*N*-(2-(1*H*-indol-3-yl)ethyl)-3-oxobutan-2-imine oxide (S31). Prepared using the general procedure described above with **29** and diacetyl (1.5 equiv) in CH_2Cl_2/MeOH (1/1) at 23 ºC for 2 h, ultimately yielding **S31** (0.137 g, 99% yield) as a yellow solid. **S31**: R_f = 0.65 (silica gel, CH_2Cl_2/MeOH = 9/1); IR (film) ν_{max} 3283, 1679, 1508, 1458, 1426, 1358, 1292, 1111, 970, 745 cm^{-1}; ^{1}H NMR (500 MHz, $CDCl_3$) δ 8.07 (br s, 1 H, exchangeable), 7.73 (d, J = 7.8 Hz, 1 H), 7.38–7.32 (m, 1 H), 7.24–7.12 (m, 2 H), 7.08 (d, J = 2.1 Hz, 1 H), 4.62 (t, J = 7.4 Hz, 2 H), 3.31 (t, J = 7.4 Hz, 2 H), 2.19 (s, 3 H), 1.96 (s, 3 H); ^{13}C NMR (101 MHz, $CDCl_3$) δ 193.3, 144.5, 136.2, 127.3, 122.8, 122.2, 119.7, 118.9, 111.7, 111.2, 64.1, 29.3, 24.9, 16.1; HRMS (ESI) calcd for $C_{14}H_{17}N_2O_2^+$ [M + H]$^+$ 245.1285, found 245.1288.

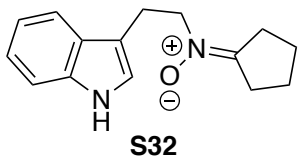

S32

***N*-(2-(1*H*-indol-3-yl)ethyl)cyclopentanimine oxide (S32).** Prepared using the general procedure described above with **29** and cyclopentanone (5.0 equiv) in CH_2Cl_2/MeOH (1/1) at 23 ºC, ultimately yielding **S32** (0.135 g, 98% yield) as a white solid. **S32**: R_f = 0.38 (silica gel, CH_2Cl_2/MeOH = 9/1); IR (film) ν_{max} 3179, 2964, 1597, 1563, 1449, 1395, 1340, 1136, 972, 798, 744 cm^{-1}; ^{1}H NMR (500 MHz, $CDCl_3$) δ 8.35 (br s, 1 H, exchangeable), 7.65 (d, J = 7.8 Hz, 1 H), 7.40–7.34 (m, 1 H), 7.22–7.16 (m, 1 H), 7.15–7.09 (m, 1 H), 7.07 (d, J = 2.4 Hz, 1 H), 4.02 (t, J = 6.7 Hz, 2 H), 3.40 (t, J = 6.7 Hz, 2 H), 2.58 (t, J = 7.4 Hz, 2 H), 1.92 (t, J = 7.2 Hz, 2 H), 1.63–1.54 (m, 2 H), 1.50–1.40 (m, 2 H); ^{13}C NMR (101 MHz, $CDCl_3$) δ 157.9, 136.5, 127.4, 123.0, 121.9, 119.3, 118.4, 111.6, 111.6,

61.7, 31.2, 31.0, 26.1, 24.4, 23.2; HRMS (CI) calcd for $C_{15}H_{19}N_2O^+$ $[M + H]^+$ 243.1492, found 243.1497.

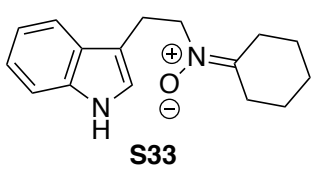

S33

***N*-(2-(1*H*-indol-3-yl)ethyl)cyclohexanimine oxide (S33).** Prepared using the general procedure described above with **29** and cyclohexanone (5.0 equiv) in CH_2Cl_2/MeOH (1/1) at 23 ºC, ultimately yielding **S33** (0.127 g, 87% yield) as a pale-yellow solid. **S33**: R_f = 0.36 (silica gel, CH_2Cl_2/MeOH = 9/1); IR (film) ν_{max} 3170, 2932, 2861, 1597, 1561, 1448, 1342, 1198, 1133, 1105, 1073, 743 cm^{-1}; ^1H NMR (500 MHz, $CDCl_3$) δ 8.60 (br s, 1 H, exchangeable), 7.63 (d, *J* = 7.8 Hz, 1 H), 7.40–7.34 (m, 1 H), 7.21–7.15 (m, 1 H), 7.15–7.09 (m, 1 H), 7.06 (d, *J* = 2.2 Hz, 1 H), 4.17 (t, *J* = 6.7 Hz, 2 H), 3.38 (t, *J* = 6.7 Hz, 2 H), 2.69 (t, *J* = 6.5 Hz, 2 H), 1.99 (t, *J* = 6.5 Hz, 2 H), 1.54–1.46 (m, 2 H), 1.37–1.29 (m, 2 H), 1.09–1.00 (m, 2 H); ^{13}C NMR (101 MHz, $CDCl_3$) δ 151.6, 136.5, 127.4, 123.1, 122.0, 119.4, 118.3, 111.6 (2 C), 59.2, 29.9, 27.1, 25.2, 24.6, 24.5, 23.7; HRMS (ESI) calcd for $C_{16}H_{21}N_2O^+$ $[M + H]^+$ 257.1648, found 257.1658.

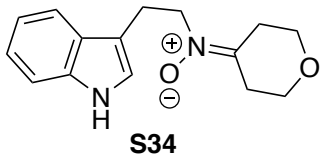

S34

***N*-(2-(1*H*-indol-3-yl)ethyl)tetrahydro-4*H*-pyran-4-imine oxide (S34).** Prepared using the general procedure described above with **29** and tetrahydro-4*H*-pyran-4-one (5.0 equiv) in CH_2Cl_2/MeOH (1/1) at 23 ºC, ultimately yielding **S34** (0.120 g, 82% yield) as a yellow solid. **S34**: R_f = 0.34 (silica gel, CH_2Cl_2/MeOH = 9/1); IR (film) ν_{max} 3179, 2860, 1597, 1562, 1457, 1388, 1341, 1139, 1102, 1009, 746 cm^{-1}; ^1H NMR (500 MHz, $CDCl_3$) δ 8.38 (br s, 1 H, exchangeable), 7.65 (d, *J* = 7.8 Hz, 1 H), 7.41–7.35 (m, 1 H), 7.23–7.17 (m, 1 H), 7.15–7.10 (m, 1 H), 7.08 (d, *J* = 2.2 Hz, 1 H), 4.14 (t, *J* = 6.3 Hz, 2 H), 3.48 (t, *J* = 5.9 Hz, 2 H), 3.41 (t, *J* = 6.3 Hz, 2 H), 2.89 (t, *J* = 5.7 Hz, 2 H), 2.77 (t, *J* = 5.9 Hz, 2 H), 1.98 (t, *J* = 5.7 Hz, 2 H); ^{13}C NMR (101 MHz, $CDCl_3$) δ 145.8, 136.4, 127.5,

123.0, 122.4, 119.8, 118.3, 111.7, 111.6, 65.9, 65.5, 59.3, 30.3, 27.6, 23.5; HRMS (CI) calcd for $C_{15}H_{19}N_2O_2^+$ $[M + H]^+$ 259.1441, found 259.1444.

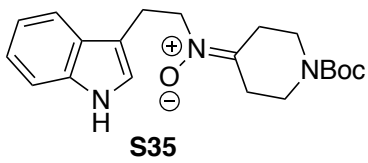

S35

***N*-(2-(1*H*-indol-3-yl)ethyl)-1-(*tert*-butoxycarbonyl)piperidin-4-imine oxide (S35).** Prepared using the general procedure described above with **29** and 1-Boc-4-piperidone (3.5 equiv) in CH_2Cl_2/MeOH (1/1) at 23 ºC, ultimately yielding **S35** (0.184 g, 91% yield) as a white solid. **S35**: R_f = 0.43 (silica gel, CH_2Cl_2/MeOH = 9/1); IR (film) ν_{max} 2972, 1695, 1597, 1564, 1394, 1363, 1223, 1148, 1000, 858, 744 cm^{-1}; ^1H NMR (500 MHz, $CDCl_3$) δ 8.18 (br s, 1 H, exchangeable), 7.64 (d, *J* = 7.8 Hz, 1 H), 7.39–7.33 (m, 1 H), 7.22–7.17 (m, 1 H), 7.15–7.09 (m, 1 H), 7.07 (d, *J* = 2.2 Hz, 1 H), 4.14 (t, *J* = 6.3 Hz, 2 H), 3.40 (t, *J* = 6.3 Hz, 2 H), 3.30–3.19 (m, 2 H), 2.75 (t, *J* = 5.7 Hz, 2 H), 2.69 (t, *J* = 6.1 Hz, 2 H), 1.99 (t, *J* = 6.0 Hz, 2 H), 1.40 (s, 9 H); ^{13}C NMR (101 MHz, $CDCl_3$) δ 154.5, 146.6, 136.3, 127.5, 122.8, 122.5, 119.8, 118.4, 111.9, 111.6, 80.2, 59.8, 41.2, 40.7, 28.9, 28.5, 27.1, 23.6; HRMS (ESI) calcd for $C_{20}H_{28}N_3O_3^+$ $[M + H]^+$ 358.2125, found 358.2133.

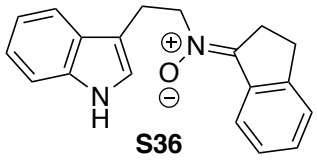

S36

(*Z*)-*N*-(2-(1*H*-indol-3-yl)ethyl)-2,3-dihydro-1*H*-inden-1-imine oxide (S36). Prepared using the general procedure described above with **29** and 1-indanone (3.0 equiv) in MeOH at 50 ºC, ultimately yielding **S36** (0.149 g, 90% yield) as a brown solid. **S36**: R_f = 0.49 (silica gel, CH_2Cl_2/MeOH = 9/1); IR (film) ν_{max} 2850, 1595, 1561, 1445, 1400, 1174, 1097, 1067, 760, 747 cm^{-1}; ^1H NMR (500 MHz, $CDCl_3$) δ 8.96 (d, *J* = 7.3 Hz, 1 H), 8.09 (br s, 1 H, exchangeable), 7.65 (d, *J* = 7.9 Hz, 1 H), 7.41–7.30 (m, 3 H), 7.24–7.16 (m, 2 H), 7.13–7.08 (m, 1 H), 7.06 (d, *J* = 2.2 Hz, 1 H), 4.17 (t, *J* = 7.0 Hz, 2 H), 3.50 (t, *J* = 7.0 Hz, 2 H), 2.93–2.86 (m, 2 H), 2.59–2.53 (m, 2 H); ^{13}C NMR (101 MHz, $CDCl_3$) δ 150.0, 148.1, 136.3, 134.8, 131.1, 127.4, 127.2, 127.2, 124.7, 122.9, 122.3, 119.7,

118.5, 112.0, 111.5, 62.3, 29.1, 28.9, 23.4; HRMS (CI) calcd for $C_{19}H_{19}N_2O^+$ $[M + H]^+$ 291.1492, found 291.1503.

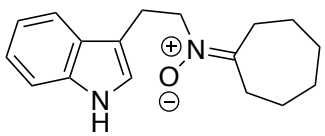

S37

***N*-(2-(1*H*-indol-3-yl)ethyl)cycloheptanimine oxide (S37).** Prepared using the general procedure described above with **29** and cycloheptanone (5.0 equiv) in CH_2Cl_2/MeOH (1/1) at 23 ºC, ultimately yielding **S37** (0.153 g, 99% yield) as a yellow solid. **S37**: R_f = 0.51 (silica gel, CH_2Cl_2/MeOH = 9/1); IR (film) ν_{max} 3173, 2924, 2854, 1597, 1564, 1449, 1211, 1140, 1105, 743 cm^{-1}; ^1H NMR (500 MHz, $CDCl_3$) δ 8.37 (br s, 1 H, exchangeable), 7.63 (d, *J* = 7.8 Hz, 1 H), 7.41–7.33 (m, 1 H), 7.22–7.16 (m, 1 H), 7.15–7.10 (m, 1 H), 7.07 (d, *J* = 2.3 Hz, 1 H), 4.17 (t, *J* = 7.0 Hz, 2 H), 3.40 (t, *J* = 6.9 Hz, 2 H), 2.79–2.71 (m, 2 H), 2.20–2.14 (m, 2 H), 1.64–1.57 (m, 2 H), 1.46–1.38 (m, 2 H), 1.35–1.28 (m, 2 H), 1.25–1.19 (m, 2 H); ^{13}C NMR (101 MHz, $CDCl_3$) δ 155.0, 136.5, 127.4, 123.0, 121.9, 119.3, 118.3, 111.6, 111.4, 59.4, 31.9, 31.2, 29.7, 29.5, 26.1, 24.6, 23.8; HRMS (CI) calcd for $C_{17}H_{23}N_2O^+$ $[M + H]^+$ 271.1805, found 271.1815.

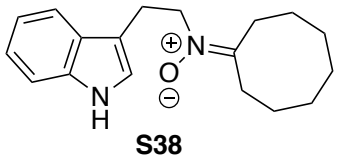

S38

***N*-(2-(1*H*-indol-3-yl)ethyl)cyclooctanimine oxide (S38).** Prepared using the general procedure described above with **29** and cyclooctanone (5.0 equiv) in CH_2Cl_2/MeOH (1/1) at 23 ºC, ultimately yielding **S38** (0.161 g, 99% yield) as a yellow solid. **S38**: R_f = 0.49 (silica gel, CH_2Cl_2/MeOH = 9/1); IR (film) ν_{max} 3173, 2924, 1597, 1562, 1448, 1400, 1355, 1217, 1142, 1109, 743 cm^{-1}; ^1H NMR (500 MHz, $CDCl_3$) δ 8.25 (br s, 1 H, exchangeable), 7.64 (d, *J* = 7.8 Hz, 1 H), 7.41–7.34 (m, 1 H), 7.23–7.17 (m, 1 H), 7.16–7.10 (m, 1 H), 7.08 (d, *J* = 2.4 Hz, 1 H), 4.13 (t, *J* = 7.2 Hz, 2 H), 3.42 (t, *J* = 7.2 Hz, 2 H), 2.69–2.60 (m, 2 H), 2.23–2.13 (m, 2 H), 1.80–1.73 (m, 2 H), 1.55–1.47 (m, 2 H), 1.45–1.38 (m, 2 H), 1.33–1.27 (m, 2 H), 1.26–1.20 (m, 2 H); ^{13}C NMR (101 MHz, $CDCl_3$)

δ 154.5, 136.6, 127.3, 123.1, 121.9, 119.2, 118.3, 111.6, 111.4, 59.0, 30.7, 29.7, 28.1, 26.8, 25.9, 25.4, 23.5, 23.3; HRMS (ESI) calcd for $C_{18}H_{25}N_2O^+$ $[M + H]^+$ 285.1961, found 285.1972.

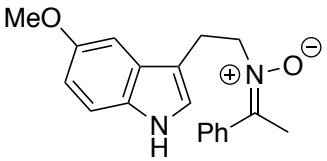

S39

(*E*)-*N*-(2-(5-methoxy-1*H*-indol-3-yl)ethyl)-1-phenylethan-1-imine oxide (S39). Prepared using the general procedure described above with **S7** and acetophenone (5.0 equiv) in CH_2Cl_2/MeOH (1/1) at 23 ºC, ultimately yielding **S39** (0.131 g, 88% yield) as a white solid. **S39**: R_f = 0.44 (silica gel, CH_2Cl_2/MeOH = 9/1); IR (film) ν_{max} 3325, 1597, 1486, 1447, 1394, 1216, 1071, 858, 798, 700 cm^{-1}; ^1H NMR (500 MHz, $CDCl_3$) δ 8.06 (br s, 1 H, exchangeable), 7.26–7.22 (m, 2 H), 7.19–7.13 (m, 2 H), 6.97 (d, *J* = 2.4 Hz, 1 H), 6.82 (dd, *J* = 8.7, 2.4 Hz, 1 H), 6.75–6.70 (m, 3 H), 4.07 (t, *J* = 6.9 Hz, 2 H), 3.74 (s, 3 H), 3.33 (t, *J* = 7.0 Hz, 2 H), 2.35 (s, 3 H); ^{13}C NMR (101 MHz, $CDCl_3$) δ 154.0, 148.4, 136.2, 131.4, 128.8, 128.7, 127.8, 127.3, 123.5, 112.6, 112.0, 111.5, 100.0, 60.1, 56.0, 23.9, 20.8; HRMS (CI) calcd for $C_{19}H_{21}N_2O_2^+$ $[M + H]^+$ 309.1598, found 309.1599.

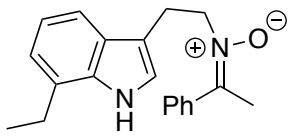

S40

(*E*)-*N*-(2-(7-ethyl-1*H*-indol-3-yl)ethyl)-1-phenylethan-1-imine oxide (S40). Prepared using the general procedure described above with **S9** and acetophenone (5.0 equiv) in CH_2Cl_2/MeOH (1/1) at 23 ºC, ultimately yielding **S40** (0.131 g, 87% yield) as a pale-yellow solid. **S40**: R_f = 0.50 (silica gel, CH_2Cl_2/MeOH = 9/1); IR (film) ν_{max} 3261, 1597, 1564, 1485, 1448, 1395, 1220, 1080, 858, 798 cm^{-1}; ^1H NMR (500 MHz, $CDCl_3$) δ 8.08 (br s, 1 H, exchangeable), 7.28–7.25 (m, 1 H), 7.22–7.15 (m, 2 H), 7.09 (d, *J* = 7.8 Hz, 1 H), 7.02–6.98 (m, 2 H), 6.97–6.92 (m, 1 H), 6.80–6.74 (m, 2 H), 4.07 (t, *J* = 7.2 Hz, 2 H), 3.36 (t, *J* = 7.2 Hz, 2 H), 2.86 (q, *J* = 7.6 Hz, 2 H), 2.37 (s, 3 H), 1.36 (t, *J* = 7.6 Hz, 3 H); ^{13}C NMR (101 MHz, $CDCl_3$) δ 148.4, 136.2, 135.1, 128.8, 128.7, 128.6, 127.2, 126.8, 122.4, 120.6, 119.7, 116.2, 112.1, 60.4, 24.1, 24.0, 20.8, 14.2; HRMS (ESI) calcd for $C_{20}H_{23}N_2O^+$ $[M + H]^+$ 307.1805, found 307.1808.

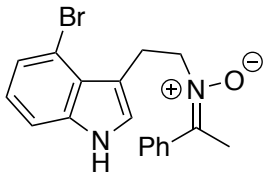

S41

(*E*)-*N*-(2-(4-bromo-1*H*-indol-3-yl)ethyl)-1-phenylethan-1-imine oxide (S41). Prepared using the general procedure described above with **S11** and acetophenone (5.0 equiv) in CH_2Cl_2/MeOH (1/1) at 23 ºC, ultimately yielding **S41** (0.127 mg, 91% yield) as a pale-yellow solid. **S41**: R_f = 0.49 (silica gel, CH_2Cl_2/MeOH = 9/1); IR (film) ν_{max} 3155, 1597, 1562, 1424, 1333, 1221, 1193, 1156, 1071, 1044, 738, 700 cm^{-1}; ^1H NMR (500 MHz, $CDCl_3$) δ 9.36 (br s, 1 H, exchangeable), 7.37 (dd, *J* = 8.1, 0.9 Hz, 1 H), 7.22–7.15 (m, 2 H), 7.09 (dd, *J* = 7.6, 0.9 Hz, 1 H), 7.05–7.00 (m, 2 H), 6.97 (t, *J* = 7.8 Hz, 1 H), 6.58–6.52 (m, 2 H), 4.25 (t, *J* = 6.4 Hz, 2 H), 3.52 (t, *J* = 6.4 Hz, 2 H), 2.31 (s, 3 H); ^{13}C NMR (101 MHz, $CDCl_3$) δ 149.7, 138.0, 135.6, 128.8, 128.6, 127.0, 125.9, 125.6, 123.5, 122.6, 114.0, 111.5, 111.0, 61.3, 24.2, 20.8; HRMS (ESI) calcd for $C_{18}H_{18}BrN_2O^+$ $[M + H]^+$ 357.0597, found 357.0610.

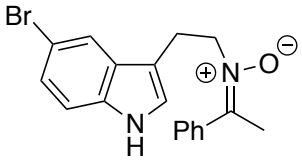

S42

(*E*)-*N*-(2-(5-bromo-1*H*-indol-3-yl)ethyl)-1-phenylethan-1-imine oxide (S42). Prepared using the general procedure described above with **S13** and acetophenone (5.0 equiv) in CH_2Cl_2/MeOH (1/1) at 23 ºC, ultimately yielding **S42** (0.114 g, 81% yield) as a white solid. **S42**: R_f = 0.68 (silica gel, CH_2Cl_2/MeOH = 9/1); IR (film) ν_{max} 3199, 1597, 1564, 1449, 1394, 1219, 1159, 1071, 882, 858, 798, 699 cm^{-1}; ^1H NMR (500 MHz, $CDCl_3$) δ 8.91 (br s, 1 H, exchangeable), 7.33–7.29 (m, 1 H), 7.28–7.27 (m, 1 H), 7.25–7.23 (m, 1 H), 7.23–7.17 (m, 3 H), 6.99 (d, *J* = 2.4 Hz, 1 H), 6.75–6.67 (m, 2 H), 4.06 (t, *J* = 6.6 Hz, 2 H), 3.29 (t, *J* = 6.9 Hz, 2 H), 2.36 (s, 3 H); ^{13}C NMR (101 MHz, $CDCl_3$) δ 148.8, 135.9, 135.0, 129.2, 129.2, 128.8, 127.1, 124.9, 124.2, 121.1, 112.8, 112.8, 111.4, 60.0, 23.8, 20.8; HRMS (ESI) calcd for $C_{18}H_{18}BrN_2O^+$ $[M + H]^+$ 357.0597, found 357.0598.

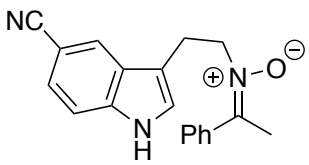

S43

(*E*)-*N*-(2-(5-cyano-1*H*-indol-3-yl)ethyl)-1-phenylethan-1-imine oxide (S43). Prepared using the general procedure described above with **S15** and acetophenone (5.0 equiv) in CH_2Cl_2/MeOH (1/1) at 23 ºC, ultimately yielding **S43** (0.094 g, 62% yield) as a white solid. **S43**: R_f = 0.40 (silica gel, CH_2Cl_2/MeOH = 9/1); IR (film) ν_{max} 3289, 2362, 2218, 1597, 1572, 1479, 1401, 1223, 1138, 1069, 802 cm^{-1}; ^1H NMR (500 MHz, $CDCl_3$) δ 9.71 (br s, 1 H, exchangeable), 7.46 (d, *J* = 8.4 Hz, 1 H), 7.42–7.39 (m, 1 H), 7.39–7.32 (m, 2 H), 7.24–7.18 (m, 2 H), 7.12 (d, *J* = 2.3 Hz, 1 H), 6.75–6.70 (m, 2 H), 4.10 (t, *J* = 6.9 Hz, 2 H), 3.33 (t, *J* = 6.9 Hz, 2 H), 2.35 (s, 3 H); ^{13}C NMR (101 MHz, $CDCl_3$) δ 149.2, 138.1, 135.8, 129.5, 128.9, 127.2, 127.1, 125.3, 124.9, 124.1, 120.7, 112.4, 112.4, 102.4, 59.8, 23.6, 20.7; HRMS (CI) calcd for $C_{19}H_{18}N_3O^+$ $[M + H]^+$ 304.1444, found 304.1446.

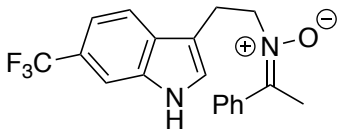

S44

(*E*)-1-phenyl-*N*-(2-(6-(trifluoromethyl)-1*H*-indol-3-yl)ethyl)ethan-1-imine oxide (S44). Prepared using the general procedure described above with **S17** and acetophenone (5.0 equiv) in CH_2Cl_2/MeOH (1/1) at 23 ºC, ultimately yielding **S44** (0.125 g, 88% yield) as a white solid. **S44**: R_f = 0.57 (silica gel, CH_2Cl_2/MeOH = 9/1); IR (film) ν_{max} 3182, 1597, 1564, 1448, 1393, 1336, 1220, 1158, 1111, 1072, 700 cm^{-1}; ^1H NMR (500 MHz, $CDCl_3$) δ 8.65 (br s, 1 H, exchangeable), 7.69–7.62 (m, 1 H), 7.29 (d, *J* = 8.4 Hz, 1 H), 7.26–7.22 (m, 1 H), 7.19 (dd, *J* = 8.4, 1.6 Hz, 1 H), 7.17–7.11 (m, 3 H), 6.70–6.63 (m, 2 H), 4.09 (t, *J* = 6.9 Hz, 2 H), 3.37 (t, *J* = 6.8 Hz, 2 H), 2.33 (s, 3 H); ^{13}C NMR (101 MHz, $CDCl_3$) δ 149.5, 135.7, 135.4, 129.6, 129.1, 128.8, 127.0, 125.8, 125.4 (q, *J* = 271.4 Hz), 123.9 (q, *J* = 31.8 Hz), 118.7, 115.9, 111.6, 109.0, 60.0, 23.6, 20.8; HRMS (CI) calcd for $C_{19}H_{18}F_3N_2O^+$ $[M + H]^+$ 347.1366, found 347.1370.

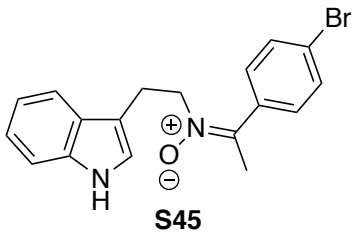

S45

(*E*)-*N*-(2-(1*H*-indol-3-yl)ethyl)-1-(4-bromophenyl)ethan-1-imine oxide (S45). Prepared using the general procedure described above with **29** and 4′-bromoacetophenone (2.5 equiv) in MeOH at 50 ºC, ultimately yielding **S45** (0.170 g, 84% yield) as a white solid. **S45**: R_f = 0.60 (silica gel, CH_2Cl_2/MeOH = 9/1); IR (film) 3184, 1577, 1484, 1457, 1221, 1165, 1075, 1009, 825, 742 ν_{max} cm^{-1}; ^1H NMR (400 MHz, $CDCl_3$) δ 8.25 (br s, 1 H, exchangeable), 7.37 (d, *J* = 8.1 Hz, 1 H), 7.28–7.24 (m, 1 H), 7.23–7.16 (m, 3 H), 7.05–7.00 (m, 1 H), 6.99 (d, *J* = 2.3 Hz, 1 H), 6.48–6.39 (m, 2 H), 4.06 (t, *J* = 6.2 Hz, 1 H), 3.35 (t, *J* = 6.2 Hz, 1 H) 2.29 (s, 3 H); ^{13}C NMR (101 MHz, $CDCl_3$) δ 147.3, 136.3, 134.9, 131.8, 128.9, 127.4, 123.1, 122.8, 122.2, 119.6, 118.5, 111.6, 111.3, 60.4, 23.7, 20.6; HRMS (CI) calcd for $C_{18}H_{18}BrN_2O^+$ $[M + H]^+$ 357.0597, found 357.0596.

General Procedure for Racemic Pictet–Spengler Reactions of Nitrones.

To a solution of nitrone (0.25 mmol, 1.0 equiv) in CH_2Cl_2 (1.25 mL, dried over 4Å MS beads) at 23 ºC was added molecular sieves (4Å, powder, ~150 mg), and the resultant slurry was stirred for 10 min under an argon atmosphere. Next, the acyl chloride (0.26 mmol, 1.05 equiv) was added and the reaction mixture was stirred for 30 min at 23 ºC. Upon completion, the contents were quenched by the addition of saturated aqueous $NaHCO_3$ (5 mL), poured into a separatory funnel, and extracted with CH_2Cl_2 (3 × 5 mL). The combined organic extracts were then dried (Na_2SO_4), filtered, and concentrated. The resultant crude material was purified by flash column chromatography (silica gel, hexanes/EtOAc = 1/0→2/1) to yield **33**, **39**, **62**. *Note:* These reactions must be run under strictly anhydrous conditions to avoid hydrolysis of the *N*-acyloxyiminium species.

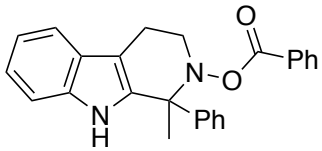

33a

1-methyl-1-phenyl-1,3,4,9-tetrahydro-2*H*-pyrido[3,4-*b*]indol-2-yl benzoate (33a). Prepared using the general procedure described above with **32** and benzoyl chloride, ultimately yielding **33a** (0.083 g, 86% yield) as a white solid. **33a**: R_f = 0.50 (silica gel, hexanes/EtOAc = 4/1); IR (film) ν_{max} 3363, 1726, 1598, 1450, 1272, 1092, 1063, 1023, 745, 700 cm^{-1}; ^1H NMR (500 MHz, $CDCl_3$) δ 8.00–7.84 (m, 3 H, 1 exchangeable), 7.63 (d, *J* = 7.7 Hz, 1 H), 7.53 (t, *J* = 7.4 Hz, 1 H), 7.43–7.35 (m, 5 H), 7.31–7.24 (m, 4 H), 7.23–7.19 (m, 1 H), 3.69–3.57 (m, 1 H), 3.44–3.26 (m, 1 H), 3.22–3.14 (m, 1 H), 2.93–2.78 (m, 1 H), 1.97 (s, 3 H); ^{13}C NMR (101 MHz, $CDCl_3$) δ 165.5, 136.2, 135.2, 133.2, 129.6, 129.3, 128.5, 128.4, 128.0, 127.9 (2 C), 127.1, 122.2, 119.8, 118.8, 111.2, 108.6, 65.9, 48.1, 25.2, 18.4; HRMS (CI) calcd for $C_{25}H_{23}N_2O_2^+$ $[M + H]^+$ 383.1754, found 383.1753.

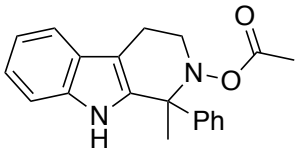

33b

1-methyl-1-phenyl-1,3,4,9-tetrahydro-2*H*-pyrido[3,4-*b*]indol-2-yl acetate (33b). Prepared using the general procedure described above with **32** and acetyl chloride, ultimately yielding **33b** (0.069 g, 86% yield) as a white solid. **33b**: R_f = 0.40 (silica gel, hexanes/EtOAc = 4/1); IR (film) ν_{max} 3363, 1238, 1744, 1597, 1448, 1366, 1297, 1221, 745, 701 cm^{-1}; ^1H NMR (500 MHz, $CDCl_3$) δ 7.76 (br s, 1 H, exchangeable), 7.57 (d, *J* = 7.8 Hz, 1 H), 7.37 (d, *J* = 8.0 Hz, 1 H), 7.35–7.30 (m, 2 H), 7.30–7.24 (m, 3 H), 7.24–7.20 (m, 1 H), 7.19–7.14 (m, 1 H), 3.58–3.44 (m, 1 H), 3.31–3.17 (m, 1 H), 3.10–3.02 (m, 1 H), 2.87–2.71 (m, 1 H), 1.98 (s, 3 H), 1.88 (s, 3 H); ^{13}C NMR (101 MHz, $CDCl_3$) δ 170.2, 136.1, 135.2, 128.4, 127.9 (2 C), 127.8, 127.0, 122.2, 119.8, 118.7, 111.1, 108.5, 65.5, 47.9, 24.7, 19.6, 18.3; HRMS (CI) calcd for $C_{20}H_{21}N_2O_2^+$ $[M + H]^+$ 321.1598, found 321.1601.

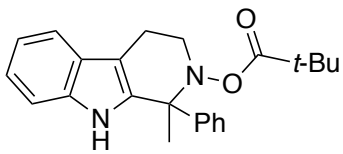

33c

1-methyl-1-phenyl-1,3,4,9-tetrahydro-2*H*-pyrido[3,4-*b*]indol-2-yl pivalate (33c). Prepared using the general procedure described above with **32** and pivaloyl chloride, ultimately yielding **33c** (0.080

g, 88% yield) as a white solid. **33c**: R_f = 0.49 (silica gel, hexanes/EtOAc = 4/1); IR (film) ν_{max} 3363, 2974, 1732, 1597, 1450, 1396, 1276, 1118, 1024, 744, 700 cm^{-1}; ^1H NMR (500 MHz, $CDCl_3$) δ 7.83 (br s, 1 H, exchangeable), 7.59 (d, *J* = 7.7 Hz, 1 H), 7.41–7.33 (m, 3 H), 7.31–7.24 (m, 3 H), 7.24–7.15 (m, 2 H), 3.56–3.43 (m, 1 H), 3.34–3.19 (m, 1 H), 3.08–2.99 (m, 1 H), 2.92–2.77 (m, 1 H), 1.91 (s, 3 H), 1.11 (s, 9 H); ^{13}C NMR (101 MHz, $CDCl_3$) δ 176.8, 136.2, 135.6, 128.3, 127.9 (2 C), 127.8, 127.0, 122.0, 119.7, 118.7, 111.1, 108.3, 65.6, 47.8, 39.0, 27.3, 24.5, 18.5; HRMS (CI) calcd for $C_{23}H_{27}N_2O_2^+$ $[M + H]^+$ 363.2067, found 363.2066.

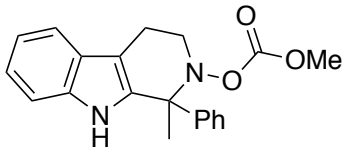

33d

Methyl (1-methyl-1-phenyl-1,3,4,9-tetrahydro-2*H*-pyrido[3,4-*b*]indol-2-yl) carbonate (33d). Prepared using the general procedure described above with **32** and methyl chloroformate, ultimately yielding **33d** (0.074 g, 87% yield) as a white solid. **33d**: R_f = 0.39 (silica gel, hexanes/EtOAc = 4/1); IR (film) ν_{max} 3380, 1755, 1597, 1440, 1229, 1128, 940, 858, 745, 700 cm^{-1}; ^1H NMR (500 MHz, $CDCl_3$) δ 7.74 (br s, 1 H, exchangeable), 7.55 (d, *J* = 7.8 Hz, 1 H), 7.38–7.30 (m, 3 H), 7.30–7.25 (m, 3 H), 7.23–7.18 (m, 1 H), 7.18–7.12 (m, 1 H), 3.78 (s, 3 H), 3.63–3.51 (m, 1 H), 3.32–3.19 (m, 1 H), 3.14–3.06 (m, 1 H), 2.86–2.73 (m, 1 H), 1.92 (s, 3 H); ^{13}C NMR (101 MHz, $CDCl_3$) δ 156.2, 136.2, 134.8, 128.4, 127.9, 127.8, 127.7, 127.0, 122.2, 119.8, 118.7, 111.1, 108.4, 66.1, 55.2, 48.1, 24.4, 18.3; HRMS (CI) calcd for $C_{20}H_{21}N_2O_3^+$ $[M + H]^+$ 337.1547, found 337.1550.

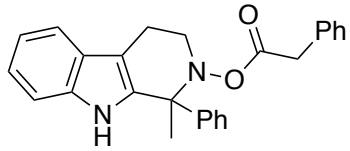

33e

1-methyl-1-phenyl-1,3,4,9-tetrahydro-2*H*-pyrido[3,4-*b*]indol-2-yl 2-phenylacetate (33e). Prepared using the general procedure described above with **32** and phenylacetyl chloride, ultimately yielding **33e** (0.095 g, 95% yield) as a white solid. **33e**: R_f = 0.44 (silica gel, hexanes/EtOAc = 4/1); IR (film) ν_{max} 3374, 3058, 1745, 1453, 1298, 1232, 1116, 1025, 745, 700 cm^{-1}; ^1H NMR (500 MHz, $CDCl_3$) δ 7.70 (br s, 1 H, exchangeable), 7.56 (d, *J* = 7.7 Hz, 1 H), 7.35 (d, *J* = 8.0 Hz, 1 H),

7.32–7.20 (m, 9 H), 7.19–7.14 (m, 3 H), 3.53 (s, 2 H), 3.48–3.41 (m, 1 H), 3.27–3.15 (m, 1 H), 3.05–2.92 (m, 1 H), 2.84–2.72 (m, 1 H), 1.78 (s, 3 H); ^{13}C NMR (101 MHz, $CDCl_3$) δ 170.4, 136.2, 135.3, 133.7, 129.3, 128.7, 128.3 (2 C), 127.8 (2 C), 127.2, 127.0, 122.1, 119.8, 118.7, 111.1, 108.4, 65.7, 48.0, 40.3, 24.3, 18.5; HRMS (ESI) calcd for $C_{26}H_{24}N_2O_2^+$ $[M + H]^+$ 397.1911, found 397.1912.

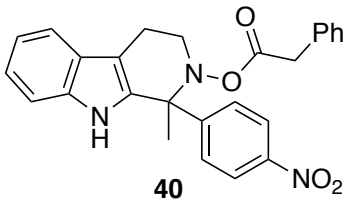

40

1-methyl-1-(4-nitrophenyl)-1,3,4,9-tetrahydro-2*H*-pyrido[3,4-*b*]indol-2-yl 2-phenylacetate (40). Prepared using the general procedure described above with **S18** and phenylacetyl chloride, ultimately yielding **40** (0.107 g, 97% yield) as a bright yellow solid. **40**: R_f = 0.34 (silica gel, hexanes/EtOAc = 4/1); IR (film) ν_{max} 3245, 1598, 1561, 1518, 1400, 1349, 1219, 1069, 857, 744 cm^{-1}; ^{1}H NMR (500 MHz, $CDCl_3$) δ 8.03 (d, J = 8.4 Hz, 2 H), 7.66 (br s, 1 H, exchangeable), 7.57 (d, J = 7.8 Hz, 1 H), 7.53–7.39 (m, 2 H), 7.35 (d, J = 8.0 Hz, 1 H), 7.28–7.21 (m, 4 H), 7.20–7.11 (m, 3 H), 3.57–3.46 (m, 3 H), 3.23–3.12 (m, 1 H), 3.05–2.95 (m, 1 H), 2.92–2.80 (m, 1 H), 1.79 (s, 3 H); ^{13}C NMR (101 MHz, $CDCl_3$) δ 170.0, 147.3, 136.4, 134.0, 133.4, 129.1, 128.8, 128.7 (2 C), 127.4, 126.7, 123.4, 122.7, 120.1, 118.9, 111.3, 108.8, 65.4, 48.3, 40.3, 23.7, 18.7; HRMS (ESI) calcd for $C_{26}H_{24}N_3O_4^+$ $[M + H]^+$ 442.1761, found 442.1759.

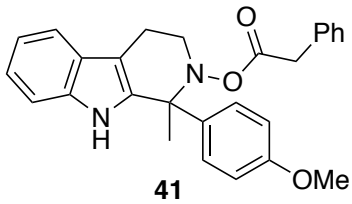

41

1-(4-methoxyphenyl)-1-methyl-1,3,4,9-tetrahydro-2*H*-pyrido[3,4-*b*]indol-2-yl 2-phenylacetate (41). Prepared using the general procedure described above with **S19** and phenylacetyl chloride, ultimately yielding **41** (0.088 g, 83% yield) as a yellow solid. **41**: R_f = 0.62 (silica gel, hexanes/EtOAc = 2/1); IR (film) ν_{max} 3373, 1746, 1607, 1510, 1454, 1299, 1249, 1180, 1116, 744 cm^{-1}; ^{1}H NMR (500 MHz, $CDCl_3$) δ 7.69 (br s, 1 H, exchangeable), 7.56 (d, J = 7.7 Hz, 1 H), 7.34 (d, J = 7.9 Hz, 1 H), 7.30–7.09 (m, 9 H), 6.79–6.72 (m, 2 H), 3.77 (s, 3 H), 3.53 (s, 2 H), 3.47–

3.39 (m, 1 H), 3.28–3.17 (m, 1 H), 3.02–2.92 (m, 1 H), 2.87–2.71 (m, 1 H), 1.77 (s, 3 H); ^{13}C NMR (101 MHz, $CDCl_3$) δ 170.4, 159.1, 136.2, 135.6, 133.8, 129.3, 129.1 (2 C), 128.6, 127.2, 127.0, 122.1, 119.7, 118.6, 113.5, 111.1, 108.2, 65.2, 55.4, 47.9, 40.3, 24.3, 18.6; HRMS (ESI) calcd for $C_{27}H_{27}N_2O_3^+$ $[M + H]^+$ 427.2016, found 427.2013.

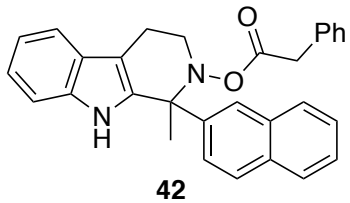

42

1-methyl-1-(naphthalen-2-yl)-1,3,4,9-tetrahydro-2*H*-pyrido[3,4-*b*]indol-2-yl 2-phenylacetate (42). Prepared using the general procedure described above with **S20** and phenylacetyl chloride, ultimately yielding **42** (0.106 g, 95% yield) as a pale-yellow solid. **42**: R_f = 0.44 (silica gel, hexanes/EtOAc = 4/1); IR (film) ν_{max} 3373, 3058, 1745, 1597, 1454, 1297, 1230, 1115, 744, 696 cm^{-1}; ^{1}H NMR (500 MHz, $CDCl_3$) δ 7.80 (d, *J* = 7.8 Hz, 1 H), 7.77–7.68 (m, 3 H), 7.67–7.62 (m, 1 H), 7.59 (d, *J* = 7.6 Hz, 1 H), 7.55 (br s, 1 H, exchangeable), 7.49–7.41 (m, 2 H), 7.36 (d, *J* = 7.9 Hz, 1 H), 7.26–7.22 (m, 1 H), 7.21–7.13 (m, 4 H), 7.12–7.05 (m, 2 H), 3.56–3.46 (m, 3 H), 3.35–3.24 (m, 1 H), 3.05–2.96 (m, 1 H), 2.91–2.78 (m, 1 H), 1.87 (s, 3 H); ^{13}C NMR (101 MHz, $CDCl_3$) δ 170.4, 136.3, 135.5, 133.7, 132.9, 129.1, 128.7, 128.6, 128.4, 128.2 (2 C), 127.6, 127.2, 127.0, 126.5, 126.4, 126.2, 125.9, 122.2, 119.8, 118.7, 111.2, 108.4, 65.8, 48.0, 40.3, 23.9, 18.7; HRMS (CI) calcd for $C_{30}H_{27}N_2O_2^+$ $[M + H]^+$ 447.2067, found 447.2064.

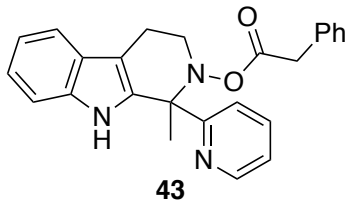

43

1-methyl-1-(pyridin-2-yl)-1,3,4,9-tetrahydro-2*H*-pyrido[3,4-*b*]indol-2-yl 2-phenylacetate (43). Prepared using the general procedure described above with **S21** and phenylacetyl chloride, ultimately yielding **43** (0.087 g, 87% yield) as a yellow solid. **43**: R_f = 0.21 (silica gel, hexanes/EtOAc = 4/1); IR (film) ν_{max} 3059, 2934, 1754, 1590, 1455, 1431, 1300, 1233, 1112, 742 cm^{-1}; ^{1}H NMR (500 MHz, $CDCl_3$, 45 ºC) δ 9.14 (br s, 1 H, exchangeable), 8.60–8.49 (m, 1 H), 7.79 (d, *J* = 8.0 Hz, 1 H), 7.56–7.47 (m, 2 H), 7.34 (d, *J* = 8.1 Hz, 1 H), 7.23–7.14 (m, 4 H), 7.14–

7.05 (m, 4 H), 3.74–3.63 (m, 2 H), 3.53–3.40 (m, 2 H), 3.10–3.02 (m, 1 H), 2.92–2.86 (m, 1 H), 1.90 (s, 3 H); ^{13}C NMR (126 MHz, $CDCl_3$, 45 ºC) δ 169.9, 163.4, 148.4, 137.1, 136.6, 136.4, 133.5, 129.2, 128.6, 127.2, 126.8, 122.2, 121.8, 120.9, 119.4, 118.5, 111.3, 106.5, 67.3, 48.5, 40.4, 22.2, 19.3; HRMS (ESI) calcd for $C_{25}H_{24}N_3O_2^+$ $[M + H]^+$ 398.1863, found 398.1867.

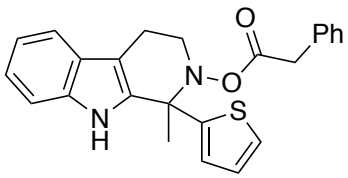

44

1-methyl-1-(thiophen-2-yl)-1,3,4,9-tetrahydro-2*H*-pyrido[3,4-*b*]indol-2-yl 2-phenylacetate (44). Prepared using the general procedure described above with **S22** and phenylacetyl chloride, ultimately yielding **44** (0.096 g, 96% yield) as a yellow solid. **44**: R_f = 0.46 (silica gel, hexanes/EtOAc = 4/1); IR (film) ν_{max} 3379, 1749, 1598, 1454, 1299, 1232, 1114, 1074, 743, 697 cm^{-1}; ^{1}H NMR (500 MHz, $CDCl_3$) δ 7.68 (br s, 1 H, exchangeable), 7.53 (d, J = 7.8 Hz, 1 H), 7.37–7.25 (m, 5 H), 7.24–7.17 (m, 3 H), 7.16–7.11 (m, 1 H), 6.92–6.81 (m, 1 H), 6.76–6.57 (m, 1 H), 3.62–3.54 (m, 2 H), 3.50–3.34 (m, 2 H), 3.09–2.93 (m, 1 H), 2.92–2.84 (m, 1 H), 1.86 (s, 3 H); ^{13}C NMR (101 MHz, $CDCl_3$) δ 170.1, 136.3, 135.1, 133.6, 129.3, 128.7, 127.2, 126.6 (2 C), 126.2, 126.1, 122.2, 119.7, 118.7, 111.2 (2 C), 107.9, 63.7, 48.4, 40.2, 25.4, 19.3; HRMS (ESI) calcd for $C_{24}H_{23}N_2O_2S^+$ $[M + H]^+$ 403.1475, found 403.1476.

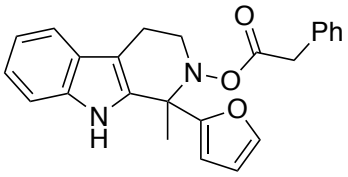

45

1-(furan-2-yl)-1-methyl-1,3,4,9-tetrahydro-2*H*-pyrido[3,4-*b*]indol-2-yl 2-phenylacetate (45). Prepared using the general procedure described above with **S23** and phenylacetyl chloride, ultimately yielding **45** (0.090 g, 93% yield) as a pale-yellow solid. **45**: R_f = 0.31 (silica gel, hexanes/EtOAc = 4/1); IR (film) ν_{max} 3373, 1750, 1496, 1454, 1300, 1233, 1157, 1115, 1011, 744, 697 cm^{-1}; ^{1}H NMR (500 MHz, $CDCl_3$) δ 7.69 (br s, 1 H, exchangeable), 7.52 (d, J = 7.7 Hz, 1 H), 7.41–7.34 (m, 1 H), 7.33–7.25 (m, 4 H), 7.25–7.21 (m, 2 H), 7.21–7.16 (m, 1 H), 7.16–7.10 (m, 1 H), 6.30–6.20 (m, 1 H), 5.97 (d, J = 3.3 Hz, 1 H), 3.60–3.52 (m, 2 H), 3.51–3.41 (m, 2 H), 3.04–

2.94 (m, 1 H), 2.93–2.86 (m, 1 H), 1.81 (s, 3 H); ^{13}C NMR (101 MHz, $CDCl_3$) δ 170.1, 154.4, 142.7, 136.3, 133.8, 133.6, 129.3, 128.6, 127.2, 126.6, 122.2, 119.6, 118.6, 111.2, 110.1, 109.7, 108.2, 62.3, 48.7, 40.2, 22.4, 19.2; HRMS (CI) calcd for $C_{24}H_{23}N_2O_3^+$ $[M + H]^+$ 387.1703, found 387.1703.

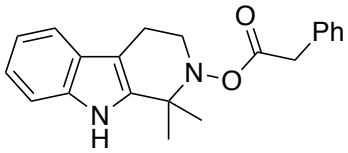

46

1,1-dimethyl-1,3,4,9-tetrahydro-2*H*-pyrido[3,4-*b*]indol-2-yl 2-phenylacetate (46). Prepared using the general procedure described above with **S24** and phenylacetyl chloride, ultimately yielding **46** (0.081 g, 97% yield) as a white solid. **46**: R_f = 0.50 (silica gel, hexanes/EtOAc = 2/1); IR (film) ν_{max} 3364, 2981, 1746, 1598, 1454, 1317, 1299, 1231, 1120, 744, 696 cm^{-1}; ^{1}H NMR (500 MHz, $CDCl_3$) δ 7.68 (br s, 1 H, exchangeable), 7.48 (d, *J* = 7.7 Hz, 1 H), 7.33 (d, *J* = 8.0 Hz, 1 H), 7.30–7.22 (m, 5 H), 7.20–7.15 (m, 1 H), 7.15–7.08 (m, 1 H), 3.61 (s, 2 H), 3.52 (t, *J* = 5.6 Hz, 2 H), 2.83 (t, *J* = 5.0 Hz, 2 H), 1.46 (s, 6 H); ^{13}C NMR (126 MHz, $CDCl_3$, 45 ºC) δ 170.3, 137.6, 136.2, 133.8, 129.3, 128.7, 127.3, 127.2, 121.9, 119.7, 118.4, 111.0, 106.3, 59.8, 48.3, 40.4, 26.2, 18.8; HRMS (ESI) calcd for $C_{21}H_{23}N_2O_2^+$ $[M + H]^+$ 335.1754, found 335.1756.

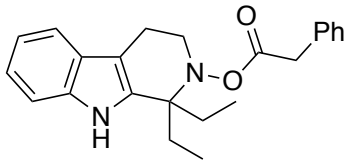

47

1,1-diethyl-1,3,4,9-tetrahydro-2*H*-pyrido[3,4-*b*]indol-2-yl 2-phenylacetate (47). Prepared using the general procedure described above with **S25** and phenylacetyl chloride, ultimately yielding **47** (0.077 g, 85% yield) as a yellow solid. **47**: R_f = 0.42 (silica gel, hexanes/EtOAc = 4/1); IR (film) ν_{max} 3387, 2972, 1746, 1597, 1496, 1454, 1339, 1231, 1119, 744 cm^{-1}; ^{1}H NMR (500 MHz, $CDCl_3$) δ 7.65 (br s, 1 H, exchangeable), 7.49 (d, *J* = 7.8 Hz, 1 H), 7.33 (d, *J* = 8.0 Hz, 1 H), 7.31–7.21 (m, 5 H), 7.20–7.15 (m, 1 H), 7.13–7.09 (m, 1 H), 3.62–3.52 (m, 4 H), 2.83 (t, *J* = 6.1 Hz, 2 H), 1.86–1.70 (m, 4 H), 0.85 (t, *J* = 7.5 Hz, 6 H); ^{13}C NMR (101 MHz, $CDCl_3$) δ 170.0, 136.1, 135.9, 133.8,

129.2, 128.7, 127.3, 126.9, 121.7, 119.5, 118.3, 110.9, 107.6, 65.6, 47.5, 40.6, 28.0, 18.9, 8.7; HRMS (ESI) calcd for $C_{23}H_{27}N_2O_2^+$ $[M + H]^+$ 363.2067, found 363.2072.

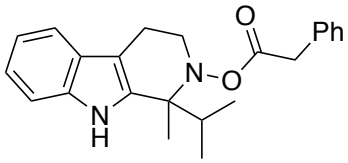

48

1-isopropyl-1-methyl-1,3,4,9-tetrahydro-2*H*-pyrido[3,4-*b*]indol-2-yl 2-phenylacetate (48). Prepared using the general procedure described above with **S26** and phenylacetyl chloride, ultimately yielding **48** (0.067 g, 74% yield) as a yellow solid. **48**: R_f = 0.40 (silica gel, hexanes/EtOAc = 4/1); IR (film) ν_{max} 3388, 2965, 1744, 1597, 1454, 1389, 1297, 1229, 1122, 744, 696 cm^{-1}; ^1H NMR (500 MHz, $CDCl_3$) δ 7.66 (br s, 1 H, exchangeable), 7.49 (d, *J* = 7.7 Hz, 1 H), 7.33 (d, *J* = 8.0 Hz, 1 H), 7.31–7.21 (m, 5 H), 7.20–7.15 (m, 1 H), 7.14–7.09 (m, 1 H), 3.58–3.50 (m, 3 H), 3.50–3.44 (m, 1 H), 2.90–2.81 (m, 1 H), 2.81–2.74 (m, 1 H), 2.03–1.94 (m, 1 H), 1.33 (s, 3 H), 1.06 (d, *J* = 6.9 Hz, 3 H), 0.95 (d, *J* = 6.8 Hz, 3 H); ^{13}C NMR (101 MHz, $CDCl_3$) δ 170.2, 137.3, 135.9, 133.8, 129.3, 128.6, 127.2, 126.8, 121.8, 119.5, 118.4, 110.8, 107.4, 65.2, 47.7, 40.4, 37.2, 18.6, 17.9, 17.4; HRMS (CI) calcd for $C_{23}H_{27}N_2O_2^+$ $[M + H]^+$ 363.2067, found 363.2066.

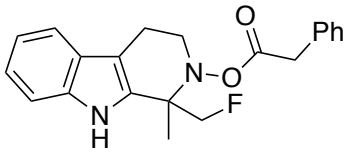

49

1-(fluoromethyl)-1-methyl-1,3,4,9-tetrahydro-2*H*-pyrido[3,4-*b*]indol-2-yl 2-phenylacetate (49). Prepared using the general procedure described above with **S27** and phenylacetyl chloride, ultimately yielding **49** (0.063 g, 71% yield) as a yellow solid. **49**: R_f = 0.26 (silica gel, hexanes/EtOAc = 4/1); IR (film) ν_{max} 3372, 1750, 1598, 1454, 1301, 1230, 1117, 1030, 745, 697 cm^{-1}; ^1H NMR (500 MHz, $CDCl_3$) δ 8.02 (br s, 1 H, exchangeable), 7.50 (d, *J* = 7.8 Hz, 1 H), 7.37–7.23 (m, 6 H), 7.23–7.16 (m, 1 H), 7.15–7.08 (m, 1 H), 4.48 (ddd, *J* = 62.2, 47.0, 8.5 Hz, 2 H), 3.61 (s, 2 H), 3.55–3.46 (m, 2 H), 3.00–2.88 (m, 1 H), 2.87–2.76 (m, 1 H), 1.54 (s, 3 H); ^{13}C NMR (126 MHz, $CDCl_3$, 45 ºC) δ 169.8, 136.5, 134.2, 133.5, 129.3, 128.9, 127.5, 126.4, 122.4,

119.8, 118.6, 111.2, 107.5, 87.97 (d, J = 172.9 Hz), 62.22 (d, J = 19.4 Hz), 48.9, 40.4, 20.0, 19.1; HRMS (CI) calcd for $C_{21}H_{22}FN_2O_2^+$ $[M + H]^+$ 353.1660, found 353.1660.

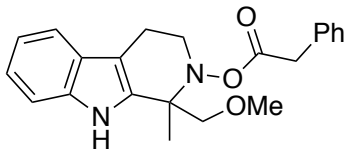

50

1-(methoxymethyl)-1-methyl-1,3,4,9-tetrahydro-2*H*-pyrido[3,4-*b*]indol-2-yl 2-phenylacetate (50). Prepared using the general procedure described above with **S28** and phenylacetyl chloride, ultimately yielding **50** (0.080 g, 87% yield) as a yellow solid. **50**: R_f = 0.53 (silica gel, hexanes/EtOAc = 2/1); IR (film) ν_{max} 3437, 2922, 1754, 1598, 1454, 1318, 1301, 1230, 1109, 745, 696 cm^{-1}; ^1H NMR (500 MHz, $CDCl_3$) δ 8.47 (br s, 1 H, exchangeable), 7.48 (d, J = 7.7 Hz, 1 H), 7.38–7.26 (m, 6 H), 7.19–7.13 (m, 1 H), 7.12–7.06 (m, 1 H), 3.61 (s, 2 H), 3.55–3.45 (m, 3 H), 3.33 (s, 4 H), 3.02–2.91 (m, 1 H), 2.81–2.72 (m, 1 H), 1.50 (s, 3 H); ^{13}C NMR (126 MHz, $CDCl_3$, 45 ºC) δ 170.0, 136.6, 136.2, 133.8, 129.4, 128.8, 127.4, 126.5, 121.8, 119.4, 118.4, 111.1, 106.1, 78.4, 62.4, 59.7, 48.7, 40.6, 21.0, 19.2; HRMS (CI) calcd for $C_{22}H_{25}N_2O_3^+$ $[M + H]^+$ 365.1860, found 365.1862.

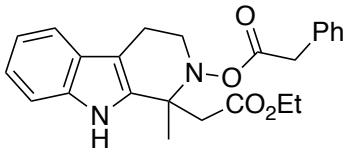

51

1-(2-ethoxy-2-oxoethyl)-1-methyl-1,3,4,9-tetrahydro-2*H*-pyrido[3,4-*b*]indol-2-yl 2-phenylacetate (51). Prepared using the general procedure described above with **S29** and phenylacetyl chloride, ultimately yielding **51** (0.097 g, 96% yield) as a white solid. **51**: R_f = 0.29 (silica gel, hexanes/EtOAc = 4/1); IR (film) ν_{max} 3364, 2903, 2383, 2315, 1760, 1597, 1454, 1226, 1117, 1031 cm^{-1}; ^1H NMR (500 MHz, $CDCl_3$) δ 9.46 (br s, 1 H, exchangeable), 7.47 (d, J = 7.8 Hz, 1 H), 7.36 (d, J = 8.1 Hz, 1 H), 7.33–7.24 (m, 5 H), 7.21–7.14 (m, 1 H), 7.13–7.05 (m, 1 H), 4.27–4.11 (m, 2 H), 3.62 (s, 2 H), 3.55–3.45 (m, 2 H), 2.96–2.85 (m, 1 H), 2.84–2.74 (m, 3 H), 1.57 (s, 3 H), 1.28 (t, J = 7.1 Hz, 3 H); ^{13}C NMR (126 MHz, $CDCl_3$, 45 ºC) δ 173.2, 169.9, 136.2, 136.0, 133.7, 129.3,

128.8, 127.4, 126.5, 122.0, 119.5, 118.4, 111.4, 106.6, 61.3, 61.2, 48.3, 43.3, 40.5, 23.0, 19.0, 14.2; HRMS (CI) calcd for $C_{24}H_{27}N_2O_4^+$ $[M + H]^+$ 407.1965, found 407.1963.

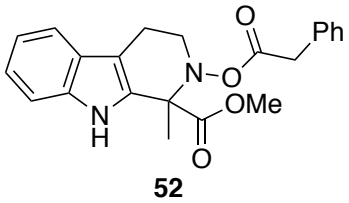

52

Methyl 1-methyl-2-(2-phenylacetoxy)-2,3,4,9-tetrahydro-1*H*-pyrido[3,4-*b*]indole-1-carboxylate (52). Prepared using the general procedure described above with **S30** and phenylacetyl chloride, ultimately yielding **52** (0.087 g, 92% yield) as a yellow solid. **52**: R_f = 0.38 (silica gel, hexanes/EtOAc = 2/1); IR (film) ν_{max} 3365, 2383, 2315, 1764, 1598, 1454, 1232, 1119, 1073, 736 cm^{-1}; ^1H NMR (500 MHz, $CDCl_3$) δ 8.50 (br s, 1 H, exchangeable), 7.50 (d, *J* = 7.8 Hz, 1 H), 7.37 (d, *J* = 8.1 Hz, 1 H), 7.34–7.23 (m, 5 H), 7.23–7.17 (m, 1 H), 7.15–7.09 (m, 1 H), 3.87–3.75 (m, 1 H), 3.59–3.47 (m, 3 H), 3.45 (s, 3 H), 3.03–2.94 (m, 1 H), 2.87–2.79 (m, 1 H), 1.74 (s, 3 H); ^{13}C NMR (126 MHz, $CDCl_3$, 45 ºC) δ 172.5, 169.4, 136.6, 133.6, 131.7, 129.3, 128.7, 127.3, 126.6, 122.5, 119.8, 118.6, 111.3, 108.1, 67.1, 52.6, 48.5, 40.3, 24.3, 18.7; HRMS (CI) calcd for $C_{22}H_{23}N_2O_4^+$ $[M + H]^+$ 379.1652, found 379.1651.

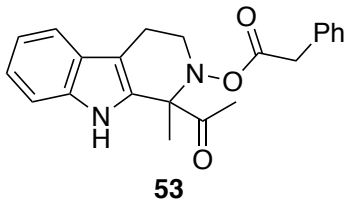

53

1-acetyl-1-methyl-1,3,4,9-tetrahydro-2*H*-pyrido[3,4-*b*]indol-2-yl 2-phenylacetate (53). Prepared using the general procedure described above with **S31** and phenylacetyl chloride, ultimately yielding **53** (0.072 g, 80% yield) as a white solid. **53**: R_f = 0.34 (silica gel, hexanes/EtOAc = 4/1); IR (film) ν_{max} 3379, 1757, 1713, 1597, 1454, 1352, 1300, 1231, 1112, 745, 695 cm^{-1}; ^1H NMR (500 MHz, $CDCl_3$) δ 8.36 (br s, 1 H, exchangeable), 7.50 (d, *J* = 7.8 Hz, 1 H), 7.36 (d, *J* = 8.1 Hz, 1 H), 7.33–7.16 (m, 6 H), 7.15–7.09 (m, 1 H), 3.76–3.66 (m, 1 H), 3.55 (s, 2 H), 3.49–3.41 (m, 1 H), 3.05–2.93 (m, 1 H), 2.83–2.73 (m, 1 H), 2.09 (s, 3 H), 1.60 (s, 3 H); ^{13}C NMR (101 MHz, $CDCl_3$) δ 209.9, 169.4, 136.6, 133.1, 132.1, 129.2, 128.8, 127.6, 126.4, 122.4, 119.7, 118.5, 111.4,

107.8, 71.7, 48.2, 40.3, 24.6, 21.1, 19.0; HRMS (CI) calcd for $C_{22}H_{23}N_2O_3^+$ [M + H]$^+$ 363.1703, found 363.1707.

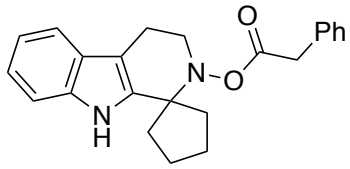

54

4',9'-dihydrospiro[cyclopentane-1,1'-pyrido[3,4-*b*]indol]-2'(3'*H*)-yl 2-phenylacetate (54). Prepared using the general procedure described above with **S32** and phenylacetyl chloride, ultimately yielding **54** (0.086 g, 95% yield) as a white solid. **54**: R_f = 0.31 (silica gel, hexanes/EtOAc = 4/1); IR (film) ν_{max} 3376, 2958, 1745, 1598, 1454, 1299, 1230, 1117, 744, 696 cm^{-1}; ^{1}H NMR (500 MHz, $CDCl_3$) δ 7.66 (br s, 1 H, exchangeable), 7.49 (d, *J* = 7.7 Hz, 1 H), 7.34 (d, *J* = 7.9 Hz, 1 H), 7.29–7.21 (m, 5 H), 7.21–7.15 (m, 1 H), 7.15–7.10 (m, 1 H), 3.74–3.60 (m, 1 H), 3.56 (s, 2 H), 3.51–3.36 (m, 1 H), 2.94–2.56 (m, 2 H), 2.12–2.05 (m, 2 H), 1.96–1.84 (m, 4 H), 1.82–1.73 (m, 2 H); ^{13}C NMR (101 MHz, $CDCl_3$) δ 170.4, 137.3, 135.9, 133.8, 129.2, 128.7, 127.3, 127.1, 121.8, 119.7, 118.3, 110.9, 106.6, 70.5, 49.1, 41.0, 40.4, 36.1, 25.7, 25.6, 17.7; HRMS (ESI) calcd for $C_{23}H_{25}N_2O_2^+$ [M + H]$^+$ 361.1911, found 361.1913.

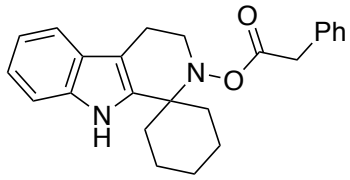

55

4',9'-dihydrospiro[cyclohexane-1,1'-pyrido[3,4-*b*]indol]-2'(3'*H*)-yl 2-phenylacetate (55). Prepared using the general procedure described above with **S33** and phenylacetyl chloride, ultimately yielding **55** (0.080 g, 86% yield) as a white solid. **55**: R_f = 0.41 (silica gel, hexanes/EtOAc = 4/1); IR (film) ν_{max} 3379, 2938, 2854, 1738, 1598, 1446, 1297, 1271, 1230, 1118, 744, 695 cm^{-1}; ^{1}H NMR (500 MHz, $CDCl_3$) δ 7.75 (br s, 1 H, exchangeable), 7.50 (d, *J* = 7.7 Hz, 1 H), 7.35 (d, *J* = 8.0 Hz, 1 H), 7.27–7.20 (m, 5 H), 7.20–7.16 (m, 1 H), 7.15–7.11 (m, 1 H), 3.80–3.66 (m, 1 H), 3.57–3.46 (m, 3 H), 2.98–2.77 (m, 1 H), 2.70–2.50 (m, 1 H), 2.02–1.88 (m, 3 H), 1.74–1.62 (m, 4 H), 1.50–1.42 (m, 1 H), 1.40–1.27 (m, 2 H); ^{13}C NMR (101 MHz, $CDCl_3$) δ 170.2, 138.0, 135.6, 133.8, 129.2, 128.6, 127.2 (2 C), 121.7, 119.6, 118.3, 111.0,

106.6, 60.9, 46.7, 40.5, 38.7, 33.2, 25.9, 21.5, 21.1, 17.2; HRMS (ESI) calcd for $C_{24}H_{27}N_2O_2^+$ [M + H]$^+$ 375.2067, found 375.2068.

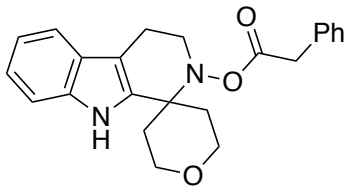

56

2,3,4',5,6,9'-hexahydrospiro[pyran-4,1'-pyrido[3,4-*b*]indol]-2'(3'*H*)-yl 2-phenylacetate (56). Prepared using the general procedure described above with **S34** and phenylacetyl chloride, ultimately yielding **56** (0.089 g, 94% yield) as a yellow solid. **56**: R_f = 0.29 (silica gel, hexanes/EtOAc = 2/1); IR (film) ν_{max} 3295, 2956, 1748, 1597, 1453, 1305, 1264, 1229, 1105, 744 cm^{-1}; ^{1}H NMR (500 MHz, $CDCl_3$) δ 7.92 (br s, 1 H, exchangeable), 7.51 (d, *J* = 7.7 Hz, 1 H), 7.36 (d, *J* = 8.0 Hz, 1 H), 7.29–7.18 (m, 6 H), 7.17–7.11 (m, 1 H), 4.19–4.00 (m, 1 H), 3.81–3.64 (m, 3 H), 3.61–3.42 (m, 4 H), 3.03–2.79 (m, 1 H), 2.75–2.51 (m, 1 H), 2.05–1.95 (m, 2 H), 1.86–1.77 (m, 2 H); ^{13}C NMR (101 MHz, $CDCl_3$) δ 169.9, 136.1, 136.0, 133.5, 129.1, 128.8, 127.4, 126.9, 122.0, 119.6, 118.4, 111.3, 107.2, 63.3, 63.1, 59.0, 47.2, 40.5, 38.0, 32.9, 17.1; HRMS (ESI) calcd for $C_{23}H_{25}N_2O_3^+$ [M + H]$^+$ 377.1860, found 377.1865.

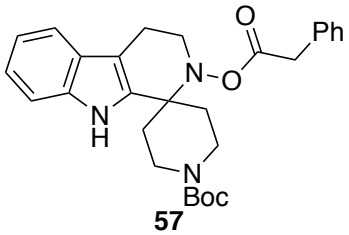

57

***tert*-butyl 2'-(2-phenylacetoxy)-2',3',4',9'-tetrahydrospiro[piperidine-4,1'-pyrido[3,4-*b*]indole]-1-carboxylate (57).** Prepared using the general procedure described above with **S35** and phenylacetyl chloride, ultimately yielding **57** (0.109 g, 91% yield) as a white solid. **57**: R_f = 0.31 (silica gel, hexanes/EtOAc = 4/1); IR (film) ν_{max} 3304, 2975, 1755, 1670, 1598, 1435, 1366, 1247, 1163, 1113, 744 cm^{-1}; ^{1}H NMR (500 MHz, $CDCl_3$) δ 8.36 (br s, 1 H, exchangeable), 7.51 (d, *J* = 7.7 Hz, 1 H), 7.36 (d, *J* = 8.0 Hz, 1 H), 7.25–7.10 (m, 7 H), 3.97–3.62 (m, 3 H), 3.58–3.32 (m, 4 H), 3.13–2.78 (m, 2 H), 2.77–2.54 (m, 1 H), 1.92–1.78 (m, 4 H), 1.48 (s, 9 H); ^{13}C NMR (101 MHz, $CDCl_3$) δ 169.9, 154.7, 136.2, 136.1, 133.5,

129.1, 128.7, 127.4, 126.7, 121.8, 119.4, 118.2, 111.5, 106.7, 79.9, 59.7, 47.2, 40.6, 40.0, 38.7, 37.4, 32.5, 28.7, 17.2; HRMS (CI) calcd for $C_{28}H_{34}N_3O_4^+$ [M + H]$^+$ 476.2544, found 476.2543.

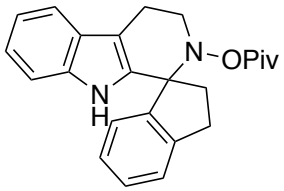

58

2,3,4',9'-tetrahydrospiro[indene-1,1'-pyrido[3,4-*b*]indol]-2'(3'*H*)-yl pivalate (58). Prepared using the general procedure described above with **S36** and pivaloyl chloride, ultimately yielding **58** (0.085 g, 90% yield) as a brown solid. **58**: R_f = 0.57 (silica gel, hexanes/EtOAc = 4/1); IR (film) ν_{max} 3388, 2970, 1739, 1597, 1478, 1460, 1396, 1303, 1274, 1125, 744 cm^{-1}; ^{1}H NMR (500 MHz, $CDCl_3$, 45 ºC) δ 7.58–7.53 (m, 1 H), 7.40 (br s, 1 H, exchangeable), 7.34–7.27 (m, 2 H), 7.23–7.18 (m, 1 H), 7.17–7.08 (m, 4 H), 3.74–3.64 (m, 1 H), 3.58–3.50 (m, 1 H), 3.40–3.29 (m, 1 H), 3.25–3.16 (m, 1 H), 3.08–2.99 (m, 1 H), 2.96–2.89 (m, 1 H), 2.85–2.73 (m, 1 H), 2.47–2.36 (m, 1 H), 1.00 (s, 9 H); ^{13}C NMR (126 MHz, $CDCl_3$, 45 ºC) δ 176.0, 145.6, 142.9, 136.5, 136.2, 129.0, 127.0, 126.9, 126.5, 124.7, 122.0, 119.7, 118.5, 111.1, 108.5, 74.6, 49.7, 38.6, 30.8, 27.2, 27.1, 19.4; HRMS (CI) calcd for $C_{24}H_{27}N_2O_2^+$ [M + H]$^+$ 375.2067, found 375.2066.

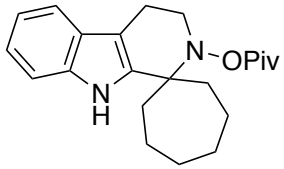

59

4',9'-dihydrospiro[cycloheptane-1,1'-pyrido[3,4-*b*]indol]-2'(3'*H*)-yl pivalate (59). Prepared using the general procedure described above with **S37** and pivaloyl chloride, ultimately yielding **59** (0.064 g, 72% yield) as a white solid. **59**: R_f = 0.54 (silica gel, hexanes/EtOAc = 4/1); IR (film) ν_{max} 3379, 2928, 1728, 1597, 1564, 1448, 1395, 1277, 1127, 744 cm^{-1}; ^{1}H NMR (500 MHz, $CDCl_3$, 45 ºC) δ 7.85 (br s, 1 H, exchangeable), 7.51 (d, J = 7.7 Hz, 1 H), 7.36 (d, J = 8.0 Hz, 1 H), 7.21–7.16 (m, 1 H), 7.15–7.11 (m, 1 H), 3.69–3.56 (m, 2 H), 2.94–2.72 (m, 2 H), 2.21–2.10 (m, 2 H), 1.98–1.88 (m, 4 H), 1.80–1.74 (m, 2 H), 1.69–1.57 (m, 4 H), 1.18 (s, 9 H); ^{13}C NMR (126 MHz, $CDCl_3$, 45 ºC) δ 176.4, 139.6, 135.9, 127.4, 121.6, 119.6, 118.4, 110.9, 105.6, 64.7, 47.1, 39.1,

30.0, 27.4, 27.3, 23.1, 17.6; HRMS (CI) calcd for $C_{22}H_{31}N_2O_2^+$ [M + H]$^+$ 355.2380, found 355.2378.

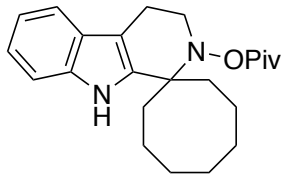

60

4',9'-dihydrospiro[cyclooctane-1,1'-pyrido[3,4-*b*]indol]-2'(3'*H*)-yl pivalate (60). Prepared using the general procedure described above with **S38** and pivaloyl chloride, ultimately yielding **60** (0.050 g, 54% yield) as a white solid. **60**: R_f = 0.58 (silica gel, hexanes/EtOAc = 4/1); IR (film) ν_{max} 3378, 2925, 1728, 1597, 1564, 1448, 1396, 1278, 1127, 1028, 743 cm^{-1}; ^{1}H NMR (500 MHz, $CDCl_3$, 45 ºC) δ 7.81 (br s, 1 H, exchangeable), 7.51 (d, *J* = 7.7 Hz, 1 H), 7.36 (d, *J* = 8.0 Hz, 1 H), 7.21–7.15 (m, 1 H), 7.14–7.09 (m, 1 H), 3.73–3.54 (m, 2 H), 2.99–2.65 (m, 2 H), 2.20–2.08 (m, 2 H), 2.05–1.95 (m, 4 H), 1.72–1.55 (m, 8 H), 1.15 (s, 9 H); ^{13}C NMR (126 MHz, $CDCl_3$, 45 ºC) δ 176.3, 139.4, 135.8, 127.4, 121.6, 119.6, 118.4, 110.9, 105.5, 64.2, 46.9, 39.1, 28.4, 27.4, 27.3, 25.3, 22.0, 17.6; HRMS (ESI) calcd for $C_{23}H_{33}N_2O_2^+$ [M + H]$^+$ 369.2537, found 369.2537.

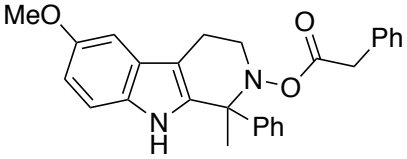

63

6-methoxy-1-methyl-1-phenyl-1,3,4,9-tetrahydro-2*H*-pyrido[3,4-*b*]indol-2-yl 2-phenylacetate (63). Prepared using the general procedure described above with **S39** and phenylacetyl chloride, ultimately yielding **63** (0.098 g, 92% yield) as a brown solid. **63**: R_f = 0.37 (silica gel, hexanes/EtOAc = 4/1); IR (film) ν_{max} 3372, 1746, 1597, 1564, 1484, 1453, 1217, 1165, 1116, 1027, 699 cm^{-1}; ^{1}H NMR (500 MHz, $CDCl_3$) δ 7.62 (br s, 1 H, exchangeable), 7.33–7.20 (m, 9 H), 7.20–7.14 (m, 2 H), 7.01 (d, *J* = 2.5 Hz, 1 H), 6.87 (dd, *J* = 8.7, 2.5 Hz, 1 H), 3.89 (s, 3 H), 3.53 (s, 2 H), 3.48–3.39 (m, 1 H), 3.25–3.14 (m, 1 H), 3.00–2.89 (m, 1 H), 2.78–2.67 (m, 1 H), 1.77 (s, 3 H); ^{13}C NMR (101 MHz, $CDCl_3$) δ 170.5, 154.2, 136.1, 133.7, 131.2, 129.2, 128.6, 128.2 (2 C), 127.9, 127.7 (2 C), 127.3, 127.2, 111.9, 108.0, 100.7, 65.7, 56.0, 47.9, 40.2, 24.3, 18.4; HRMS (ESI) calcd for $C_{27}H_{27}N_2O_3^+$ [M + H]$^+$ 427.2016, found 427.2015.

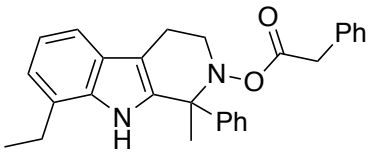

64

8-ethyl-1-methyl-1-phenyl-1,3,4,9-tetrahydro-2*H*-pyrido[3,4-*b*]indol-2-yl 2-phenylacetate (64). Prepared using the general procedure described above with **S40** and phenylacetyl chloride, ultimately yielding **64** (0.096 g, 90% yield) as a yellow solid. **64**: R_f = 0.50 (silica gel, hexanes/EtOAc = 4/1); IR (film) ν_{max} 3382, 2965, 1742, 1597, 1564, 1494, 1446, 1393, 1236, 1116, 700 cm^{-1}; ^1H NMR (500 MHz, $CDCl_3$) δ 7.60 (br s, 1 H, exchangeable), 7.43 (d, *J* = 7.8 Hz, 1 H), 7.32–7.22 (m, 8 H), 7.21–7.17 (m, 2 H), 7.17–7.12 (m, 1 H), 7.11–7.05 (m, 1 H), 3.53 (s, 2 H), 3.47–3.40 (m, 1 H), 3.24–3.14 (m, 1 H), 3.03–2.93 (m, 1 H), 2.85 (q, *J* = 7.6 Hz, 2 H), 2.79–2.68 (m, 1 H), 1.81 (s, 3 H), 1.36 (t, *J* = 7.6 Hz, 3 H); ^{13}C NMR (101 MHz, $CDCl_3$) δ 170.4, 135.0, 134.7, 133.7, 129.2, 128.6, 128.3, 128.0, 127.8 (2 C), 127.2, 126.7, 126.5, 120.7, 120.1, 116.4, 109.0, 65.7, 47.9, 40.2, 24.5, 24.0, 18.4, 13.9; HRMS (CI) calcd for $C_{28}H_{29}N_2O_2^+$ $[M + H]^+$ 425.2224, found 425.2225.

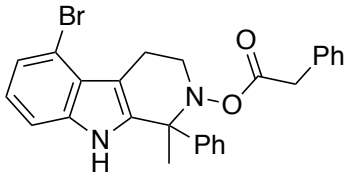

65

5-bromo-1-methyl-1-phenyl-1,3,4,9-tetrahydro-2*H*-pyrido[3,4-*b*]indol-2-yl 2-phenylacetate (65). Prepared using the general procedure described above with **S41** and phenylacetyl chloride, ultimately yielding **65** (0.099 g, 83% yield) as a white solid. **65**: R_f = 0.44 (silica gel, hexanes/EtOAc = 4/1); IR (film) ν_{max} 3357, 1743, 1597, 1494, 1446, 1317, 1237, 1118, 729, 700 cm^{-1}; ^1H NMR (500 MHz, $CDCl_3$) δ 7.85 (br s, 1 H, exchangeable), 7.32–7.20 (m, 10 H), 7.20–7.14 (m, 2 H), 7.01 (t, *J* = 7.9 Hz, 1 H), 3.54 (s, 2 H), 3.47–3.39 (m, 1 H), 3.34–3.24 (m, 1 H), 3.23–3.11 (m, 2 H), 1.77 (s, 3 H); ^{13}C NMR (101 MHz, $CDCl_3$) δ 170.4, 137.1, 136.3, 133.6, 129.3, 128.7, 128.4, 127.9, 127.7, 127.6, 127.3, 125.9, 123.7, 122.9, 114.3, 110.3, 109.2, 65.6, 47.9, 40.3, 24.4, 20.5; HRMS (ESI) calcd for $C_{26}H_{24}BrN_2O_2^+$ $[M + H]^+$ 475.1016, found 475.1017.

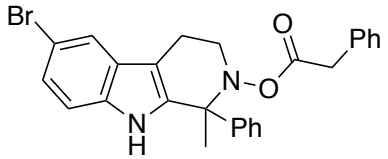

66

6-bromo-1-methyl-1-phenyl-1,3,4,9-tetrahydro-2*H*-pyrido[3,4-*b*]indol-2-yl 2-phenylacetate (66). Prepared using the general procedure described above with **S42** and phenylacetyl chloride, ultimately yielding **66** (0.089 g, 74% yield) as a white solid. **66**: R_f = 0.44 (silica gel, hexanes/EtOAc = 2/1); IR (film) ν_{max} 3362, 1743, 1597, 1447, 1301, 1220, 1117, 858, 798, 700 cm^{-1}; ^1H NMR (500 MHz, $CDCl_3$) δ 7.76 (br s, 1 H, exchangeable), 7.67 (d, *J* = 1.9 Hz, 1 H), 7.31–7.27 (m, 1 H), 7.26–7.19 (m, 9 H), 7.18–7.12 (m, 2 H), 3.53 (s, 2 H), 3.47–3.38 (m, 1 H), 3.24–3.12 (m, 1 H), 2.97–2.86 (m, 1 H), 2.78–2.65 (m, 1 H), 1.76 (s, 3 H); ^{13}C NMR (101 MHz, $CDCl_3$) δ 170.3, 136.7, 134.8, 133.6, 129.2, 128.7, 128.7, 128.4, 128.0, 127.7, 127.6, 127.3, 124.9, 121.3, 113.0, 112.6, 108.0, 65.6, 47.7, 40.3, 24.3, 18.3; HRMS (ESI) calcd for $C_{26}H_{24}BrN_2O_2^+$ [M + H]$^+$ 475.1016, found 475.1014.

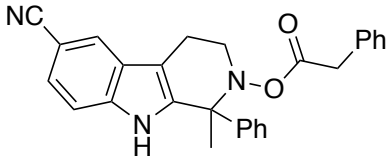

67

6-cyano-1-methyl-1-phenyl-1,3,4,9-tetrahydro-2*H*-pyrido[3,4-*b*]indol-2-yl 2-phenylacetate (67). Prepared using the general procedure described above with **S43** and phenylacetyl chloride, ultimately yielding **67** (0.069 g, 65% yield) as a white solid. **67**: R_f = 0.44 (silica gel, hexanes/EtOAc = 2/1); IR (film) ν_{max} 3328, 2219, 1747, 1598, 1473, 1446, 1319, 1232, 1184, 1116, 699 cm^{-1}; ^1H NMR (500 MHz, $CDCl_3$) δ 8.20 (br s, 1 H, exchangeable), 7.92–7.84 (m, 1 H), 7.46–7.35 (m, 2 H), 7.31–7.17 (m, 8 H), 7.17–7.11 (m, 2 H), 3.53 (s, 2 H), 3.48–3.40 (m, 1 H), 3.25–3.15 (m, 1 H), 2.98–2.89 (m, 1 H), 2.81–2.68 (m, 1 H), 1.78 (s, 3 H); ^{13}C NMR (101 MHz, $CDCl_3$) δ 170.3, 138.0, 137.8, 133.5, 129.2, 128.7, 128.4, 128.1, 127.6, 127.6, 127.3, 126.8, 125.1, 124.1, 120.9, 112.0, 109.0, 102.6, 65.6, 47.6, 40.2, 24.3, 18.1; HRMS (ESI) calcd for $C_{27}H_{24}N_3O_2^+$ [M + H]$^+$ 422.1863, found 422.1863.

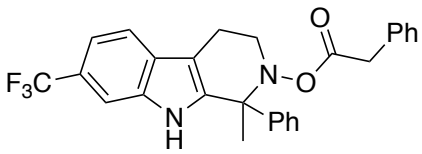

68

1-methyl-1-phenyl-7-(trifluoromethyl)-1,3,4,9-tetrahydro-2*H*-pyrido[3,4-*b*]indol-2-yl 2-phenylacetate (68). Prepared using the general procedure described above with **S44** and phenylacetyl chloride, ultimately yielding **68** (0.072 g, 62% yield) as a white solid. **68**: R_f = 0.44 (silica gel, hexanes/EtOAc = 4/1); IR (film) ν_{max} 3355, 1743, 1597, 1564, 1448, 1392, 1336, 1220, 1159, 1114, 1052, 699 cm^{-1}; ^1H NMR (500 MHz, $CDCl_3$) δ 7.95 (br s, 1 H, exchangeable), 7.66–7.59 (m, 2 H), 7.40 (d, *J* = 8.4 Hz, 1 H), 7.29–7.20 (m, 8 H), 7.18–7.12 (m, 2 H), 3.53 (s, 2 H), 3.49–3.42 (m, 1 H), 3.28–3.16 (m, 1 H), 3.01–2.91 (m, 1 H), 2.83–2.71 (m, 1 H), 1.79 (s, 3 H); ^{13}C NMR (101 MHz, $CDCl_3$) δ 170.4, 138.3, 135.1, 133.6, 129.2, 129.0, 128.7, 128.4, 128.3, 128.0, 127.8, 127.7, 127.3, 125.3 (q, *J* = 271.2 Hz), 124.1 (q, *J* = 31.9 Hz), 119.0, 116.6, 108.6, 65.7, 47.7, 40.3, 24.3, 18.3; HRMS (ESI) calcd for $C_{27}H_{24}F_3N_2O_2^+$ $[M + H]^+$ 465.1784, found 465.1784.

Identification of Hydrolysis By-product.

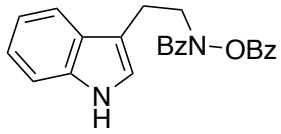

S46

***N*-(2-(1*H*-indol-3-yl)ethyl)-*N*-(benzoyloxy)benzamide (S46)**: R_f = 0.16 (silica gel, hexanes/EtOAc = 4/1); IR (film) ν_{max} 3406, 3059, 2925, 1762, 1654, 1451, 1239, 1010, 742, 704 cm^{-1}; ^1H NMR (400 MHz, $CDCl_3$) δ 8.16 (br s, 1 H, exchangeable), 7.93 (d, *J* = 7.5 Hz, 2 H), 7.64–7.57 (m, 1 H), 7.50–7.39 (m, 5 H), 7.37–7.30 (m, 2 H), 7.26–7.14 (m, 3 H), 7.09–7.02 (m, 2 H), 4.20 (t, *J* = 7.2 Hz, 2 H), 3.23 (t, *J* = 7.2 Hz, 2 H); ^{13}C NMR (101 MHz, $CDCl_3$) δ 170.5, 164.4, 136.4, 134.2, 133.7, 130.9, 130.0, 128.8, 128.3, 127.8, 127.4, 127.1, 122.6, 122.2, 119.6, 118.6, 112.1, 111.4, 51.2, 23.4; HRMS (ESI) calcd for $C_{24}H_{21}N_2O_3^+$ $[M + H]^+$ 385.1547, found 385.1547.

General Procedure for Racemic Pictet–Spengler Reaction without BzCl.

To a solution of hydroxylamine **29** (0.044 g, 0.25 mmol, 1.0 equiv) in MeOH (1.66 mL) at 23 ºC was added the requisite ketone (0.50 mmol, 2.0 equiv), AcOH (0.007 mL, 0.13 mmol, 0.5 equiv, via microsyringe), and $MgSO_4$ (0.120 g, 0.75 mmol, 3.0 equiv). The resultant mixture was stirred for 16 h at 23 ºC. Upon completion, the contents were diluted with CH_2Cl_2 (5 mL), quenched by the addition of saturated aqueous $NaHCO_3$ (5 mL), poured into a separatory funnel, and extracted with CH_2Cl_2 (3 × 5 mL). The combined organic extracts were then dried (Na_2SO_4), filtered, and concentrated. The resultant crude material was purified by flash column chromatography (silica gel, CH_2Cl_2/MeOH = 1/0→9/1) to yield **71-73**.

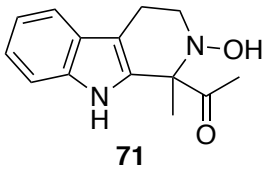

71

1-(2-hydroxy-1-methyl-2,3,4,9-tetrahydro-1*H*-pyrido[3,4-*b*]indol-1-yl)ethan-1-one (71). Prepared using the general procedure described above with **29** and diacetyl, ultimately yielding **71** (0.060 g, 98% yield) as a solid. **71**: ^{1}H NMR (500 MHz, $CDCl_3$) δ 8.30 (br s, 1 H, exchangeable), 7.50 (d, *J* = 8.7 Hz, 1 H), 7.33 (d, *J* = 8.1 Hz, 1 H), 7.22–7.15 (m, 1 H), 7.14–7.08 (m, 1 H), 4.91 (br s, 1 H, exchangeable), 3.56–3.48 (m, 1 H), 3.48–3.41 (m, 1 H), 3.14–3.03 (m, 1 H), 2.88–2.78 (m, 1 H), 2.38 (s, 3 H), 1.60 (s, 3 H).

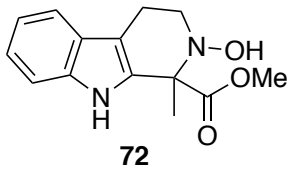

72

methyl 2-hydroxy-1-methyl-2,3,4,9-tetrahydro-1*H*-pyrido[3,4-*b*]indole-1-carboxylate (72). Prepared using the general procedure described above with **29** and methyl pyruvate, ultimately yielding **72** (0.057 g, 88% yield) as a solid. ^{1}H NMR (500 MHz, $CDCl_3$) δ 8.31 (br s, 1 H, exchangeable), 7.49 (d, *J* = 8.9 Hz, 1 H), 7.35 (d, *J* = 8.1 Hz, 1 H), 7.22–7.16 (m, 1 H), 7.14–7.08 (m, 1 H), 5.86 (br s,

1 H, exchangeable), 3.85 (s, 3 H), 3.64–3.56 (m, 1 H), 3.49–3.40 (m, 1 H), 3.06–2.98 (m, 1 H), 2.91–2.83 (m, 1 H), 1.80 (s, 3 H).

General Procedure for Enantioselective Pictet–Spengler Reactions of Nitrones.

Molecular sieves (4Å, powder 1.25 g) were flame-dried *in vacuo* and then allowed to cool to 23 °C before being suspended in toluene (25.0 mL) under an argon atmosphere. Nitrone (0.25 mmol, 1.0 equiv) and catalyst **74**[16] (0.015 g, 0.025 mmol, 0.1 equiv) were added sequentially. The reaction contents were then cooled to –78 ºC and stirred for 10 min before benzoyl bromide (0.031 mL, 0.26 mmol, 1.05 equiv) was added. The reaction mixture was then stirred for an additional 30 min at –78 ºC. Upon completion, the contents were quenched by the addition of saturated aqueous $NaHCO_3$ (25 mL), warmed to 23 ºC, poured into a separatory funnel, and extracted with EtOAc (3 × 75 mL). The combined organic extracts were then dried (Na_2SO_4), filtered, and concentrated. The resultant crude material was purified by flash column chromatography (silica gel, hexanes/Et_2O = 1/0→4/1) to yield ***ent*-33a** and **101**-**108**. *Note:* These reactions must be run under strictly anhydrous conditions to avoid hydrolysis of the *N*-acyloxyiminium species. In addition, the enantiomeric excess was determined by chiral HPLC (ChiralPak AD-H, 90:10 hexanes/*i*-PrOH, 1 mL/min, 254 nm).

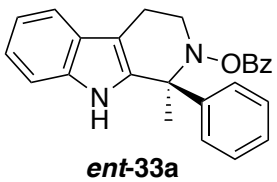

***ent*-33a**

(*S*)-1-methyl-1-phenyl-1,3,4,9-tetrahydro-2*H*-pyrido[3,4-*b*]indol-2-yl benzoate (*ent*-33a). Prepared using the general procedure described above with **32**, ultimately yielding ***ent*-33a** (0.080 g, 83% yield, 82% *ee*) as a white solid. ***ent*-33a**: see above for data; $[\alpha]_D^{25}$ = –24.6º (c = 1.00, CHCl3).

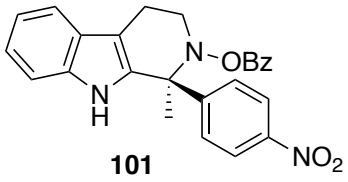

101

(*S*)-1-methyl-1-(4-nitrophenyl)-1,3,4,9-tetrahydro-2*H*-pyrido[3,4-*b*]indol-2-yl benzoate (101). Prepared using the general procedure described above with **S18**, ultimately yielding **101** (0.080 g, 75% yield, 81% *ee*) as a yellow solid. **101**: R_f = 0.38 (silica gel, hexanes/EtOAc = 4/1); $[\alpha]_D^{25}$ = –11.0º (c = 1.00, CHCl3); IR (film) ν_{max} 3370, 1726, 1520, 1450, 1348, 1233, 1058, 1023, 746, 708 cm^{-1}; ^1H NMR (400 MHz, $CDCl_3$) δ 8.13 (d, *J* = 9.1 Hz, 2 H), 7.90 (d, *J* = 8.2 Hz, 2 H), 7.86 (br s, 1 H, exchangeable), 7.69–7.60 (m, 3 H), 7.58–7.51 (m, 1 H), 7.45–7.36 (m, 3 H), 7.31–7.26 (m, 1 H), 7.25–7.19 (m, 1 H), 3.71–3.61 (m, 1 H), 3.32–3.13 (m, 2 H), 2.95–2.82 (m, 1 H), 1.97 (s, 3 H); ^{13}C NMR (101 MHz, $CDCl_3$) δ 165.4, 147.4, 136.4, 133.7, 133.5, 129.6, 129.4, 128.9, 128.7, 126.9, 124.0, 123.5, 122.7, 120.1, 119.0, 111.4, 109.0, 65.7, 48.5, 24.8, 18.5; HRMS (ESI) calcd for $C_{25}H_{22}N_3O_4^+$ $[M + H]^+$ 428.1605, found 428.1604.

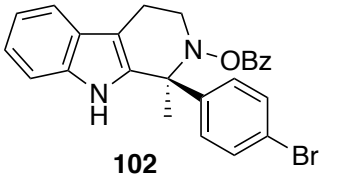

102

(*S*)-1-(4-bromophenyl)-1-methyl-1,3,4,9-tetrahydro-2*H*-pyrido[3,4-*b*]indol-2-yl benzoate (102). Prepared using the general procedure described above with **S45**, ultimately yielding **102** (0.093 g, 80% yield, 80% *ee*) as a white solid. **102**: R_f = 0.58 (silica gel, hexanes/EtOAc = 4/1); $[\alpha]_D^{25}$ = –9.6º (c = 1.00, CHCl3); IR (film) ν_{max} 3361, 1725, 1485, 1450, 1271, 1177, 1059, 1009, 745, 709 cm^{-1}; ^1H NMR (400 MHz, $CDCl_3$) δ 7.90 (d, *J* = 8.1 Hz, 2 H), 7.80 (br s, 1 H, exchangeable), 7.61 (d, *J* = 7.8 Hz, 1 H), 7.57–7.49 (m, 1 H), 7.44–7.34 (m, 5 H), 7.31–7.27 (m, 2 H), 7.25–7.17 (m, 2 H), 3.68–3.56 (m, 1 H), 3.37–3.25 (m, 1 H), 3.21–3.11 (m, 1 H), 2.91–2.78 (m, 1 H), 1.93 (s, 3 H); ^{13}C NMR (101 MHz, $CDCl_3$) δ 165.5, 136.3, 134.6, 133.3, 131.5 (2 C), 129.6, 129.6, 129.1, 128.6, 127.0, 122.4, 122.0, 119.9, 118.9, 111.3, 108.7, 65.5, 48.2, 24.9, 18.5; HRMS (ESI) calcd for $C_{25}H_{22}BrN_2O_2^+$ $[M + H]^+$ 461.0859, found 461.0855.

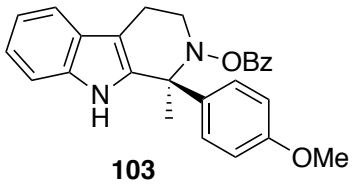

103

(*S*)-1-(4-methoxyphenyl)-1-methyl-1,3,4,9-tetrahydro-2*H*-pyrido[3,4-*b*]indol-2-yl benzoate (103). Prepared using the general procedure described above with **S19**, ultimately yielding **103** (0.079 g, 77% yield, 83% *ee*) as a white solid. **103**: R_f = 0.33 (silica gel, hexanes/EtOAc = 4/1); $[\alpha]_D^{25}$ = –20.8º (c = 1.00, CHCl3); IR (film) ν_{max} 3364, 2934, 1726, 1508, 1451, 1248, 1179, 1024, 745, 710 cm^{-1}; ^1H NMR (400 MHz, $CDCl_3$) δ 7.91 (d, *J* = 8.2 Hz, 2 H), 7.82 (br s, 1 H, exchangeable), 7.61 (d, *J* = 7.5 Hz, 1 H), 7.56–7.49 (m, 1 H), 7.42–7.34 (m, 3 H), 7.32–7.27 (m, 2 H), 7.25–7.16 (m, 2 H), 6.81 (d, *J* = 9.1 Hz, 2 H), 3.77 (s, 3 H), 3.66–3.56 (m, 1 H), 3.42–3.29 (m, 1 H), 3.21–3.11 (m, 1 H), 2.91–2.78 (m, 1 H), 1.94 (s, 3 H); ^{13}C NMR (101 MHz, $CDCl_3$) δ 165.5, 159.1, 136.2, 135.5, 133.1, 129.6 (2 C), 129.4, 129.1, 128.5, 127.1, 122.1, 119.7, 118.7, 113.6, 111.2, 108.4, 65.4, 55.4, 48.0, 25.1, 18.5; HRMS (CI) calcd for $C_{26}H_{25}N_2O_3^+$ $[M + H]^+$ 413.1860, found 413.1860.

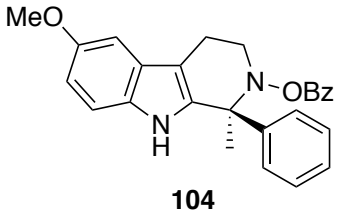

104

(*S*)-6-methoxy-1-methyl-1-phenyl-1,3,4,9-tetrahydro-2*H*-pyrido[3,4-*b*]indol-2-yl benzoate (104). Prepared using the general procedure described above with **S39** in toluene:CH_2Cl_2 (4:1), ultimately yielding **104** (0.083 g, 81% yield, 80% *ee*) as a white solid. **104**: R_f = 0.35 (silica gel, hexanes/EtOAc = 4/1); $[\alpha]_D^{25}$ = –37.0º (c = 1.00, CHCl3); IR (film) ν_{max} 3362, 2936, 1728, 1486, 1451, 1246, 1166, 1062, 1023, 709 cm^{-1}; ^1H NMR (400 MHz, $CDCl_3$) δ 7.90 (d, *J* = 7.1 Hz, 2 H), 7.70 (br s, 1 H, exchangeable), 7.55–7.49 (m, 1 H), 7.41–7.34 (m, 4 H), 7.32–7.24 (m, 4 H), 7.06 (d, *J* = 2.4 Hz, 1 H), 6.90 (dd, *J* = 8.7, 2.4 Hz, 1 H), 3.90 (s, 3 H), 3.66–3.58 (m, 1 H), 3.38–3.27 (m, 1 H), 3.18–3.08 (m, 1 H), 2.86–2.74 (m, 1 H), 1.95 (s, 3 H); ^{13}C NMR (101 MHz, $CDCl_3$) δ 165.5, 154.3, 136.1, 133.2, 131.3, 129.6, 129.3, 128.5, 128.4 (2 C), 127.9 (2 C), 127.5, 112.0,

111.9, 108.4, 100.9, 66.0, 56.1, 48.1, 25.1, 18.5; HRMS (ESI) calcd for $C_{26}H_{25}N_2O_3^+$ $[M + H]^+$ 413.1860, found 413.1861.

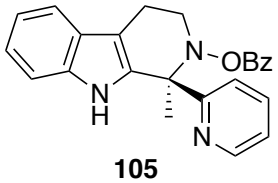

105

(*R*)-1-methyl-1-(pyridin-2-yl)-1,3,4,9-tetrahydro-2*H*-pyrido[3,4-*b*]indol-2-yl benzoate (105). Prepared using the general procedure described above with **S21** in toluene:CH_2Cl_2 (4:1), ultimately yielding **105** (0.069 g, 72% yield, 55% *ee*) as a white solid. **105**: R_f = 0.21 (silica gel, hexanes/EtOAc = 4/1); $[\alpha]_D^{25}$ = +21.2 (c = 1.00, CHCl3); IR (film) ν_{max} 3395, 2991, 2937, 1739, 1588, 1451, 1245, 1058, 737, 709 cm^{-1}; ^1H NMR (400 MHz, $CDCl_3$) δ 8.62–8.55 (m, 1 H), 8.02–7.92 (m, 1 H), 7.91–7.70 (m, 2 H), 7.66–7.58 (m, 1 H), 7.57–7.46 (m, 2 H), 7.43–7.29 (m, 3 H), 7.21–7.06 (m, 4 H), 3.92–3.69 (m, 2 H), 3.22–3.10 (m, 1 H), 3.05–2.94 (m, 1 H), 2.05 (s, 3 H); ^{13}C NMR (101 MHz, $CDCl_3$) δ 165.3, 163.4, 148.5, 137.3, 136.6, 136.3, 133.2, 129.5, 129.2, 128.5, 126.7, 122.3, 121.8, 120.9, 119.4, 118.5, 111.3, 106.6, 67.5, 48.5, 24.0, 19.5; HRMS (ESI) calcd for $C_{24}H_{22}N_3O_2^+$ $[M + H]^+$ 384.1707, found 384.1707.

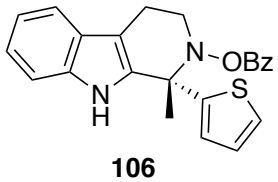

106

(*S*)-1-methyl-1-(thiophen-2-yl)-1,3,4,9-tetrahydro-2*H*-pyrido[3,4-*b*]indol-2-yl benzoate (106). Prepared using the general procedure described above with **S22**, ultimately yielding **106** (0.080 g, 82% yield, -53% *ee*) as a white solid. **106**: R_f = 0.43 (silica gel, hexanes/EtOAc = 4/1); $[\alpha]_D^{25}$ = +11.1° (c = 1.00, CHCl3); IR (film) ν_{max} 3365, 2924, 1730, 1451, 1265, 1177, 1062, 1024, 740, 708 cm^{-1}; ^1H NMR (400 MHz, $CDCl_3$) δ 7.97 (d, *J* = 7.2 Hz, 2 H), 7.78 (br s, 1 H, exchangeable), 7.62–7.51 (m, 2 H), 7.44–7.33 (m, 3 H), 7.31 (d, *J* = 5.4 Hz, 1 H), 7.25–7.13 (m, 2 H), 6.94–6.87 (m, 1 H), 6.79 (s, 1 H), 3.68–3.49 (m, 2 H), 3.25–3.11 (m, 1 H), 3.01–2.91 (m, 1 H), 2.06 (s, 3 H); ^{13}C NMR (101 MHz, $CDCl_3$) δ 165.2, 136.4, 135.1, 133.2, 129.7 (2 C), 129.2, 128.5 (2 C), 126.7, 126.3, 126.2,

122.3, 119.8, 118.8, 111.3, 108.1, 63.9, 48.5, 26.3, 19.4; HRMS (CI) calcd for $C_{23}H_{21}N_2O_2S^+$ [M + H]$^+$ 389.1318, found 389.1317.

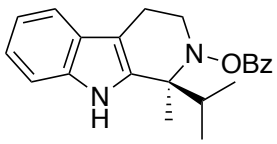

107

(*S*)-1-isopropyl-1-methyl-1,3,4,9-tetrahydro-2*H*-pyrido[3,4-*b*]indol-2-yl benzoate (107). Prepared using the general procedure described above with **S26**, ultimately yielding **107** (0.052 g, 60% yield, 62% *ee*) as a white solid. **107**: R_f = 0.50 (silica gel, hexanes/EtOAc = 4/1); $[\alpha]_D^{25}$ = –30.8º (c = 1.00, CHCl3); IR (film) ν_{max} 3383, 2965, 1724, 1451, 1270, 1089, 1064, 1024, 738, 710 cm^{-1}; ^{1}H NMR (500 MHz, $CDCl_3$) δ 7.96–7.91 (m, 2 H), 7.76 (br s, 1 H, exchangeable), 7.57–7.50 (m, 2 H), 7.43–7.35 (m, 3 H), 7.23–7.18 (m, 1 H), 7.17–7.11 (m, 1 H), 3.75–3.62 (m, 2 H), 3.04–2.96 (m, 1 H), 2.96–2.88 (m, 1 H), 2.18–2.09 (m, 1 H), 1.54 (s, 3 H), 1.16 (d, *J* = 6.8 Hz, 3 H), 1.05 (d, *J* = 6.8 Hz, 3 H); ^{13}C NMR (101 MHz, $CDCl_3$) δ 165.3, 137.4, 136.0, 133.1, 129.6 (2 C), 128.6, 126.9, 121.8, 119.5, 118.5, 110.9, 107.6, 65.5, 48.1, 37.4, 18.9, 18.7, 18.1, 18.0; HRMS (CI) calcd for $C_{22}H_{25}N_2O_2^+$ [M + H]$^+$ 349.1911, found 349.1910.

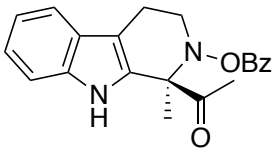

108

(*R*)-1-acetyl-1-methyl-1,3,4,9-tetrahydro-2*H*-pyrido[3,4-*b*]indol-2-yl benzoate (108). Prepared using the general procedure described above with **S31**, ultimately yielding **108** (0.064 g, 74% yield, 16% *ee*) as a white solid. **108**: R_f = 0.38 (silica gel, hexanes/EtOAc = 4/1); $[\alpha]_D^{25}$ = –6.2º (c = 1.00, CHCl3); IR (film) ν_{max} 3378, 2943, 1745, 1631, 1452, 1244, 1057, 1024, 737, 709 cm^{-1}; ^{1}H NMR (400 MHz, $CDCl_3$) δ 8.49 (br s, 1 H, exchangeable), 7.90 (d, *J* = 8.1 Hz, 2 H), 7.60–7.51 (m, 2 H), 7.45–7.35 (m, 3 H), 7.25–7.19 (m, 1 H), 7.17–7.11 (m, 1 H), 3.98–3.85 (m, 1 H), 3.65–3.52 (m, 1 H), 3.21–3.09 (m, 1 H), 2.96–2.83 (m, 1 H), 2.35 (s, 3 H), 1.77 (s, 3 H); ^{13}C NMR (101 MHz, $CDCl_3$) δ 210.0, 164.8, 136.7, 133.7, 132.2, 129.6, 128.7, 128.7, 126.5, 122.5, 119.8, 118.6, 111.5, 108.0, 72.1, 48.4, 24.9, 21.3, 19.0; HRMS (ESI) calcd for $C_{21}H_{21}N_2O_3^+$ [M + H]$^+$ 349.1547, found 349.1546.

Derivatizations of Pictet–Spengler Products.

Scheme 3.11. N–O bond cleavage.

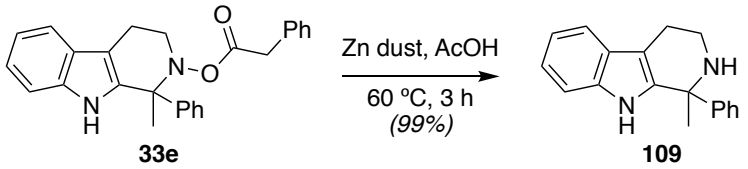

33e **109**

1-methyl-1-phenyl-2,3,4,9-tetrahydro-1*H*-pyrido[3,4-*b*]indole (109).[7,17] To a solution of **33e** (0.041 g, 0.10 mmol, 1.0 equiv) in AcOH (1.5 mL) at 23 ºC was added activated Zn dust (0.101 g, 1.55 mmol, 15.0 equiv) in a microwave tube open to air. The microwave tube was then sealed and the reaction was heated to 60 ºC with stirring for 3 h. Upon completion, the contents were cooled to 23 ºC, filtered through a pad of Celite, washed with MeOH, and concentrated. The crude product was then diluted with CH_2Cl_2 (10 mL) and washed with a 1:1 mixture of aqueous NH_3 (5 mL, 30 wt. %) and saturated aqueous $NaHCO_3$ (5 mL). The remaining aqueous layer was extracted with CH_2Cl_2 (3 × 10 mL). Next, the combined organic extracts were washed with saturated aqueous $NaHCO_3$ (10 mL) and the new aqueous layer was extracted with CH_2Cl_2 (2 × 10 mL). The combined organic extracts were then dried (Na_2SO_4), filtered, and concentrated to yield pure **109** (0.027 g, 99% yield) as a white solid. **109**: R_f = 0.29 (silica gel, CH_2Cl_2/MeOH = 9/1); IR (film) ν_{max} 3404, 1597, 1564, 1449, 1392, 1295, 1121, 858, 744, 700 cm^{-1}; ^1H NMR (400 MHz, $CDCl_3$) δ 7.94 (br s, 1 H, exchangeable), 7.56 (d, *J* = 6.8 Hz, 1 H), 7.32–7.22 (m, 5 H), 7.21–7.10 (m, 2 H), 3.19–3.07 (m, 1 H), 2.95–2.69 (m, 3 H), 1.91 (br s, 1 H, exchangeable), 1.84 (s, 3 H); ^{13}C NMR (101 MHz, $CDCl_3$) δ 146.2, 138.2, 135.8, 128.4, 127.4, 127.4, 127.0, 121.9, 119.5, 118.5, 111.0, 109.7, 57.0, 39.8, 28.3, 22.8; HRMS (ESI) calcd for $C_{18}H_{19}N_2^+$ $[M + H]^+$ 263.1543, found 263.1545.

Scheme 3.12. One-pot N–O bond cleavage and reductive amination.

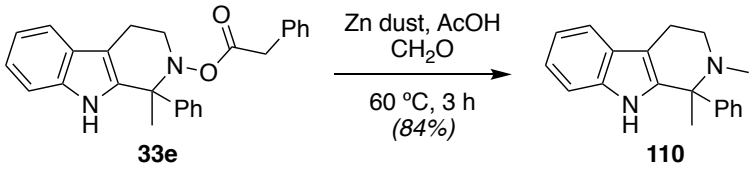

1,2-dimethyl-1-phenyl-2,3,4,9-tetrahydro-1*H*-pyrido[3,4-*b*]indole (110).[7,18] To a solution of **33e** (0.041 g, 0.10 mmol, 1.0 equiv) in AcOH (1.5 mL) at 23 ºC sequentially added CH_2O (0.050 mL, 37 wt. % in H_2O, 0.62 mmol, 6.0 equiv) and activated Zn powder (0.101 g, 1.55 mmol, 15.0 equiv) in a microwave tube open to air. The microwave tube was then sealed and the reaction was heated to 60 ºC with stirring for 3 h. Upon completion, the contents were cooled to 23 ºC, filtered through a pad of Celite, washed with MeOH, and concentrated. The crude product was then diluted with CH_2Cl_2 (10 mL) and washed with a 1:1 mixture of aqueous NH_3 (5 mL, 30 wt. %) and saturated aqueous $NaHCO_3$ (5 mL). The remaining aqueous layer was extracted with CH_2Cl_2 (3 × 10 mL). Next, the combined organic extracts were washed with saturated aqueous $NaHCO_3$ (10 mL) and the new aqueous layer was extracted with CH_2Cl_2 (2 × 10 mL). The combined organic extracts were then dried (Na_2SO_4), filtered, and concentrated to yield pure **110** (0.024 g, 84% yield) as a yellow solid. **110**: R_f = 0.44 (silica gel, CH_2Cl_2/MeOH = 9/1); IR (film) ν_{max} 3412, 2942, 1447, 1297, 1251, 1179, 1026, 909, 741, 702 cm^{-1}; ^1H NMR (500 MHz, $CDCl_3$) δ 7.57–7.53 (m, 1 H), 7.45–7.40 (m, 2 H), 7.34–7.29 (m, 3 H), 7.29–7.24 (m, 1 H), 7.22–7.19 (m, 1 H), 7.16–7.09 (m, 2 H), 3.04–2.94 (m, 3 H), 2.94–2.86 (m, 1 H), 2.27 (s, 3 H), 1.79 (s, 3 H); ^{13}C NMR (101 MHz, $CDCl_3$) δ 144.5, 139.4, 136.3, 128.2, 127.9, 127.4, 127.2, 121.6, 119.4, 118.5, 110.9, 108.3, 61.0, 47.9, 37.7, 21.2, 19.3; HRMS (ESI) calcd for $C_{19}H_{21}N_2^+$ $[M + H]^+$ 277.1699, found 277.1698.

Scheme 3.13. Copper-catalyzed electrophilic amination with a diorganozinc reagent.

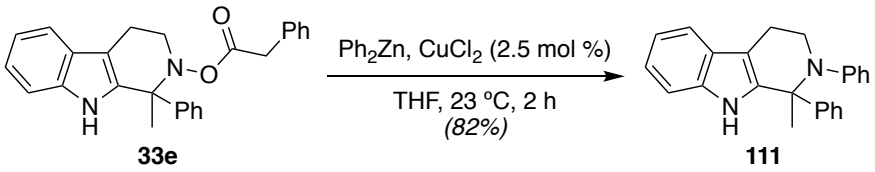

1-methyl-1,2-diphenyl-2,3,4,9-tetrahydro-1*H*-pyrido[3,4-*b*]indole (111).[19a] To a solution of PhMgBr (1.0 M in THF, 1.50 mL, 1.5 mmol, 1.0 equiv) in THF (1.5 mL) at 0 ºC was added a freshly prepared solution of $ZnCl_2$ (1.0 M in THF, 0.75 mL, 0.75 mmol, 0.5 equiv) under an argon atmosphere. The resultant mixture warmed to 23 ºC and stirred for 15 min. Upon completion, the diorganozinc reagent was titrated using iodine to determine the concentration (here as 0.19 M).[19c] Then, the freshly prepared solution of Ph_2Zn (0.19 M, 0.73 mL, 0.14 mmol, 1.1 equiv) was added to a solution of **33e** (0.050 g, 0.13 mmol, 1.0 equiv) and $CuCl_2$ (0.4 mg, 0.003 mmol, 0.025 equiv) in THF (1.0 mL) at 23 ºC under an argon atmosphere. The resultant mixture was stirred at 23 ºC for 2 h. Upon completion, the contents were quenched with saturated aqueous $NaHCO_3$ (5 mL), poured into a separatory funnel, and extracted with EtOAc (3 × 5 mL). The combined organic extracts were then dried (Na_2SO_4), filtered, and concentrated. The resultant crude material was purified by flash column chromatography (silica gel, hexanes/EtOAc = 1/0→4/1) to yield **111** (0.035 g, 82% yield) as a white solid. **111**: R_f = 0.74 (silica gel, hexanes/EtOAc = 4/1); IR (film) ν_{max} 3413, 2909, 1594, 1490, 1449, 1288, 1231, 908, 739, 701 cm^{-1}; ^1H NMR (500 MHz, $CDCl_3$) δ 7.65–7.57 (m, 1 H), 7.40 (br s, 1 H, exchangeable), 7.29–7.19 (m, 6 H), 7.19–7.08 (m, 4 H), 7.03 (t, *J* = 7.3 Hz, 1 H), 6.75 (d, *J* = 7.8 Hz, 2 H), 3.55 (t, *J* = 6.0 Hz, 2 H), 3.10–2.96 (m, 2 H), 1.80 (s, 3 H); ^{13}C NMR (101 MHz, $CDCl_3$) δ 149.5, 145.0, 139.8, 136.4, 128.8, 128.2, 128.0, 127.4, 127.1, 126.8, 123.9, 121.8, 119.5, 118.5, 111.0, 109.2, 62.1, 47.4, 22.3, 22.2; HRMS (ESI) calcd for $C_{24}H_{23}N_2^+$ $[M + H]^+$ 339.1856, found 339.1869.

Scheme 3.14. Deprotection of acetyl group.

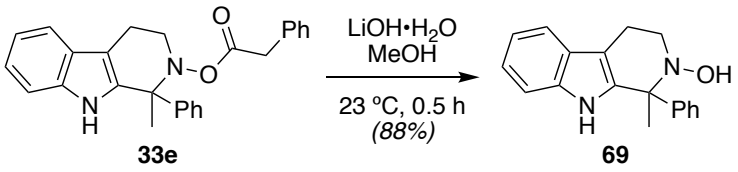

1-methyl-1-phenyl-1,3,4,9-tetrahydro-2*H*-pyrido[3,4-*b*]indol-2-ol (69).[20] To a solution of **33e** (0.100 g, 0.25 mmol, 1.0 equiv) in MeOH (2.0 mL) at 23 ºC was added LiOH•H_2O (0.012 mg, 0.28 mmol, 1.1 equiv) open to air. The resultant mixture was stirred at 23 ºC for 30 min, during which time the product crashed out as a white precipitate. Upon completion, the reaction contents were concentrated directly and then diluted with CH_2Cl_2/MeOH (9/1, 10 mL). Deionized H_2O (5 mL) was then added, the contents were poured into a separatory funnel, and the product was extracted with CH_2Cl_2/MeOH (9/1, 3 × 10 mL). The combined organic extracts were then dried (Na_2SO_4), filtered, and concentrated. The resultant crude material was purified by flash column chromatography (silica gel, hexanes/EtOAc = 1/0→2/1) or recrystallization (CH_2Cl_2) to yield **69** (0.062 mg, 88% yield) as a white solid. **69**: R_f = 0.59 (silica gel, CH_2Cl_2/MeOH = 9/1); IR (film) ν_{max} 3410, 1597, 1564, 1449, 1393, 1232, 858, 799, 735, 700 cm^{-1}; ^1H NMR (500 MHz, DMSO-d_6) δ 10.75 (br s, 1 H, exchangeable), 7.94 (br s, 1 H, exchangeable), 7.42 (d, J = 7.7 Hz, 1 H), 7.32–7.23 (m, 3 H), 7.22–7.12 (m, 3 H), 7.07–7.01 (m, 1 H), 7.00–6.94 (m, 1 H), 3.21–3.05 (m, 1 H), 2.99–2.84 (m, 2 H), 2.66–2.52 (m, 1 H), 1.81 (s, 3 H); ^{13}C NMR (101 MHz, DMSO-d_6) δ 137.3, 136.2, 127.8, 127.5, 127.1, 126.7, 126.3, 120.6, 118.3, 117.8, 111.0, 106.3, 64.6, 49.0, 24.1, 18.4; HRMS (ESI) calcd for $C_{18}H_{19}N_2O^+$ $[M + H]^+$ 279.1492, found 279.1495.

Scheme 3.15. Oxidation of hydroxylamine to aldonitrone.

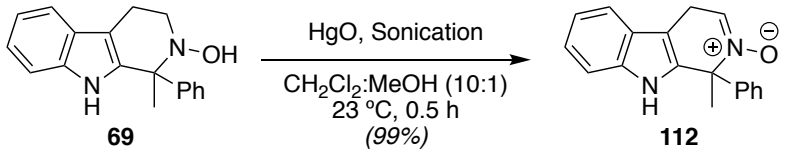

69 112

1-methyl-1-phenyl-4,9-dihydro-1*H*-pyrido[3,4-*b*]indole 2-oxide (112).[21] To a solution of **69** (0.042 g, 0.15 mmol, 1.0 equiv) in CH_2Cl_2/MeOH (10/1, 1.5 mL) at 23 ºC was added yellow HgO (0.098 g, 0.44 mmol, 3.0 equiv) under an argon atmosphere. The reaction contents were then sonicated for 0.5 h. Upon completion, $MgSO_4$ (0.055 g, 0.45 mmol, 3.0 equiv) was added and the reaction contents were stirred for an additional 10 min. The resulting grey heterogeneous mixture was filtered through a pad of Celite with a layer of $MgSO_4$ on top, washed with CH_2Cl_2 (15 mL), and then concentrated to afford nitrone **112** (0.041 g, 99% yield) as a yellow solid that was carried forward without further purification. **112**: ^{1}H NMR (500 MHz, $CDCl_3$) δ 7.60 (s, 1 H), 7.57 (d, *J* = 7.6 Hz, 1 H), 7.49–7.45 (m, 1 H), 7.43–7.38 (m, 2 H), 7.37–7.31 (m, 3 H), 7.30–7.27 (m, 1 H), 7.25–7.16 (m, 2 H), 4.01–3.87 (m, 2 H), 2.35 (s, 3 H).

Scheme 3.16. Grignard reaction.

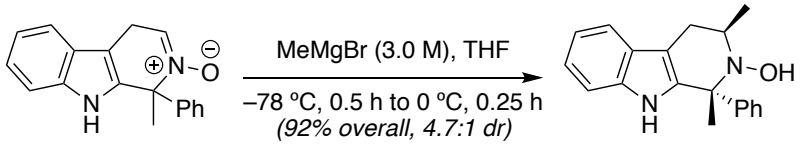

112 (±)-113

To a solution of **112** (0.041 g, 0.15 mmol, 1.0 equiv) in THF (3.0 mL) at –78 ºC was added dropwise MeMgBr (3.0 M in Et_2O, 0.49 mL, 1.49 mmol, 10 equiv) over the course of 15 min under an argon atmosphere. The resultant mixture was then stirred at –78 ºC for an additional 30 min before being warmed to 0 ºC and stirred for 15 min. Upon completion, the reaction contents were quenched with saturated aqueous NH_4Cl (5 mL) and extracted with EtOAc (3 × 5 mL). The

combined organic extracts were then dried (Na_2SO_4), filtered, and concentrated. The resultant crude material was purified by flash column chromatography (silica gel, hexanes/EtOAc = 1/0→3/1) to yield **113a** (0.033 g, 76% yield) and **113b** (0.007 g, 16% yield) as white solids (0.040 g combined, 92% yield overall, 4.7:1 *dr*).[23]

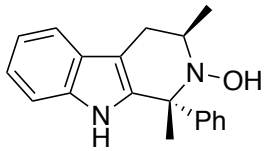

(±)-113a

(±)-(1*R*,3*R*)-1,3-dimethyl-1-phenyl-1,3,4,9-tetrahydro-2*H*-pyrido[3,4-*b*]indol-2-ol (113a): R_f = 0.25 (silica gel, hexanes/EtOAc = 4/1); IR (film) ν_{max} 3410, 2975, 2932, 1449, 1299, 1234, 1184, 910, 738, 700 cm^{-1}; ^1H NMR (500 MHz, $CDCl_3$) δ 7.89 (br s, 1 H, exchangeable), 7.56 (d, *J* = 7.8 Hz, 1 H), 7.39 (d, *J* = 8.1 Hz, 1 H), 7.26–7.18 (m, 6 H), 7.18–7.13 (m, 1 H), 4.52 (br s, 1 H, exchangeable), 3.20–3.09 (m, 1 H), 2.85–2.77 (m, 1 H), 2.70–2.56 (m, 1 H), 1.94 (s, 3 H), 1.26 (d, *J* = 6.6 Hz, 3 H); ^{13}C NMR (101 MHz, $CDCl_3$) δ 136.6, 133.7, 128.4, 127.8, 127.4, 127.3, 126.9, 122.2, 119.8, 118.8, 111.2, 109.1, 67.4, 52.7, 29.8, 26.1, 19.5; HRMS (ESI) calcd for $C_{19}H_{21}N_2O^+$ $[M + H]^+$ 293.1648, found 293.1658.

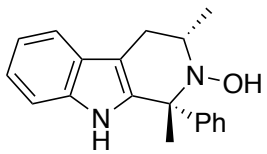

(±)-113b

(±)-(1*R*,3*S*)-1,3-dimethyl-1-phenyl-1,3,4,9-tetrahydro-2*H*-pyrido[3,4-*b*]indol-2-ol (113b): R_f = 0.37 (silica gel, hexanes/EtOAc = 4/1); IR (film) ν_{max} 3532, 3399, 2928, 1452, 1374, 1303, 1238, 908, 734, 701 cm^{-1}; ^1H NMR (500 MHz, $CDCl_3$) δ 7.56–7.47 (m, 3 H), 7.36–7.28 (m, 3 H), 7.25–7.15 (m, 2 H), 7.14–7.07 (m, 2 H), 4.48 (br s, 1 H, exchangeable), 3.63–3.52 (m, 1 H), 2.99–2.89 (m, 1 H), 2.85–2.76 (m, 1 H), 1.90 (s, 3 H), 1.43 (d, *J* = 6.1 Hz, 3 H); ^{13}C NMR (101 MHz, $CDCl_3$) δ 144.5, 138.9, 136.5, 130.6, 128.4, 127.6, 126.7, 121.7, 119.5, 118.5, 111.0, 107.3, 66.1, 53.5, 29.9, 29.3, 20.5; HRMS (ESI) calcd for $C_{19}H_{21}N_2O^+$ $[M + H]^+$ 293.1648, found 293.1648.

Scheme 3.17. Strecker-type reaction.

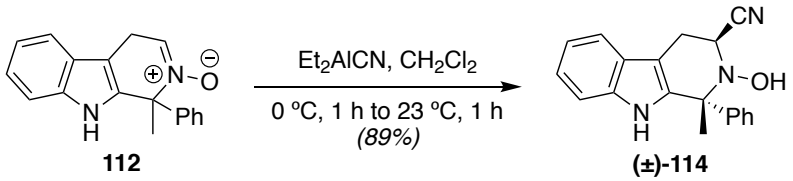

(±)-(1*R*,3*S*)-2-hydroxy-1-methyl-1-phenyl-2,3,4,9-tetrahydro-1*H*-pyrido[3,4-*b*]indole-3-carbonitrile (114).[24] To a solution of **112** (0.041 g, 0.15 mmol, 1.0 equiv) in CH_2Cl_2 (3.0 mL) at 0 ºC was added Et_2AlCN (1.0 M in toluene, 0.45 mL, 0.45 mmol, 3.0 equiv) under an argon atmosphere. The resultant mixture was stirred at 0 ºC for 1 h and then warmed to 23 ºC and stirred for an additional 1 h. Upon completion, the reaction contents were quenched with saturated aqueous $NaHCO_3$ (5 mL), poured into a separatory funnel, and extracted with CH_2Cl_2 (3 × 5 mL). The combined organic extracts were then dried (Na_2SO_4), filtered, and concentrated. The resultant crude material was purified by flash column chromatography (silica gel, hexanes/EtOAc = 1/0→3/1) to yield **114** (0.40 mg, 89% yield) as a white solid. **114**: R_f = 0.24 (silica gel, hexanes/EtOAc = 4/1); IR (film) ν_{max} 3404, 3058, 2920, 2258, 1453, 1300, 1183, 1028, 739, 701 cm^{-1}; ^1H NMR (500 MHz, $CDCl_3$) δ 7.93 (br s, 1 H, exchangeable), 7.56 (d, *J* = 7.9 Hz, 1 H), 7.40 (d, *J* = 8.1 Hz, 1 H), 7.30–7.26 (m, 3 H), 7.26–7.23 (m, 1 H), 7.21–7.12 (m, 3 H), 5.26 (br s, 1 H, exchangeable), 4.09–4.00 (m, 1 H), 3.57–3.47 (m, 1 H), 3.06–2.97 (m, 1 H), 1.96 (s, 3 H); ^{13}C NMR (101 MHz, $CDCl_3$) δ 136.2, 133.6, 128.7, 128.4, 127.3, 127.1, 126.4, 122.7, 120.3, 119.7, 118.7, 111.3, 106.2, 66.3, 50.2, 25.6, 22.1; HRMS (ESI) calcd for $C_{19}H_{18}N_3O^+$ $[M + H]^+$ 304.1444, found 304.1454.

Scheme 3.18. [3+2] cycloaddition.

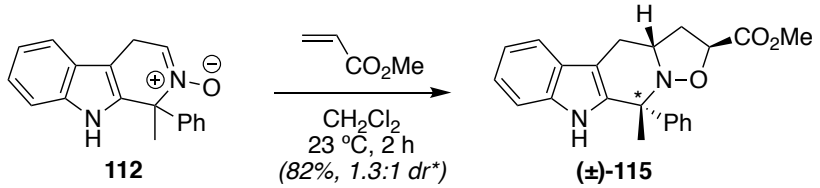

112 **(±)-115**

To a solution of **112** (0.041 g, 0.15 mmol, 1.0 equiv) in CH_2Cl_2 (3.0 mL) at 23 ºC was added methyl acrylate (0.13 mL, 1.5 mmol, 10 equiv) under an argon atmosphere and stirred for 2 h. Upon completion, the reaction contents were quenched with saturated aqueous $NaHCO_3$ (5 mL) and extracted with CH_2Cl_2 (3 × 5 mL). The combined organic extracts were then dried (Na_2SO_4), filtered, and concentrated. The resultant crude material was purified by preparative thin layer chromatography (silica gel, CH_2Cl_2/MeOH = 15/1) to yield **115a** (0.025 mg, 46% yield) and **115b** (0.019 mg, 35% yield) as yellow solids (0.044 mg combined, 82% yield overall, 1.3:1 *dr*).[25]

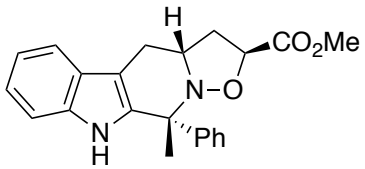

(±)-115a

(±)-methyl (2*S*,3a*R*,10*R*)-10-methyl-10-phenyl-2,3,3a,4,9,10-hexahydroisoxazolo[2',3':1,6]pyrido[3,4-*b*]indole-2-carboxylate (115a): R_f = 0.32 (silica gel, hexanes/EtOAc = 4/1); IR (film) ν_{max} 3386, 2924, 1741, 1454, 1373, 1213, 1102, 1028, 742, 703 cm^{-1}; ^1H NMR (500 MHz, $CDCl_3$) δ 7.61–7.54 (m, 2 H), 7.52–7.46 (m, 1 H), 7.38–7.26 (m, 4 H), 7.21–7.17 (m, 1 H), 7.16–7.07 (m, 2 H), 4.61 (dd, *J* = 8.0, 5.4 Hz, 1 H), 3.76 (s, 3 H), 3.65–3.56 (m, 1 H), 3.23–3.14 (m, 1 H), 2.89–2.79 (m, 1 H), 2.63–2.56 (m, 2 H), 1.99 (s, 3 H); ^{13}C NMR (101 MHz, $CDCl_3$) δ 172.3, 143.9, 139.6, 136.9, 128.6, 127.8, 127.5, 126.4, 122.0, 119.7, 118.4, 111.2, 107.8, 74.4, 64.7, 55.7, 52.3, 38.9, 26.1, 17.6; HRMS (ESI) calcd for $C_{22}H_{23}N_2O_3^+$ $[M + H]^+$ 363.1703, found 363.1717.

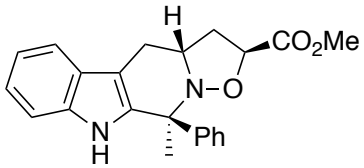

(±)-115b

(±)-methyl (2*S*,3a*R*,10*S*)-10-methyl-10-phenyl-2,3,3a,4,9,10-hexahydroisoxazolo[2',3':1,6]pyrido[3,4-*b*]indole-2-carboxylate (115b): R_f = 0.26 (silica gel, hexanes/EtOAc = 4/1); IR (film) ν_{max} 3373, 2924, 1738, 1453, 1376, 1210, 1103, 1029, 741, 700 cm^{-1}; ^1H NMR (500 MHz, $CDCl_3$) δ 7.75 (br s, 1 H, exchangeable), 7.54 (d, *J* = 8.7 Hz, 1 H), 7.34 (d, *J* = 7.9 Hz, 1 H), 7.26–7.11 (m, 7 H), 4.62 (dd, *J* = 9.2, 4.0 Hz, 1 H), 3.52 (s, 3 H), 3.22–3.01 (m, 2 H), 2.81–2.71 (m, 1 H), 2.52–2.36 (m, 2 H), 2.09 (s, 3 H); ^{13}C NMR (101 MHz, $CDCl_3$) δ 171.6, 137.0, 136.5, 130.1, 130.0, 127.7, 127.3, 126.4, 122.2, 119.9, 118.6, 111.3, 109.3, 74.4, 64.9, 55.0, 52.2, 38.4, 26.0, 25.2; HRMS (ESI) calcd for $C_{22}H_{23}N_2O_3^+$ $[M + H]^+$ 363.1703, found 363.1714.

3.8 References

[1] For selected reviews on β-carbolines and their syntheses, see: (a) *The Alkaloids, Chemistry and Physiology* (Ed.: Manske, R. H. F.), Academic Press, New York, *vol. XX*, **1981**; (b) Love, B. E. *Org. Prep. Proced. Int.* **1996**, *28*, 1; (c) Grate, J. W.; Frye, G. C. in *Sensors Update* (Ed.: Baltes, H.; Gopel, W.; Hesse, J.), Wiley-VCH, Weinheim, *vol. 2*, **1996**, p. 10; (d) Hesse, M. in *Alkaloids: Nature's Curse or Blessing* Wiley-VCH, Zürich, Switzerland, **2002**, p. 14; (e) Cao, R. H.; Peng, W. L.; Wang, Z. H.; Xu, A. L. *Curr. Med. Chem.* **2007**, *14*, 479; (f) Dai, J. K.; Dan, W. J.; Schneider, U.; Wang, J. R. *Eur. J. Med. Chem.* **2018**, *157*, 622; (g) Maity, P.; Adhikari, D.; Jana, A. K. *Tetrahedron* **2019**, *75*, 965.

[2] (a) Pictet, A.; Spengler, T. *Ber. Dtsch. Chem. Ges.* **1911**, *44*, 2030; (b) Tatsui, G. *Yakugaku Zasshi* **1928**, *48*, 453.

[3] For selected reviews on the Pictet–Spengler reaction, see: (a) Cox, E. D.; Cook, J. M. *Chem. Rev.* **1995**, *95*, 1797; (b) Stöckigt, J; Antonchick, A, P.; Wu, F.; Waldmann, H. *Angew. Chem. Int. Ed.* **2011**, *50*, 8538; (c) Dalpozzo, R. *Molecules* **2016**, *21*, 69.

[4] For examples based on thioureas, see: (a) Taylor, M. S.; Jacobsen, E. N. *J. Am. Chem. Soc.* **2004**, *126*, 10558; (b) Raheem, I. T.; Thiara, P. S.; Peterson, E. A.; Jacobsen, E. N. *J. Am. Chem. Soc.* **2007**, *129*, 13404; (c) Klausen, R. S.; Jacobsen, E. N. *Org. Lett.* **2009**, *11*, 887; (d) Mittal, N.; Sun, D. X.; Seidel, D. *Org. Lett.* **2014**, *16*, 1012; (e) Klausen, R. S.; Kennedy, C. R.; Hyde, A. M.; Jacobsen, E. N. *J. Am. Chem. Soc.* **2017**, *139*, 12299. For examples based on phosphoric acids, see: (f) Seayad, J.; Seayad, A. M.; List, B. *J. Am. Chem. Soc.* **2006**, *128*, 1086; (g) Wanner, M. J.; van der Haas, R. N.; de Cuba, K. R.; van Maarseveen, J. H.; Hiemstra, H. *Angew. Chem. Int. Ed.* **2007**, *46*, 7485; (h) Sewgobind, N. V.; Wanner, M. J.; Ingemann, S.; de Gelder, R.; van Maarseveen, J. H.; Hiemstra, H. *J. Org. Chem.* **2008**, *73*, 6405; (i) Muratore, M. E.; Holloway, C. A.; Pilling, A. W.; Storer, R. I.; Trevitt, G.; Dixon, D.-J. *J. Am. Chem. Soc.* **2009**, *131*, 10796; (j) Holloway, C.-A.; Muratore, M. E.; Storer, R. I.; Dixon, D. J. *Org. Lett.* **2010**, *12*, 4720; (k) Huang, D.; Xu, F.; Lin, X.; Wang, Y. *Chem.–Eur. J.* **2012**, *18*, 3148; (l) Wang, S.-G.; Xia, Z.-L.; Xu, R.-Q.; Liu, X.-J.; Zheng, C.; You, S.-L. *Angew. Chem. Int. Ed.* **2017**, *56*, 7440. For an additional case using gold under non-hydrogen bonding catalysis, see: (m) Glinsky-Olivier, N.; Yang, S.; Retailleau, P.; Gandon, V.; Guinchard, X. *Org. Lett.* **2019**, *21*, 9446.

[5] For the isolation or discovery of **1**-**4**, see: (a) Kobayashi, J.; Sekiguchi, M.; Shimamoto, S.; Shigemori, H.; Ishiyama, H.; Ohsaki, H. *J. Org. Chem.* **2002**, *67*, 6449; (b) Feng, T.; Duan, K.-T.; He, S.-J; Wu, B.; Zheng, Y.-S.; Ai, H.-L.; Li, Z.-H.; He, J.; Zuo, J.-P.; Liu, J.-K. *Org. Lett.* **2018**, *20*, 7926; (c) Yeung, B. K. S.; Zou, B.; Rottmann, M.; Lakshminarayana, S. B.; Ang, S. H.; Leong, S. Y.; Tan, J.; Wong, J.; Keller-Maerki, S.; Fischli, C.; Goh, A.; Schmitt, E. K.; Krastel, P.; Francotte, E.; Kuhen, K.; Plouffe, D.; Henson, K.; Wagner, T.; Winzeler, E. A.; Petersen, F.; Brun, R.; Dartois, V.; Diagana, T. T.; Keller, T. H. *J. Med. Chem.* **2010**, *53*, 5155; (d) Rottmann, M.; McNamara, C.; Yeung, B. K. S.; Lee, M. C. S.; Zou, B.; Russell, B.; Seitz, P.; Plouffe, D. M.; Dharia, N. V.; Tan, J.; Cohen, S. B.; Spencer, K. R.; González-Páez, G. E.; Lakshminarayana, S. B.; Goh, A.; Suwanarusk, R.; Jegla, T.; Schmitt, E. K.; Beck, H.-P.; Brun, R.; Nosten, F.; Renia, L.; Dartois, V.; Keller, T. H.; Fidock, D. A.; Winzeler, E. A.; Diagana, T. T. *Science* **2010**, *329*, 1175; (e) Wong, S.-P.; Chone, K.-W.; Lim, K.-H.; Lime, S.-H.; Low, Y.-Y.; Kam, T.-S. *Org. Lett.* **2016**, *18*, 1618. For total syntheses of **1** and **4**, see: (f) Liu, Y.; Luo, S.; Fu, X.; Fang, F.; Zhuang, Z.; Xiong, W.; Jia, X.; Zhai, H. *Org. Lett*. **2006**, *8*, 115; (g) Suzuki, K.; Takayama, H. *Org. Lett.* **2006**,

8, 4605; (h) Zhou, Z.; Gao, A. X.; Snyder, S. A. *J. Am. Chem. Soc.* **2019**, *141*, 7715; (i) Andres, R.; Wang, Q.; Zhu, J. *J. Am. Chem. Soc.* **2020**, *142*, 14726.

[6] For selected, racemic versions to access aza-quaternary centers within tetrahydro-β-carbolines, see: (a) Hester, J. B. *J. Org. Chem.* **1964**, *29*, 2864; (b) Mayer, J. P.; Davis, D. B.; Zhang, J.; Beaton, G.; Bjergarde, K.; Andersen, C. M.; Goodman, B. A.; Herrera, C. J. *Tetrahedron Lett.* **1996**, *37*, 5633; (c) Horiguchi, Y.; Nakamura, M.; Saitoh, T.; Sano, T. *Chem. Pharm. Bull.* **2003**, *51*, 1368; (d) Kuo, F.-M.; Tseng, M.-C.; Yen, Y.-H.; Chu, Y.-H. *Tetrahedron* **2004**, *60*, 12075; (e) Lingam, Y.; Rao, D. M.; Bhowmik, D. R.; Santu, P. S.; Rao, K. R.; Islam, A. *Tetrahedron Lett*. **2007**, *48*, 7243; (f) Mumford, P. M.; Shiers, J. J.; Tarver, G. J.; Hayes, J. F.; Shipman, M. *Tetrahedron Lett.* **2008**, *49*, 3489; (g) Ryabukhin, S. V.; Panov, D. M.; Plaskon, A. S.; Tolmachev, A. A.; Smaliy, R. V. *Monatsh. Chem.* **2012**, *143*, 1507; (h) Wang, L.-N.; Shen, S.-L.; Qu, J. *RSC Adv.* **2014**, *4*, 30733; (i) Riesco-Domínguez, A.; van der Zwaluw, N.; Blanco-Ania, D.; Rutjes, F. P. J. T. *Eur. J. Org. Chem.* **2017**, 662; (j) Wang, Z.; Niu, J.; Zeng, H.; Li, C.-J. *Org. Lett.* **2019**, *21*, 7033. For enantioselective variants, see: (k) Bou-Hamdan, F. R.; Leighton, J. L. *Angew. Chem. Int. Ed.* **2009**, *48*, 2403; (l) Badillo, J. J.; Silva-Garcia, A.; Shupe, B. H.; Fettinger J. C.; Franz, A. K. *Tetrahedron Lett.* **2011**, *52*, 5550; (m) Duce, A.; Pesciaioli, F.; Gramigna, L.; Bernardi, L.; Mazzanti, A.; Ricci, A.; Bartoli, G.; Bencivenni, G. *Adv. Synth. Catal.* **2011**, *353*, 860; (n) Dai, W.; Lu, H.; Li, X.; Shi, F.; Tu, S. J. *Chem.–Eur. J.* **2014**, *20*, 11382; (o) Piemontesi, C.; Wang, Q.; Zhu, J. *J. Am. Chem. Soc.* **2016**, *138*, 11148.

[7] Lisnyak, V. G.; Lynch-Colameta, T.; Snyder, S. A. *Angew. Chem. Int. Ed.* **2018**, *57*, 15162.

[8] For selected racemic versions, see: (a) Han, S.-Y.; Lakshmikantham, M. V.; Cava, M. P. *Heterocycles*, **1985**, *23*, 1671; (b) Plate, R.; Van Hout, R. H. M.; Behm, H.; Ottenheijm, H. C. J. *J. Org. Chem.* **1987**, *52*, 555; (c) Sandrin, J.; Hollinshead, S. P.; Cook, J. M. *J. Org. Chem.* **1989**, *54*, 5636; (d) Still, I. W. J.; Strautmanis, J. R. *Can. J. Chem.* **1990**, *68*, 1408; (e) Hermkens, P. H. H.; van Maarseveen, J. H.; Cobben, P. L. H. M.; Ottenheijm, H. C. J.; Kruse, C. G.; Scheeren, H. W. *Tetrahedron* **1990**, *46*, 833; (f) Hino, T.; Hasegawa, A.; Liu, J.-J.; Nakagawa M. *Chem. Pharm. Bull.* **1990**, *38*, 59; (g) Liu, J.; Nakagawa, M.; Ogata, K.; Hino, T.; *Chem. Pharm. Bull.* **1991**, *39*, 1672; (h) Tsuji, R.; Yamanaka, M.; Nishida, A.; Nakagawa, M. *Chem. Lett.* **2002**, *428*. For enantioselective versions, see: (i) Kawate, T.; Yamada, H.; Soe, T.; Nakagawa, M. *Tetrahedron: Asymmetry* **1996**, *7*, 1249; (j) Kawate, T.; Yamada, H.; Matsumizu, M.; Nishida, A.; Nakagawa, M. *Synlett* **1997**, 1761; (k) Yamada, H.; Kawate, T.; Matsumizu, M.; Nishida, A.; Yamaguchi, K.; Nakagawa, M. *J. Org. Chem.* **1998**, *63*, 6348. For a review, see: (l) Hino, T.; Nakagawa, M. *Heterocycles* **1998**, *49*, 499.

[9] (a) Heine, H. W.; Zibuck, R.; VandenHeuvel, W. J. A. *J. Am. Chem. Soc.* **1982**, *104*, 3691; (b) Kawakami, T.; Ohtake, H.; Arakawa, H.; Okachi, T.; Imada, Y.; Murahashi, S.-I. *Org. Lett.* **1999**, *1*, 107; (c) Kawakami, T.; Ohtake, H.; Arakawa, H.; Okachi, T.; Imada, Y.; Murahashi, S.-I. *Chem. Lett.* **1999**, 795; (d) Kawakami, T.; Ohtake, H.; Arakawa, H.; Okachi, T.; Imada, Y.; Murahashi, S.-I. *Bull. Chem. Soc. Jpn.* **2000**, *73*, 2423.

[10] Kerkouvius, J. K.; Kerr, M. A. *J. Am. Chem. Soc.* **2018**, *140*, 8415.

[11] Winter, C.; Krause, N. *Angew. Chem. Int. Ed.* **2009**, *48*, 6339.

[12] Teruhiko, I.; Keita, N.; Senzaki, M.; Tatsukawa, A.; Saito, S. *Tetrahedron* **1998**, *54*, 2433.

[13] (a) Rodríguez, J. G.; Gil-Lopetegui, P. *Heterocycl. Chem.* **1993**, *30*, 373; (b) Horiguchi, Y.; Nakamura, M.; Kida, A.; Kodama, H.; Saitoh, T.; Sano, T. *Heterocycles* **2003**, *59*, 691; (c)

Murai, K.; Kobayashi, T.; Miyoshi, M.; Fujioka, H. *Org. Lett.* **2018**, *20*, 2333; (d) Zeng, H.; Wang, Z.; Li, C.-J. *Angew. Chem. Int. Ed.* **2019**, *58*, 2859.
[14] (a) Viti, F.; Bellinvia, S.; Demartis, S. WO2015/197861A1, **2015**; (b) Chen, Y.; Yihua, L.; Luo, J.; Zhang, Y.; Zheng, C.; Tong, W.; Liu, M. CN102977091B, **2016**.
[15] For selected, recent reviews, see: (a) Takemoto, Y. *Org. Biomol. Chem.* **2005**, *3*, 4299; (b) Zhang, Z.; Schreiner, P. R. *Chem. Soc. Rev.* **2009**, *38*, 1187; (c) Siau, W.-Y.; Wang, J. *Catal. Sci. Technol.* **2011**, *1*, 1298; (d) Serdyuk, O. V.; Heckel, C. M.; Tsogoeva, S. B. *Org. Biomol. Chem.* **2013**, *11*, 7051; (e) Brak, K.; Jacobsen, E. N. *Angew. Chem. Int. Ed.* **2013**, *52*, 534; (f) Fang, X.; Wang, C.-J. *Chem. Commun.* **2015**, *51*, 1185.
[16] Jacobsen, E. N.; Zuend, S. J. *US Pat.* 2013/66109A1, **2013**.
[17] King, G. S.; Magnus, P. D.; Rzepa, H. S. *J. Chem. Soc., Perkin Trans. 1* **1972**, 437.
[18] da Silva, R. A.; Estevam, I. H. S.; Bieber, L. W. *Tetrahedron Lett.* **2007**, *48*, 7680.
[19] (a) Berman, A. M.; Johnson, J. S. *J. Am. Chem. Soc.* **2004**, *126*, 5680; (b) Graßl, S.; Chen, Y.-H.; Hamze, C.; Tüllmann, C. P.; Knochel, P. *Org. Lett.* **2019**, *21*, 494; (c) Krasovskiy, A.; Knochel, P. *Synthesis* **2006**, 890.
[20] Banerjee, A.; Yamamoto, H. *Chem. Sci.* **2019**, *10*, 2124.
[21] (a) Gössinger, E. *Tetrahedron Lett.* **1980**, *21*, 2229; (b) Cicchi, S.; Goti, A.; Brandi, A. *J. Org. Chem.* **1995**, *60*, 4743.
[22] See Chapter 1. For general reviews about nucleophilic additions to nitrones, see: (a) Lombardo, M.; Trombini, C. *Synthesis* **2000**, *6*, 759; (b) Merino, P.; Franco, S.; Merchan, F. L.; Tejero, T. *Synlett*, **2000**, 442; (c) Merino, P. *C. R. Chim.* **2005**, *8*, 775; (d) Murahashi, S.-I.; Imada, Y. *Chem. Rev.* **2019**, *119*, 4684.
[23] Merino, P.; Mannucci, V.; Tejero, T. *Eur. J. Org. Chem.* **2008**, 3943.
[24] (a) Merchan, F. L.; Merino, P.; Tejero, T. *Tetrahedron Lett.* **1995**, *36*, 6949; (b) Merino, P.; Lanaspa, A.; Merchan, F. L.; Tejero, T. *J. Org. Chem.* **1996**, *61*, 9028; (c) Goti, A.; Cicchi, S.; Mannucci, V.; Cardona, F.; Guarna, F.; Merino, P.; Tejero, T. *Org. Lett.* **2003**, *5*, 4235.
[25] (a) Ali, S. A.; Wazeer, M. I. M. *J. Chem. Soc., Perkin Trans. 2* **1986**, 1789; (b) Ali, S. A.; Wazeer, M. I. M. *J. Chem. Soc., Perkin Trans. 1* **1988**, 597; (c) Ali, S. A.; Wazeer, M. I. M. *Tetrahedron* **1988**, *44*, 187.
[26] (a) Jackson, A. H.; Smith, A. E. *Tetrahedron* **1968**, *24*, 403; (b) Ungemach, F.; Cook, J. M. *Heterocycles* **1978**, *9*, 1089; (c) Bailey, P. D. *J. Chem. Res*. **1987**, 202; (d) Czerwinski, K. M.; Deng, L.; Cook, J. M. *Tetrahedron Lett.* **1992**, *33*, 4721; (e) Zheng, C.; Xia, Z.-L. You, S.-L. *Chem* **2018**, *4*, 1952; (f) Zheng, C.; You, S.-L. *Acc. Chem. Res.* **2020**, *53*, 974.
[27] (a) Kowalski, P.; Bojarski, A. J.; Mokrosz, J. L. *Tetrahedron* **1995**, *51*, 2737; (b) Maresh, J. J.; Giddings, L.-A.; Friedrich, A.; Loris, E. A.; Panjikar, S.; Trout, B. L.; Stöckigt, J.; Peters, B.; O'Connor, S. E. *J. Am. Chem. Soc.* **2008**, *130*, 710; (c) Overvoorde, L. M.; Grayson, M. N.; Luo, Y.; Goodman, J. M. *J. Org. Chem.* **2015**, *80*, 2634.
[28] (a) Figerio, M.; Santagostino, M.; Sputore, S. *J. Org. Chem.* **1999**, *64*, 4537; b) Relevant, G.; Dundand, S.; Hesse, S.; Kirsh, G. *Synthesis* **2011**, *18*, 2935.
[29] Oppolzer, W.; Siles, S.; Snowden, R. L.; Bakker, B. H.; Petrzilka, M. *Tetrahedron* **1985**, *41*, 3497.
[30] Liu, W.; Wang, H.; Li, X.; Xu, Y.; Zhang, J.; Wang, W.; Gong, Q.; Qiu, X.; Zhu, J.; Mao, F.; Zhang, H.; Li, J. *Bioorg. Med. Chem*. **2018**, *26*, 3117.
[31] Fu, L.; Davies, H. M. L. *Org. Lett*. **2017**, *19*, 1504.

3.9 NMR Spectra

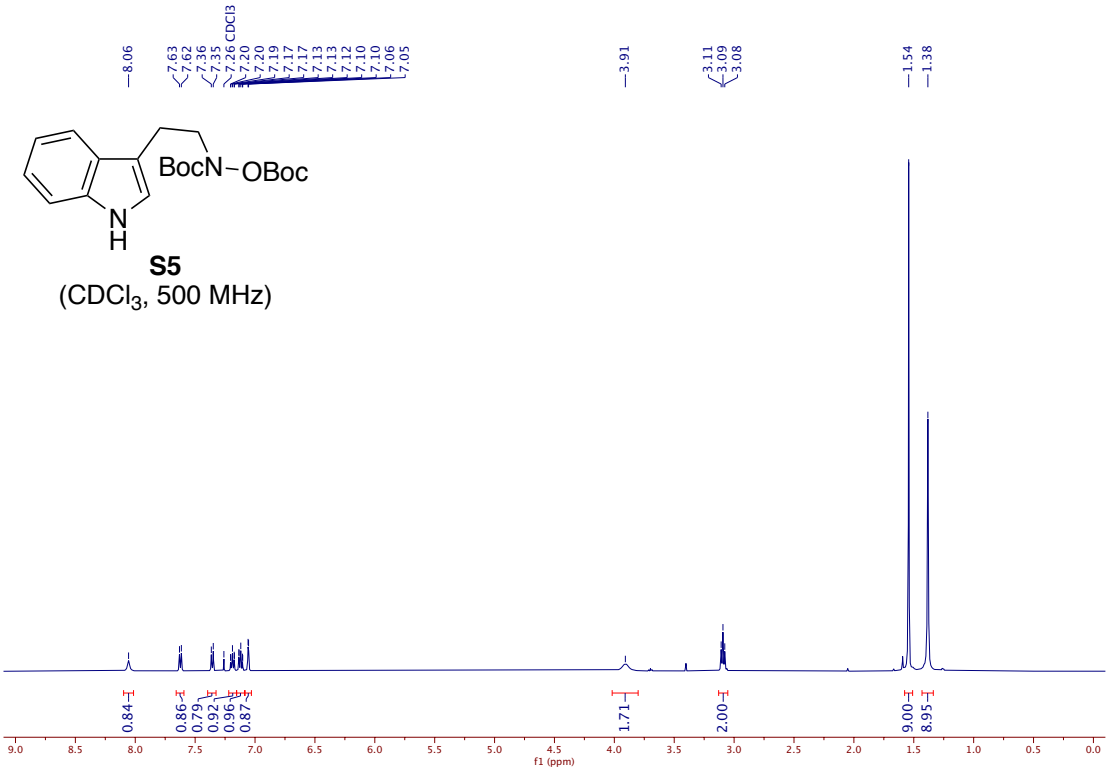

S5
($CDCl_3$, 500 MHz)

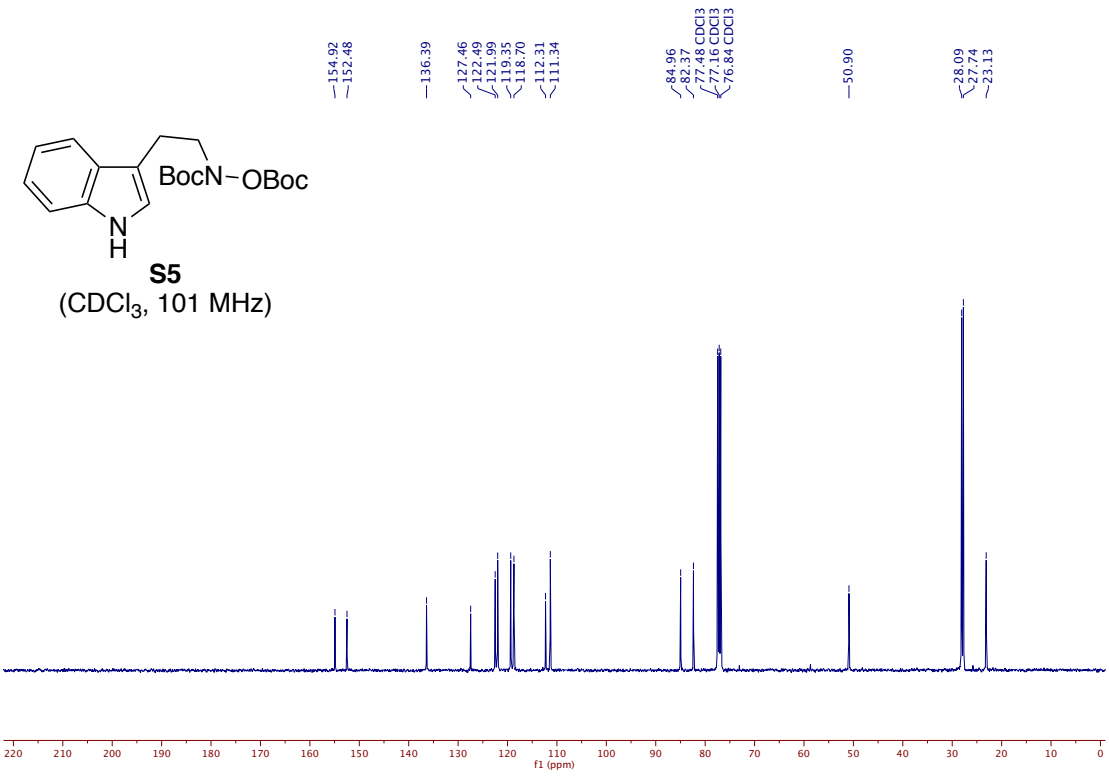

S5
($CDCl_3$, 101 MHz)

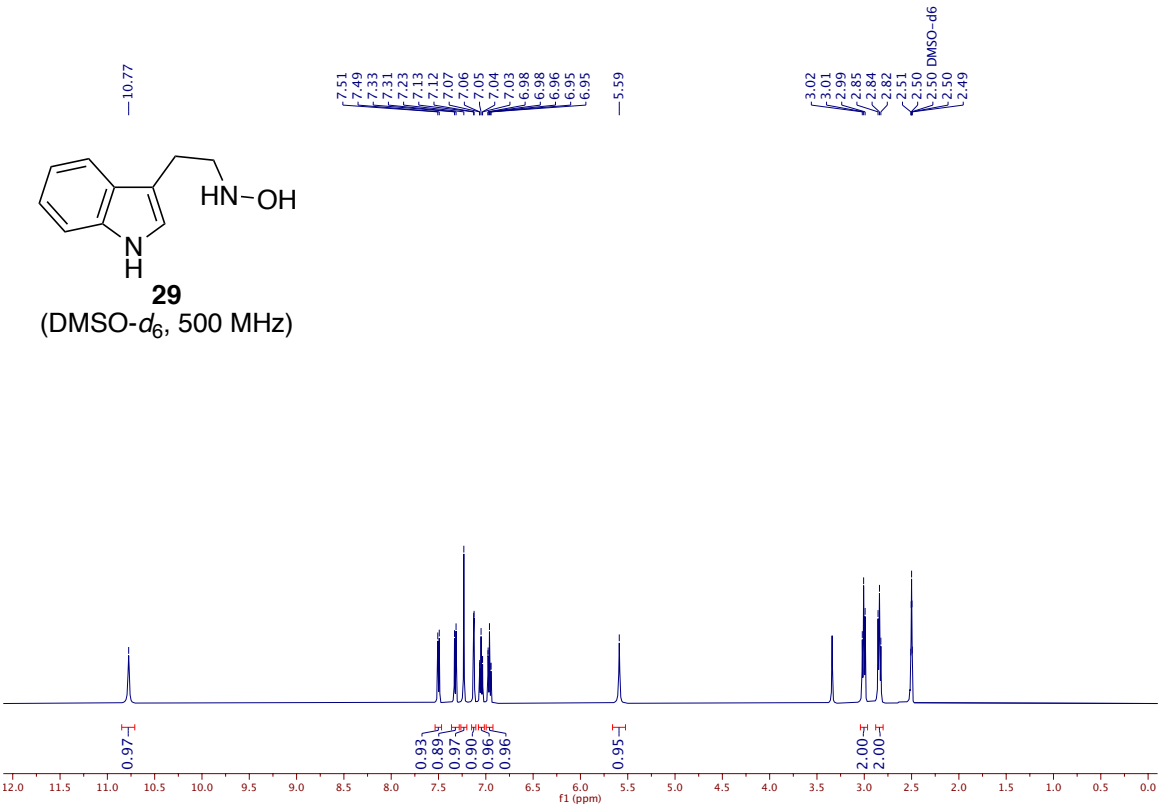

29

(DMSO-d_6, 500 MHz)

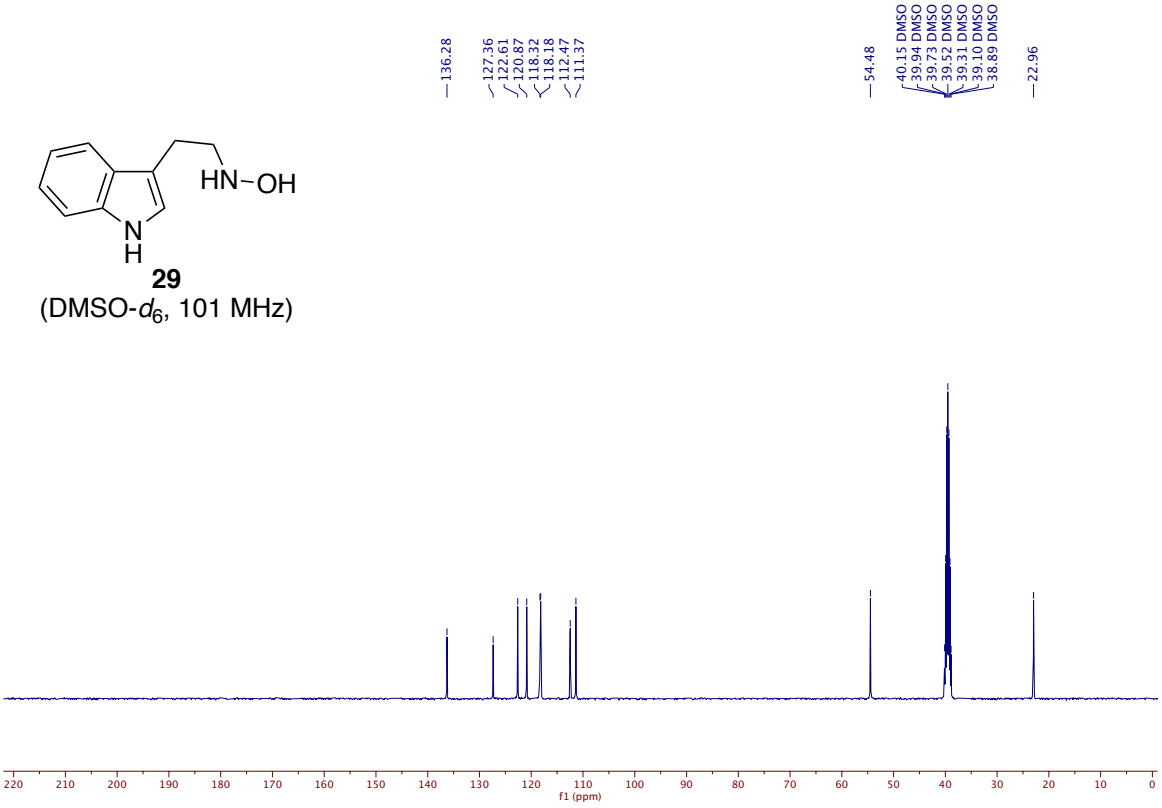

29

(DMSO-d_6, 101 MHz)

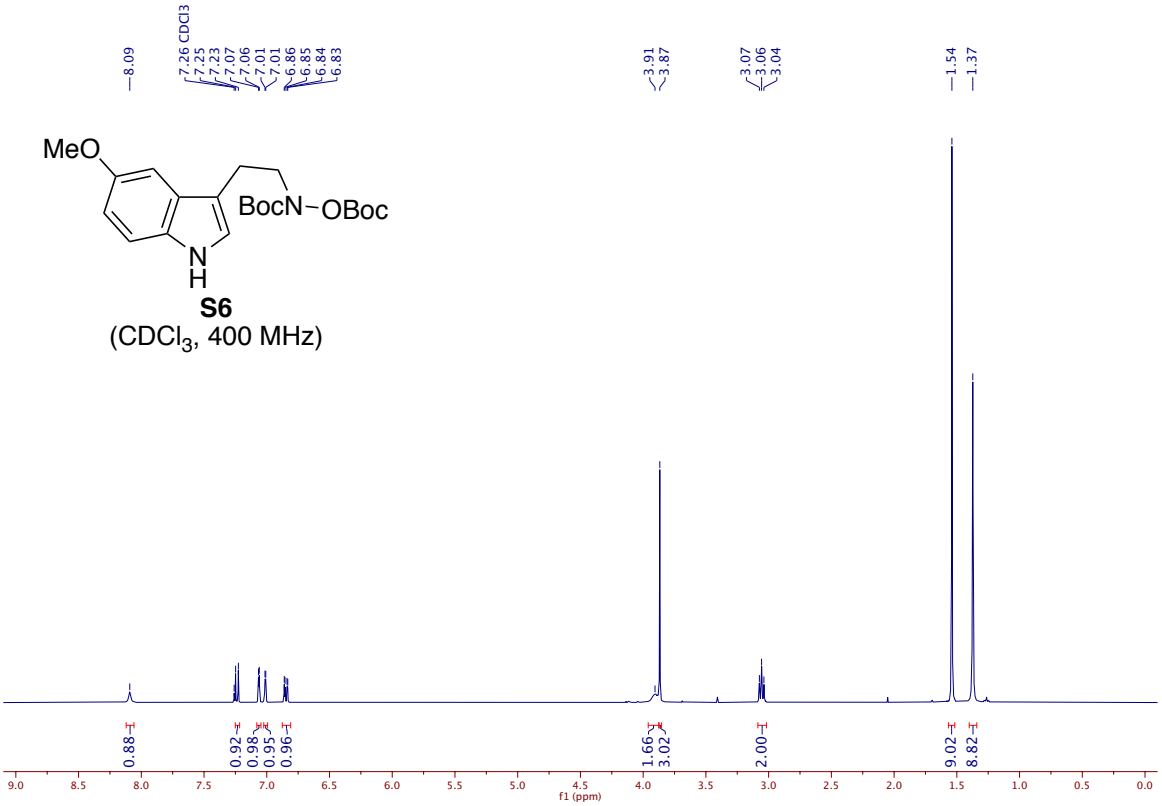

S6

($CDCl_3$, 400 MHz)

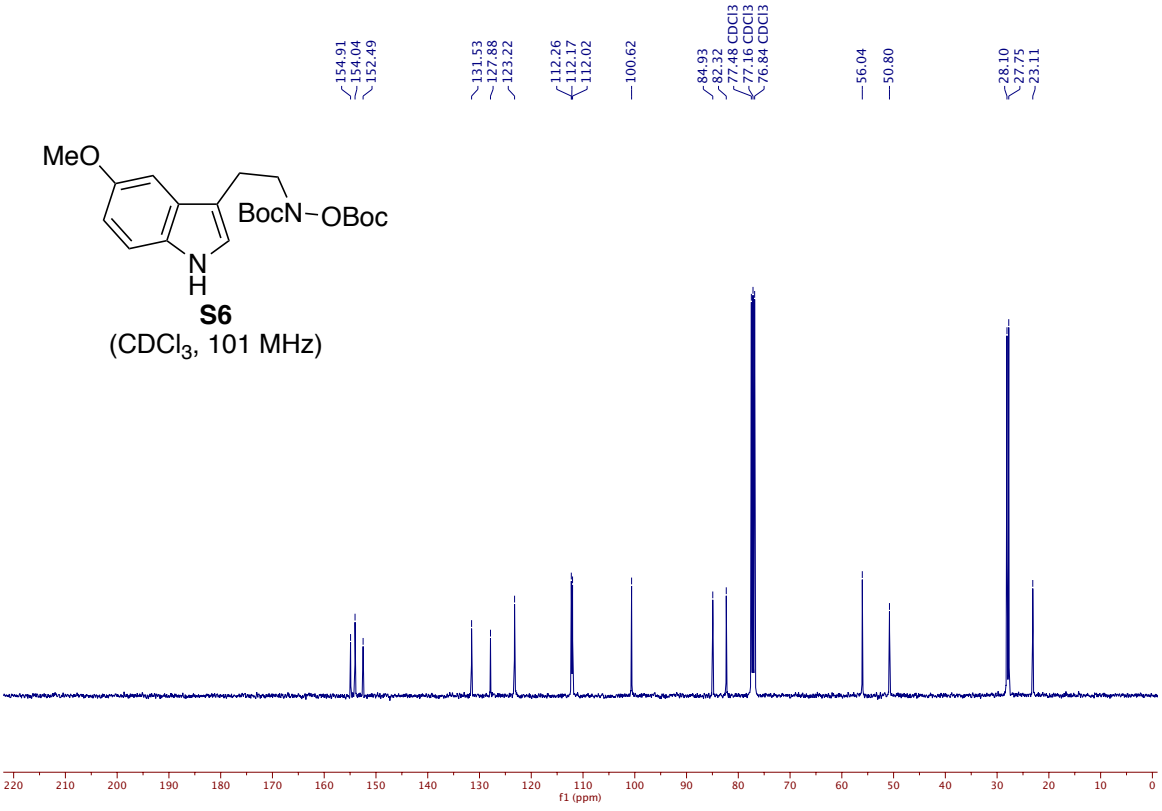

S6

($CDCl_3$, 101 MHz)

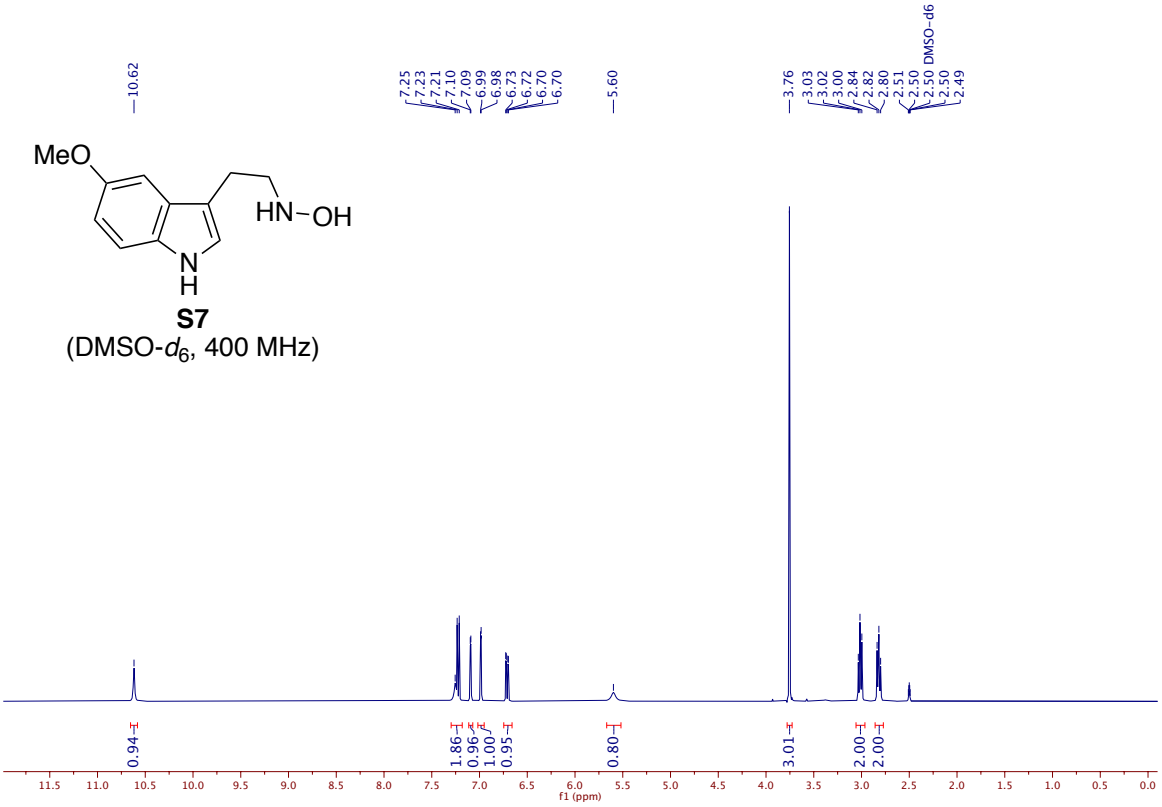

S7

(DMSO-d_6, 400 MHz)

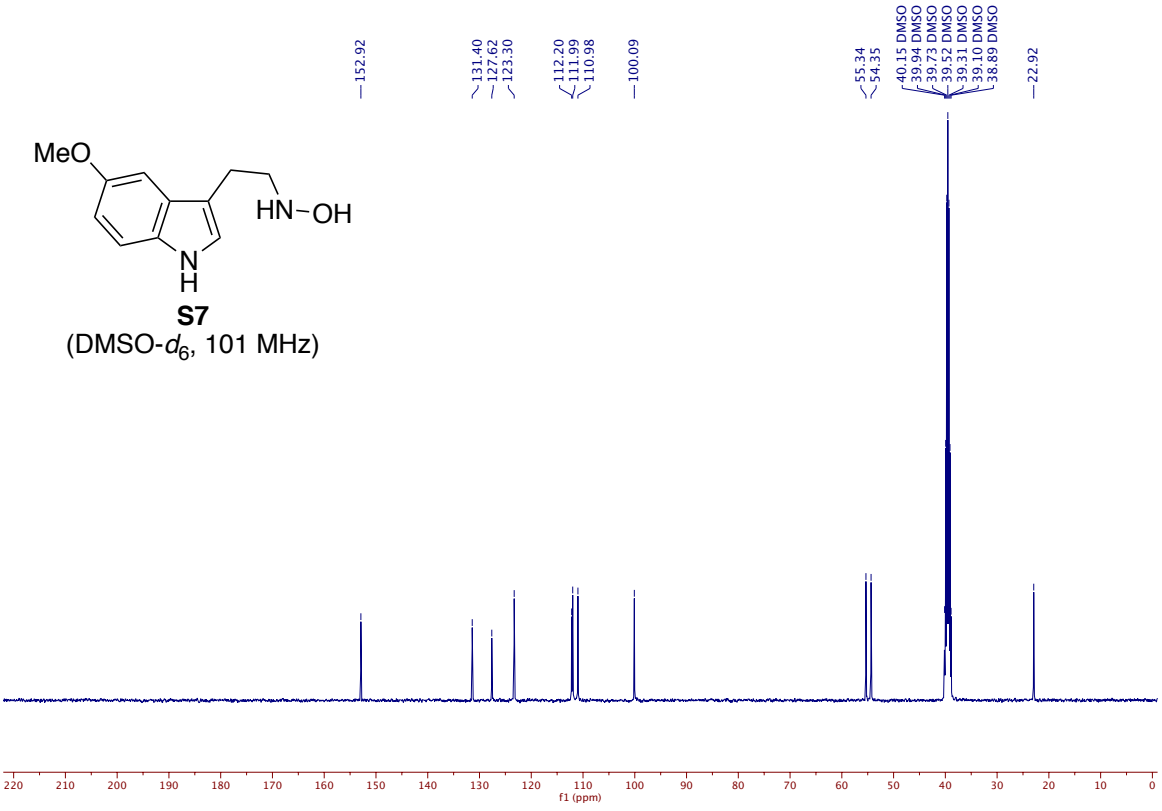

S7

(DMSO-d_6, 101 MHz)

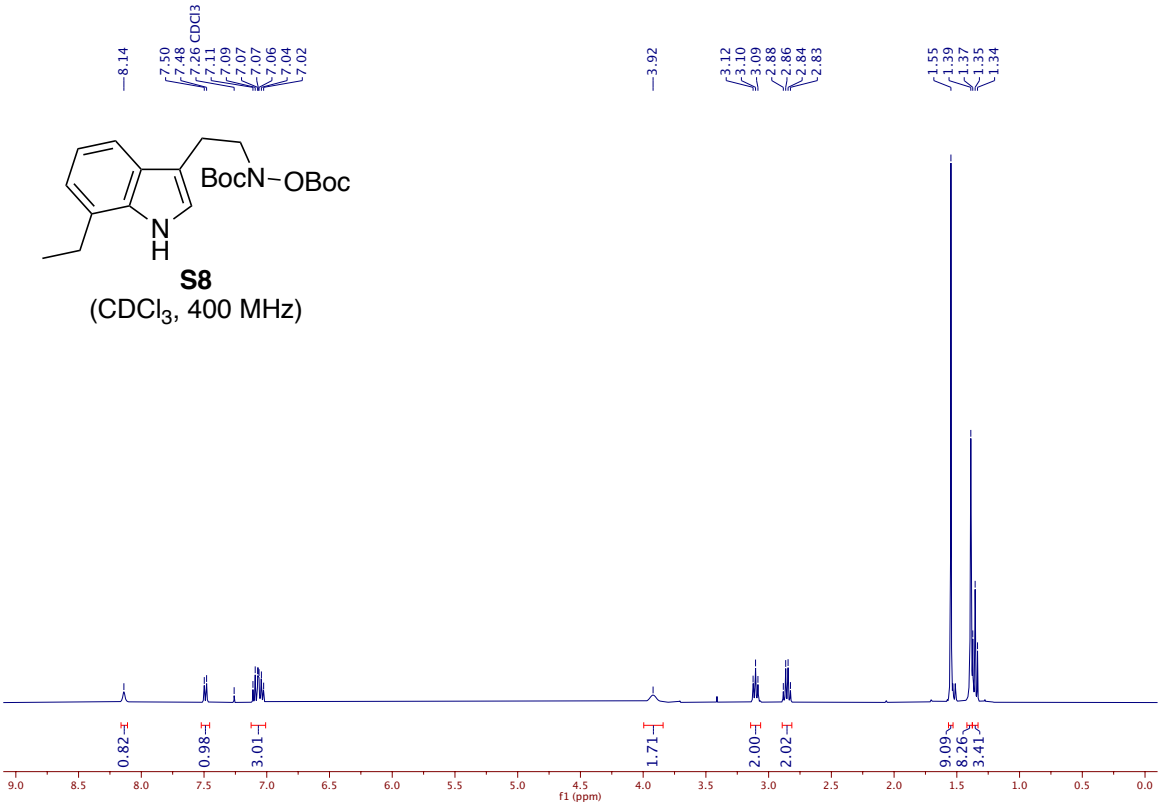

S8

($CDCl_3$, 400 MHz)

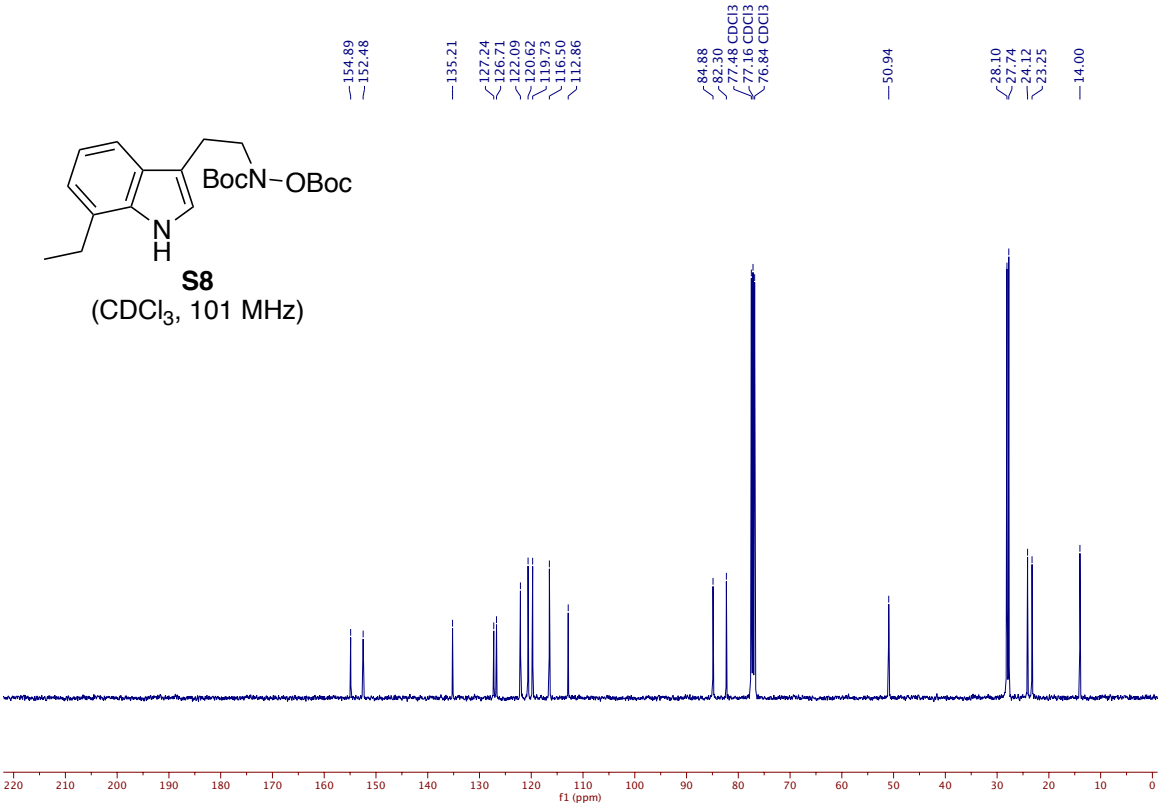

S8

($CDCl_3$, 101 MHz)

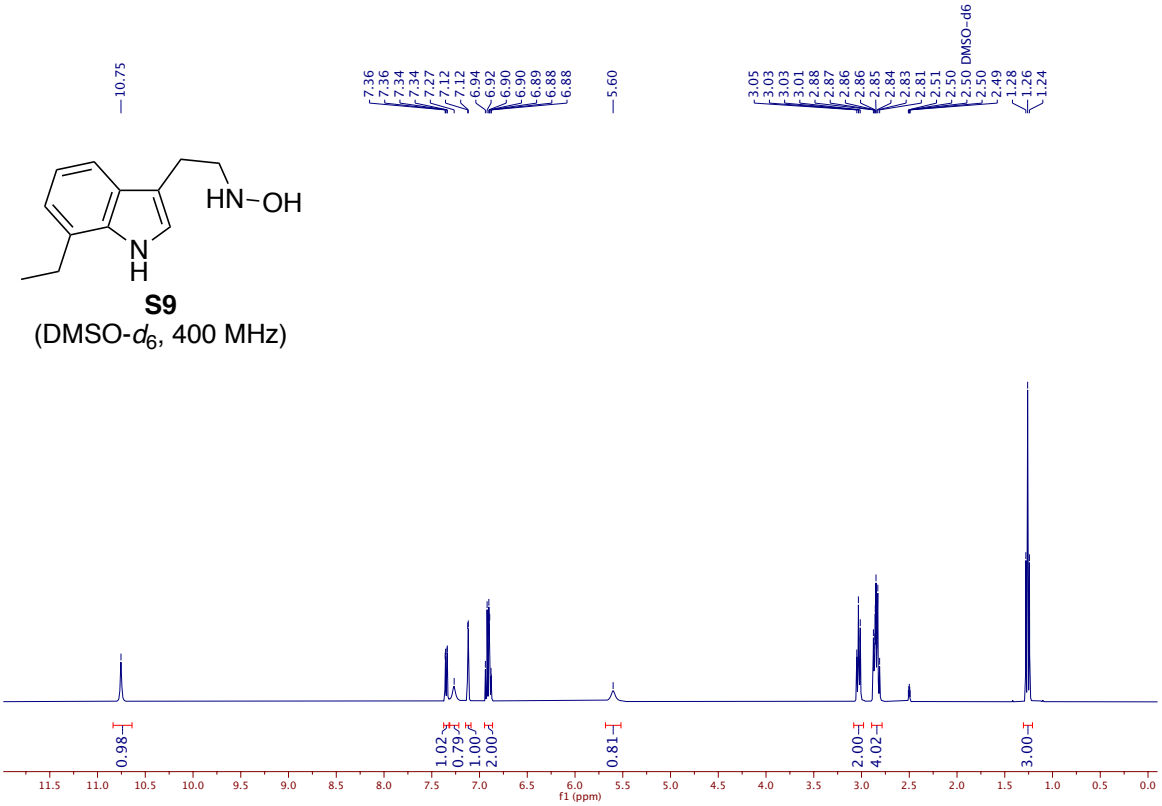

S9

(DMSO-d_6, 400 MHz)

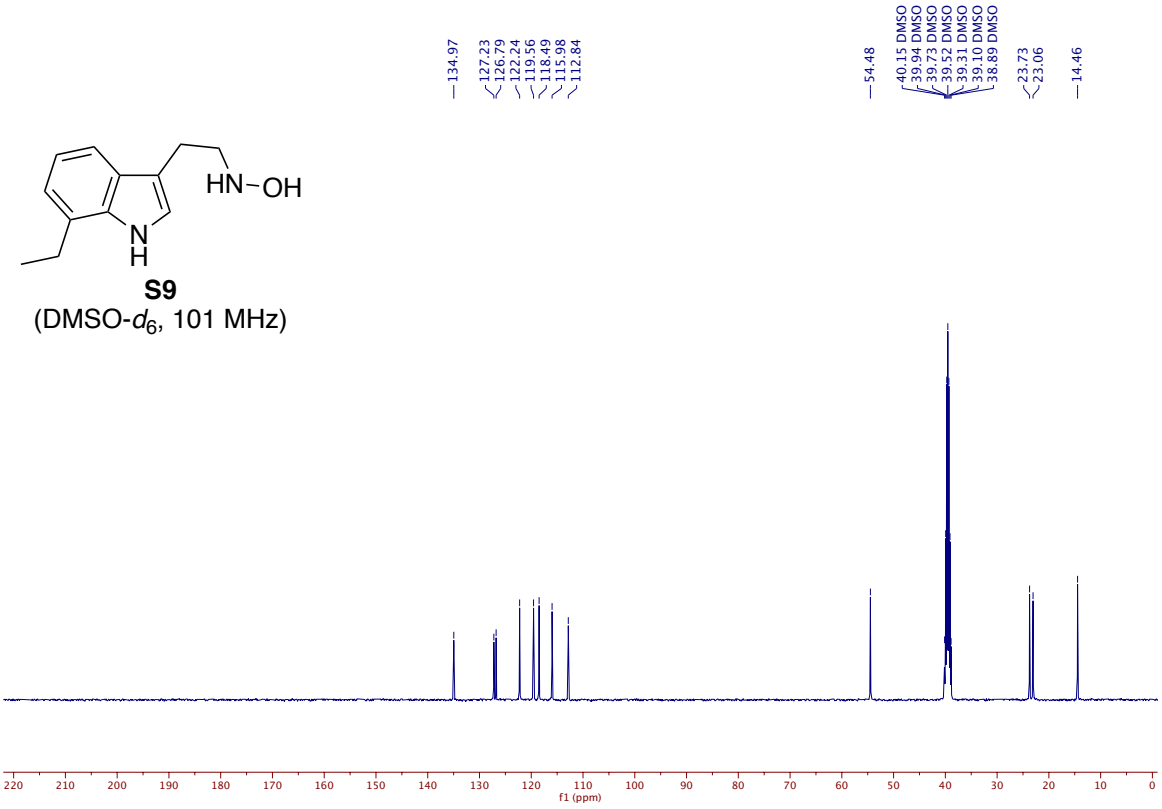

S9

(DMSO-d_6, 101 MHz)

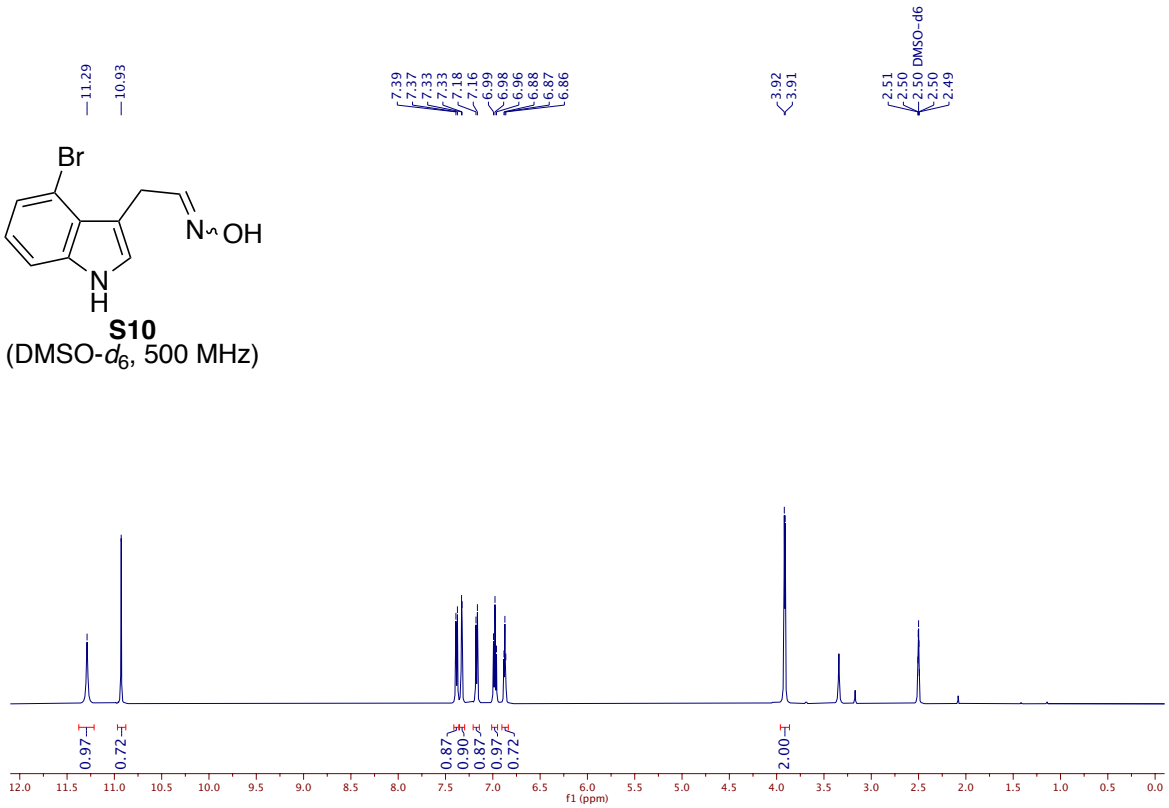

S10
(DMSO-d_6, 500 MHz)

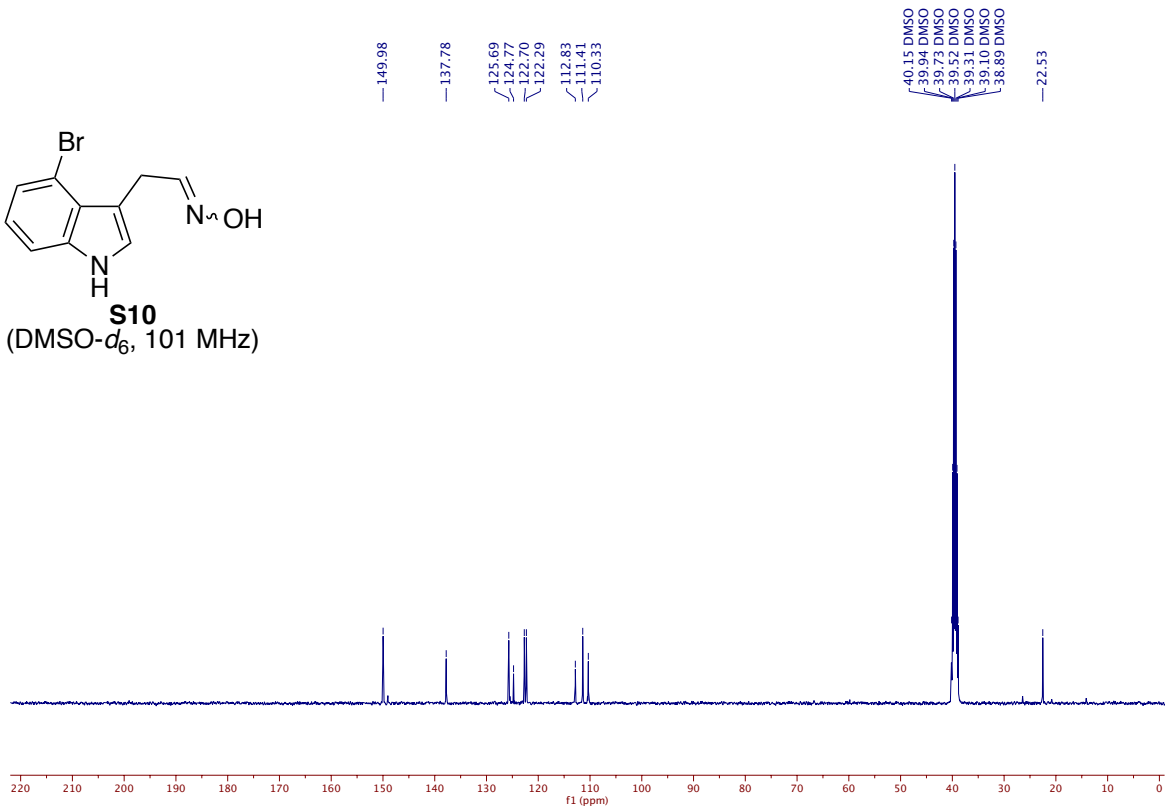

S10
(DMSO-d_6, 101 MHz)

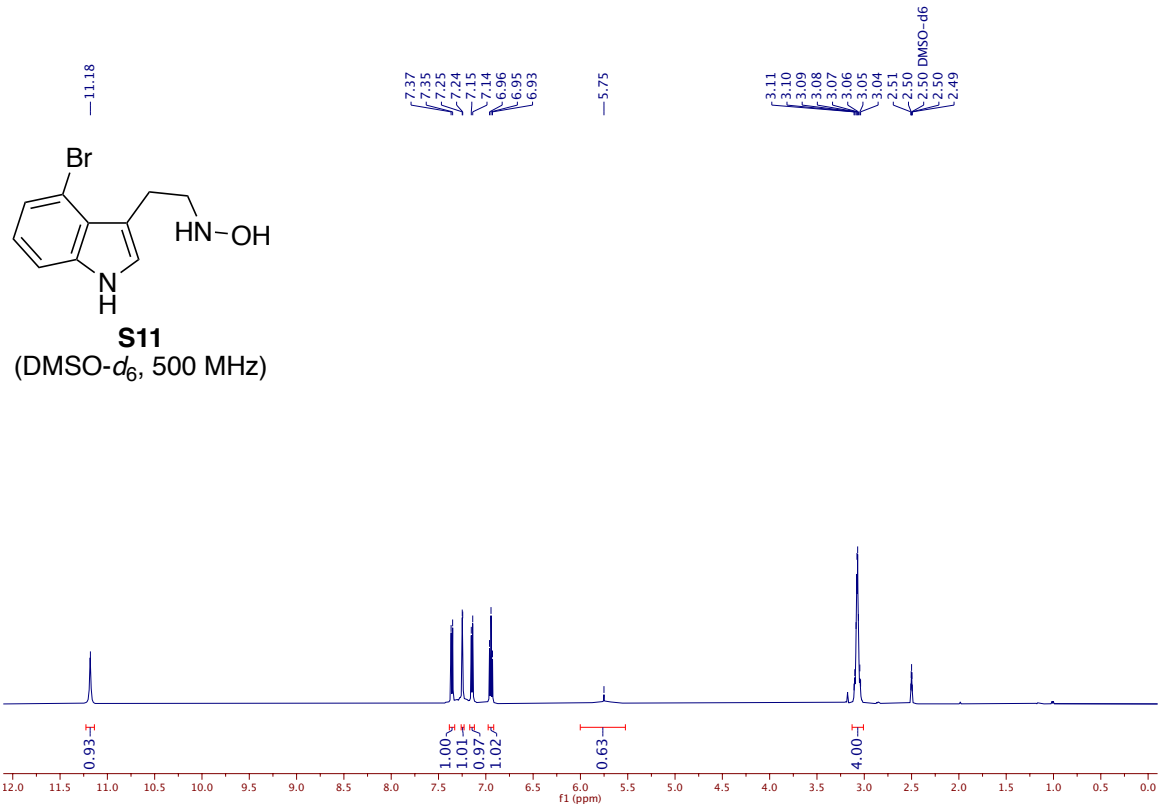

S11
(DMSO-d_6, 500 MHz)

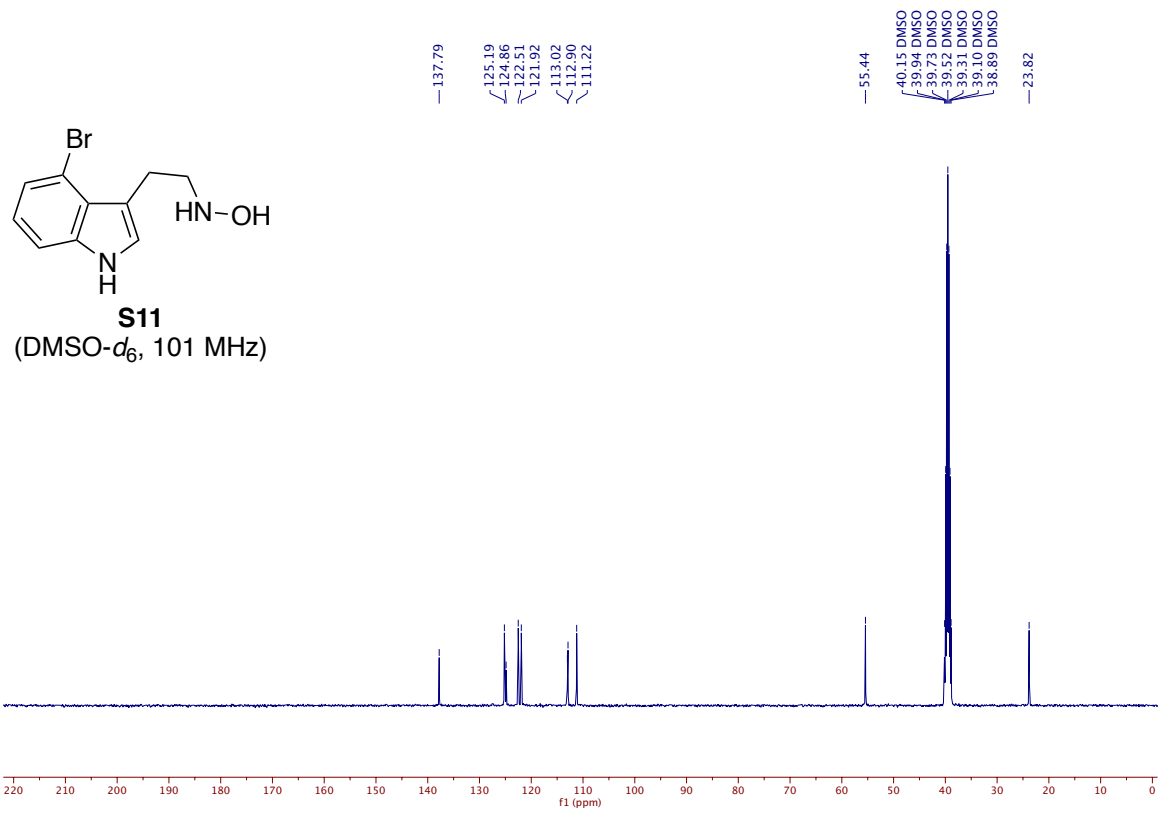

S11
(DMSO-d_6, 101 MHz)

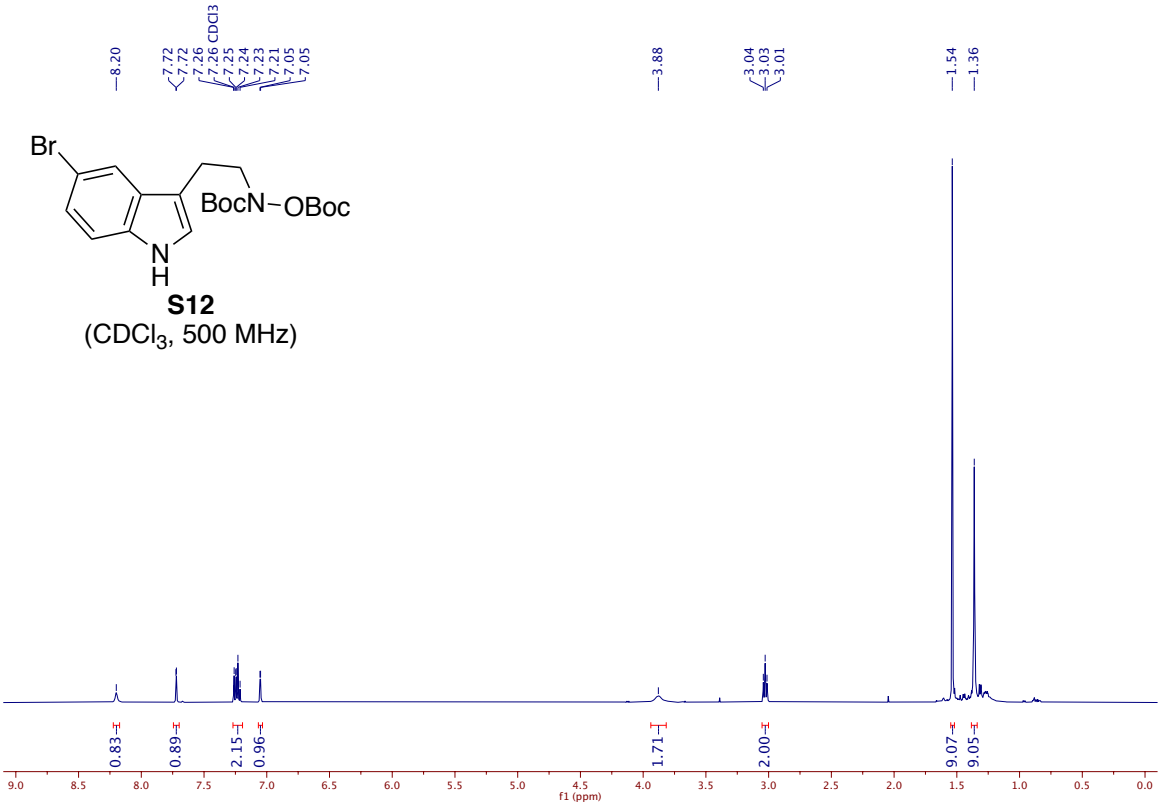

S12
($CDCl_3$, 500 MHz)

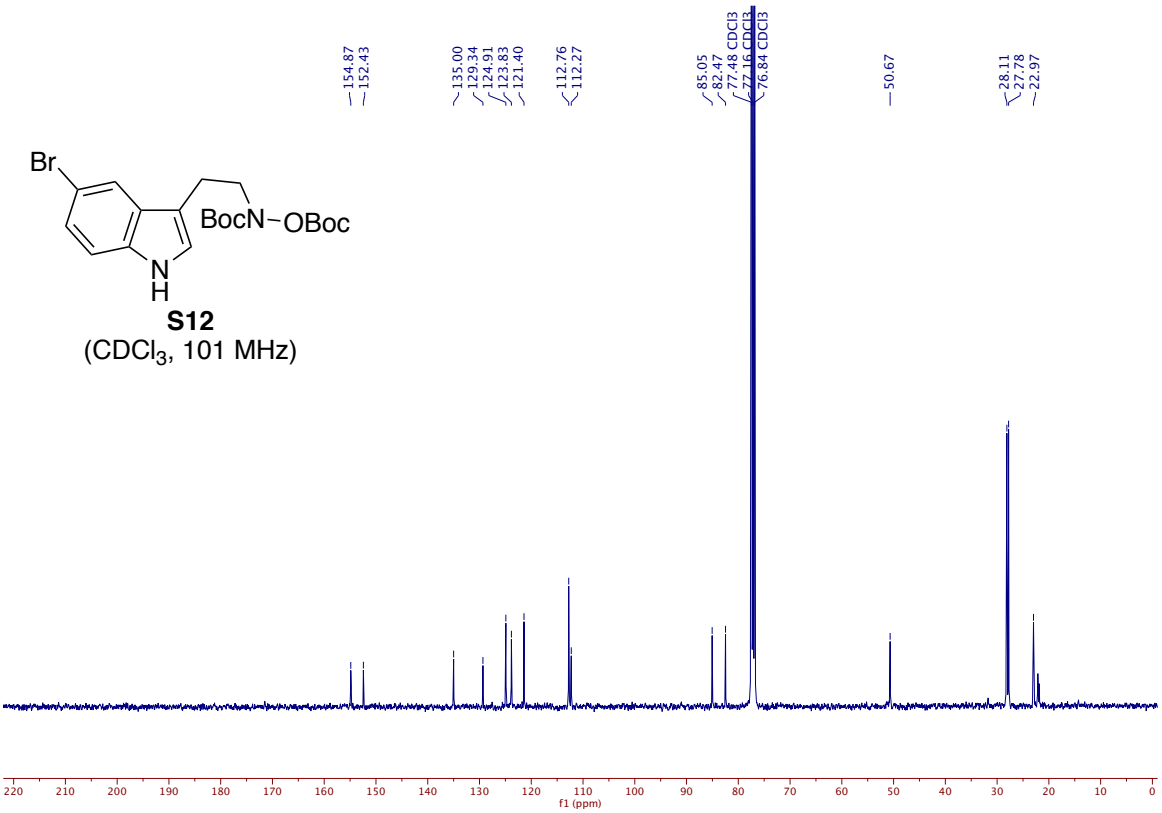

S12
($CDCl_3$, 101 MHz)

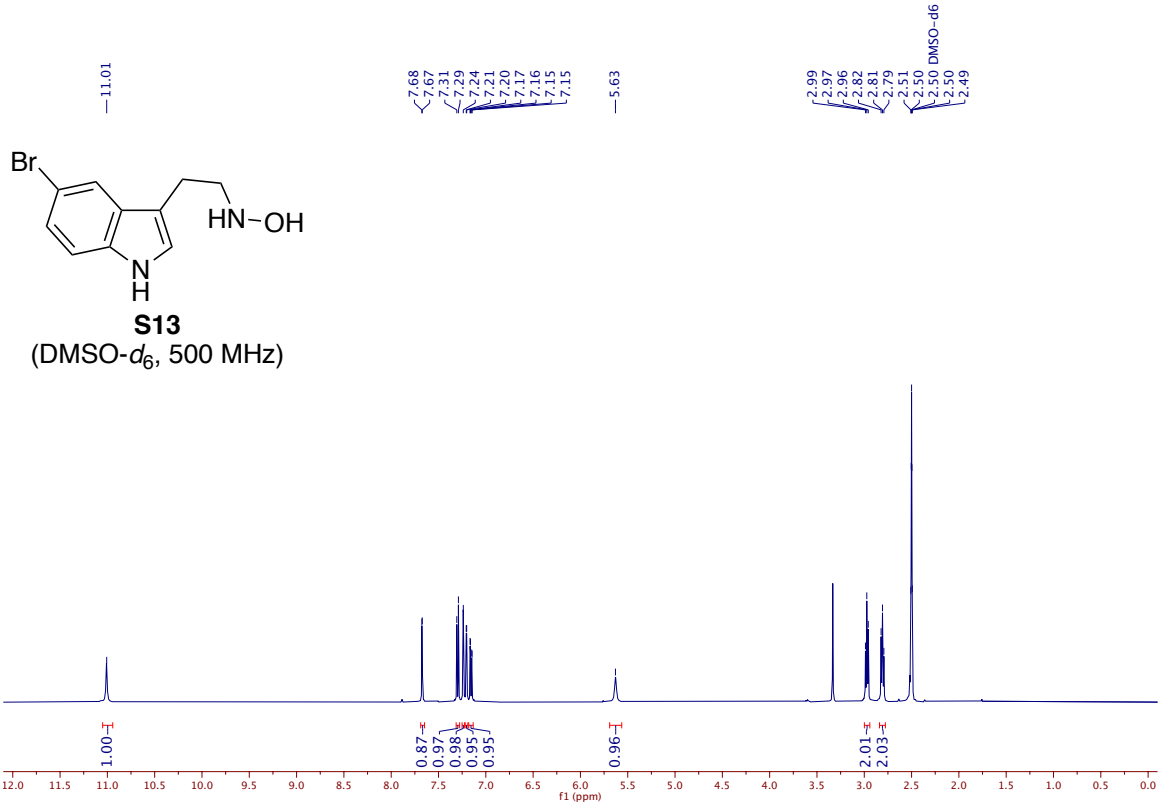

S13
(DMSO-d_6, 500 MHz)

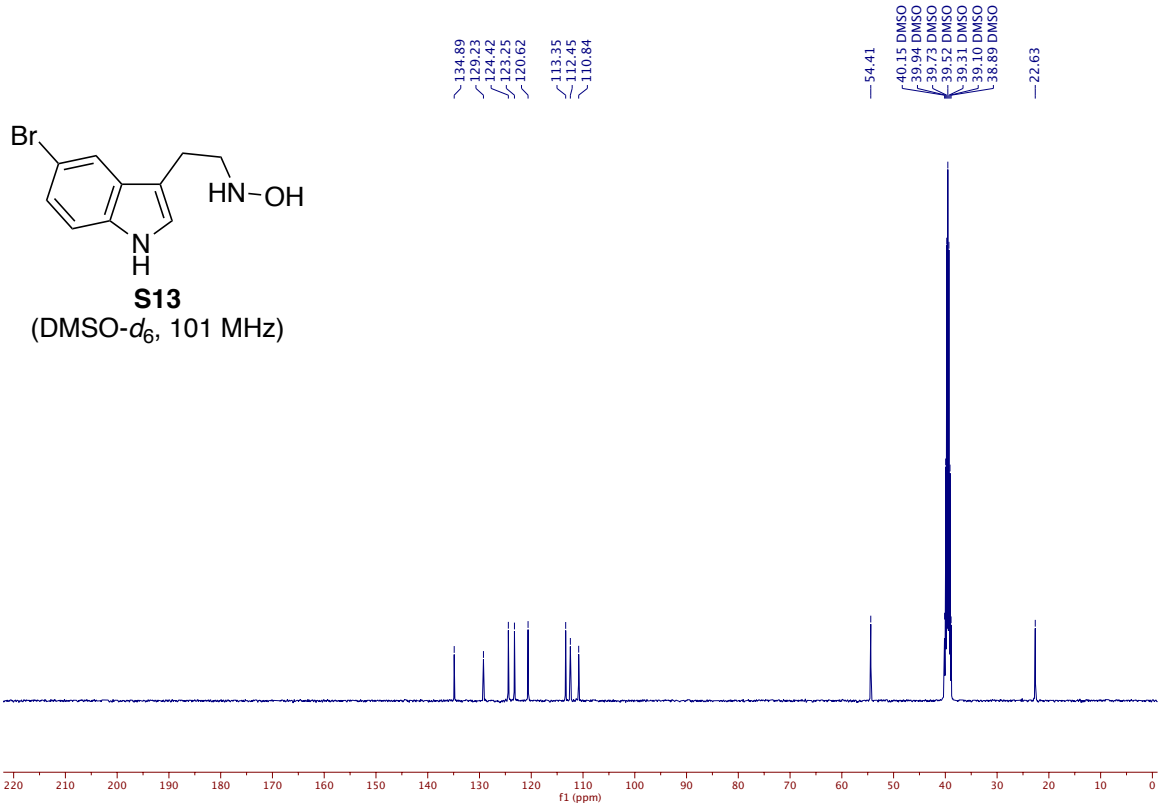

S13
(DMSO-d_6, 101 MHz)

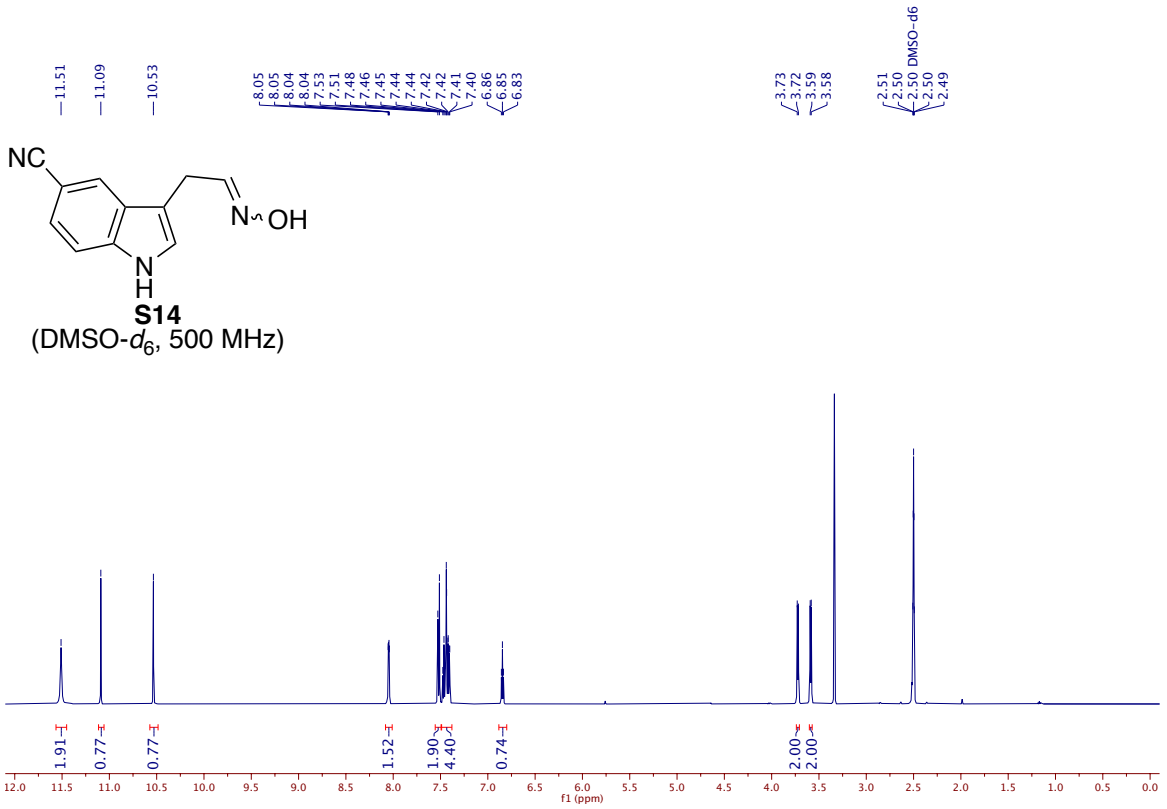

S14
(DMSO-d_6, 500 MHz)

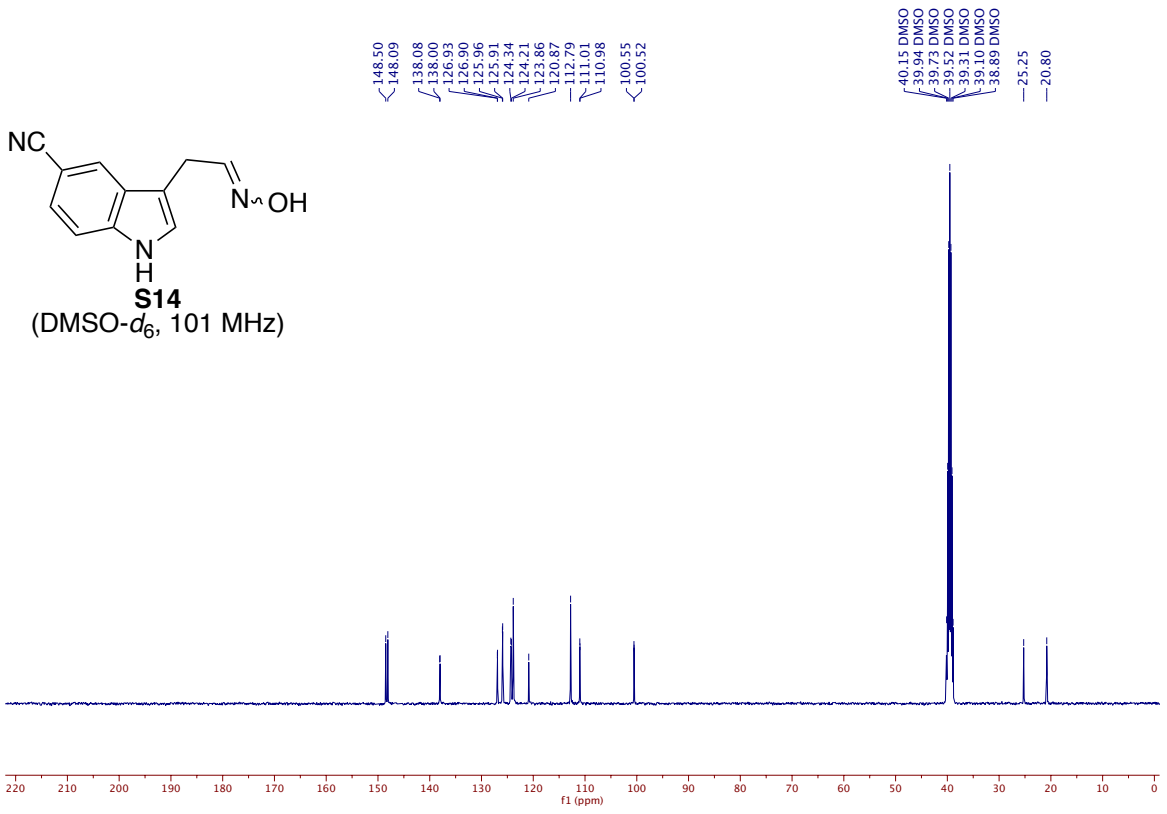

S14
(DMSO-d_6, 101 MHz)

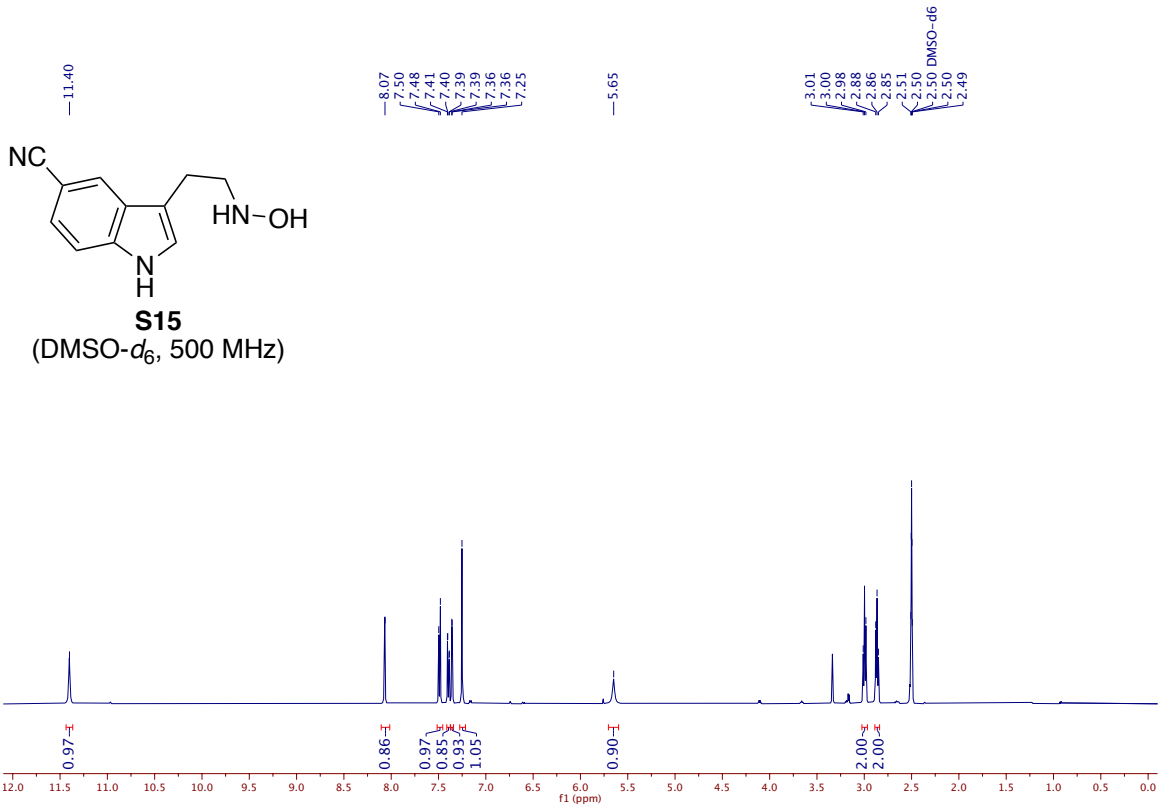

S15
(DMSO-d_6, 500 MHz)

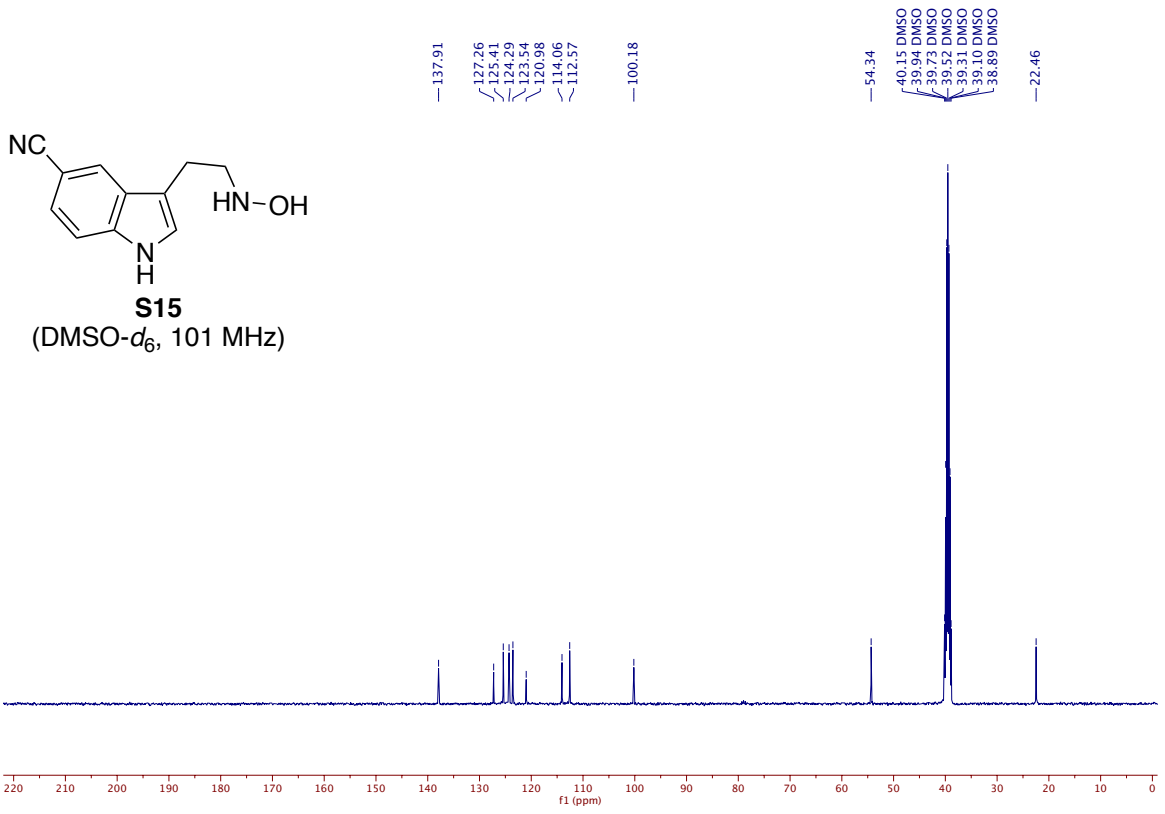

S15
(DMSO-d_6, 101 MHz)

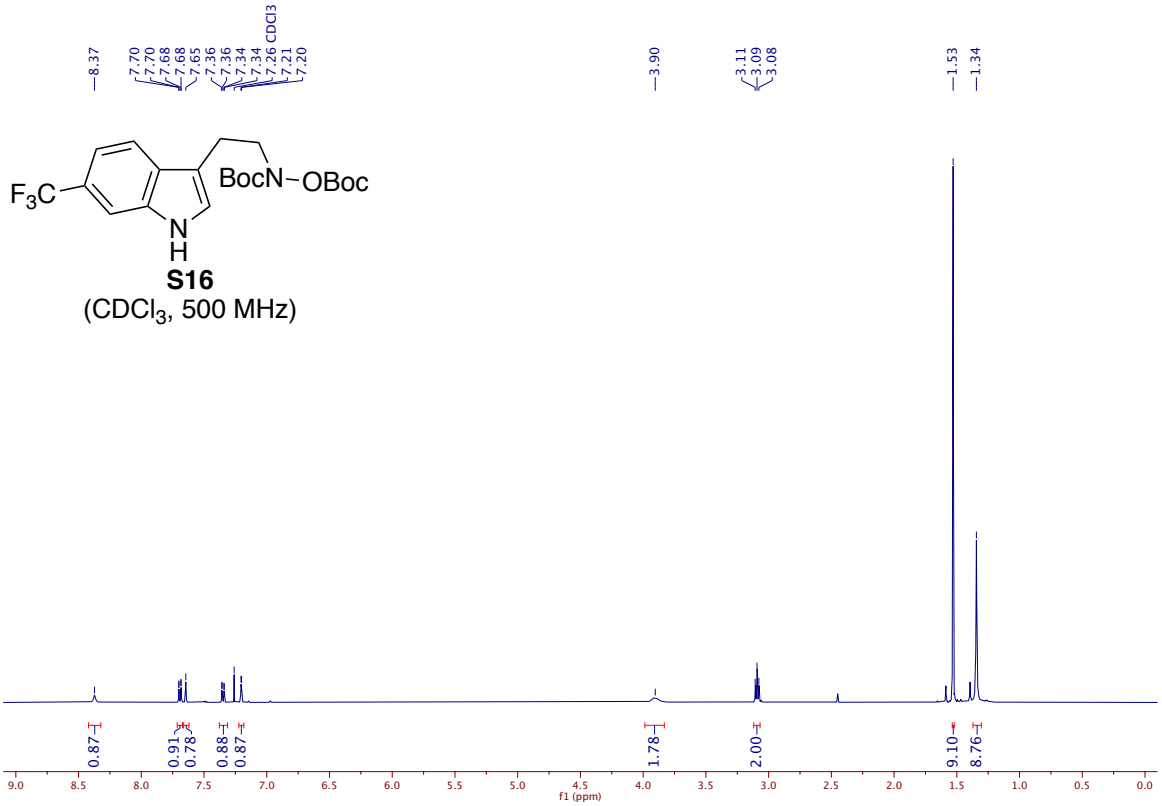

S16

($CDCl_3$, 500 MHz)

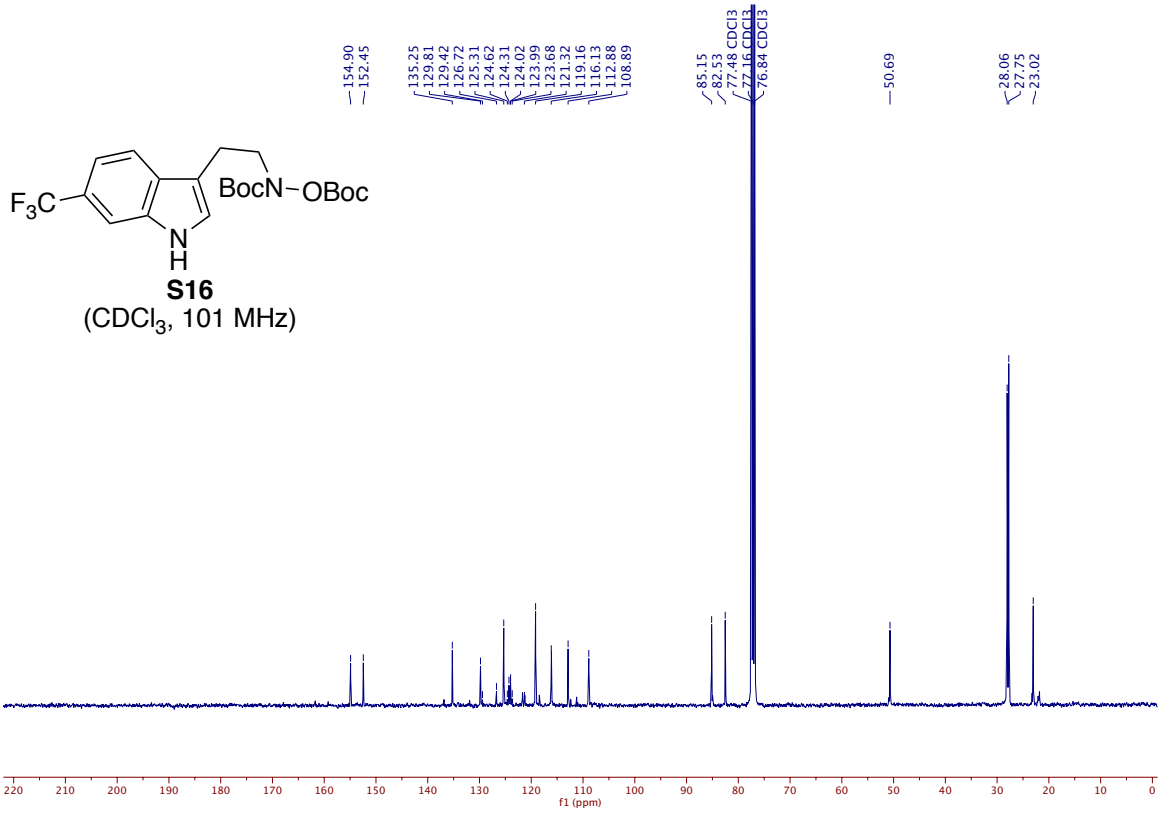

S16

($CDCl_3$, 101 MHz)

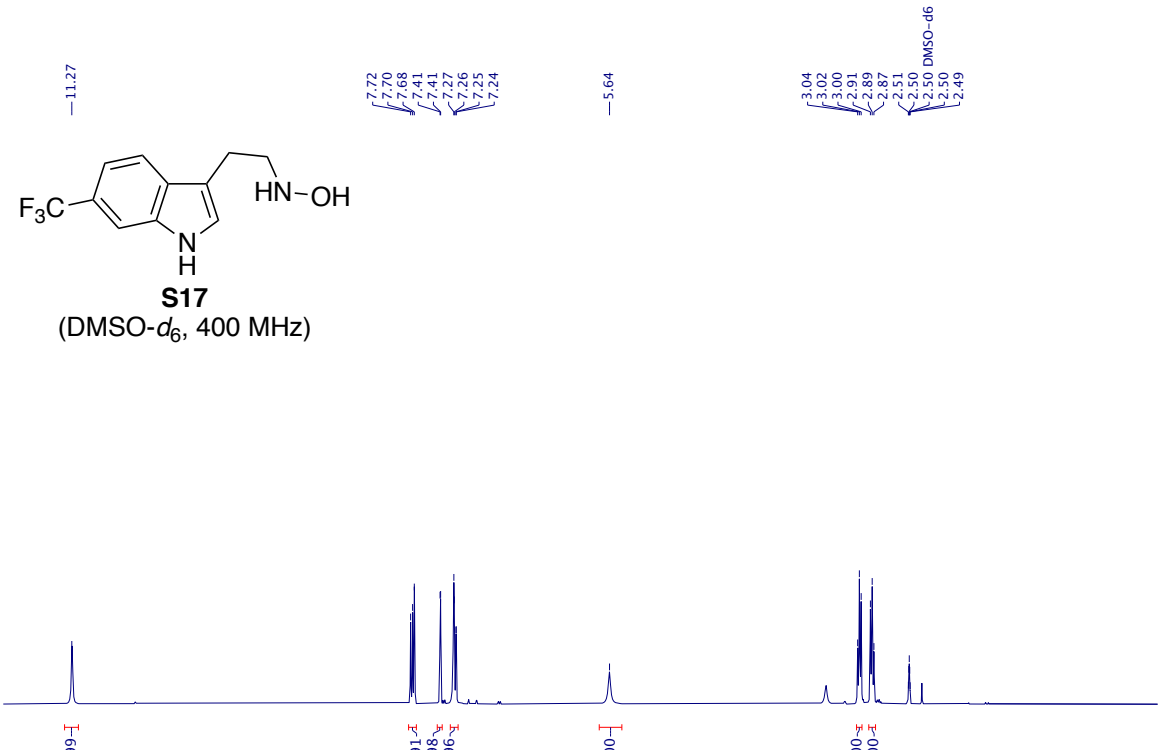

S17
(DMSO-d_6, 400 MHz)

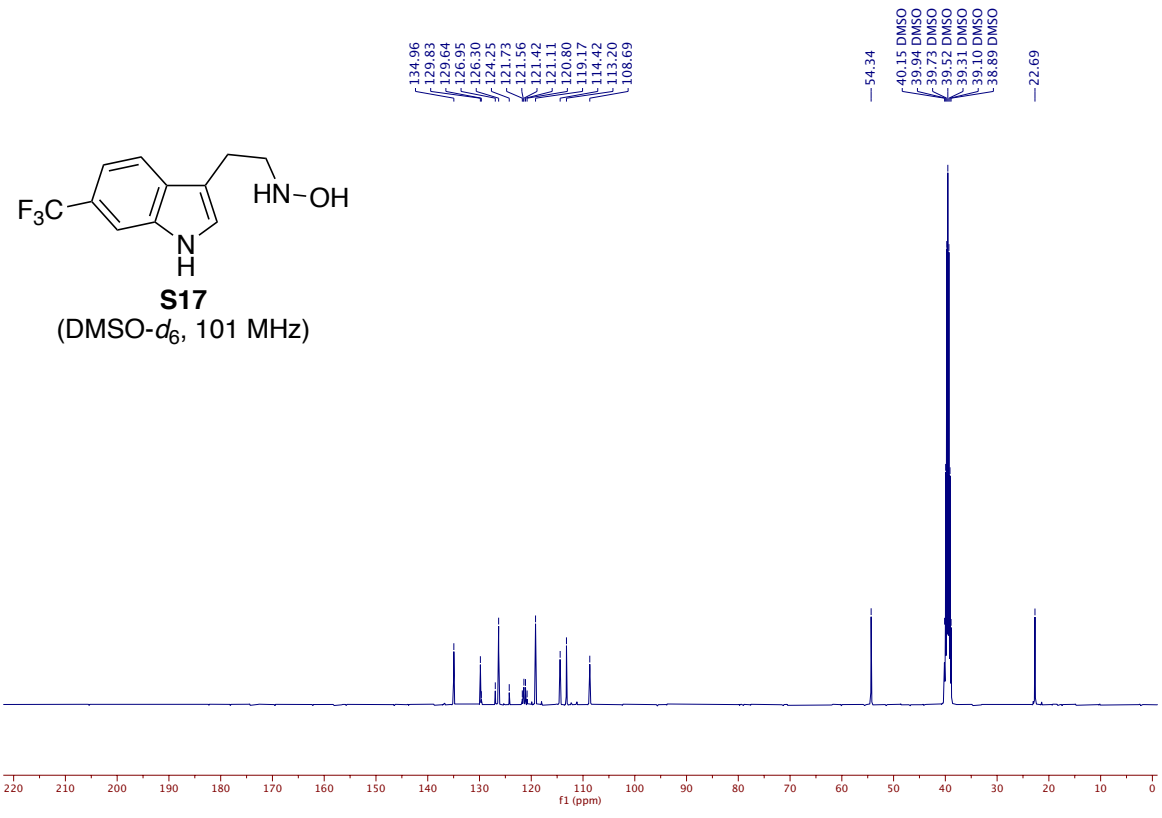

S17
(DMSO-d_6, 101 MHz)

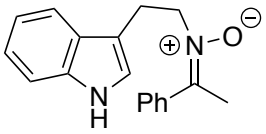

32
($CDCl_3$, 500 MHz)

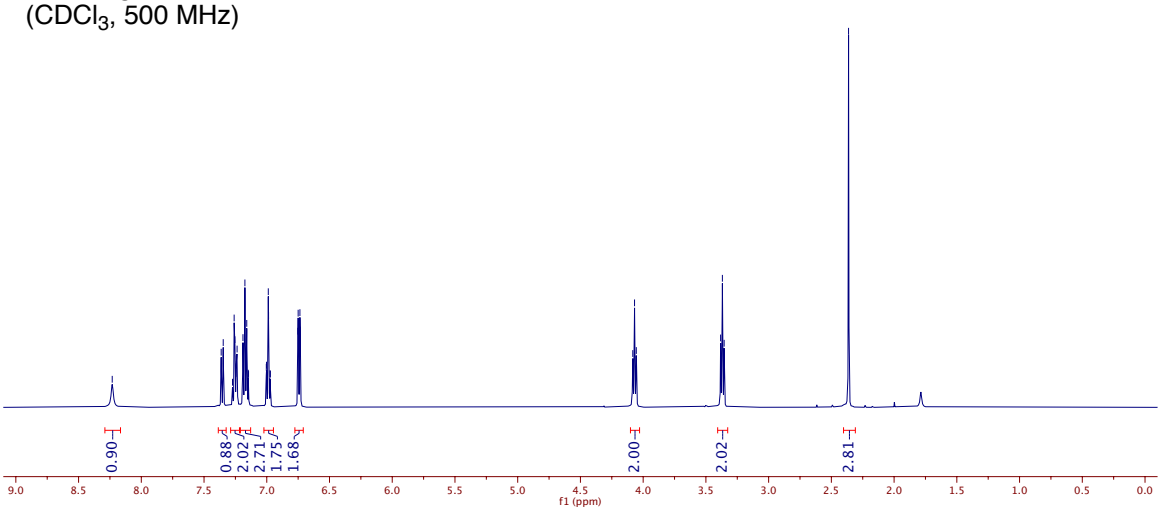

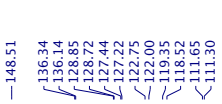

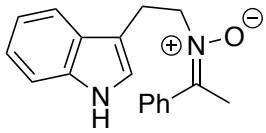

32
($CDCl_3$, 101 MHz)

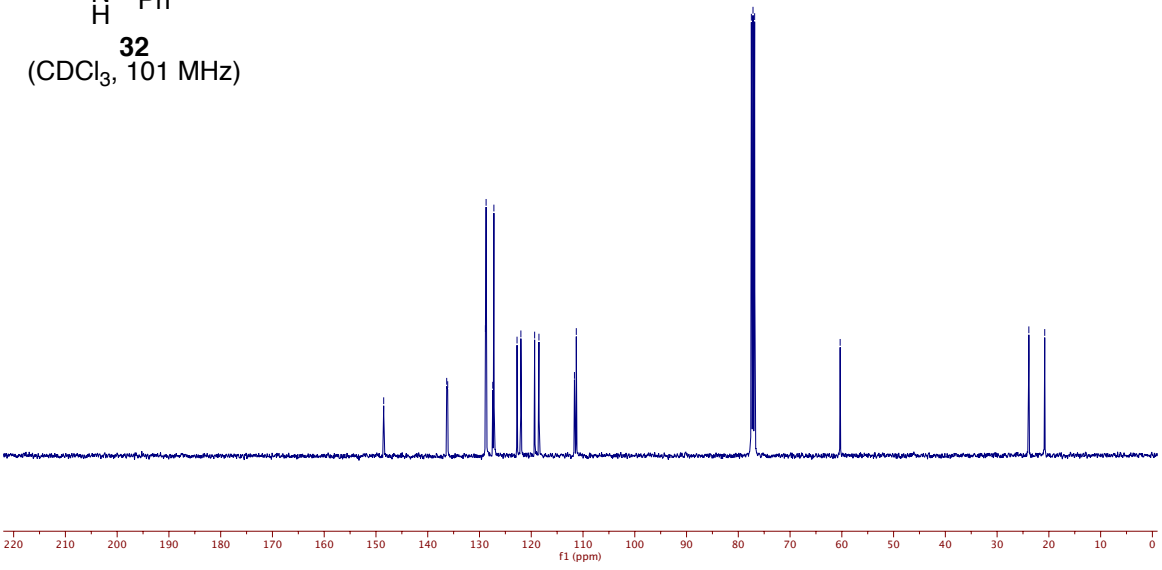

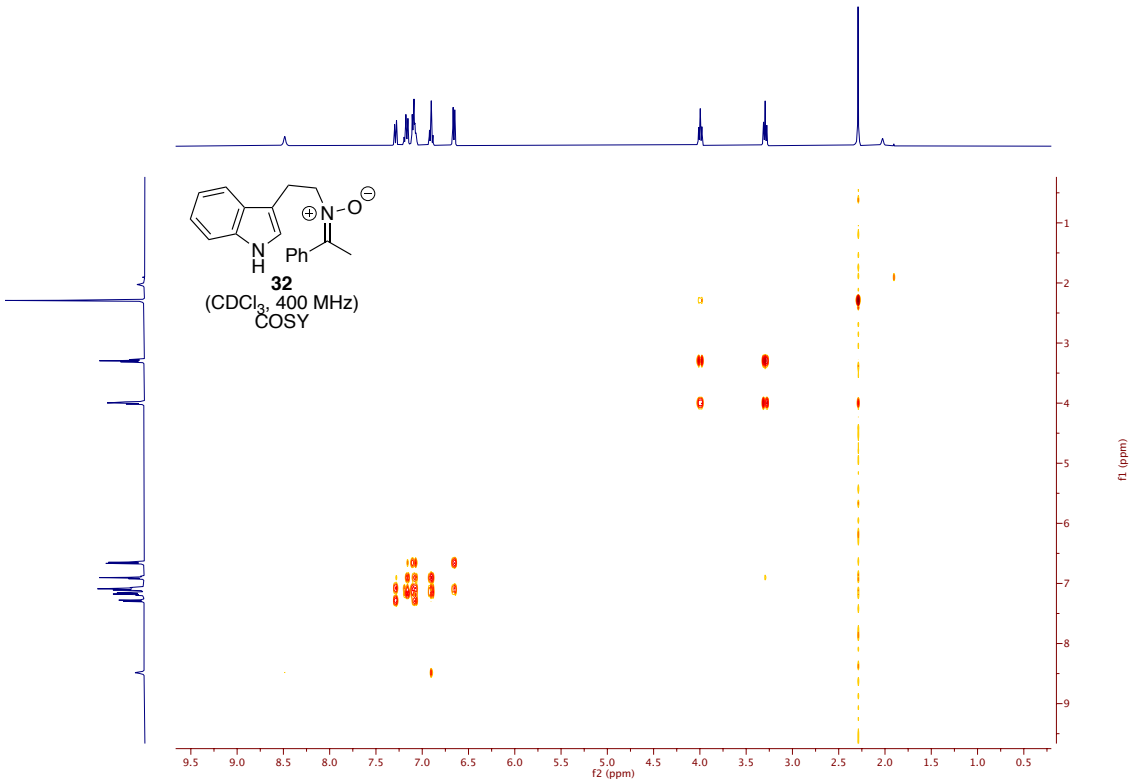
32
(CDCl3, 400 MHz)
COSY
f2 (ppm)
f1 (ppm)

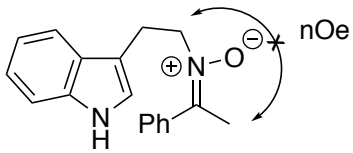
nOe

32

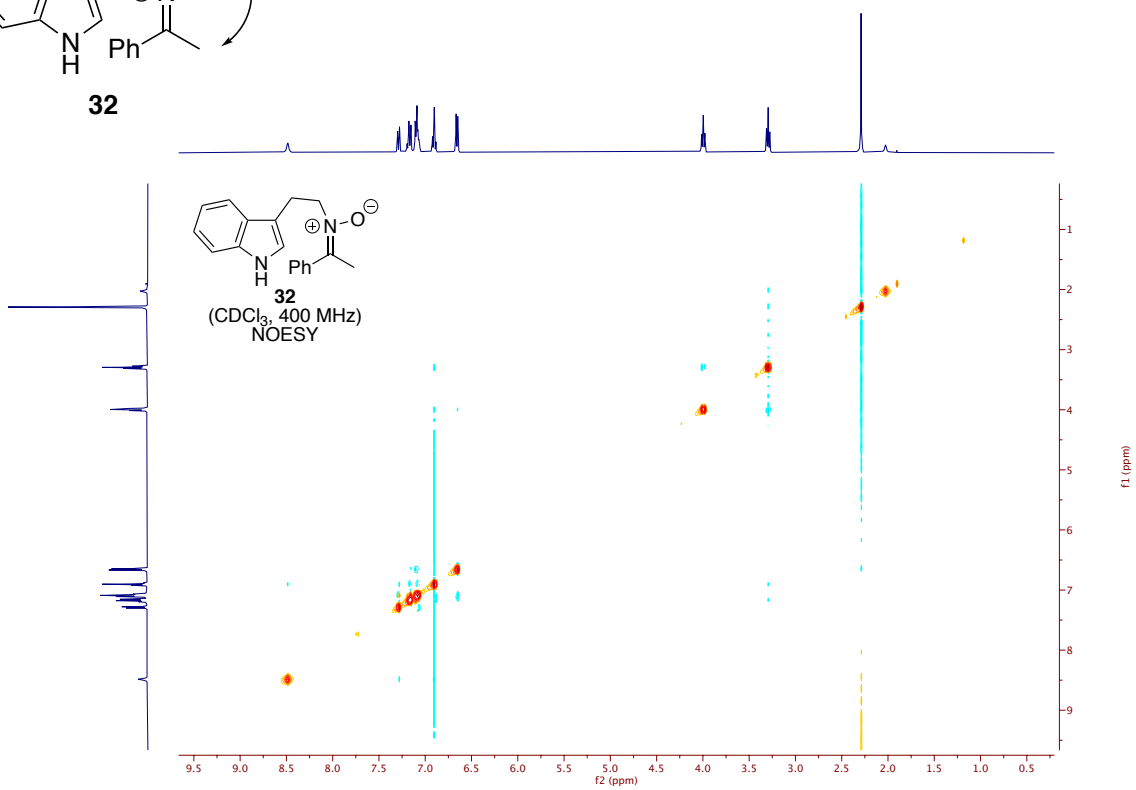
32
(CDCl3, 400 MHz)
NOESY
f2 (ppm)
f1 (ppm)

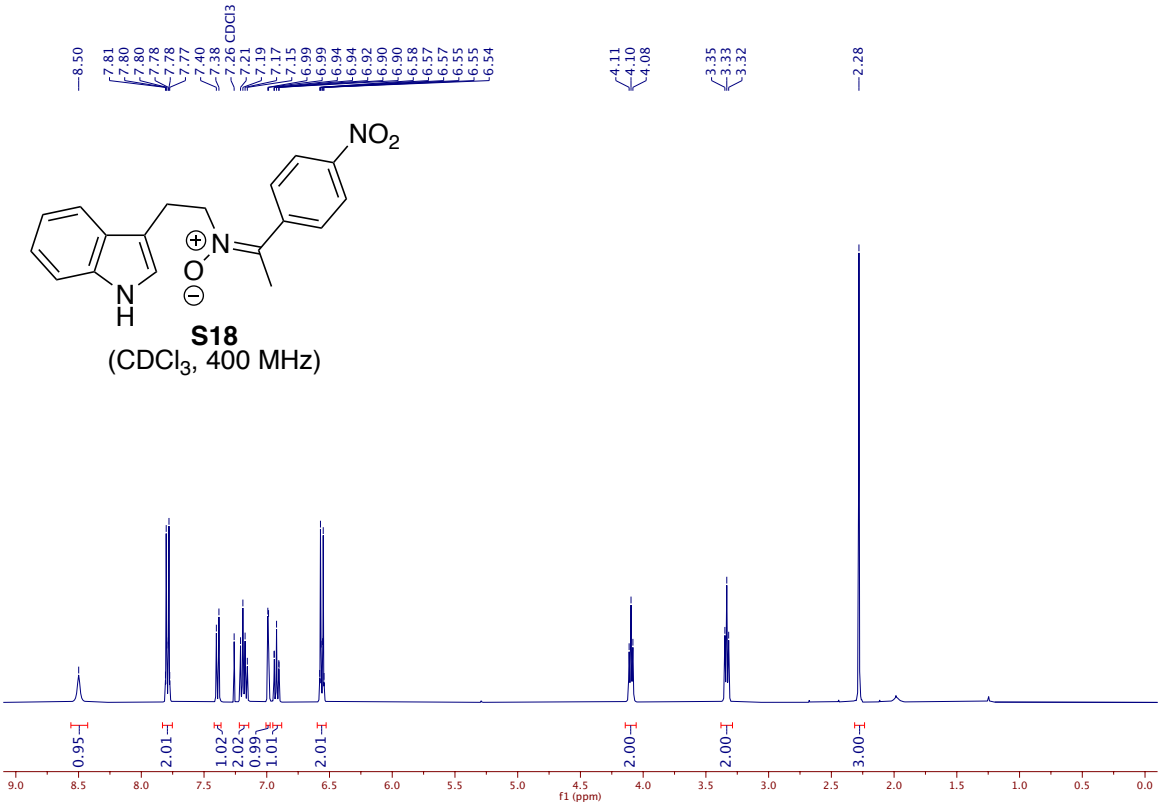

S18
($CDCl_3$, 400 MHz)

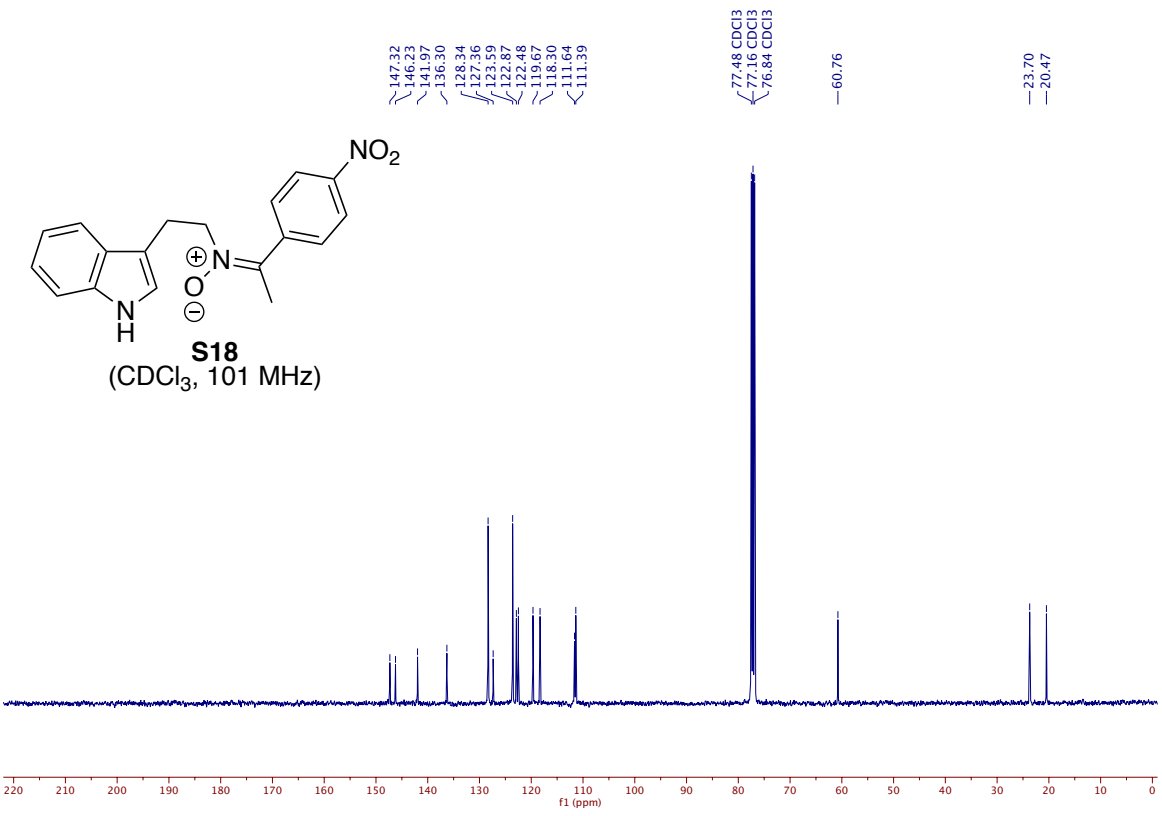

S18
($CDCl_3$, 101 MHz)

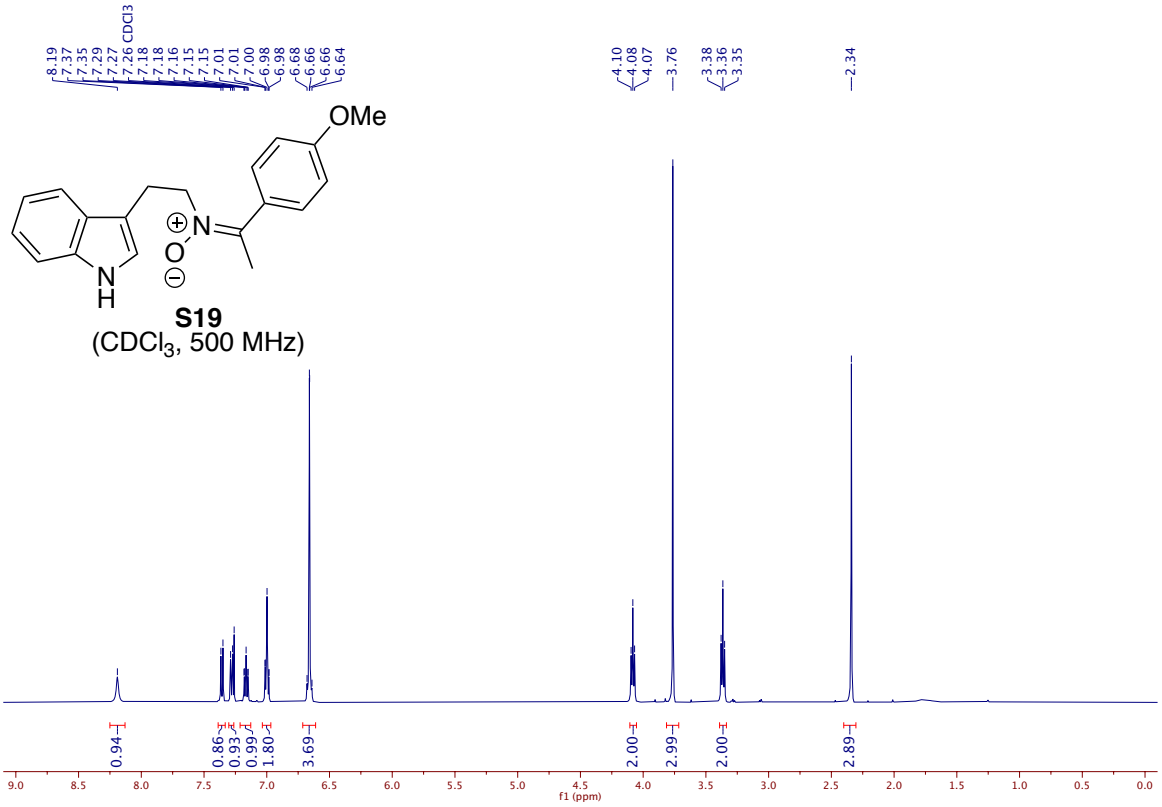

S19
($CDCl_3$, 500 MHz)

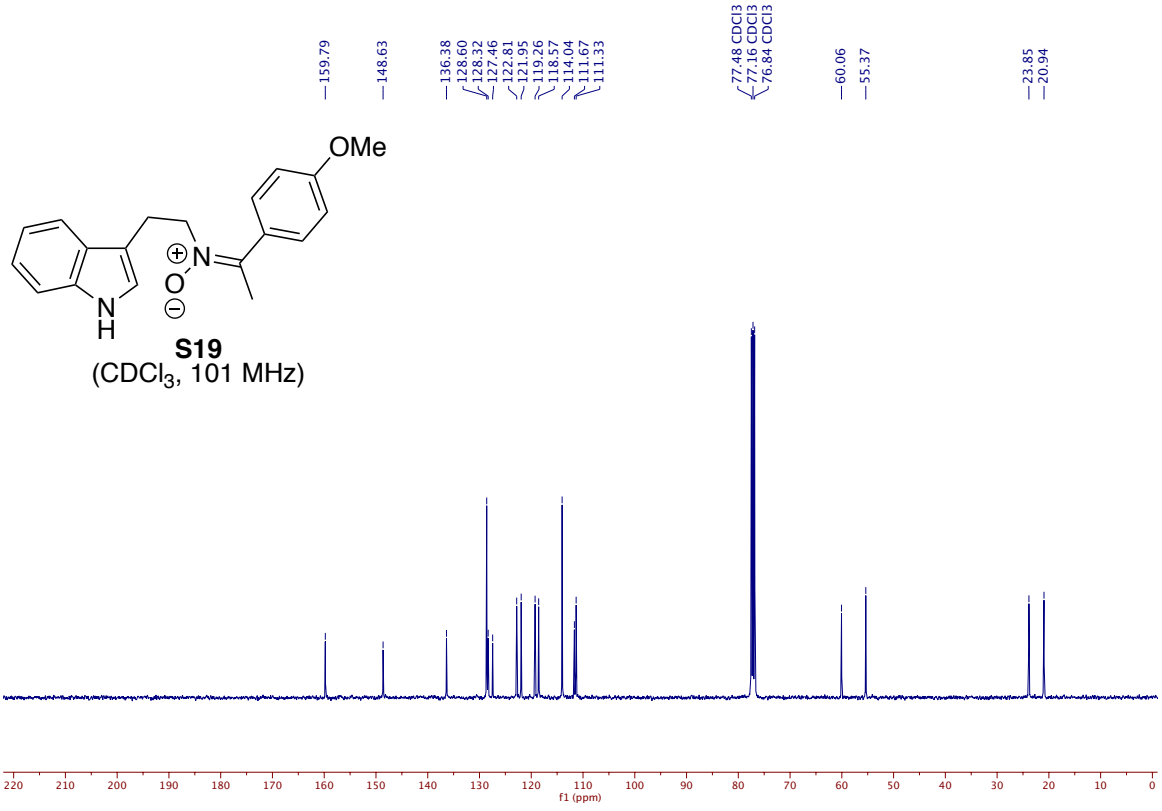

S19
($CDCl_3$, 101 MHz)

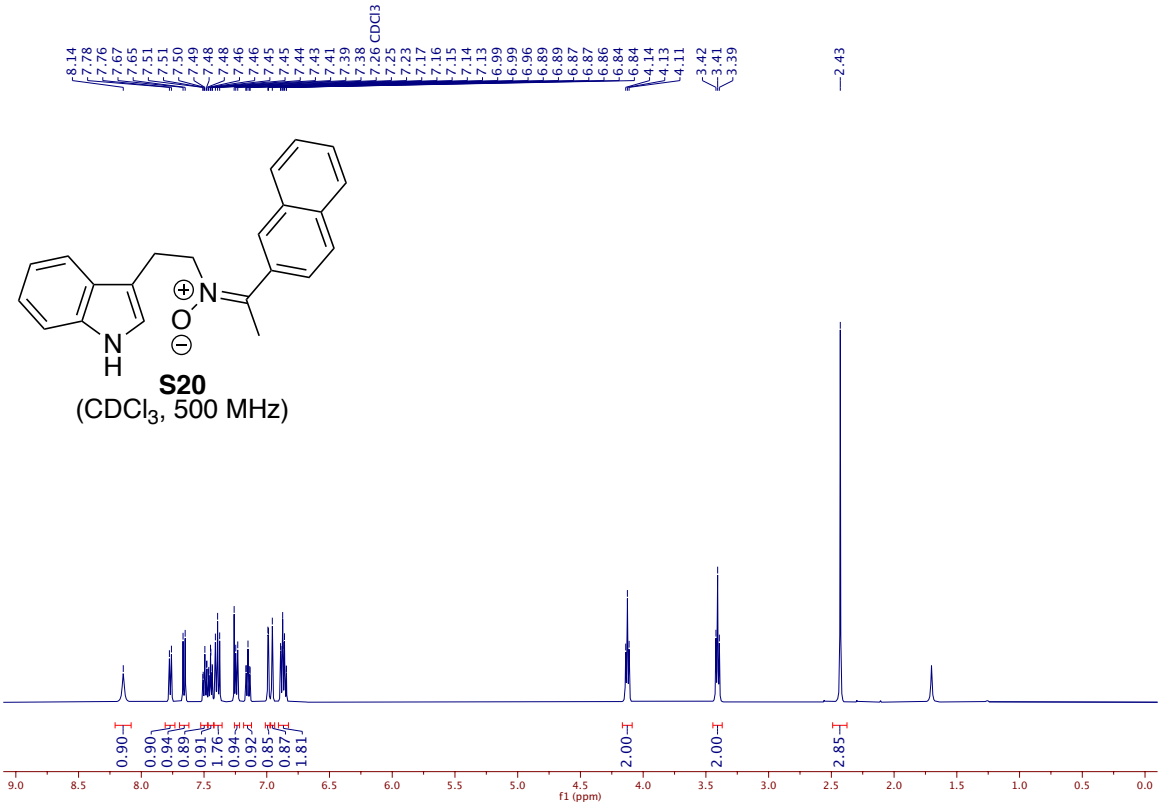

S20
($CDCl_3$, 500 MHz)

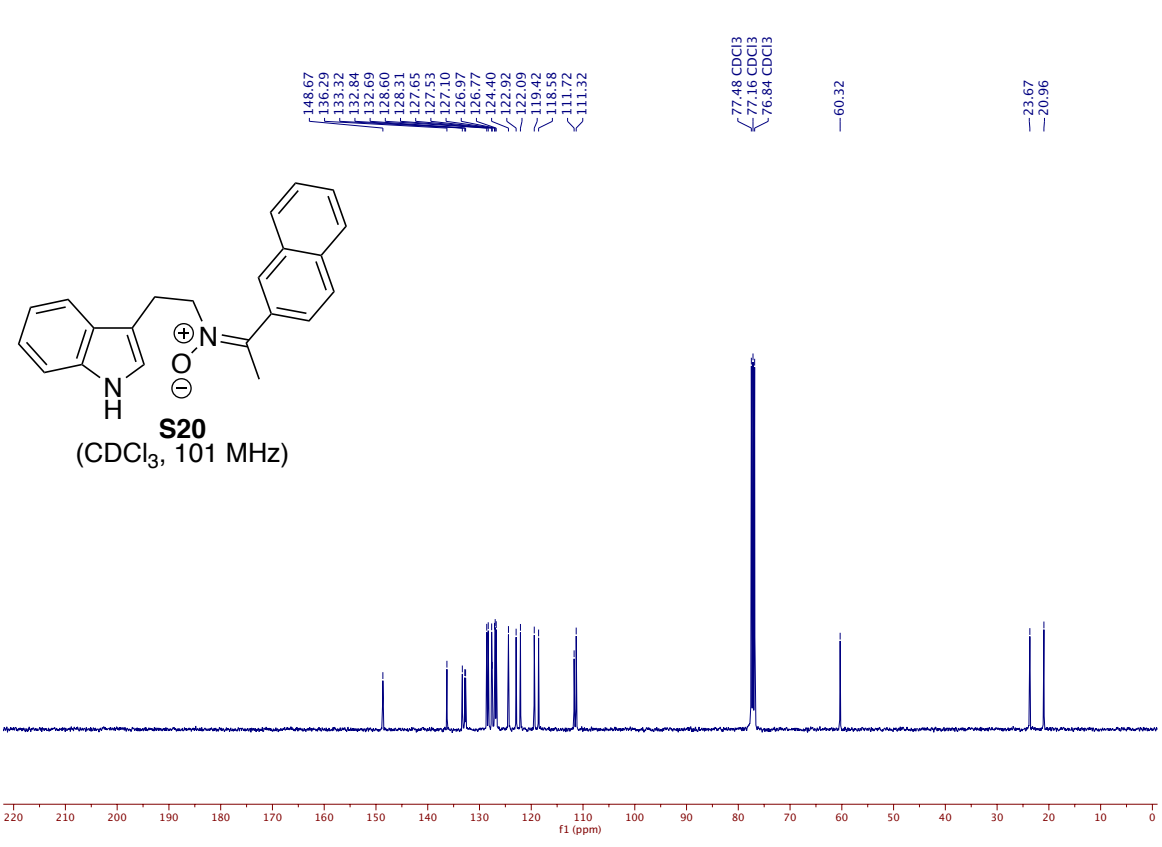

S20
($CDCl_3$, 101 MHz)

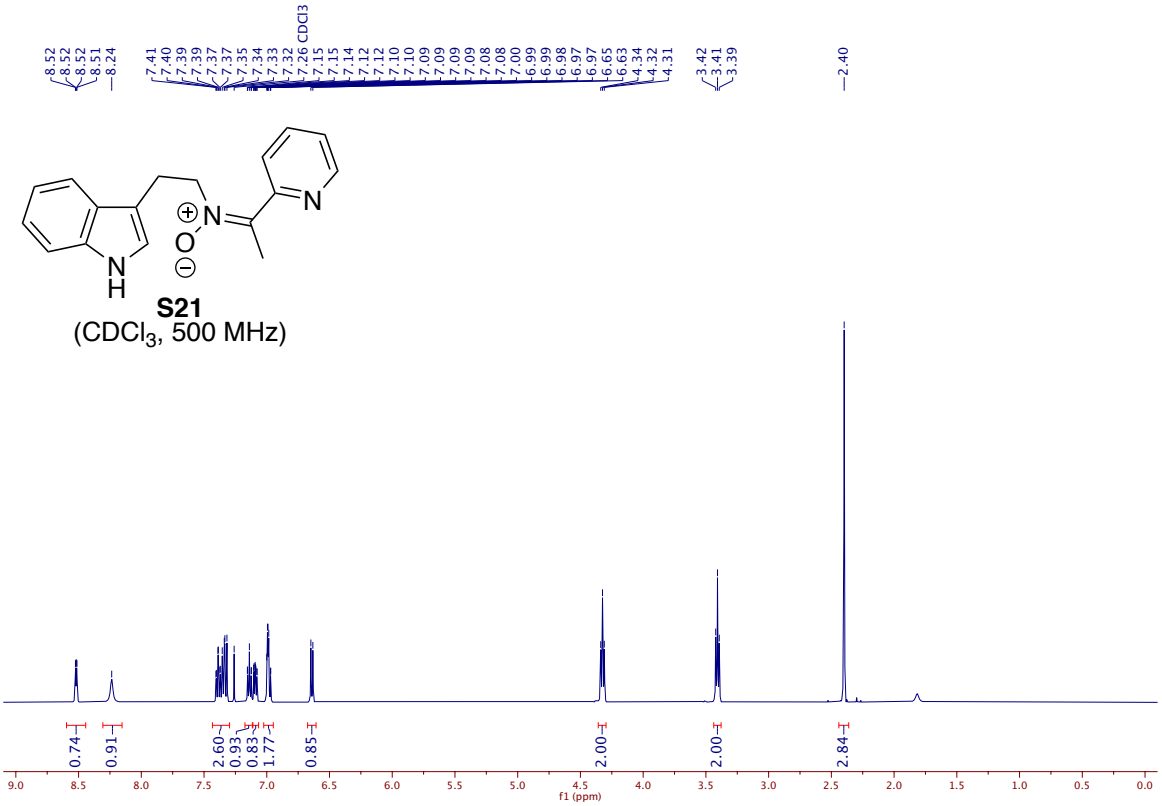

S21
($CDCl_3$, 500 MHz)

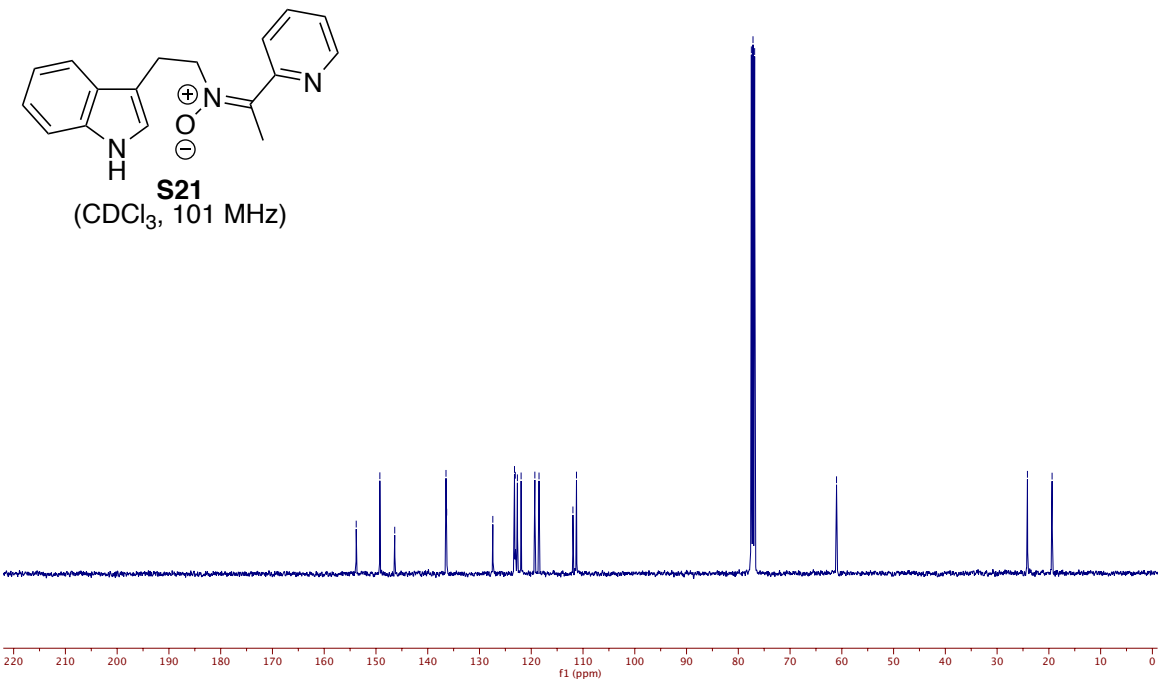

S21
($CDCl_3$, 101 MHz)

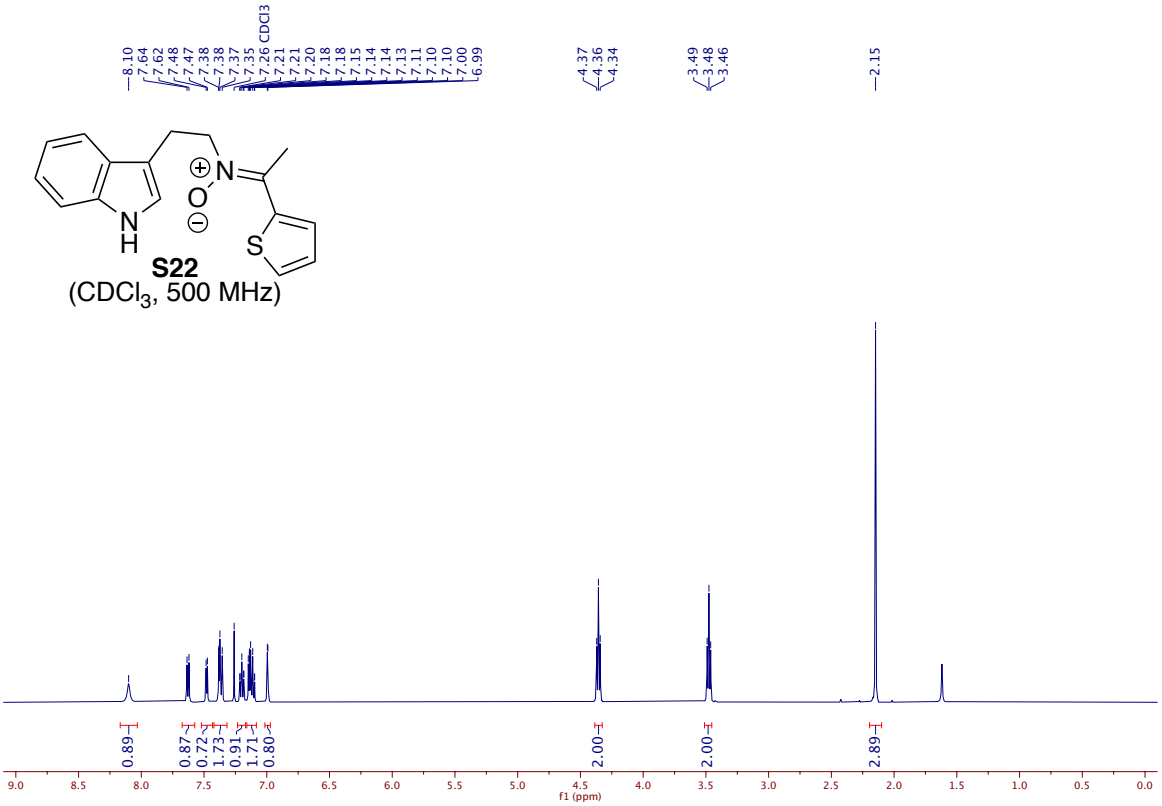
8.10
7.64
7.62
7.48
7.47
7.38
7.38
7.37
7.35
7.26 CDCl3
7.21
7.21
7.20
7.18
7.18
7.15
7.14
7.14
7.13
7.11
7.10
7.10
7.00
6.99
4.37
4.36
4.34
3.49
3.48
3.46
2.15
S22
(CDCl3, 500 MHz)
0.89
0.87
0.72
1.73
0.91
1.71
0.80
2.00
2.00
2.89
f1 (ppm)

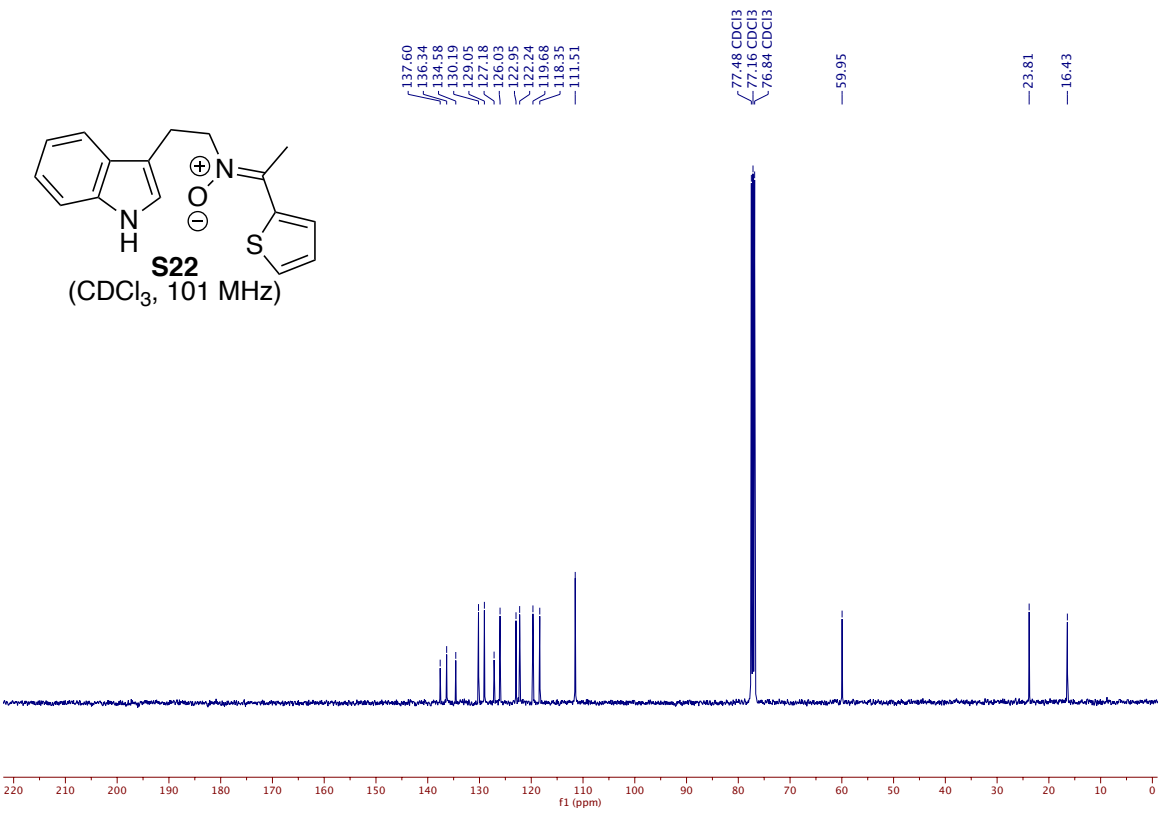
137.60
136.34
134.58
130.19
129.05
127.18
126.03
122.95
122.24
119.68
118.35
111.51
77.48 CDCl3
77.16 CDCl3
76.84 CDCl3
59.95
23.81
16.43
S22
(CDCl3, 101 MHz)
f1 (ppm)

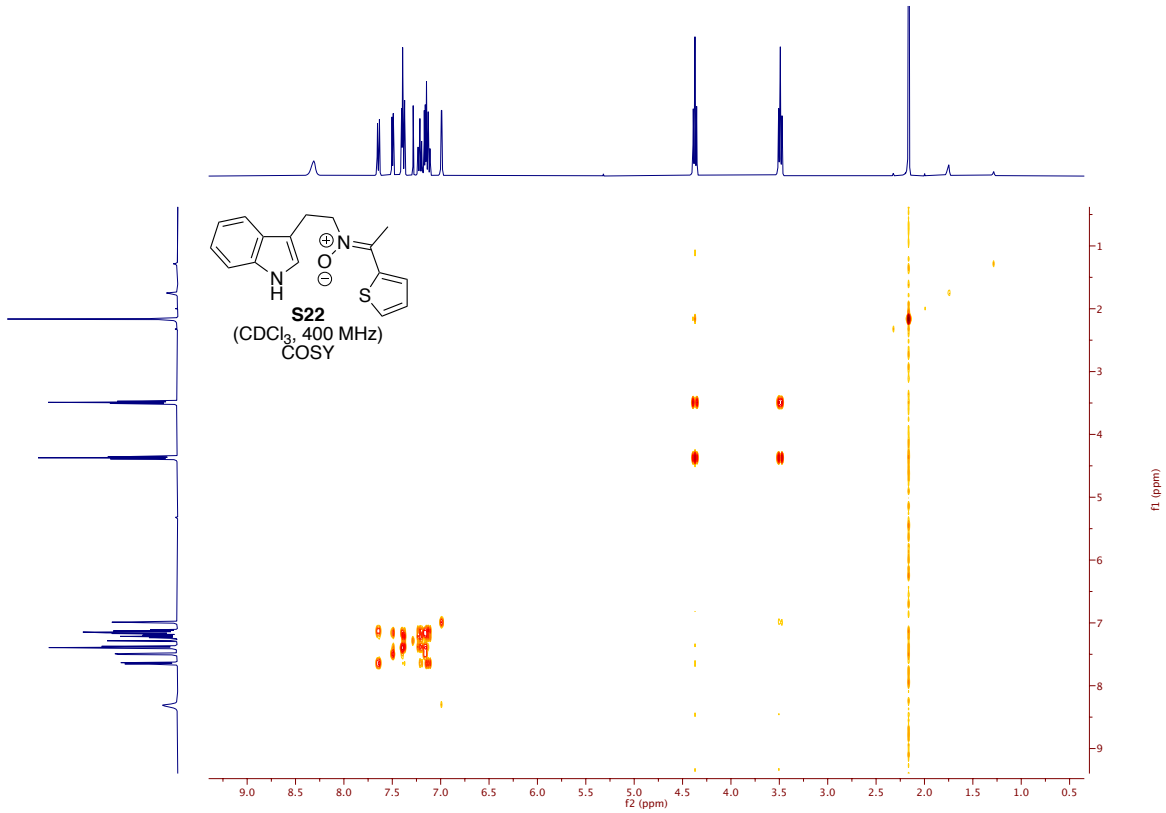
S22
(CDCl3, 400 MHz)
COSY
f2 (ppm)
f1 (ppm)

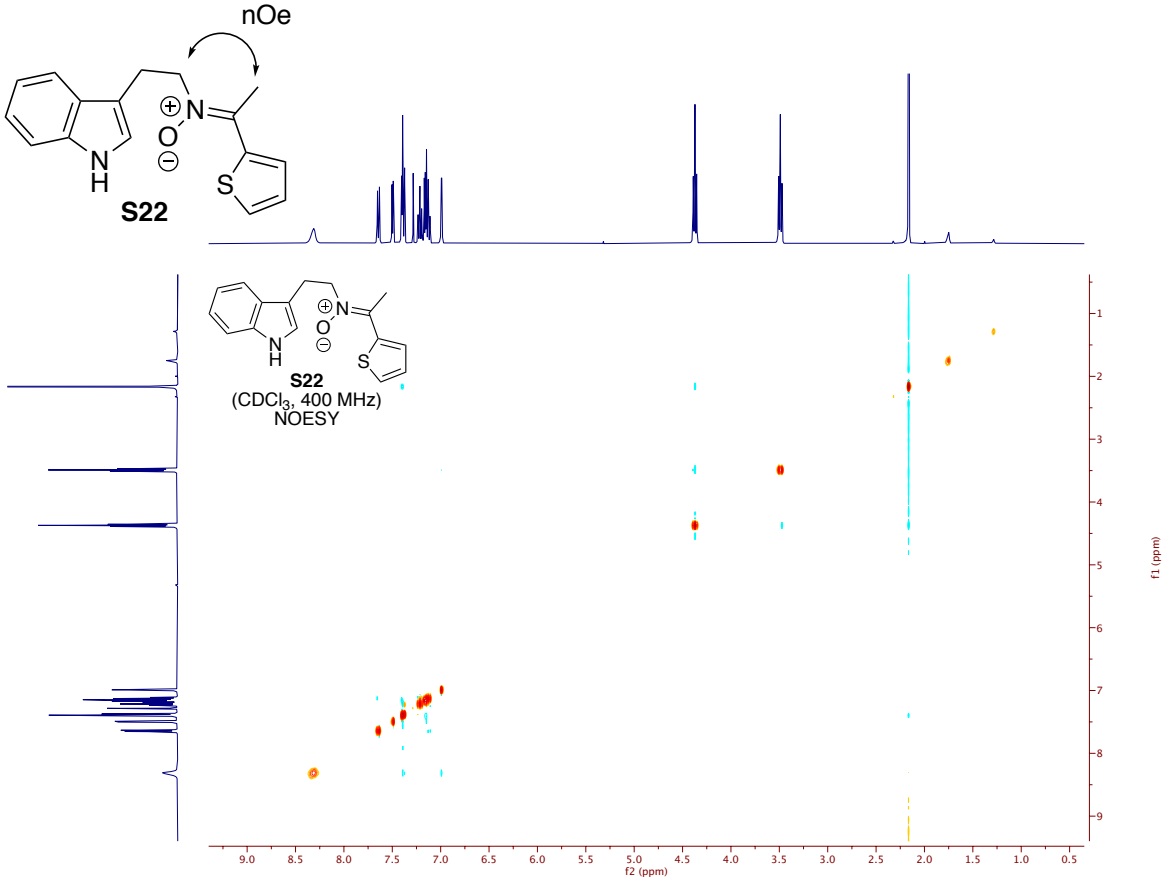
nOe
S22
S22
(CDCl3, 400 MHz)
NOESY
f2 (ppm)
f1 (ppm)

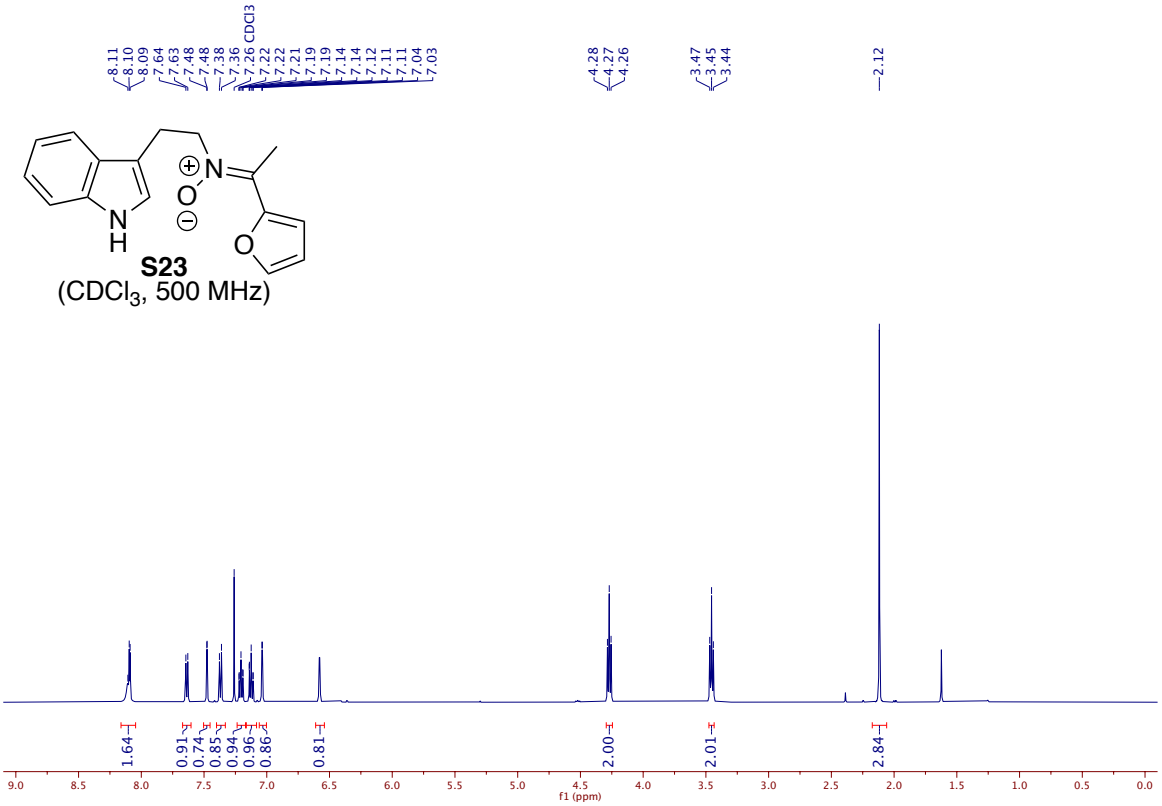

S23
($CDCl_3$, 500 MHz)

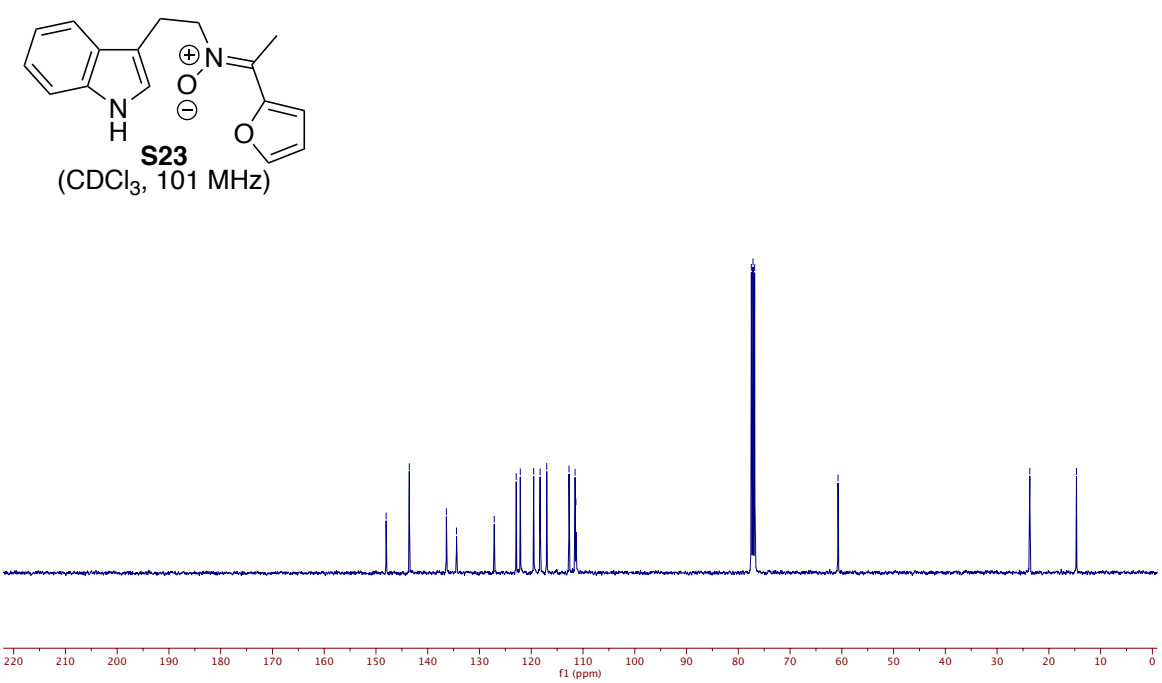

S23
($CDCl_3$, 101 MHz)

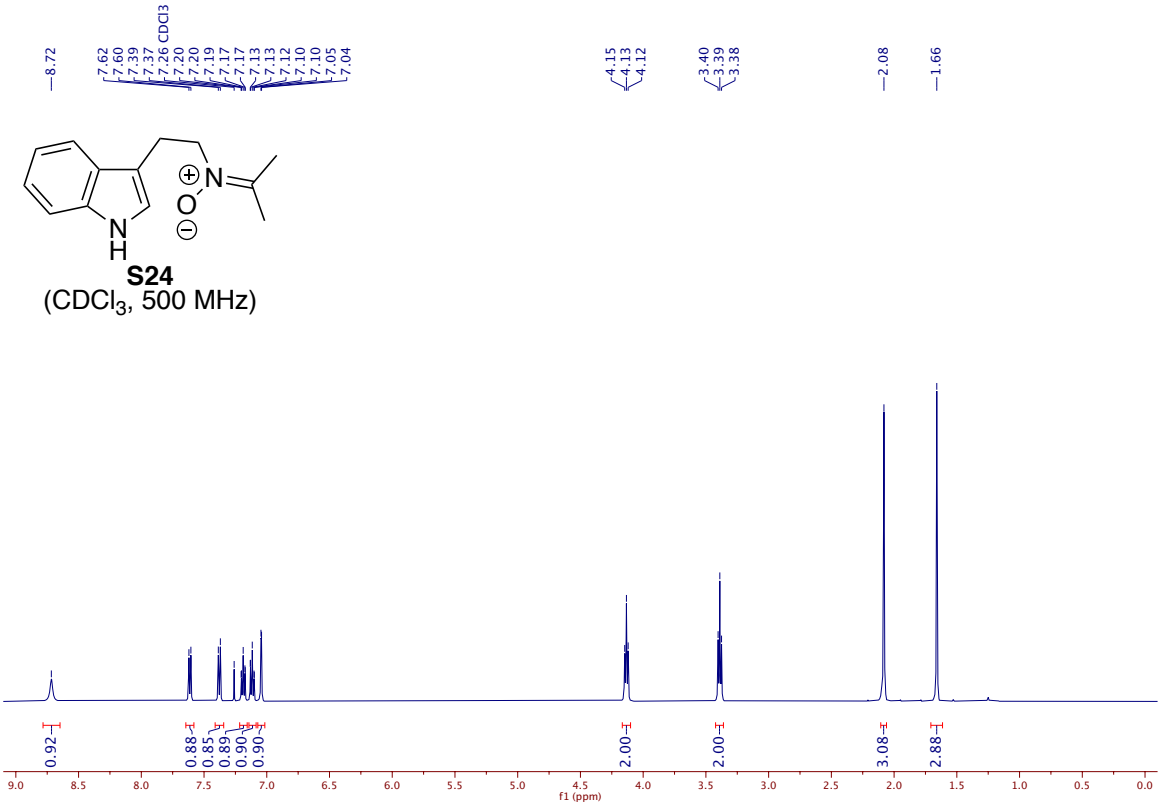

S24
($CDCl_3$, 500 MHz)

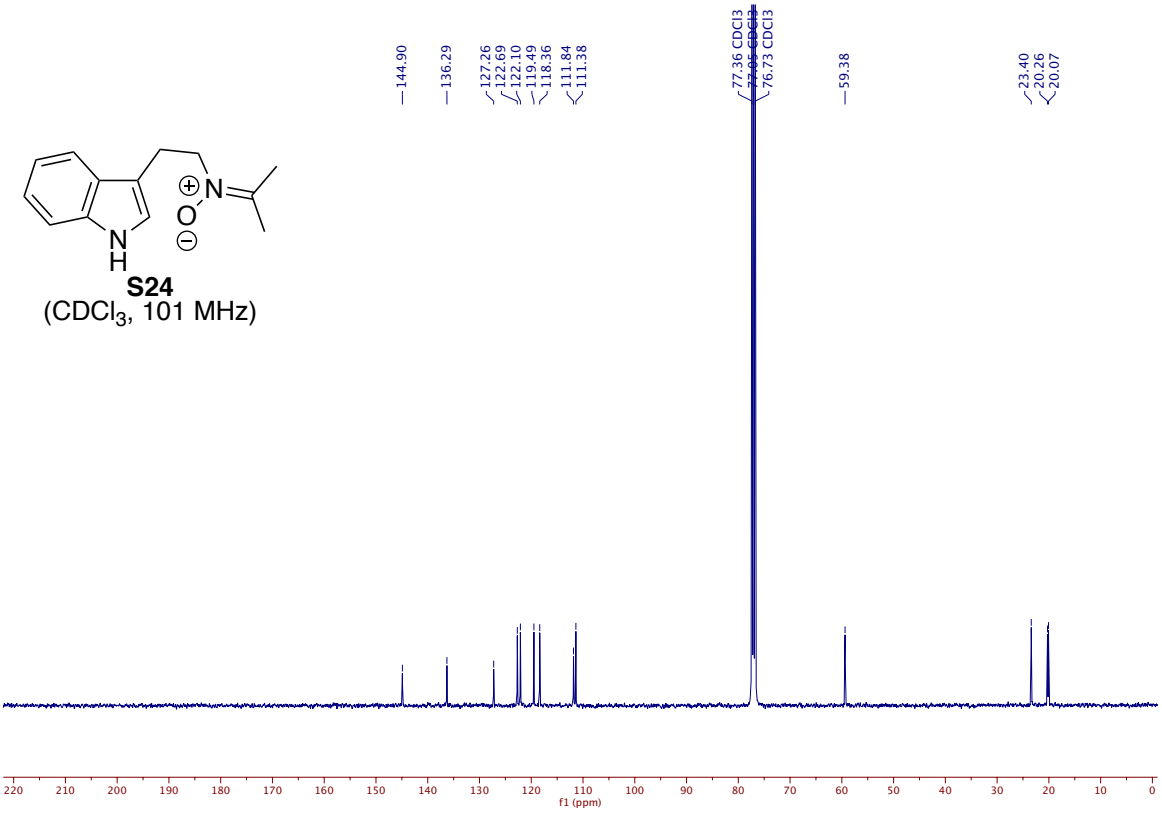

S24
($CDCl_3$, 101 MHz)

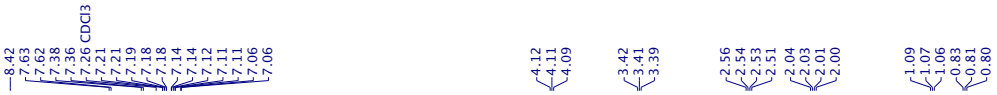

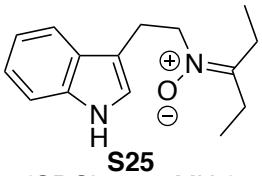

S25
($CDCl_3$, 500 MHz)

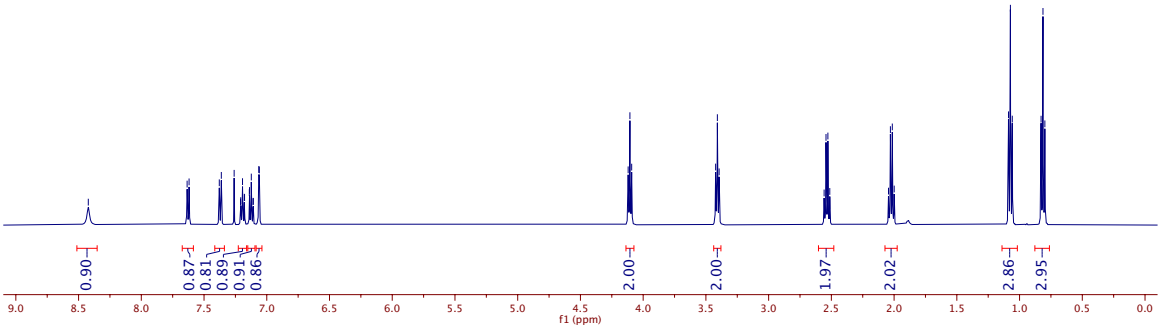

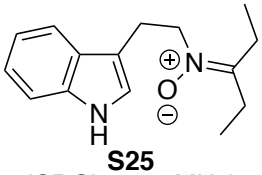

S25
($CDCl_3$, 101 MHz)

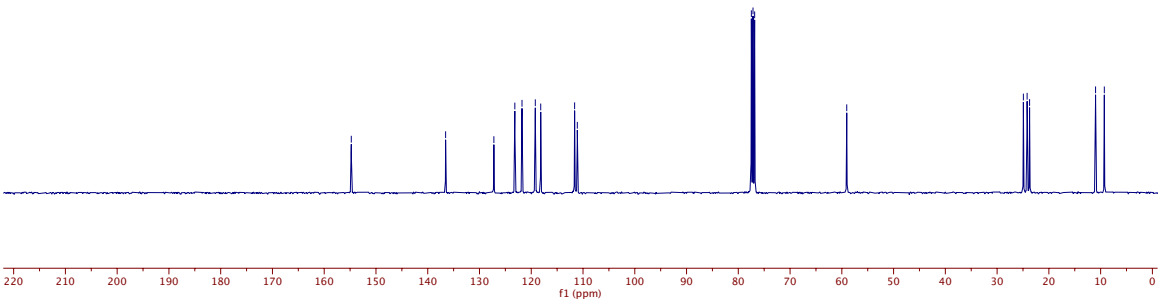

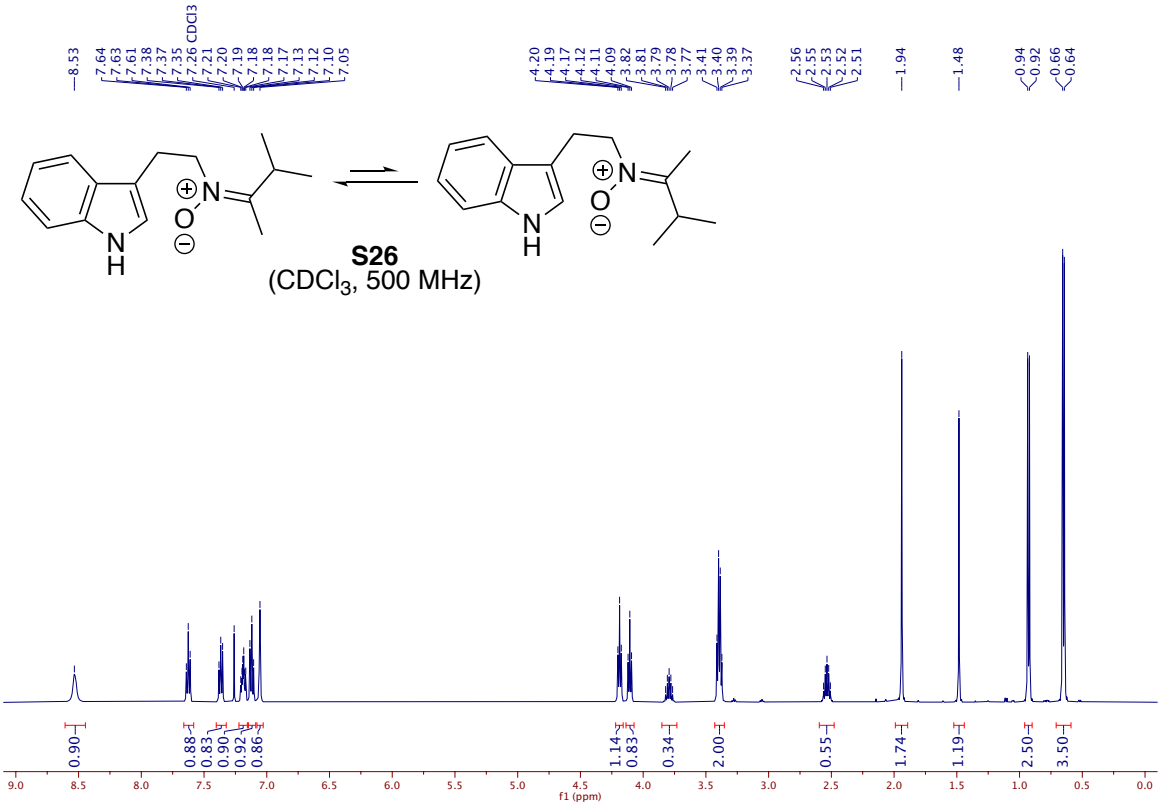
8.53
7.64
7.63
7.61
7.38
7.37
7.35
7.26 CDCl3
7.21
7.20
7.19
7.18
7.18
7.17
7.13
7.12
7.10
7.05
4.20
4.19
4.17
4.12
4.11
4.09
3.82
3.81
3.79
3.78
3.77
3.41
3.40
3.39
3.37
2.56
2.55
2.53
2.52
2.51
1.94
1.48
0.94
0.92
0.66
0.64
S26
(CDCl3, 500 MHz)
0.90
0.88
0.83
0.90
0.92
0.86
1.14
0.83
0.34
2.00
0.55
1.74
1.19
2.50
3.50
f1 (ppm)

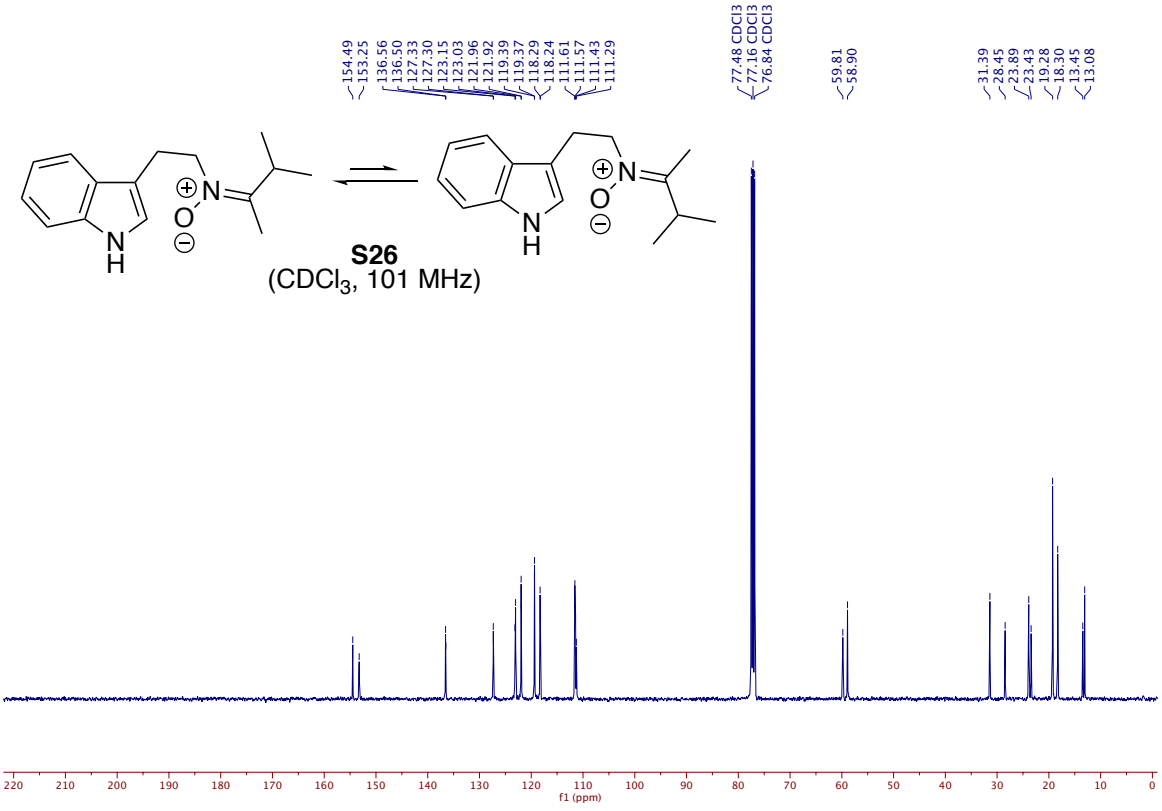
154.49
153.25
136.56
136.50
127.33
127.30
123.15
123.03
121.96
121.92
119.39
119.37
118.29
118.24
111.61
111.57
111.43
111.29
77.48 CDCl3
77.16 CDCl3
76.84 CDCl3
59.81
58.90
31.39
28.45
23.89
23.43
19.28
18.30
13.45
13.08
S26
(CDCl3, 101 MHz)
f1 (ppm)

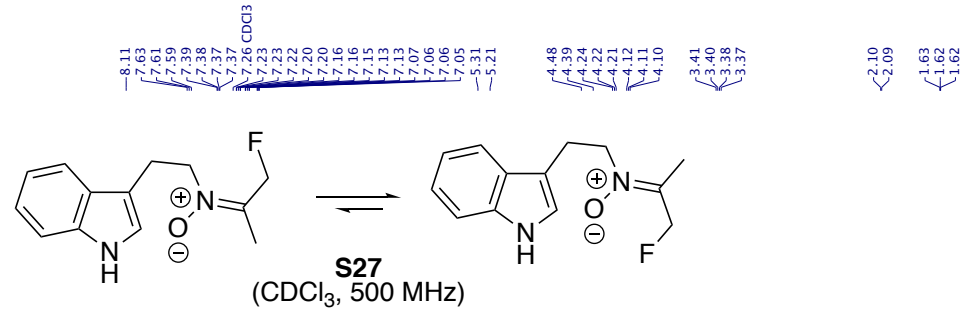

S27
($CDCl_3$, 500 MHz)

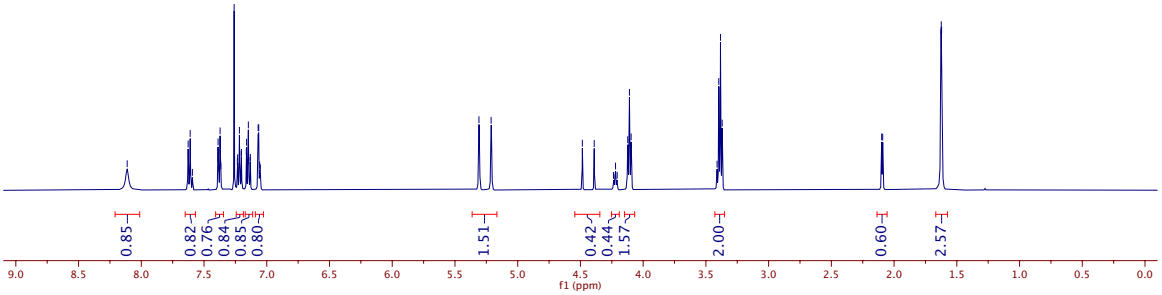

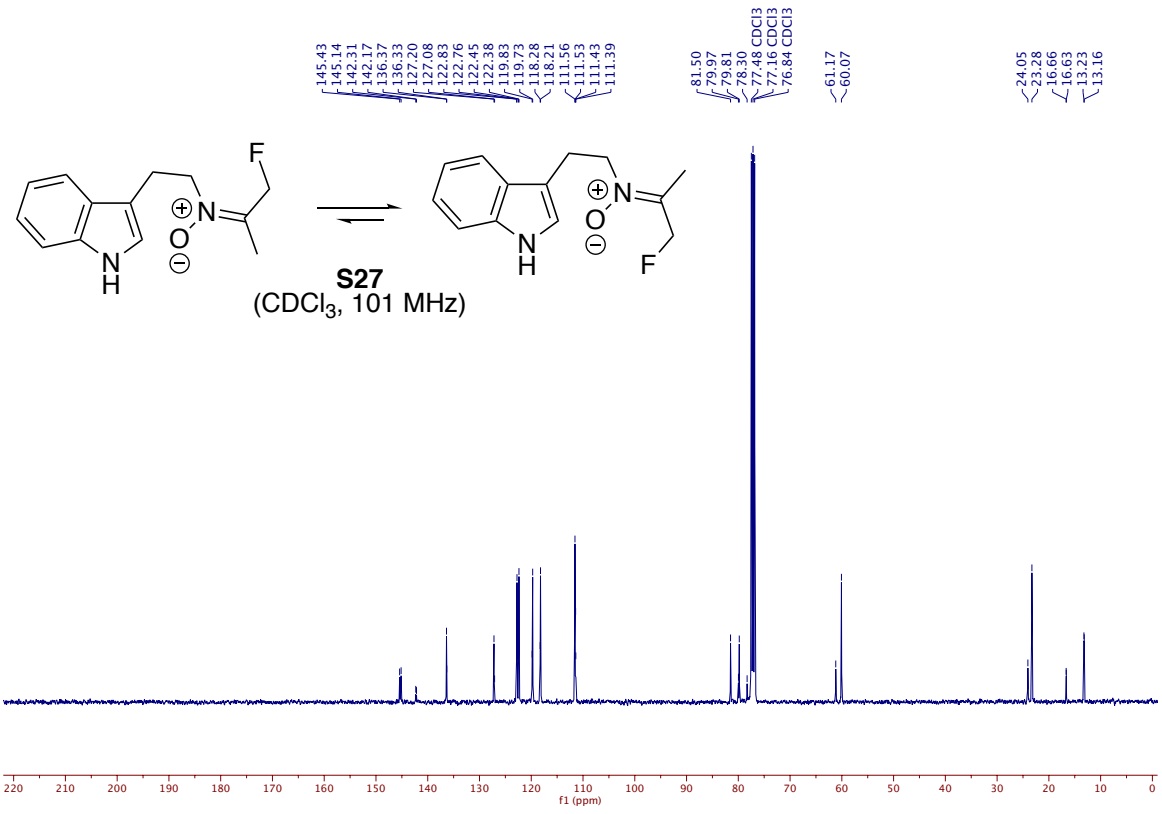

S27
($CDCl_3$, 101 MHz)

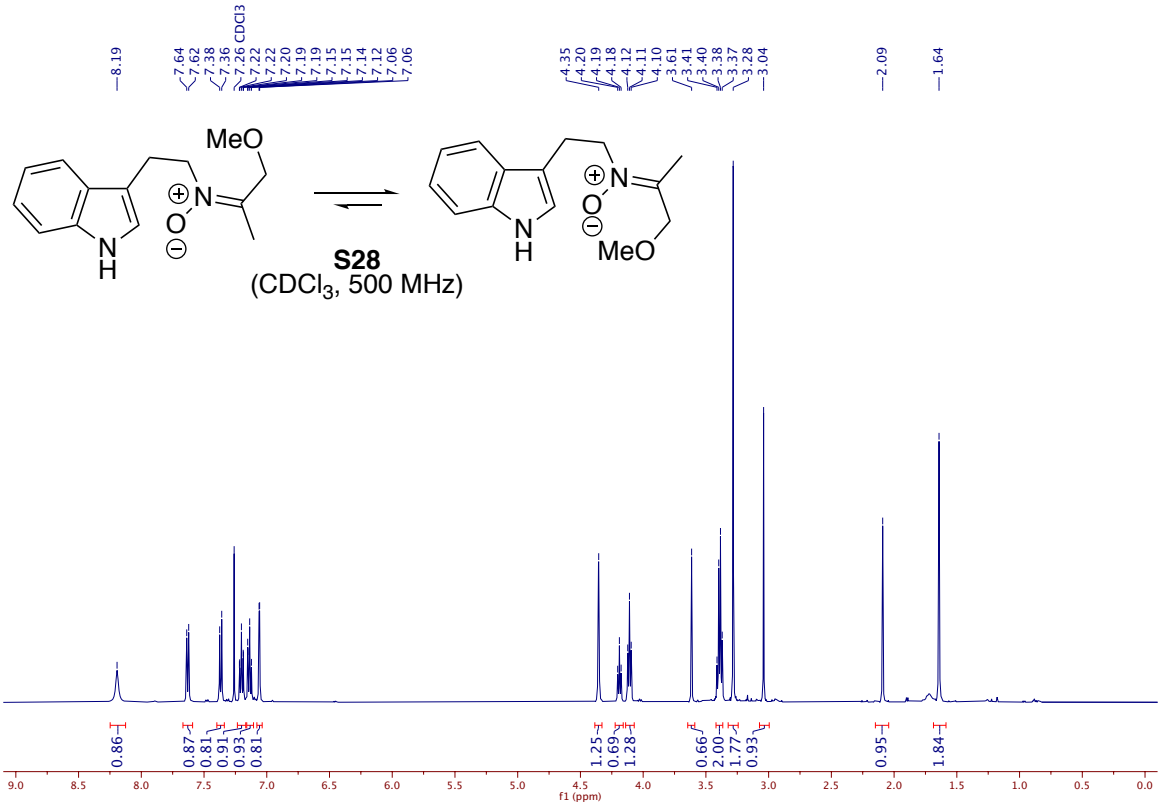
MeO
N
H
N
O
MeO
S28
(CDCl3, 500 MHz)
f1 (ppm)

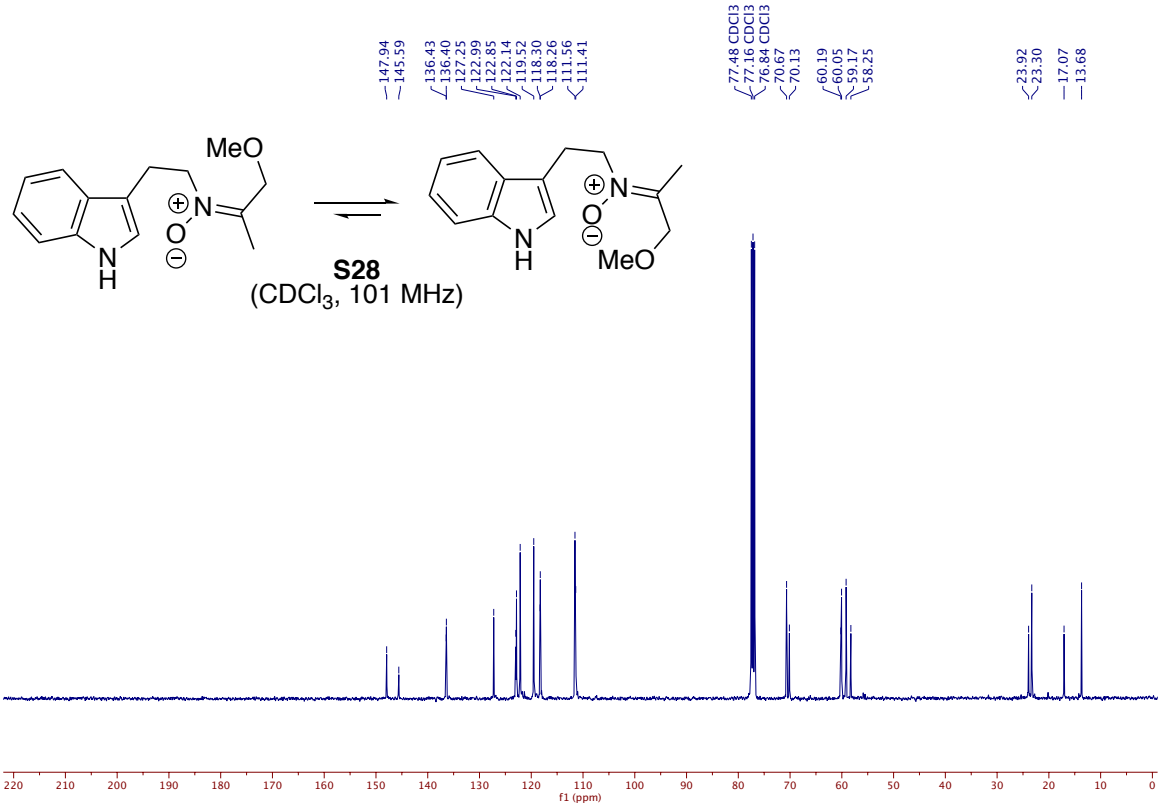
MeO
N
H
N
O
MeO
S28
(CDCl3, 101 MHz)
f1 (ppm)

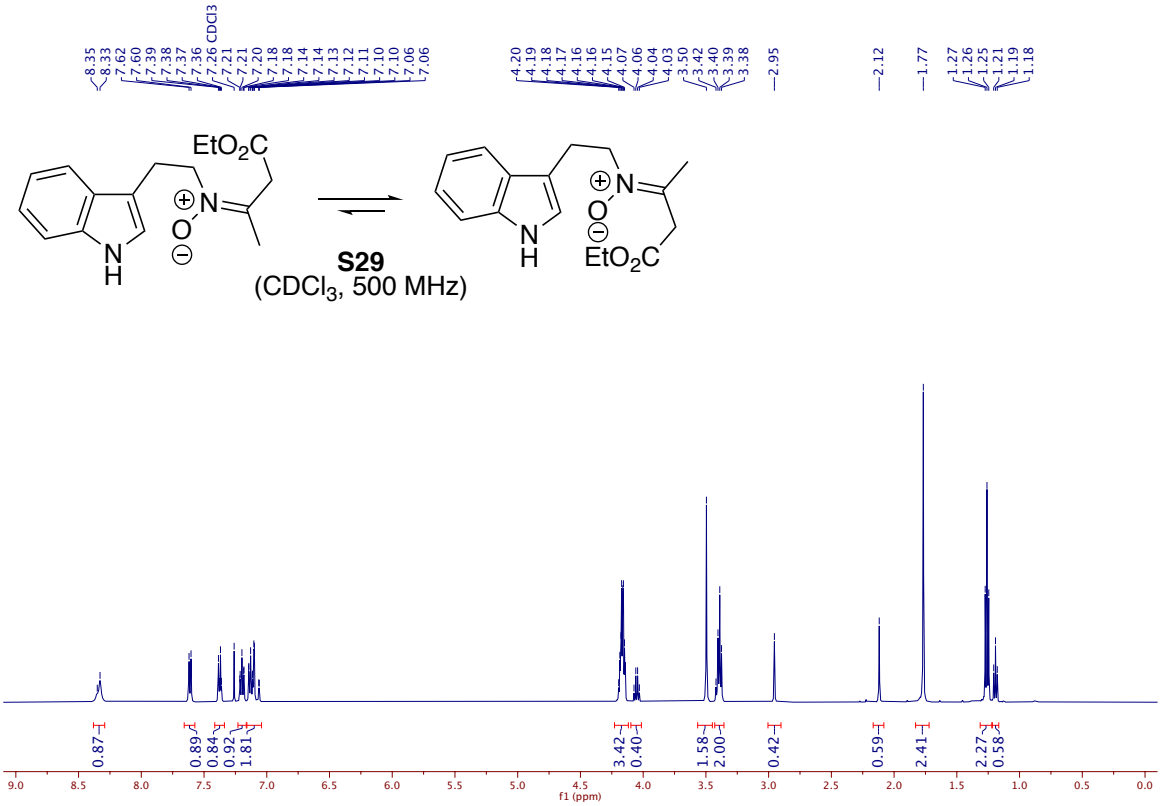
8.35
8.33
7.62
7.60
7.39
7.38
7.37
7.36
7.26 CDCl3
7.21
7.21
7.20
7.18
7.18
7.14
7.14
7.13
7.12
7.11
7.10
7.10
7.06
7.06
4.20
4.19
4.18
4.17
4.16
4.16
4.15
4.07
4.06
4.04
4.03
3.50
3.42
3.40
3.39
3.38
2.95
2.12
1.77
1.27
1.26
1.25
1.21
1.19
1.18
EtO2C
N
H
O
EtO2C
S29
(CDCl3, 500 MHz)
0.87
0.89
0.84
0.92
1.81
3.42
0.40
1.58
2.00
0.42
0.59
2.41
2.27
0.58
f1 (ppm)

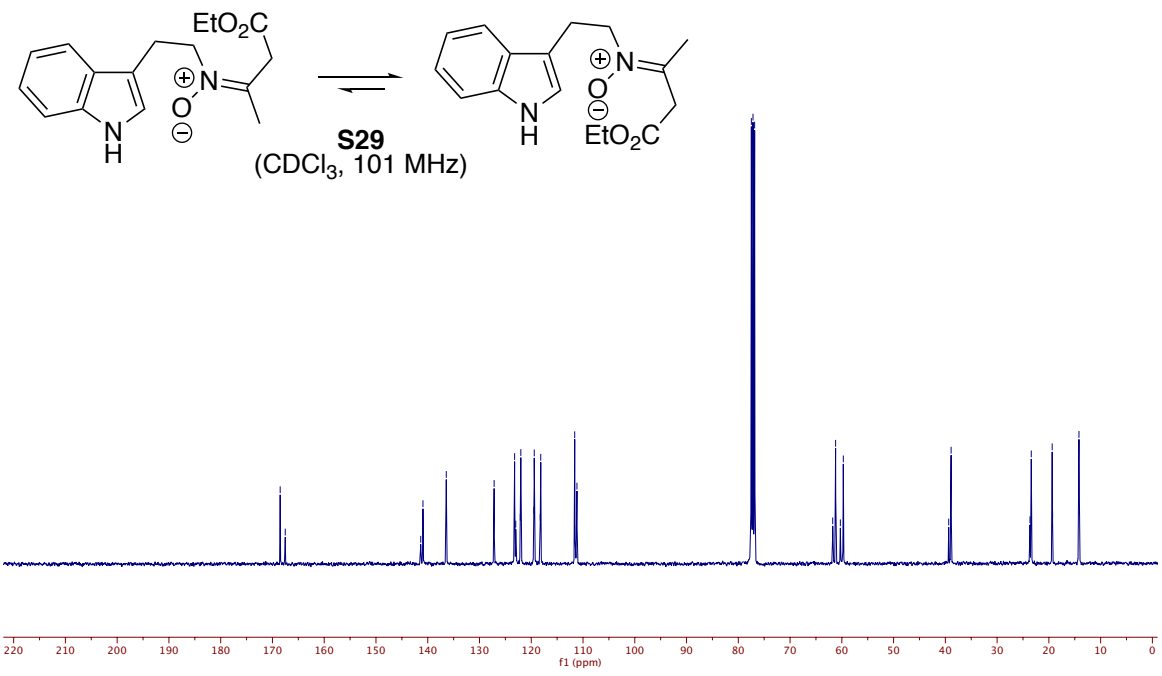
168.51
167.53
141.35
140.92
136.42
127.17
123.21
123.00
122.11
122.02
119.49
119.42
118.27
118.17
111.60
111.28
111.17
77.48 CDCl3
77.16 CDCl3
76.84 CDCl3
61.76
61.20
60.28
59.72
39.35
38.89
23.64
23.40
19.36
19.29
14.19
14.10
EtO2C
N
H
O
EtO2C
S29
(CDCl3, 101 MHz)
f1 (ppm)

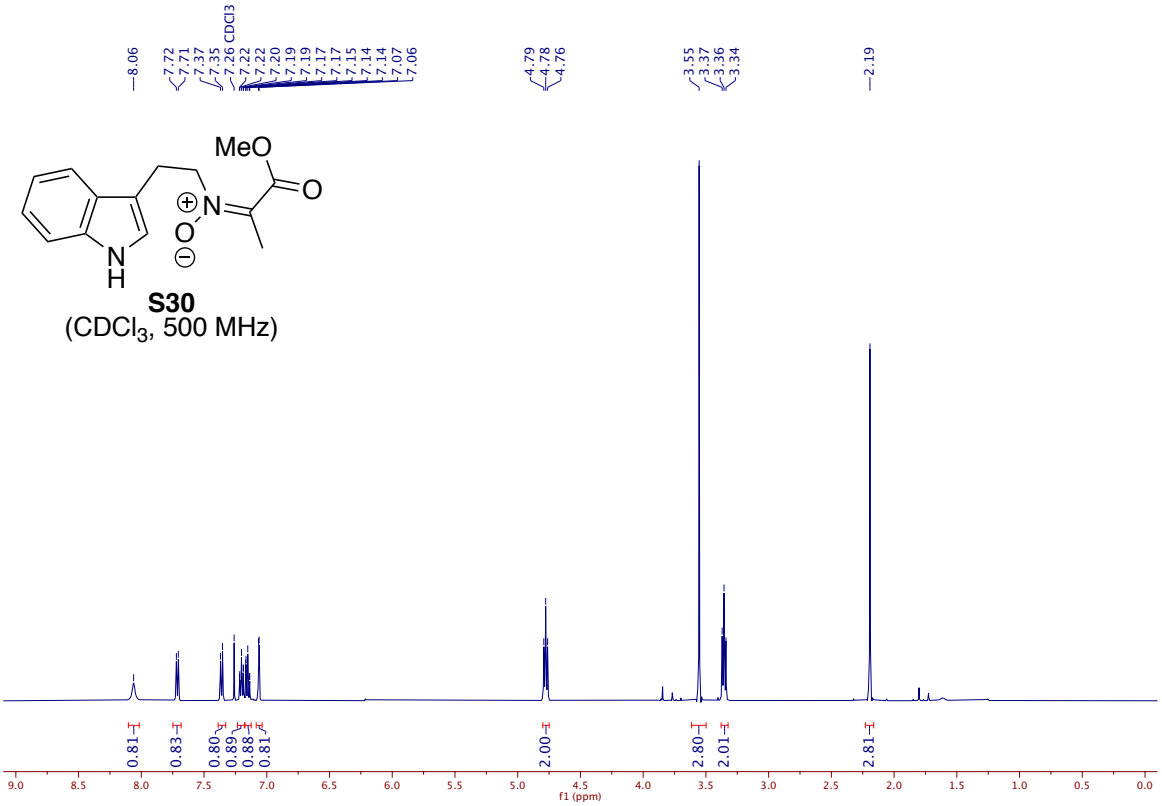

S30
($CDCl_3$, 500 MHz)

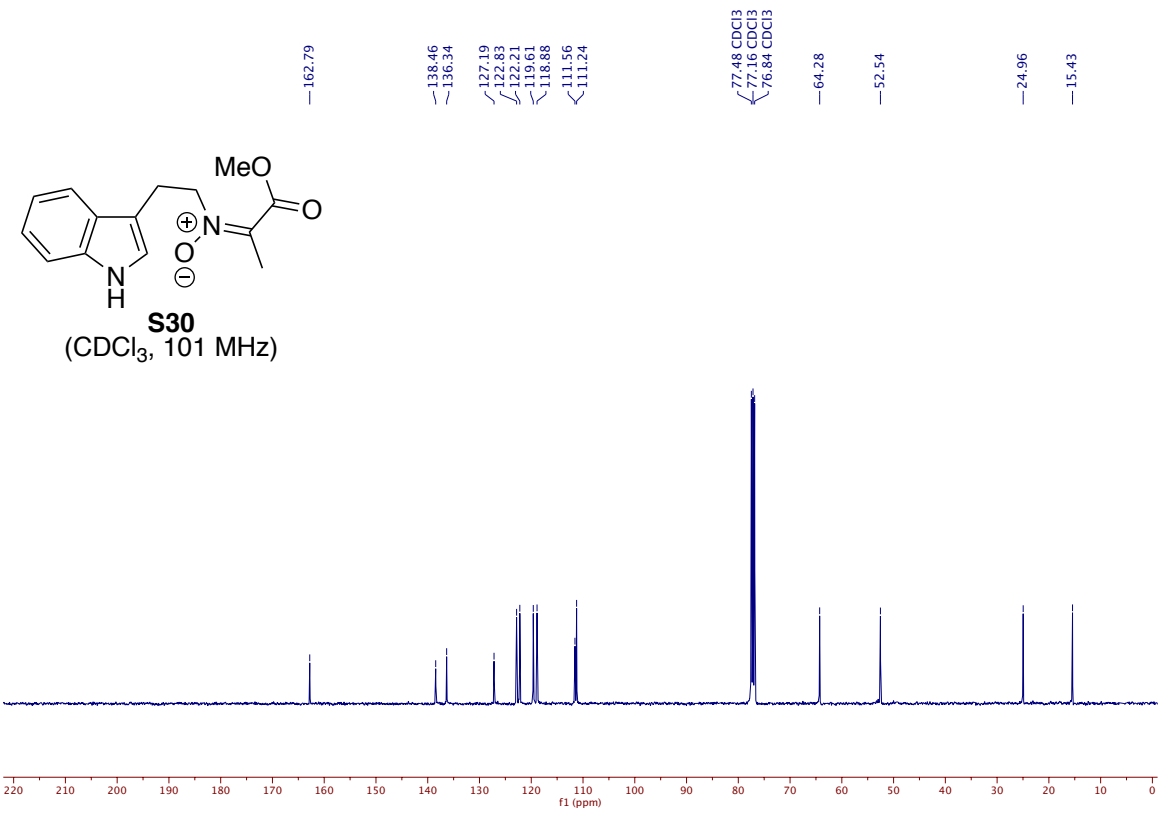

S30
($CDCl_3$, 101 MHz)

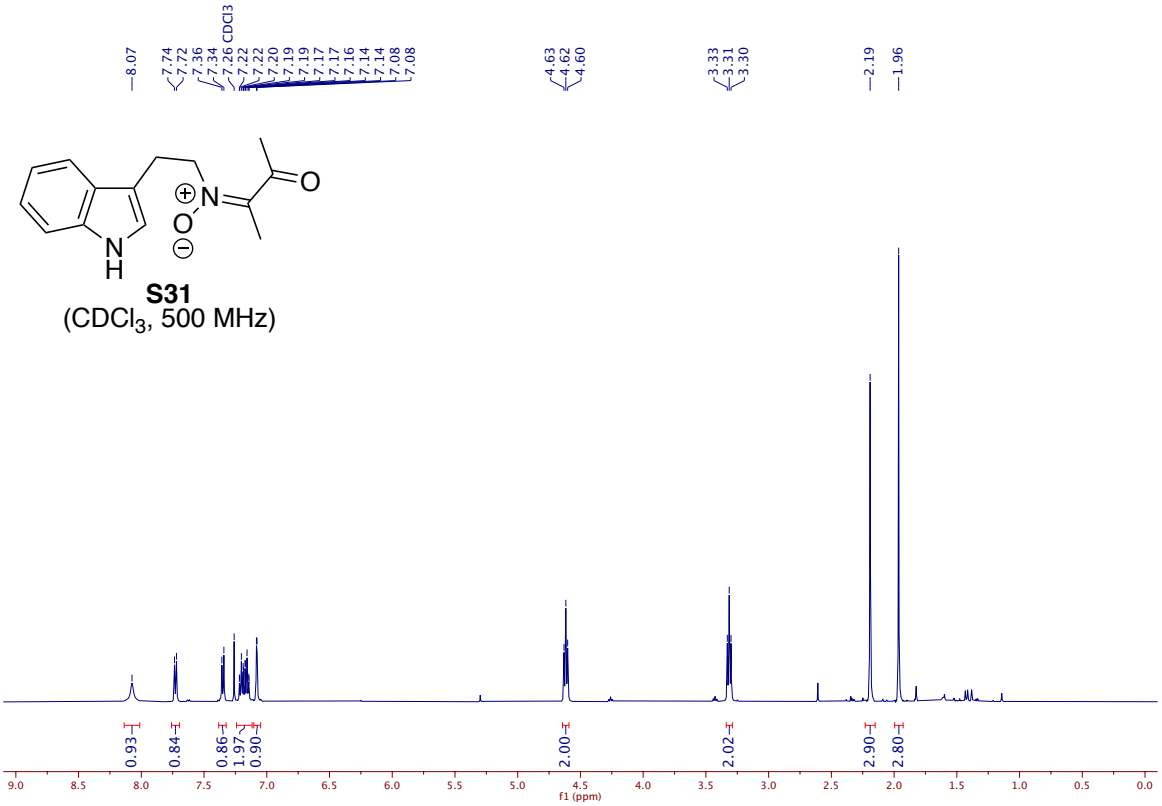

S31
($CDCl_3$, 500 MHz)

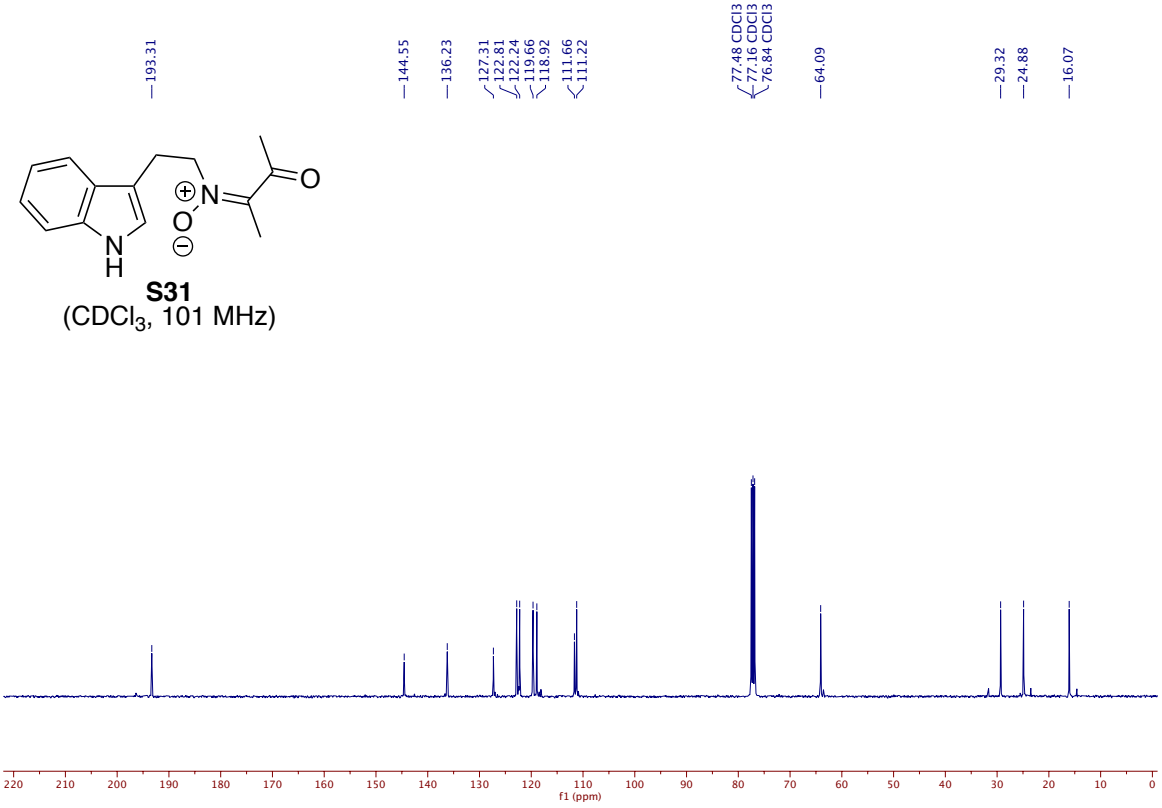

S31
($CDCl_3$, 101 MHz)

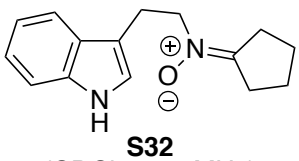

S32
($CDCl_3$, 500 MHz)

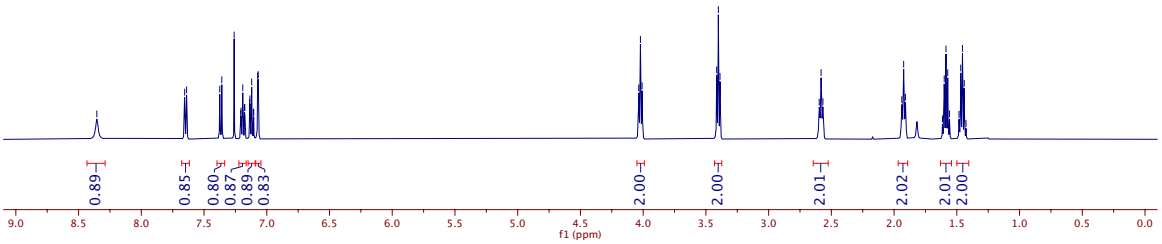

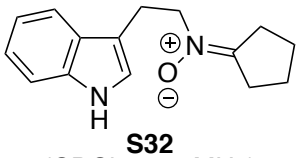

S32
($CDCl_3$, 101 MHz)

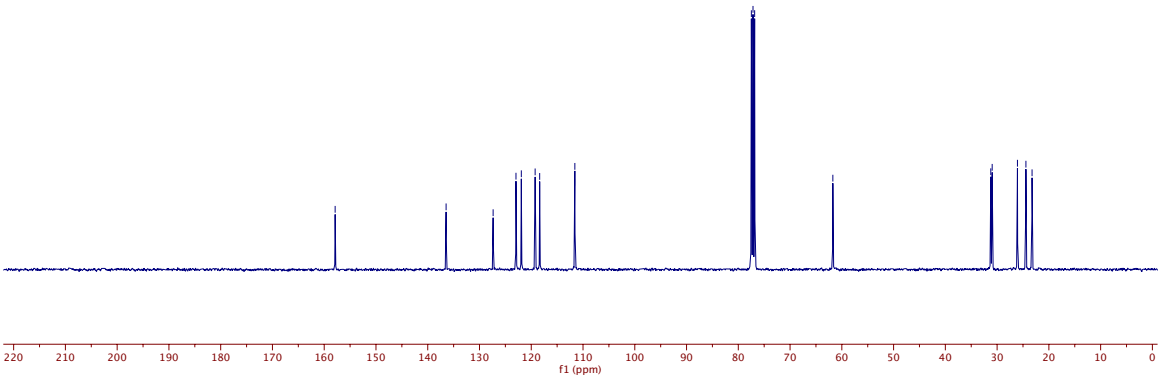

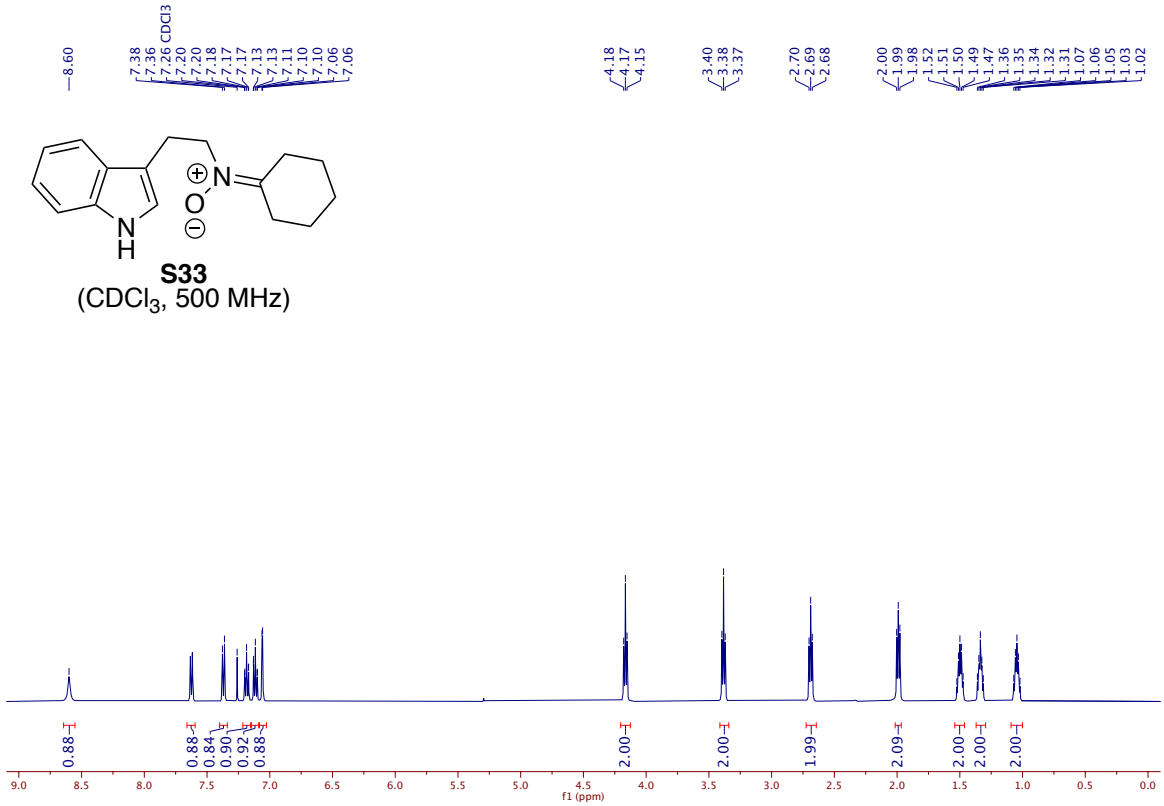

S33
($CDCl_3$, 500 MHz)

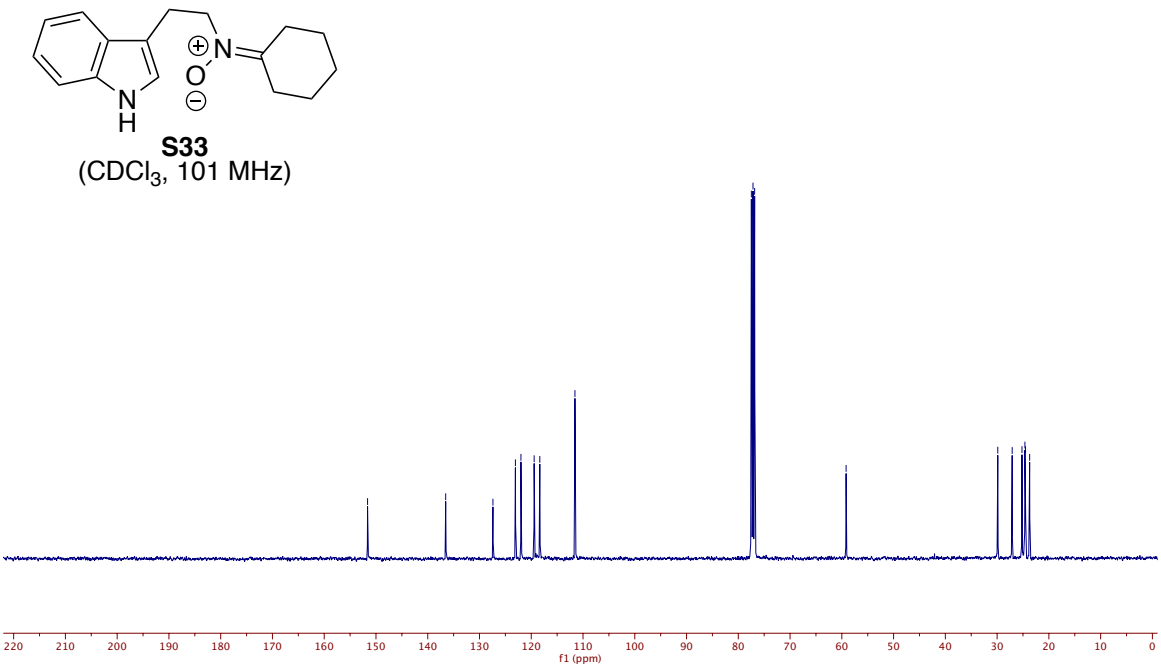

S33
($CDCl_3$, 101 MHz)

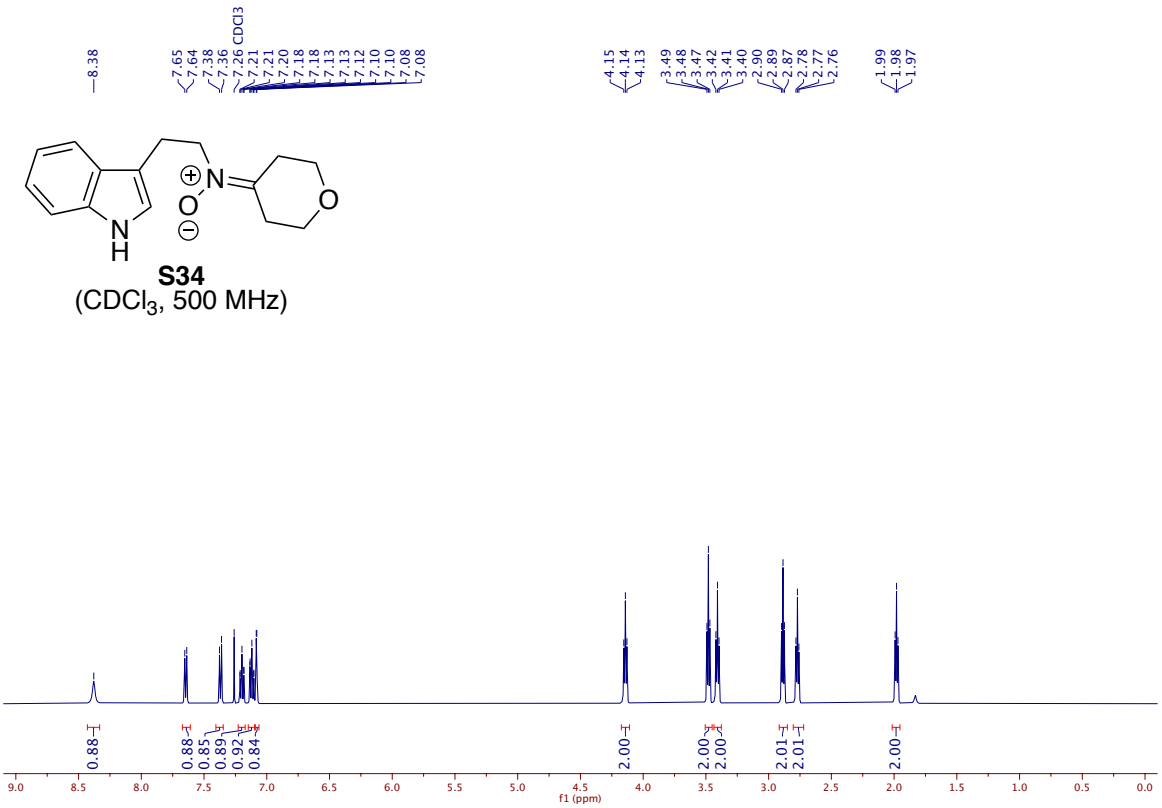

S34
($CDCl_3$, 500 MHz)

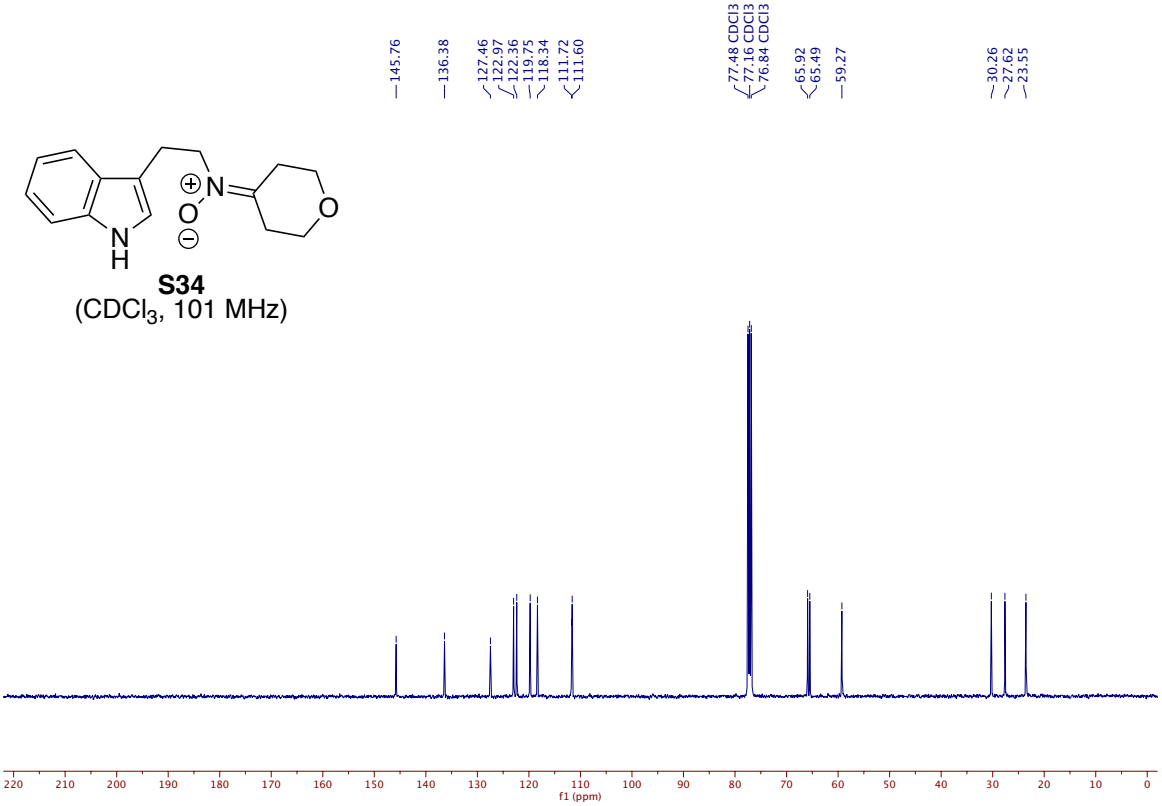

S34
($CDCl_3$, 101 MHz)

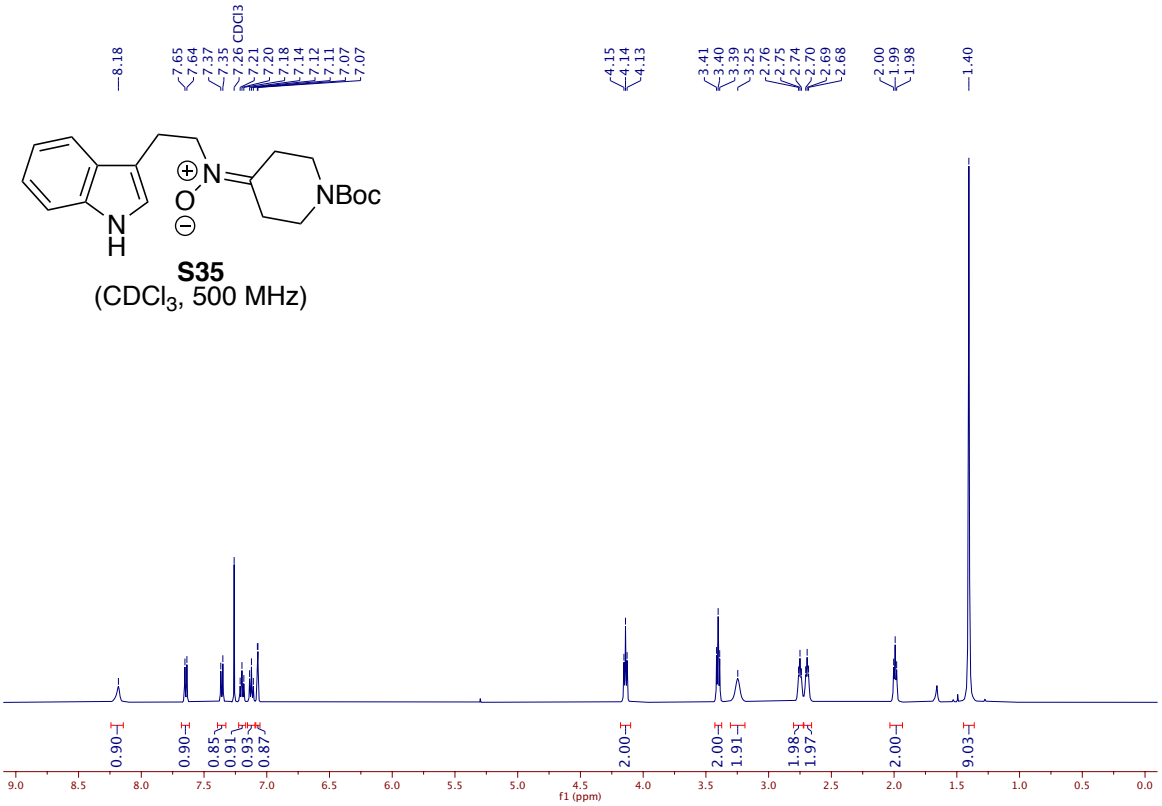

S35
($CDCl_3$, 500 MHz)

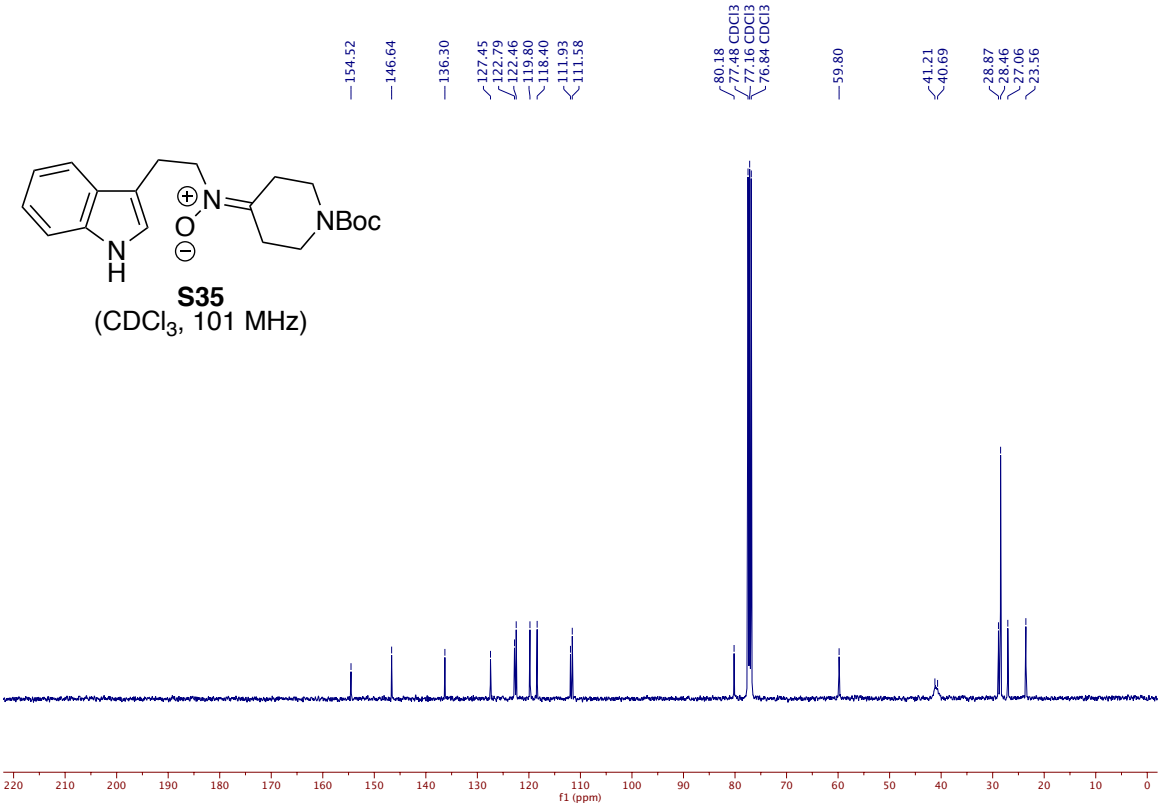

S35
($CDCl_3$, 101 MHz)

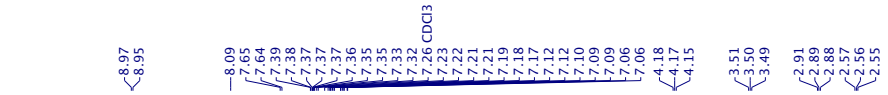

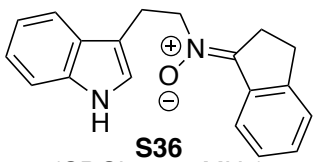

S36
($CDCl_3$, 500 MHz)

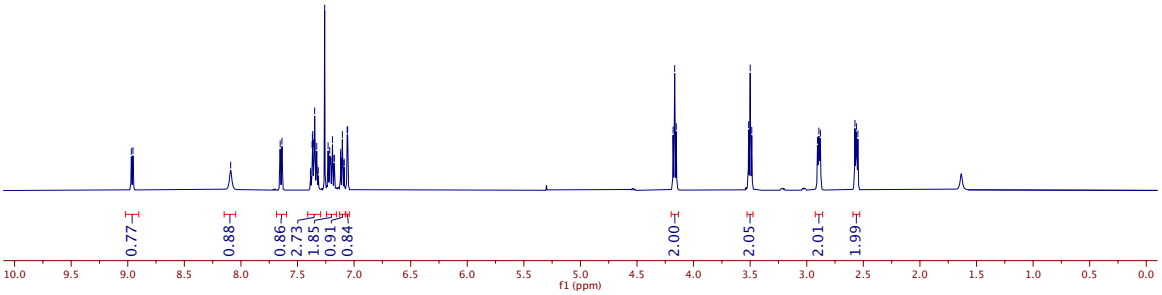

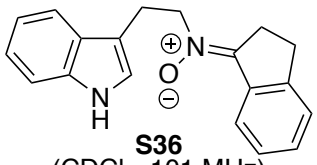

S36
($CDCl_3$, 101 MHz)

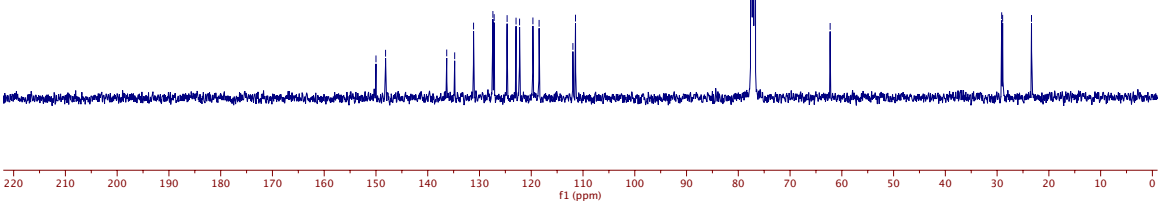

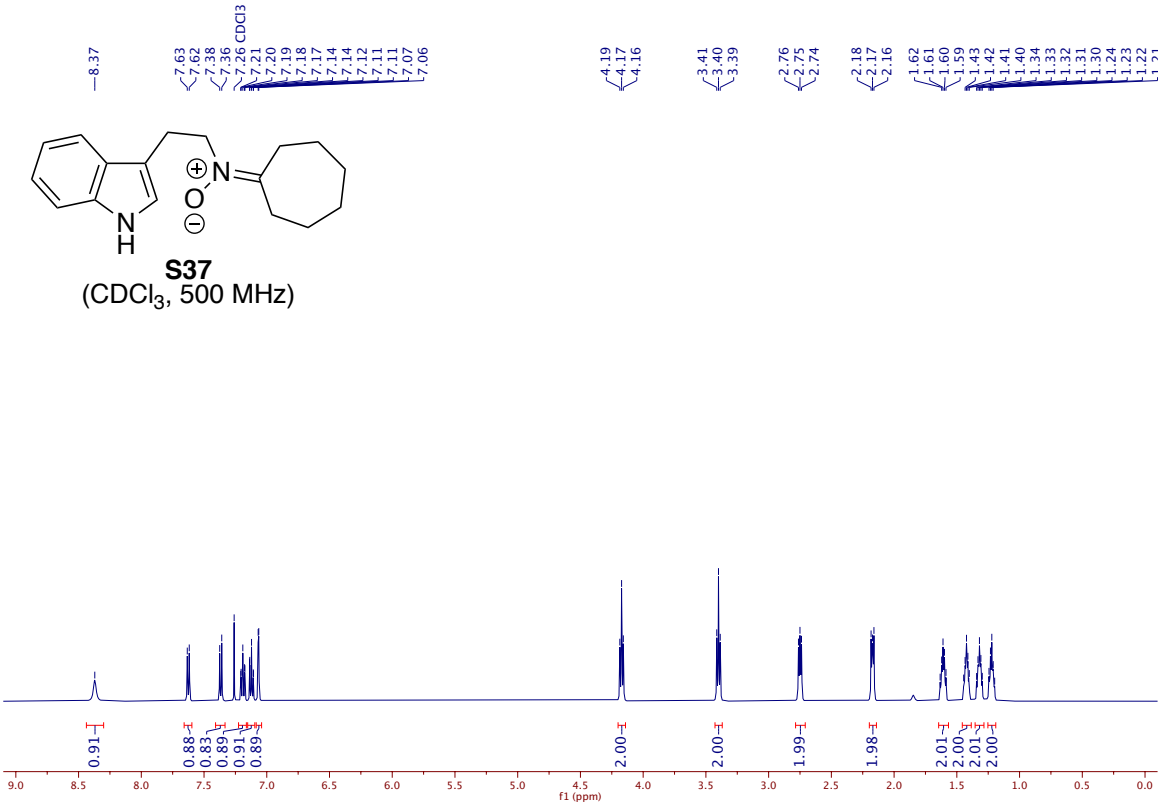

S37
($CDCl_3$, 500 MHz)

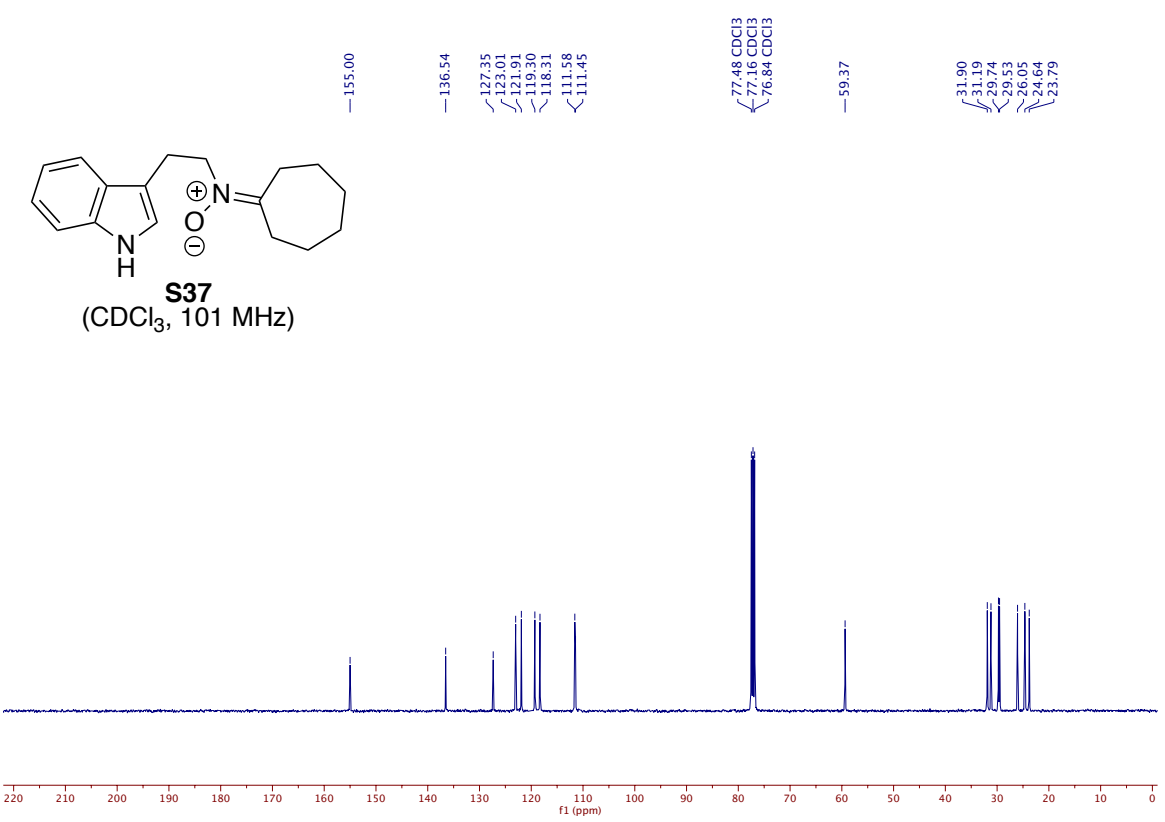

S37
($CDCl_3$, 101 MHz)

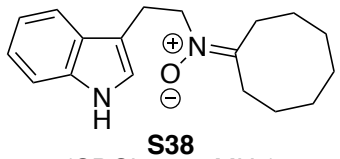

S38
($CDCl_3$, 500 MHz)

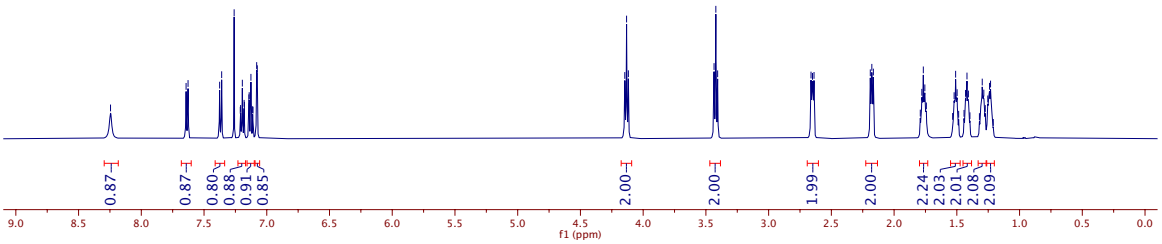

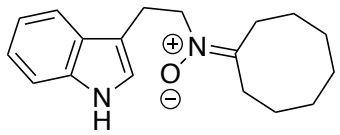

S38
($CDCl_3$, 101 MHz)

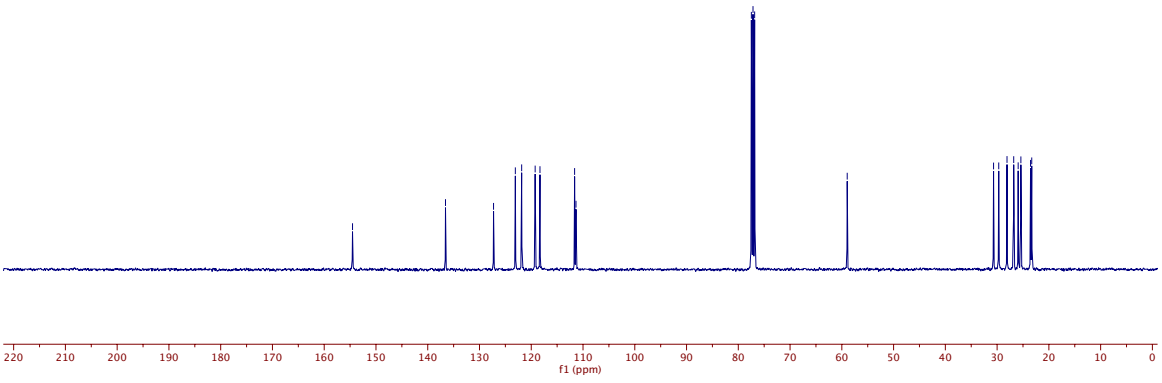

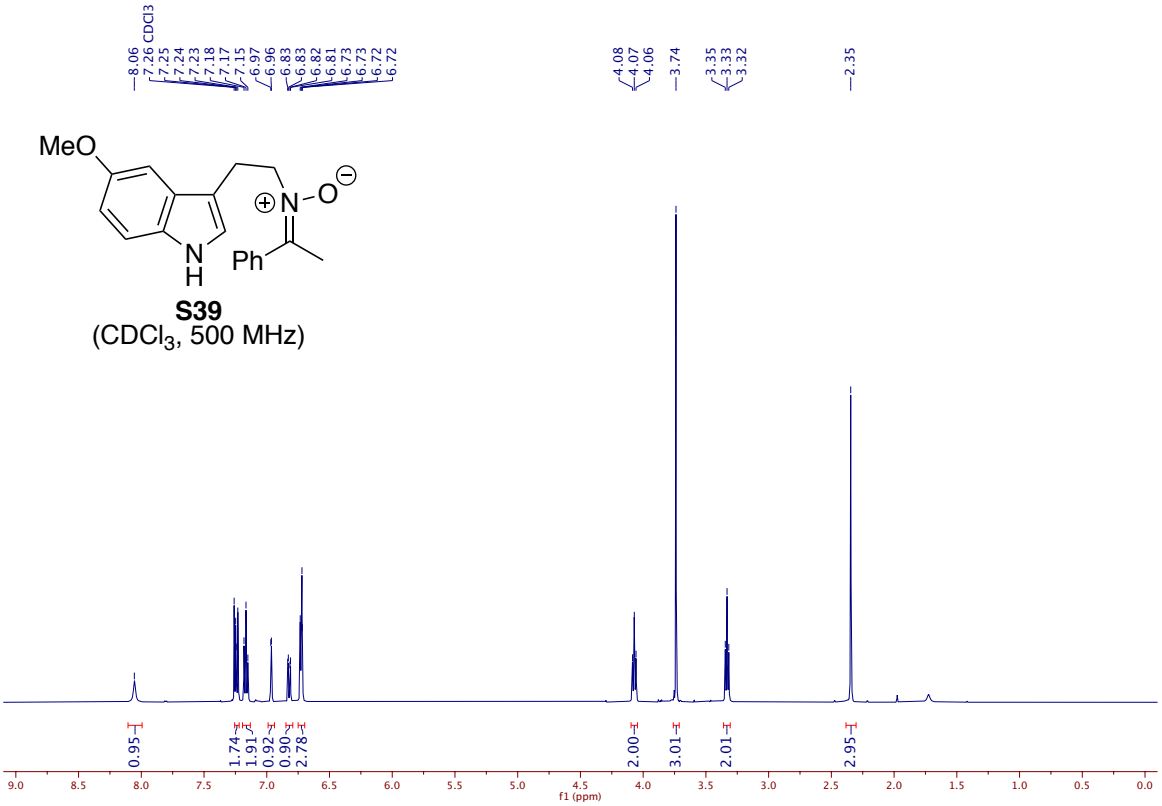

S39
($CDCl_3$, 500 MHz)

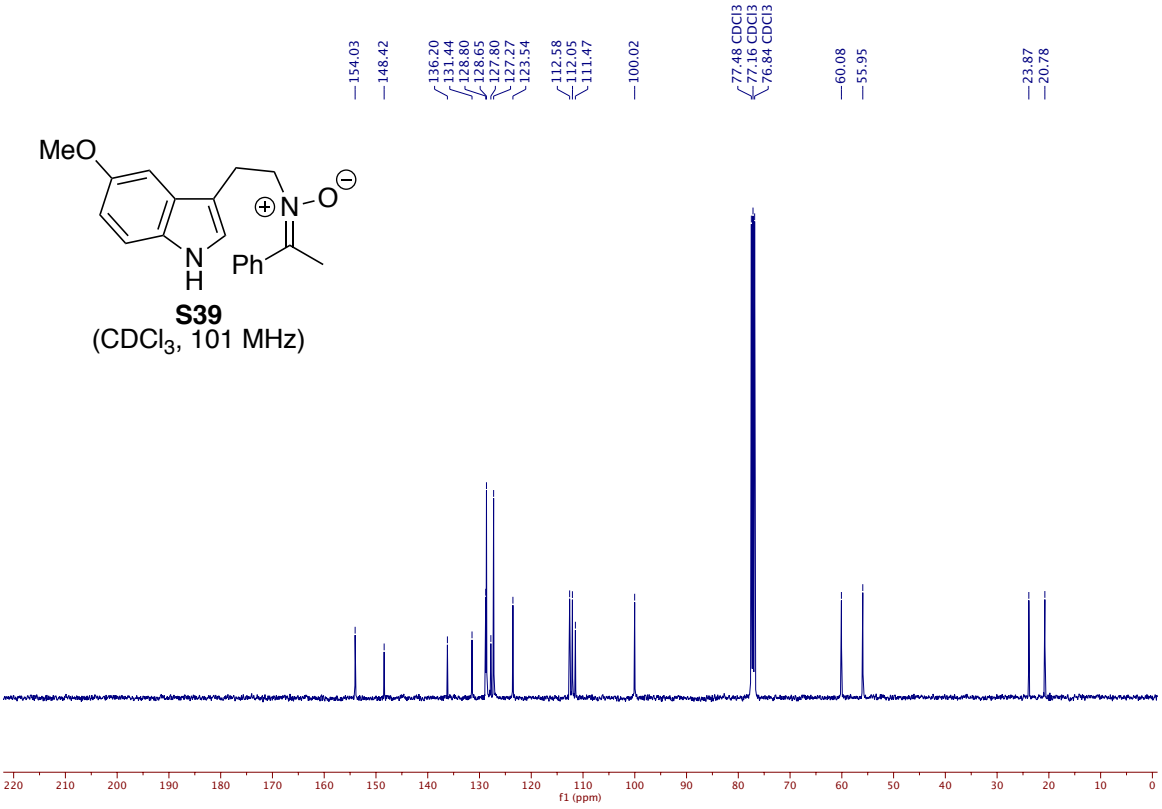

S39
($CDCl_3$, 101 MHz)

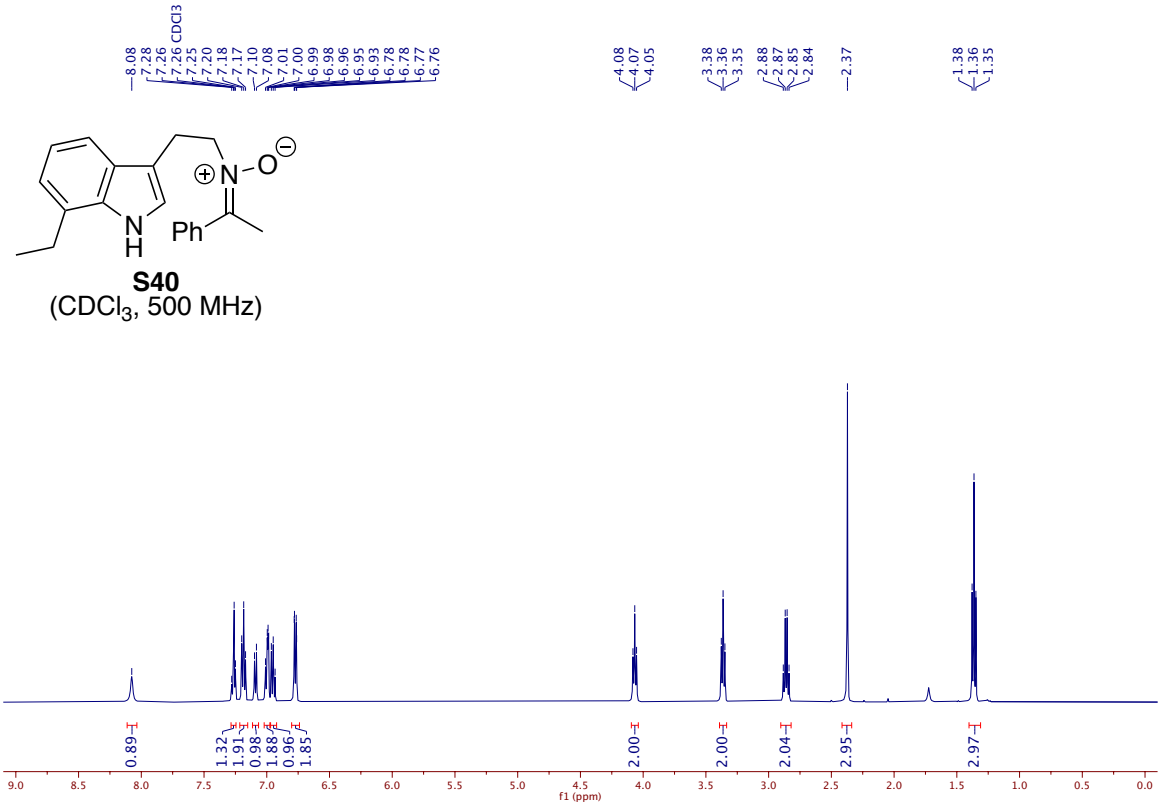

S40
($CDCl_3$, 500 MHz)

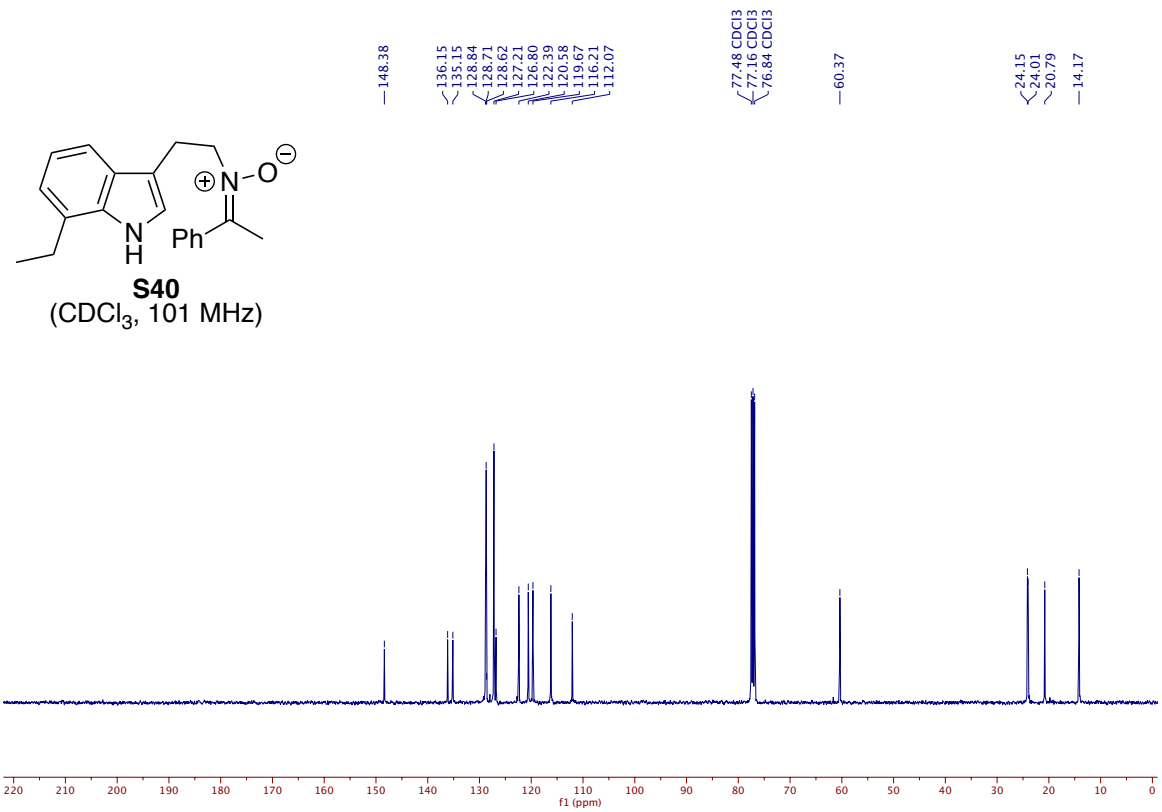

S40
($CDCl_3$, 101 MHz)

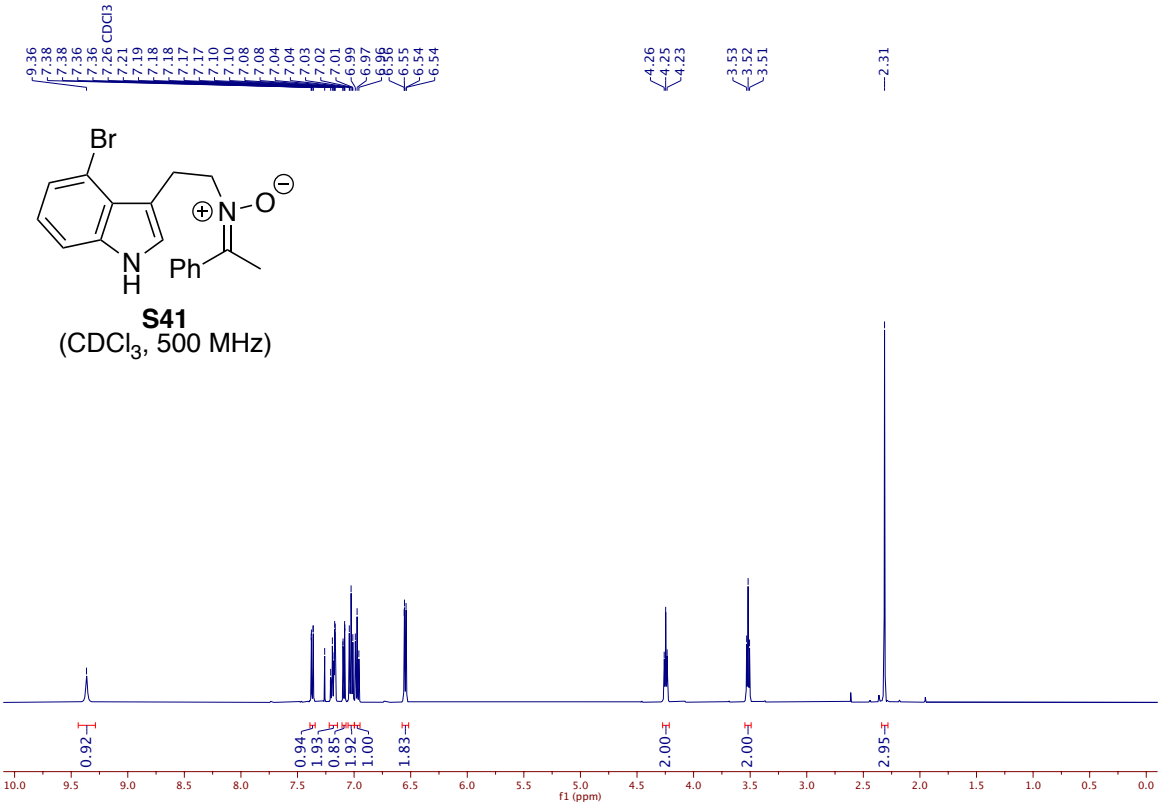

S41
($CDCl_3$, 500 MHz)

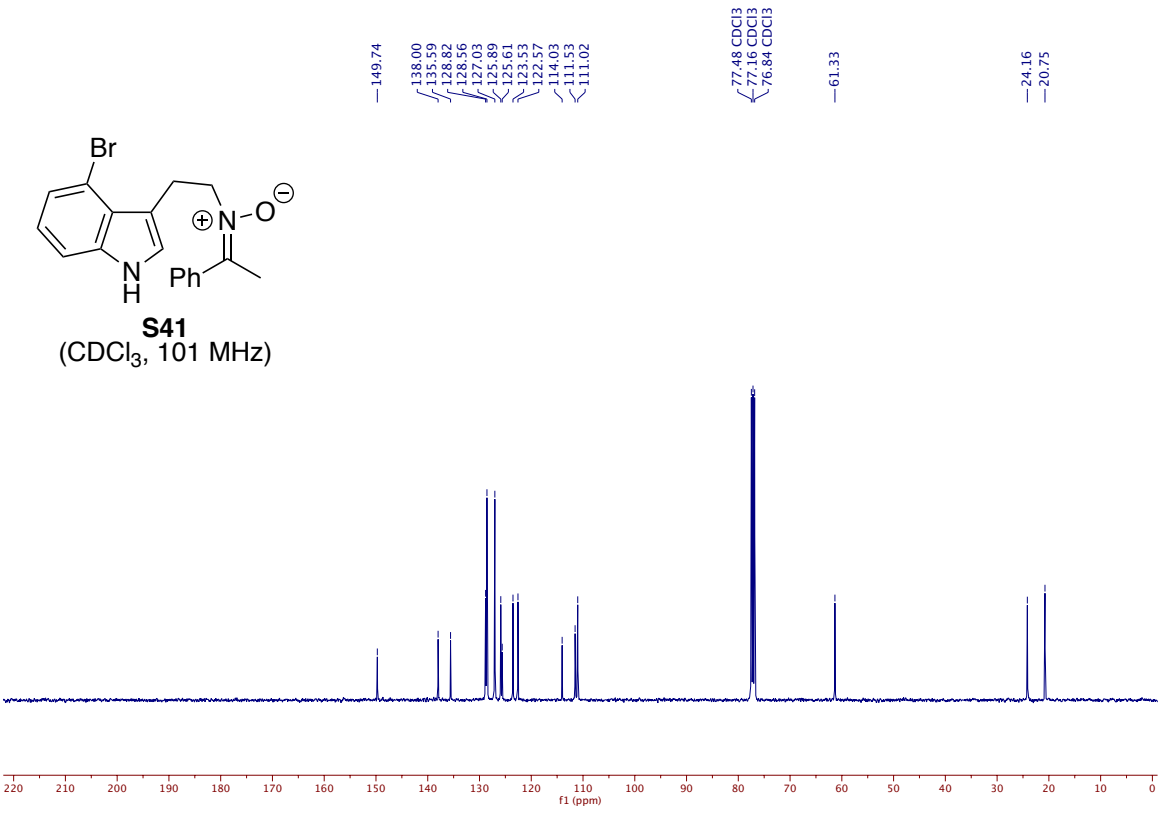

S41
($CDCl_3$, 101 MHz)

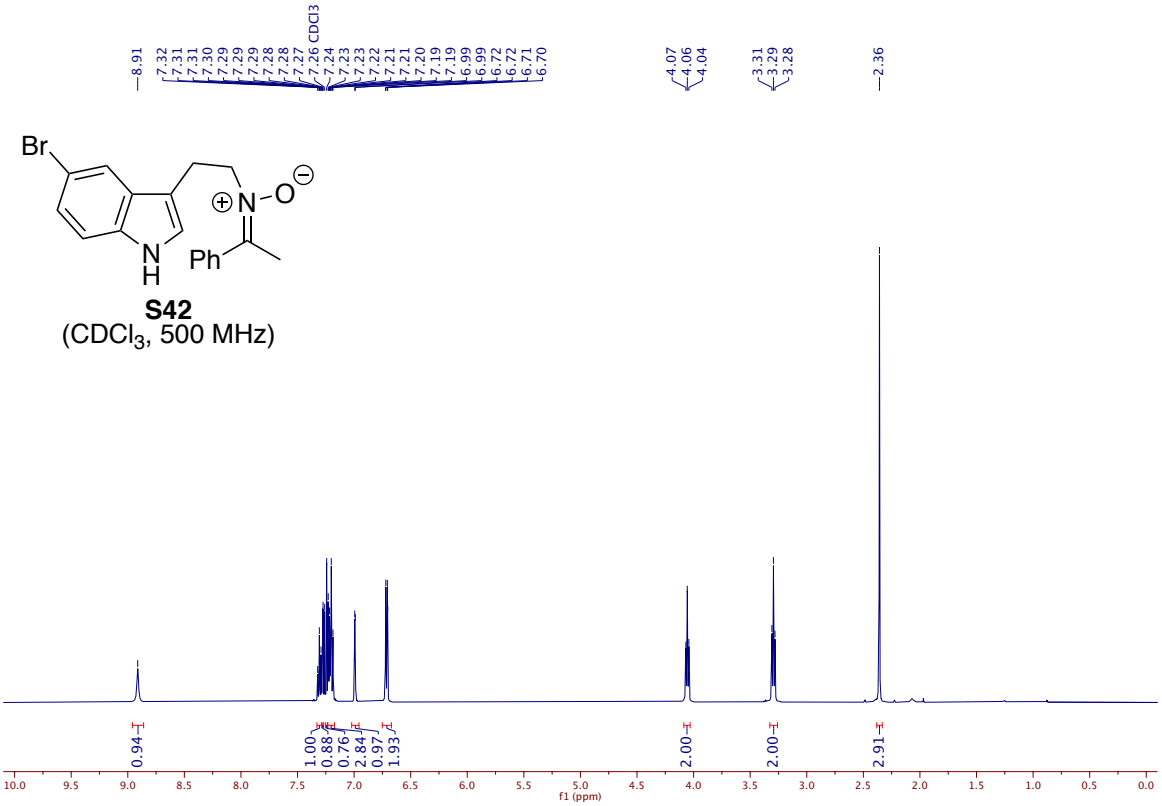

S42
($CDCl_3$, 500 MHz)

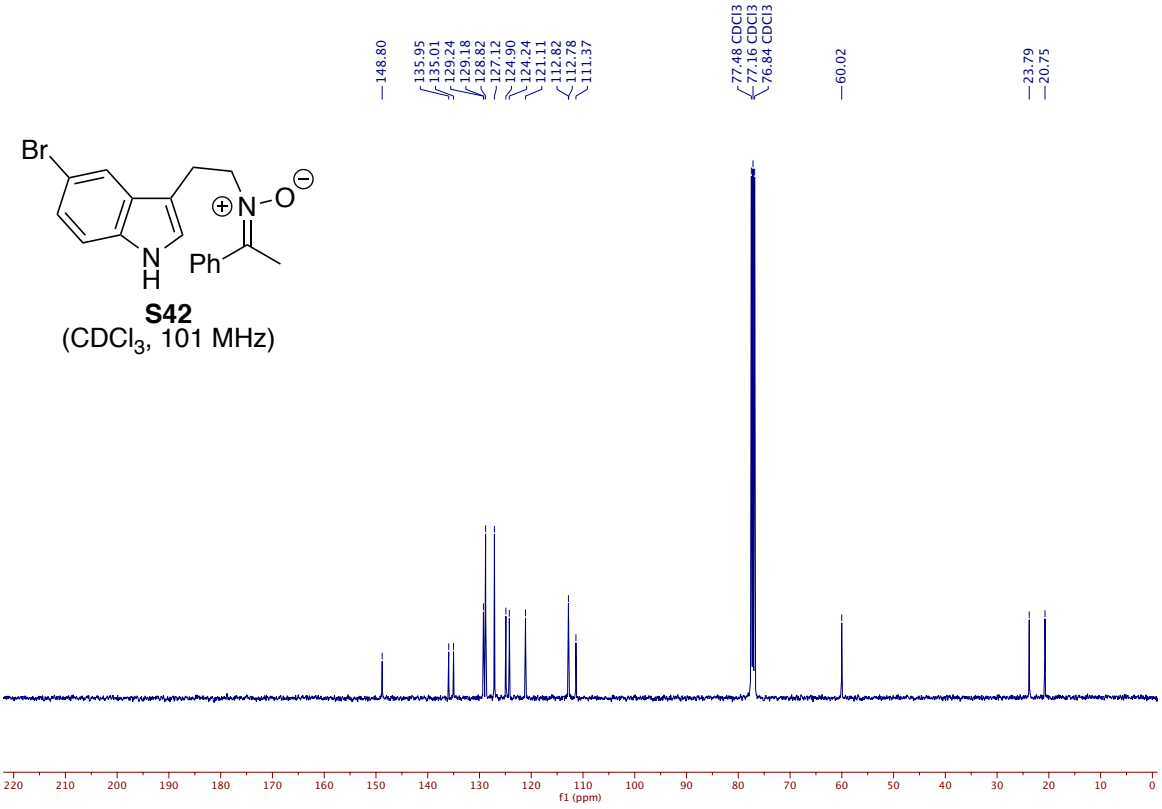

S42
($CDCl_3$, 101 MHz)

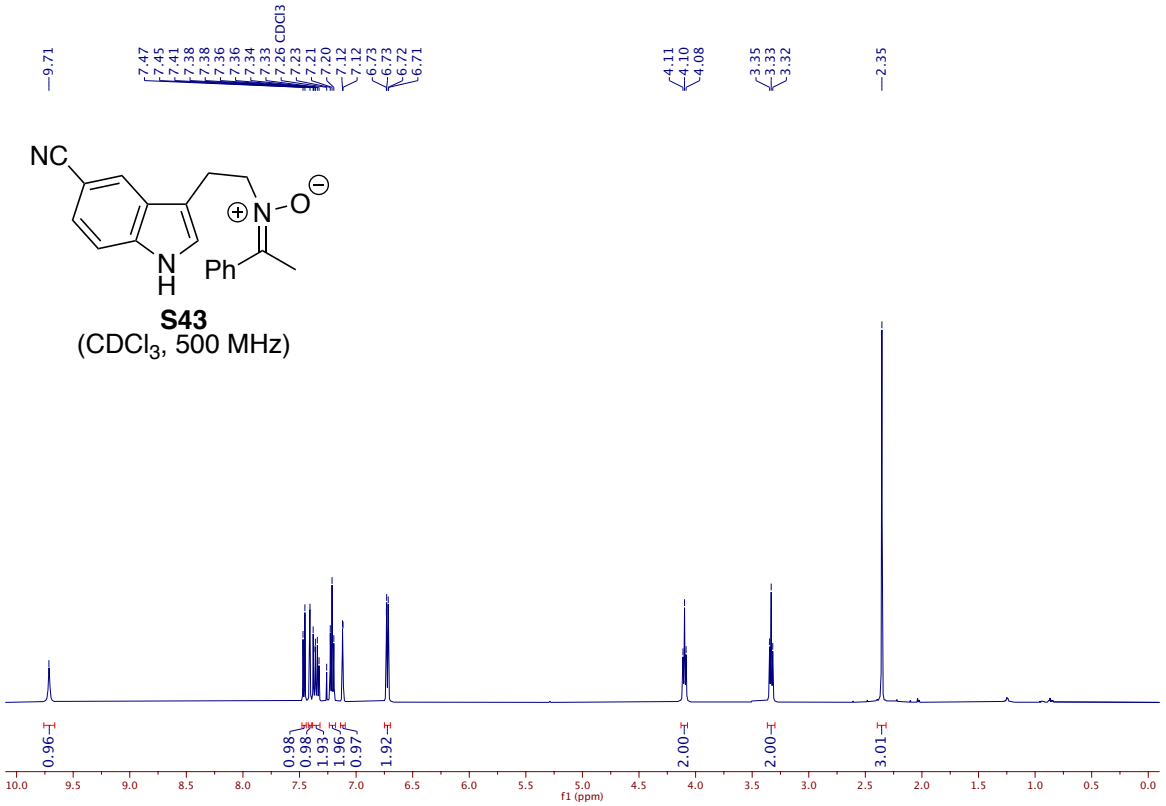

S43
($CDCl_3$, 500 MHz)

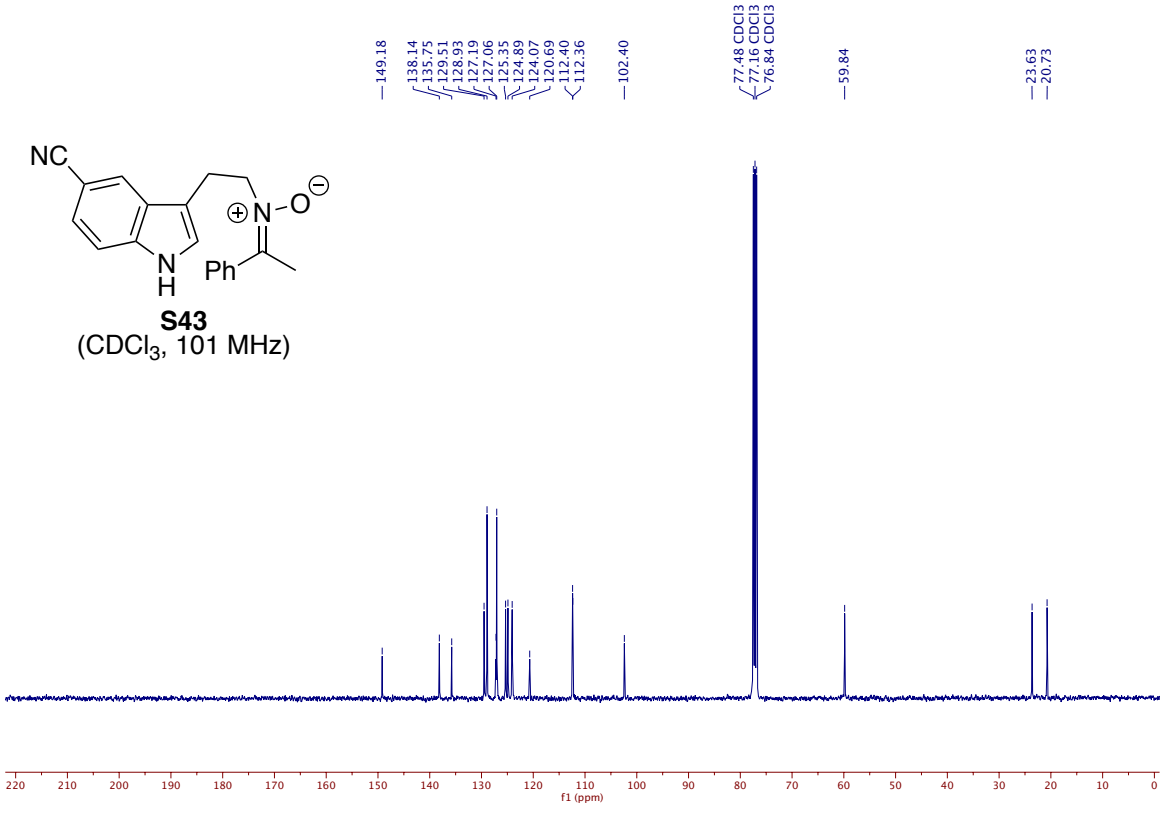

S43
($CDCl_3$, 101 MHz)

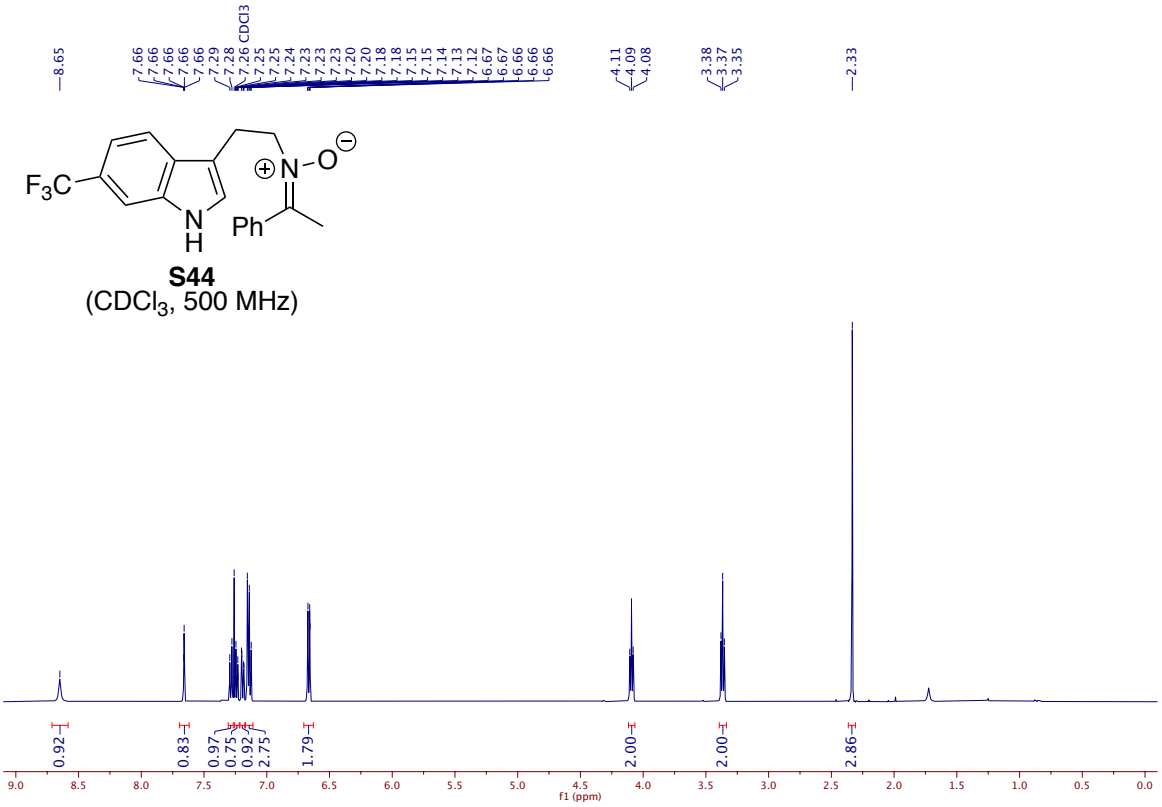

S44
($CDCl_3$, 500 MHz)

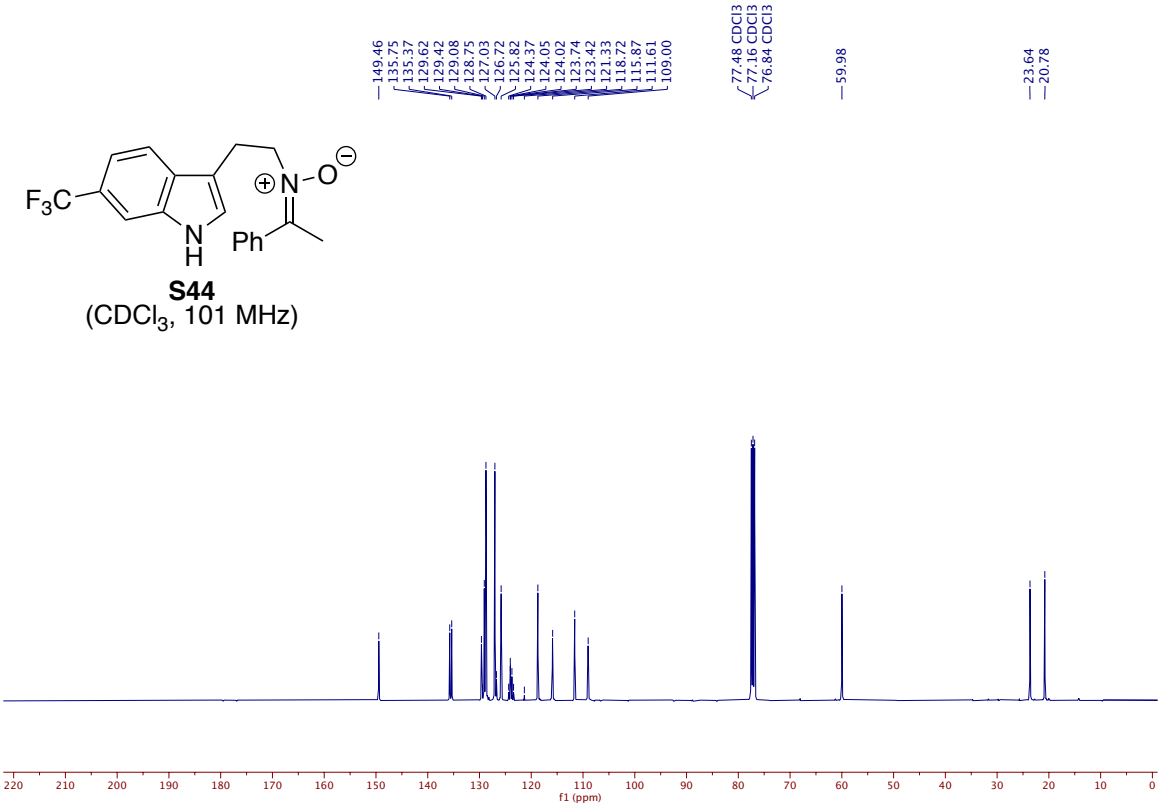

S44
($CDCl_3$, 101 MHz)

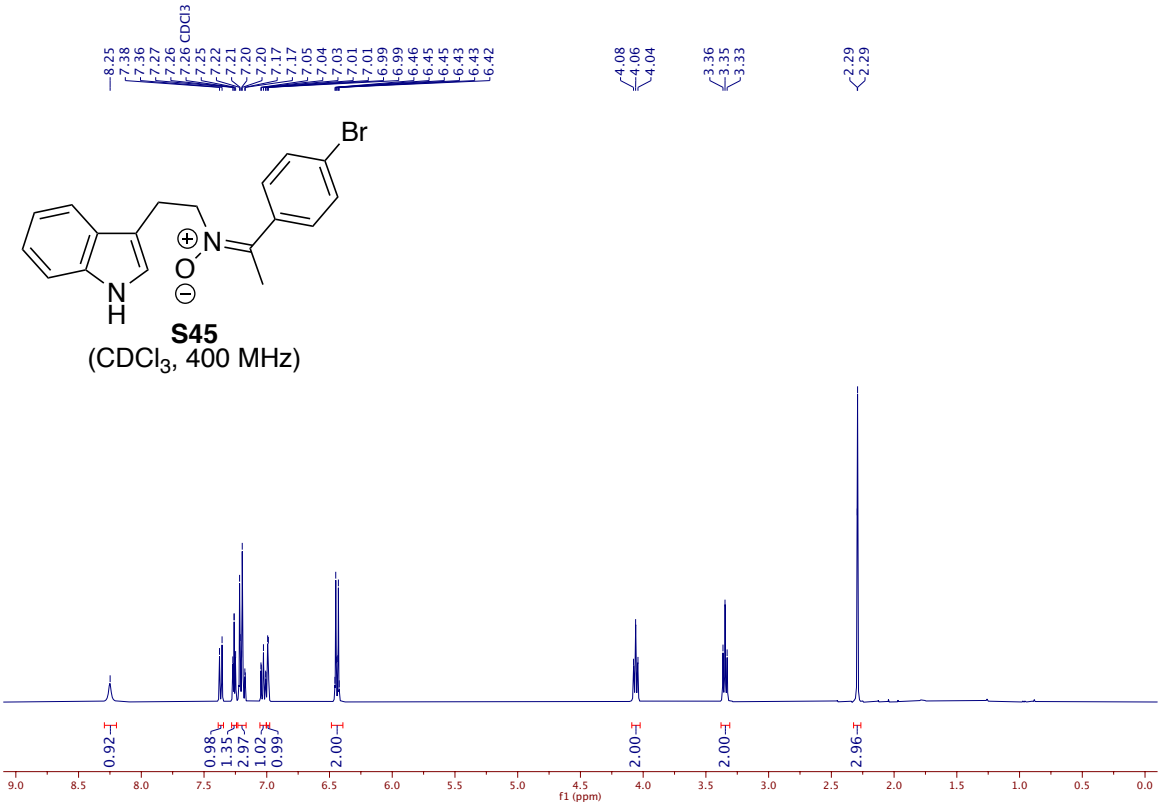

S45
($CDCl_3$, 400 MHz)

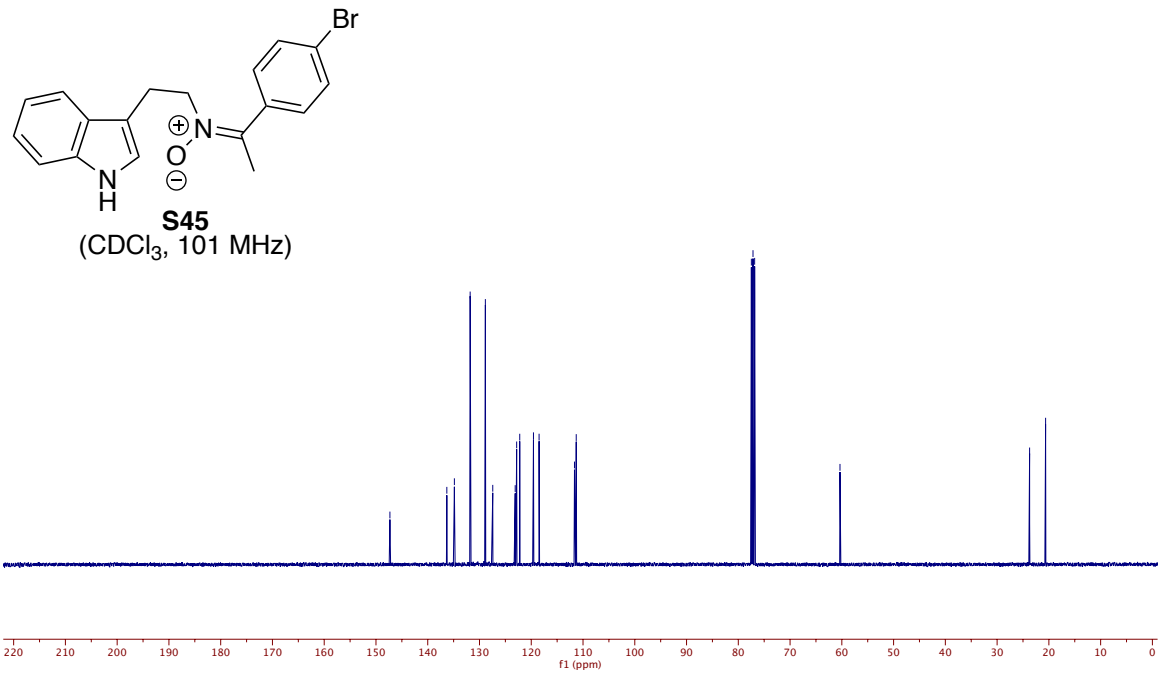

S45
($CDCl_3$, 101 MHz)

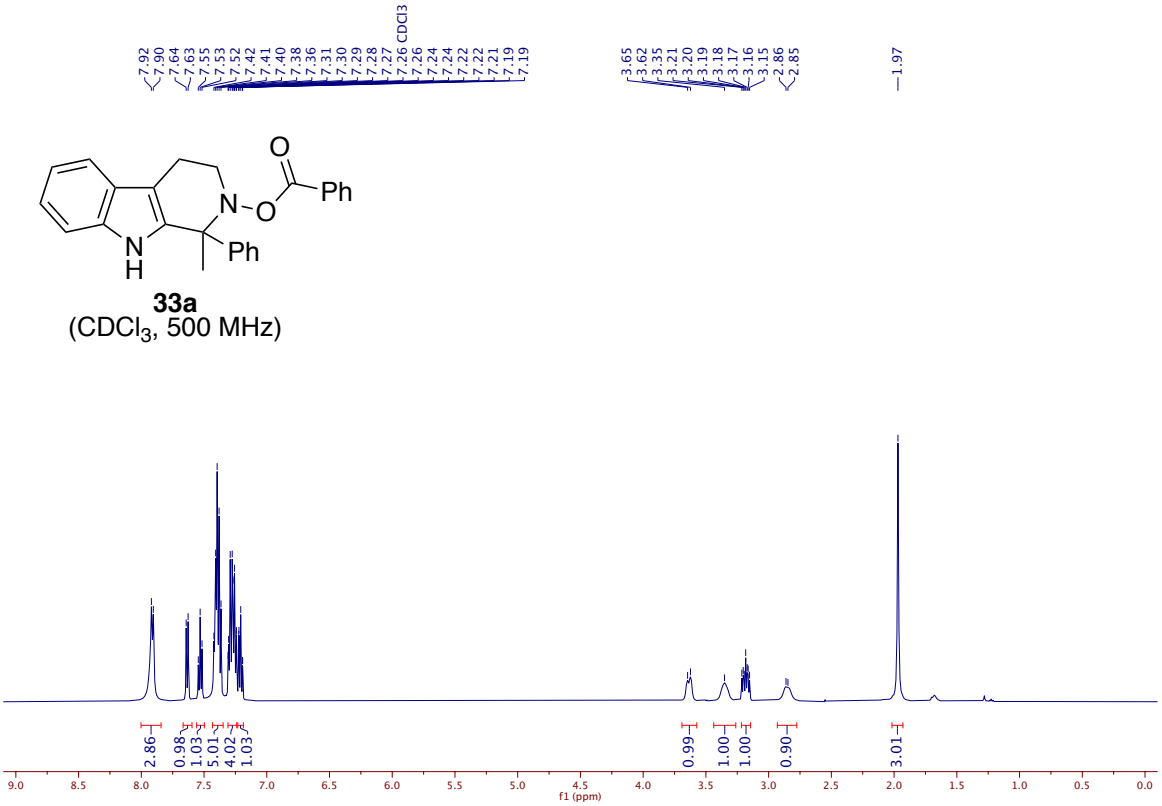

33a
($CDCl_3$, 500 MHz)

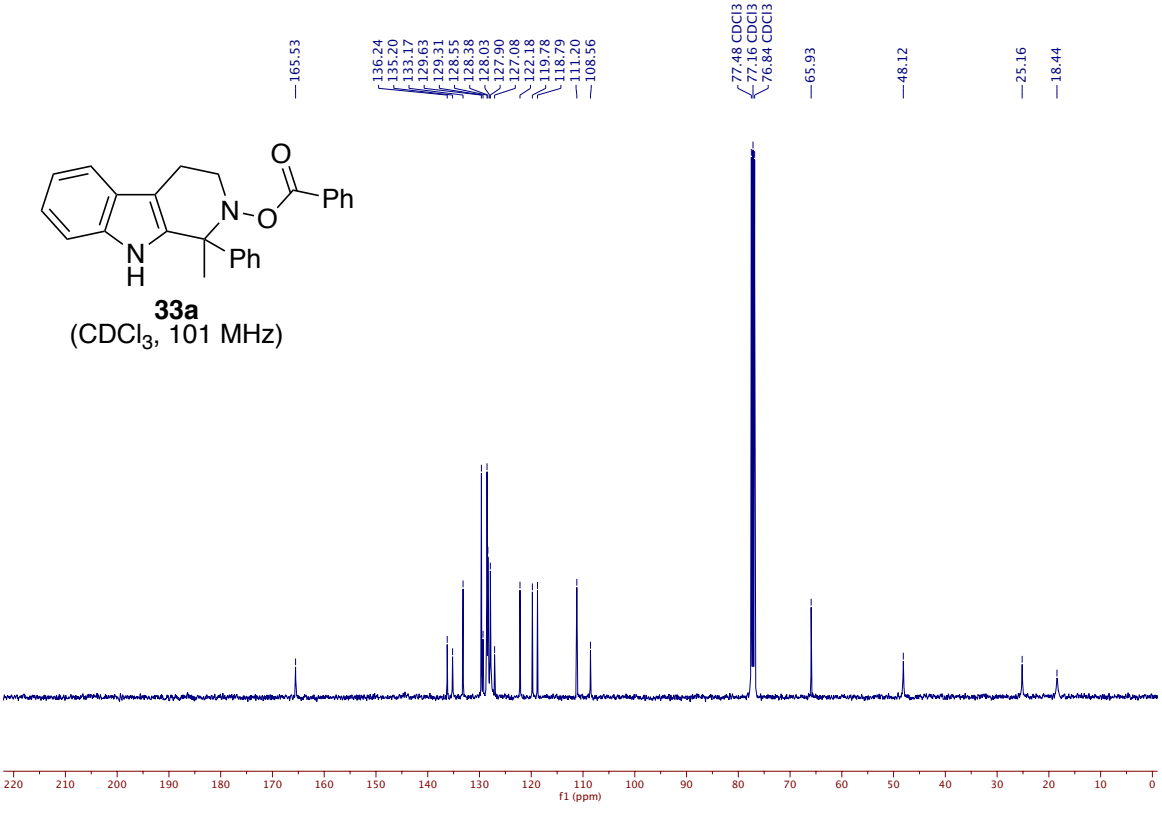

33a
($CDCl_3$, 101 MHz)

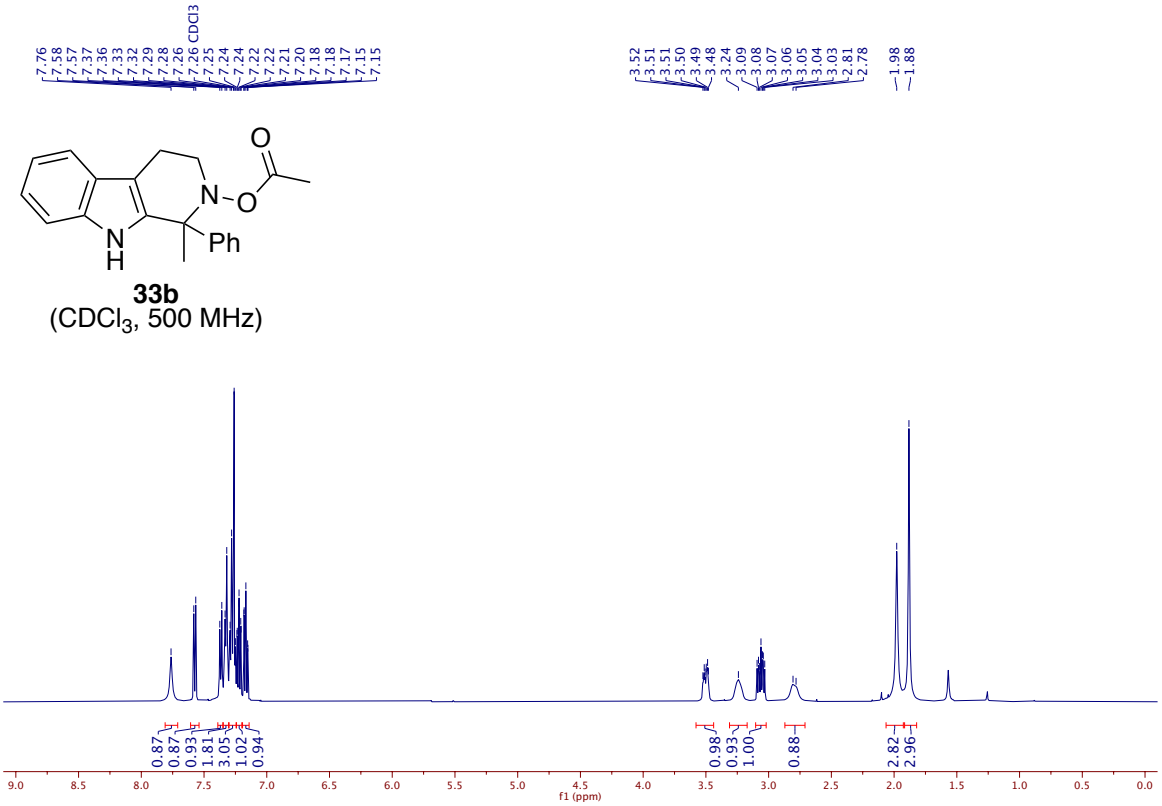

33b
($CDCl_3$, 500 MHz)

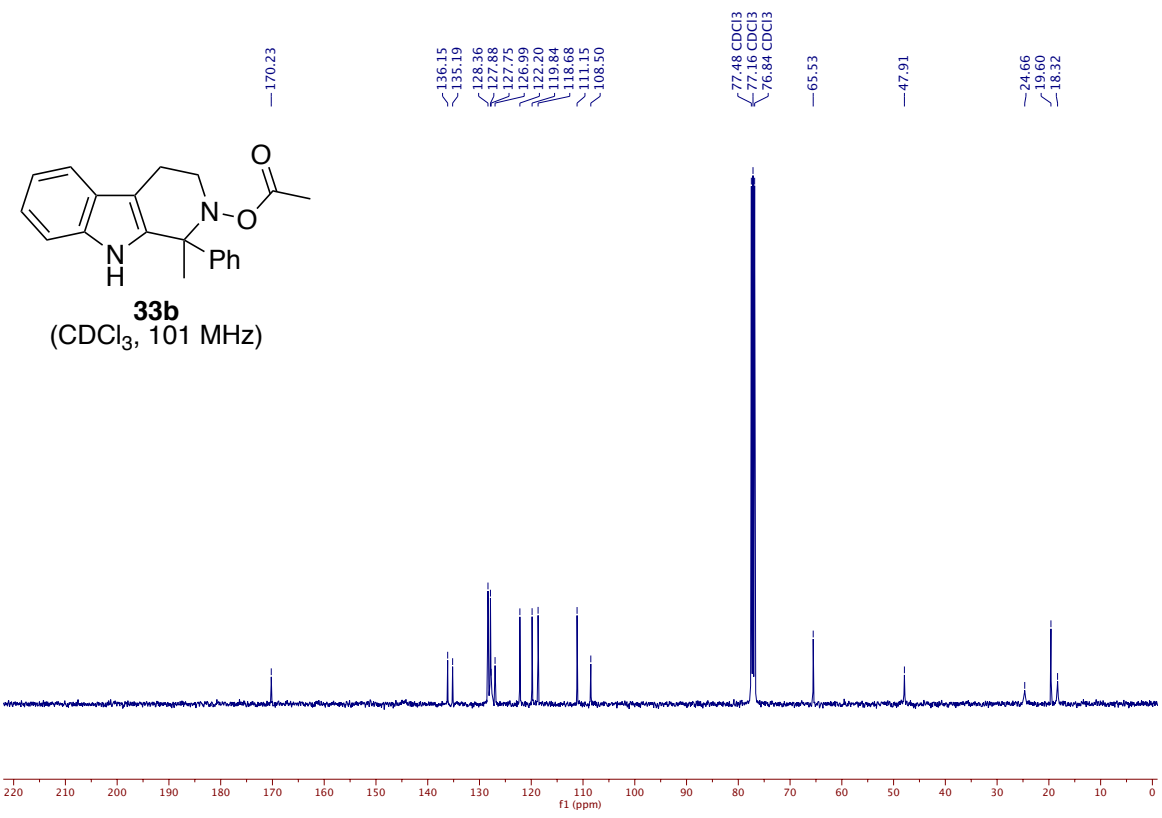

33b
($CDCl_3$, 101 MHz)

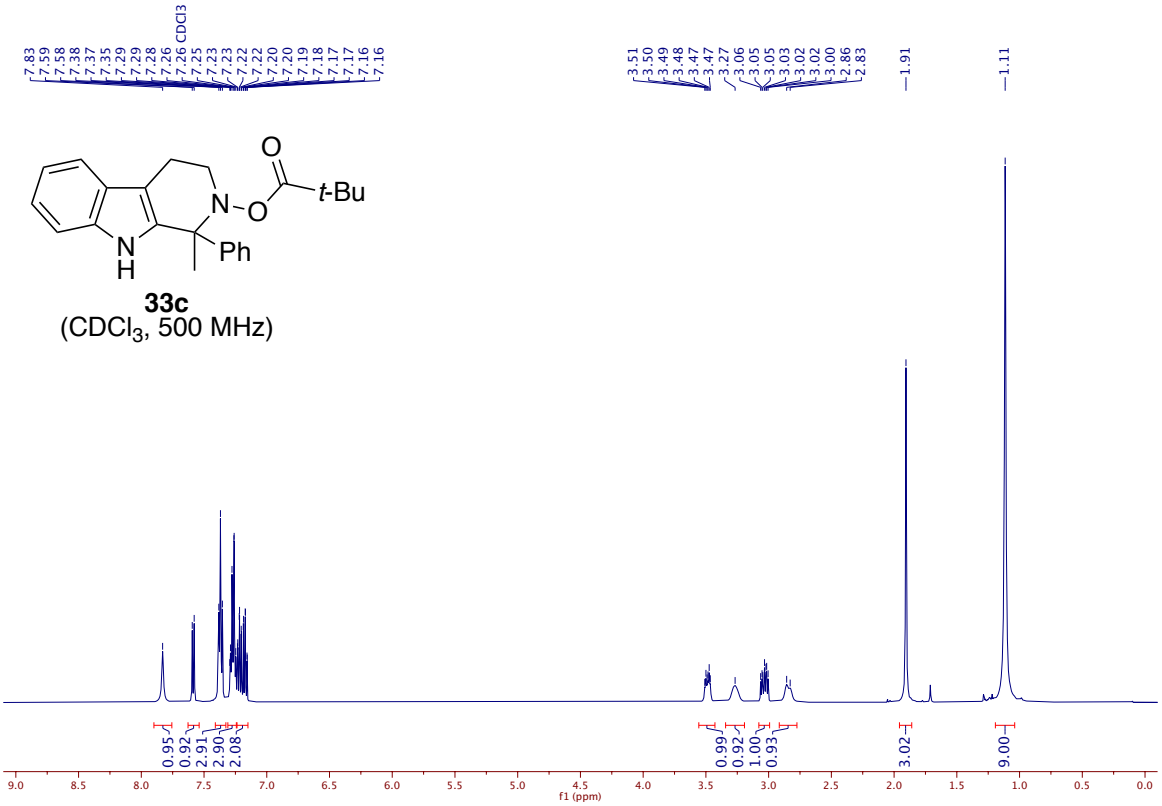

33c
($CDCl_3$, 500 MHz)

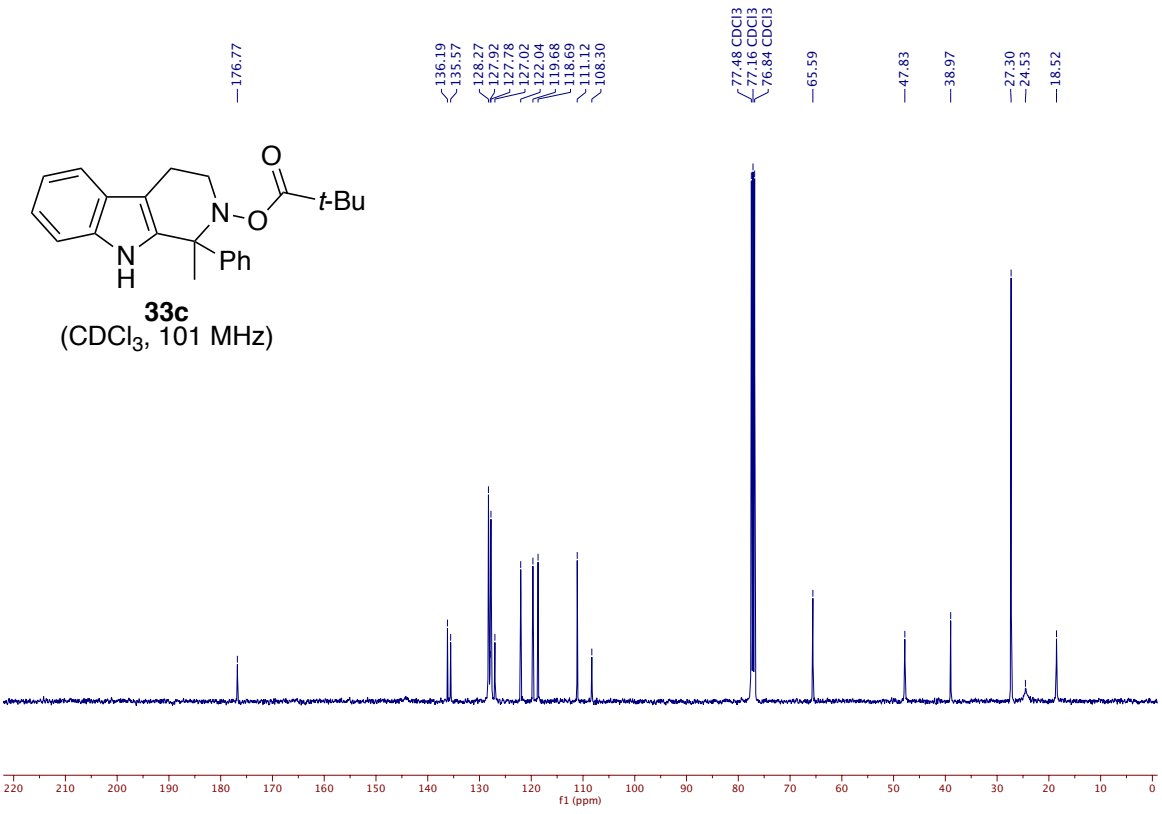

33c
($CDCl_3$, 101 MHz)

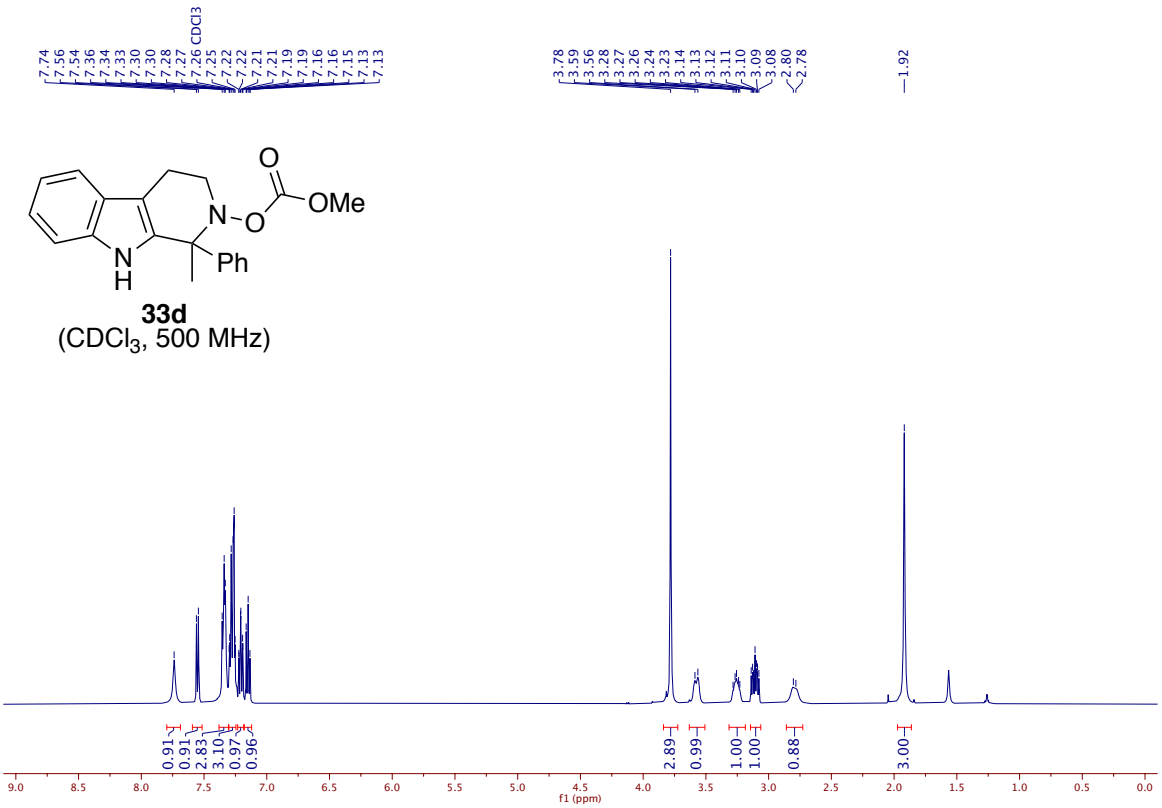

33d
($CDCl_3$, 500 MHz)

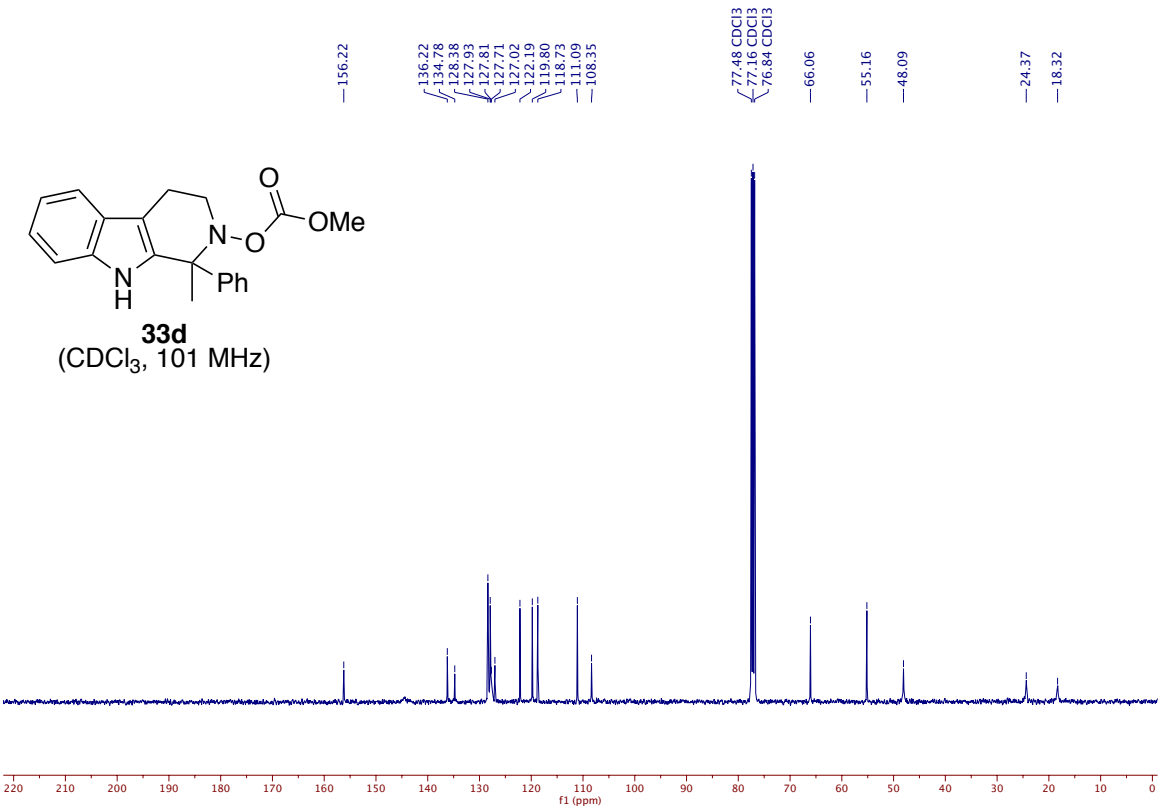

33d
($CDCl_3$, 101 MHz)

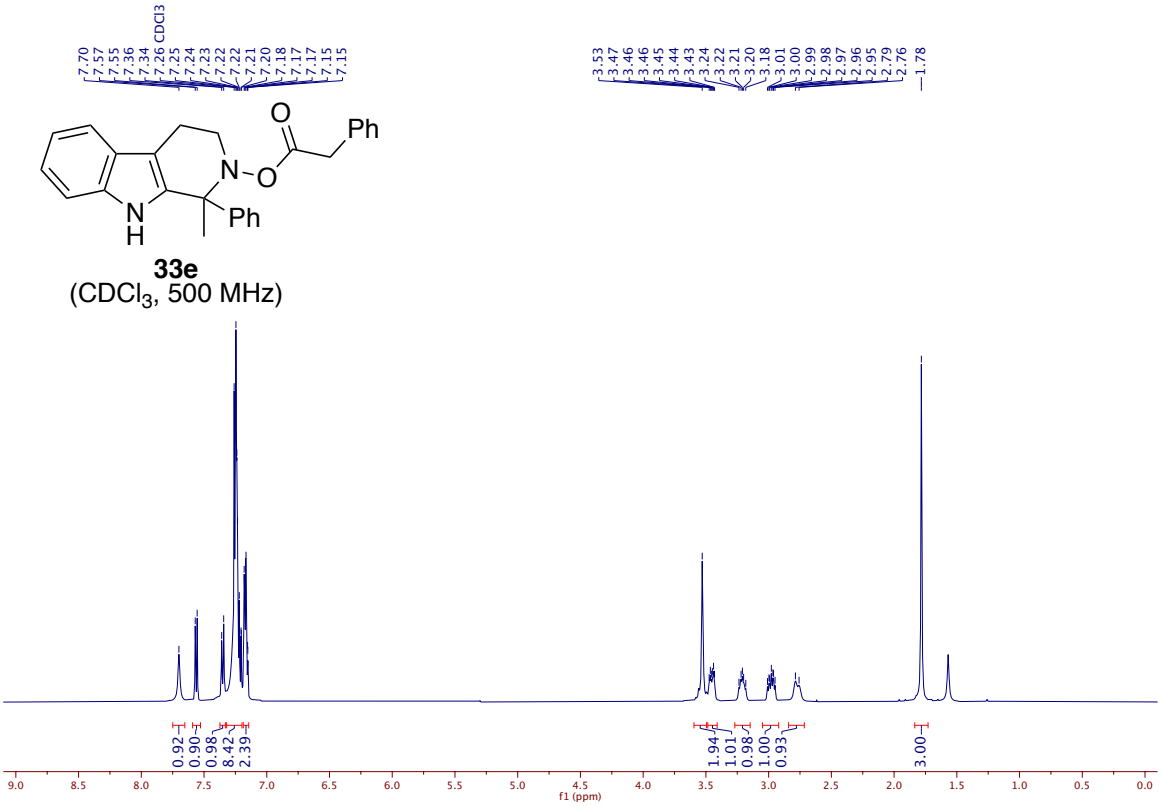

33e
($CDCl_3$, 500 MHz)

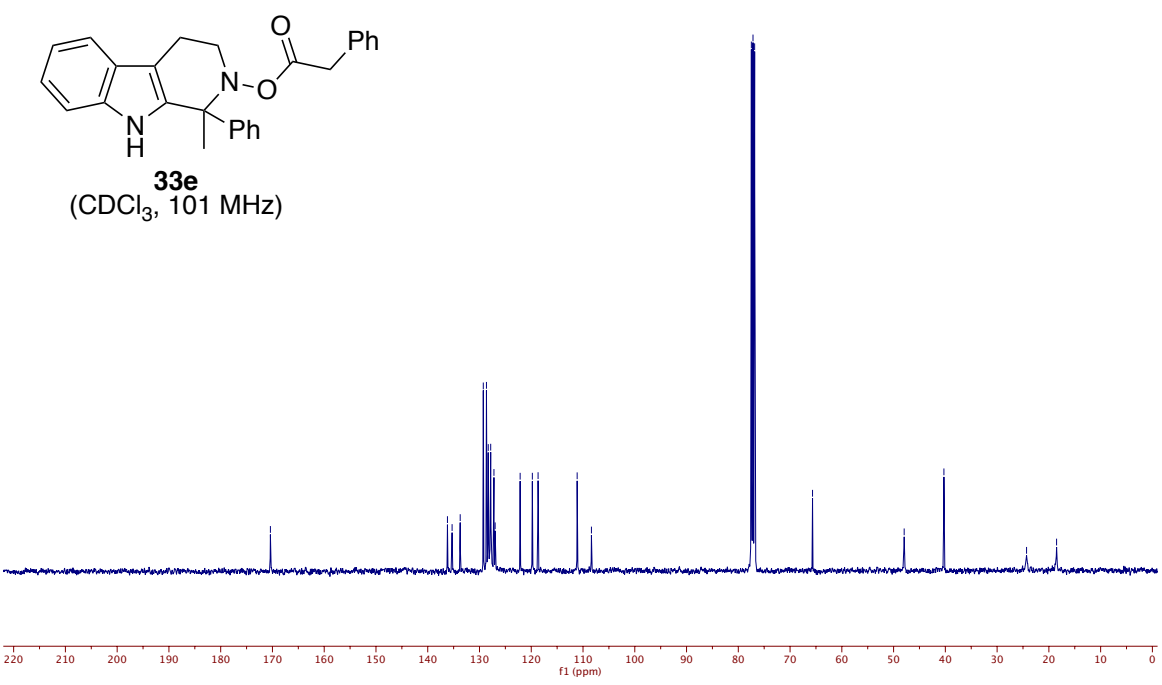

33e
($CDCl_3$, 101 MHz)

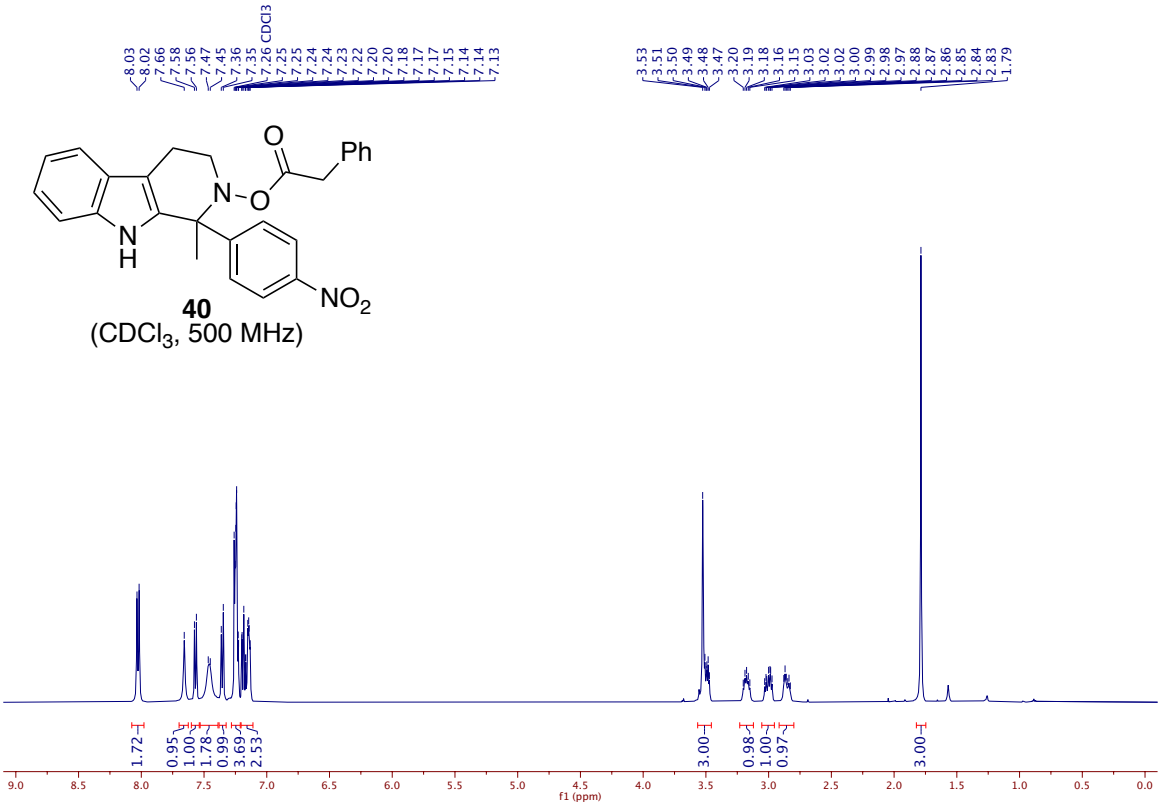
8.03
8.02
7.66
7.58
7.56
7.47
7.45
7.36
7.35
7.26 CDCl3
7.25
7.24
7.24
7.23
7.22
7.20
7.18
7.17
7.17
7.15
7.14
7.14
7.13
3.53
3.51
3.50
3.49
3.48
3.47
3.20
3.19
3.18
3.16
3.15
3.03
3.02
3.02
3.00
2.99
2.98
2.97
2.88
2.87
2.86
2.85
2.84
2.83
1.79
O
Ph
N
O
N
H
NO2
40
(CDCl3, 500 MHz)
1.72
0.95
1.00
1.78
0.99
3.69
2.53
3.00
0.98
1.00
0.97
3.00
f1 (ppm)

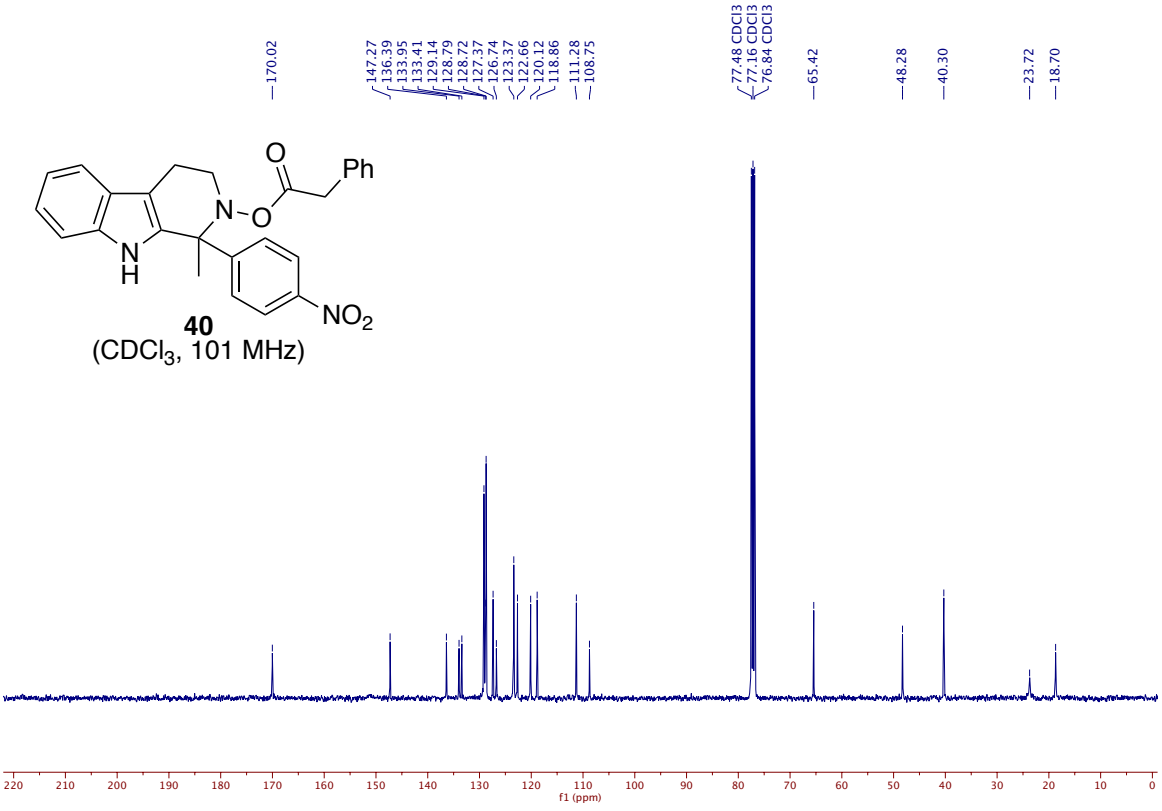
170.02
147.27
136.39
133.95
133.41
129.14
128.79
128.72
127.37
126.74
123.37
122.66
120.12
118.86
111.28
108.75
77.48 CDCl3
77.16 CDCl3
76.84 CDCl3
65.42
48.28
40.30
23.72
18.70
O
Ph
N
O
N
H
NO2
40
(CDCl3, 101 MHz)
f1 (ppm)

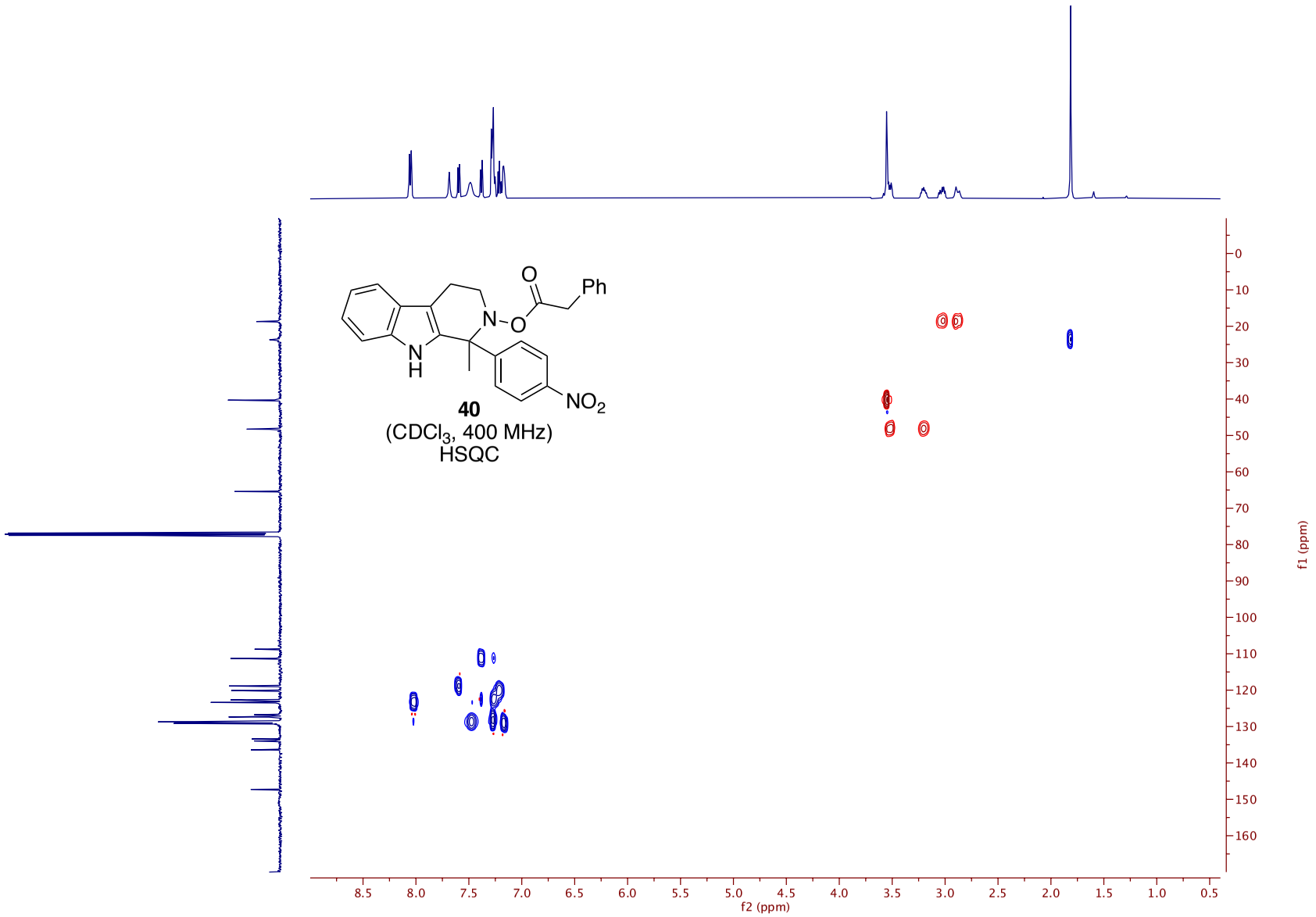
O
Ph
N
O
N
H
NO2
40
(CDCl3, 400 MHz)
HSQC
f2 (ppm)
f1 (ppm)

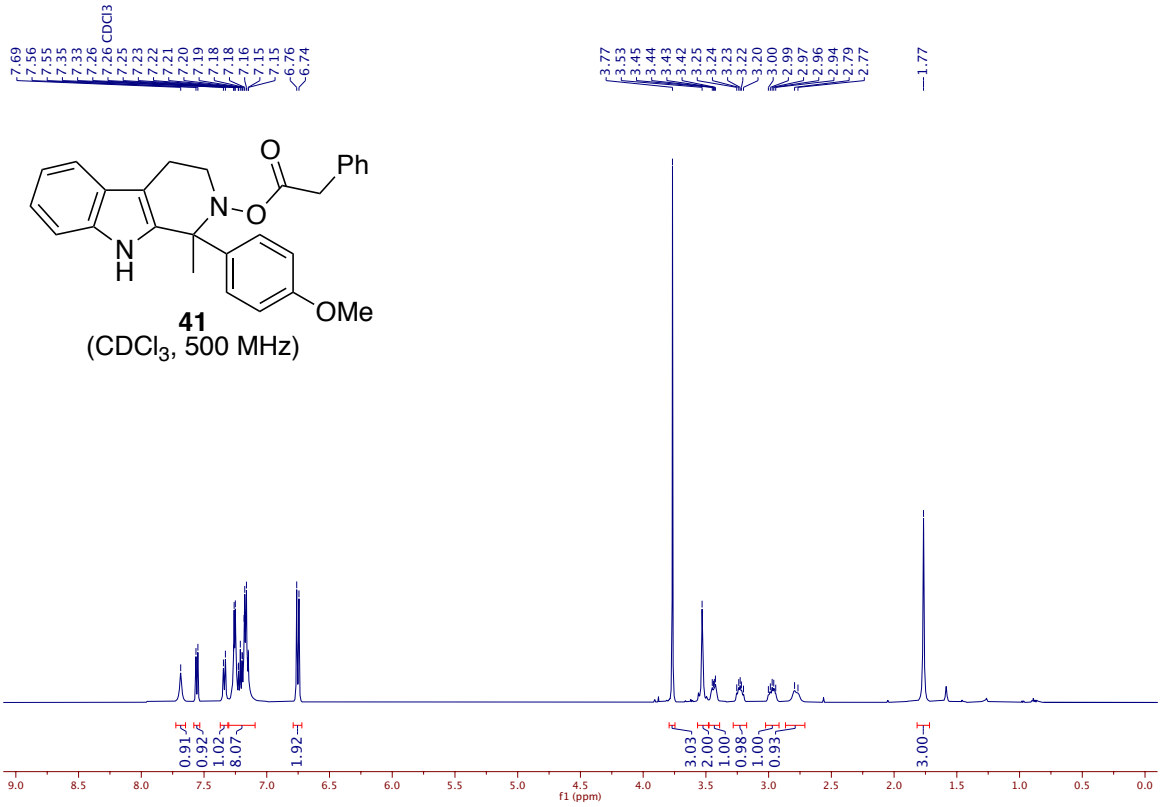

41
($CDCl_3$, 500 MHz)

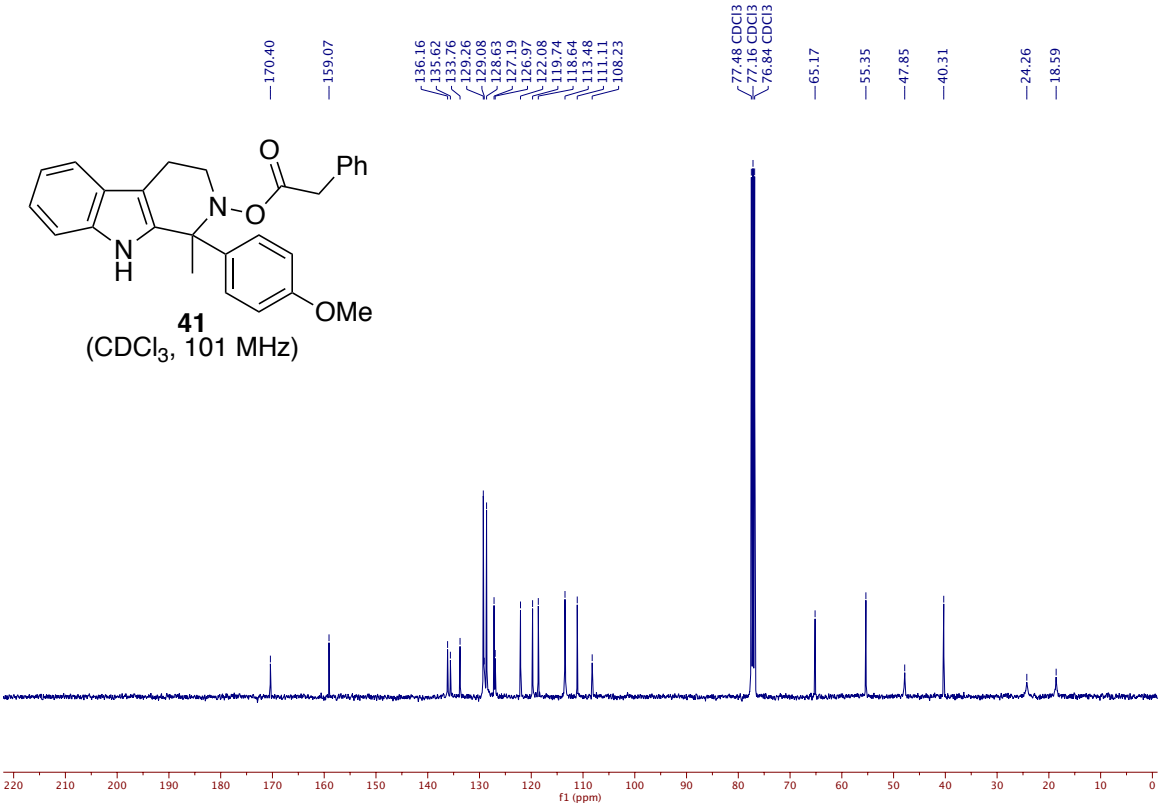

41
($CDCl_3$, 101 MHz)

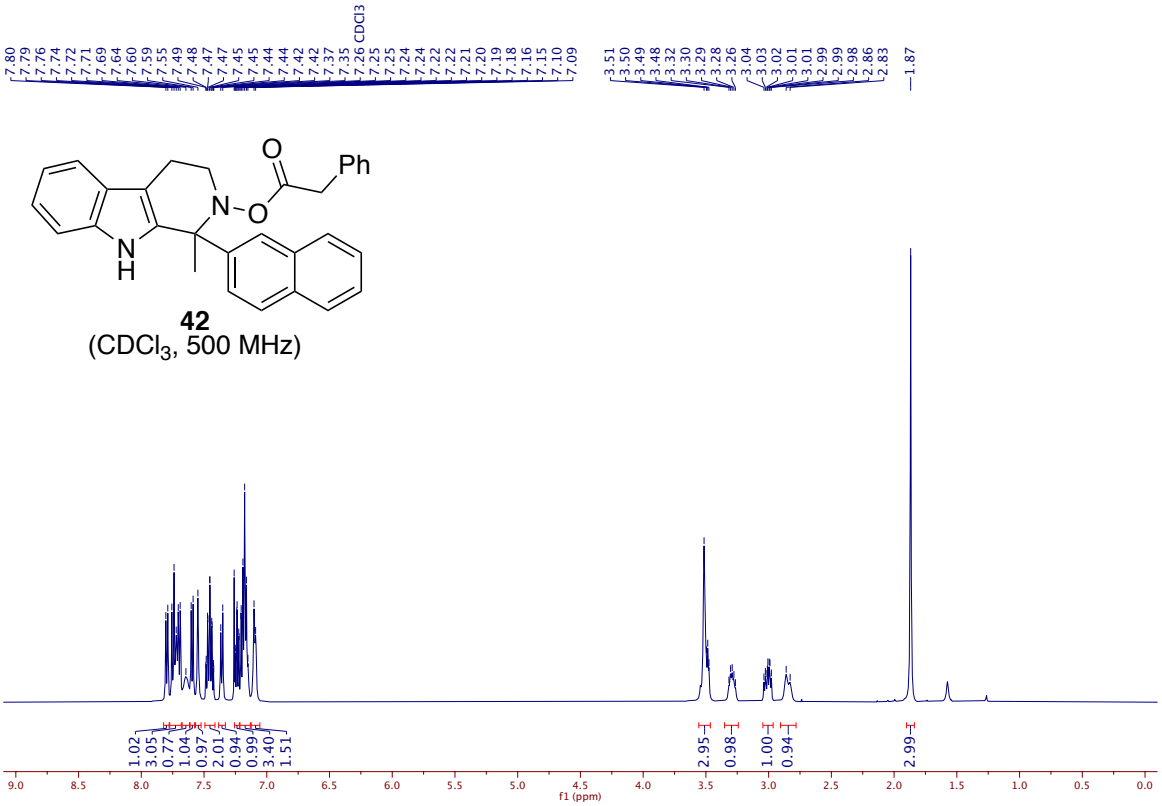

42
($CDCl_3$, 500 MHz)

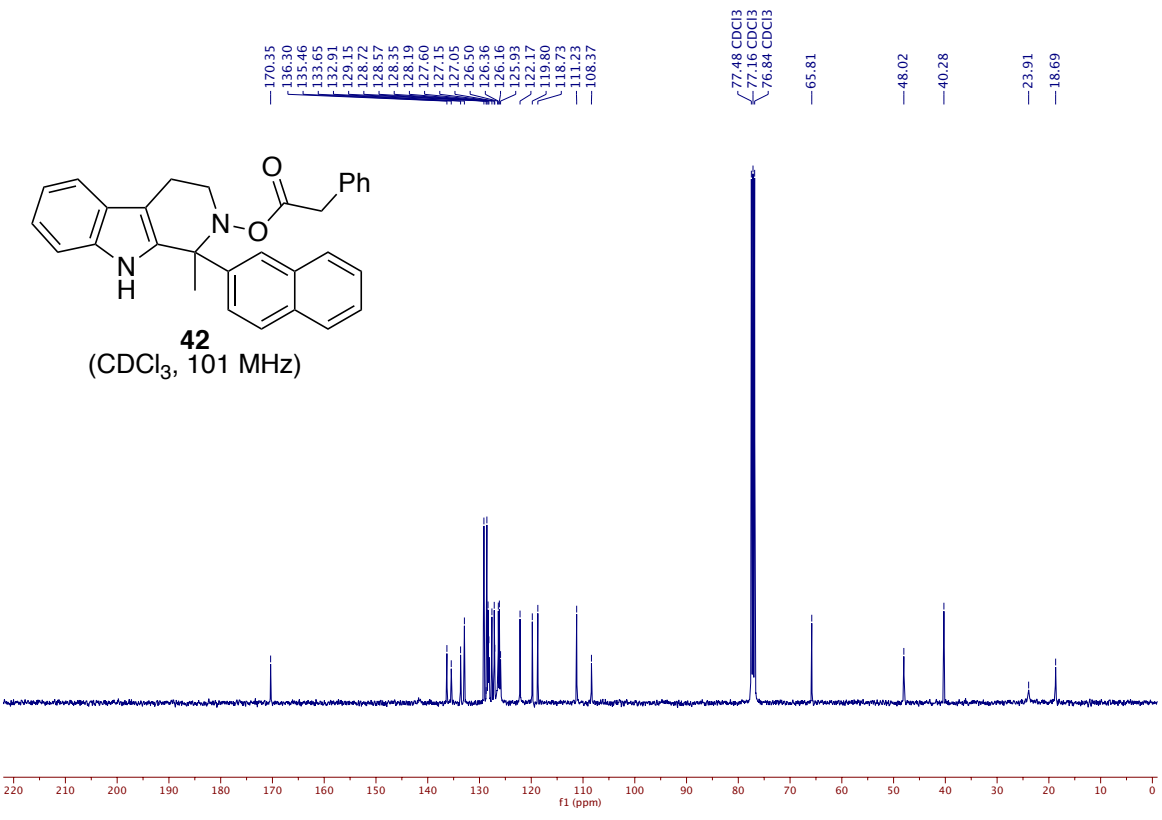

42
($CDCl_3$, 101 MHz)

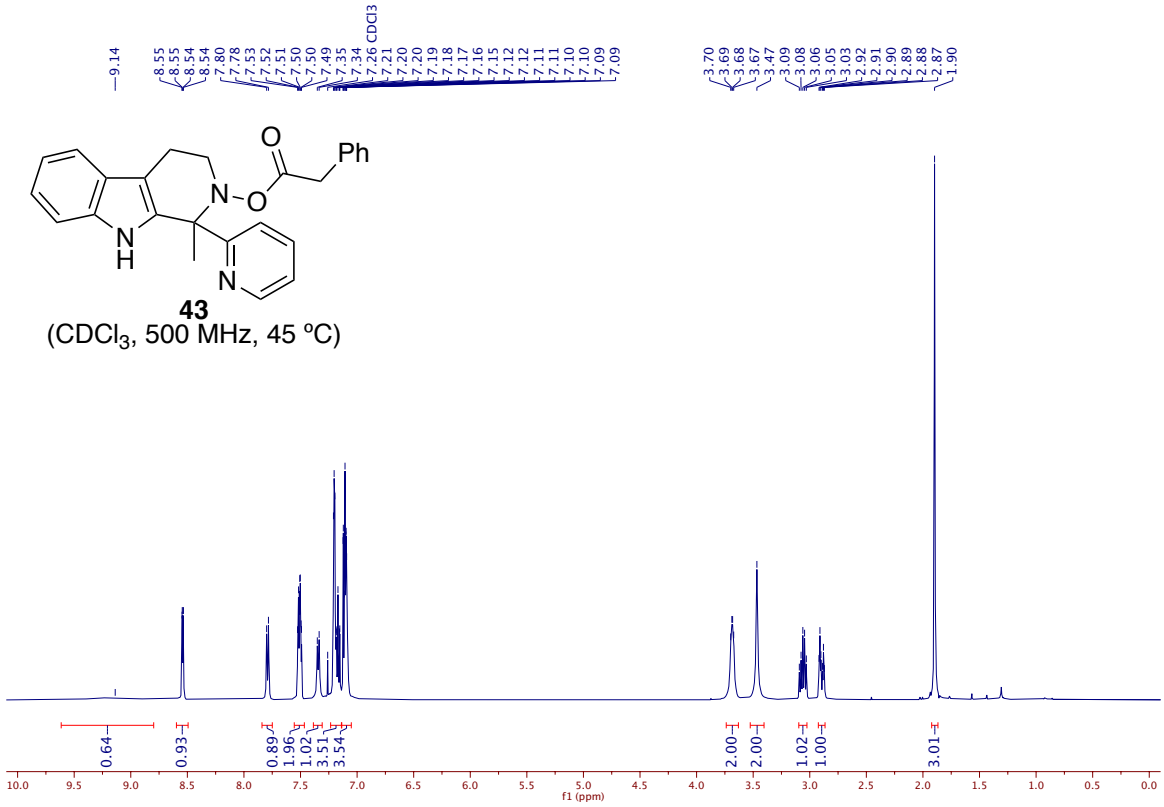
9.14
8.55
8.55
8.54
8.54
7.80
7.78
7.53
7.52
7.51
7.50
7.50
7.49
7.35
7.34
7.26 CDCl3
7.21
7.20
7.20
7.19
7.18
7.17
7.16
7.15
7.12
7.12
7.11
7.10
7.10
7.09
7.09
3.70
3.69
3.68
3.67
3.47
3.09
3.08
3.06
3.05
3.03
2.92
2.91
2.90
2.89
2.88
2.87
1.90
O
Ph
N
O
N
H
N
43
(CDCl3, 500 MHz, 45 ºC)
0.64
0.93
0.89
1.96
1.02
3.51
3.54
2.00
2.00
1.02
1.00
3.01
f1 (ppm)

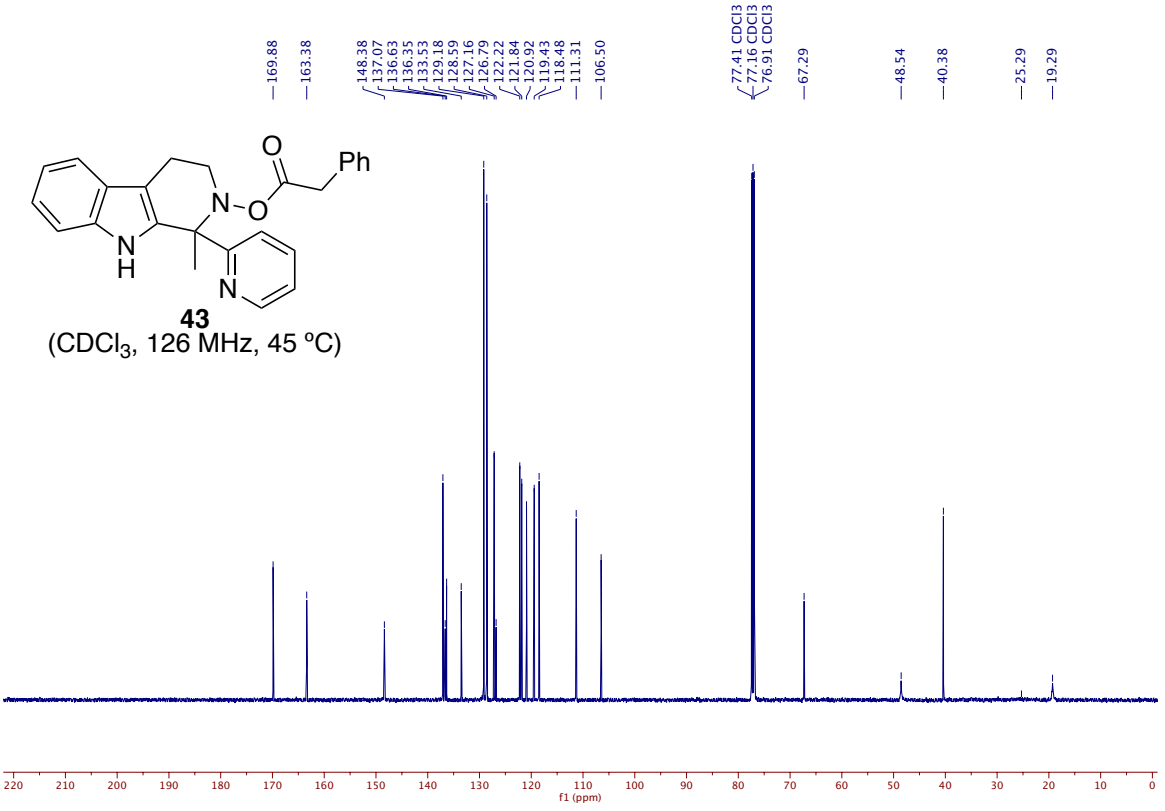
169.88
163.38
148.38
137.07
136.63
136.35
133.53
129.18
128.59
127.16
126.79
122.22
121.84
120.92
119.43
118.48
111.31
106.50
77.41 CDCl3
77.16 CDCl3
76.91 CDCl3
67.29
48.54
40.38
25.29
19.29
O
Ph
N
O
N
H
N
43
(CDCl3, 126 MHz, 45 ºC)
f1 (ppm)

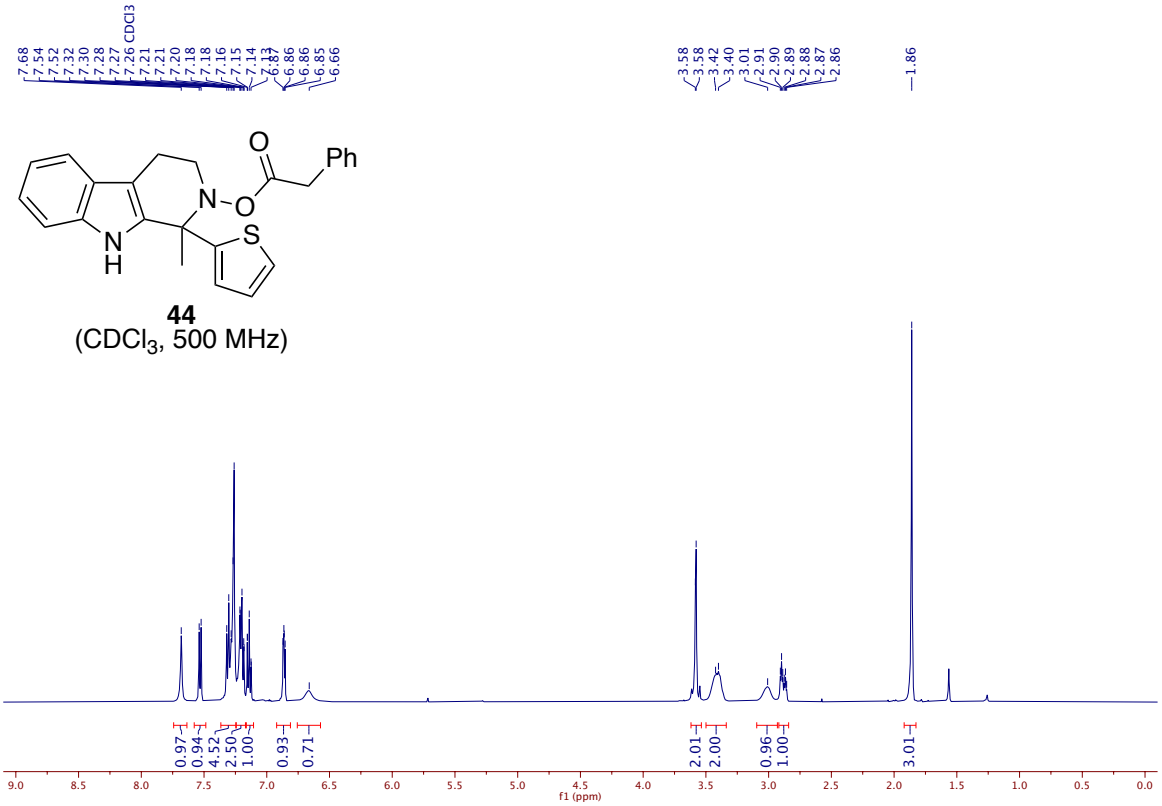

44
($CDCl_3$, 500 MHz)

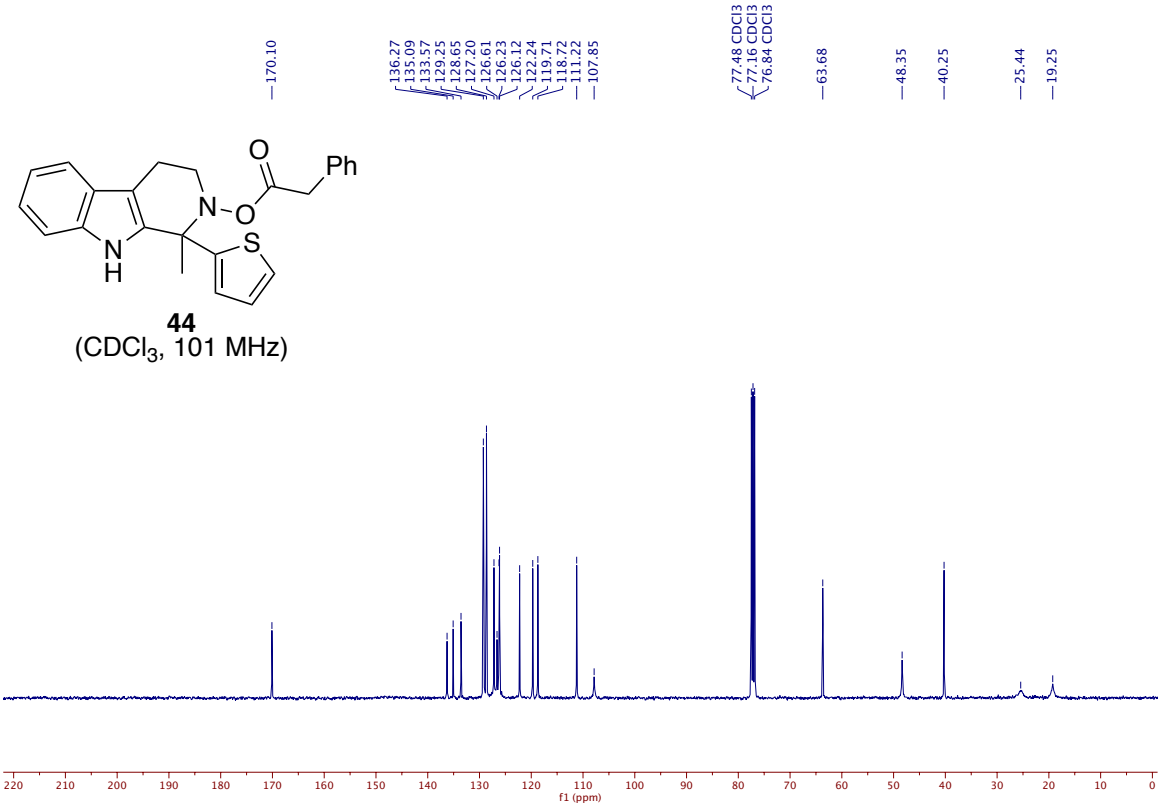

44
($CDCl_3$, 101 MHz)

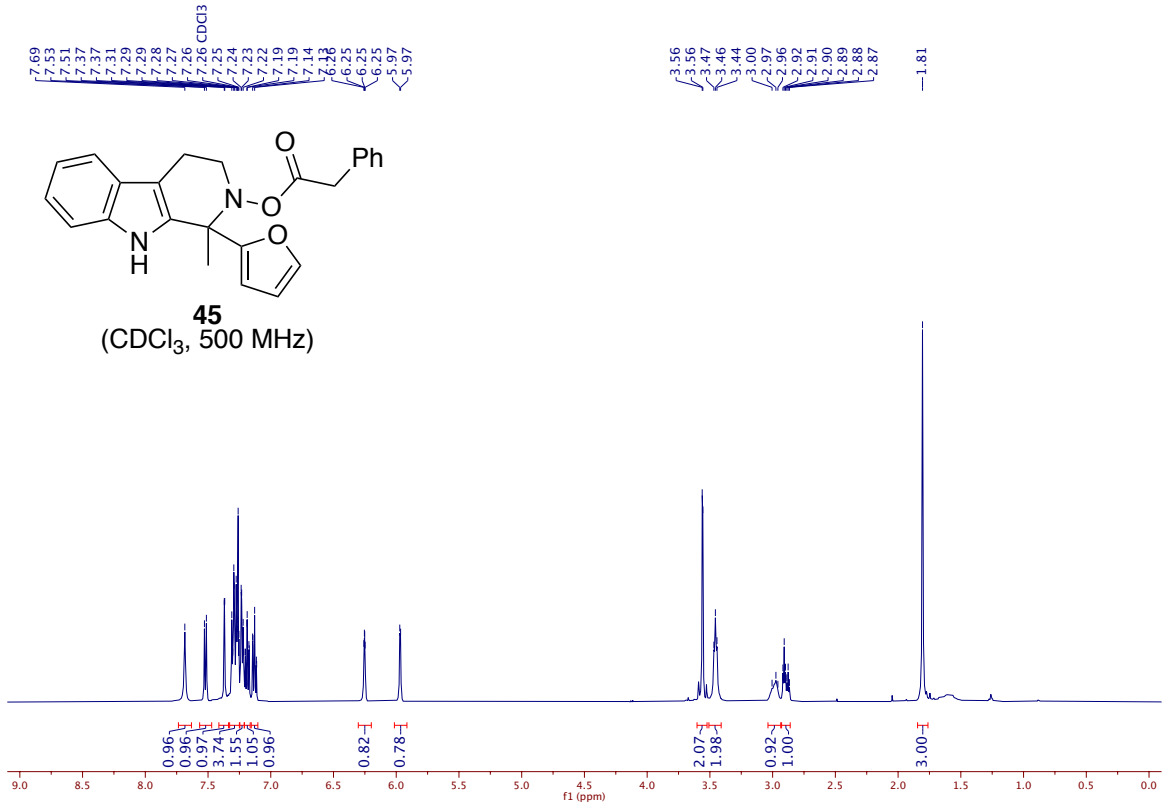

45
($CDCl_3$, 500 MHz)

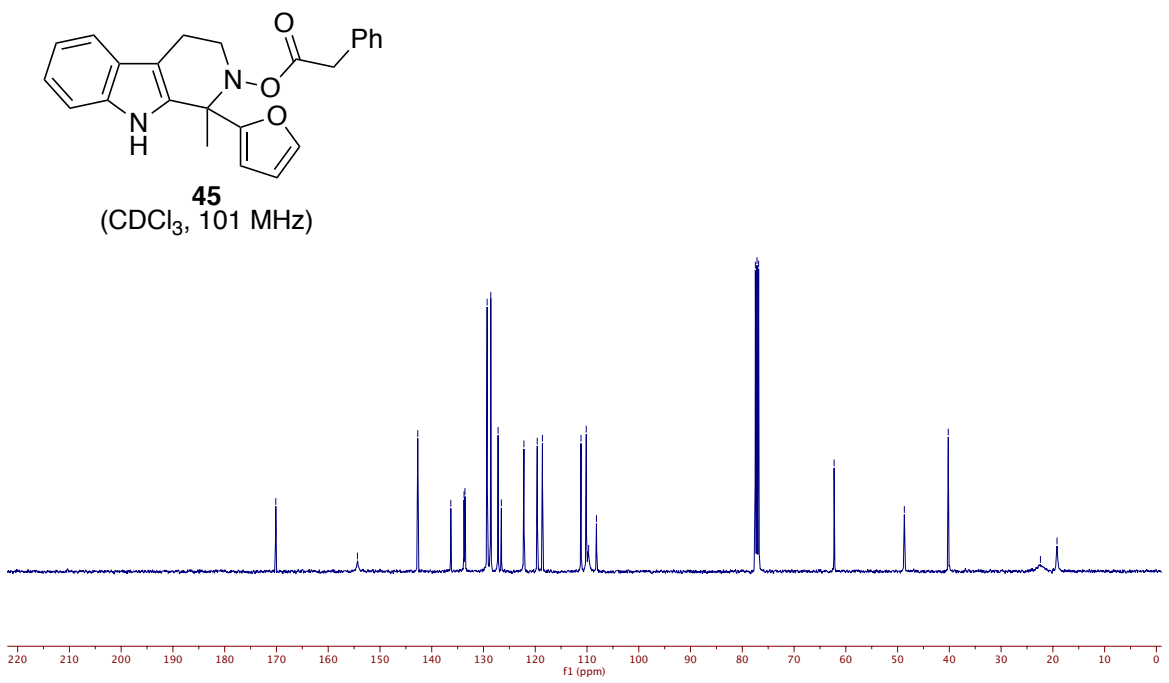

45
($CDCl_3$, 101 MHz)

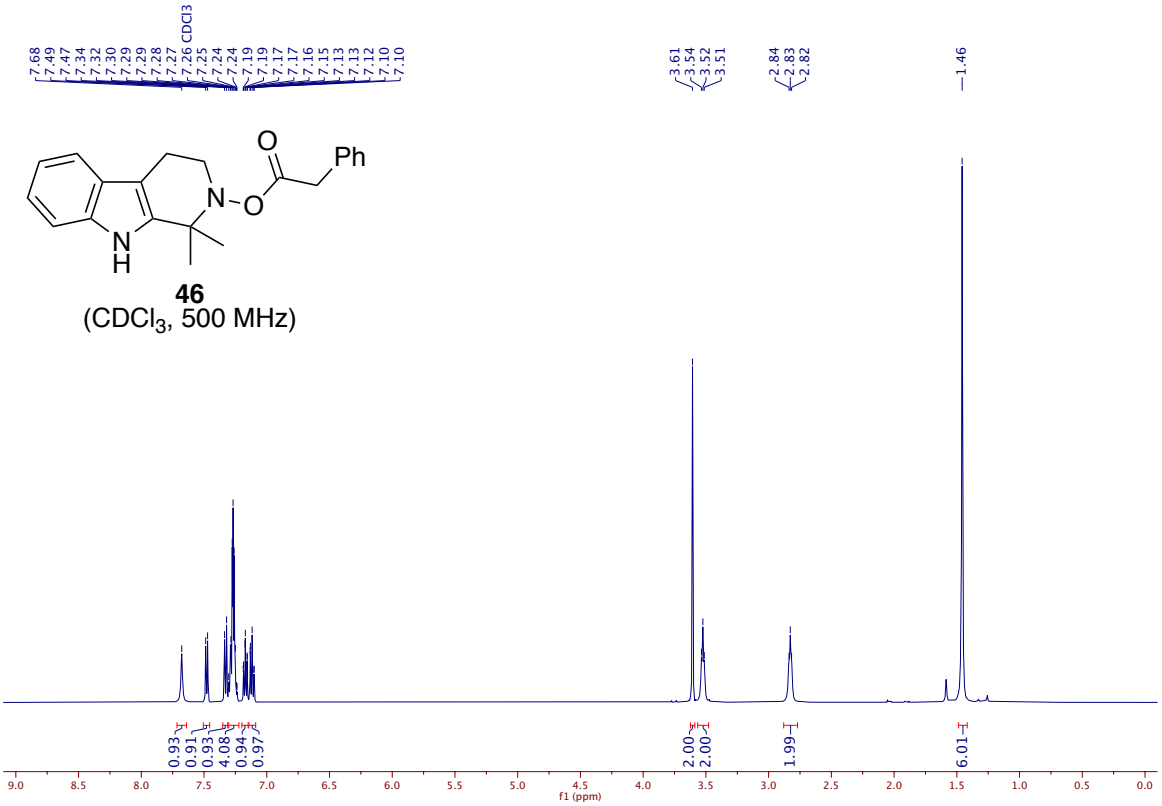

46
($CDCl_3$, 500 MHz)

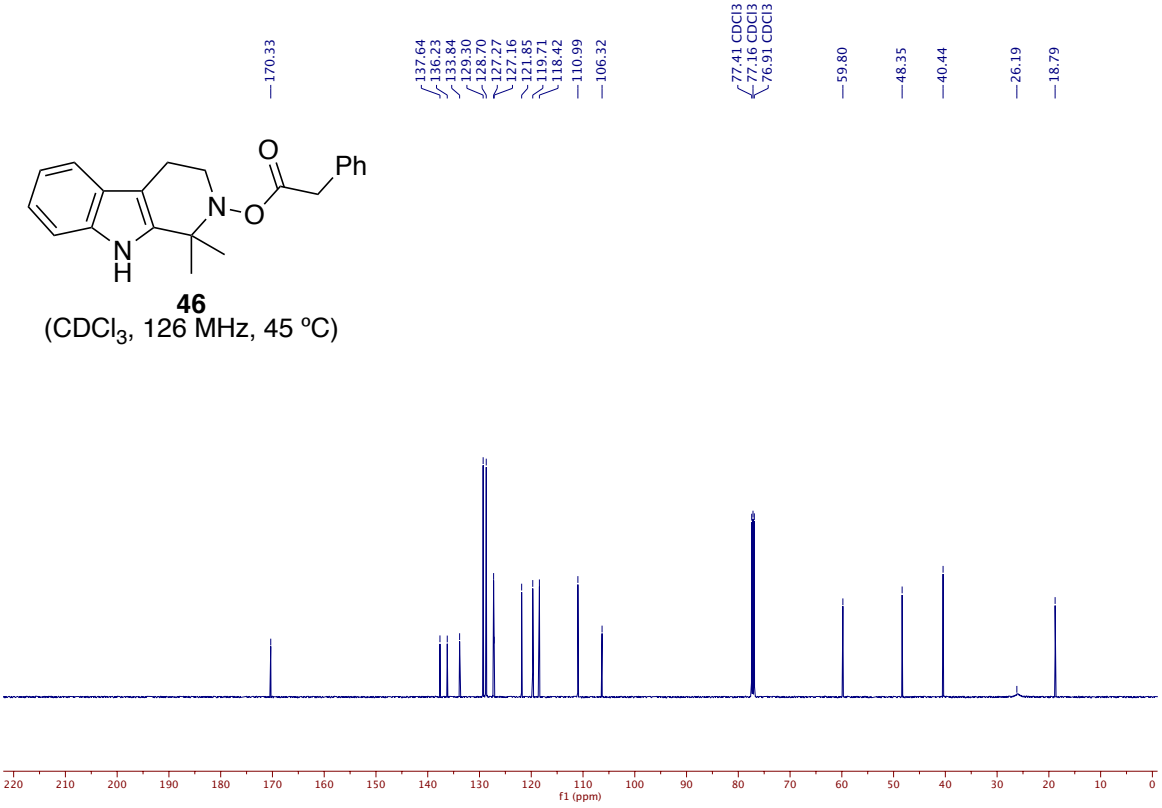

46
($CDCl_3$, 126 MHz, 45 ºC)

47
($CDCl_3$, 500 MHz)

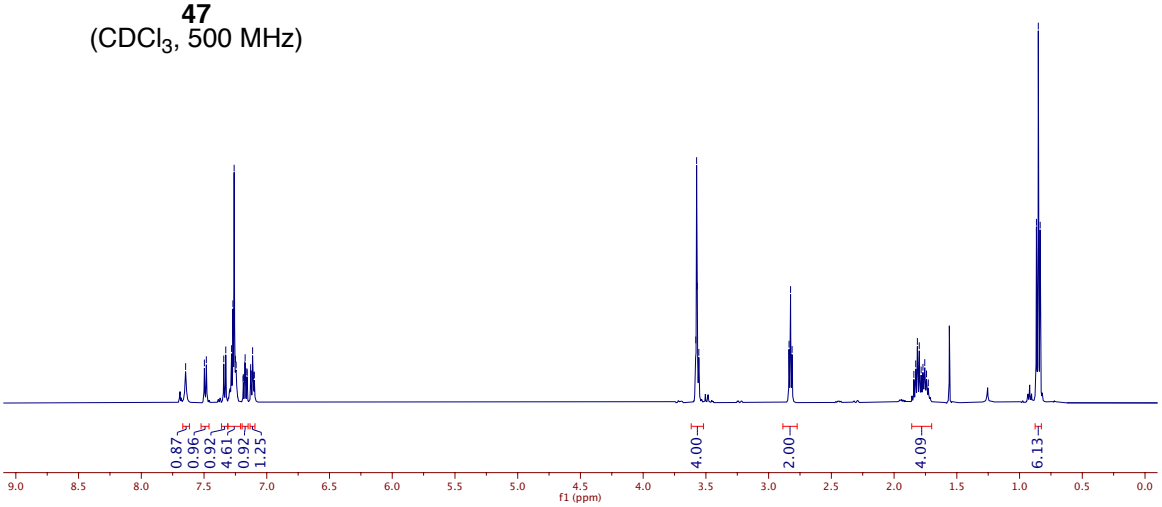

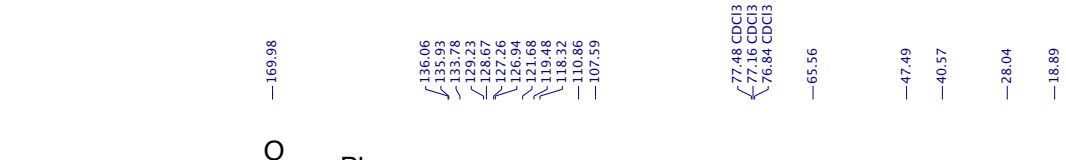

47
($CDCl_3$, 101 MHz)

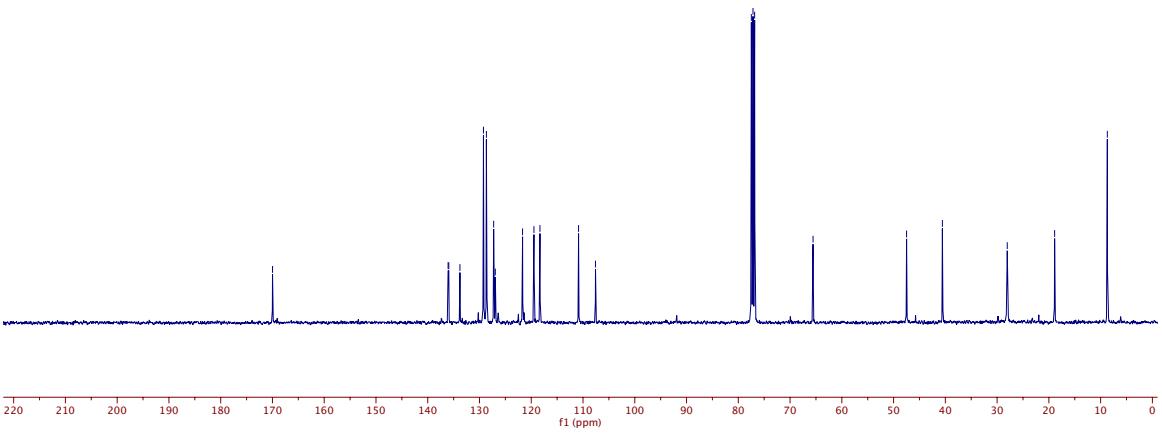

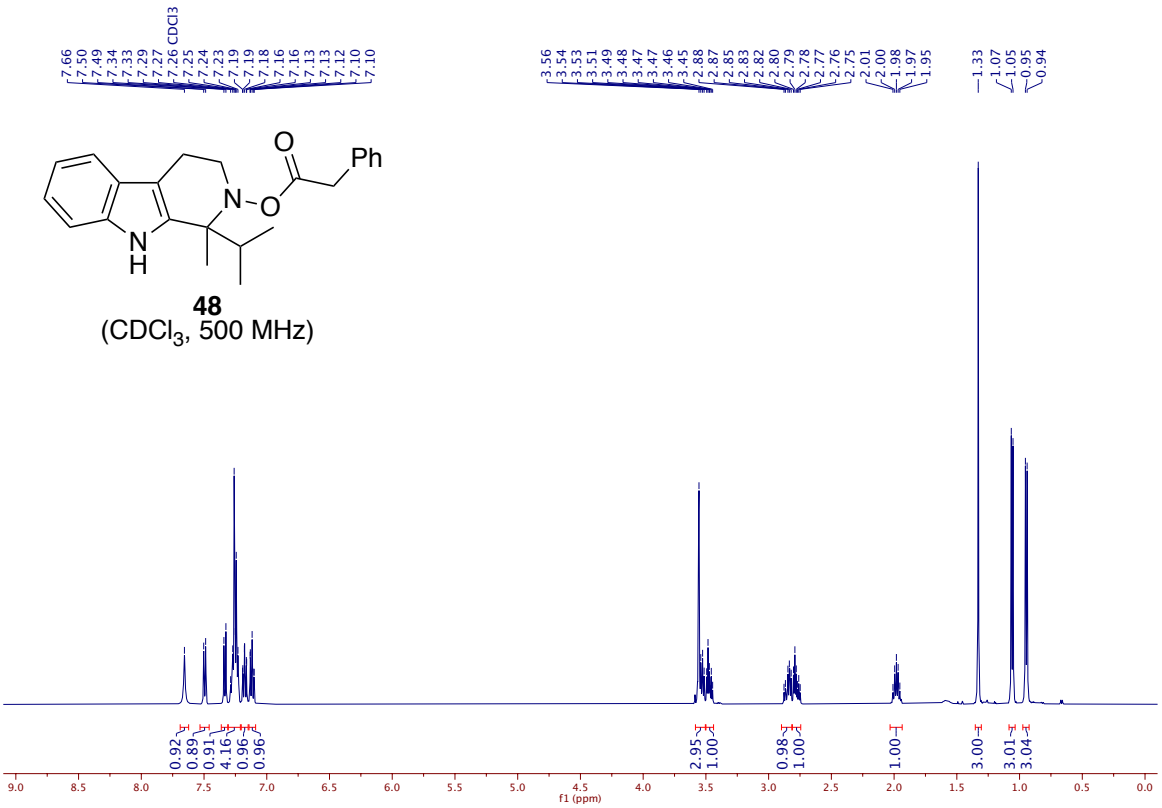

48
($CDCl_3$, 500 MHz)

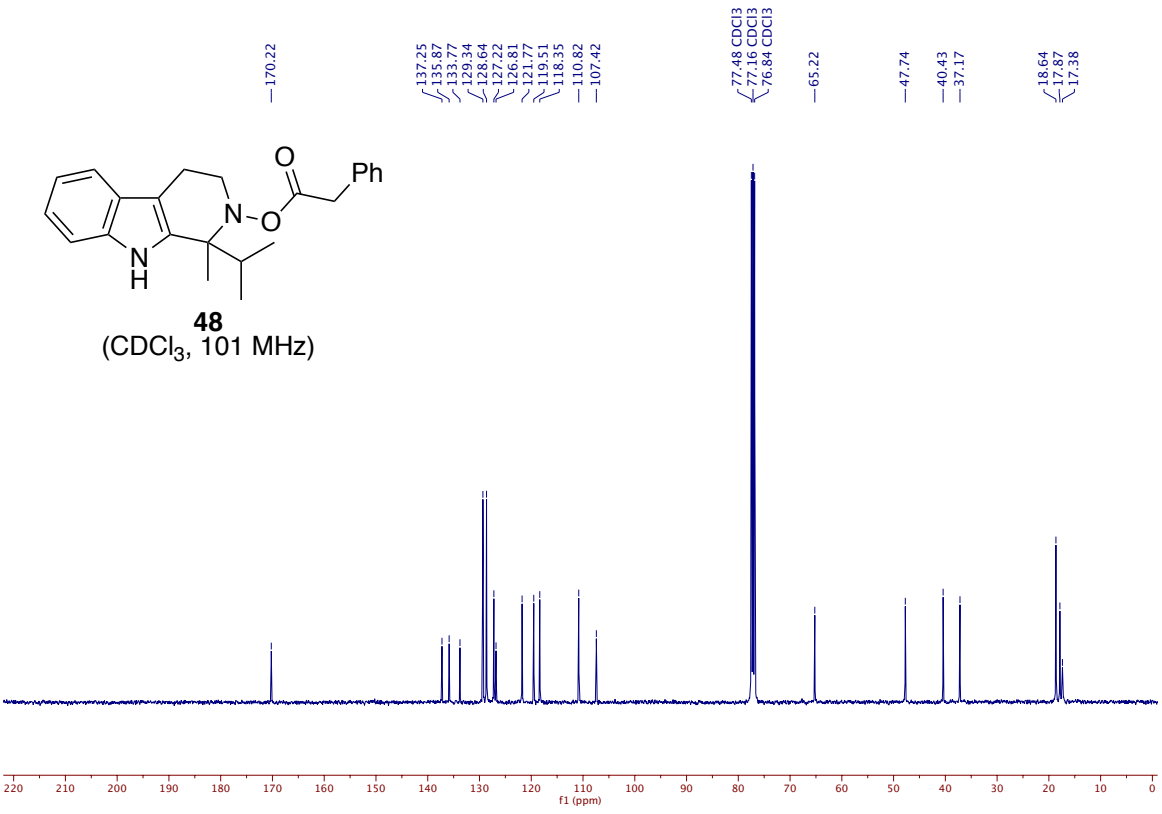

48
($CDCl_3$, 101 MHz)

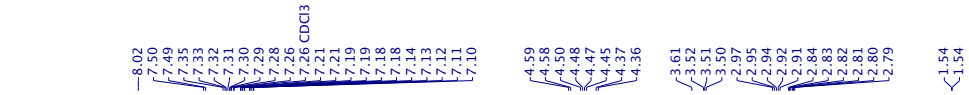

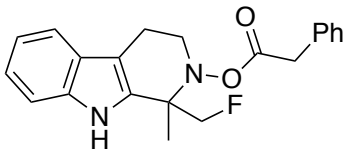

49
($CDCl_3$, 500 MHz)

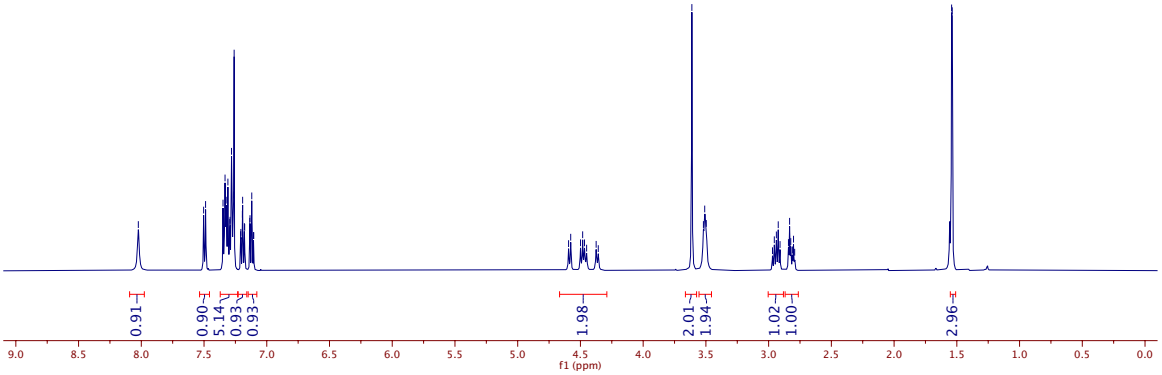

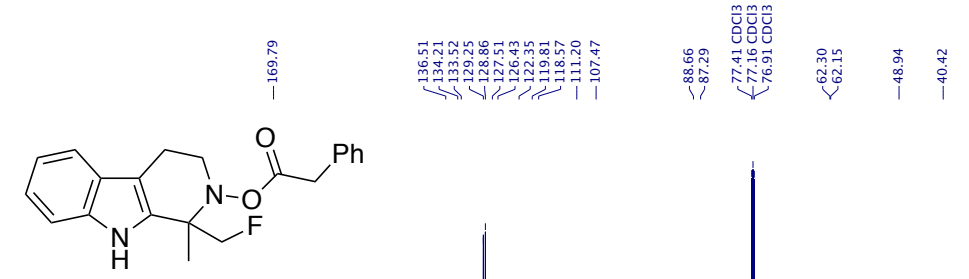

49
($CDCl_3$, 126 MHz, 45 °C)

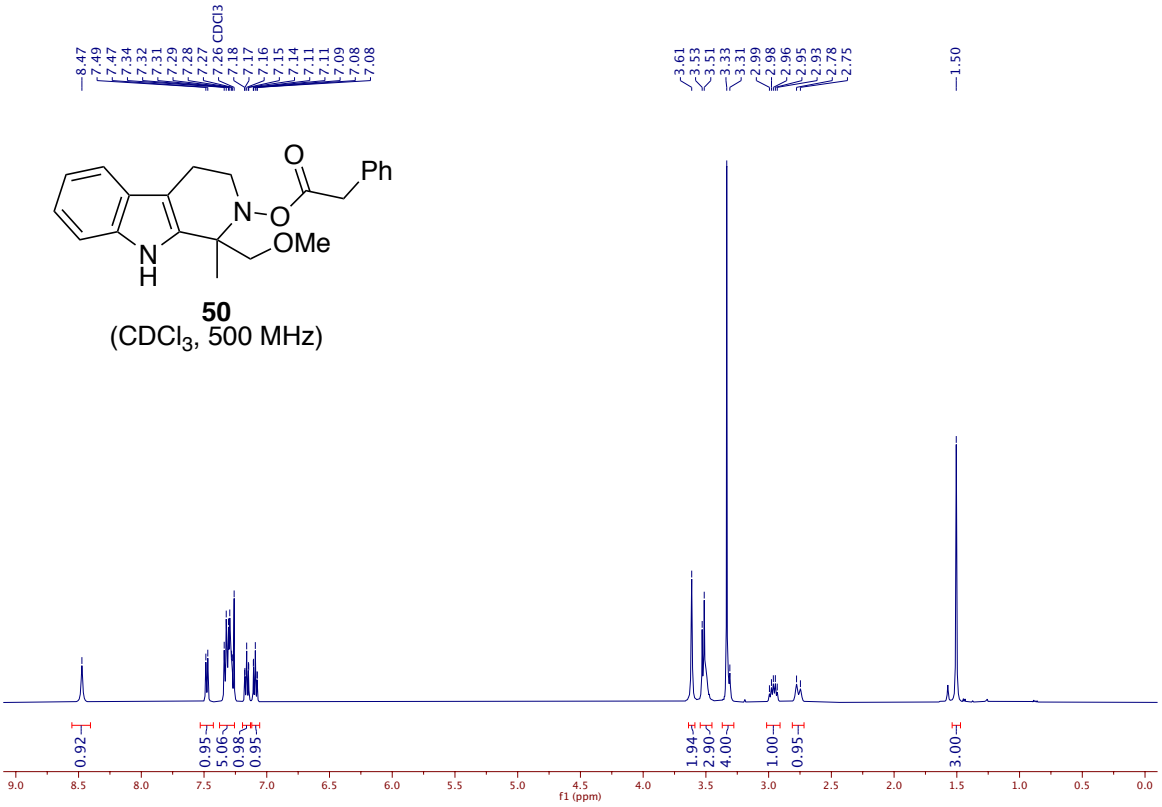

50
($CDCl_3$, 500 MHz)

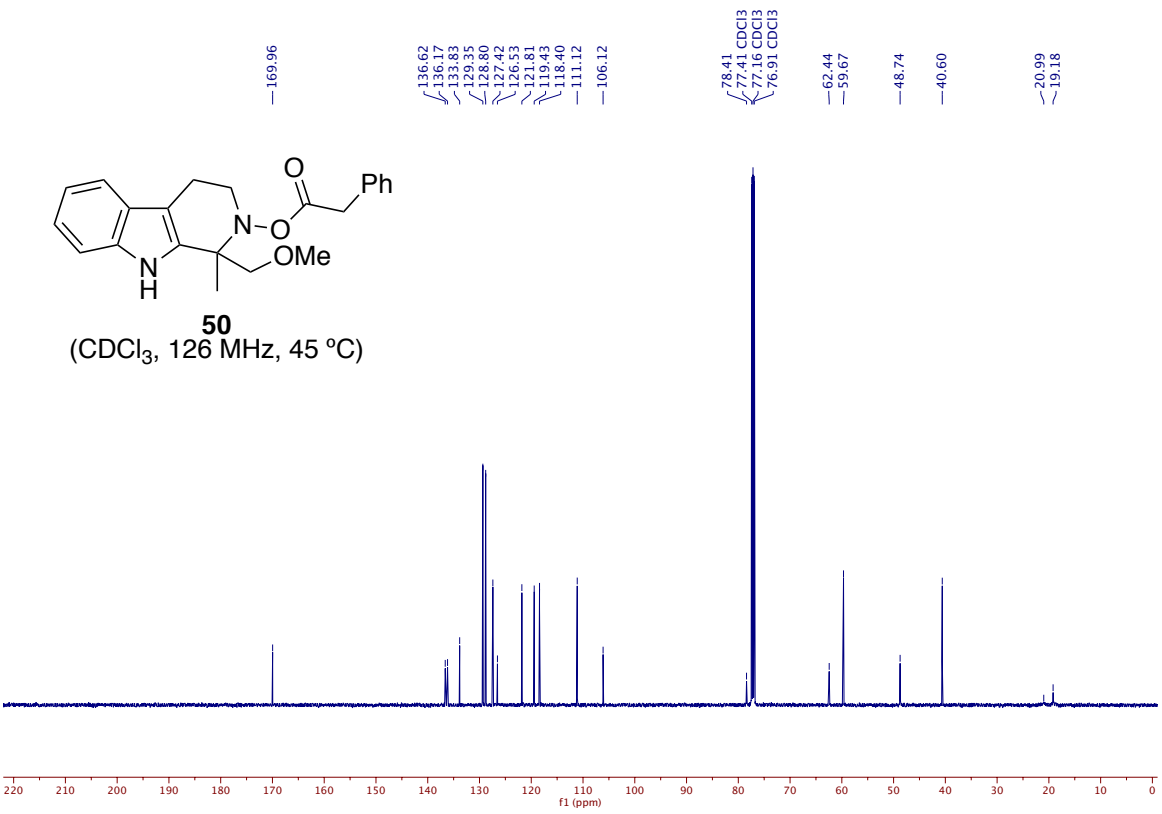

50
($CDCl_3$, 126 MHz, 45 °C)

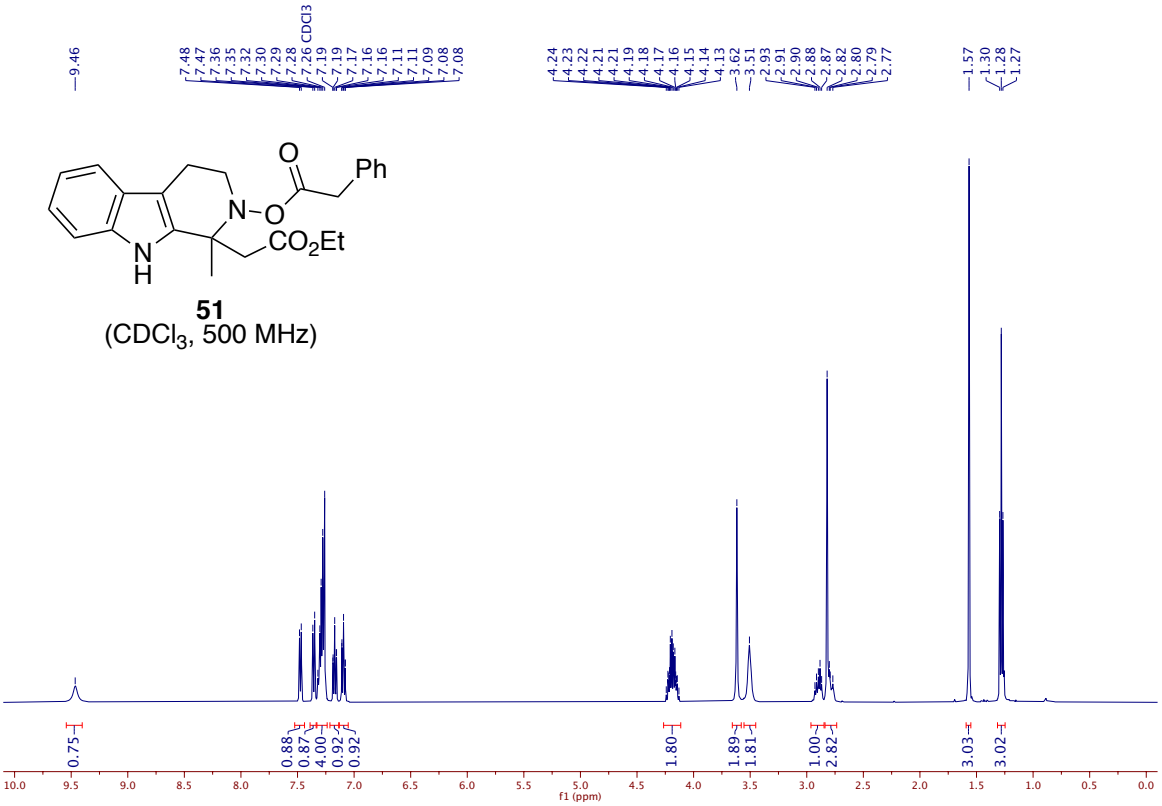

51
($CDCl_3$, 500 MHz)

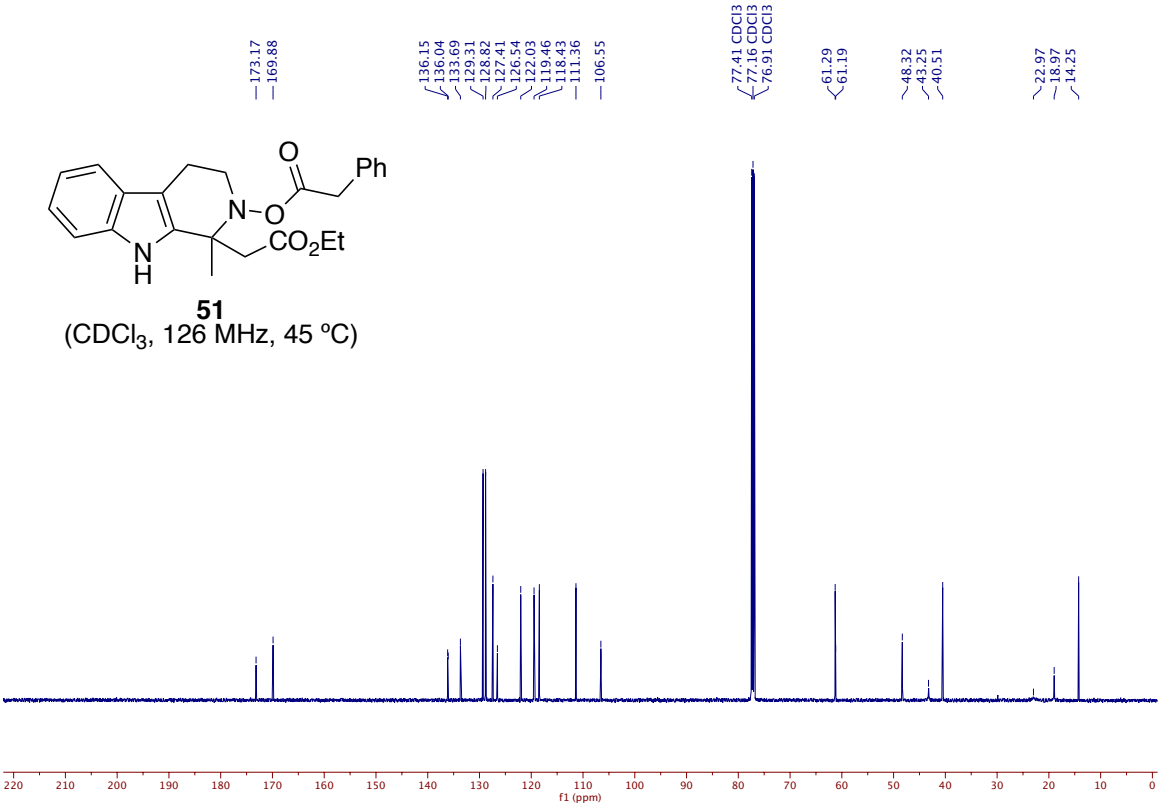

51
($CDCl_3$, 126 MHz, 45 °C)

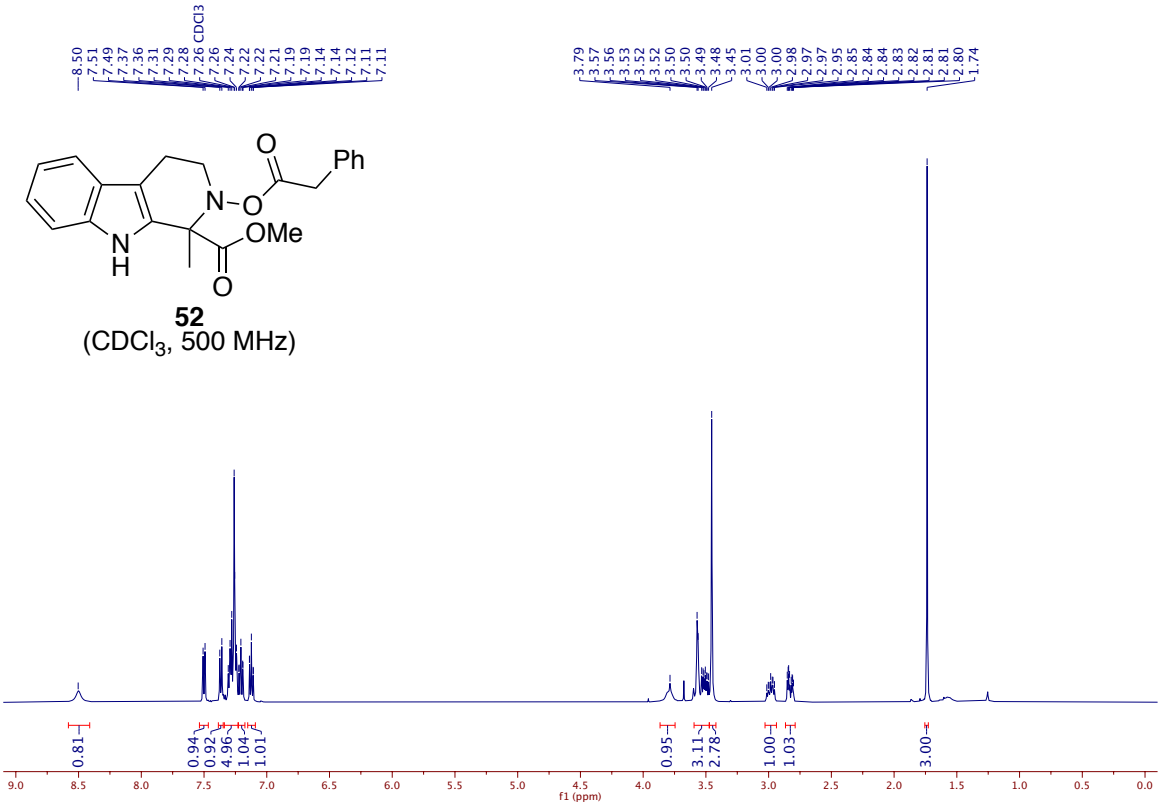

52
($CDCl_3$, 500 MHz)

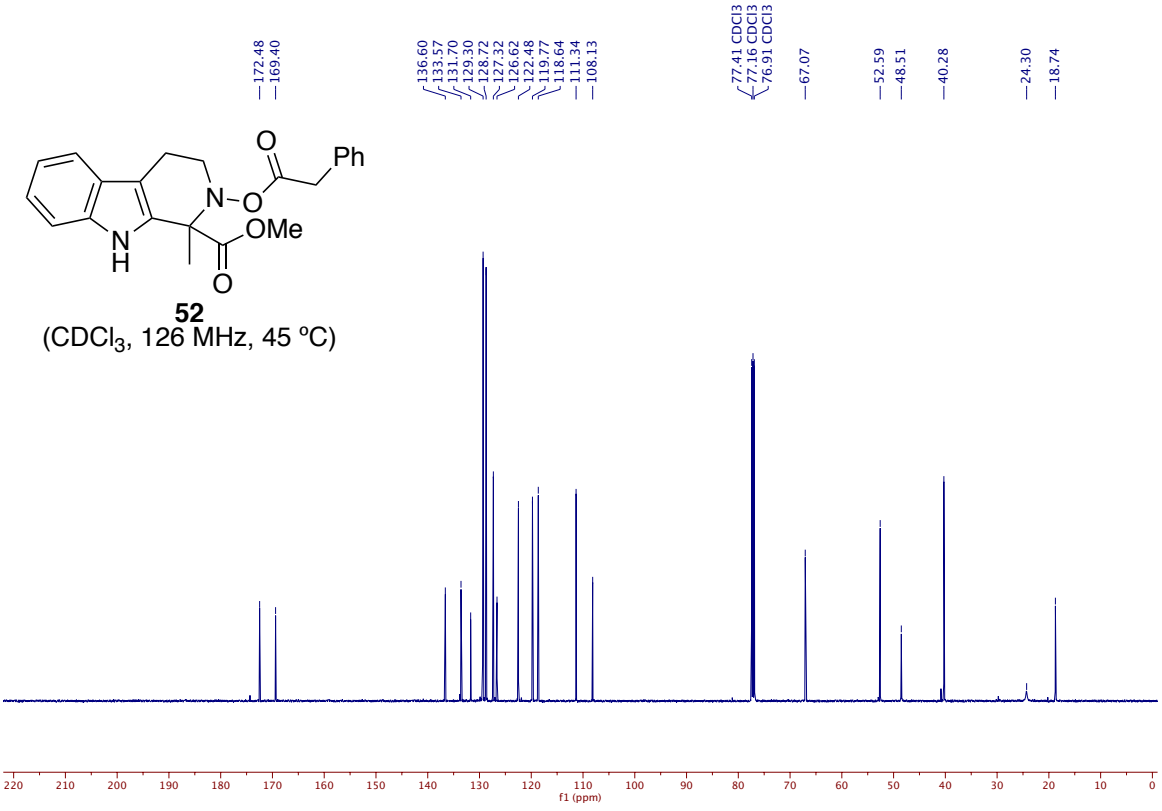

52
($CDCl_3$, 126 MHz, 45 ºC)

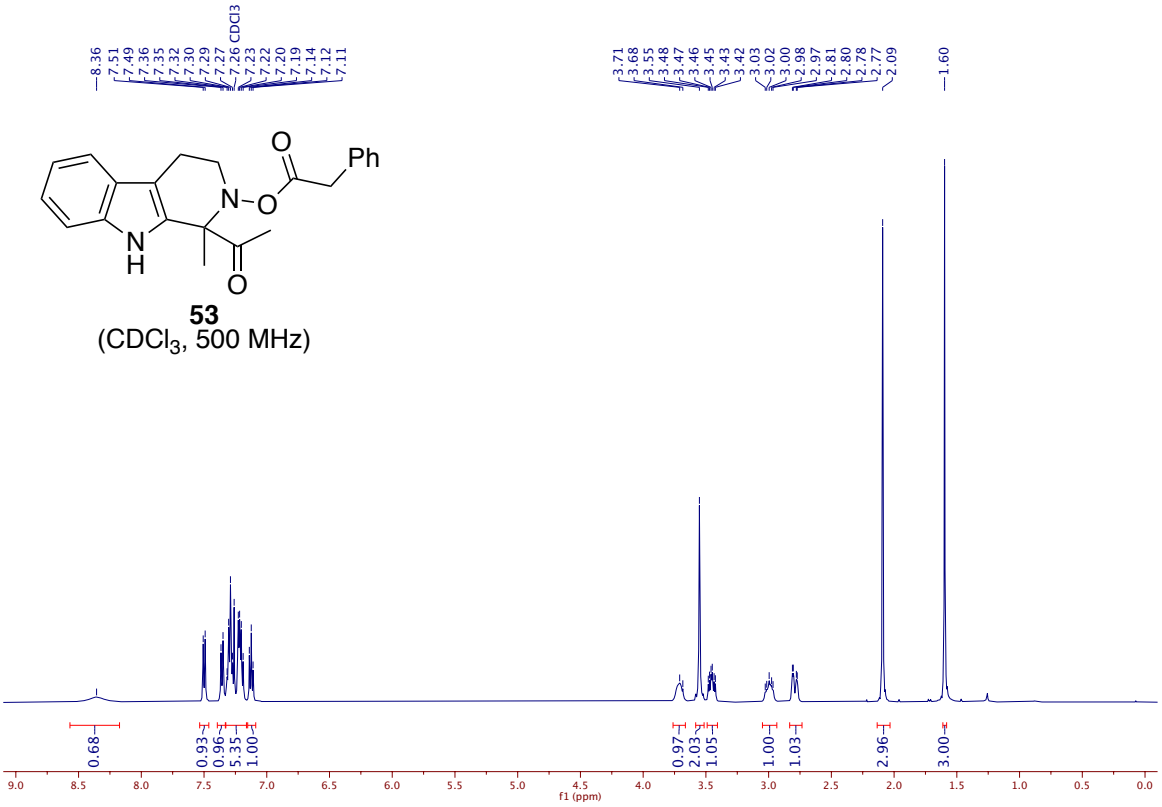

53
($CDCl_3$, 500 MHz)

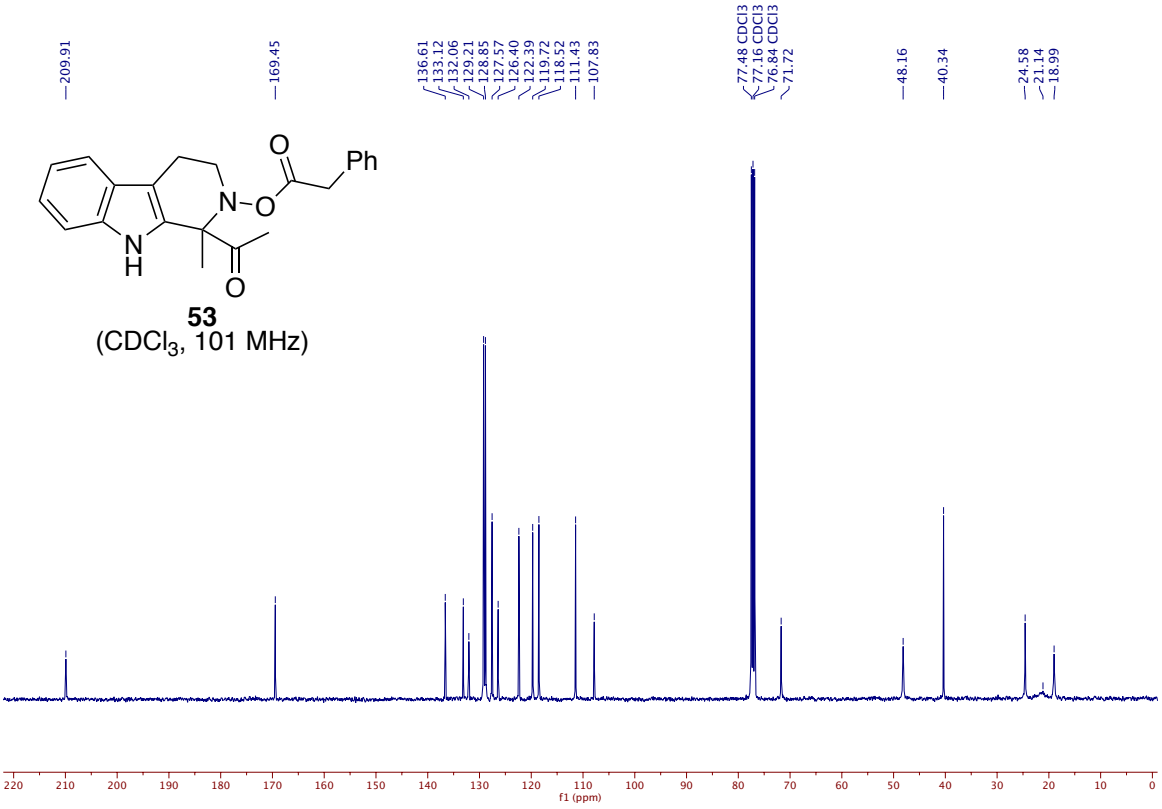

53
($CDCl_3$, 101 MHz)

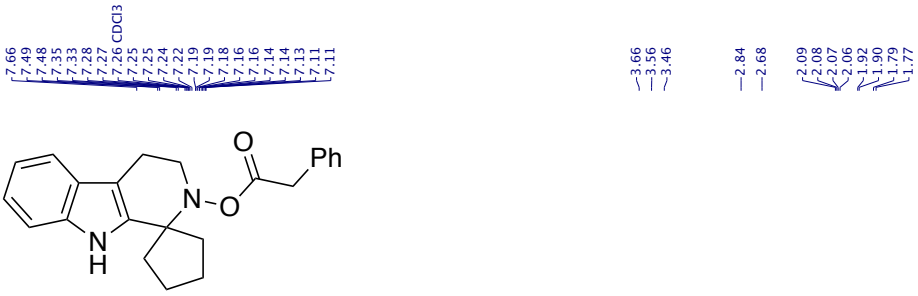

54
($CDCl_3$, 500 MHz)

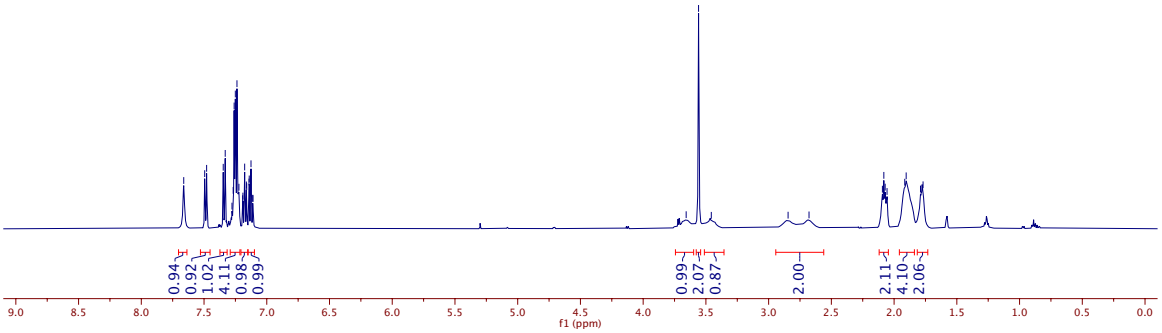

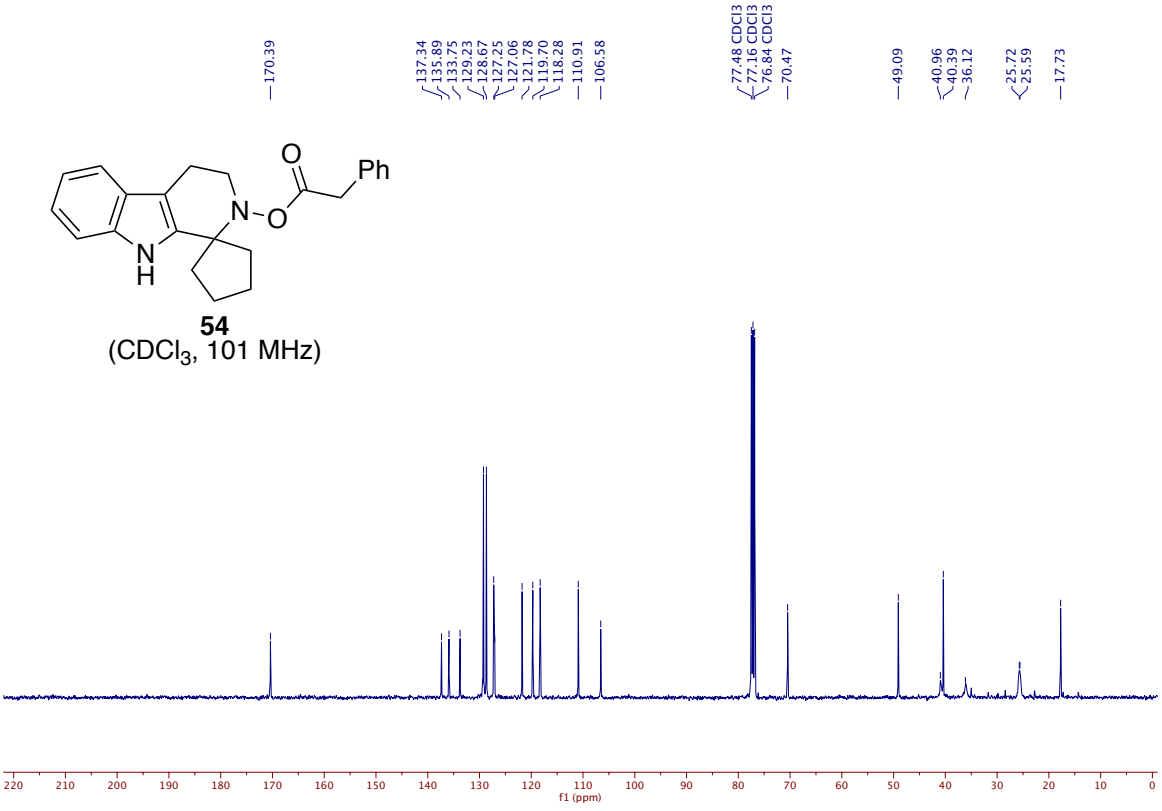

54
($CDCl_3$, 101 MHz)

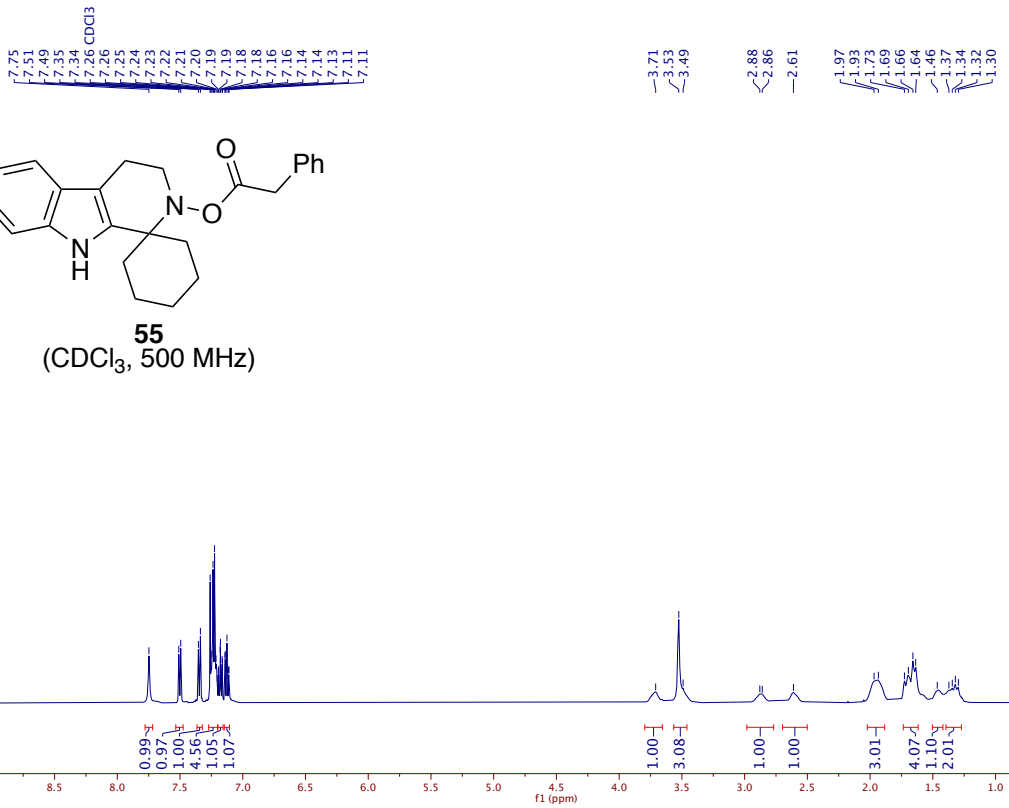

55
($CDCl_3$, 500 MHz)

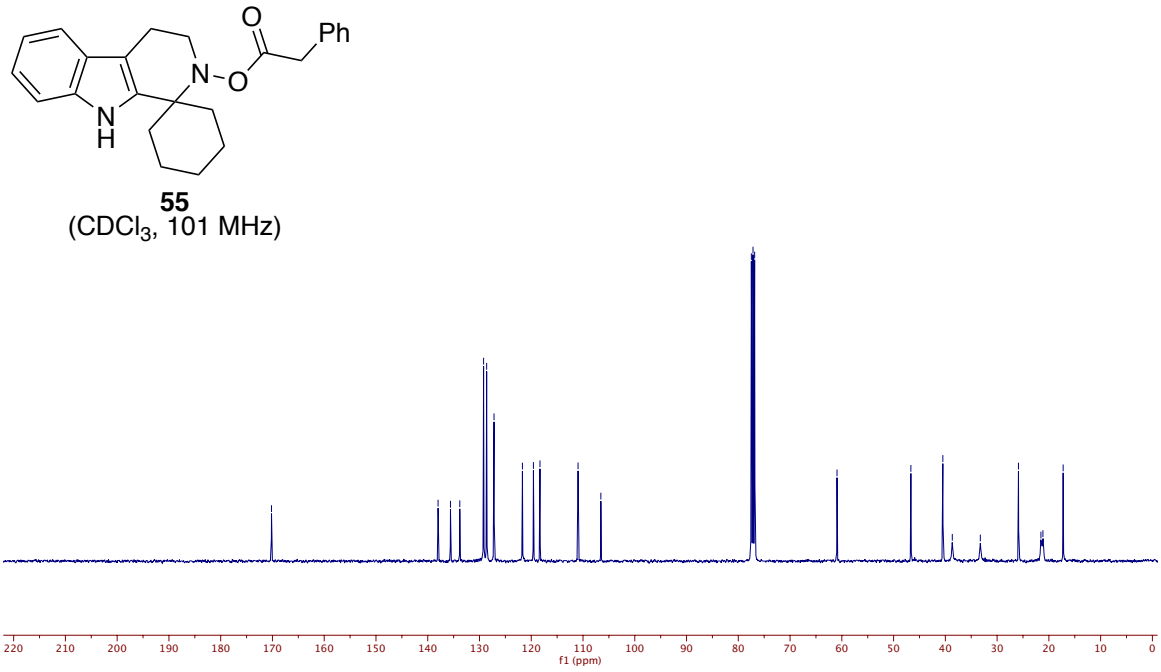

55
($CDCl_3$, 101 MHz)

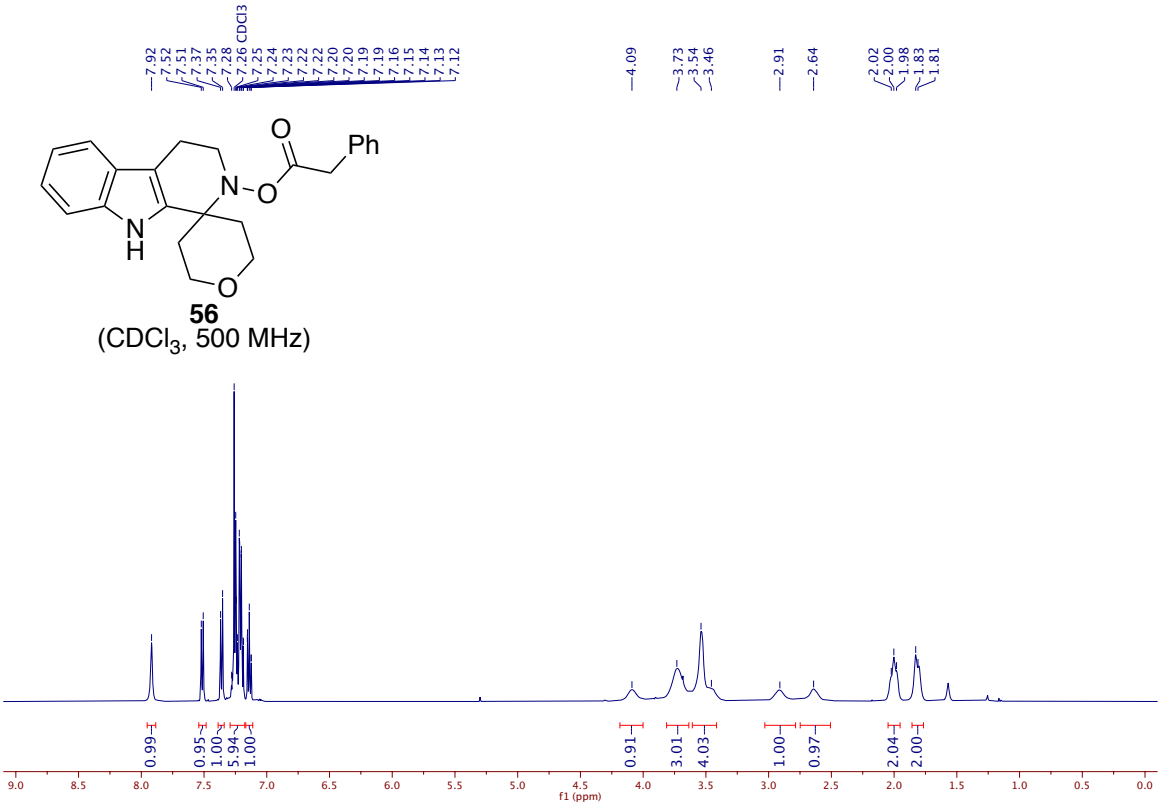

56

($CDCl_3$, 500 MHz)

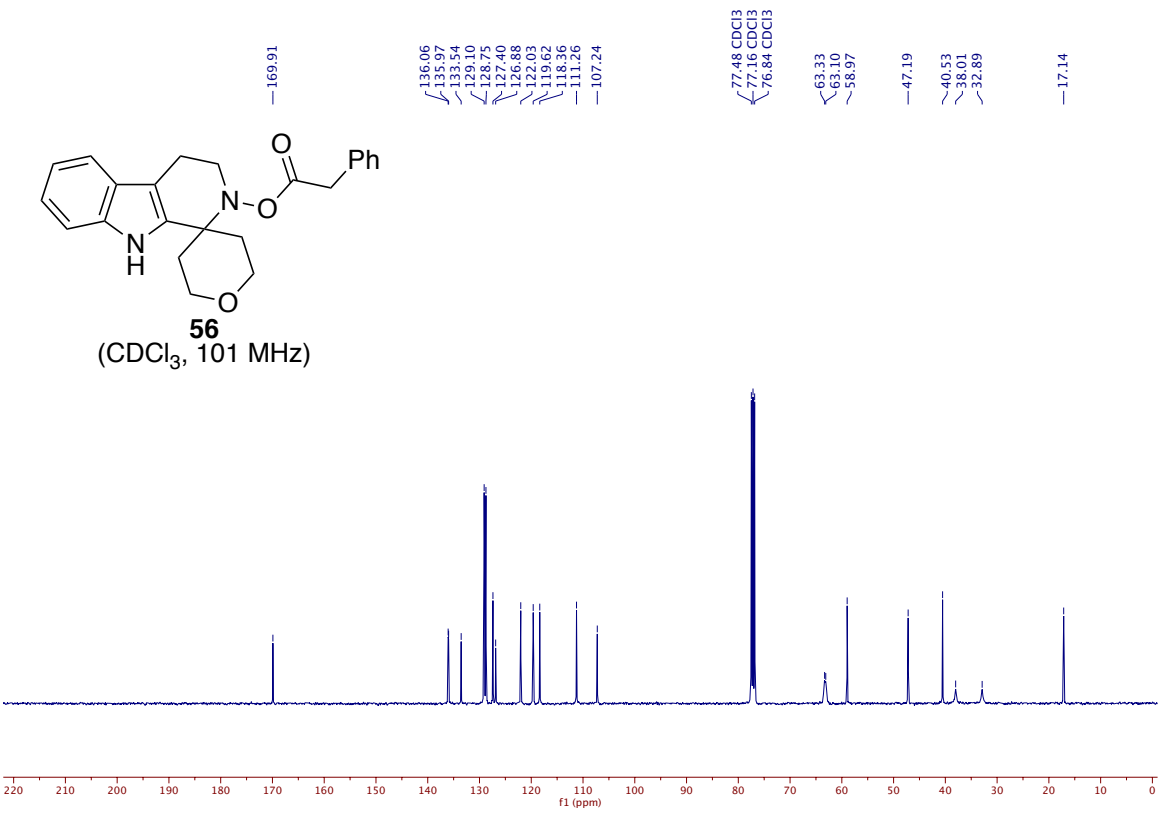

56

($CDCl_3$, 101 MHz)

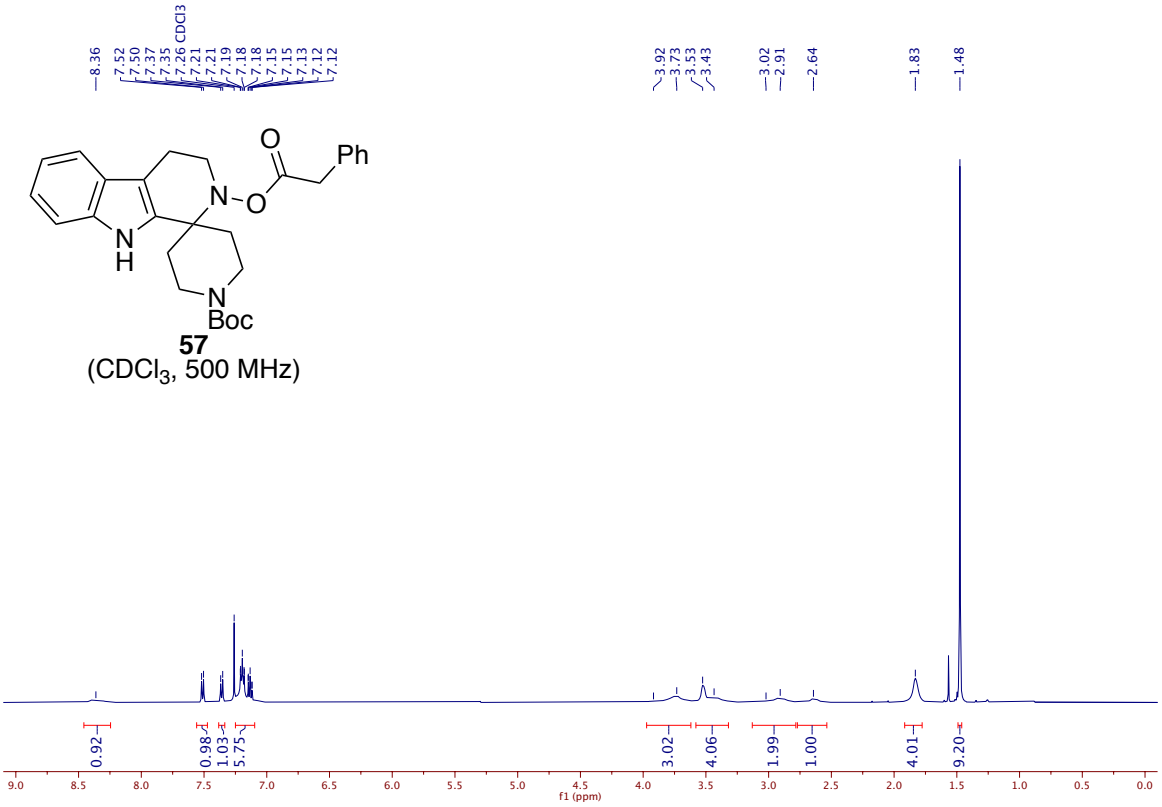

57

($CDCl_3$, 500 MHz)

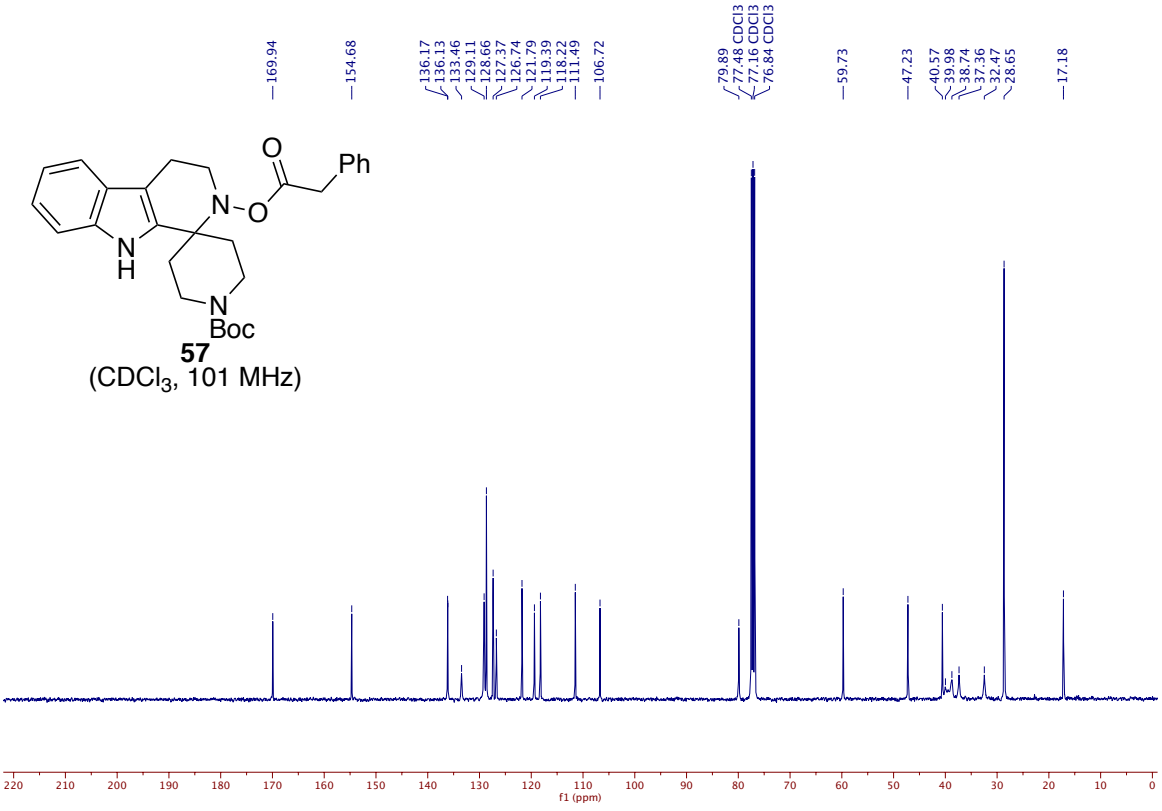

57

($CDCl_3$, 101 MHz)

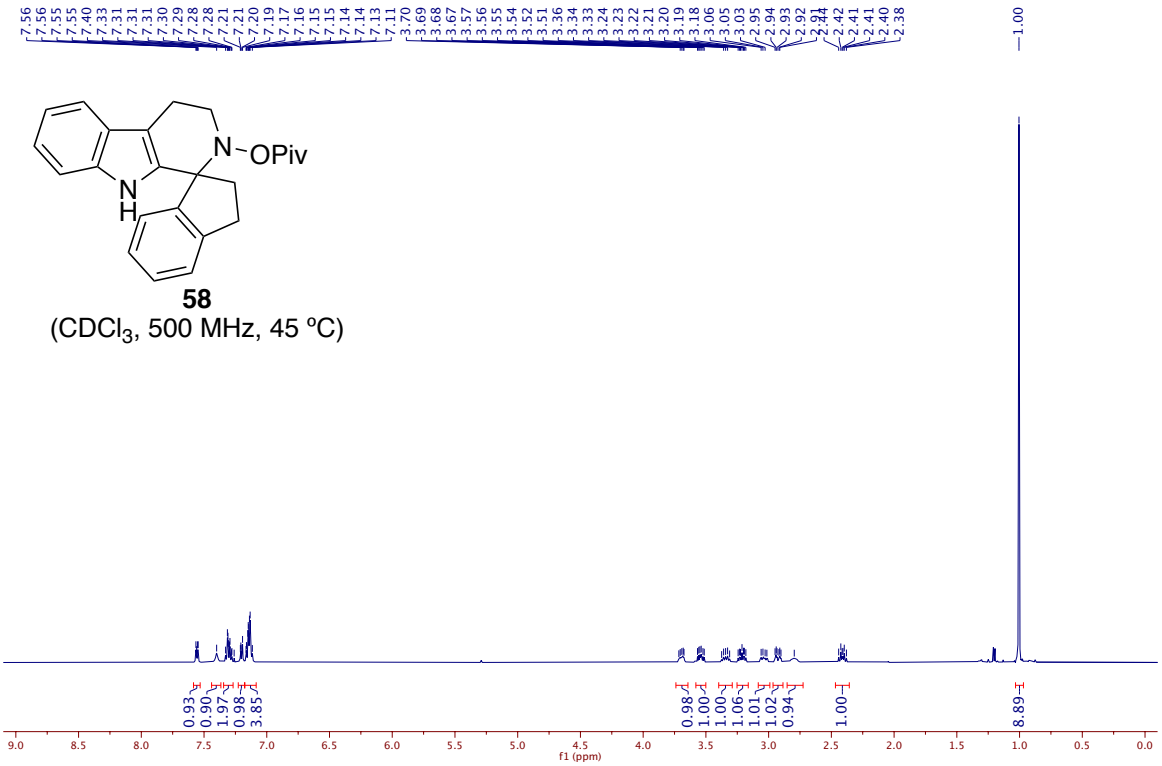
N–OPiv
N
H
58
(CDCl3, 500 MHz, 45 °C)
f1 (ppm)

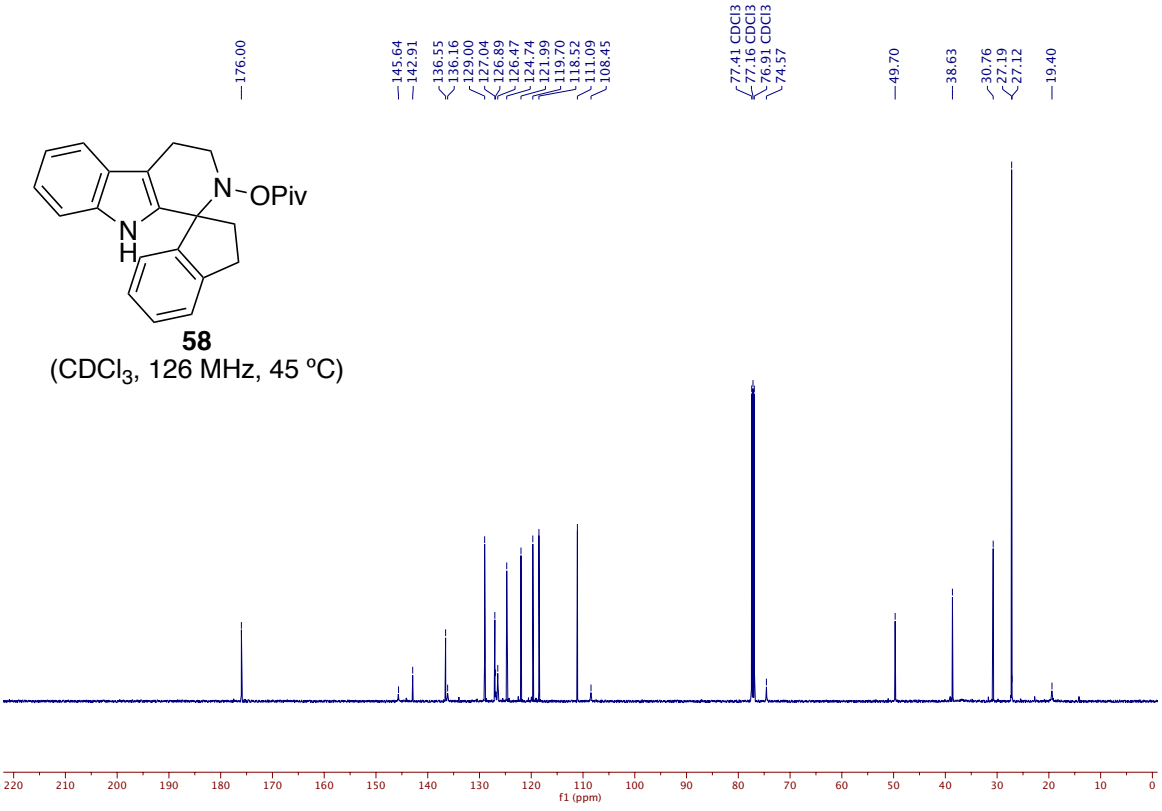
N–OPiv
N
H
58
(CDCl3, 126 MHz, 45 °C)
f1 (ppm)

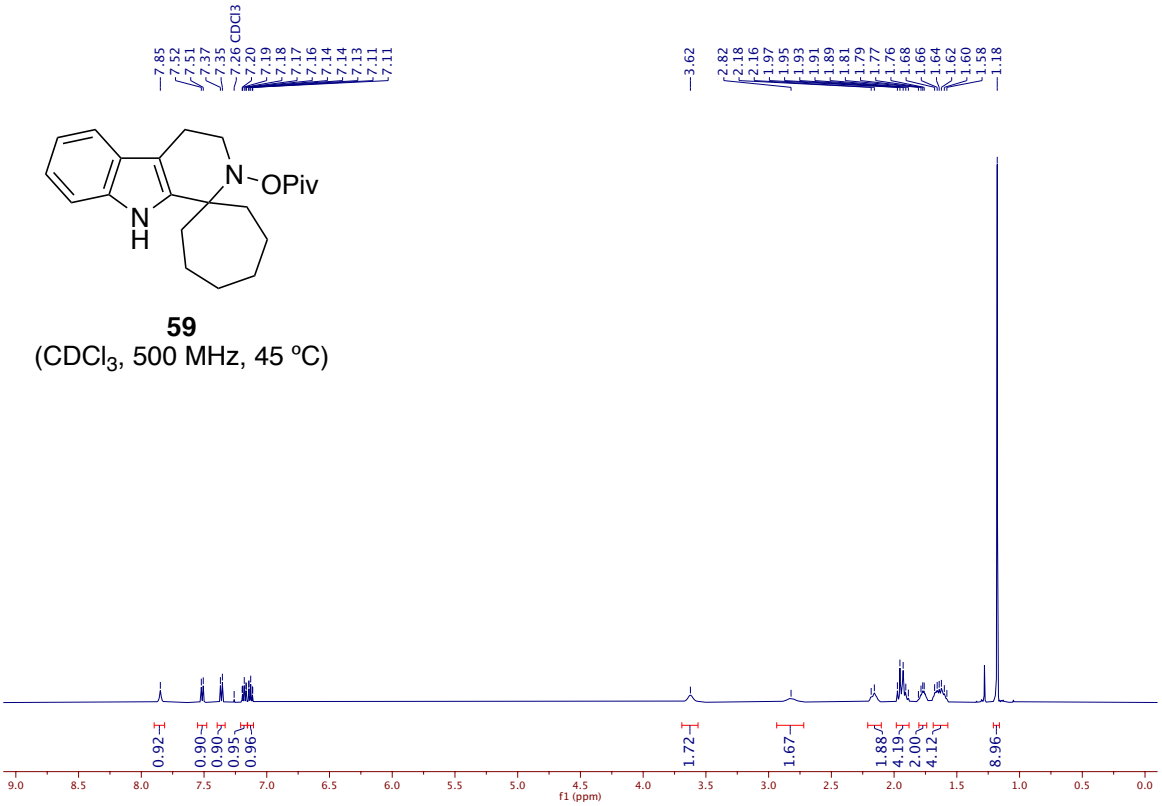

59
($CDCl_3$, 500 MHz, 45 °C)

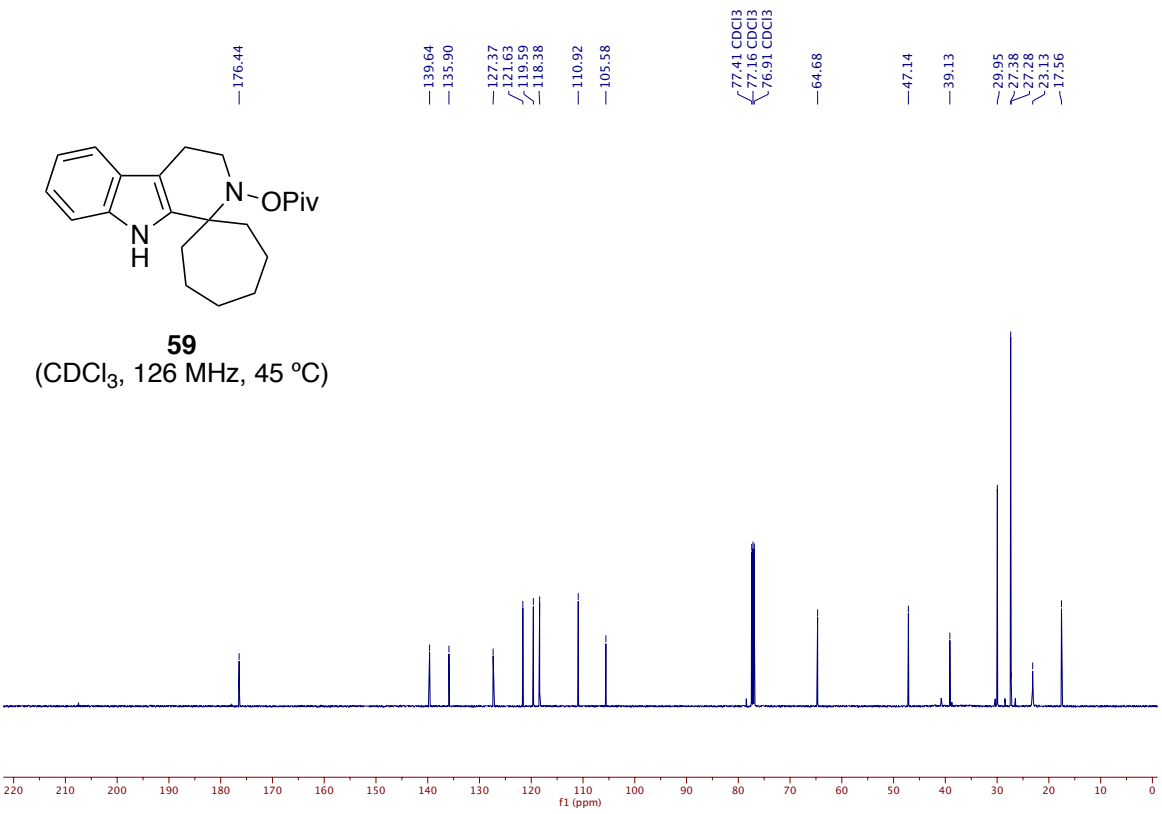

59
($CDCl_3$, 126 MHz, 45 °C)

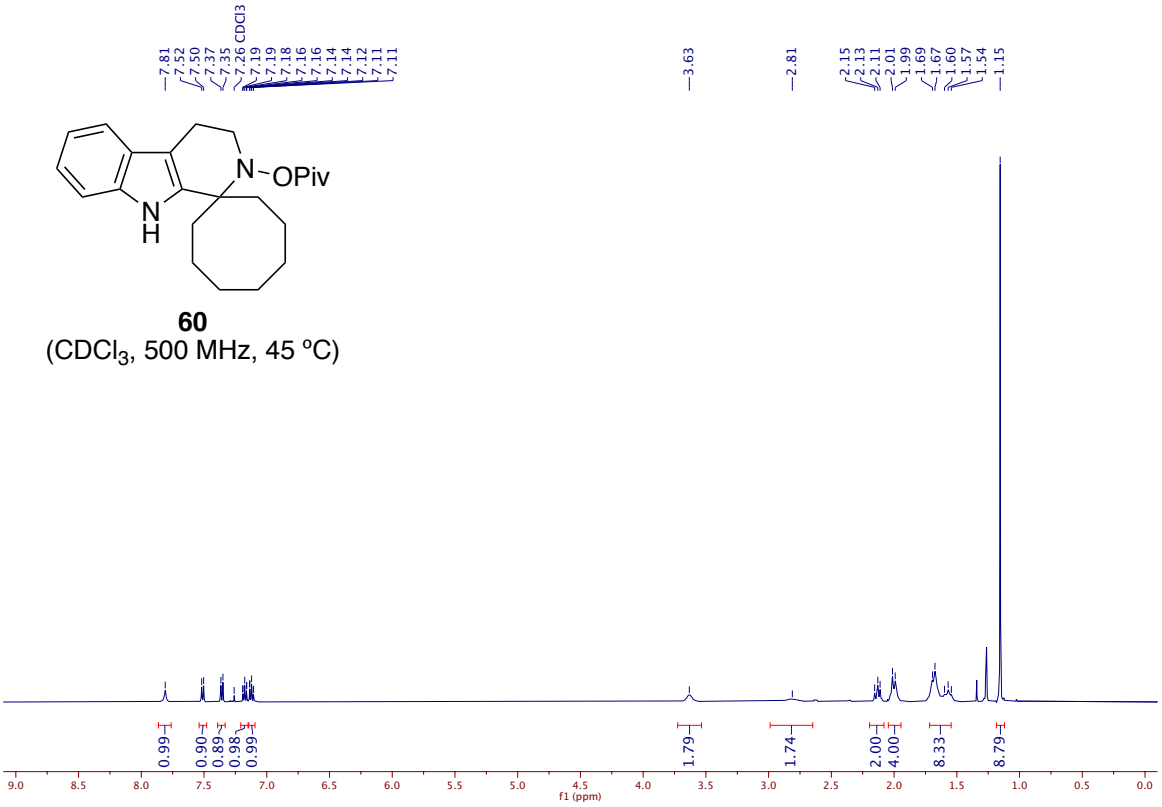

60
($CDCl_3$, 500 MHz, 45 ºC)

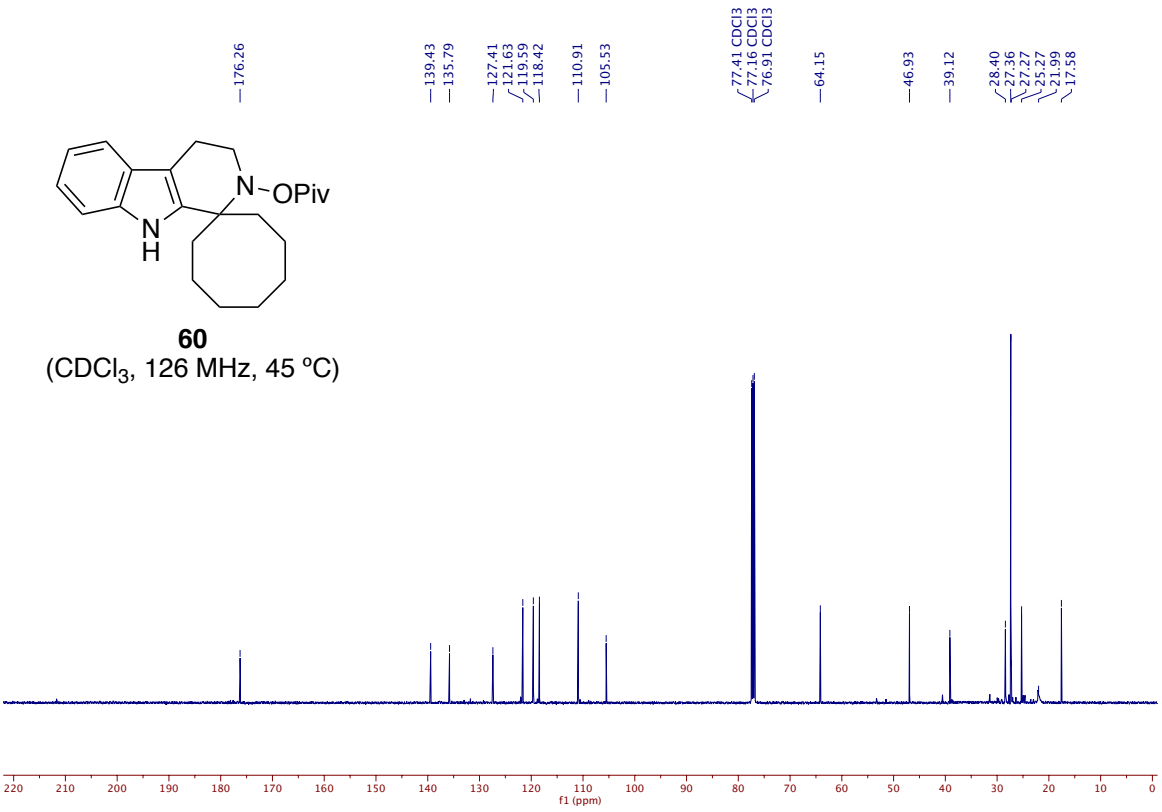

60
($CDCl_3$, 126 MHz, 45 ºC)

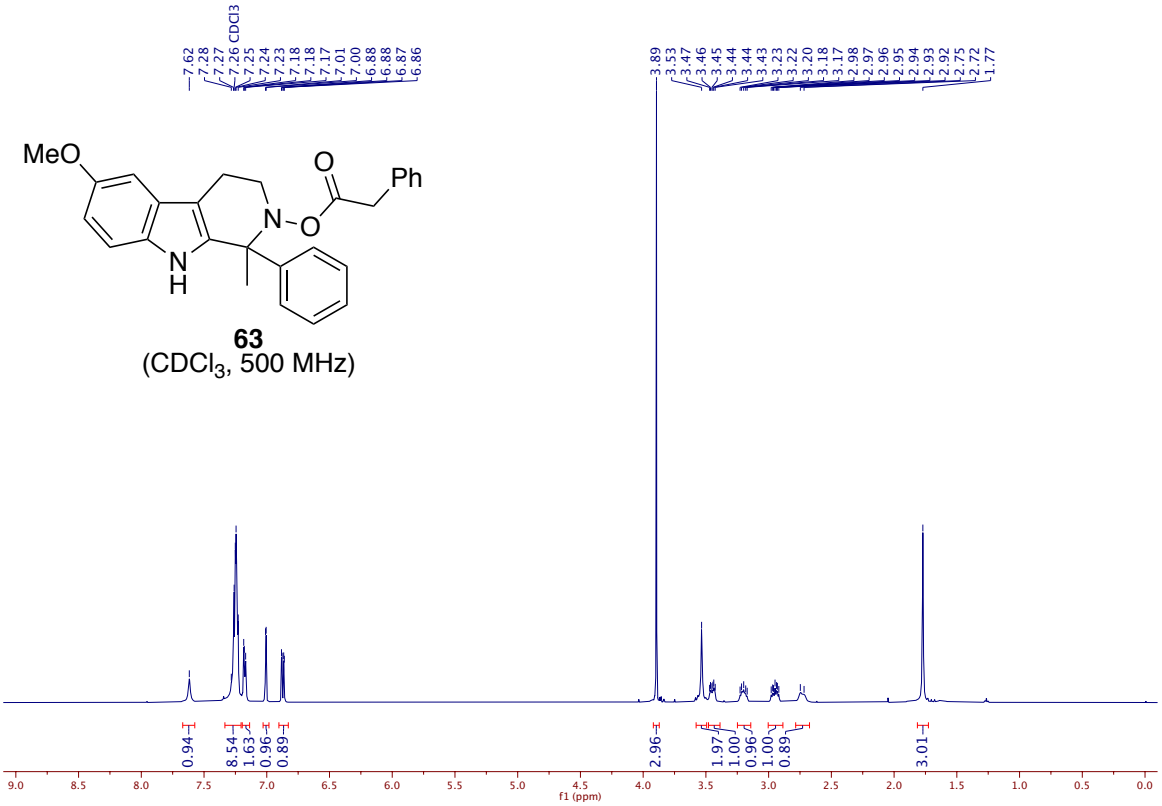

63
($CDCl_3$, 500 MHz)

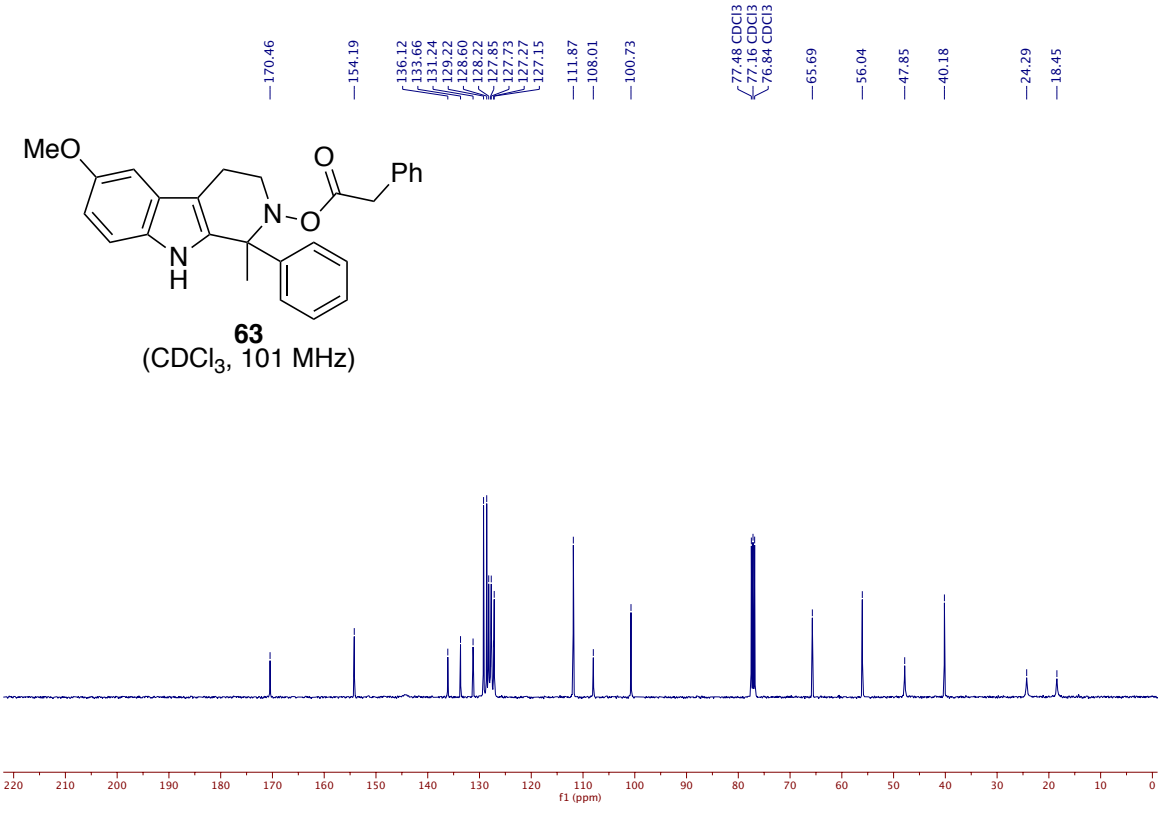

63
($CDCl_3$, 101 MHz)

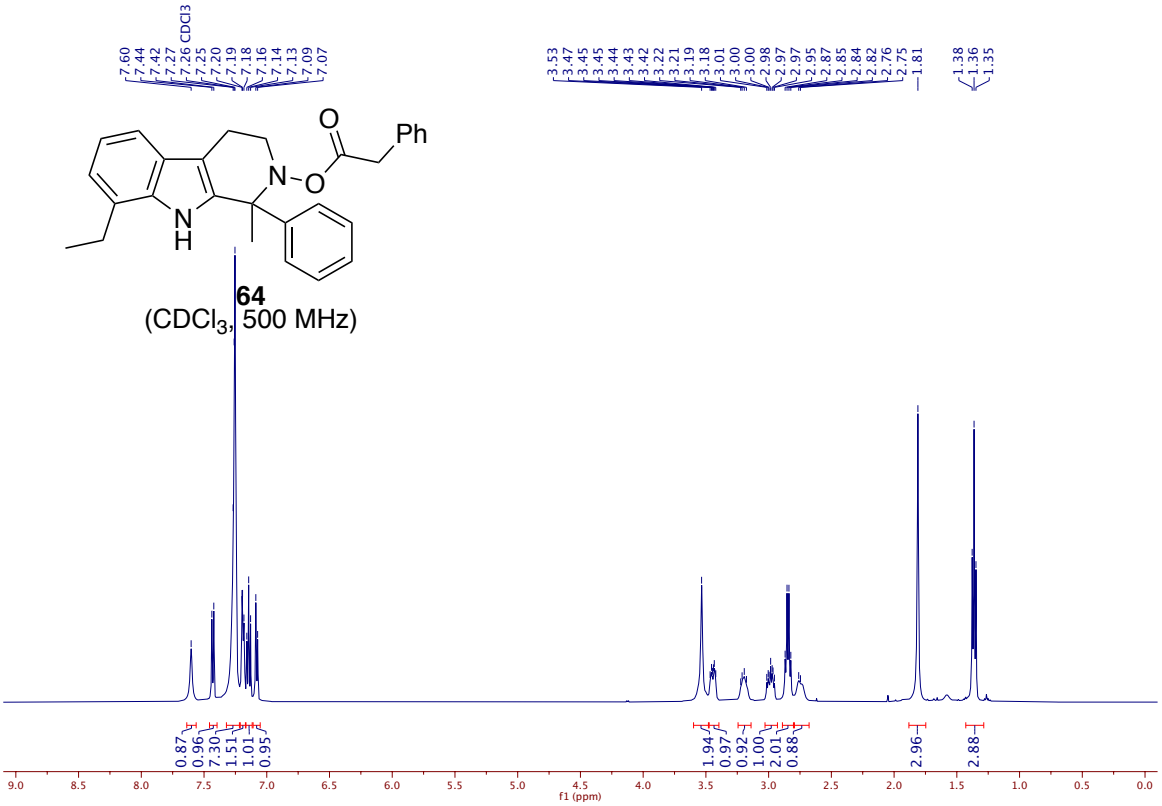

64
($CDCl_3$, 500 MHz)

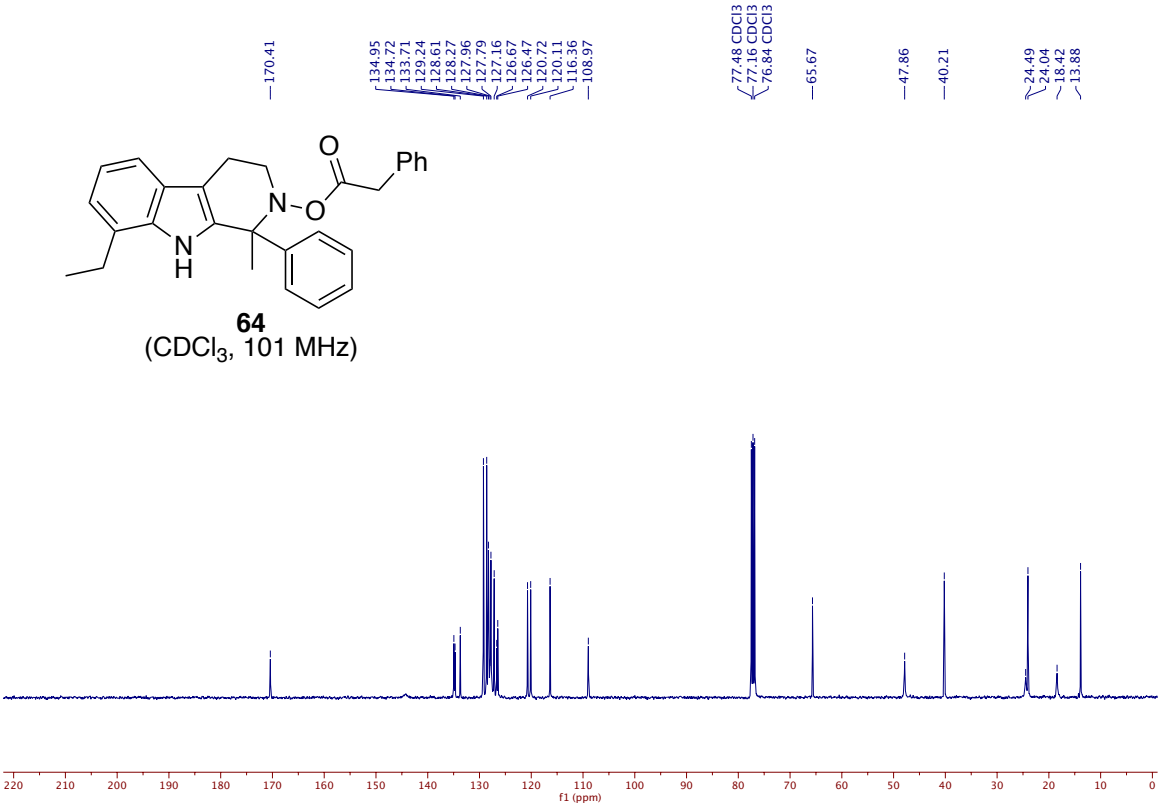

64
($CDCl_3$, 101 MHz)

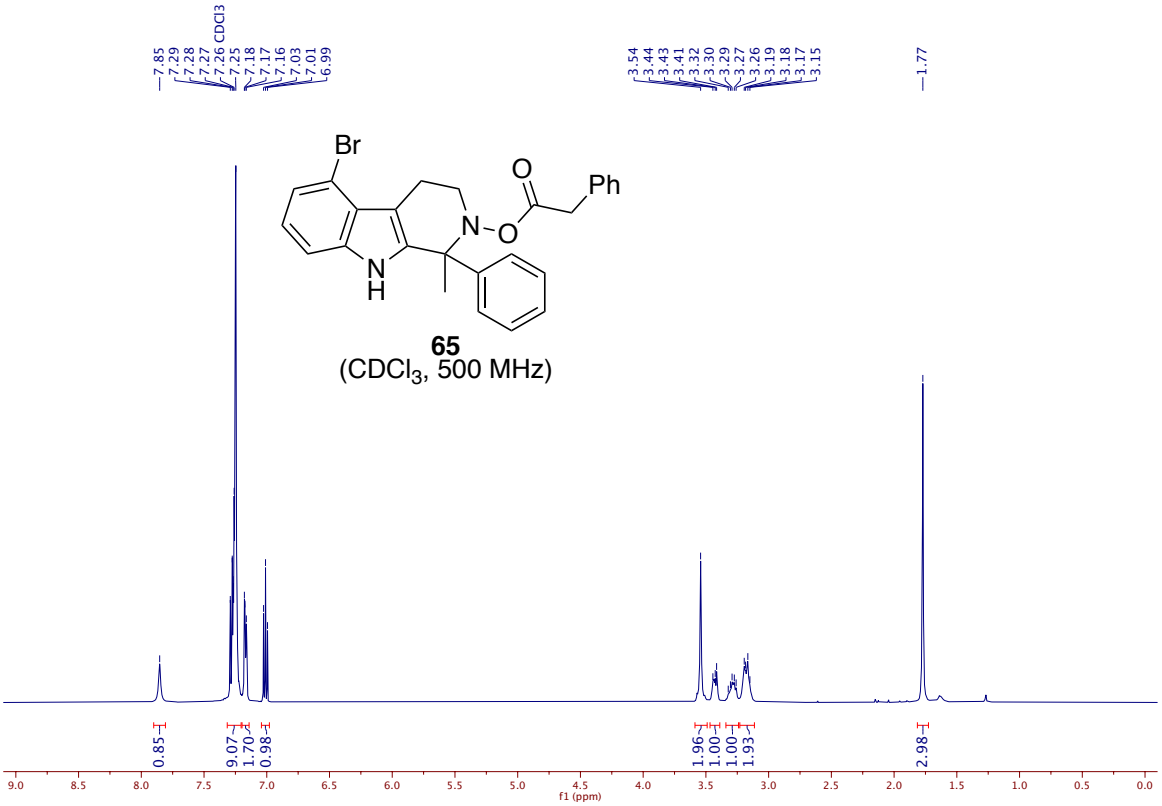

65

($CDCl_3$, 500 MHz)

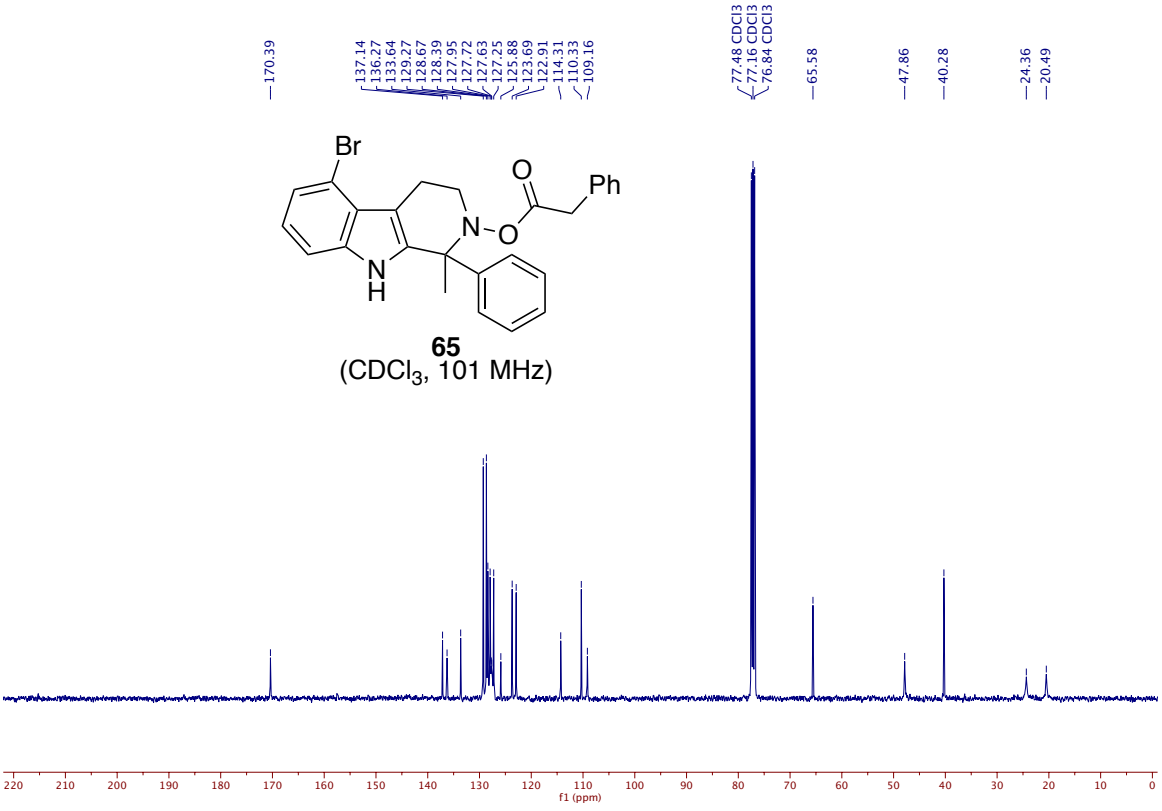

65

($CDCl_3$, 101 MHz)

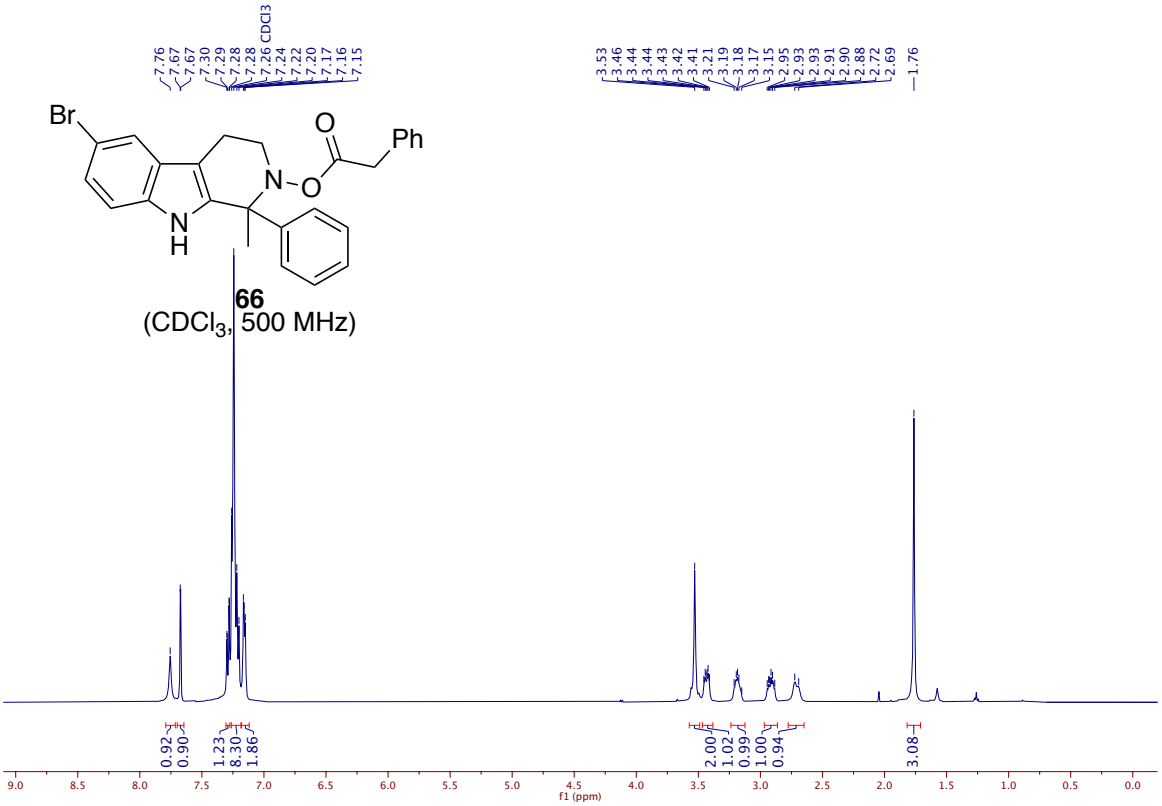

66
($CDCl_3$, 500 MHz)

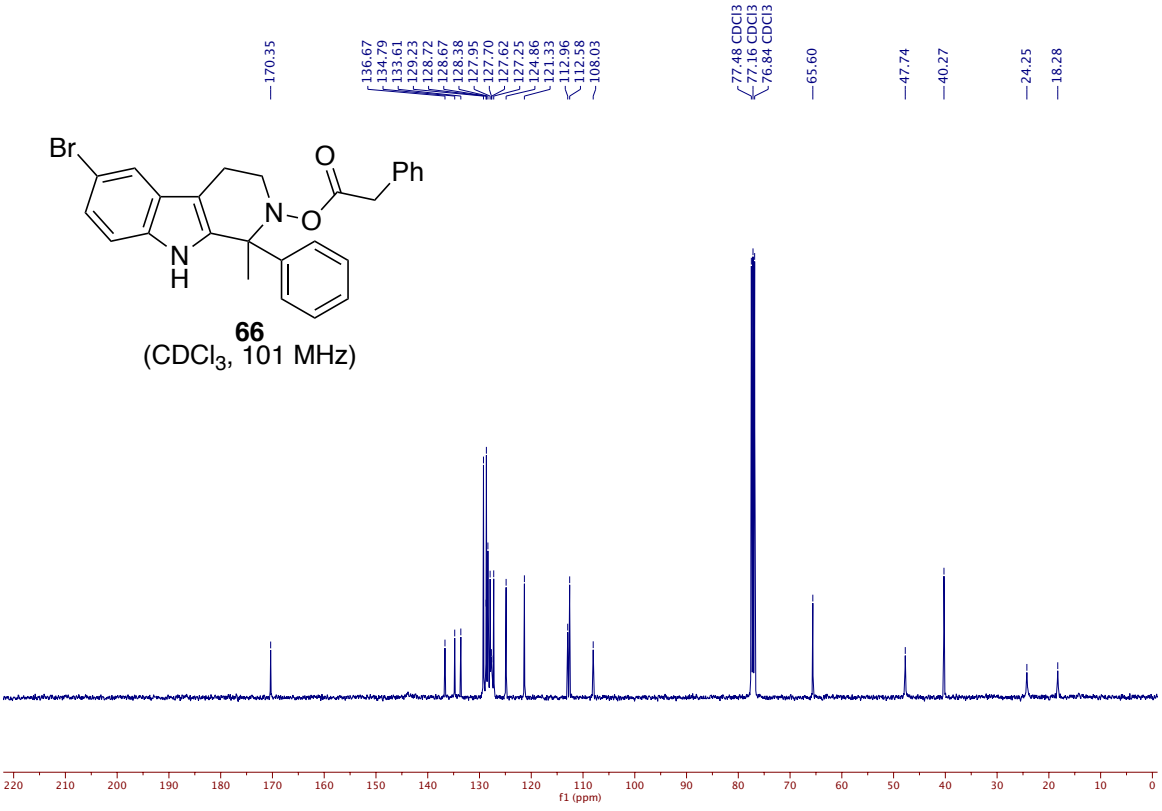

66
($CDCl_3$, 101 MHz)

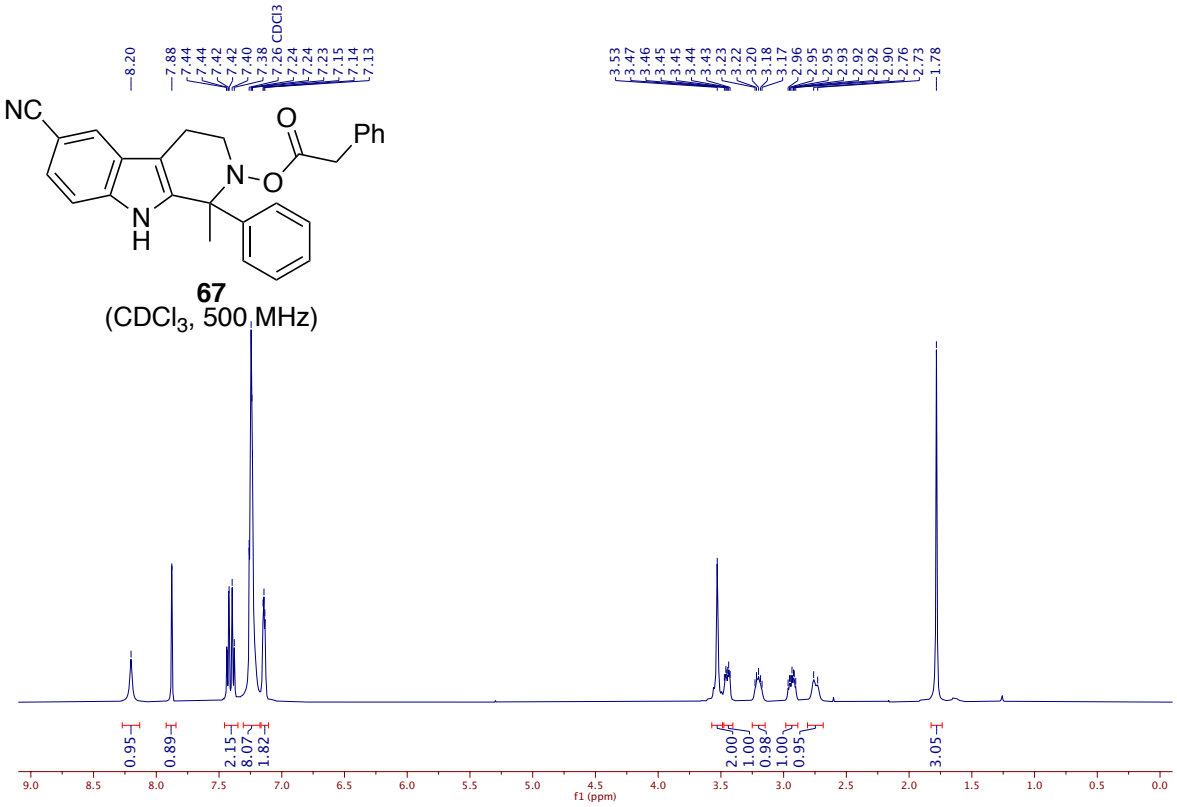
NC
O
Ph
N
O
N
H
67
(CDCl3, 500 MHz)
f1 (ppm)

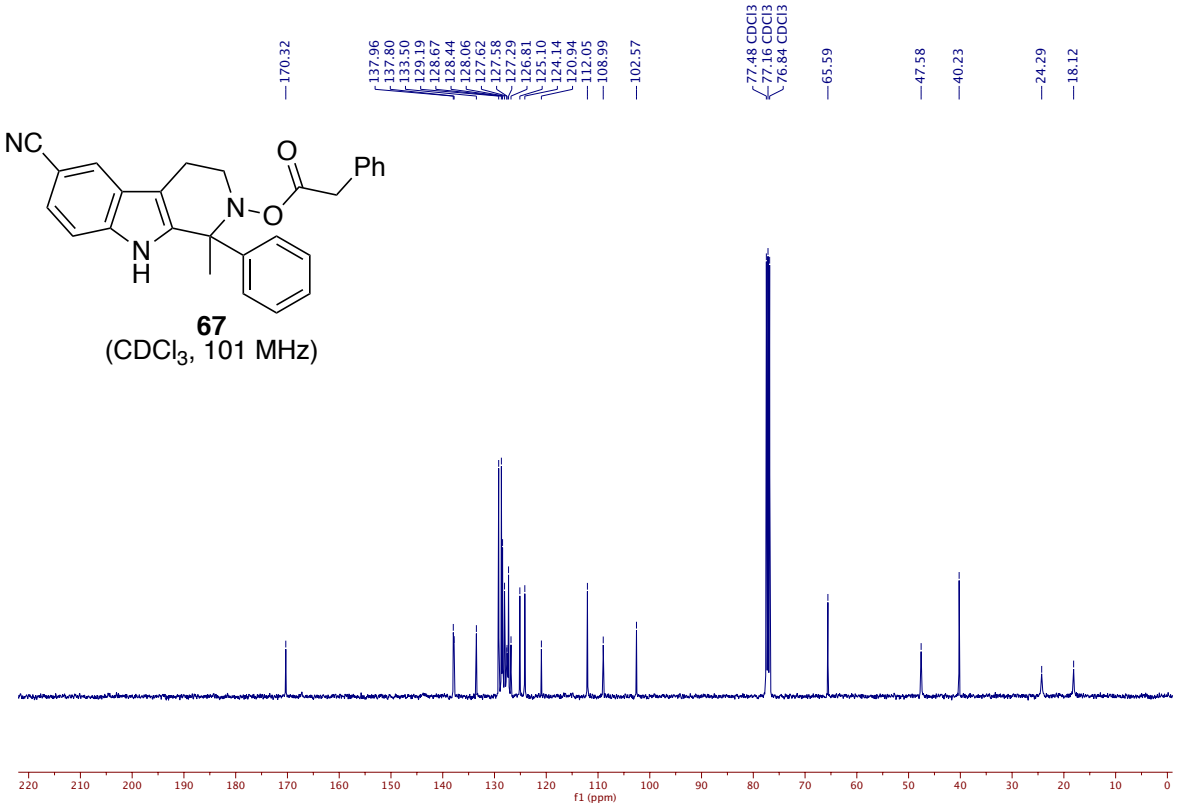
NC
O
Ph
N
O
N
H
67
(CDCl3, 101 MHz)
f1 (ppm)

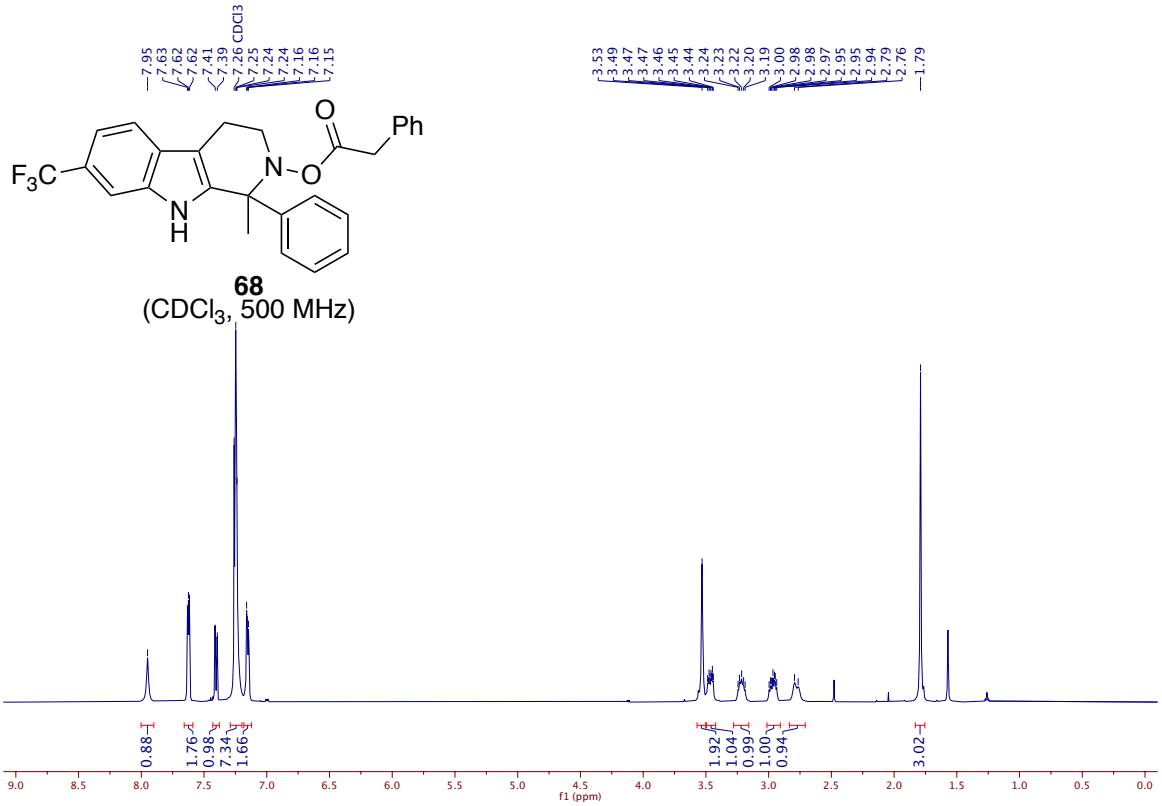

68
($CDCl_3$, 500 MHz)

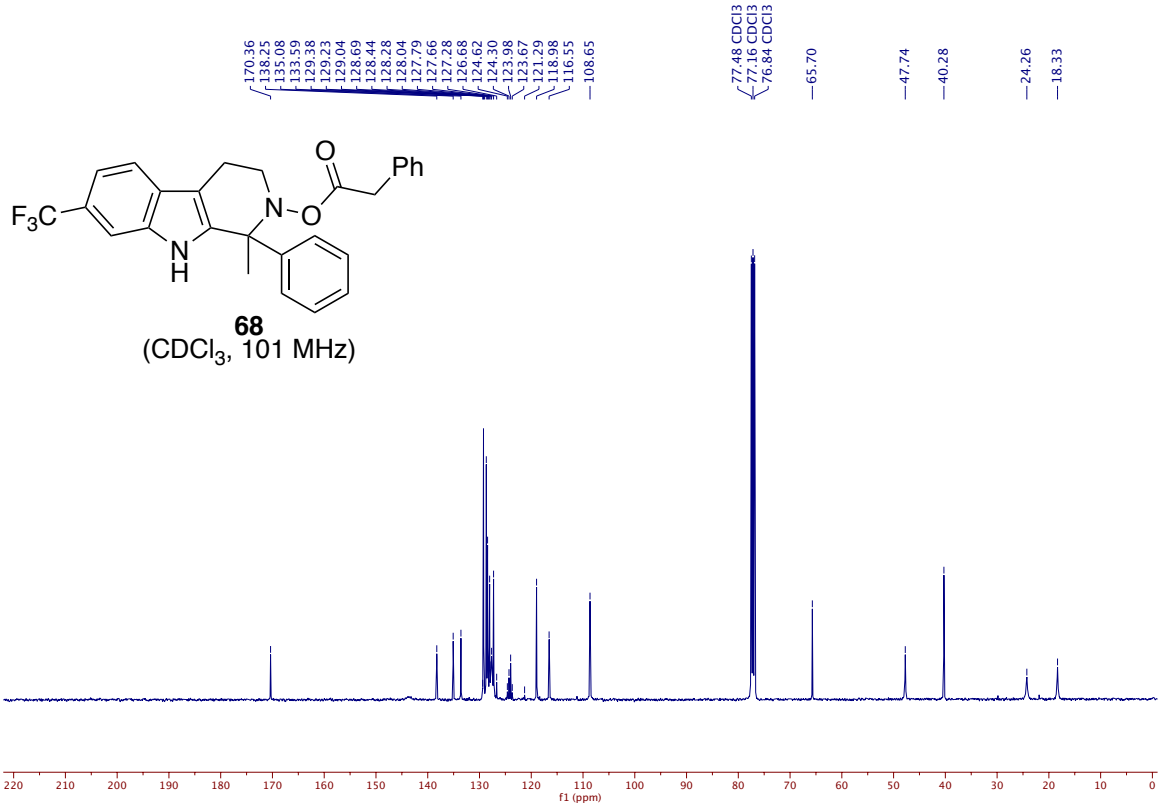

68
($CDCl_3$, 101 MHz)

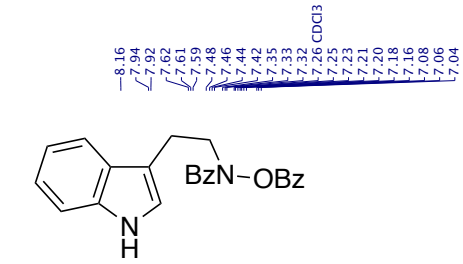

S46
($CDCl_3$, 400 MHz)

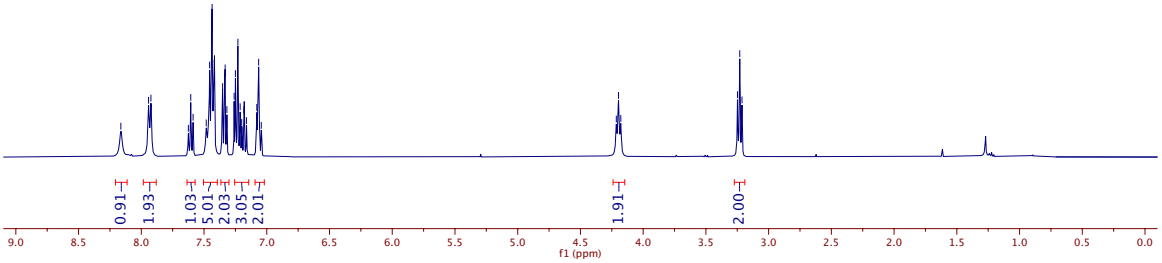

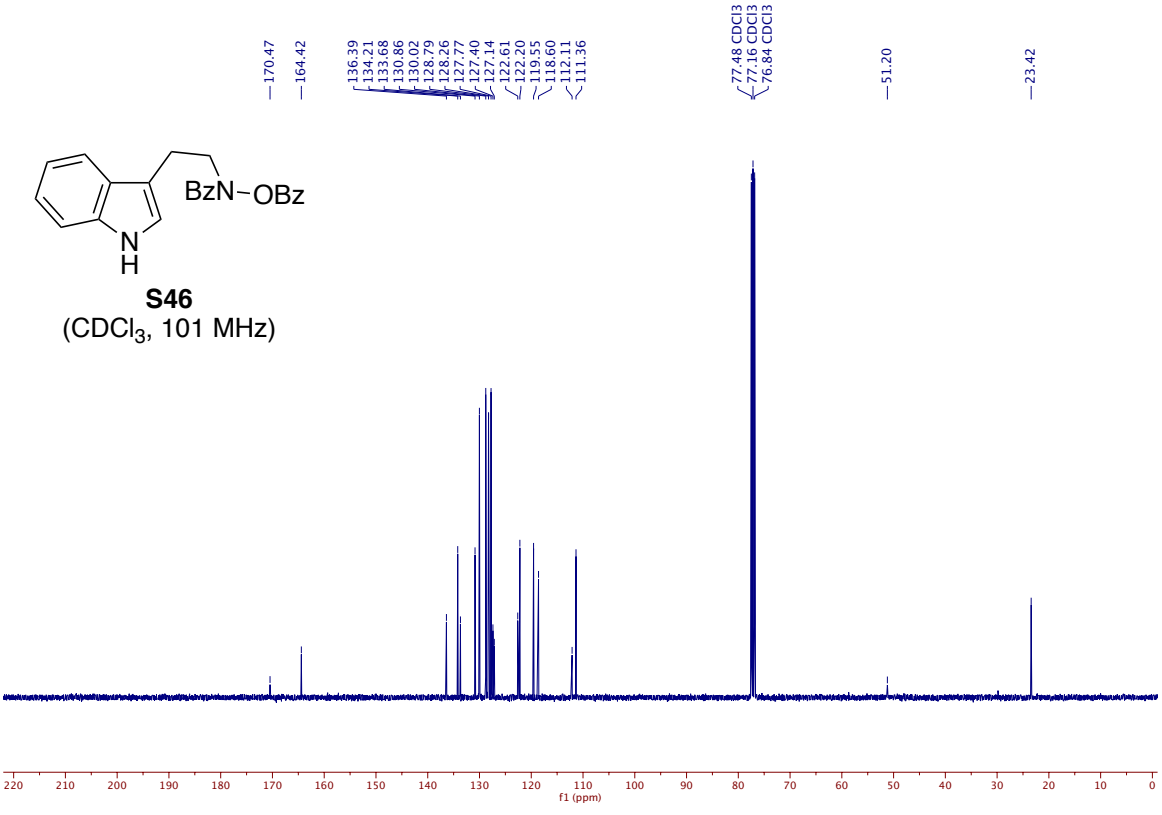

S46
($CDCl_3$, 101 MHz)

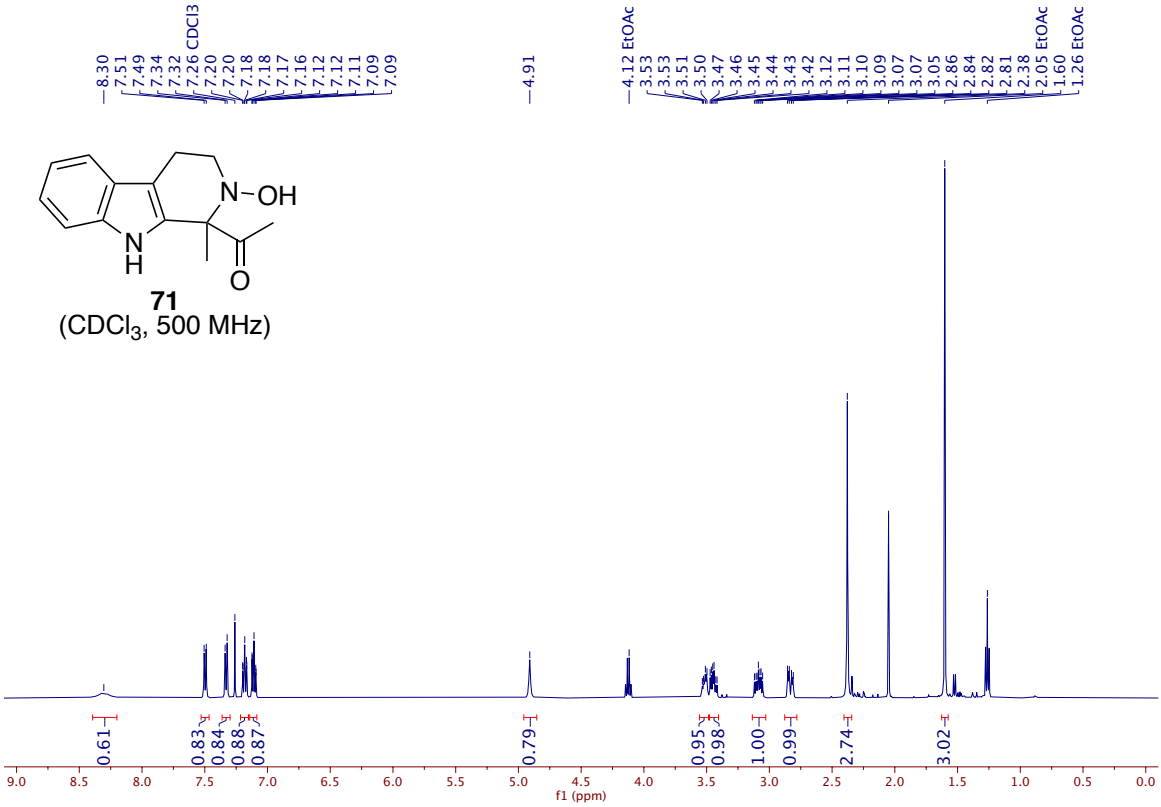

71
($CDCl_3$, 500 MHz)

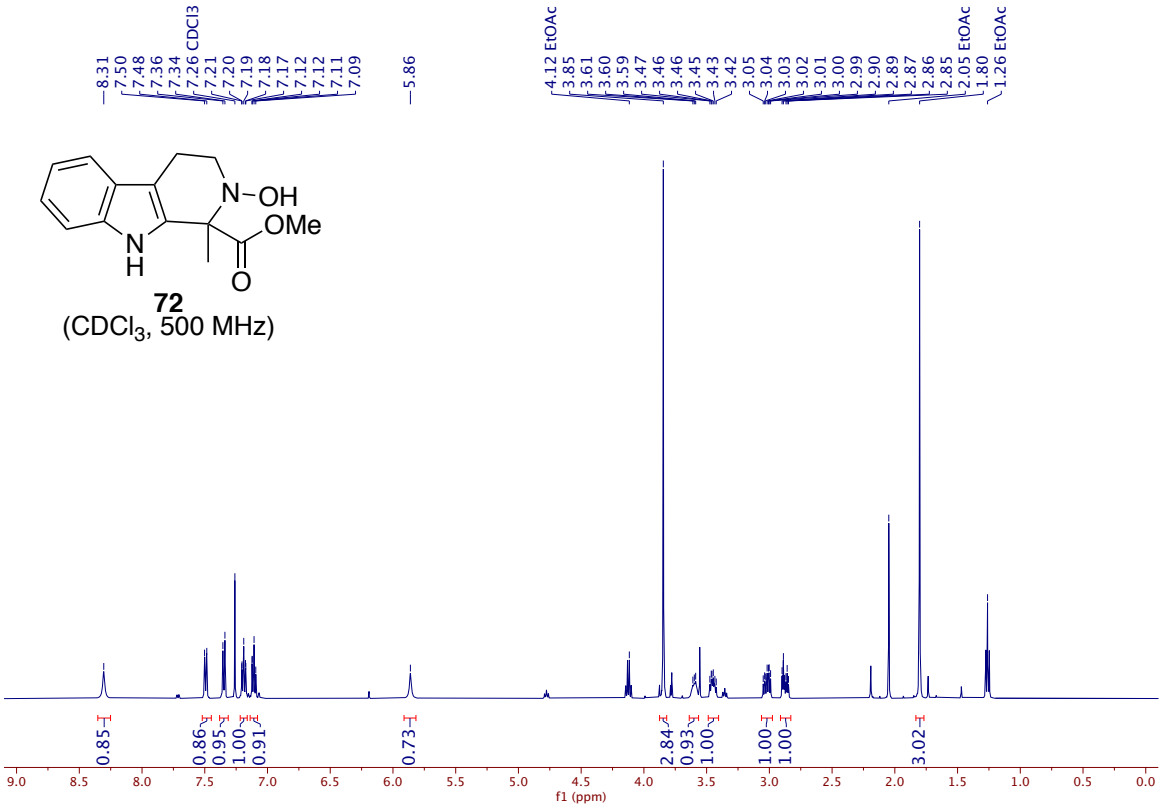

72
($CDCl_3$, 500 MHz)

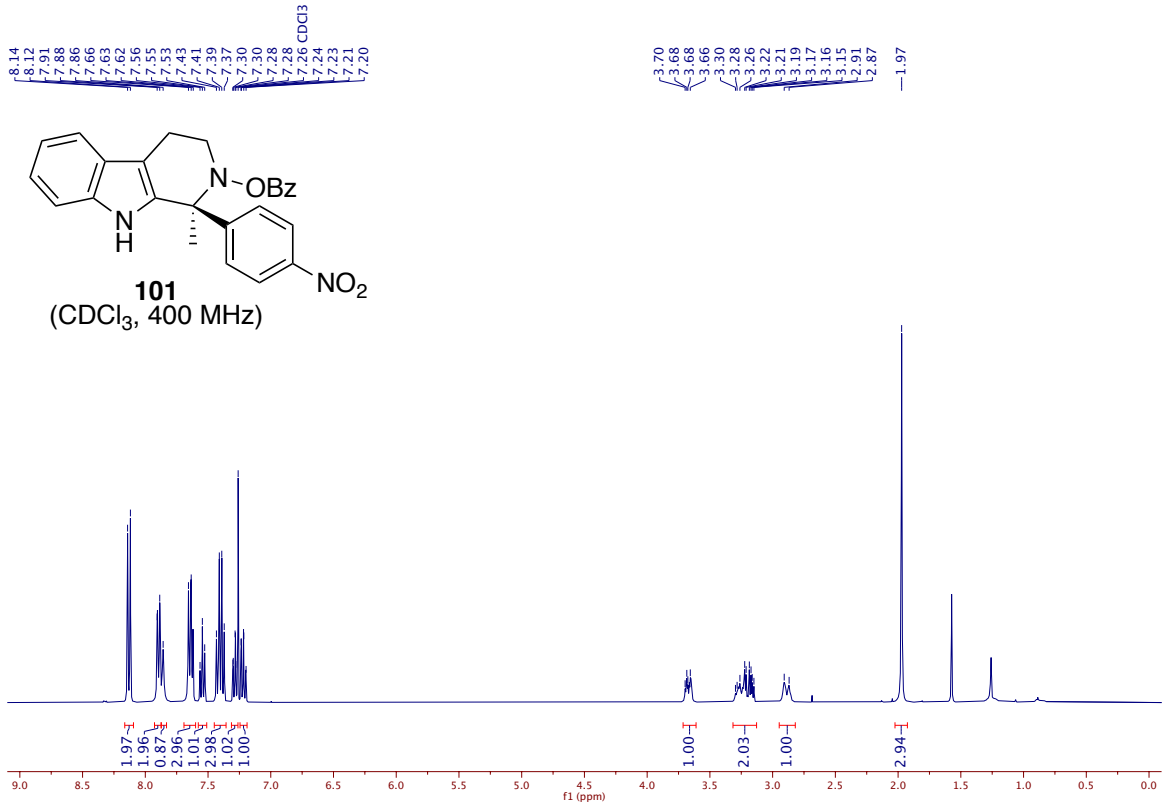
8.14
8.12
7.91
7.88
7.86
7.66
7.63
7.62
7.56
7.55
7.53
7.43
7.41
7.39
7.37
7.30
7.28
7.28
CDCl3
7.24
7.23
7.21
7.20
3.70
3.68
3.68
3.66
3.30
3.28
3.26
3.22
3.21
3.19
3.17
3.16
3.15
2.91
2.87
1.97
N
OBz
H
NO2
101
(CDCl3, 400 MHz)
1.97
1.96
0.87
2.96
1.01
2.98
1.02
1.00
1.00
2.03
1.00
2.94
f1 (ppm)

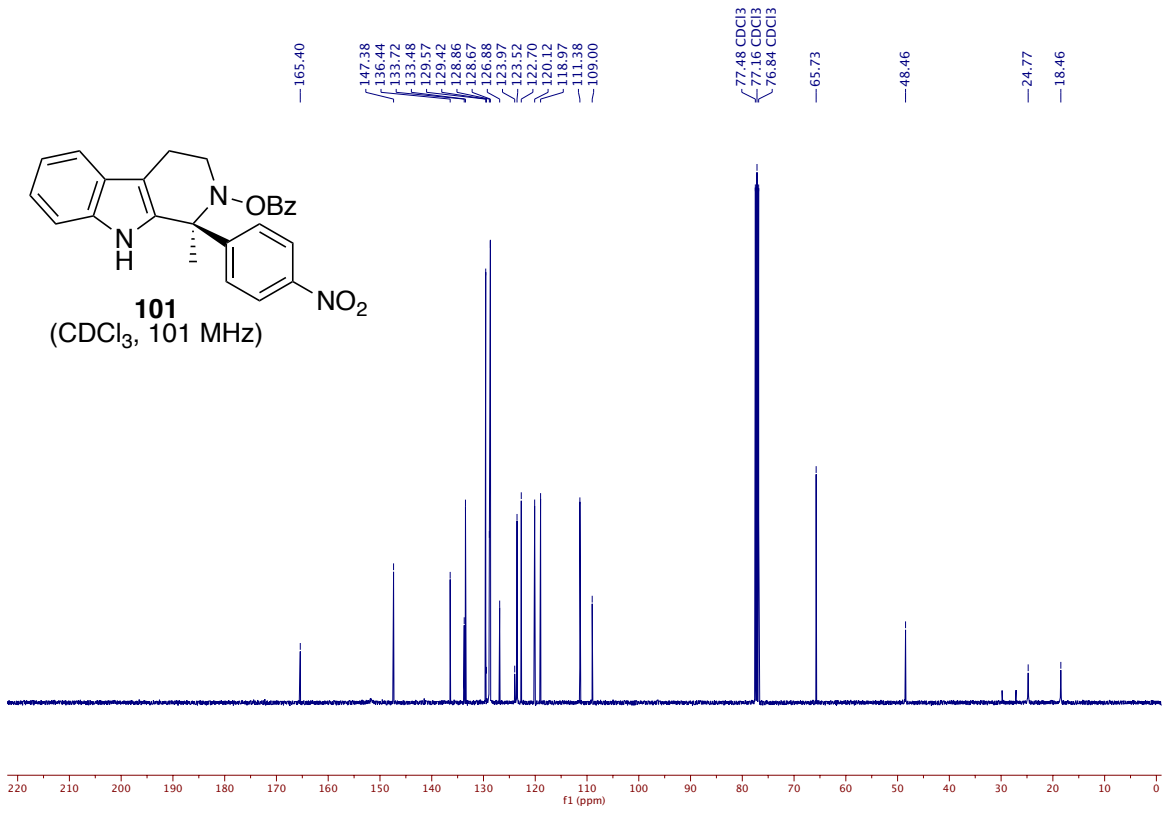
165.40
147.38
136.44
133.72
133.48
129.57
129.42
128.86
128.67
126.88
123.97
123.52
122.70
120.12
118.97
111.38
109.00
77.48 CDCl3
77.16 CDCl3
76.84 CDCl3
65.73
48.46
24.77
18.46
N
OBz
H
NO2
101
(CDCl3, 101 MHz)
f1 (ppm)

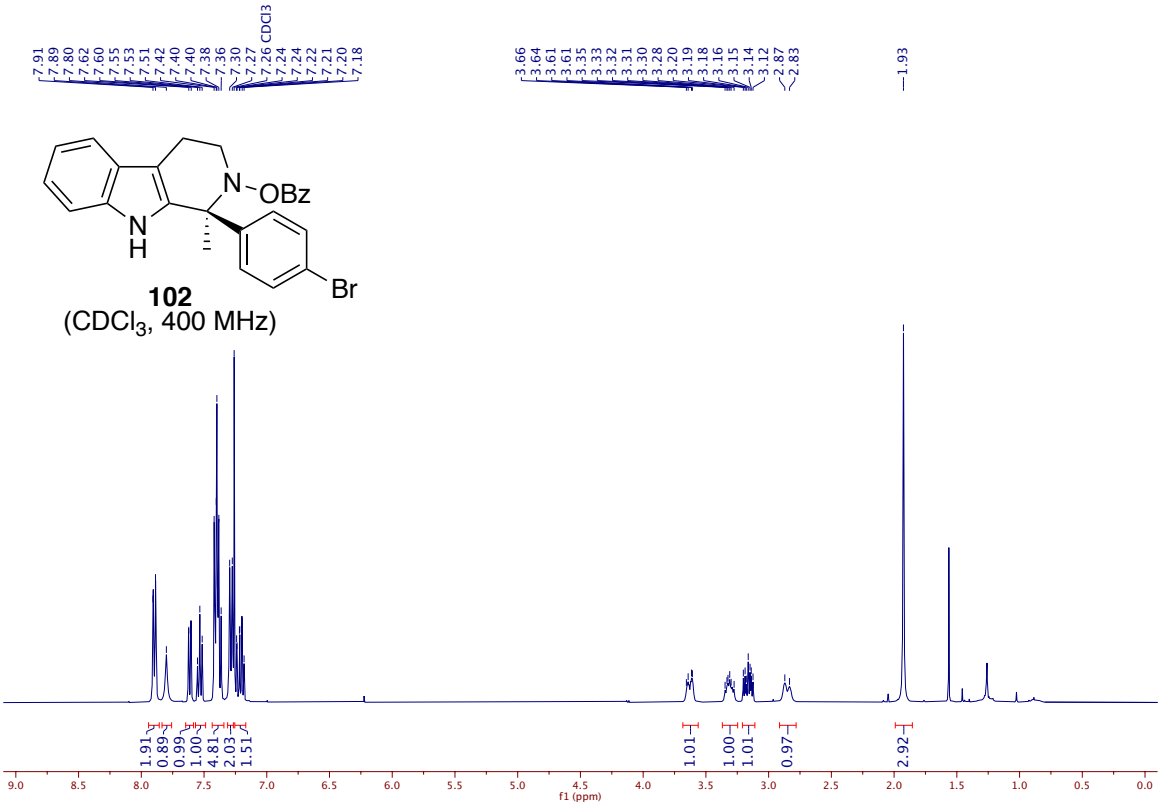
7.91
7.89
7.80
7.62
7.60
7.55
7.53
7.51
7.42
7.40
7.40
7.38
7.36
7.30
7.27
7.26 CDCl3
7.24
7.24
7.22
7.21
7.20
7.18
3.66
3.64
3.61
3.61
3.35
3.33
3.32
3.31
3.30
3.28
3.20
3.19
3.18
3.16
3.15
3.14
3.12
2.87
2.83
1.93
N
OBz
N
H
Br
102
(CDCl3, 400 MHz)
1.91
0.89
0.99
1.00
4.81
2.03
1.51
1.01
1.00
1.01
0.97
2.92
f1 (ppm)

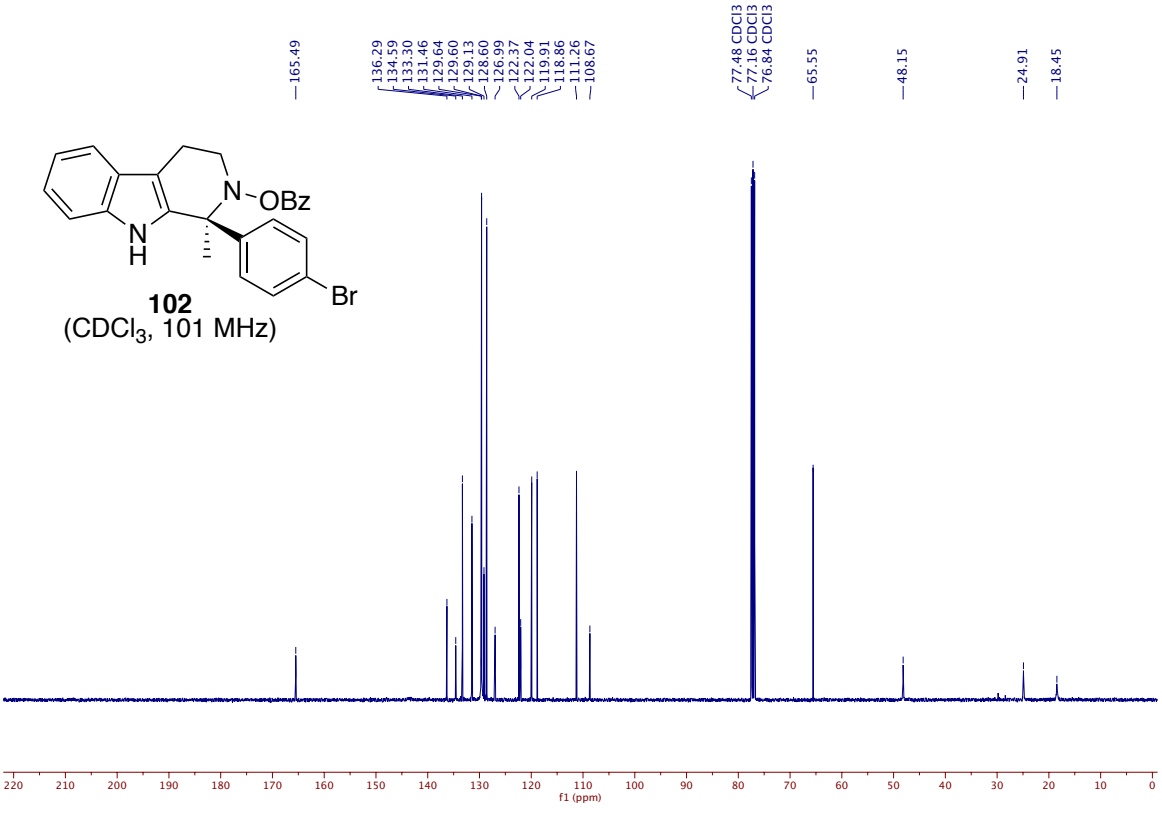
165.49
136.29
134.59
133.30
131.46
129.64
129.60
129.13
128.60
126.99
122.37
122.04
119.91
118.86
111.26
108.67
77.48 CDCl3
77.16 CDCl3
76.84 CDCl3
65.55
48.15
24.91
18.45
N
OBz
N
H
Br
102
(CDCl3, 101 MHz)
f1 (ppm)

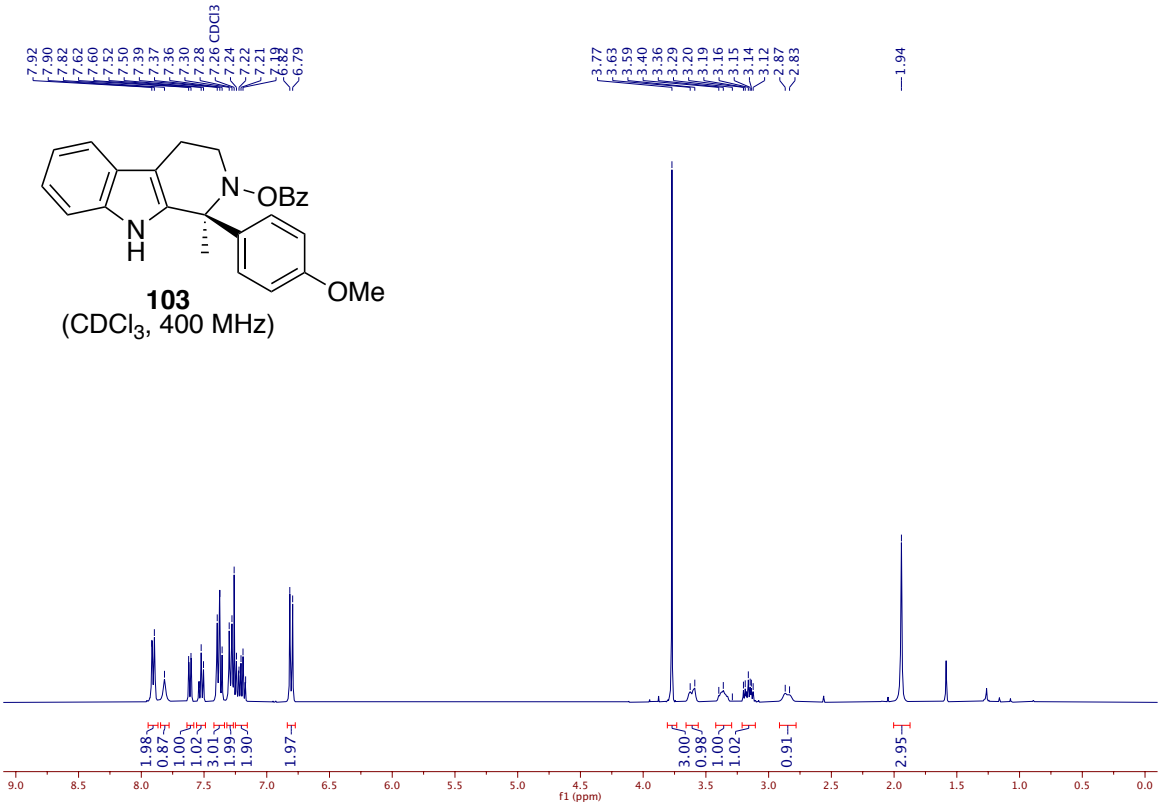
7.92
7.90
7.82
7.62
7.60
7.52
7.50
7.39
7.37
7.36
7.30
7.28
7.26 CDCl3
7.24
7.22
7.21
7.19
6.82
6.79
3.77
3.63
3.59
3.40
3.36
3.29
3.20
3.19
3.16
3.15
3.14
3.12
2.87
2.83
1.94
N
OBz
N
H
OMe
103
(CDCl3, 400 MHz)
1.98
0.87
1.00
1.02
3.01
1.99
1.90
1.97
3.00
0.98
1.00
1.02
0.91
2.95
f1 (ppm)

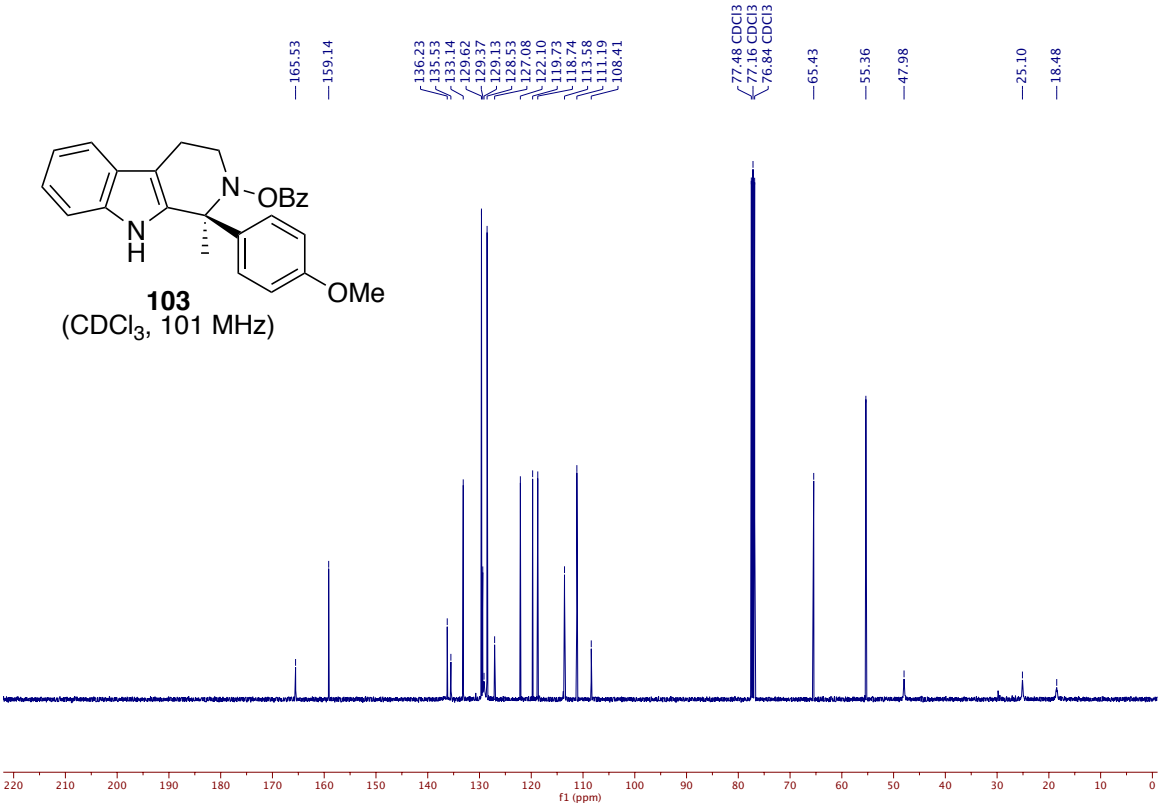
165.53
159.14
136.23
135.53
133.14
129.62
129.37
129.13
128.53
127.08
122.10
119.73
118.74
113.58
111.19
108.41
77.48 CDCl3
77.16 CDCl3
76.84 CDCl3
65.43
55.36
47.98
25.10
18.48
N
OBz
N
H
OMe
103
(CDCl3, 101 MHz)
f1 (ppm)

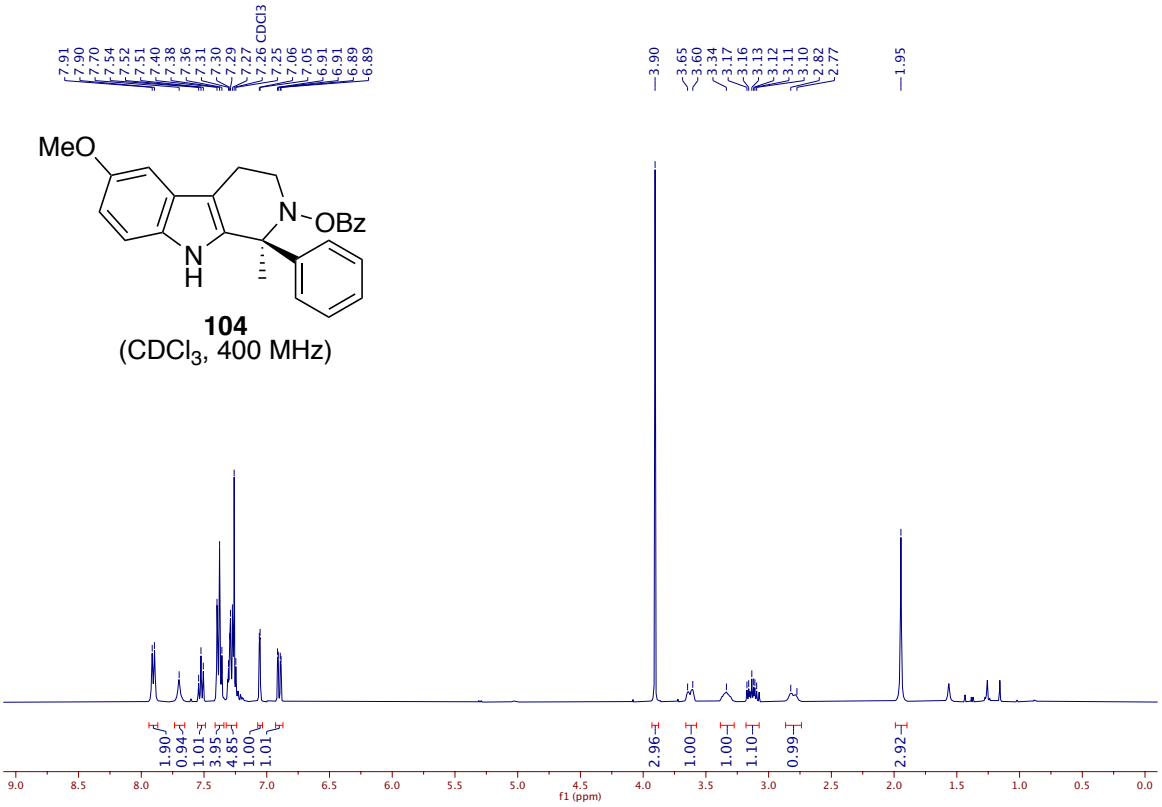
MeO
N
OBz
N
H
104
(CDCl3, 400 MHz)
f1 (ppm)

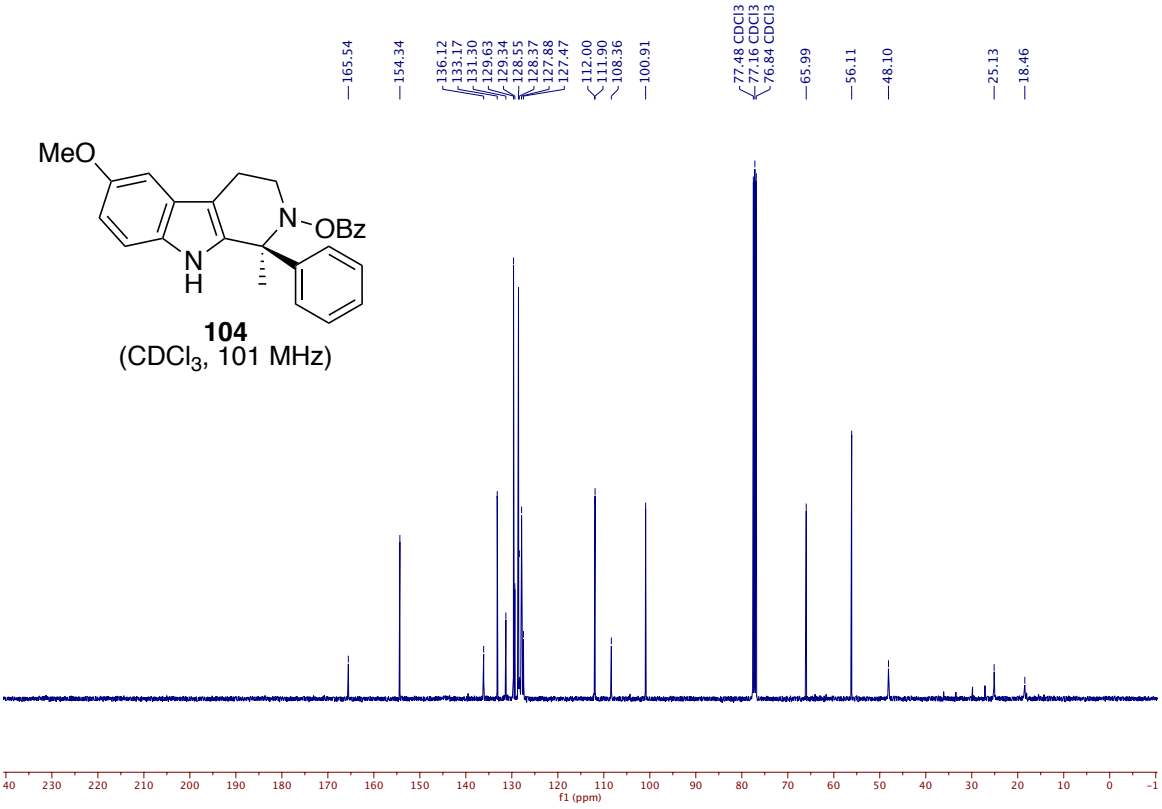
MeO
N
OBz
N
H
104
(CDCl3, 101 MHz)
f1 (ppm)

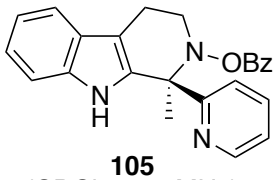

105
($CDCl_3$, 400 MHz)

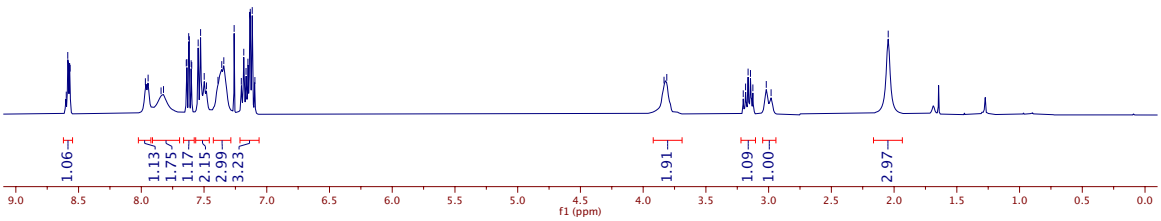

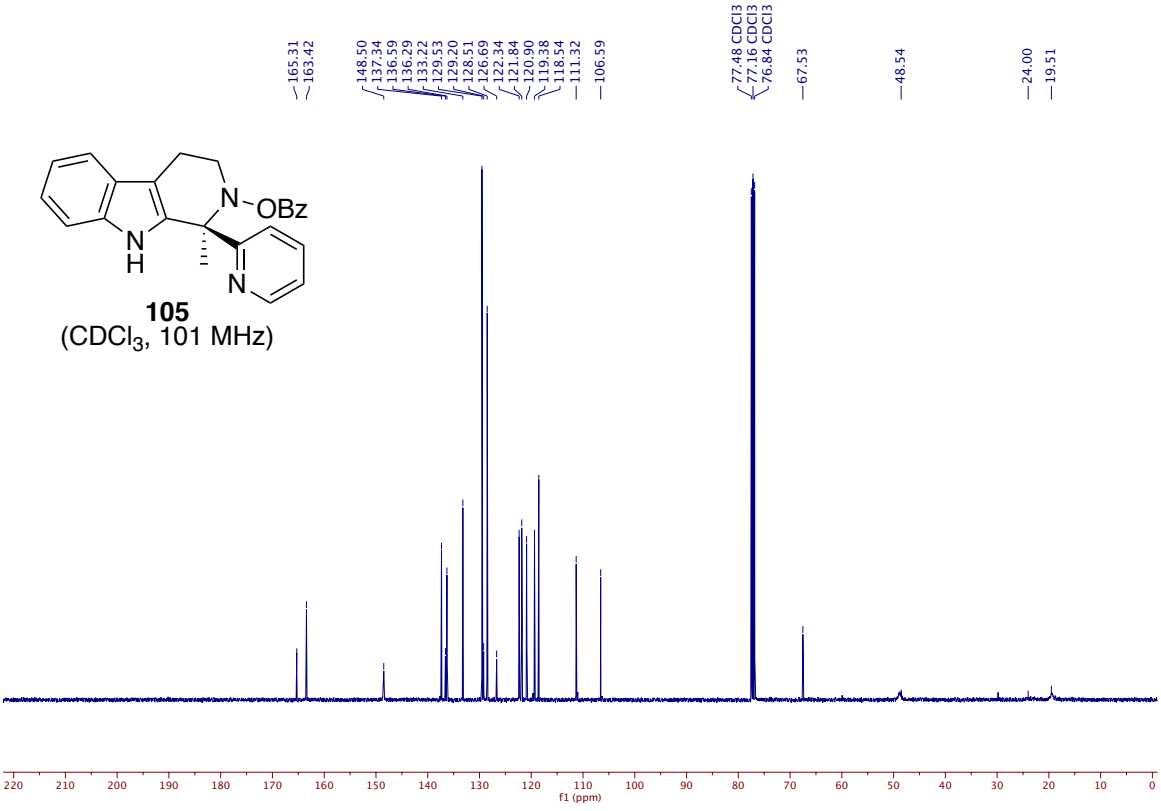

105
($CDCl_3$, 101 MHz)

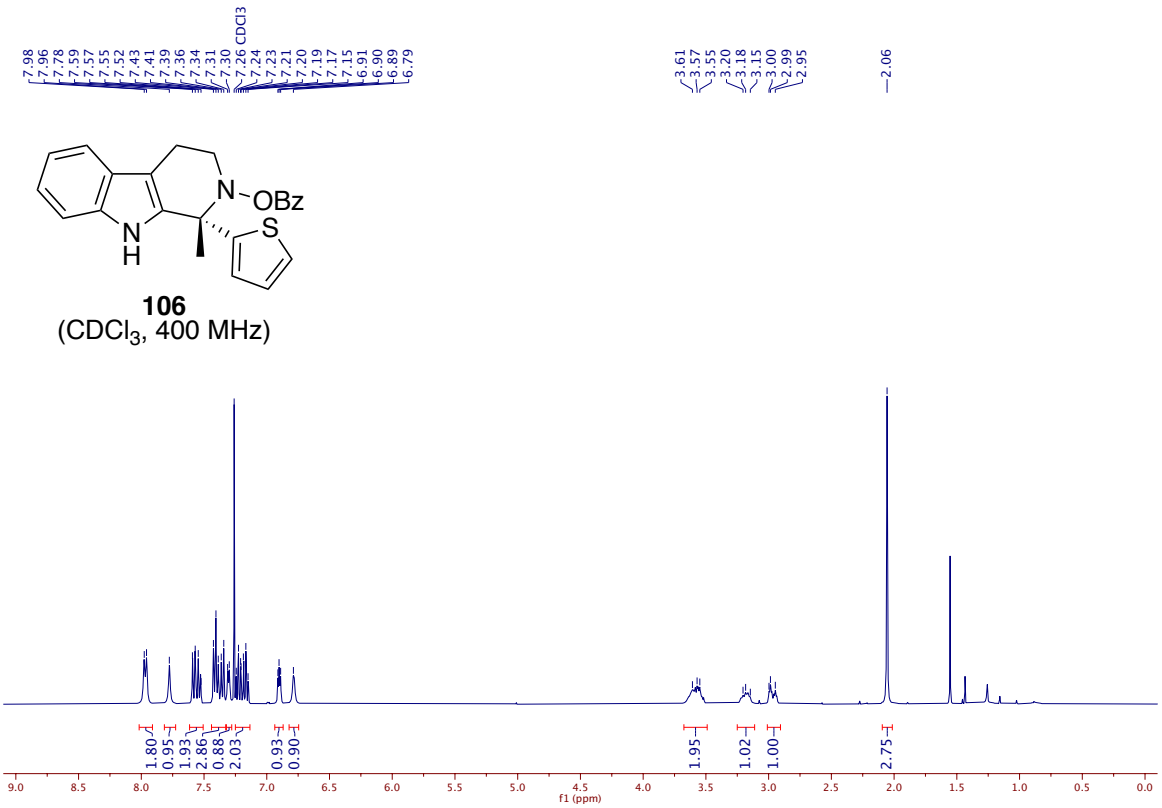

106
($CDCl_3$, 400 MHz)

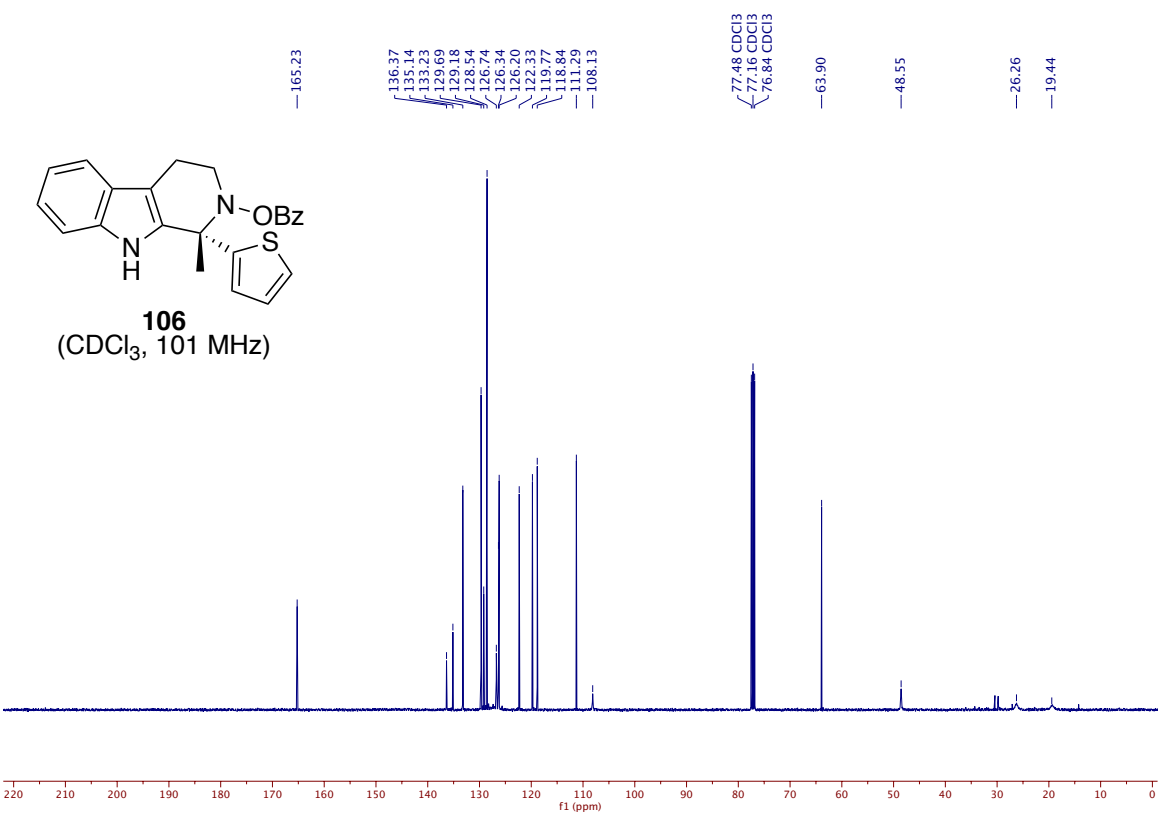

106
($CDCl_3$, 101 MHz)

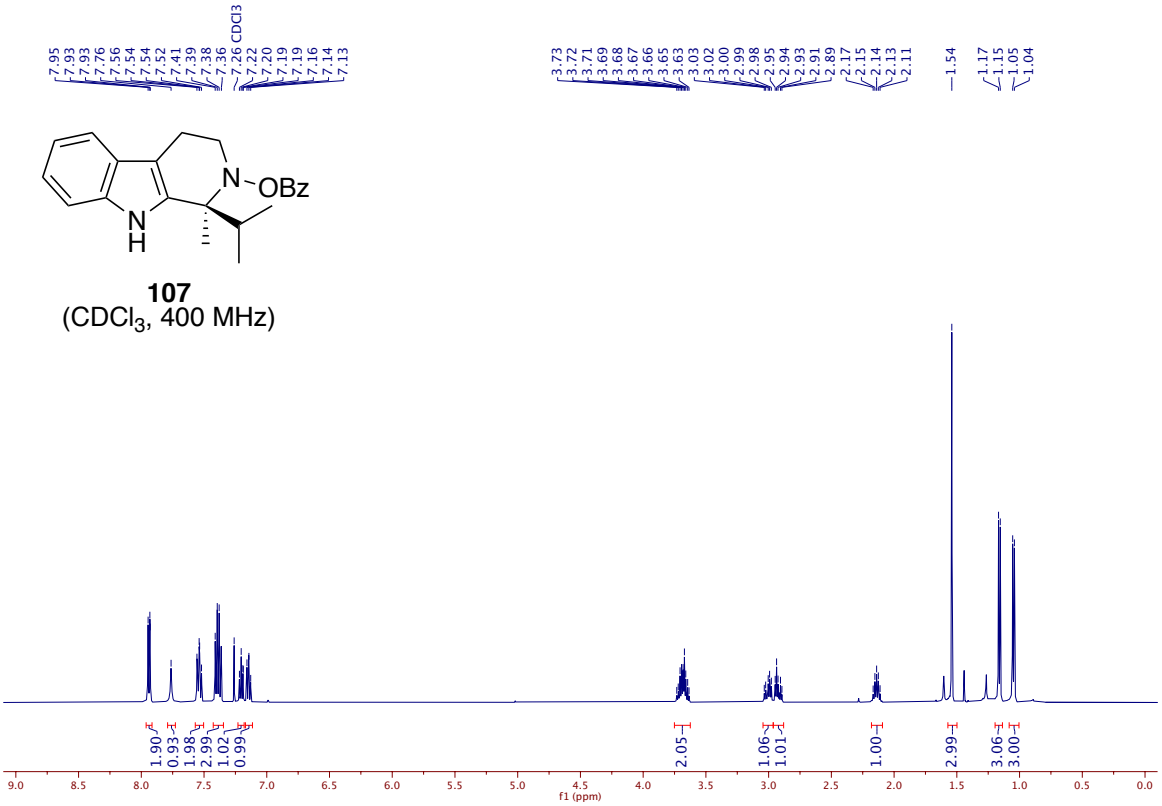

107
($CDCl_3$, 400 MHz)

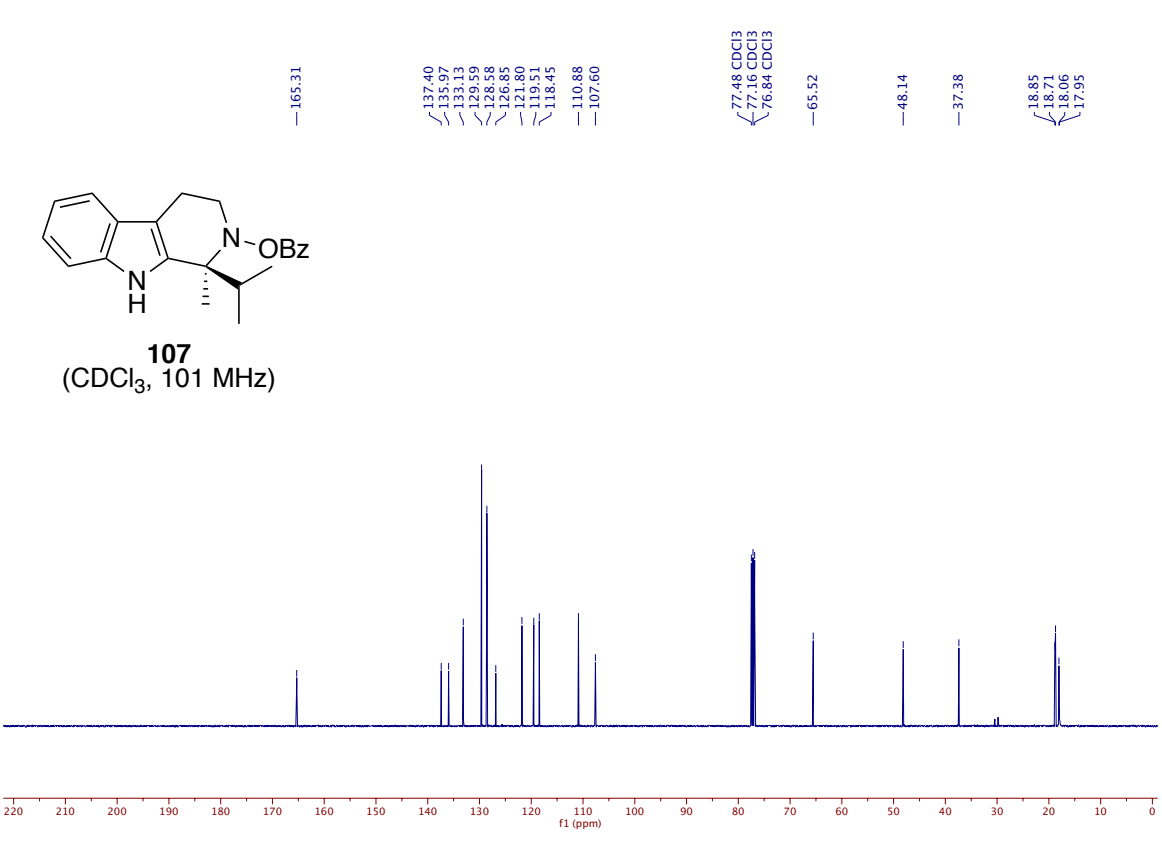

107
($CDCl_3$, 101 MHz)

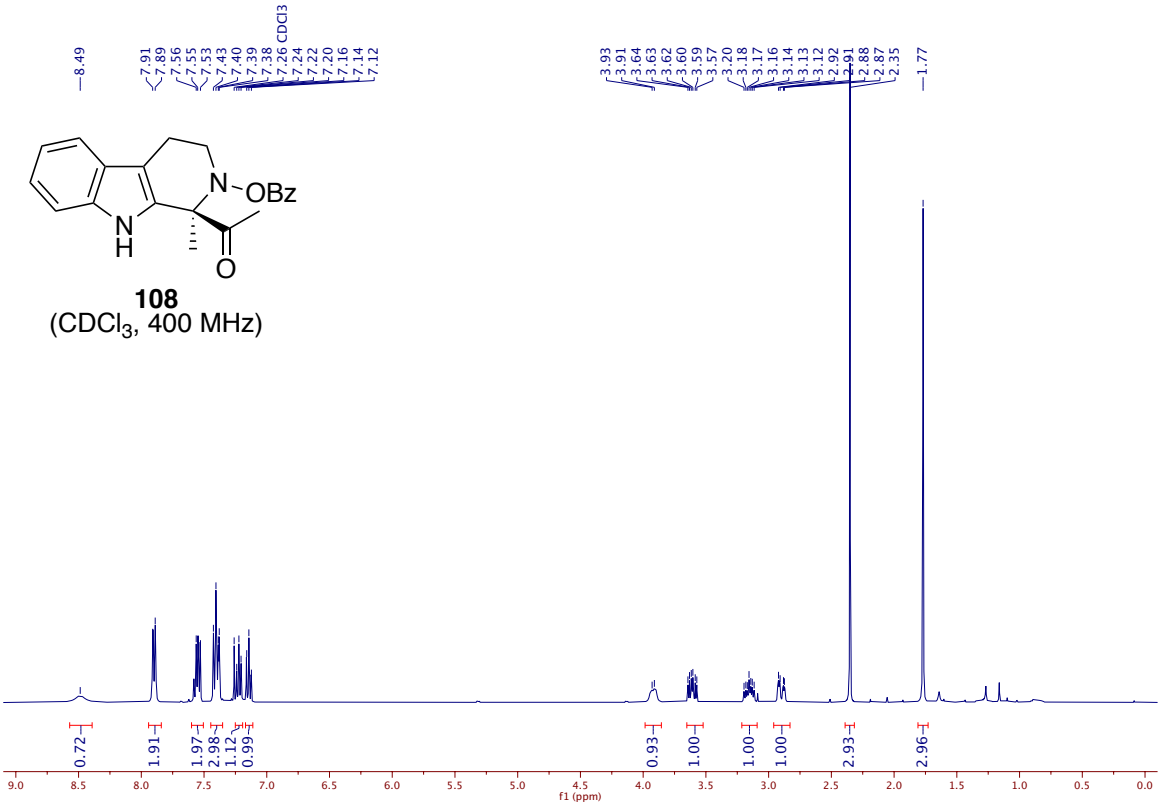

108
($CDCl_3$, 400 MHz)

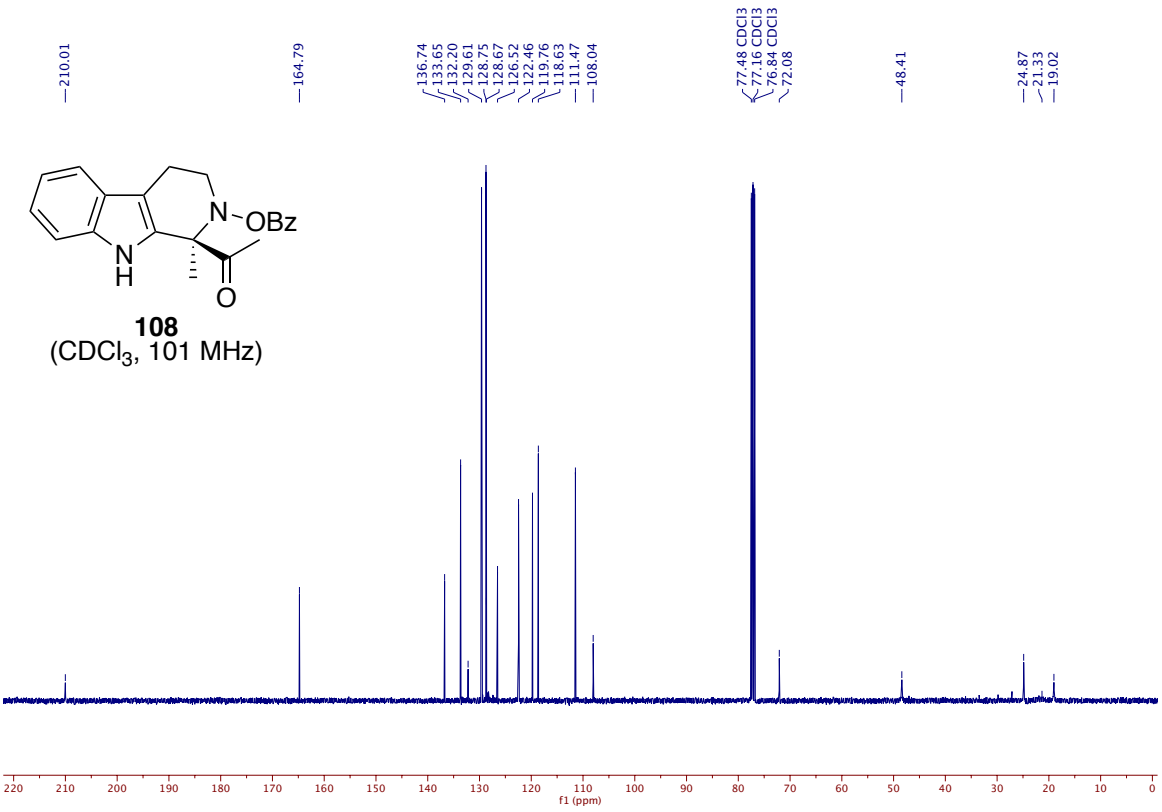

108
($CDCl_3$, 101 MHz)

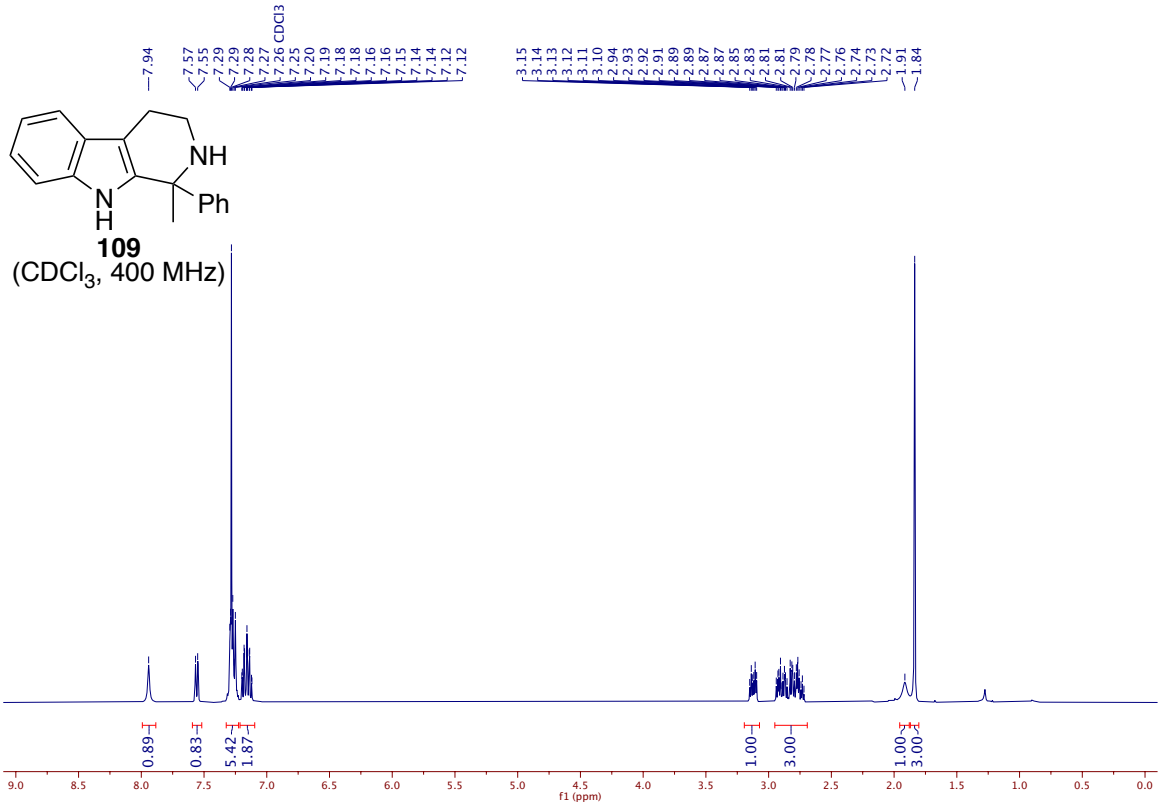

109
($CDCl_3$, 400 MHz)

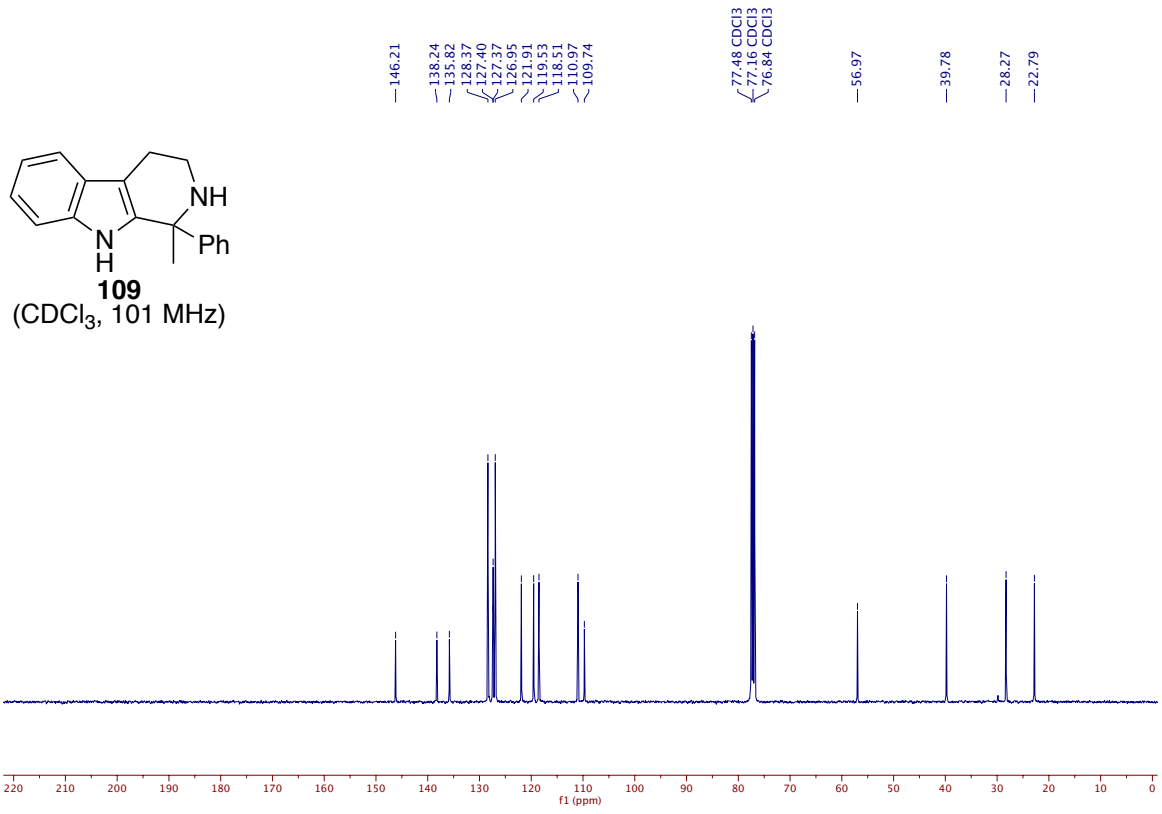

109
($CDCl_3$, 101 MHz)

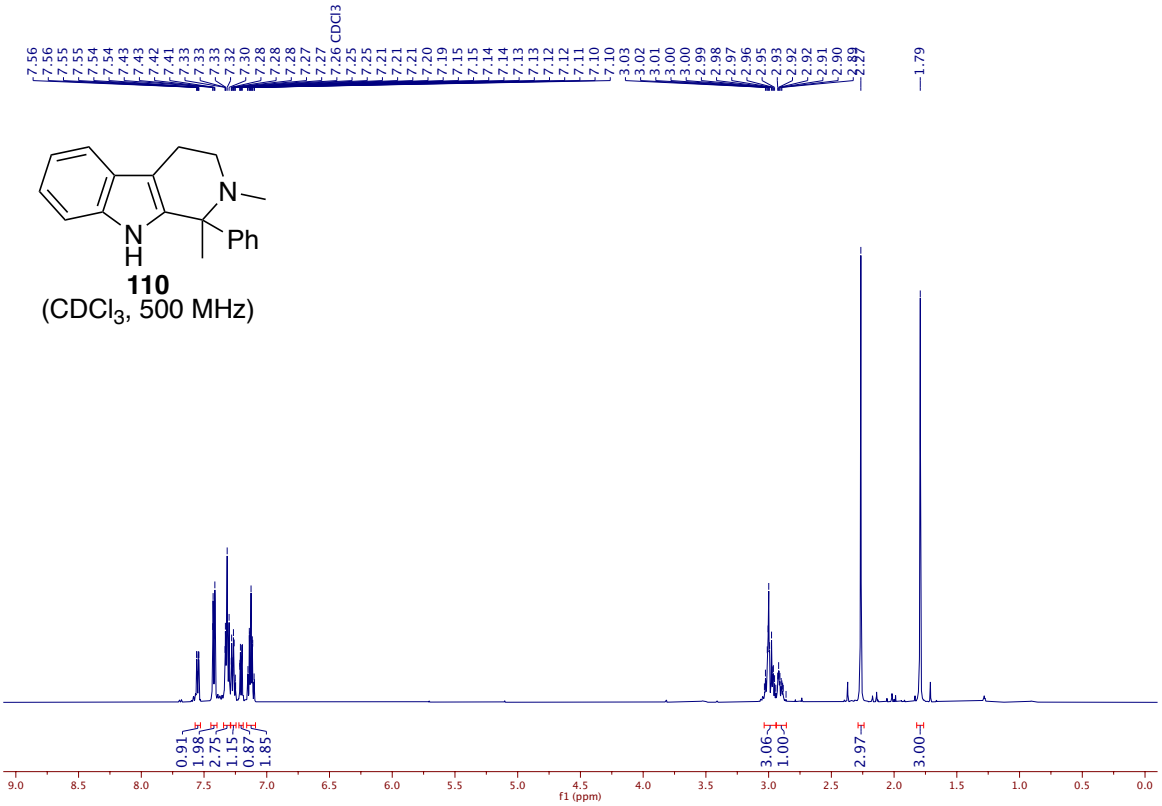

110
($CDCl_3$, 500 MHz)

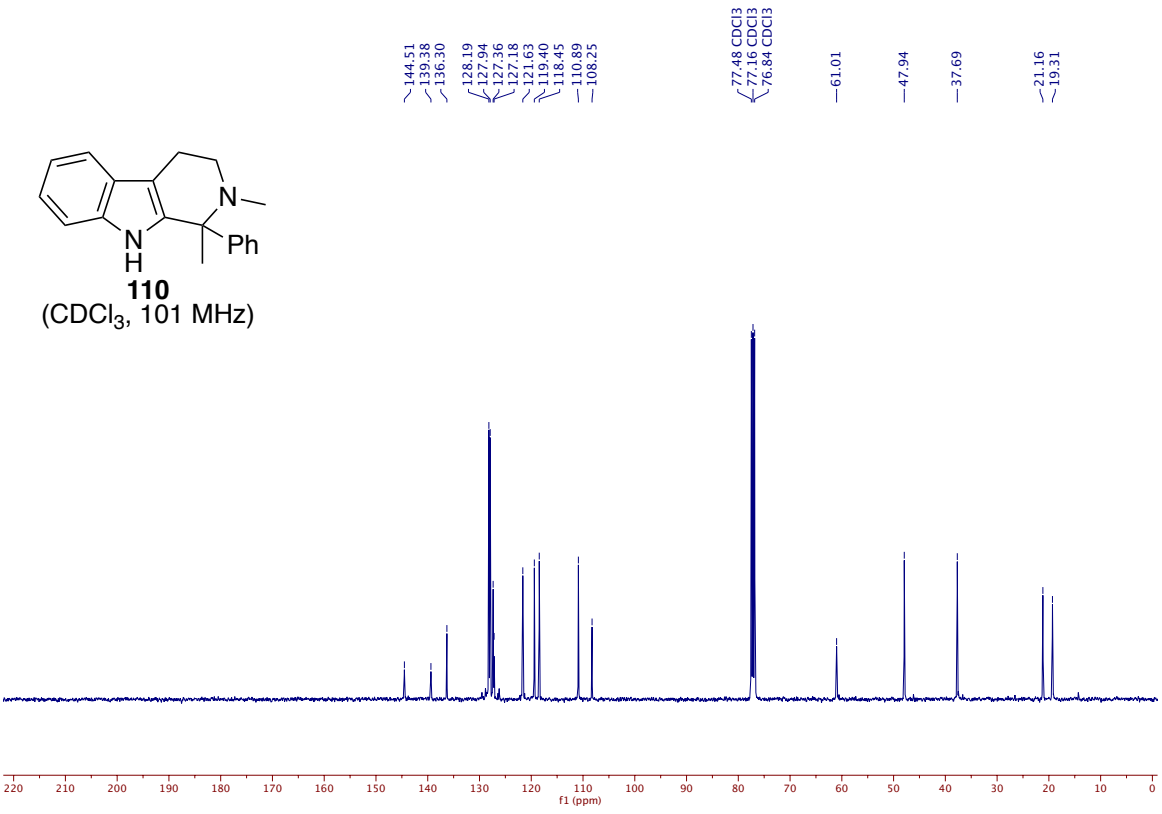

110
($CDCl_3$, 101 MHz)

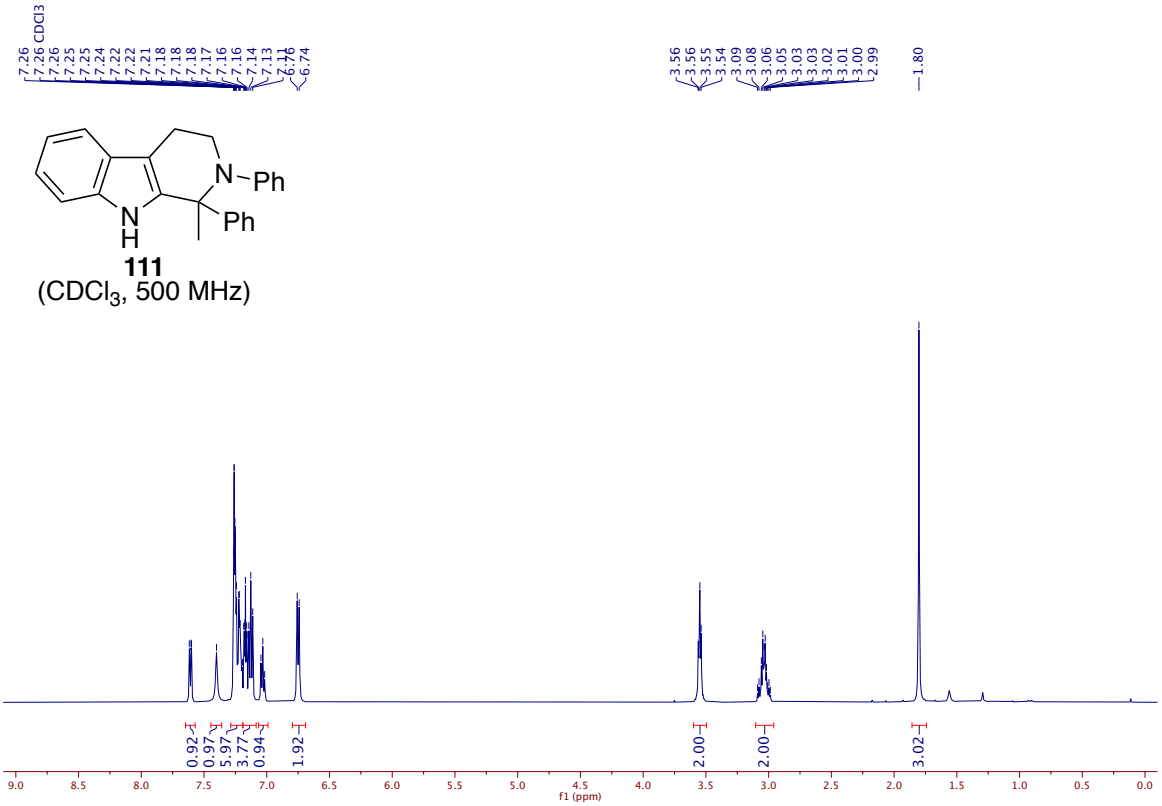

111

($CDCl_3$, 500 MHz)

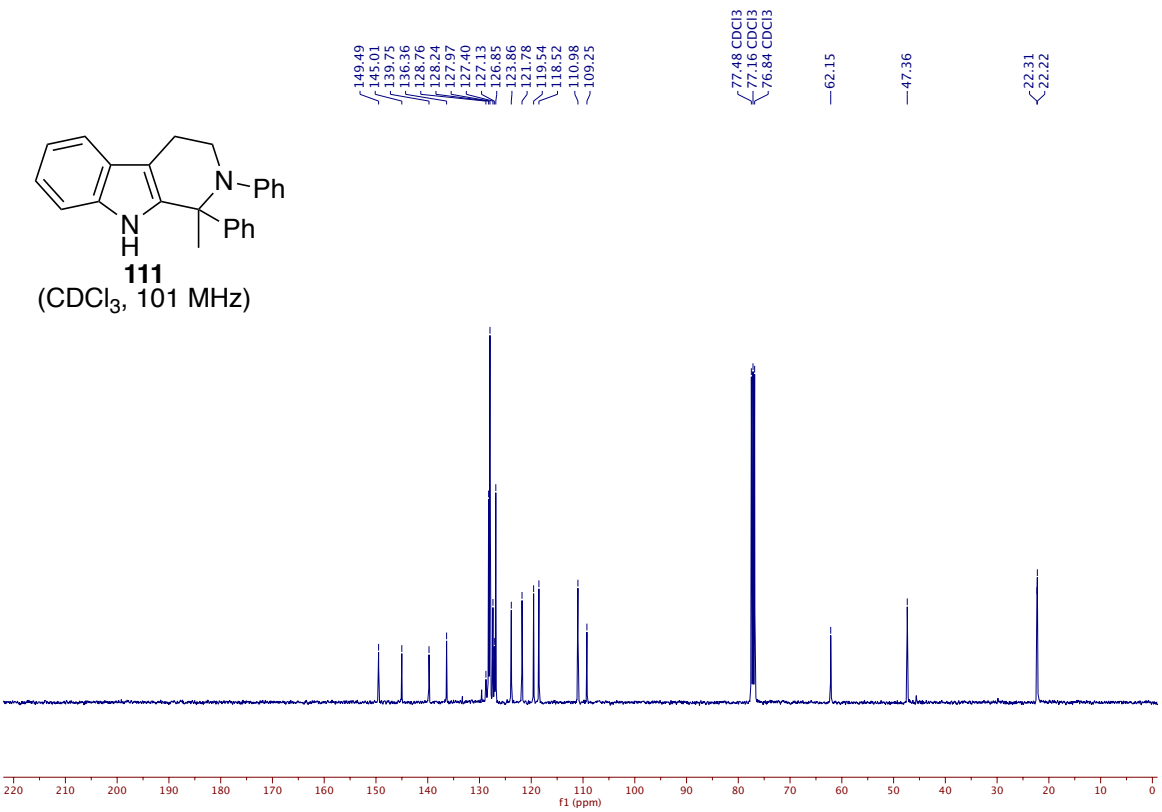

111

($CDCl_3$, 101 MHz)

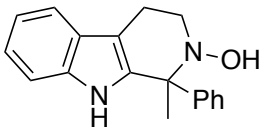

69

(DMSO-d_6, 500 MHz)

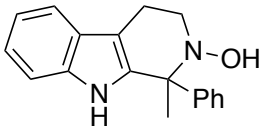

69

(DMSO-d_6, 101 MHz)

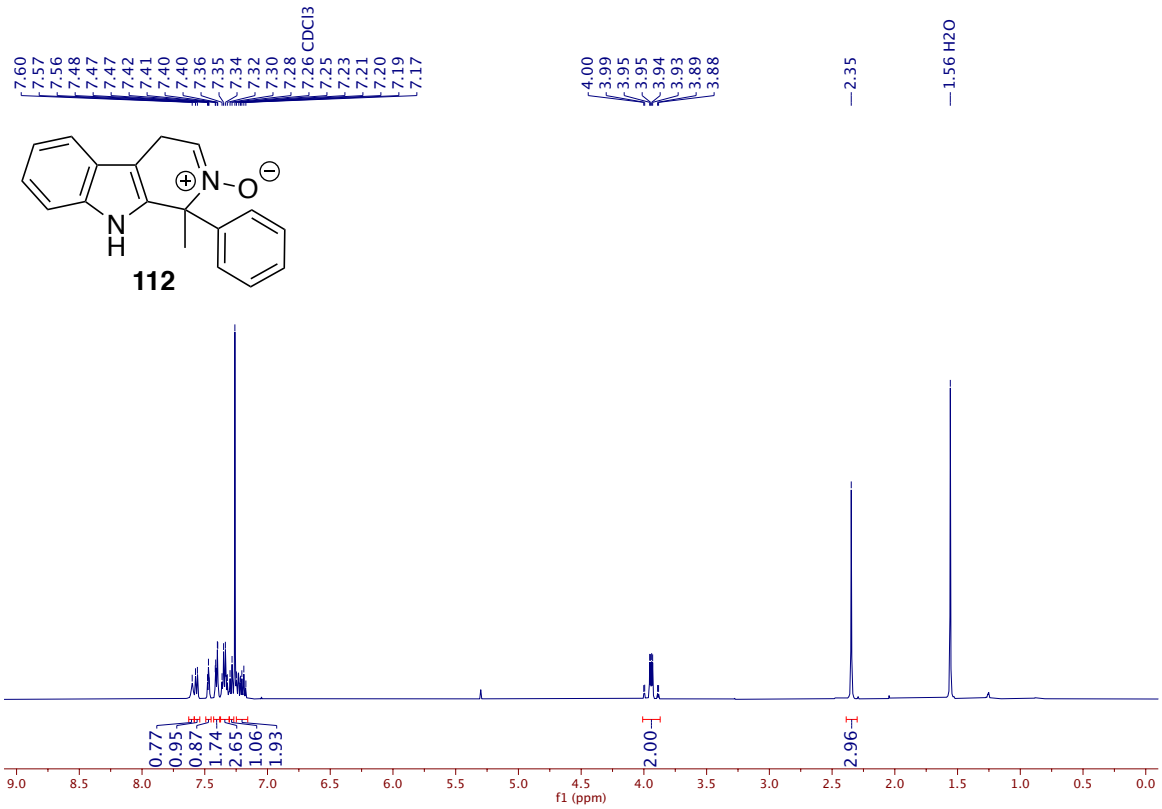
7.60
7.57
7.56
7.48
7.47
7.47
7.42
7.41
7.40
7.40
7.36
7.35
7.34
7.32
7.30
7.28
CDCl3
7.26
7.25
7.23
7.21
7.20
7.19
7.17
4.00
3.99
3.95
3.95
3.94
3.93
3.89
3.88
2.35
1.56 H2O
N
O
N
H
112
0.77
0.95
0.87
1.74
2.65
1.06
1.93
2.00
2.96
9.0
8.5
8.0
7.5
7.0
6.5
6.0
5.5
5.0
4.5
4.0
3.5
3.0
2.5
2.0
1.5
1.0
0.5
0.0
f1 (ppm)

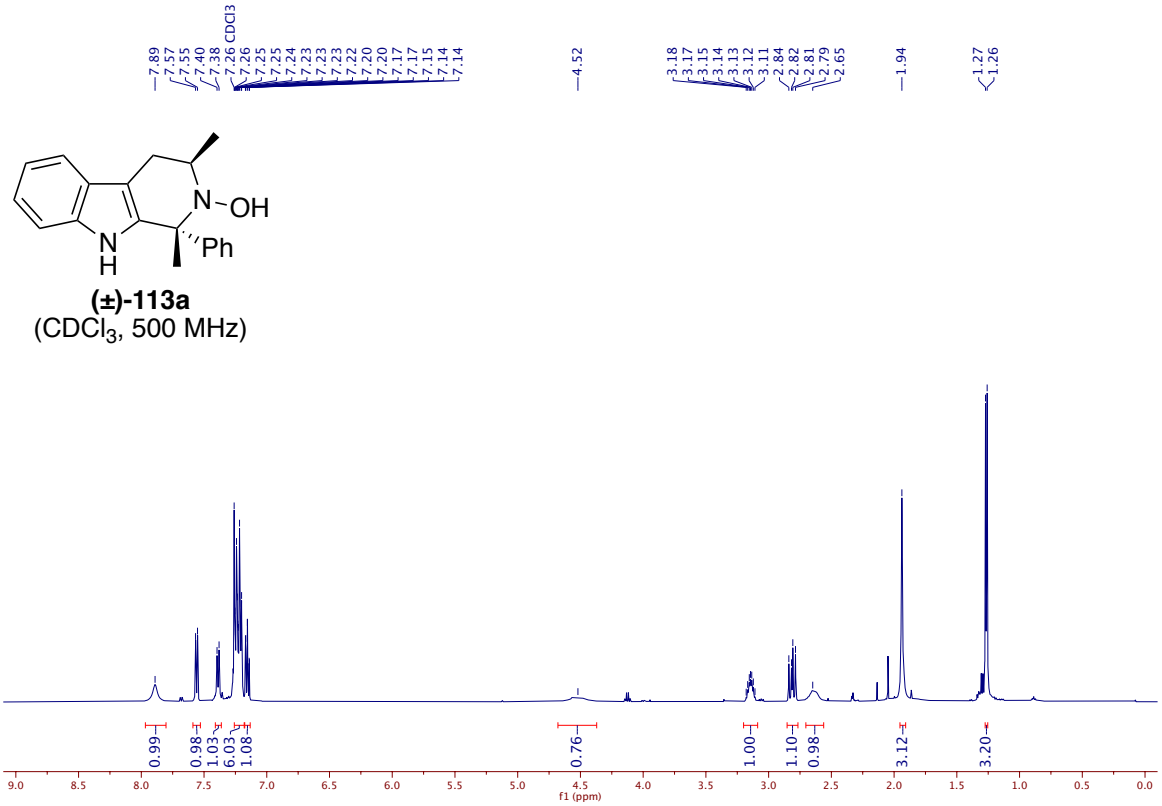

(±)-113a
($CDCl_3$, 500 MHz)

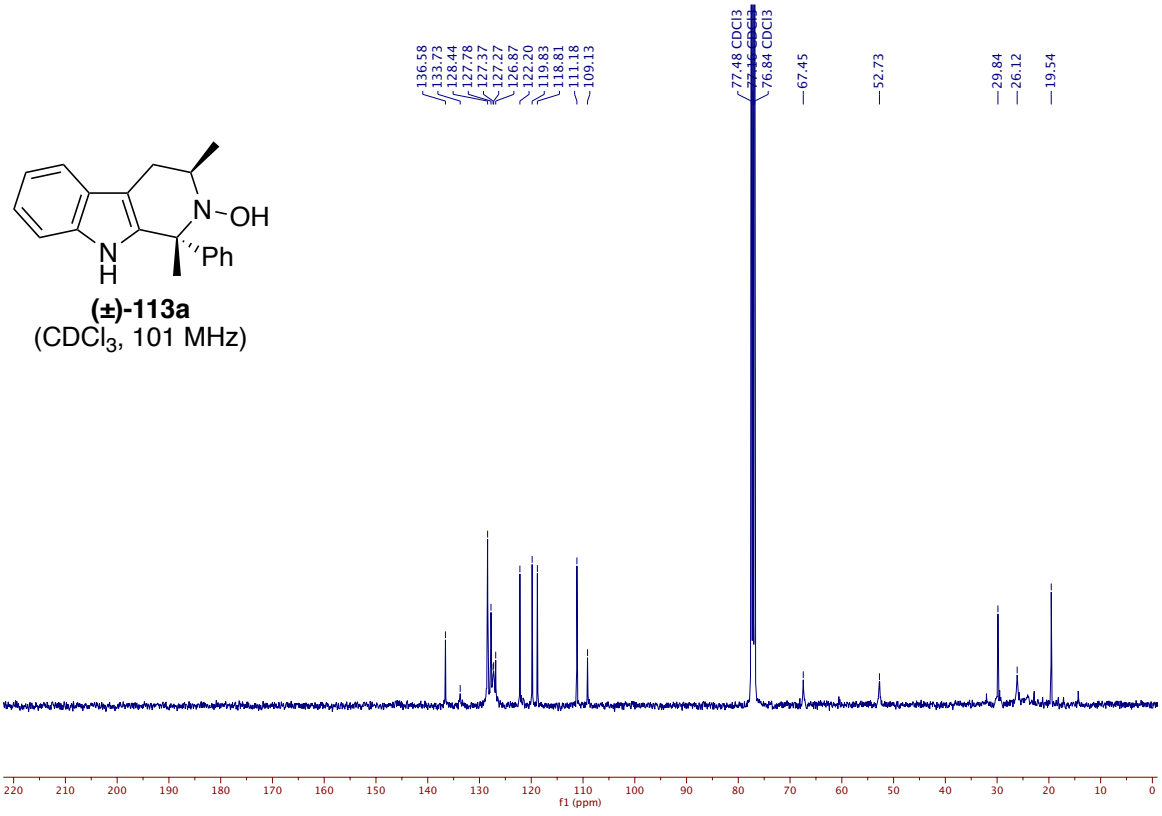

(±)-113a
($CDCl_3$, 101 MHz)

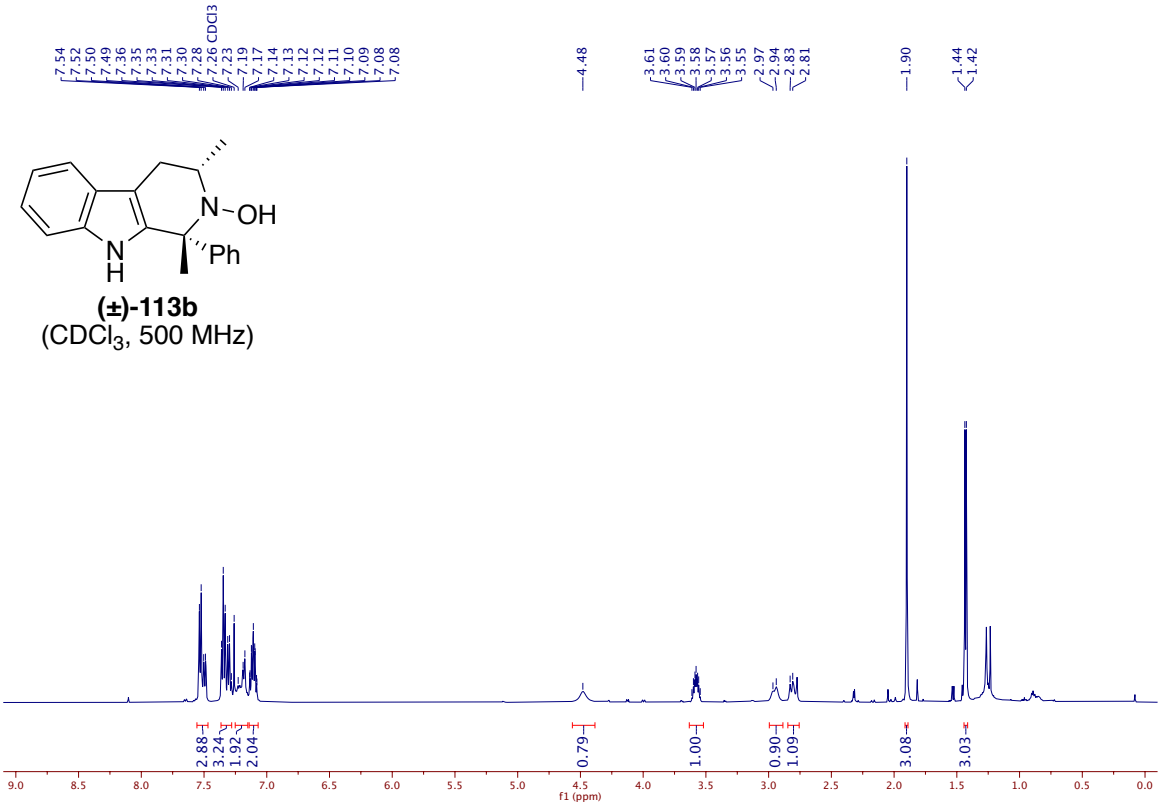

(±)-113b
($CDCl_3$, 500 MHz)

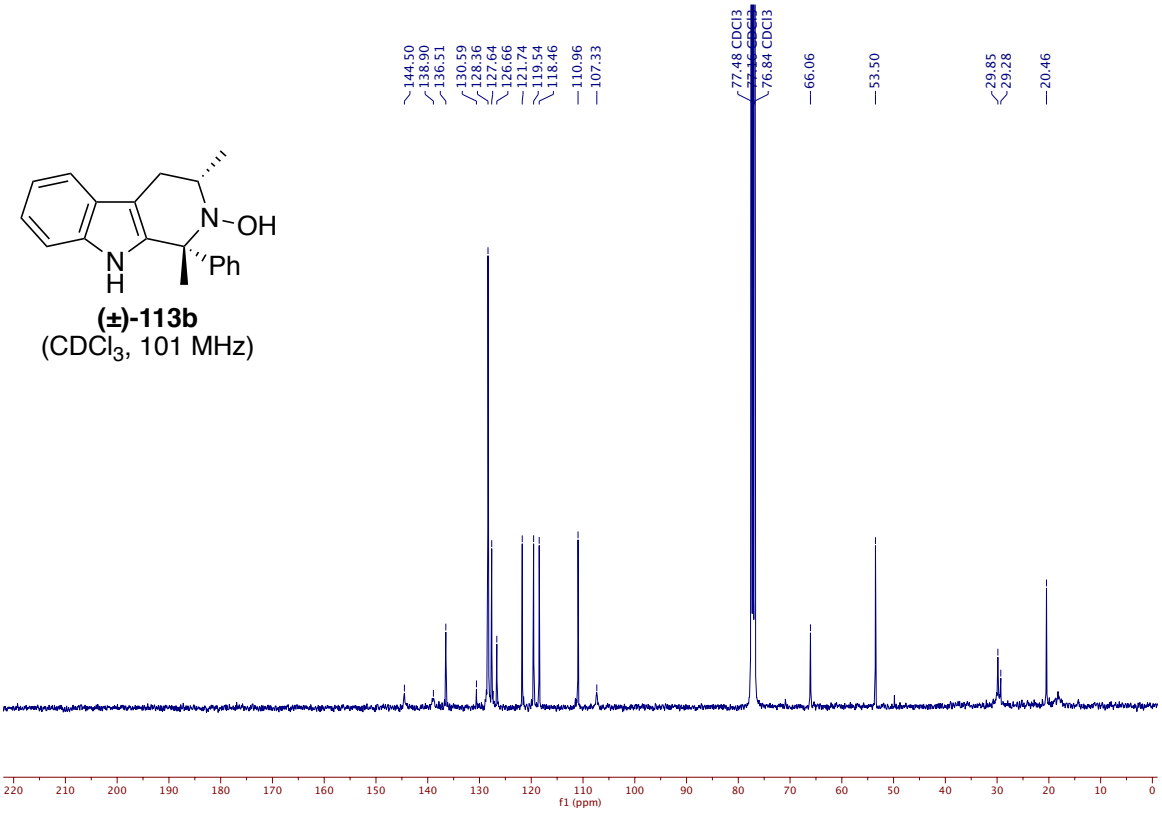

(±)-113b
($CDCl_3$, 101 MHz)

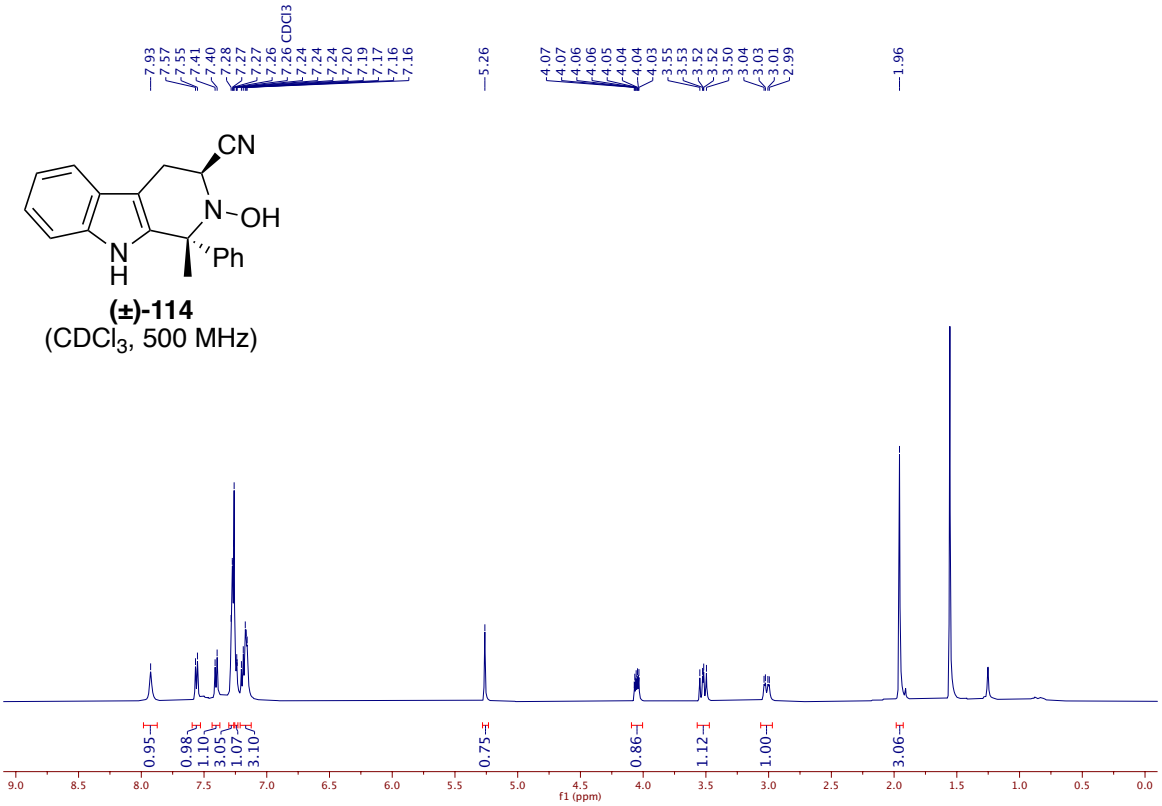

(±)-114
($CDCl_3$, 500 MHz)

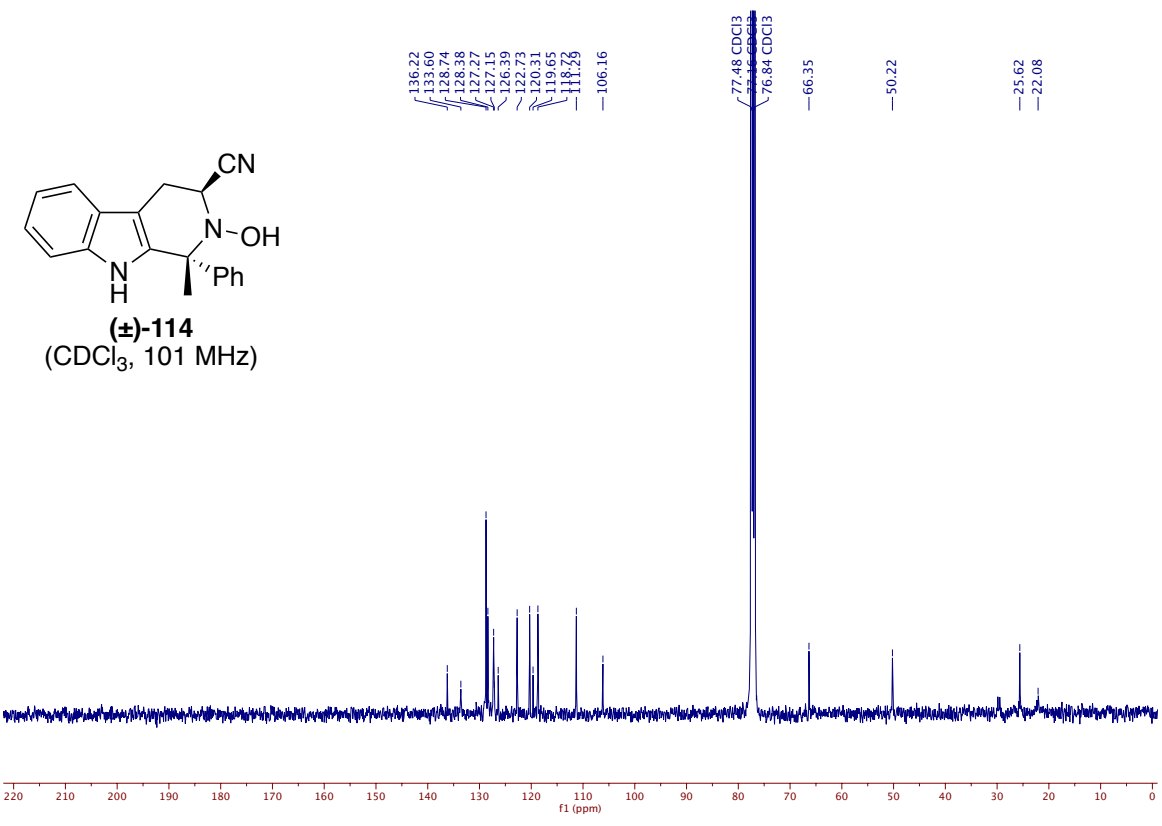

(±)-114
($CDCl_3$, 101 MHz)

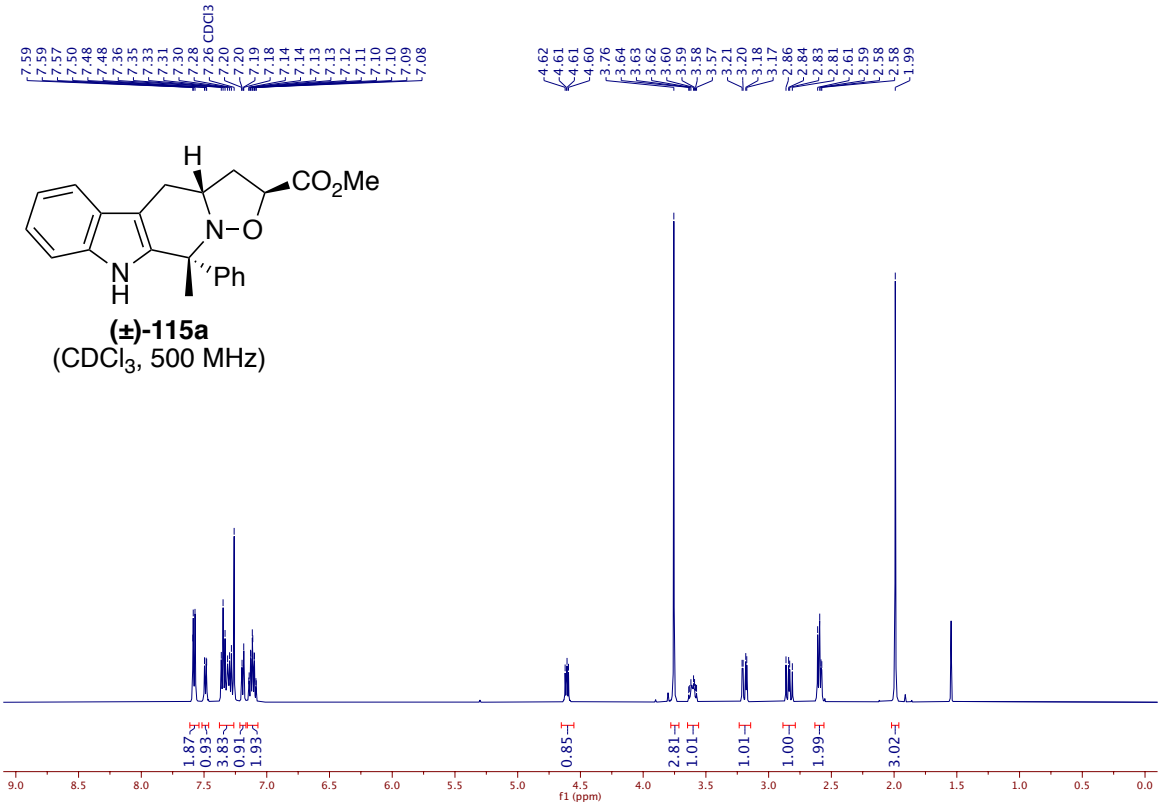
7.59
7.59
7.57
7.50
7.48
7.48
7.36
7.35
7.33
7.31
7.30
7.28
7.26 CDCl3
7.20
7.20
7.19
7.18
7.14
7.14
7.13
7.13
7.12
7.11
7.10
7.10
7.09
7.08
4.62
4.61
4.61
4.60
3.76
3.64
3.63
3.62
3.60
3.59
3.58
3.57
3.21
3.20
3.18
3.17
2.86
2.84
2.83
2.81
2.61
2.59
2.58
2.58
1.99
H
CO2Me
N–O
N
H
Ph
(±)-115a
(CDCl3, 500 MHz)
1.87
0.93
3.83
0.91
1.93
0.85
2.81
1.01
1.01
1.00
1.99
3.02
f1 (ppm)

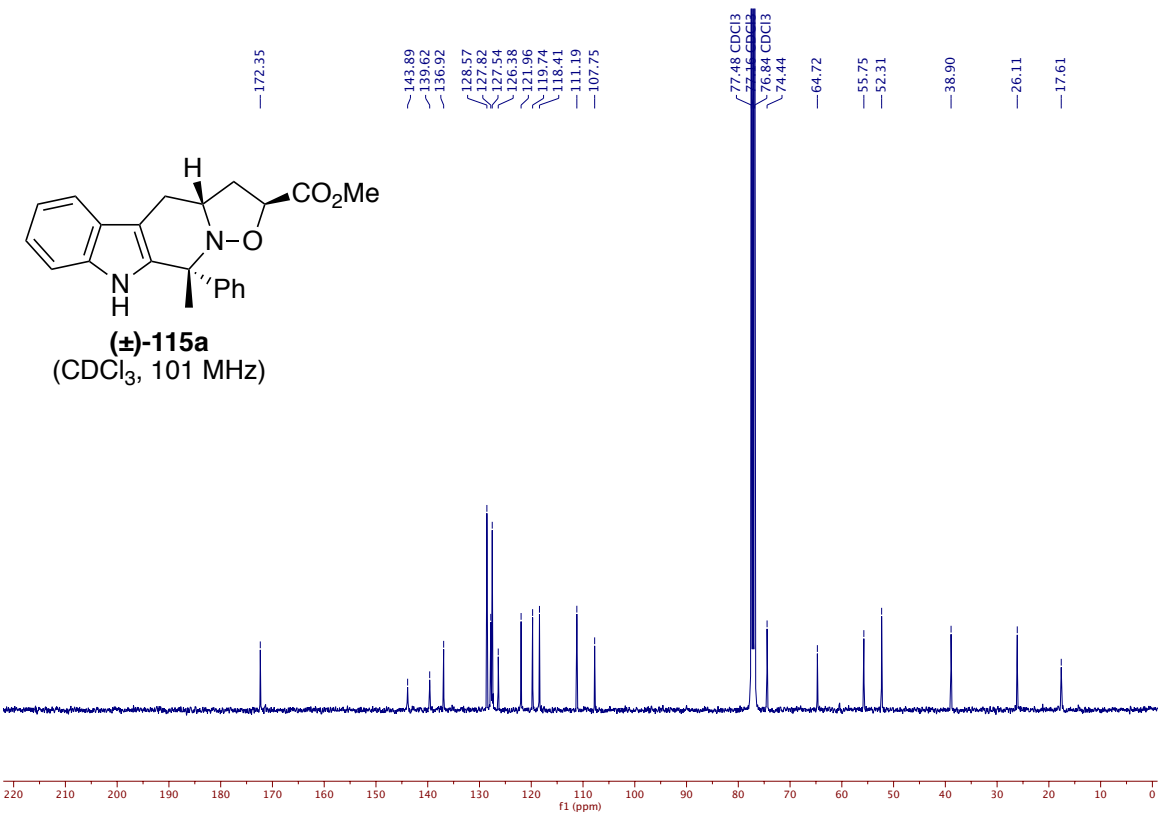
172.35
143.89
139.62
136.92
128.57
127.82
127.54
126.38
121.96
119.74
118.41
111.19
107.75
77.48 CDCl3
77.16 CDCl3
76.84 CDCl3
74.44
64.72
55.75
52.31
38.90
26.11
17.61
H
CO2Me
N–O
N
H
Ph
(±)-115a
(CDCl3, 101 MHz)
f1 (ppm)

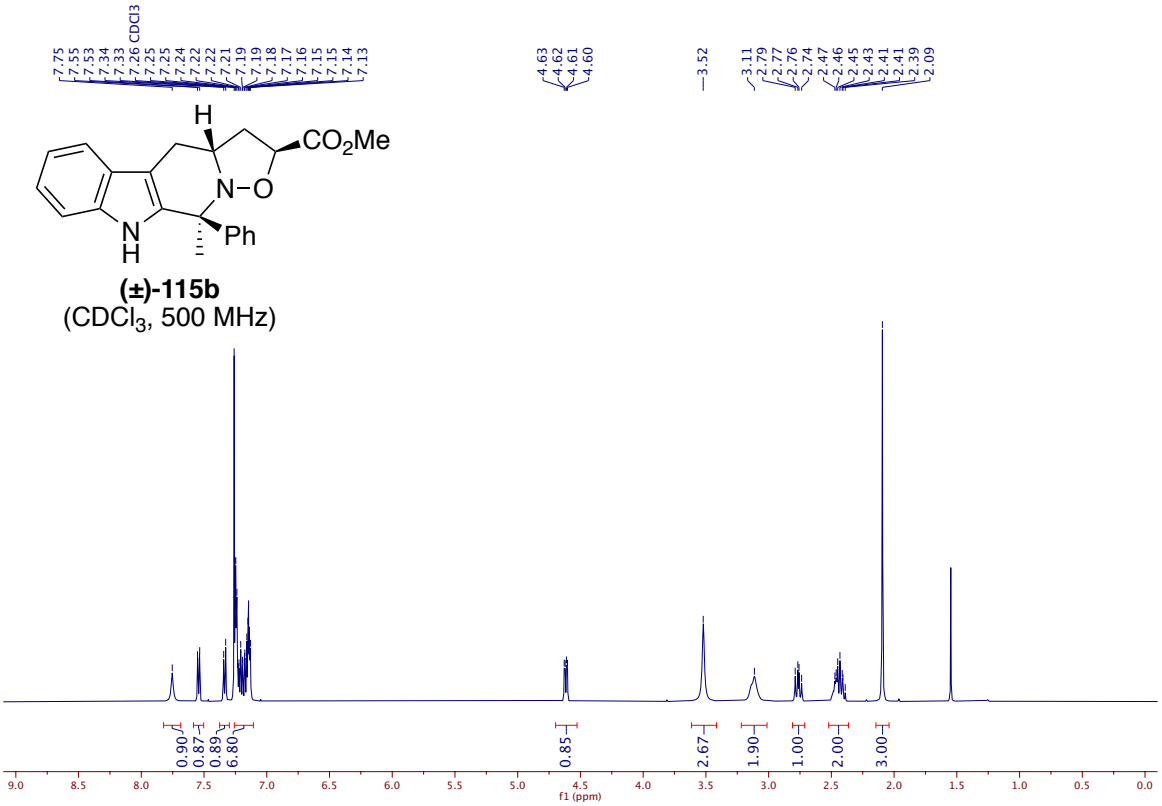

(±)-115b
($CDCl_3$, 500 MHz)

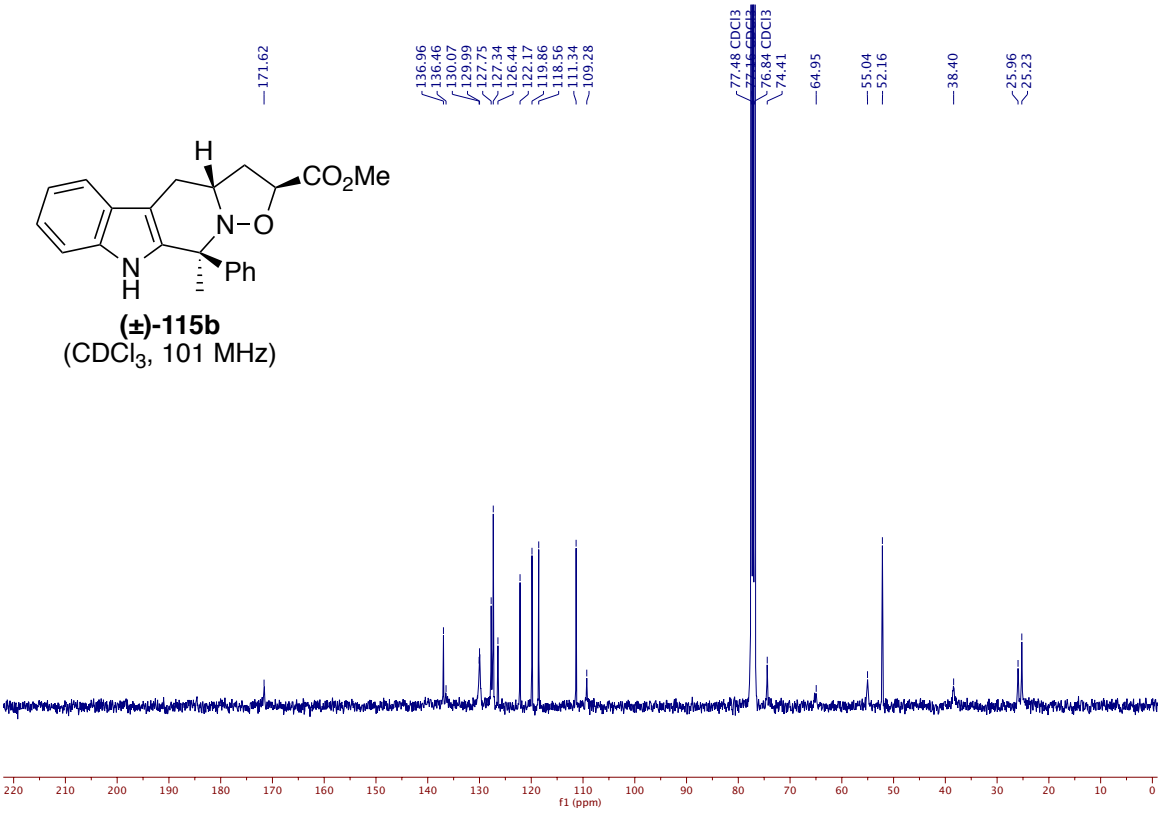

(±)-115b
($CDCl_3$, 101 MHz)

3.10 HPLC Traces

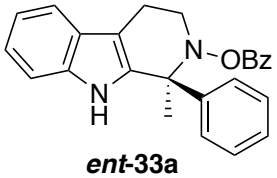

***ent*-33a**

Conditions: HPLC (ChiralPak AD-H, 90:10 hexanes/i-PrOH, 1 mL/min, 254 nm)

Racemic Sample:

<Chromatogram>

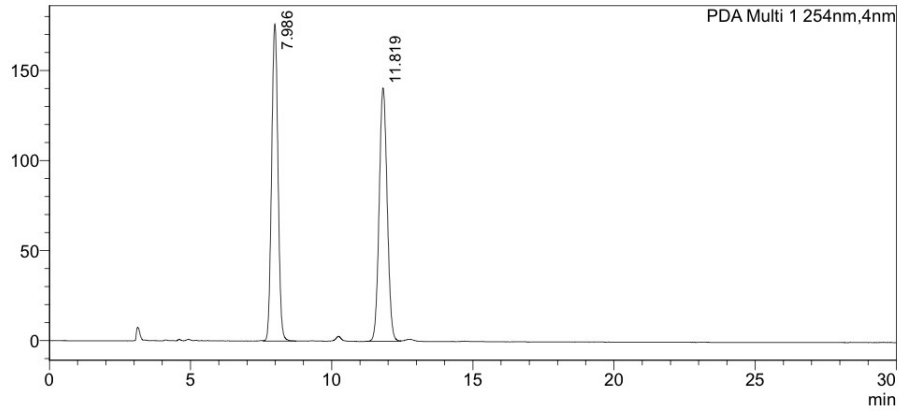

<Peak Table>

PDA Ch1 254nm

Peak#	Ret. Time	Height	Area	Height%	Area%
1	7.986	176267	2749666	55.582	49.673
2	11.819	140861	2785819	44.418	50.327
Total		317128	5535485	100.000	100.000

Enantioenriched Sample:

<Chromatogram>

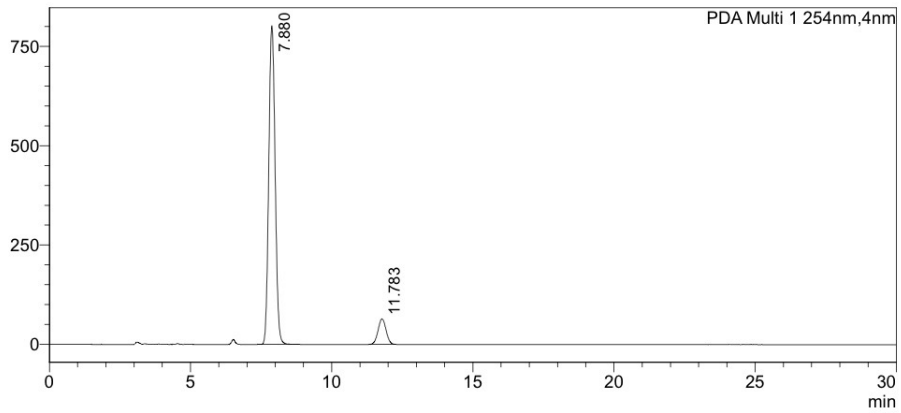

<Peak Table>

PDA Ch1 254nm

Peak#	Ret. Time	Height	Area	Height%	Area%
1	7.880	802274	12518070	92.580	90.783
2	11.783	64304	1270991	7.420	9.217
Total		866578	13789061	100.000	100.000

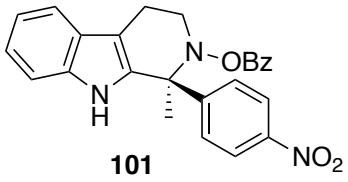

101

Conditions: HPLC (ChiralPak AD-H, 90:10 hexanes/i-PrOH, 1 mL/min, 254 nm)

Racemic Sample:

<Chromatogram>

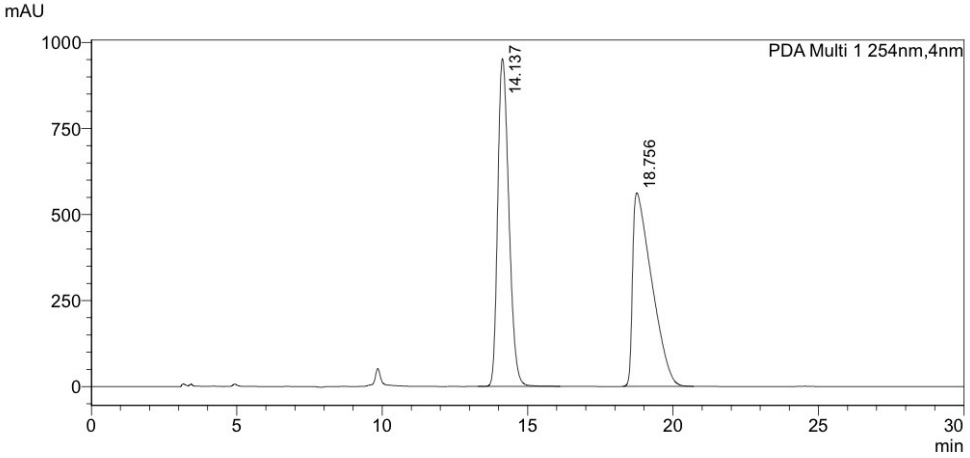

<Peak Table>

PDA Ch1 254nm

Peak#	Ret. Time	Height	Area	Height%	Area%
1	14.137	952894	25421779	62.900	49.773
2	18.756	562034	25654098	37.100	50.227
Total		1514928	51075878	100.000	100.000

Enantioenriched Sample:

<Chromatogram>

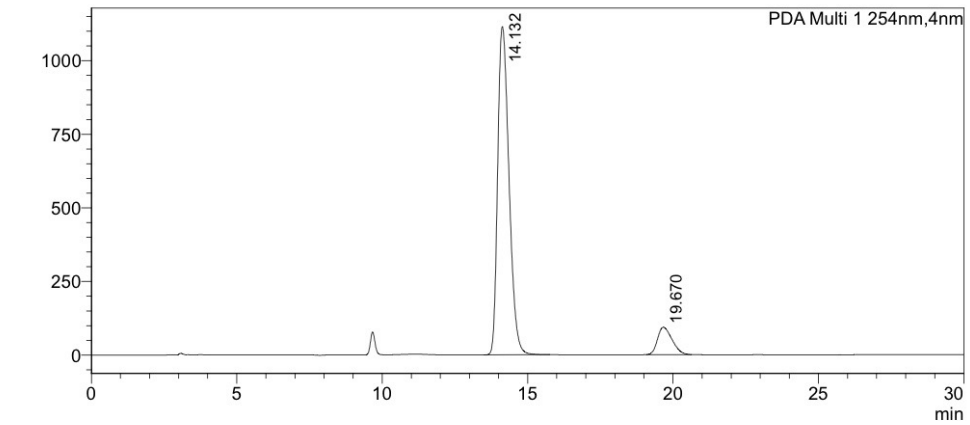

<Peak Table>

PDA Ch1 254nm

Peak#	Ret. Time	Height	Area	Height%	Area%
1	14.132	1115363	30219406	92.306	90.376
2	19.670	92969	3218078	7.694	9.624
Total		1208332	33437484	100.000	100.000

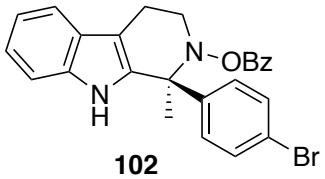

102

Conditions: HPLC (ChiralPak AD-H, 90:10 hexanes/i-PrOH, 1 mL/min, 254 nm)

Racemic Sample:

<Chromatogram>

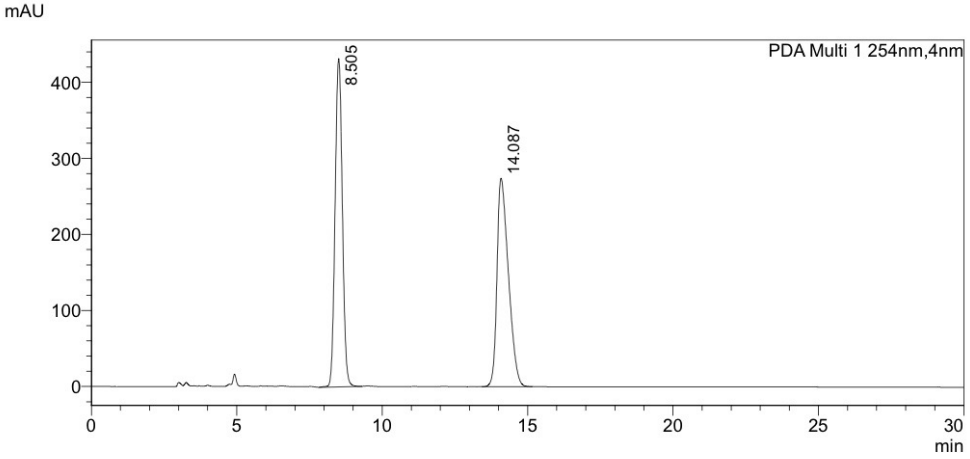

<Peak Table>

PDA Ch1 254nm

Peak#	Ret. Time	Height	Area	Height%	Area%
1	8.505	431813	7476611	61.157	50.000
2	14.087	274260	7476740	38.843	50.000
Total		706073	14953351	100.000	100.000

Enantioenriched Sample:

<Chromatogram>

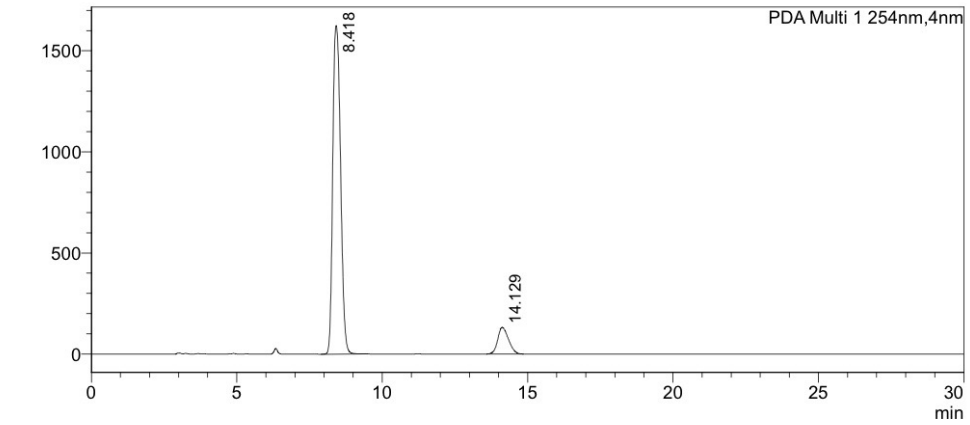

<Peak Table>

PDA Ch1 254nm

Peak#	Ret. Time	Height	Area	Height%	Area%
1	8.418	1625324	30373382	92.499	89.951
2	14.129	131804	3393250	7.501	10.049
Total		1757128	33766632	100.000	100.000

Crystallization Sample:

<Chromatogram>

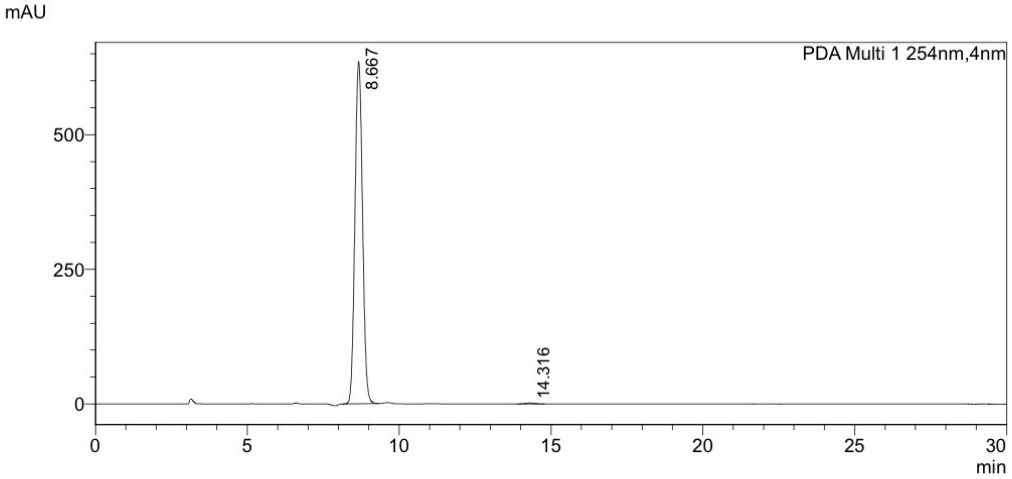

<Peak Table>

PDA Ch1 254nm

Peak#	Ret. Time	Height	Area	Height%	Area%
1	8.667	635186	10994403	99.703	99.590
2	14.316	1893	45287	0.297	0.410
Total		637078	11039691	100.000	100.000

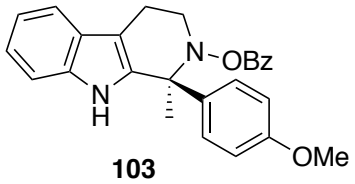

103

Conditions: HPLC (ChiralPak AD-H, 90:10 hexanes/i-PrOH, 1 mL/min, 254 nm)

Racemic Sample:

<Chromatogram>

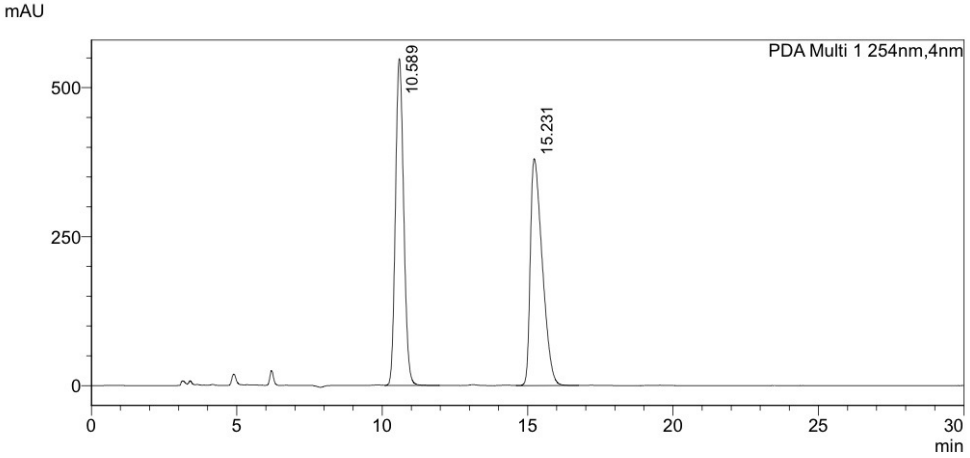

<Peak Table>

PDA Ch1 254nm

Peak#	Ret. Time	Height	Area	Height%	Area%
1	10.589	548849	10821368	59.038	49.840
2	15.231	380801	10890847	40.962	50.160
Total		929651	21712215	100.000	100.000

Enantioenriched Sample:

<Chromatogram>

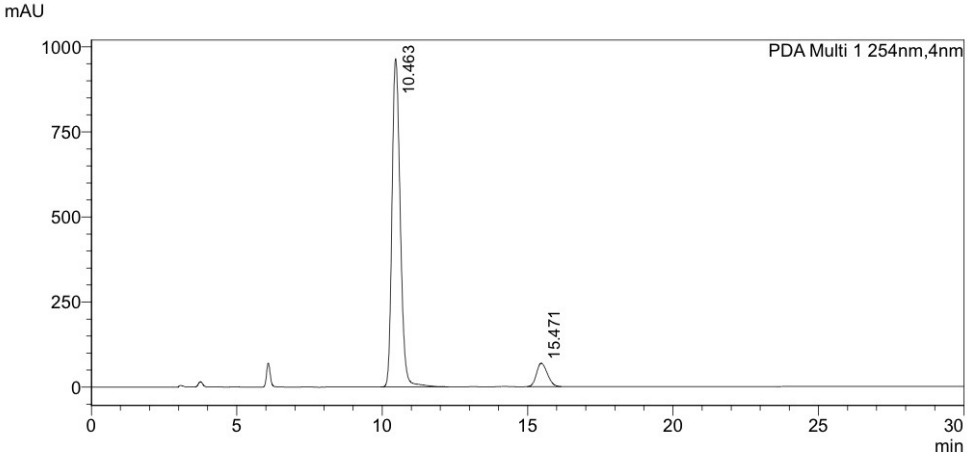

<Peak Table>

PDA Ch1 254nm

Peak#	Ret. Time	Height	Area	Height%	Area%
1	10.463	964866	19025086	93.357	91.455
2	15.471	68658	1777665	6.643	8.545
Total		1033524	20802751	100.000	100.000

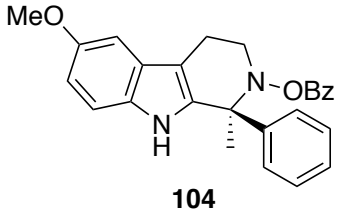

104

Conditions: HPLC (ChiralPak AD-H, 90:10 hexanes/i-PrOH, 1 mL/min, 254 nm)

Racemic Sample:

<Chromatogram>

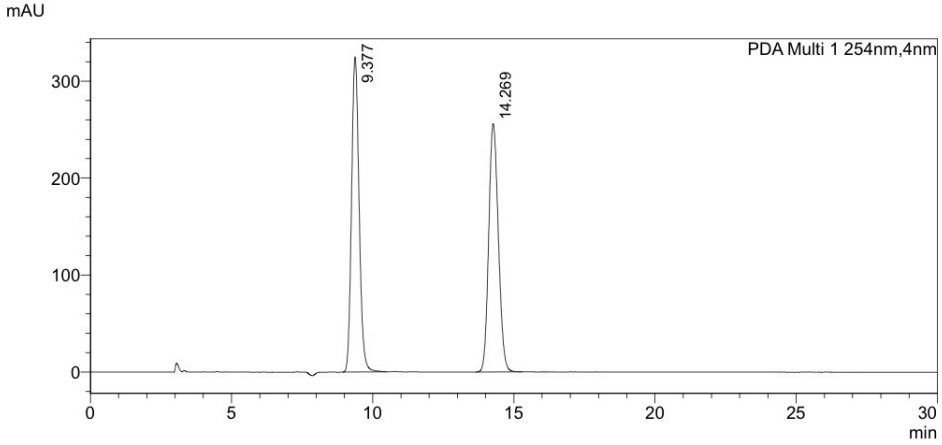

<Peak Table>

PDA Ch1 254nm

Peak#	Ret. Time	Height	Area	Height%	Area%
1	9.377	325055	6031388	55.957	49.822
2	14.269	255845	6074544	44.043	50.178
Total		580900	12105932	100.000	100.000

Enantioenriched Sample:

<Chromatogram>

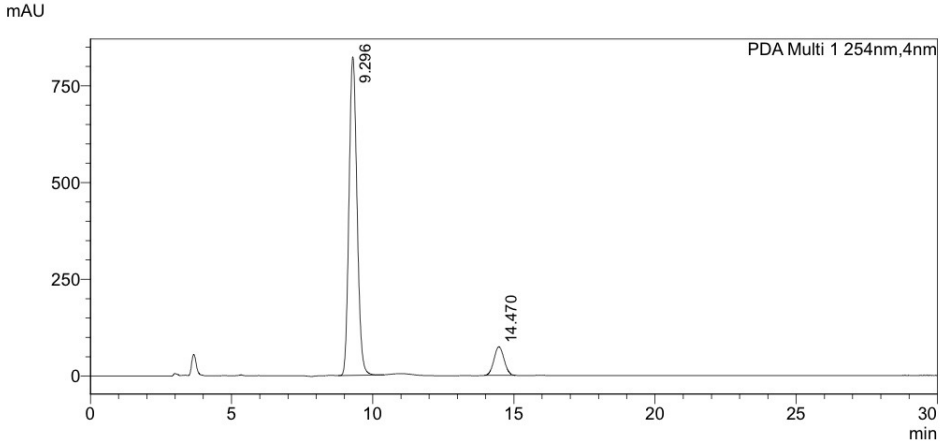

<Peak Table>

PDA Ch1 254nm

Peak#	Ret. Time	Height	Area	Height%	Area%
1	9.296	822941	16240677	91.771	89.871
2	14.470	73796	1830399	8.229	10.129
Total		896737	18071077	100.000	100.000

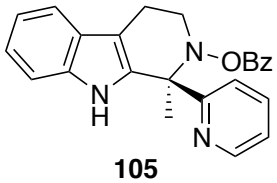

105

Conditions: HPLC (ChiralPak AD-H, 90:10 hexanes/i-PrOH, 1 mL/min, 254 nm)

Racemic Sample:

<Chromatogram>

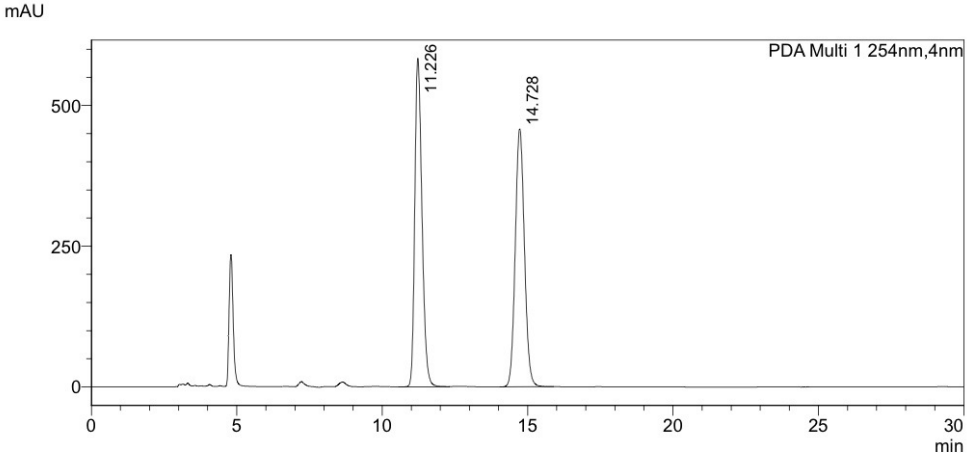

<Peak Table>

PDA Ch1 254nm

Peak#	Ret. Time	Height	Area	Height%	Area%
1	11.226	583381	10071262	55.997	49.998
2	14.728	458435	10072209	44.003	50.002
Total		1041816	20143471	100.000	100.000

Enantioenriched Sample:

<Chromatogram>

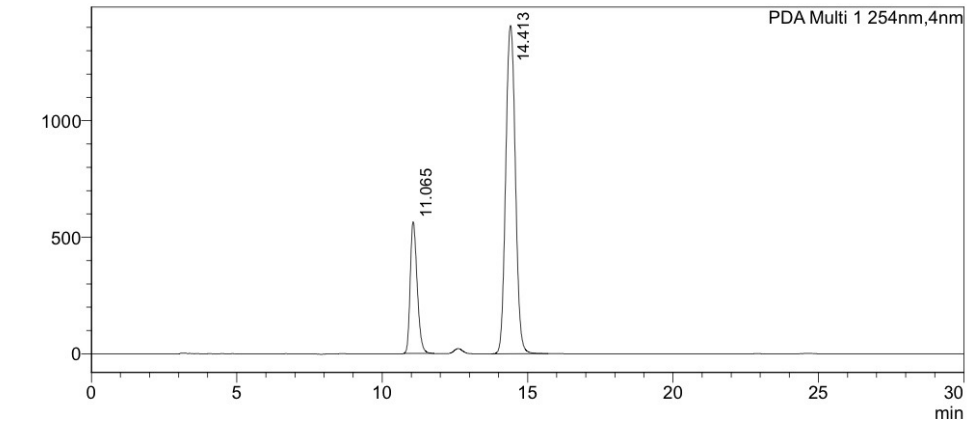

<Peak Table>

PDA Ch1 254nm

Peak#	Ret. Time	Height	Area	Height%	Area%
1	11.065	564622	9387200	28.623	22.444
2	14.413	1407970	32437761	71.377	77.556
Total		1972593	41824961	100.000	100.000

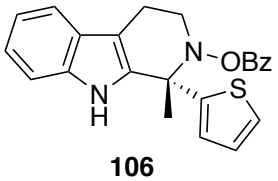

106

Conditions: HPLC (ChiralPak AD-H, 90:10 hexanes/i-PrOH, 1 mL/min, 254 nm)

Racemic Sample:

<Chromatogram>

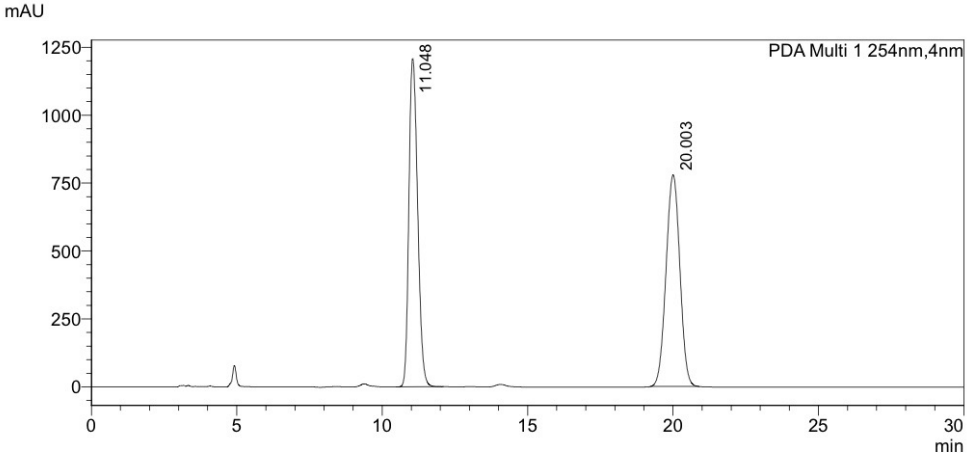

<Peak Table>

PDA Ch1 254nm

Peak#	Ret. Time	Height	Area	Height%	Area%
1	11.048	1208916	25351279	60.817	49.617
2	20.003	778873	25742938	39.183	50.383
Total		1987789	51094216	100.000	100.000

Enantioenriched Sample:

<Chromatogram>

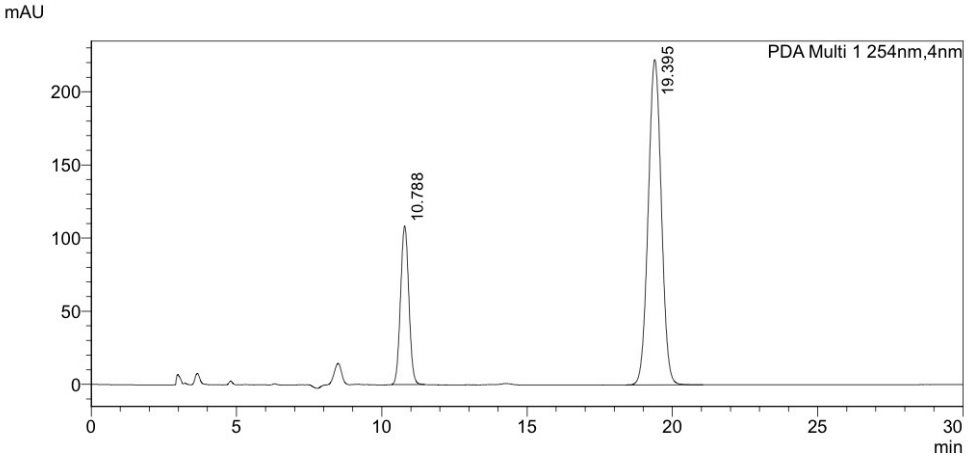

<Peak Table>

PDA Ch1 254nm

Peak#	Ret. Time	Height	Area	Height%	Area%
1	10.788	108314	2152604	32.748	23.595
2	19.395	222432	6970402	67.252	76.405
Total		330746	9123006	100.000	100.000

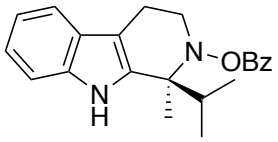

107

Conditions: HPLC (ChiralPak AD-H, 90:10 hexanes/i-PrOH, 1 mL/min, 254 nm)

Racemic Sample:

<Chromatogram>

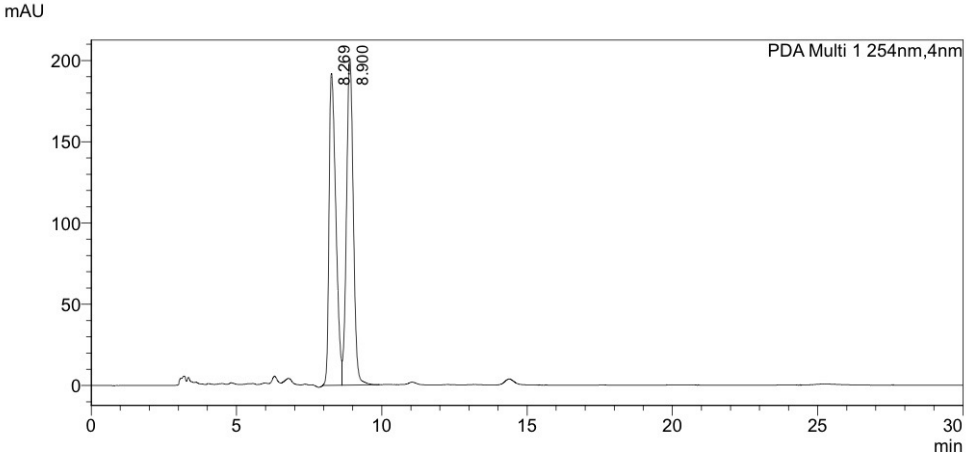

<Peak Table>

PDA Ch1 254nm

Peak#	Ret. Time	Height	Area	Height%	Area%
1	8.269	192083	3130806	48.871	48.895
2	8.900	200956	3272371	51.129	51.105
Total		393039	6403177	100.000	100.000

Enantioenriched Sample:

<Chromatogram>

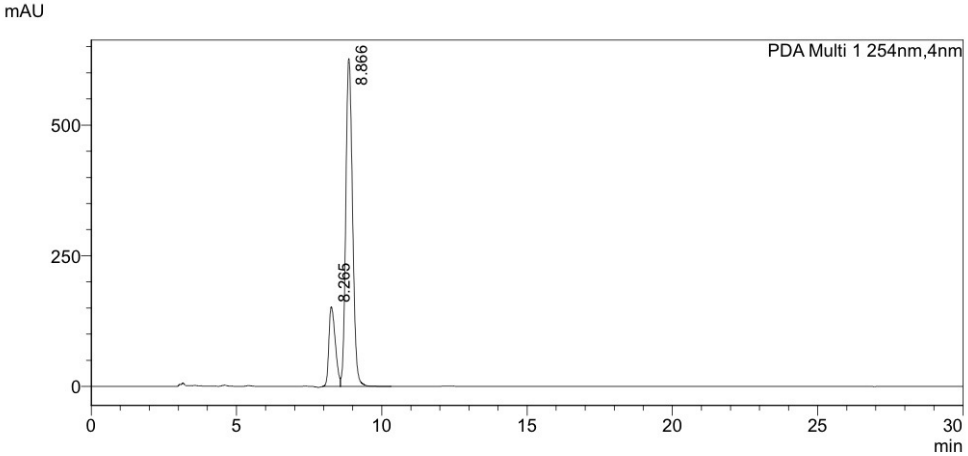

<Peak Table>

PDA Ch1 254nm

Peak#	Ret. Time	Height	Area	Height%	Area%
1	8.265	152396	2350053	19.545	18.775
2	8.866	627305	10166924	80.455	81.225
Total		779701	12516977	100.000	100.000

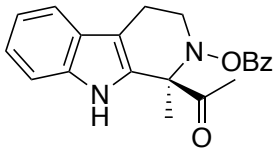

108

Conditions: HPLC (ChiralPak AD-H, 90:10 hexanes/i-PrOH, 1 mL/min, 254 nm)

Racemic Sample:

<Chromatogram>

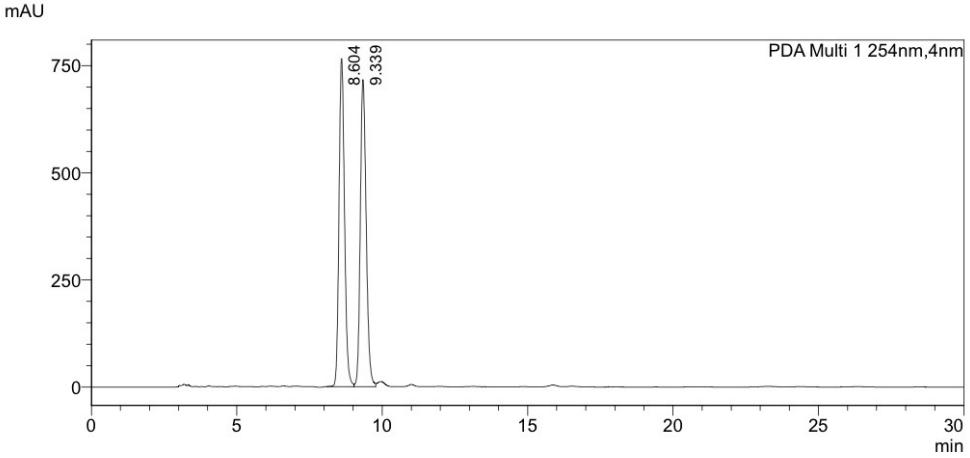

<Peak Table>

PDA Ch1 254nm

Peak#	Ret. Time	Height	Area	Height%	Area%
1	8.604	765554	10079971	51.669	49.982
2	9.339	716089	10087227	48.331	50.018
Total		1481642	20167198	100.000	100.000

Enantioenriched Sample:

<Chromatogram>

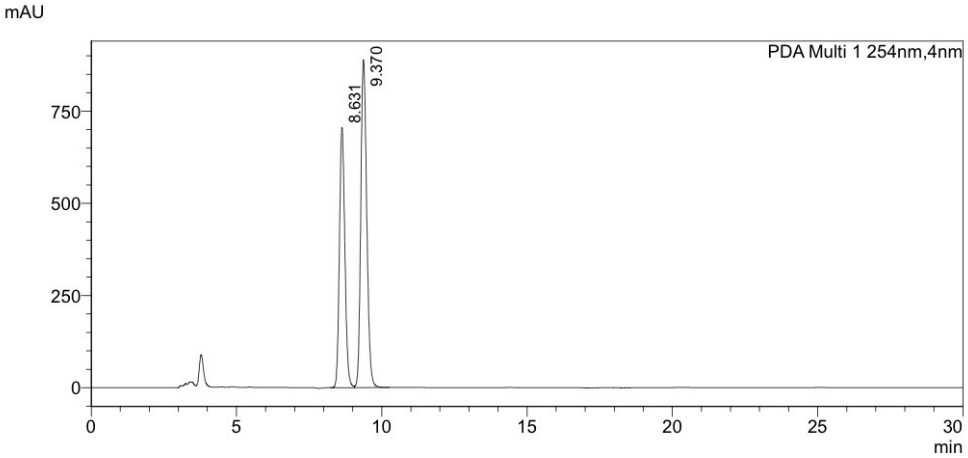

<Peak Table>

PDA Ch1 254nm

Peak#	Ret. Time	Height	Area	Height%	Area%
1	8.631	705922	9185569	44.244	42.134
2	9.370	889606	12615307	55.756	57.866
Total		1595528	21800876	100.000	100.000

3.11 X-Ray Crystallography Data

General information: The diffraction data were measured at 100 K on a Bruker D8 VENTURE diffractometer equipped with a microfocus Mo-target X-ray tube (λ = 0.71073 Å) and PHOTON 100 CMOS detector. Data were collected using ϕ and ω scans to survey a hemisphere of reciprocal space. Data reduction and integration were performed with the Bruker APEX3 software package (Bruker AXS, version 2017.3-0, 2018). Data were scaled and corrected for absorption effects using the multi-scan procedure as implemented in SADABS (Bruker AXS, version 2014/5, Krause, Herbst-Irmer, Sheldrick & Stalke, *J. Appl. Cryst.* **2015**, *48*, 3-10). The structure was solved by SHELXT (Version 2014/5: Sheldrick, G. M. *Acta Crystallogr*. **2015**, *A71*, 3-8) and refined by a full-matrix least-squares procedure using OLEX2 (O. V. Dolomanov, L. J. Bourhis, R. J. Gildea, J. A. K. Howard and H. Puschmann. J. Appl. Crystallogr. **2009**, *42*, 339-341) (XL refinement program version 2018/3, *Sheldrick, G. M. Acta Crystallogr.* **2015**, *C71*, 3-8).

Crystal Structure of 33a

Specific details for structure refinement: All atoms were refined with anisotropic thermal parameters. Hydrogen atoms were included in idealized positions for structure factor calculations except atom H2 attached to nitrogen atom N2. This hydrogen atom was located in the difference Fourier map and allowed to be refined without any additional restraints. All structures are drawn with thermal ellipsoids at 50% probability.

Crystal Structure of 43

Specific details for structure refinement: All atoms were refined with anisotropic thermal parameters. Hydrogen atoms were included in idealized positions for structure factor calculations

except an H-atom attached to an indole nitrogen atom. This hydrogen atom was located in the difference Fourier map and allowed to be freely refined with the thermal parameter being constrained to be 1.2 times of the Ueq value of the N atom. All structures are drawn with thermal ellipsoids at 50% probability.

Crystal Structure of 102

Specific details for structure refinement: All atoms were refined with anisotropic thermal parameters. All hydrogen atoms were included in idealized positions for structure factor calculations except the hydrogen atom of the NH group. This atom was found in the difference Fourier map and refined without geometric restraints. All structures are drawn with thermal ellipsoids at 50% probability.

Crystal Structure of ±113a

Specific details for structure refinement: All atoms were refined with anisotropic thermal parameters. Hydrogen atoms were included in idealized positions for structure factor calculations except atom H1O and H1N attached to oxygen and nitrogen atoms, respectively. These hydrogen atoms were located in the difference Fourier map. All structures are drawn with thermal ellipsoids at 50% probability.

Crystal Structure of ±114

Specific details for structure refinement: All atoms were refined with anisotropic thermal parameters. Hydrogen atoms were included in idealized positions for structure factor calculations except atom H1O and H3N attached to oxygen and nitrogen atoms, respectively. These hydrogen

atoms were located in the difference Fourier map. All structures are drawn with thermal ellipsoids at 50% probability.

Crystal Structure of ±115a

Specific details for structure refinement: All atoms were refined with anisotropic thermal parameters. Hydrogen atoms were included in idealized positions for structure factor calculations except H-atoms attached to nitrogen atoms. These hydrogen atoms (H1 and H3) were located in the difference Fourier map and allowed to be refined at 0.88 Å within a default 0.02 Å standard deviation with their thermal parameters being constrained to be 1.2 times of the Ueq value of the N atoms. All structures are drawn with thermal ellipsoids at 50% probability.

Crystal Structure of ±115b

Specific details for structure refinement: The structure was first solved and refined using HKLF 4 file format. The final refinement cycles were carried out with HKLF 5. Refined fractional volume contribution for the second twin component is 0.46. All atoms were refined with anisotropic thermal parameters. Hydrogen atoms were included in idealized positions for structure factor calculations except H-atoms attached to nitrogen atoms. These hydrogen atoms (H1 and H3) were located in the difference Fourier map and allowed to be refined at 0.88 Å within a default 0.02 Å standard deviation with their thermal parameters being constrained to be 1.2 times of the Ueq value of the N atoms. All structures are drawn with thermal ellipsoids at 40% probability.

Figure 3.3. ORTEP representation of **33a**.

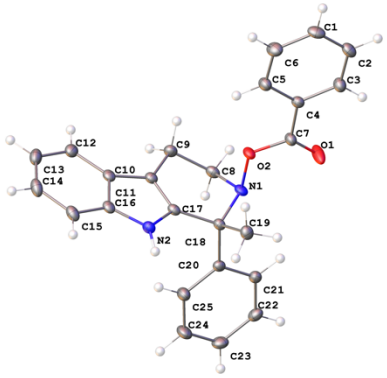

Crystal data and structure refinement for 0732_LC.

Identification code	0732_LC
Empirical formula	$C_{25}H_{22}N_2O_2$
Formula weight	382.44
Temperature/K	100(2)
Crystal system	monoclinic
Space group	$P2_1/c$
a/Å	9.5752(5)
b/Å	12.0481(7)
c/Å	17.8268(10)
α/°	90
β/°	101.373(2)
γ/°	90
Volume/Å^3	2016.17(19)
Z	4
ρ_{calc}g/cm^3	1.260
μ/mm^{-1}	0.080
F(000)	808.0
Crystal size/mm^3	0.307 × 0.108 × 0.107
Radiation	MoKα (λ = 0.71073)
2Θ range for data collection/°	4.662 to 53.01
Index ranges	$-12 \le h \le 12$, $-15 \le k \le 15$, $-22 \le l \le 22$
Reflections collected	50007
Independent reflections	4167 [R_{int} = 0.0400, R_{sigma} = 0.0184]
Data/restraints/parameters	4167/0/267
Goodness-of-fit on F^2	1.023
Final R indexes [I>=2σ (I)]	R_1 = 0.0357, wR_2 = 0.0812
Final R indexes [all data]	R_1 = 0.0481, wR_2 = 0.0879
Largest diff. peak/hole / e Å^{-3}	0.27/-0.18

$R_{int} = \Sigma \mid F_o^2 - \langle F_o^2 \rangle \mid / \Sigma \mid F_o^2 \mid$

$R1 = \Sigma \mid \mid F_o \mid - \mid F_c \mid \mid / \Sigma \mid F_o \mid$

$wR2 = [\Sigma [w (F_o^2 - F_c^2)^2] / \Sigma [w (F_o^2)^2]]^{1/2}$

Goodness-of-fit = $[\Sigma [w (F_o^2 - F_c^2)^2] / (n-p)]^{1/2}$

n: number of independent reflections; p: number of refined parameters

Figure 3.4. ORTEP representation of **43**.

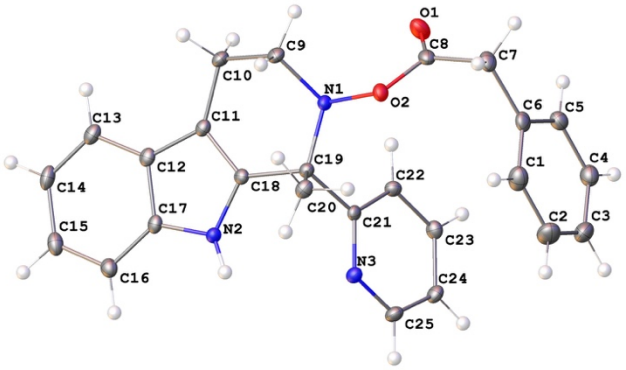

Crystal data and structure refinement for mo_0877_tes.

Identification code	mo_0877_tes
Empirical formula	$C_{25}H_{23}N_3O_2$
Formula weight	397.46
Temperature/K	100(2)
Crystal system	triclinic
Space group	P-1
a/Å	7.7539(3)
b/Å	10.3038(5)
c/Å	13.4620(6)
α/°	107.202(2)
β/°	98.294(2)
γ/°	96.619(2)
Volume/Å^3	1002.39(8)
Z	2
ρ_{calc}g/cm^3	1.317
μ/mm^{-1}	0.085
F(000)	420.0
Crystal size/mm^3	0.41 × 0.28 × 0.14
Radiation	MoKα (λ = 0.71073)
2Θ range for data collection/°	4.406 to 56.86
Index ranges	-10 ≤ h ≤ 10, -13 ≤ k ≤ 13, -17 ≤ l ≤ 18
Reflections collected	32154
Independent reflections	5032 [R_{int} = 0.0383, R_{sigma} = 0.0309]
Data/restraints/parameters	5032/0/275
Goodness-of-fit on F^2	1.032
Final R indexes [I>=2σ (I)]	R_1 = 0.0425, wR_2 = 0.0965
Final R indexes [all data]	R_1 = 0.0618, wR_2 = 0.1050
Largest diff. peak/hole / e Å^{-3}	0.35/-0.21

$R_{int} = \Sigma \mid F_o^2 - \langle F_o^2 \rangle \mid / \Sigma \mid F_o^2 \mid$

$R1 = \Sigma \mid \mid F_o \mid - \mid F_c \mid \mid / \Sigma \mid F_o \mid$

$wR2 = [\Sigma [w (F_o^2 - F_c^2)^2] / \Sigma [w (F_o^2)^2]]^{1/2}$

Goodness-of-fit = $[\Sigma [w (F_o^2 - F_c^2)^2] / (n-p)]^{1/2}$

n: number of independent reflections; p: number of refined parameters

Figure 3.5. ORTEP representation of **102**.

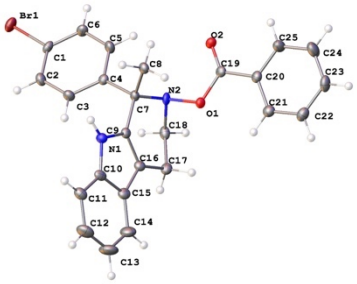

Crystal data and structure refinement for 0953_TLC_Snyder_2.

Identification code	0953_TLC_Snyder_2
Empirical formula	$C_{25}H_{21}BrN_2O_2$
Formula weight	461.35
Temperature/K	100(2)
Crystal system	orthorhombic
Space group	$P2_12_12_1$
a/Å	9.8948(6)
b/Å	10.3781(6)
c/Å	20.5618(13)
α/°	90
β/°	90
γ/°	90
Volume/Å^3	2111.5(2)
Z	4
ρ_{calc}g/cm^3	1.451
μ/mm^{-1}	1.971
F(000)	944.0
Crystal size/mm^3	0.12 × 0.051 × 0.045
Radiation	MoKα (λ = 0.71073)
2Θ range for data collection/°	4.396 to 57.446
Index ranges	-13 ≤ h ≤ 12, -14 ≤ k ≤ 13, -27 ≤ l ≤ 27
Reflections collected	43364
Independent reflections	5432 [R_{int} = 0.0474, R_{sigma} = 0.0470]
Data/restraints/parameters	5432/0/275
Goodness-of-fit on F^2	1.056
Final R indexes [I>=2σ (I)]	R_1 = 0.0338, wR_2 = 0.0616
Final R indexes [all data]	R_1 = 0.0468, wR_2 = 0.0646
Largest diff. peak/hole / e Å^{-3}	0.73/-0.36
Flack parameter	0.012(3)

$R_{int} = \Sigma \mid F_o^2 - \langle F_o^2 \rangle \mid / \Sigma \mid F_o^2 \mid$

$R1 = \Sigma \mid \mid F_o \mid - \mid F_c \mid \mid / \Sigma \mid F_o \mid$

$wR2 = [\Sigma [w (F_o^2 - F_c^2)^2] / \Sigma [w (F_o^2)^2]]^{1/2}$

Goodness-of-fit = $[\Sigma [w (F_o^2 - F_c^2)^2] / (n-p)]^{1/2}$

n: number of independent reflections; p: number of refined parameters

Figure 3.6. ORTEP representation of **±113a**.

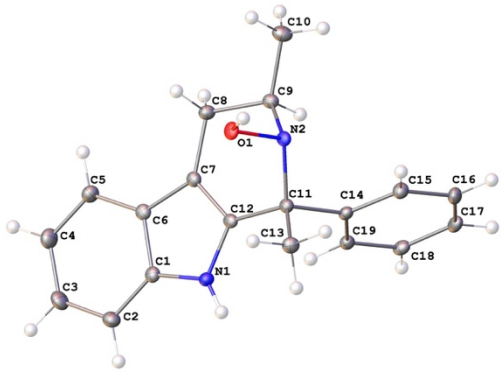

Crystal data and structure refinement for 0812_T.

Identification code	0812_T
Empirical formula	$C_{19}H_{20}N_2O$
Formula weight	292.37
Temperature/K	100(2)
Crystal system	triclinic
Space group	P-1
a/Å	8.5841(6)
b/Å	10.1481(7)
c/Å	10.2458(8)
α/°	112.745(2)
β/°	103.325(2)
γ/°	99.118(2)
Volume/Å^3	769.88(10)
Z	2
ρ_{calc}g/cm^3	1.261
μ/mm^{-1}	0.079
F(000)	312.0
Crystal size/mm^3	0.6 × 0.27 × 0.15
Radiation	MoKα (λ = 0.71073)
2Θ range for data collection/°	4.528 to 57.228
Index ranges	-11 ≤ h ≤ 11, -13 ≤ k ≤ 13, -13 ≤ l ≤ 13
Reflections collected	28347
Independent reflections	3937 [R_{int} = 0.0470, R_{sigma} = 0.0339]
Data/restraints/parameters	3937/2/209
Goodness-of-fit on F^2	1.031
Final R indexes [I>=2σ (I)]	R_1 = 0.0453, wR_2 = 0.1035
Final R indexes [all data]	R_1 = 0.0654, wR_2 = 0.1129
Largest diff. peak/hole / e Å^{-3}	0.39/-0.19

$R_{int} = \Sigma \mid F_o^2 - \langle F_o^2 \rangle \mid / \Sigma \mid F_o^2 \mid$

$R1 = \Sigma \mid \mid F_o \mid - \mid F_c \mid \mid / \Sigma \mid F_o \mid$

$wR2 = [\Sigma [w (F_o^2 - F_c^2)^2] / \Sigma [w (F_o^2)^2]]^{1/2}$

Goodness-of-fit = $[\Sigma [w (F_o^2 - F_c^2)^2] / (n-p)]^{1/2}$

n: number of independent reflections; p: number of refined parameters

Figure 3.7. ORTEP representation of **±114**.

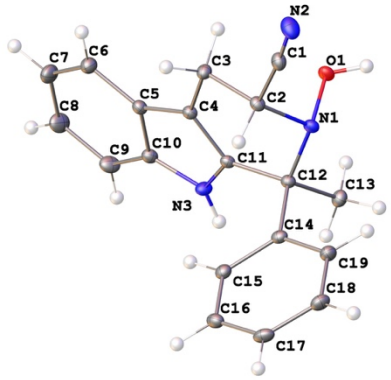

Crystal data and structure refinement for 0814_t.

Identification code	0814_t
Empirical formula	$C_{19}H_{17}N_3O$
Formula weight	303.35
Temperature/K	100(2)
Crystal system	monoclinic
Space group	$P2_1/c$
a/Å	8.5899(4)
b/Å	18.3551(8)
c/Å	10.2741(5)
α/°	90
β/°	102.416(2)
γ/°	90
Volume/Å^3	1582.02(13)
Z	4
ρ_{calc}g/cm^3	1.274
μ/mm^{-1}	0.081
F(000)	640.0
Crystal size/mm^3	0.426 × 0.202 × 0.106
Radiation	MoKα (λ = 0.71073)
2Θ range for data collection/°	4.438 to 61.224
Index ranges	$-12 \leq h \leq 12$, $-26 \leq k \leq 25$, $-14 \leq l \leq 14$
Reflections collected	43653
Independent reflections	4749 [R_{int} = 0.0455, R_{sigma} = 0.0375]
Data/restraints/parameters	4749/2/217
Goodness-of-fit on F^2	1.044
Final R indexes [I>=2σ (I)]	R_1 = 0.0477, wR_2 = 0.1095
Final R indexes [all data]	R_1 = 0.0730, wR_2 = 0.1192
Largest diff. peak/hole / e Å^{-3}	0.39/-0.21

$R_{int} = \Sigma \mid F_o^2 - \langle F_o^2 \rangle \mid / \Sigma \mid F_o^2 \mid$

$R1 = \Sigma \mid \mid F_o \mid - \mid F_c \mid \mid / \Sigma \mid F_o \mid$

$wR2 = [\Sigma [w (F_o^2 - F_c^2)^2] / \Sigma [w (F_o^2)^2]]^{1/2}$

Goodness-of-fit = $[\Sigma [w (F_o^2 - F_c^2)^2] / (n-p)]^{1/2}$

n: number of independent reflections; p: number of refined parameters

Figure 3.8. ORTEP representation of **±115a**.

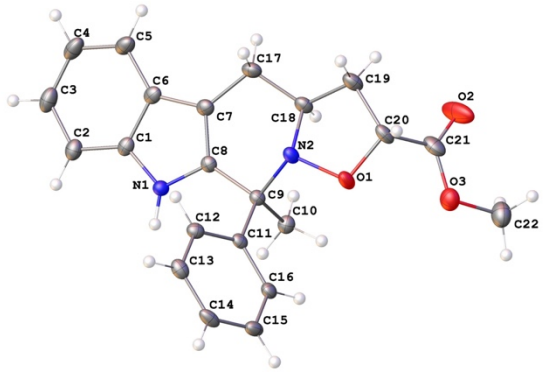

Crystal data and structure refinement for 0869_tessa_top.

Identification code	0869_tessa_top
Empirical formula	$C_{22}H_{22.3}N_2O_{3.15}$
Formula weight	365.12
Temperature/K	100(2)
Crystal system	monoclinic
Space group	$P2_1/c$
a/Å	20.9936(14)
b/Å	10.3069(7)
c/Å	17.3090(11)
α/°	90
β/°	99.457(2)
γ/°	90
Volume/Å^3	3694.4(4)
Z	8
ρ_{calc}g/cm^3	1.313
μ/mm^{-1}	0.088
F(000)	1548.0
Crystal size/mm^3	0.22 × 0.16 × 0.12
Radiation	MoKα (λ = 0.71073)
2Θ range for data collection/°	4.414 to 52.836
Index ranges	-26 ≤ h ≤ 26, -12 ≤ k ≤ 12, -21 ≤ l ≤ 20
Reflections collected	96894
Independent reflections	7298 [R_{int} = 0.0519, R_{sigma} = 0.0343]
Data/restraints/parameters	7298/2/504
Goodness-of-fit on F^2	1.053
Final R indexes [I>=2σ (I)]	R_1 = 0.0464, wR_2 = 0.0956
Final R indexes [all data]	R_1 = 0.0758, wR_2 = 0.1049
Largest diff. peak/hole / e Å^{-3}	0.30/-0.37

$R_{int} = \Sigma \mid F_o^2 - \langle F_o^2 \rangle \mid / \Sigma \mid F_o^2 \mid$

$R1 = \Sigma \mid \mid F_o \mid - \mid F_c \mid \mid / \Sigma \mid F_o \mid$

$wR2 = [\Sigma [w (F_o^2 - F_c^2)^2] / \Sigma [w (F_o^2)^2]]^{1/2}$

Goodness-of-fit = $[\Sigma [w (F_o^2 - F_c^2)^2] / (n-p)]^{1/2}$

n: number of independent reflections; p: number of refined parameters

Figure 3.9. ORTEP representation of **±115b**.

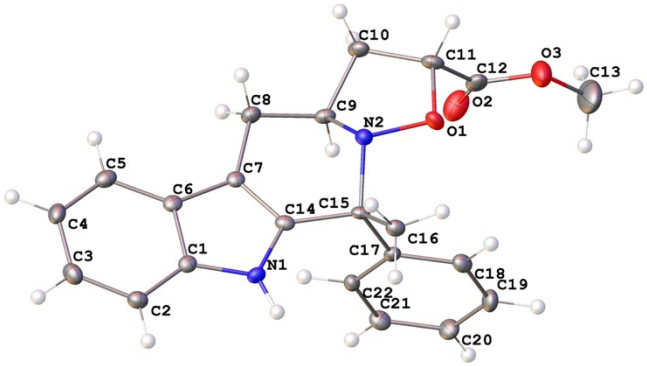

Crystal data and structure refinement for 0872_tes_btm.

Identification code	0872_tes_btm
Empirical formula	$C_{44.5}H_{45}ClN_4O_6$
Formula weight	767.29
Temperature/K	100(2)
Crystal system	triclinic
Space group	P-1
a/Å	12.3351(7)
b/Å	13.1435(7)
c/Å	13.7758(7)
α/°	93.491(2)
β/°	101.268(2)
γ/°	116.875(2)
Volume/Å^3	1925.16(18)
Z	2
ρ_{calc}g/cm^3	1.324
μ/mm^{-1}	0.155
F(000)	810.0
Crystal size/mm^3	0.32 × 0.19 × 0.14
Radiation	MoKα (λ = 0.71073)
2Θ range for data collection/°	4.256 to 52.882
Index ranges	-15 ≤ h ≤ 14, -16 ≤ k ≤ 16, 0 ≤ l ≤ 17
Reflections collected	7910
Independent reflections	7910 [R_{int} = 0.0610, R_{sigma} = 0.0562]
Data/restraints/parameters	7910/3/522
Goodness-of-fit on F^2	1.090
Final R indexes [I>=2σ (I)]	R_1 = 0.0559, wR_2 = 0.1025
Final R indexes [all data]	R_1 = 0.0856, wR_2 = 0.1125
Largest diff. peak/hole / e Å^{-3}	0.36/-0.59

$R_{int} = \Sigma \mid F_o^2 - \langle F_o^2 \rangle \mid / \Sigma \mid F_o^2 \mid$

$R1 = \Sigma \mid \mid F_o \mid - \mid F_c \mid \mid / \Sigma \mid F_o \mid$

$wR2 = [\Sigma [w (F_o^2 - F_c^2)^2] / \Sigma [w (F_o^2)^2]]^{1/2}$

Goodness-of-fit = $[\Sigma [w (F_o^2 - F_c^2)^2] / (n-p)]^{1/2}$

n: number of independent reflections; p: number of refined parameters

CHAPTER 4

DEVELOPMENT OF ASYMMETRIC ISO-PICTET–SPENGLER REACTIONS OF KETONITRONES TO GENERATE AZA-QUATERNARY CENTERS

4.1 Introduction

The indole core is an important structural motif found in an array of bioactive natural products, agrochemicals, and pharmaceuticals.[1] Indeed, this privileged scaffold has attracted the attention of medicinal and organic chemists alike due to its prevalence in modern drug discovery and alkaloid total synthesis. Despite this, the majority of methods currently available tend to focus on a select subset of indole skeletons. As discussed in Chapter 3, tetrahydro-β-carbolines (**1**, Figure 4.1) have been exhaustively investigated and a multitude of methods for their synthesis have been disclosed,[2] with the Pictet–Spengler reaction being arguably the most powerful.[3,4] However, there are only a limited number of Pictet–Spengler-type reactions reported that synthesize other related indole congeners,[5] such as tetrahydro-γ-carbolines (**2**),[6] tetrahydropyrazino[1,2-*a*]indoles (**3**),[7] and tetrahydropyrrolo[4,3,2-*de*]isoquinolines (**4**),[8] which have diverse therapeutic potentials.

Figure 4.1. Selected indole analogs of interest.

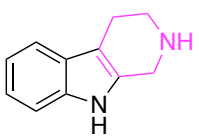

1: tetrahydro-β-carboline

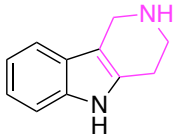

2: tetrahydro-γ-carboline

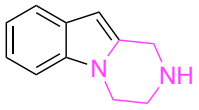

3: tetrahydropyrazino[1,2-*a*]indole

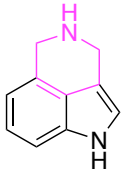

4: tetrahydropyrrolo[4,3,2-*de*]isoquinoline

The term "iso-Pictet–Spengler reaction" was coined by Jacobsen in 2011, when he reported the first enantioselective method to access tetrahydro-γ-carbolines (**8**, Scheme 4.1).[6d] They applied chiral thiourea **7** and BzOH as a highly effective cocatalyst system to enable one-pot reactions of isotryptamines (**5**) with various aldehydes (**6**) and Boc_2O, leading to products (61-92% *ee*) with extremely high enantioselectivities after trituration or recrystallization (>98% *ee*). Nonetheless,

the yields of the methodology greatly suffered from the trituration or recrystallization process and the synthesis of the isotryptamine starting material was not simple (4 steps). Additionally, there was only one successful example incorporating a ketone (4′-chloroacetophenone) that required prolonged reaction times (14 days) to obtain the product in a 76% *ee*, though the enantiomeric excess could be increased to 98% *ee* after trituration at the expense of yield (95% to 53%). The following year, Leighton and co-workers published two highly enantioselective, one-pot iso-Pictet–Spengler reactions to construct compounds of type **13** and **14**.[7e] Nevertheless, this protocol required superstoichiometric quantities of a chiral silicon Lewis acid (**12**) to promote the cyclization and was only compatible with α-ketoamides, limiting the substrate scope of the reaction. Since these seminal works, numerous other groups have taken interest in iso-Pictet–Spengler reactions, but efficient methods to access aza-quaternary centers are still needed.[5-8]

Scheme 4.1. Key precedents for Iso-Pictet–Spengler reactions developed by the (a) Jacobsen group and (b) Leighton group.

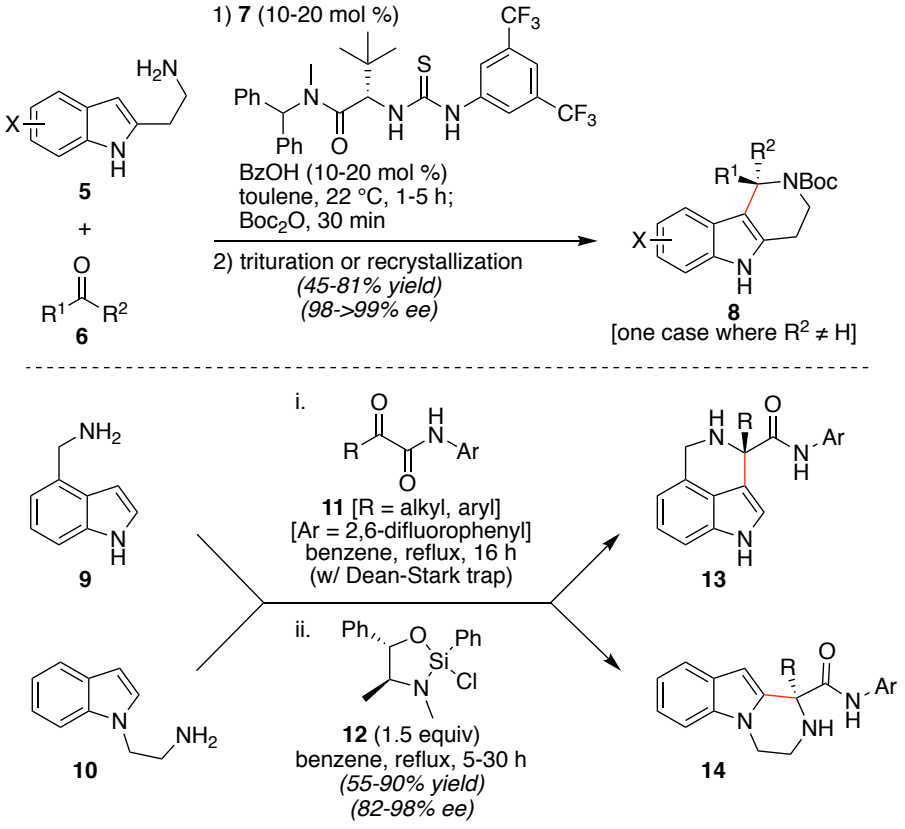

Inspired by our recent work utilizing nitrones in Mannich-type reactions (Chapter 2)[9] and Pictet–Spengler reactions (Chapter 3),[10] we envisioned that such substrates might also be effective for establishing novel iso-Pictet–Spengler reactions to forge indole analogs **2**-**4** bearing aza-quaternary centers. Herein, we delineate our current progress on the development of three unique approaches using ketonitrones to access tetrahydro-γ-carbolines (**2**), tetrahydropyrazino[1,2-*a*]indoles (**3**), and tetrahydropyrrolo[4,3,2-*de*]isoquinolines (**4**), with the former two exhibiting promising results employing organocatalysis to induce enantiocontrol. Although the scope of the reactions has yet to be explored, we believe that, once optimized, these procedures can be applied to build a diverse collection of heterocyclic products that can be screened for biological activities.

4.2 Starting Material Preparation

To begin, we employed a 3-step route that was previously developed for our ketonitrone-based Pictet–Spengler reaction to obtain the relevant starting materials.[10] The three alkyl alcohols (**15**), attached at the *N*-, C2-, or C4-atom of the indole ring, were either commercially available or known compounds easily synthesized in 1 step. As shown in Scheme 4.2, alcohol **15** smoothly underwent a Mitsunobu reaction with *N*,*O*-Di-Boc-hydroxylamine,[11] followed by a facile Boc-deprotection to afford hydroxylamine **16**,[12] and finally condensation of the requisite ketone (**6**) to form the desired ketonitrone (**17**, *N*- and C4-subsituted indoles only).[13] Due to the varying electronics of the proposed iso-Pictet–Spengler reactions, we considered multiple organocatalytic systems[14] to see which could provide the highest level of conversion and enantioselection.

Scheme 4.2. Preparation of ketonitrones for subsequent methods.

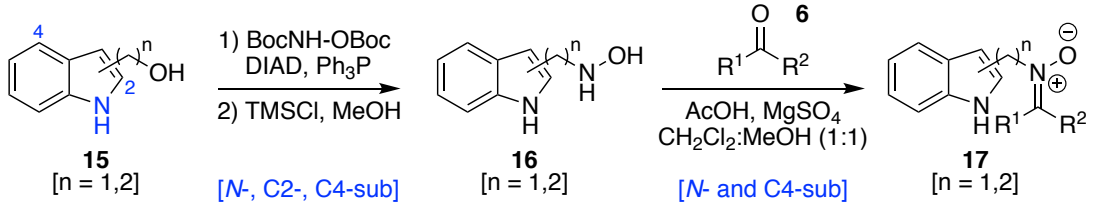

4.3 Investigation into the Synthesis of Tetrahydro-γ-Carboline Derivatives

With the required starting materials in hand, we decided to investigate the C2-iso-Pictet–Spengler reaction first. Interestingly, when we attempted to condense acetophenone (**19**) onto hydroxylamine **20**, instead of isolating the predicted ketonitrone (**18**), tetrahydro-γ-carboline **21** was obtained exclusively in quantitative yield (Scheme 4.3). Even with shortened reaction times or a change in solvent to CH_2Cl_2 alone, the ketonitrone continued to rapidly undergo cyclization to **21** without the need for additional promoters beyond the catalytic AcOH (>80% yield). Traditional iso-Pictet–Spengler reactions applying imines usually require strong acid and/or high temperatures to affect the formation of aza-quaternary centers,[6] demonstrating how this approach can provide a more mild, complementary way to access compounds of this type. We plan to study the scope of this highly efficient one-pot, racemic protocol to construct other tetrahydro-γ-carbolines with aza-quaternary centers in the future.

Scheme 4.3. Initial discovery of a racemic synthesis of tetrahydro-γ-carbolines.

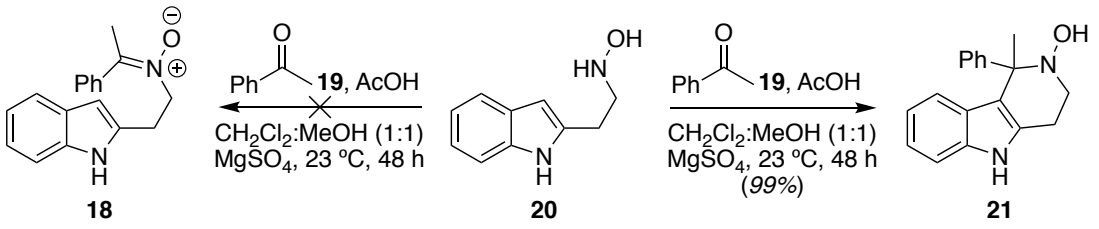

Encouraged by these results and the literature precedents discussed earlier, we then examined if chiral thiourea catalysis[15] could promote an enantioselective variant of the one-pot conversion of **20** to **21**. Unfortunately, all endeavors to exploit the same thiourea reported by Jacobsen and co-workers (**7**)[6d] only yielded a racemic product (Table 4.1, entry 1). Motivated by reports of chiral phosphoric acids being proficient organocatalyts,[16] especially in traditional Pictet–Spengler reactions, we anticipated that they may prove efficacious in our system as well.

Pleasingly, after screening an assortment of phosphoric acids, **22e** was able to catalyze the desired condensation with **19** and subsequent cyclization to **21** in a moderate 56% *ee* (entry 6). Efforts to improve the enantioselectivity by lowering the temperature were fruitless, as the reaction was completely shut down below 5 °C. Due to the demonstrated improvements in reactivity and scope with more acidic chiral Brønsted acids in other reactions,[17] our next focus will be to synthesize and test phosphoramidic acid and imidodiphosphorimidate derivatives of **22e** in hopes of enhancing the modest enantioselectivity currently observed.

Table 4.1. Exploration of thiourea and phosphoric acid catalysts to promote enantioselection.

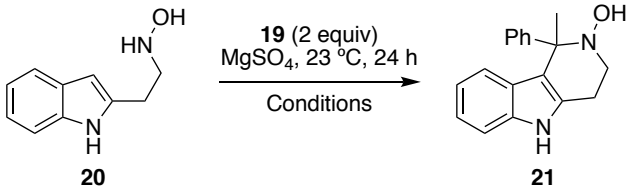

20 **21**

Entry	Solvent	Concentration (M)	Catalyst (20 mol %)	*ee* (%)
1	CH_2Cl_2 or toluene	0.10	**7**, AcOH	racemic
2	toluene	0.05	**22a**	2
3	toluene	0.05	**22b**	5
4	toluene	0.05	**22c**	18
5	toluene	0.05	**22d**	20
6	toluene	0.05	**22e**	56
7	toluene	0.05	**22f**	N/A

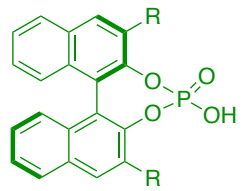

22a: R = Ph
22b: R = 2-naphthyl
22c: R = 3,5-$(CF_3)_2C_6H_3$
22d: R = 2,4,6-$(Me)_3C_6H_2$
22e: R = 2,4,6-$(i\text{-}Pr)_3C_6H_2$
22f: R = $SiPh_3$

4.4 Study of the Tetrahydropyrazino[1,2-a]indole Scaffold

We next embarked on the study of *N*-iso-Pictet–Spengler reactions of ketonitrones to produce tetrahydropyrazino[1,2-*a*]indoles. Initial inquiries quickly showed that phosphoric acids or chiral thiourea and carboxylic acid cocatalyst systems were not effective at promoting the desired cyclization. Therefore, we opted to employ the same tactic used in our previous Pictet–Spengler reaction, which is to increase the reactivity of the ketonitrone via formation of an *N*-

acyloxyiminium species *in situ*.[18] To our delight, this method proved capable of delivering tetrahydropyrazino[1,2-*a*]indole **24**, albeit in only a 30-40% yield depending if BzCl or BzBr was utilized (Scheme 4.4). As presented in Table 4.2, a collection of chiral thiourea catalysts was screened in combination with BzCl to see if enantiocontrol was possible within this system. While most catalysts tested thus far have provided only low enantioselectivity (0-34% *ee*), there have been some general trends detected. For example, catalysts containing a 2,5-substituted pyrrole group (**28** and **29**) afforded the lowest conversions and very little enantiocontrol when the product could be isolated. Although varying the chiral backbone of the catalysts led to higher conversion, it did not provide any dramatic increase in the enantioselectivity of **24**. Nonetheless, an interesting observation was made when the thiourea functional group of the catalyst was changed to a urea; this switch (**35** to **36**) led to a complete reversal in enantioselectivity (14% *ee* to –17% *ee*). To confirm this result, we then probed catalysts **37** and **38**, and again noted equal but opposite enantioselectivities (34% *ee* and –31% *ee*). These aryl pyrrolidinoamido-thiourea and -urea represent our best results to date. Disappointingly, any attempts for optimization have been unsuccessful; lowering the temperature, changing the solvent, diluting the reaction, or switching BzCl to BzBr did not impact the enantioselectivity of the reaction. Our next steps are to synthesize additional aryl pyrrolidinoamido-thioureas, with a focus on bulky aryl groups that have proven advantageous in other reactions due to their ability to stabilize cation-π interactions.[19]

Scheme 4.4. Preliminary results for the racemic formation of **24**.

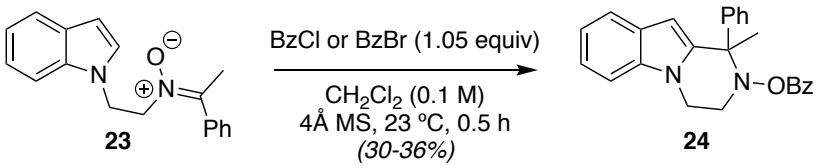

23 **24**

Table 4.2. Exploration of varied catalysts to achieve asymmetric cyclization of nitrone **23** using BzCl.

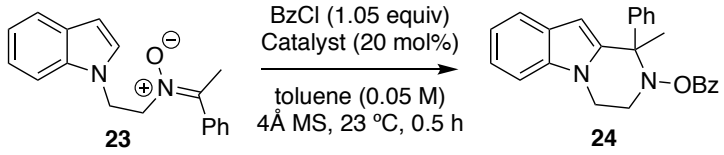

23 **24**

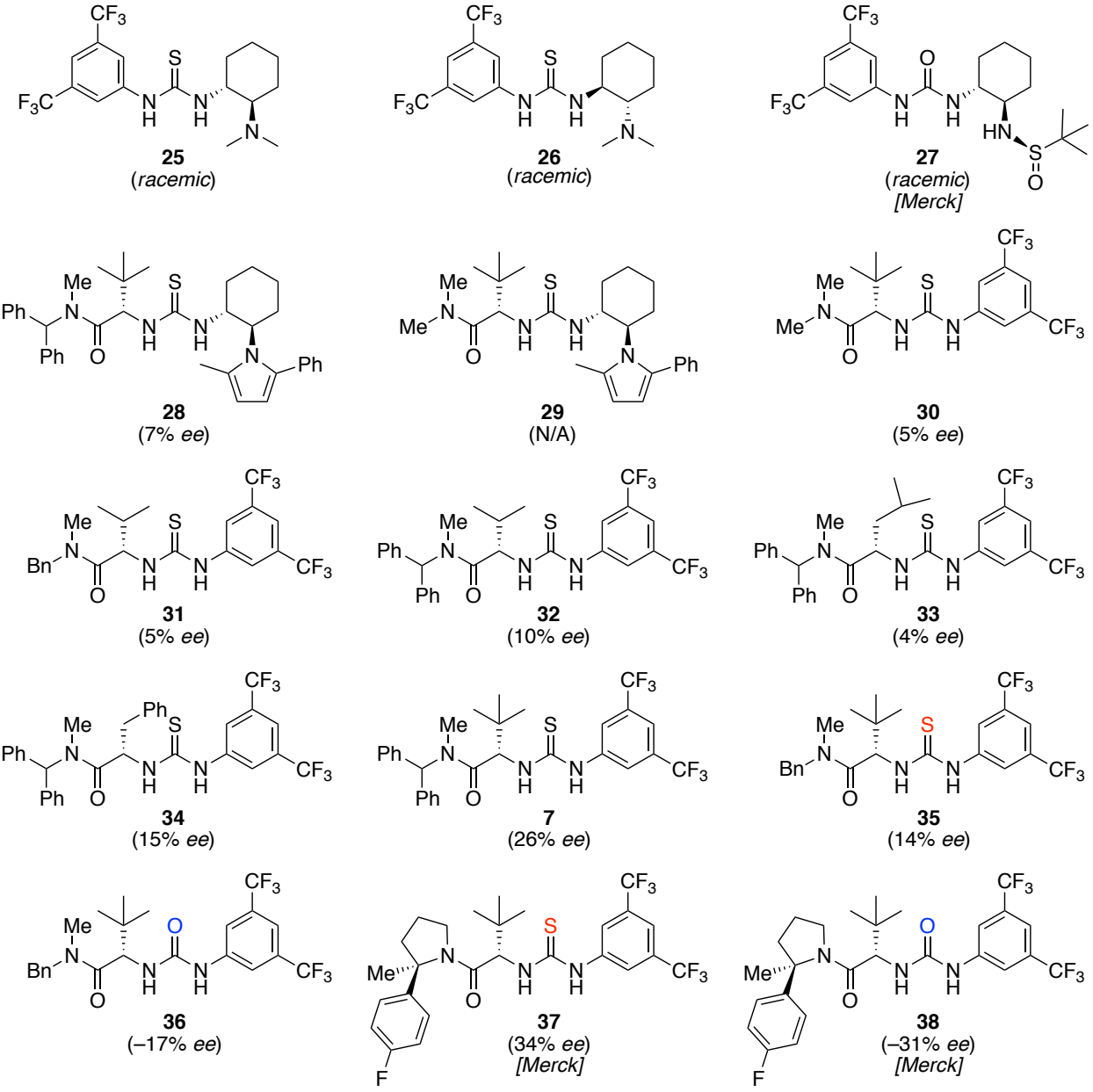

4.5 Exploration of the Tetrahydropyrrolo[4,3,2-de]isoquinoline System

The final scaffold of interest was the tetrahydropyrrolo[4,3,2-*de*]isoquinoline, which we envisioned could be built by a C4-iso-Pictet–Spengler reaction of nitrones. We began our

explorations by trying to affect a racemic reaction using acetophenone-derived ketonitrone **39** as our model substrate (Scheme 4.5). Gratifyingly, **39** could be transformed into the corresponding, more reactive *N*-acyloxyiminium ion using BzBr and subsequently cyclized to **40** in CH_2Cl_2 after only 30 minutes at 23 ºC. Notwithstanding this, a major side-product (**41**) was readily formed via hydrolysis of the *N*-acyloxyiminium species. Moving forward without optimizing this result further, we attempted to render the reaction asymmetric. Yet, all catalytic systems evaluated (thioureas/*N*-acyloxyiminium ion, thioureas/carboxylic acids, or phosphoric acids) were unsuccessful at providing any significant enantiocontrol. Due to what appears to be less favorable electronics for this iso-Pictet–Spengler reaction, we plan to optimize and report a racemic variant that can still provide synthetic value and access to new chemical space.

Scheme 4.5. Racemic reaction of **39** rendered competent by *N*-acyloxyiminium species.

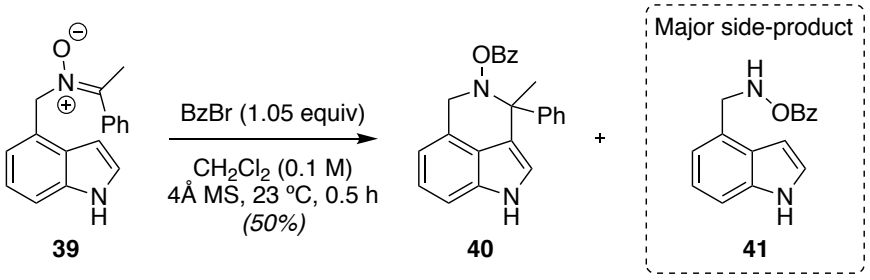

4.6 Conclusion

In conclusion, we have commenced explorations of three variations of iso-Pictet–Spengler reactions of ketonitrones to efficiently generate indole heterocycles with aza-quaternary centers. To achieve this, we are utilizing the power of organocatalysis in combination with the unique reactivity of nitrones. Thus far, we have had moderate success developing catalytic, enantioselective procedures employing phosphoric acids for the tetrahydro-γ-carboline derivatives and using thioureas in combination with *N*-acyloxyiminium species for the tetrahydropyrazino[1,2-*a*]indole scaffolds. Although not optimized, these preliminary findings are

encouraging for the validity of our proposal. Unfortunately, no significant enantiocontrol has been observed for the tetrahydropyrrolo[4,3,2-*de*]isoquinoline system. Investigations to increase the both the enantioselectivities of the reactions and the substrate scope are the subject of current endeavors.

4.7 Experimental Section

General Procedures. All reactions were carried out under an argon atmosphere with dry solvents under anhydrous conditions, unless otherwise noted. Dry tetrahydrofuran (THF), toluene, acetonitrile (MeCN), and dichloromethane (CH_2Cl_2) were obtained by passing commercially available pre-dried, oxygen-free formulations through activated alumina columns. Yields refer to chromatographically and spectroscopically (^1H and ^{13}C NMR) homogeneous materials, unless otherwise stated. Reagents were purchased at the highest commercial quality and used without further purification, unless otherwise stated. Reactions were magnetically stirred and monitored by thin-layer chromatography (TLC) carried out on 0.25 mm E. Merck silica gel plates (60F-254) using UV light as visualizing agent, and an aqueous solution of ceric ammonium sulfate, ammonium molybdate, and sulfuric acid or aqueous solution of potassium permanganate and sodium bicarbonate and heat as a developing agent. SiliCycle silica gel (60, academic grade, particle size 0.040–0.063 mm) was used for flash column chromatography. Preparative thin-layer chromatography separations were carried out on 0.50 mm E. Merck silica gel plates (60F-254). NMR spectra were recorded on Bruker 400 and 500 MHz instruments and calibrated using residual undeuterated solvent as an internal reference. The following abbreviations were used to explain the multiplicities: s = singlet, d = doublet, t = triplet, q = quartet, br = broad, m = multiplet. IR spectra were recorded on a Nicolet iS5 FT-IR spectrometer using neat thin film technique. High-resolution mass spectra (HRMS) were recorded on Agilent 6244 TOF-MS using ESI (Electrospray Ionization) or CI (Chemical Ionization) at the University of Chicago Mass Spectroscopy Core Facility. Chiral high-performance liquid chromatography (HPLC) analysis was performed using a Shimadzu Prominence analytical chromatograph with commercial ChiralPak columns (OD-H).

The X-ray diffraction data were measured on a Bruker D8 VENTURE diffractometer at the University of Chicago X-ray Laboratory.

General Procedure for Preparation of Hydroxylamines.[11,12]

Scheme 4.6. Preparation of hydroxylamines.

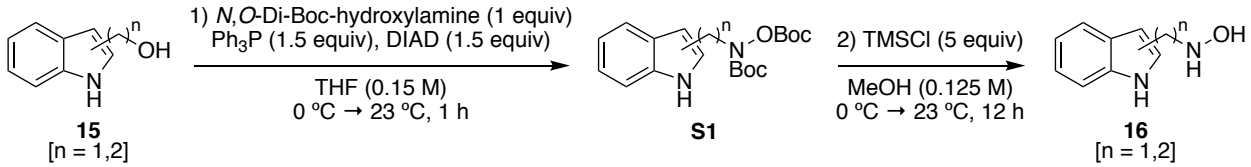

Step 1: To a solution of alcohol **15** (1.0 equiv), Ph_3P (1.5 equiv), *N*,*O*-Di-Boc-hydroxylamine (1.0 equiv) in THF (0.15 M) at 0 ºC was added DIAD (1.5 equiv) dropwise under an argon atmosphere. The resultant mixture was warmed to 23 ºC and stirred for 1 h. Upon completion, MeOH (10.0 equiv) was added and the reaction was stirred for 15 min. The reaction contents were then concentrated directly and the resultant crude material was purified by flash column chromatography (silica gel, hexanes/EtOAc = 1/0→2/1) to yield **S1**. *Step 2:* Next, to a solution of the newly-formed **S1** (1.0 equiv) in MeOH (0.125 M) at 0 ºC was added TMSCl (5.0 equiv) dropwise under an argon atmosphere. The resultant mixture was slowly warmed to 23 ºC and stirred for 12 h. Upon completion, the reaction contents were concentrated directly and then diluted with CH_2Cl_2:MeOH (9:1). Saturated aqueous Na_2CO_3 was added, the contents were poured into a separatory funnel, and then the product was extracted with CH_2Cl_2 (3 ×). The combined organic extracts were then dried (Na_2SO_4), filtered, and concentrated. The resultant crude material was purified either by flash column chromatography (silica gel, CH_2Cl_2/MeOH = 1/0→9/1) or recrystallization (CH_2Cl_2) to afford **16**.

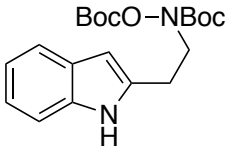

S2

***tert*-butyl (2-(1*H*-indol-2-yl)ethyl)((*tert*-butoxycarbonyl)oxy)carbamate (S2).** Prepared using the general procedure described above with 2-(1*H*-indol-2-yl)ethan-1-ol[20] (1.84 g, 11.41 mmol), ultimately yielding **S2** (3.74 g, 87% yield) as a white solid. **S2**: R_f = 0.50 (silica gel, hexanes/EtOAc = 4/1); IR (film) ν_{max} 3390, 3057, 2981, 2934, 1785, 1715, 1370, 1252, 1148, 749 cm^{-1}; ^1H NMR (400 MHz, $CDCl_3$) δ 9.11 (br s, 1 H, exchangeable), 7.53 (d, *J* = 7.7 Hz, 1 H), 7.34 (d, *J* = 7.9 Hz, 1 H), 7.15–7.09 (m, 1 H), 7.08–7.02 (m, 1 H), 6.29–6.24 (m, 1 H), 3.89 (t, *J* = 6.2 Hz, 2 H), 3.02 (t, *J* = 6.1 Hz, 2 H), 1.56 (s, 9 H), 1.37 (s, 9 H); ^{13}C NMR (101 MHz, $CDCl_3$) δ 155.0, 153.3, 136.7, 136.4, 128.5, 121.1, 119.9, 119.4, 110.9, 100.3, 85.6, 83.1, 50.9, 28.0, 27.7, 26.3; HRMS (ESI) calcd for $C_{20}H_{29}N_2O_5^+$ $[M + H]^+$ 377.2071, found 377.2073.

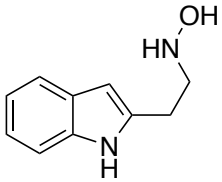

20

***N*-(2-(1*H*-indol-2-yl)ethyl)hydroxylamine (20).** Prepared using the general procedure described above with **S2** (3.74 g, 9.94 mmol), ultimately yielding **20** (1.40 g, 80% yield) as a pale-yellow solid. **20**: R_f = 0.43 (silica gel, CH_2Cl_2/MeOH = 9/1); IR (film) ν_{max} 3274, 2925, 1549, 1457, 1341, 1291, 1048, 855, 785, 749 cm^{-1}; ^1H NMR (400 MHz, DMSO) δ 10.87 (br s, 1 H, exchangeable), 7.41 (d, *J* = 8.7 Hz, 1 H), 7.32 (br s, 1 H, exchangeable), 7.29 (d, *J* = 7.9 Hz, 1 H), 7.03–6.97 (m, 1 H), 6.96–6.89 (m, 1 H), 6.20–6.12 (m, 1 H), 5.73 (br s, 1 H, exchangeable), 3.09 (t, *J* = 7.3 Hz, 2 H), 2.91 (t, *J* = 7.4 Hz, 2 H); ^{13}C NMR (101 MHz, DMSO) δ 138.4, 136.0, 128.4, 120.0, 119.1, 118.6, 110.6, 98.6, 53.2, 26.1; HRMS (CI) calcd for $C_{10}H_{13}N_2O^+$ $[M + H]^+$ 177.1022, found 177.1022.

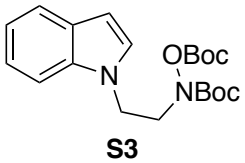

S3

***tert*-butyl (2-(1*H*-indol-1-yl)ethyl)((*tert*-butoxycarbonyl)oxy)carbamate (S3).** Prepared using the general procedure described above with 2-(1*H*-indol-1-yl)ethan-1-ol[21] (2.00 g, 12.41 mmol), ultimately yielding **S3** (4.41 g, 94% yield) as a pale-yellow oil. **S3**: R_f = 0.55 (silica gel, hexanes/EtOAc = 4/1); IR (film) ν_{max}

2981, 2934, 1785, 1727, 1478, 1370, 1239, 1151, 1109, 741 cm^{-1}; ^1H NMR (400 MHz, $CDCl_3$) δ 7.62 (d, *J* = 7.9 Hz, 1 H), 7.37 (d, *J* = 8.2 Hz, 1 H), 7.24–7.18 (m, 1 H), 7.15 (d, *J* = 3.1 Hz, 1 H), 7.13–7.07 (m, 1 H), 6.51–6.47 (m, 1 H), 4.37 (t, *J* = 6.4 Hz, 2 H), 3.97 (t, 2 H), 1.54 (s, 9 H), 1.27 (s, 9 H); ^{13}C NMR (101 MHz, $CDCl_3$) δ 154.2, 152.3, 136.0, 128.9, 128.3, 121.8, 121.1, 119.6, 109.2, 101.8, 85.4, 82.8, 50.1, 43.7, 27.9, 27.7; HRMS (ESI) calcd for $C_{20}H_{29}N_2O_5^+$ $[M + H]^+$ 377.2071, found 377.2071.

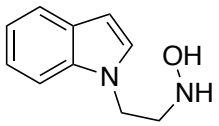

S4

***N*-(2-(1*H*-indol-1-yl)ethyl)hydroxylamine (S4).** Prepared using the general procedure described above with **S3** (4.26 g, 11.32 mmol), ultimately yielding **S4** (1.31 g, 66% yield) as a yellow oil. **S4**: R_f = 0.53 (silica gel, CH_2Cl_2/MeOH = 9/1); IR (film) ν_{max} 3259, 2928, 1512, 1464, 1315, 1251, 1195, 1014, 883, 742 cm^{-1}; ^1H NMR (500 MHz, $CDCl_3$) δ 7.65 (d, *J* = 7.9 Hz, 1 H), 7.40 (d, *J* = 8.2 Hz, 1 H), 7.25–7.20 (m, 1 H), 7.15 (d, *J* = 3.1 Hz, 1 H), 7.14–7.10 (m, 1 H), 6.56–6.51 (m, 1 H), 4.38 (t, *J* = 5.8 Hz, 2 H), 3.29 (t, *J* = 6.1, 5.7 Hz, 2 H); ^{13}C NMR (101 MHz, $CDCl_3$) δ 136.2, 128.8, 128.3, 121.8, 121.2, 119.6, 109.3, 101.8, 53.1, 43.0; HRMS (ESI) calcd for $C_{10}H_{13}N_2O^+$ $[M + H]^+$ 177.1022, found 177.1022.

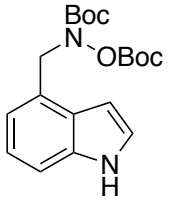

S5

***tert*-butyl ((1*H*-indol-4-yl)methyl)((*tert*-butoxycarbonyl)oxy)carbamate (S5).** Prepared using the general procedure described above with (1*H*-indol-4-yl)methanol (1.00 g, 6.80 mmol), ultimately yielding **S5** (1.16 g, 47% yield) as a white solid. **S5**: R_f = 0.33 (silica gel, hexanes/EtOAc = 4/1); IR (film) ν_{max} 3370, 3058, 2981, 2934, 1779, 1713, 1370, 1275, 1148, 754 cm^{-1}; ^1H NMR (400 MHz, $CDCl_3$) δ 8.24 (br s, 1 H, exchangeable), 7.34 (d, *J* = 7.9 Hz, 1 H), 7.23–7.19 (m, 1 H), 7.17–7.08 (m, 2 H), 6.70–6.63 (m, 1 H), 5.07 (s, 2 H), 1.50 (s, 9 H), 1.39 (s, 9 H); ^{13}C NMR (101 MHz, $CDCl_3$) δ 154.9, 152.3, 136.0, 127.2, 127.1, 124.5, 121.8, 119.7, 111.0, 100.7, 84.7, 82.5, 52.2, 28.3, 27.5; HRMS (CI) calcd for $C_{19}H_{27}N_2O_5^+$ $[M + H]^+$ 363.1914, found 363.1908.

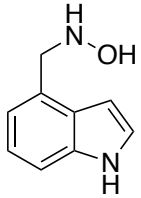

S6

***N*-((1*H*-indol-4-yl)methyl)hydroxylamine (S6).** Prepared using the general procedure described above with **S5** (0.39 g, 1.08 mmol), ultimately yielding **S6** (0.072 g, 41% yield) as a yellow solid. **S6**: R_f = 0.47 (silica gel, CH_2Cl_2/MeOH = 9/1); IR (film) ν_{max} 3406, 2923, 1502, 1415, 1343, 1282, 1101, 940, 897, 753 cm^{-1}; ^1H NMR (400 MHz, DMSO) δ 11.05 (br s, 1 H, exchangeable), 7.43–7.24 (m, 3 H), 7.08–6.97 (m, 2 H), 6.59–6.48 (m, 1 H), 5.85 (br s, 1 H, exchangeable), 4.16 (s, 2 H); ^{13}C NMR (101 MHz, DMSO) δ 135.8, 129.8, 127.2, 124.7, 120.7, 118.7, 110.1, 99.6, 55.8; HRMS (ESI) calcd for $C_9H_{11}N_2O^+$ [M + H]$^+$ 163.0866, found 163.0856.

General Procedure for Preparation of Nitrones.[13]

To a solution of hydroxylamine **16** (1.0 equiv) in CH_2Cl_2/MeOH (1/1, 0.15 M) at 23 ºC was added acetophenone (5.0 equiv), AcOH (~5 drops, from a syringe fitted with 3" needle), and $MgSO_4$ (3.0 equiv) under an argon atmosphere. The resultant mixture was stirred for 12 h at 23 ºC. Upon completion, the contents were quenched at 23 ºC with saturated aqueous $NaHCO_3$, poured into a separatory funnel, and extracted with CH_2Cl_2 (3 ×). The combined organic extracts were then dried (Na_2SO_4), filtered, and concentrated. The resultant crude material was purified by flash column chromatography (silica gel, CH_2Cl_2/MeOH = 1/0→9/1) to yield nitrone **23** and **39**. *Note:* The ratio of mixed *E-/Z-* isomers can vary depending on conditions (time, temperature, and equivalents). In addition, the *E-/Z-* ratio for each nitrone was determined by NOESY experiments.

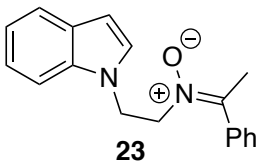

23

(*E*)-*N*-(2-(1*H*-indol-1-yl)ethyl)-1-phenylethan-1-imine oxide (23). Prepared using the general procedure described above with **S4** (0.95 g, 0.54 mmol) ultimately yielding **23** (0.133 g, 89% yield) as a yellow oil. **23**: R_f =

0.60 (silica gel, CH_2Cl_2/MeOH = 9/1); IR (film) ν_{max} 3054, 2945, 1579, 1464, 1314, 1220, 1178, 1072, 743, 701 cm^{-1}; ^1H NMR (400 MHz, $CDCl_3$) δ 7.65–7.62 (m, 1 H), 7.15–7.08 (m, 4 H), 7.04 (d, *J* = 3.1 Hz, 1 H), 6.97–6.92 (m, 2 H), 6.51–6.46 (m, 1 H), 6.23–6.17 (m, 2 H), 4.68 (t, *J* = 5.5, 4.8 Hz, 2 H), 4.08 (t, *J* = 5.3 Hz, 2 H), 2.26 (s, 3 H); ^{13}C NMR (101 MHz, $CDCl_3$) δ 150.5, 136.1, 135.3, 128.8, 128.8, 128.6, 128.3, 126.9, 121.9, 121.0, 119.8, 109.1, 101.9, 59.0, 43.5, 20.8; HRMS (ESI) calcd for $C_{18}H_{19}N_2O^+$ $[M + H]^+$ 279.1492, found 279.1497.

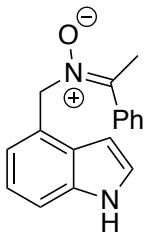

39

(*E*)-*N*-((1*H*-indol-4-yl)methyl)-1-phenylethan-1-imine oxide (39). Prepared using the general procedure described above with **S6** (0.70 g, 0.43 mmol) ultimately yielding **39** (0.100 g, 88% yield) as a pale-yellow solid. **39**: R_f = 0.53 (silica gel, CH_2Cl_2/MeOH = 9/1); IR (film) ν_{max} 3186, 2925, 2854, 1580, 1346, 1182, 1072, 897, 756, 699 cm^{-1}; ^1H NMR (400 MHz, $CDCl_3$) δ 8.40 (br s, 1 H, exchangeable), 7.40–7.36 (m, 3 H), 7.34–7.31 (m, 1 H), 7.29–7.26 (m, 2 H), 7.17–7.09 (m, 3 H), 6.36–6.31 (m, 1 H), 5.34 (s, 2 H), 2.51 (s, 3 H); ^{13}C NMR (101 MHz, $CDCl_3$) δ 148.3, 136.5, 136.1, 129.3, 129.1, 127.8, 126.7, 126.0, 124.7, 121.9, 119.6, 111.3, 100.4, 77.5, 76.8, 62.5, 21.0; HRMS (ESI) calcd for $C_{17}H_{17}N_2O^+$ $[M + H]^+$ 265.1335, found 265.1336.

Iso-Pictet–Spengler Reactions.

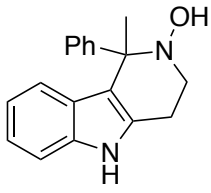

21

1-methyl-1-phenyl-1,3,4,5-tetrahydro-2*H*-pyrido[4,3-*b*]indol-2-ol (21). To a solution of hydroxylamine **20** (0.14 g, 0.79 mmol, 1.0 equiv) in CH_2Cl_2/MeOH (5.30 mL) at 23 ºC was added acetophenone (0.46 mL, 3.97 mmol, 5.0 equiv), AcOH (~5 drops, from a syringe fitted with 3" needle), and $MgSO_4$ (0.29 g, 2.38 mmol, 3.0 equiv) under an argon atmosphere. The resultant mixture was stirred for 48 h at 23

ºC. Upon completion, the contents were quenched at 23 ºC with saturated aqueous $NaHCO_3$ (5 mL), poured into a separatory funnel, and extracted with CH_2Cl_2 (3 × 5 mL). The combined organic extracts were then dried (Na_2SO_4), filtered, and concentrated. The resultant crude material was purified by flash column chromatography (silica gel, hexanes/EtOAc = 1/0→1/1) to yield **21** (0.22 g, quantitative yield) as a red solid. *Note:* These reactions must be run under strictly anhydrous conditions. **21**: R_f = 0.33 (silica gel, hexanes/EtOAc = 1/1); IR (film) ν_{max} 3400, 3056, 2982, 2940, 1460, 1328, 1265, 1025, 742, 701 cm^{-1}; ^1H NMR (400 MHz, DMSO) δ 10.86 (br s, 1 H, exchangeable), 7.76 (br s, 1 H, exchangeable), 7.39–7.26 (m, 3 H), 7.25–7.18 (m, 2 H), 7.18–7.13 (m, 1 H), 7.03–6.92 (m, 2 H), 6.83–6.75 (m, 1 H), 3.29–3.14 (m, 1 H), 3.08–2.90 (m, 2 H), 2.80–2.65 (m, 1 H), 1.85 (s, 3 H); ^{13}C NMR (101 MHz, DMSO) δ 136.1, 132.2, 127.8 (2 C), 127.3, 126.2, 126.1, 119.9, 118.6, 118.2, 113.1, 110.8, 64.6, 48.7, 23.5, 20.8; HRMS (CI) calcd for $C_{18}H_{19}N_2O^+$ $[M + H]^+$ 279.1492, found 279.1492.

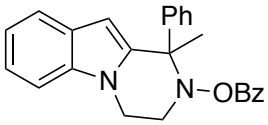

24

1-methyl-1-phenyl-3,4-dihydropyrazino[1,2-*a*]indol-2(1*H*)-yl benzoate (24). To a solution of nitrone **23** (0.045 g, 0.16 mmol, 1.0 equiv) in CH_2Cl_2 (1.6 mL) at 23 ºC was added molecular sieves (4Å, powder, ~90 mg), and the resultant slurry was stirred for 10 min under an argon atmosphere. Next, BzBr (0.020 mL, 0.17 mmol, 1.05 equiv) was added and the reaction mixture was stirred for 30 min at 23 ºC. Upon completion, the contents were quenched by the addition of saturated aqueous $NaHCO_3$ (5 mL), poured into a separatory funnel, and extracted with CH_2Cl_2 (3 × 5 mL). The combined organic extracts were then dried (Na_2SO_4), filtered, and concentrated. The resultant crude material was purified by flash column chromatography (silica gel, hexanes/EtOAc = 1/0→5/1) to yield **24** (0.022 g, 36% yield) as a pale-yellow oil. *Note:* This reaction must be run under strictly anhydrous

conditions to avoid hydrolysis of the *N*-acyloxyiminium species. **24**: R_f = 0.45 (silica gel, hexanes/EtOAc = 5/1); IR (film) ν_{max} 3058, 2990, 2927, 1746, 1450, 1247, 1082, 1051, 1024, 708 cm^{-1}; ^1H NMR (400 MHz, $CDCl_3$) δ 7.91–7.83 (m, 2 H), 7.72 (d, *J* = 6.8 Hz, 1 H), 7.56–7.50 (m, 1 H), 7.43–7.33 (m, 5 H), 7.30–7.21 (m, 5 H), 6.59 (s, 1 H), 4.29–4.19 (m, 1H), 4.10–4.00 (m, 1 H), 3.79–3.70 (m, 1 H), 3.63–3.53 (m, 1 H), 1.99 (s, 3 H); ^{13}C NMR (101 MHz, $CDCl_3$) δ 165.3, 144.8, 138.0, 137.1, 133.4, 129.7, 128.9, 128.7, 128.5, 128.1, 127.9, 127.3, 121.6, 120.7, 120.5, 109.4, 101.3, 66.8, 46.7, 37.3, 27.9; HRMS (CI) calcd for $C_{25}H_{23}N_2O_2^+$ $[M + H]^+$ 383.1754, found 383.1755.

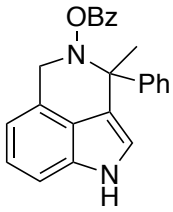

40

3-methyl-3-phenyl-1,5-dihydropyrrolo[4,3,2-*de*]isoquinolin-4(3*H*)-yl benzoate (40). To a solution of nitrone **39** (0.030 g, 0.076 mmol, 1.0 equiv) in CH_2Cl_2 (1.1 mL) at 23 ºC was added molecular sieves (4Å, powder, ~60 mg), and the resultant slurry was stirred for 10 min under an argon atmosphere. Next, BzBr (0.009 mL, 0.079 mmol, 1.05 equiv) was added and the reaction mixture was stirred for 30 min at 23 ºC. Upon completion, the contents were quenched by the addition of saturated aqueous $NaHCO_3$ (5 mL), poured into a separatory funnel, and extracted with CH_2Cl_2 (3 × 5 mL). The combined organic extracts were then dried (Na_2SO_4), filtered, and concentrated. The resultant crude material was purified by flash column chromatography (silica gel, hexanes/EtOAc = 1/0→3/1) to yield **40** (0.014 g, 50% yield) as a white solid. *Note:* This reaction must be run under strictly anhydrous conditions to avoid hydrolysis of the *N*-acyloxyiminium species. **40**: R_f = 0.18 (silica gel, hexanes/EtOAc = 5/1); IR (film) ν_{max} 3322, 3059, 2982, 2931, 1731, 1450, 1268, 1088, 1025, 707 cm^{-1}; ^1H NMR (400 MHz, $CDCl_3$) δ 8.23 (br s, 1 H, exchangeable), 7.76–7.62 (m, 2 H), 7.51–7.37 (m, 3 H), 7.33–7.26 (m, 4 H), 7.25–7.06 (m, 4 H), 6.86–6.74 (m, 1 H), 4.58–4.44 (m, 1 H), 4.37–

4.19 (m, 1 H), 1.95 (s, 3 H); ^{13}C NMR (101 MHz, $CDCl_3$) δ 165.8, 133.7, 132.9, 129.6, 128.4, 128.3, 128.0, 127.5, 126.5, 124.8, 123.3, 115.4, 109.2, 52.8, 29.8 (some carbons missing due to overlap); HRMS (ESI) calcd for $C_{24}H_{21}N_2O_2^+$ $[M + H]^+$ 369.1598, found 369.1598.

4.8 References

[1] (a) Kawasaki, T.; Higuchi, K. *Nat. Prod. Rep*. **2005**, *22*, 761; (b) Gul, W.; Hamann, M. T. *Life Sci*. **2005**, *78*, 442; (c) O'Connor, S. E.; Maresh, J. J. *Nat. Prod. Rep*. **2006**, *23*, 532; (d) de Sá Alves, F. R.; Barreiro, E. J.; Fraga C. A. M. *Mini-Rev. Med. Chem*. **2009**, *9*, 782; (e) Singh, T. P.; Singh, O. M. *Mini-Rev. Med. Chem*. **2018**, *18*, 9.

[2] For selected reviews on β-carbolines in general and their syntheses, see: (a) *The Alkaloids, Chemistry and Physiology* (Ed.: Manske, R. H. F.), Academic Press, New York, *vol. XX*, **1981**; (b) Love, B. E. *Org. Prep. Proced. Int.* **1996**, *28*, 1; (c) Grate, J. W.; Frye, G. C. in *Sensors Update* (Ed.: Baltes, H.; Gopel, W.; Hesse, J.), Wiley-VCH, Weinheim, *vol. 2*, **1996**, p. 10; (d) Hesse, M. in *Alkaloids: Nature's Curse or Blessing* Wiley-VCH, Zürich, Switzerland, **2002**, p. 14; (e) Cao, R. H.; Peng, W. L.; Wang, Z. H.; Xu, A. L. *Curr. Med. Chem.* **2007**, *14*, 479; (f) Dai, J. K.; Dan, W. J.; Schneider, U.; Wang, J. R. *Eur. J. Med. Chem.* **2018**, *157*, 622; (g) Maity, P.; Adhikari, D.; Jana, A. K. *Tetrahedron* **2019**, *75*, 965.

[3] (a) Pictet, A.; Spengler, T. *Ber. Dtsch. Chem. Ges.* **1911**, *44*, 2030; (b) Tatsui, G. *Yakugaku Zasshi* **1928**, *48*, 453.

[4] For selected reviews on the Pictet–Spengler reaction, see: (a) Cox, E. D.; Cook, J. M. *Chem. Rev.* **1995**, *95*, 1797; (b) Stöckigt, J; Antonchick, A, P.; Wu, F.; Waldmann, H. *Angew. Chem. Int. Ed.* **2011**, *50*, 8538; (c) Dalpozzo, R. *Molecules* **2016**, *21*, 69.

[5] For Iridium-catalyzed reactions, see: (a) Xu, S.-M.; Wei, L.; Shen, C.; Xiao, L.; Tao, H.-Y.; Wang, C-J. *Nat. Commun.* **2019**, *10*, 5553; (b) Xiao, F.; Xu, S.-M.; Dong, X.-Q.; Wang, C.-J. *Org. Lett.* **2021**, *23*, 706; (c) Cooksey, J. P.; Saidi, O.; Williams, J. M. J.; Blacker, A. J.; Marsden, S. P. *Tetrahedron* **2021**, *78*, 131785.

[6] (a) Komzolova, N. N.; Kucherova, N. F.; Zagorevskii, V. A. *Khim. Geterotsikl. Soedin.* **1968**, *4*, 668; (b) Molina, P.; Alcántara, J.; López-Leonardo, C. *Tetrahedron* **1996**, *52*, 5833; (c) Grigg, R.; Sridharan, V.; Sykes, D. A. *Tetrahedron* **2008**, *64*, 8952; (d) Lee, Y.; Klausen, R. S.; Jacobsen, E. N. *Org. Lett.* **2011**, *13*, 5564; (e) Subba Reddy, B. V.; Swain, M.; Reddy, S. M.; Yadav, J. S.; Sridhar, B. *J. Org. Chem.* **2012**, *77*, 11355; (f) Huang, L.; Dai, L.-X.; You, S.-L. *J. Am. Chem. Soc.* **2016**, *138*, 5793; (g) Riesco-Domínguez, A.; van der Zwaluw, N.; Blanco-Ania, D.; Rutjes, F. P. J. T. *Eur. J. Org. Chem*. **2017**, *2017*, 662; (h) Urmode, T. D.; Dawange, M. A.; Shinde, V. S.; Kusurkar, R. S. *Tetrahedron* **2017**, *73*, 4348; (i) Voznesenskaia, N. G.; Shmatova, O. I.; Nenajdenko, V. G. *Inorg. Chim. Acta* **2018**, *482*, 491.

[7] (a) Katritzky, A. R.; Verma, A. K.; He, H.-Y.; Chandra, R. *J. Org. Chem*. **2003**, *68*, 4938; (b) Tiwari, R. K.; Singh, J.; Singh, D.; Verma, A. K.; Chandra, R. Tetrahedron **2005**, *61*, 9513; (c) Tiwari, R. K.; Verma, A. K.; Chhillar, A. K.; Singh, D.; Singh, J.; Kasi Sankar, V.; Yadav, V.; Sharma, G. L.; Chandra, R. *Bioorg. Med. Chem.* **2006**, *14*, 2747; (d) Xu, H.; Fan, L.-l. *Eur. J. Med. Chem*. **2011**, *46*, 1919; (e) Schönherr, H.; Leighton, J. L. *Org. Lett*. **2012**, *14*, 2610; (f) Wu, F.; Zhu, H.; Sun, L.; Rajendran, C.; Wang, M.; Ren, X.; Panjikar, S.; Cherkasov, A.; Zou, H.; Stöckigt, J. *J. Am. Chem. Soc*. **2012**, *134*, 1498; (g) Preetam, A.; Nath, M. *RSC Adv.* **2015**, *5*, 21843; (h) Huo, H.-r.; Tang, X.-Y.; Gong, Y.-f. *Synthesis* **2018**, *50*, 2727;

[8] (a) Demerson, C. A.; Philipp, A. H.; Humber, L. G. *J. Med. Chem.* **1974**, *17*, 1140; (b) Patil, N. T.; Shinde, V. S.; Sridhar, B. *Angew. Chem. Int. Ed*. **2013**, *52*, 2251; (c) Milcendeau, P.; Zhang, Z.; Glinsky-Olivier, N.; van Elslande, E.; Guinchard, X. *J. Org. Chem.* **2021**, *86*, 6406.

[9] Lisnyak, V. G.; Lynch-Colameta, T.; Snyder, S. A. *Angew. Chem. Int. Ed.* **2018**, *57*, 15162.
[10] Lynch-Colameta, T.; Greta, S.; Snyder, S. A. *Chem. Sci.* **2021**, *12*, 6181.
[11] Kerkouvius, J. K.; Kerr, M. A. *J. Am. Chem. Soc.* **2018**, *140*, 8415.
[12] Winter, C.; Krause, N. *Angew. Chem. Int. Ed.* **2009**, *48*, 6339.
[13] Han, S.-Y.; Lakshmikantham, M. V.; Cava, M. P. *Heterocycles*, **1985**, *23*, 1671.
[14] For selected reviews on organocatalysis, see: (a) List, B. *Chem. Rev.* **2007**, *107*, 5413; (b) Dondoni, A.; Massi, A. *Angew. Chem. Int. Ed.* **2008**, *47*, 4638; (c) Bertelsen, S.; Jørgensen, K. A. *Chem. Soc. Rev*. **2009**, *38*, 2178; (d) Buckley, B. R. *Annu. Rep. Prog. Chem., Sect. B: Org. Chem.* **2009**, *105*, 113; (e) Hernández, J. G.; Juaristi, E. *Chem. Commun*. **2012**, *48*, 5396; (f) Alemán, J.; Cabrera, S. *Chem. Soc. Rev.* **2013**, *42*, 774.
[15] For selected reviews on thiourea catalysis, see: (a) Takemoto, Y. *Org. Biomol. Chem.* **2005**, *3*, 4299; (b) Zhang, Z.; Schreiner, P. R. *Chem. Soc. Rev.* **2009**, *38*, 1187; (c) Siau, W.-Y.; Wang, J. *Catal. Sci. Technol.* **2011**, *1*, 1298; (d) Serdyuk, O. V.; Heckel, C. M.; Tsogoeva, S. B. *Org. Biomol. Chem.* **2013**, *11*, 7051; (e) Fang, X.; Wang, C.-J. *Chem. Commun.* **2015**, *51*, 1185.
[16] For selected reviews on phosphoric acid catalysis, see: (a) Terada, M. *Chem. Commun.* **2008**, 4097; (b) Parmar, D.; Sugiono, E.; Raja, S.; Rueping, M. *Chem. Rev.* **2014**, *114*, 9047; (c) Wu, H.; He, Y-P.; Shi, F. *Synthesis* **2015**, *47*, 1990; (d) Maji, R.; Mallojjala, S. C.; Wheeler, S. E. *Chem. Soc. Rev.* **2018**, *47*, 1142.
[17] Schreyer, L.; Properzi, R.; List, B. *Angew. Chem. Int. Ed*. **2019**, *58*, 12761.
[18] (a) Heine, H. W.; Zibuck, R.; VandenHeuvel, W. J. A. *J. Am. Chem. Soc.* **1982**, *104*, 3691; (b) Kawakami, T.; Ohtake, H.; Arakawa, H.; Okachi, T.; Imada, Y.; Murahashi, S.-I. *Org. Lett.* **1999**, *1*, 107; (c) Kawakami, T.; Ohtake, H.; Arakawa, H.; Okachi, T.; Imada, Y.; Murahashi, S.-I. *Chem. Lett.* **1999**, 795; (d) Kawakami, T.; Ohtake, H.; Arakawa, H.; Okachi, T.; Imada, Y.; Murahashi, S.-I. *Bull. Chem. Soc. Jpn.* **2000**, *73*, 2423.
[19] (a) Knowles, R. R.; Lin, S.; Jacobsen, E. N. *J. Am. Chem. Soc.* **2010**, *132*, 5030; (b) Yeung, C. S.; Ziegler, R. E.; Porco, J. A. Jr.; Jacobsen, E. N. *J. Am. Chem. Soc.* **2014**, *136*, 13614; (c) Park, Y.; Schindler, C. S.; Jacobsen, E. N. *J. Am. Chem. Soc.* **2016**, *138*, 14848.
[20] Attia, M. I.; Güclü, D.; Hertlein, B.; Julius, J.; Witt-Enderby, P. A.; Zlotos, D. P. *Org. Biomol. Chem.* **2007**, *5*, 2129.
[21] Xiao, X.; Chen, H.; Dong, X.; Ren, D.; Deng, Q.; Wang, D.; Tian, W. *Angew. Chem. Int. Ed*. **2020**, *59*, 9534.

4.9 NMR Spectra

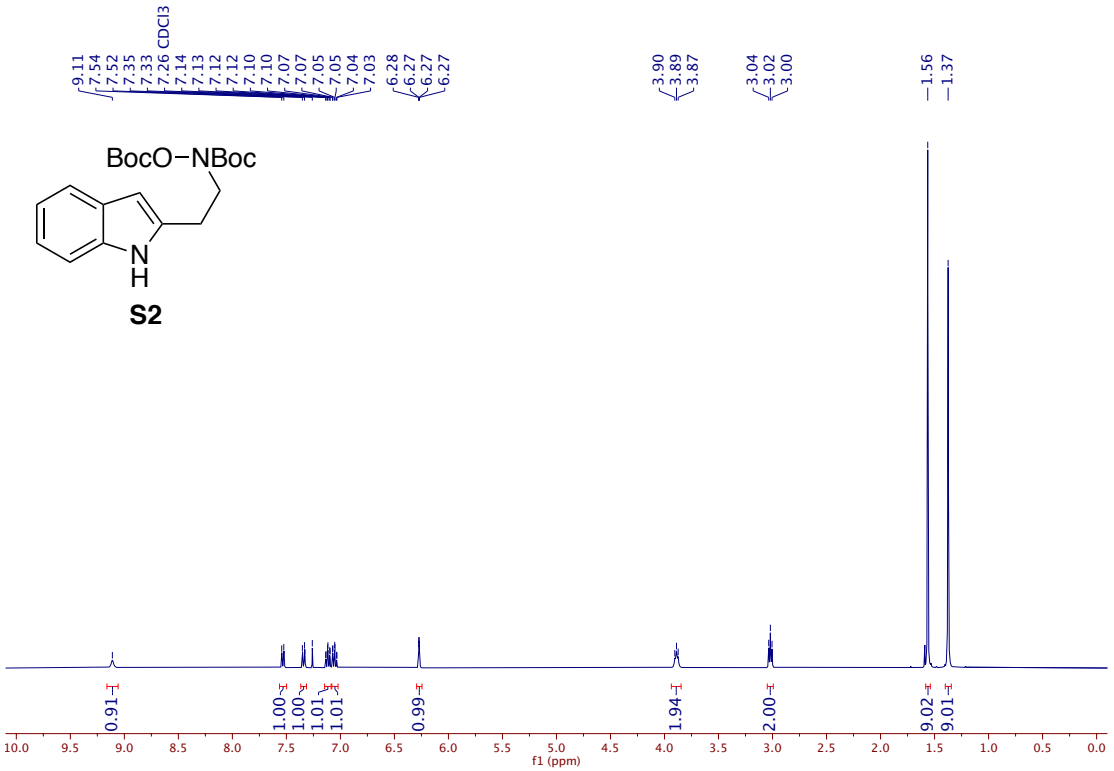

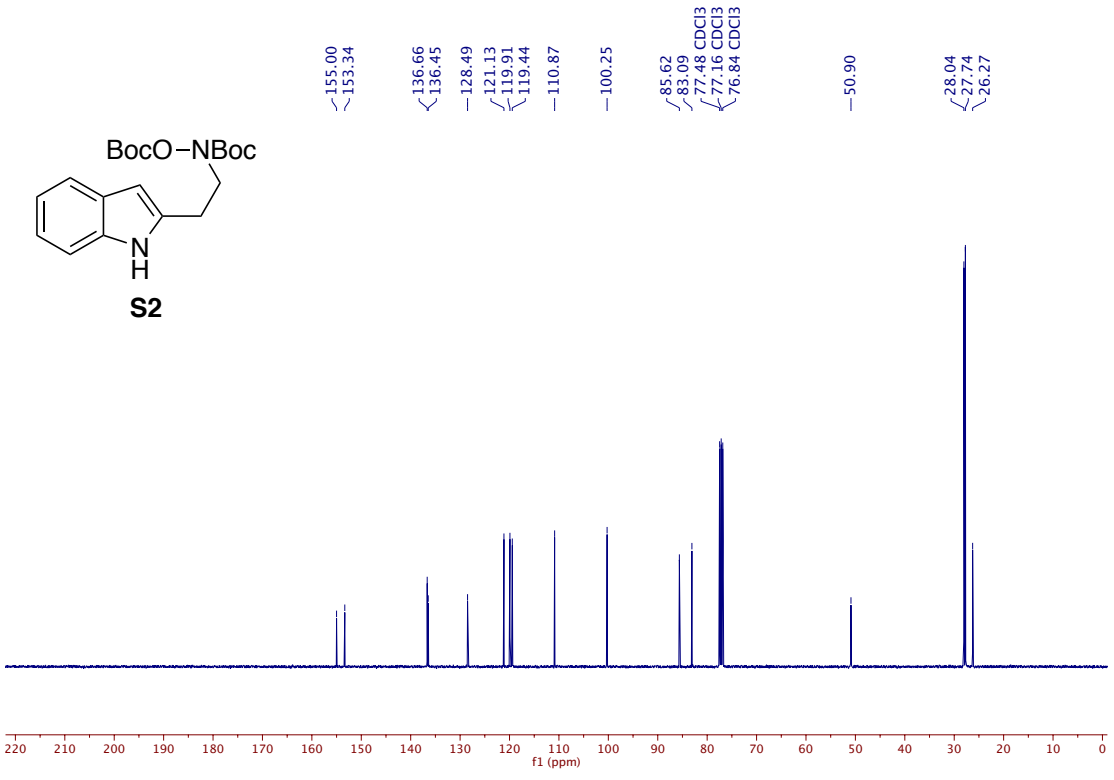

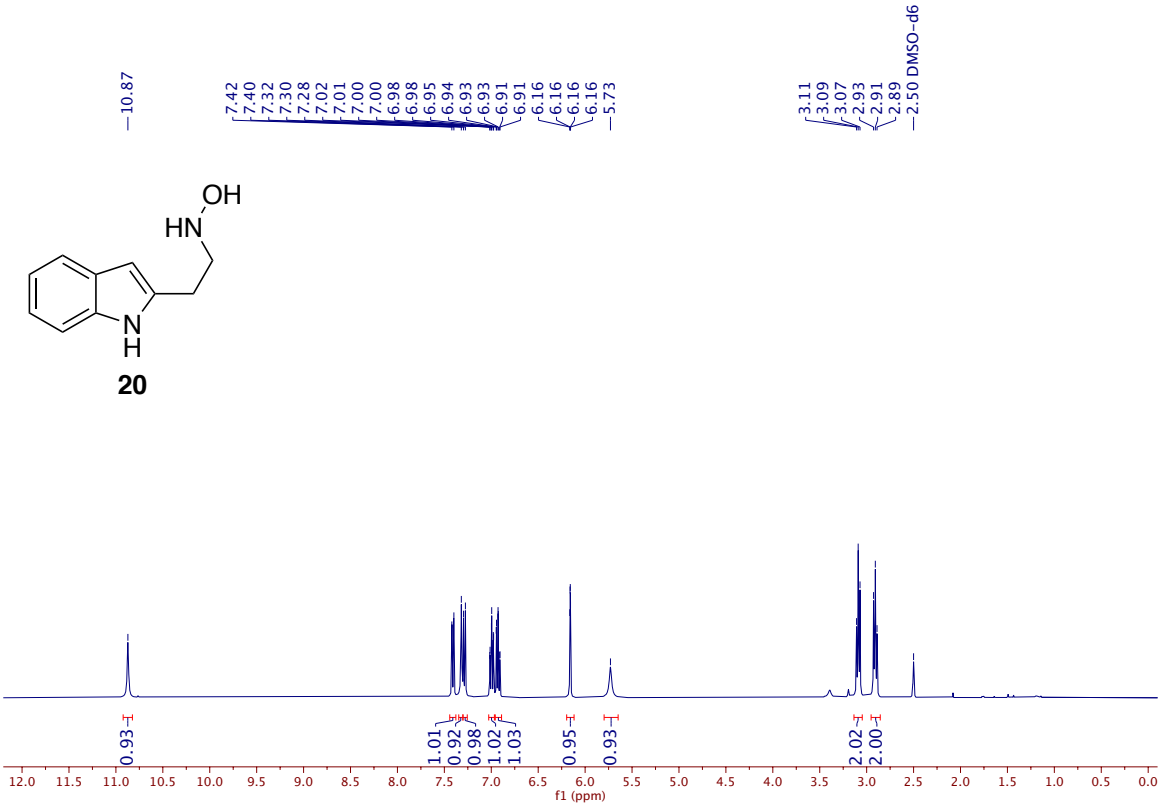
10.87
7.42
7.40
7.32
7.30
7.28
7.02
7.01
7.00
7.00
6.98
6.95
6.94
6.93
6.93
6.91
6.91
6.16
6.16
6.16
6.16
5.73
3.11
3.09
3.07
2.93
2.91
2.89
2.50 DMSO-d6
OH
HN
N
H
20
0.93
1.01
0.92
0.98
1.02
1.03
0.95
0.93
2.02
2.00
f1 (ppm)

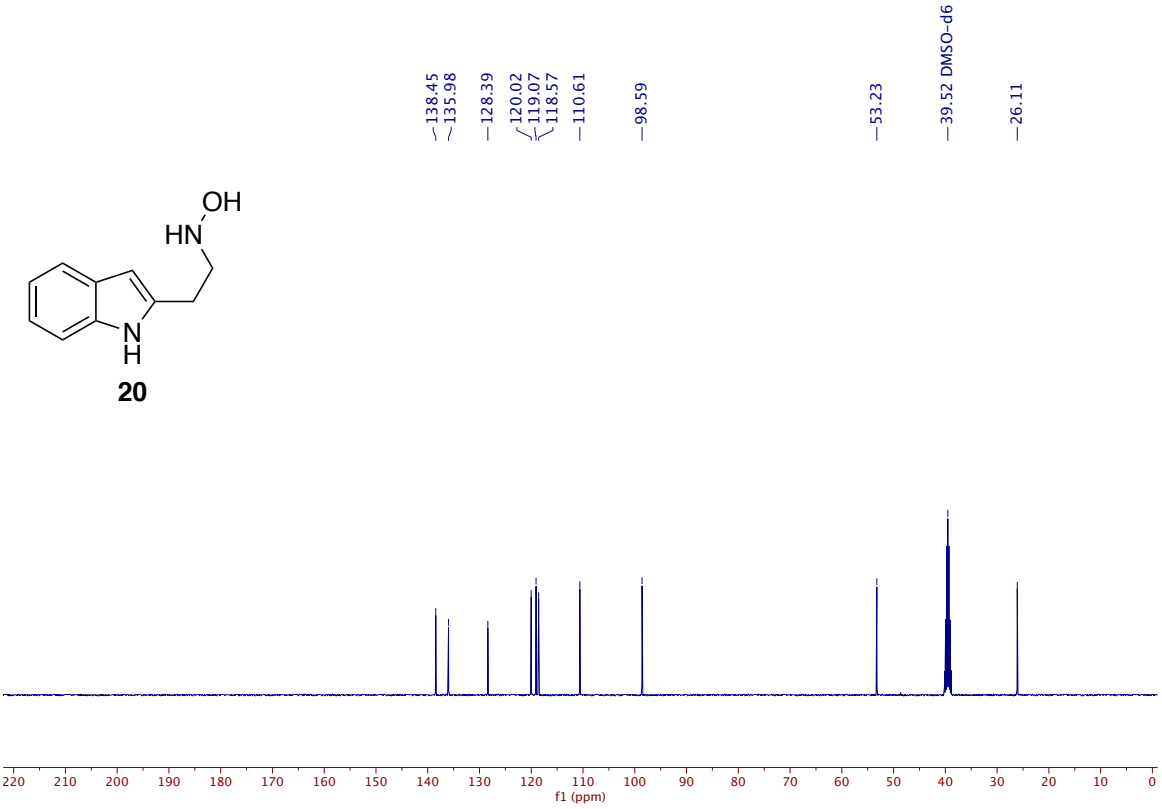
138.45
135.98
128.39
120.02
119.07
118.57
110.61
98.59
53.23
39.52 DMSO-d6
26.11
OH
HN
N
H
20
f1 (ppm)

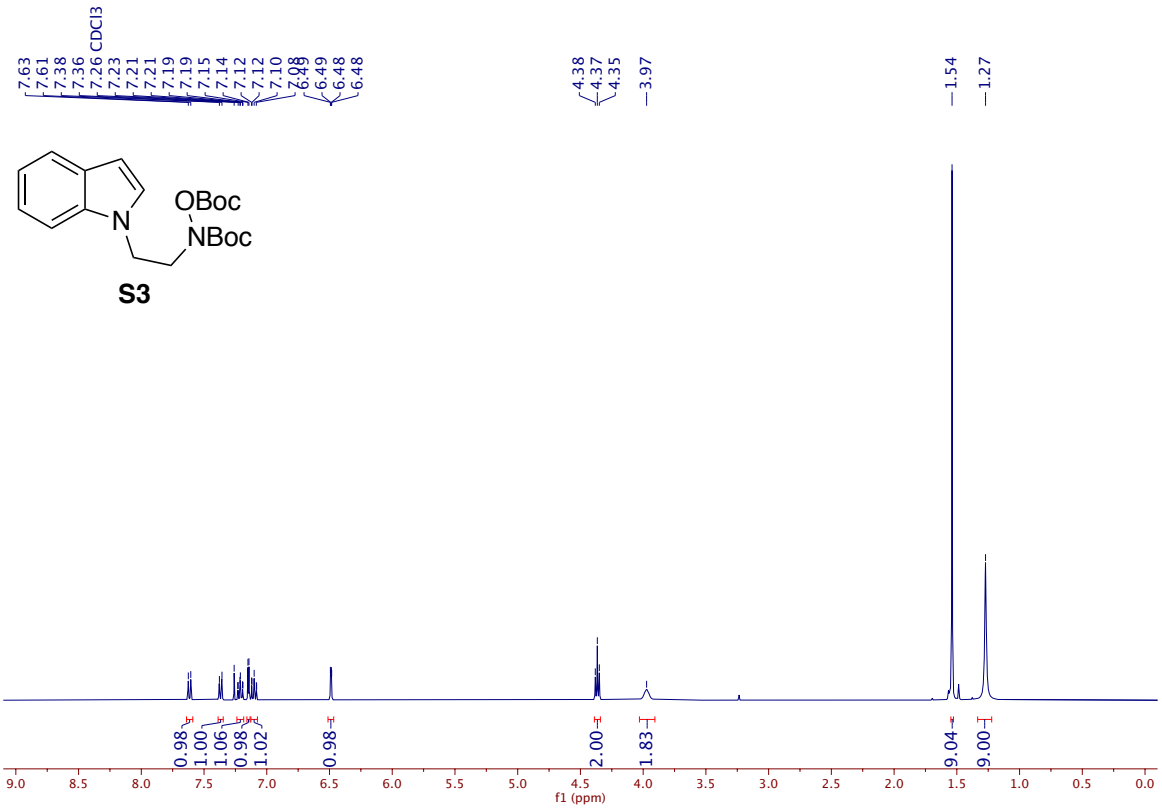
7.63
7.61
7.38
7.36
7.26 CDCl3
7.23
7.21
7.21
7.19
7.19
7.15
7.14
7.12
7.12
7.10
6.49
6.48
6.48
4.38
4.37
4.35
3.97
1.54
1.27
OBoc
NBoc
N
S3
0.98
1.00
1.06
0.98
1.02
0.98
2.00
1.83
9.04
9.00
f1 (ppm)

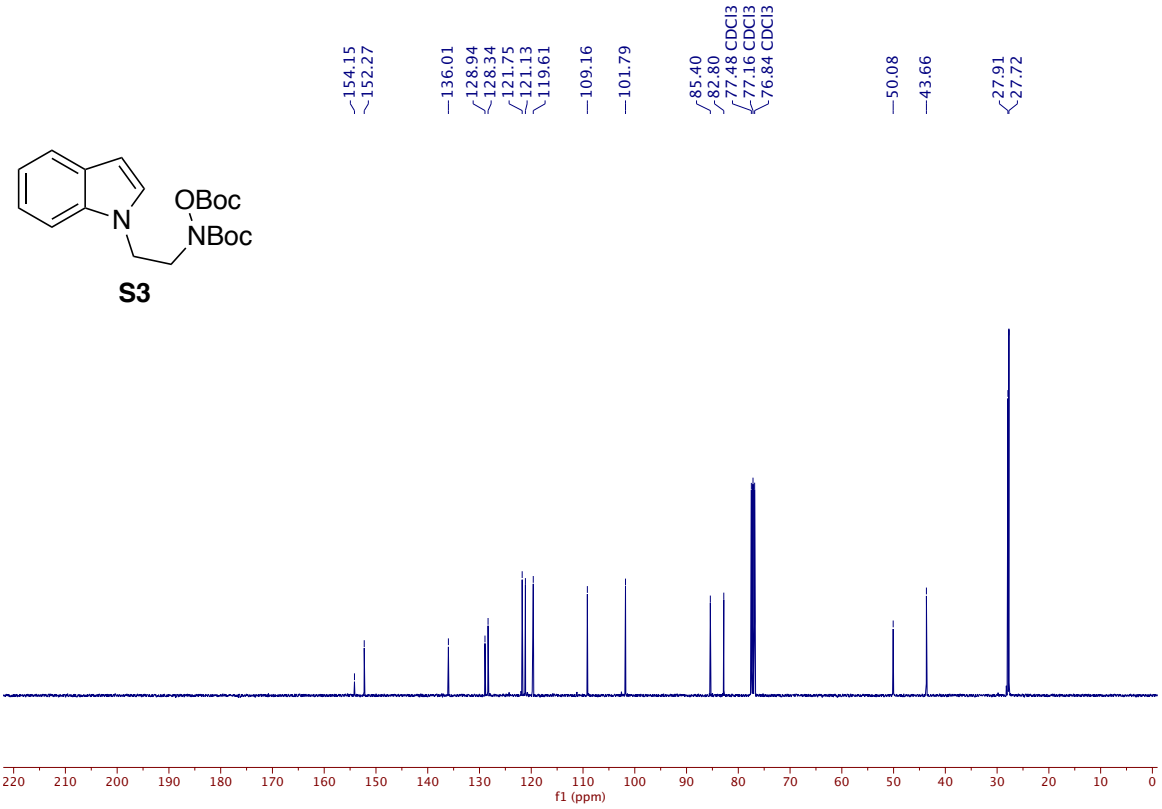
154.15
152.27
136.01
128.94
128.34
121.75
121.13
119.61
109.16
101.79
85.40
82.80
77.48 CDCl3
77.16 CDCl3
76.84 CDCl3
50.08
43.66
27.91
27.72
OBoc
NBoc
N
S3
f1 (ppm)


7.65
7.64
7.41
7.39
7.26 CDCl3
7.24
7.22
7.21
7.21
7.16
7.15
7.14
7.14
7.12
7.11
6.54
6.53
6.53
6.53
5.30 CH2Cl2
4.39
4.38
4.37
3.30
3.29
3.28

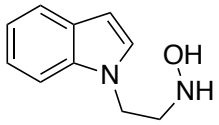
OH
N
NH

S4

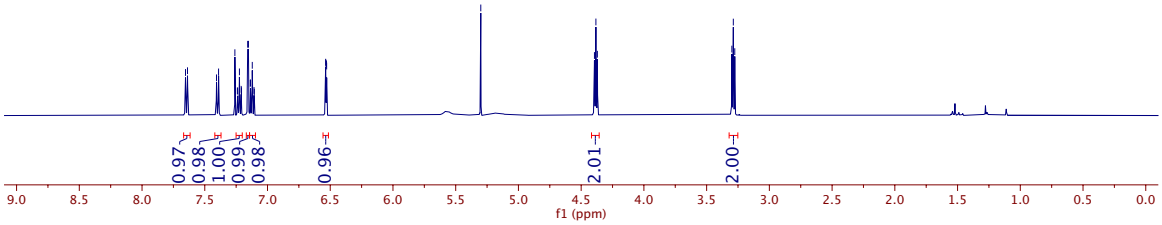
0.97
0.98
1.00
0.99
0.98
0.96
2.01
2.00
9.0
8.5
8.0
7.5
7.0
6.5
6.0
5.5
5.0
4.5
4.0
3.5
3.0
2.5
2.0
1.5
1.0
0.5
0.0
f1 (ppm)

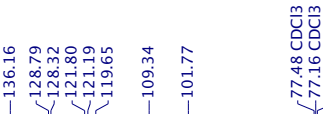
136.16
128.79
128.32
121.80
121.19
119.65
109.34
101.77
77.48 CDCl3
77.16 CDCl3
76.84 CDCl3
53.13
43.02

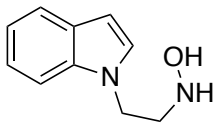
OH
N
NH

S4

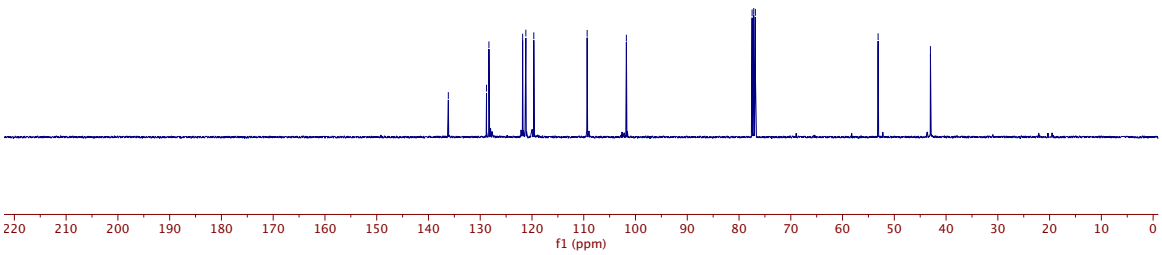
220
210
200
190
180
170
160
150
140
130
120
110
100
90
80
70
60
50
40
30
20
10
0
f1 (ppm)

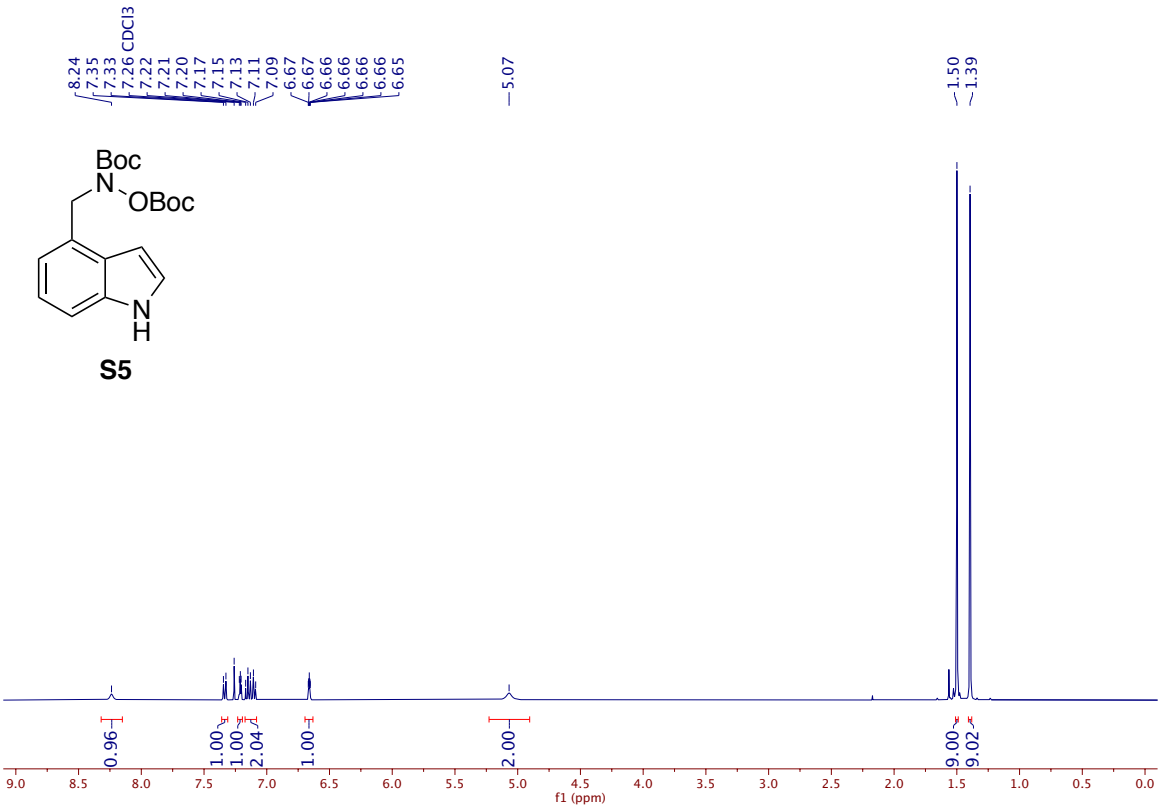
8.24
7.35
7.33
7.26 CDCl3
7.22
7.21
7.20
7.17
7.15
7.13
7.11
7.09
6.67
6.67
6.66
6.66
6.66
6.66
6.65
5.07
1.50
1.39
Boc
N
OBoc
N
H
S5
0.96
1.00
1.00
2.04
1.00
2.00
9.00
9.02
f1 (ppm)

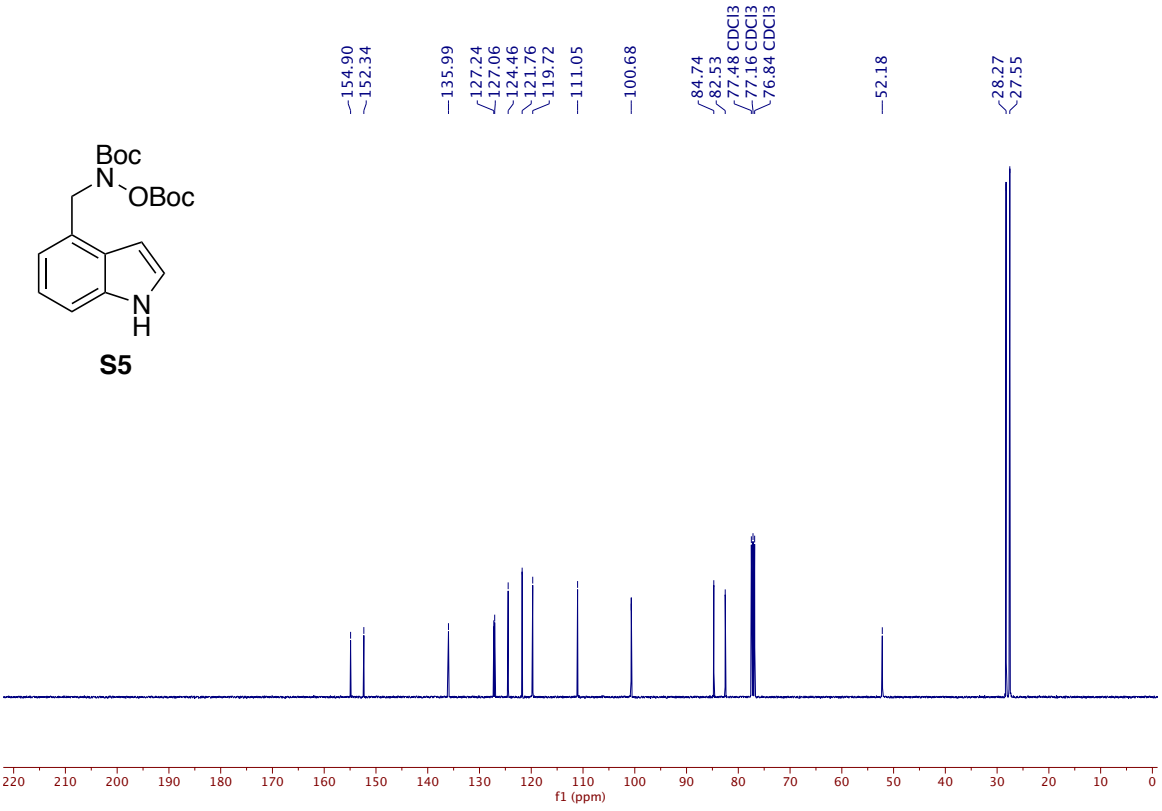
154.90
152.34
135.99
127.24
127.06
124.46
121.76
119.72
111.05
100.68
84.74
82.53
77.48 CDCl3
77.16 CDCl3
76.84 CDCl3
52.18
28.27
27.55
Boc
N
OBoc
N
H
S5
f1 (ppm)

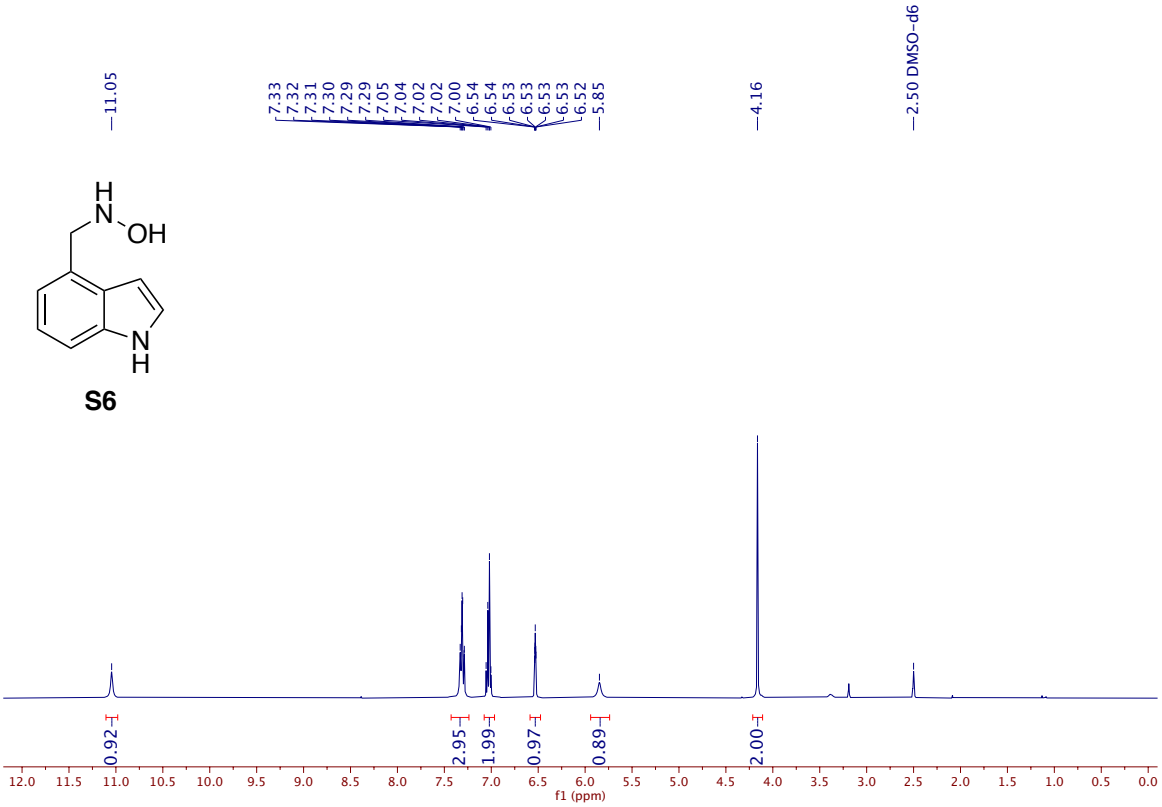
11.05
7.33
7.32
7.31
7.30
7.29
7.29
7.05
7.04
7.02
7.02
7.00
6.54
6.54
6.53
6.53
6.53
6.53
6.52
5.85
4.16
2.50 DMSO-d6
H
N
OH
N
H
S6
0.92
2.95
1.99
0.97
0.89
2.00
12.0 11.5 11.0 10.5 10.0 9.5 9.0 8.5 8.0 7.5 7.0 6.5 6.0 5.5 5.0 4.5 4.0 3.5 3.0 2.5 2.0 1.5 1.0 0.5 0.0
f1 (ppm)

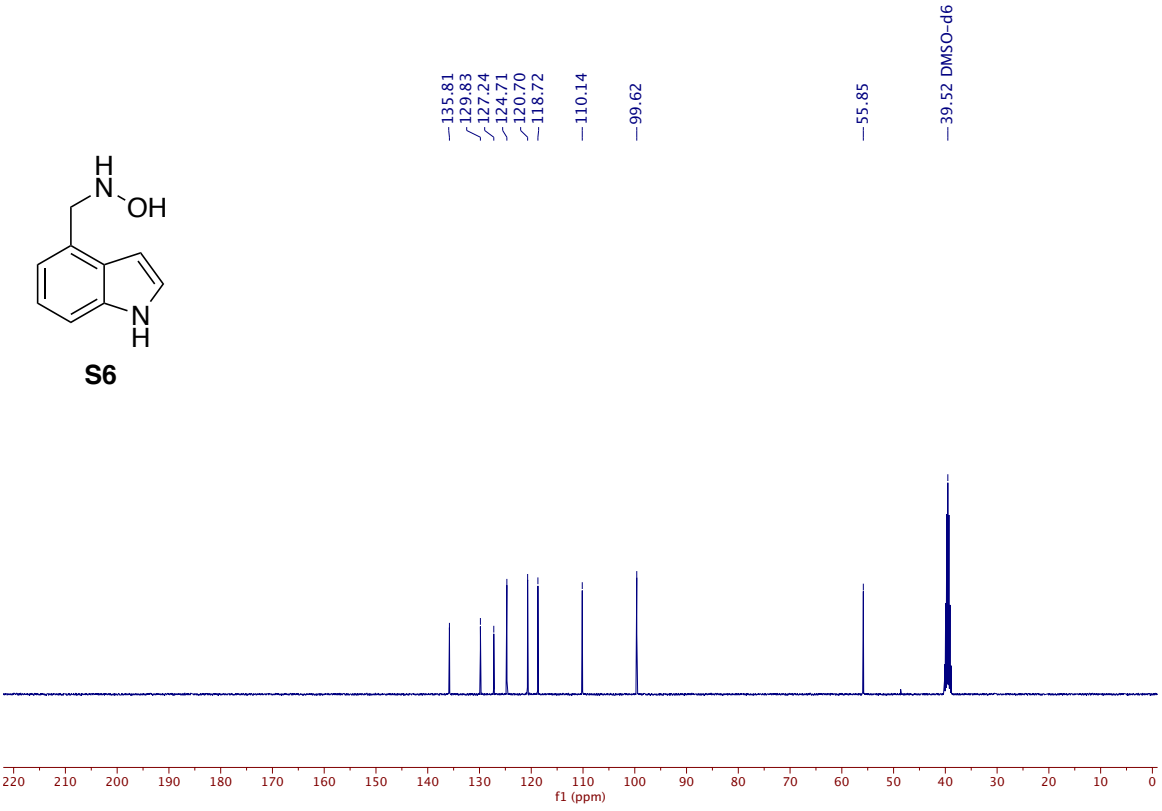
135.81
129.83
127.24
124.71
120.70
118.72
110.14
99.62
55.85
39.52 DMSO-d6
H
N
OH
N
H
S6
220 210 200 190 180 170 160 150 140 130 120 110 100 90 80 70 60 50 40 30 20 10 0
f1 (ppm)

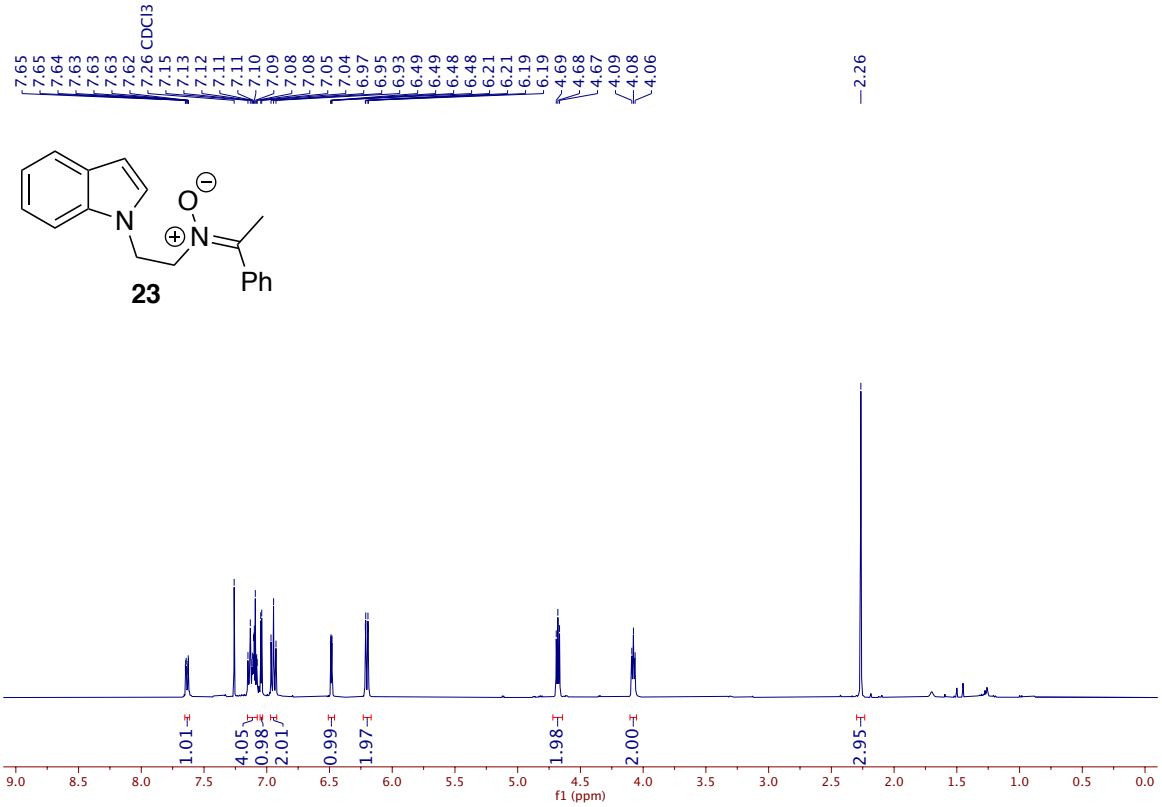
7.65
7.65
7.64
7.63
7.63
7.63
7.62
7.26 CDCl3
7.15
7.13
7.12
7.11
7.11
7.10
7.09
7.08
7.08
7.05
7.04
6.97
6.95
6.93
6.49
6.49
6.48
6.48
6.21
6.21
6.19
6.19
4.69
4.68
4.67
4.09
4.08
4.06
2.26
O
N
N
Ph
23
1.01
4.05
0.98
2.01
0.99
1.97
1.98
2.00
2.95
9.0
8.5
8.0
7.5
7.0
6.5
6.0
5.5
5.0
4.5
4.0
3.5
3.0
2.5
2.0
1.5
1.0
0.5
0.0
f1 (ppm)

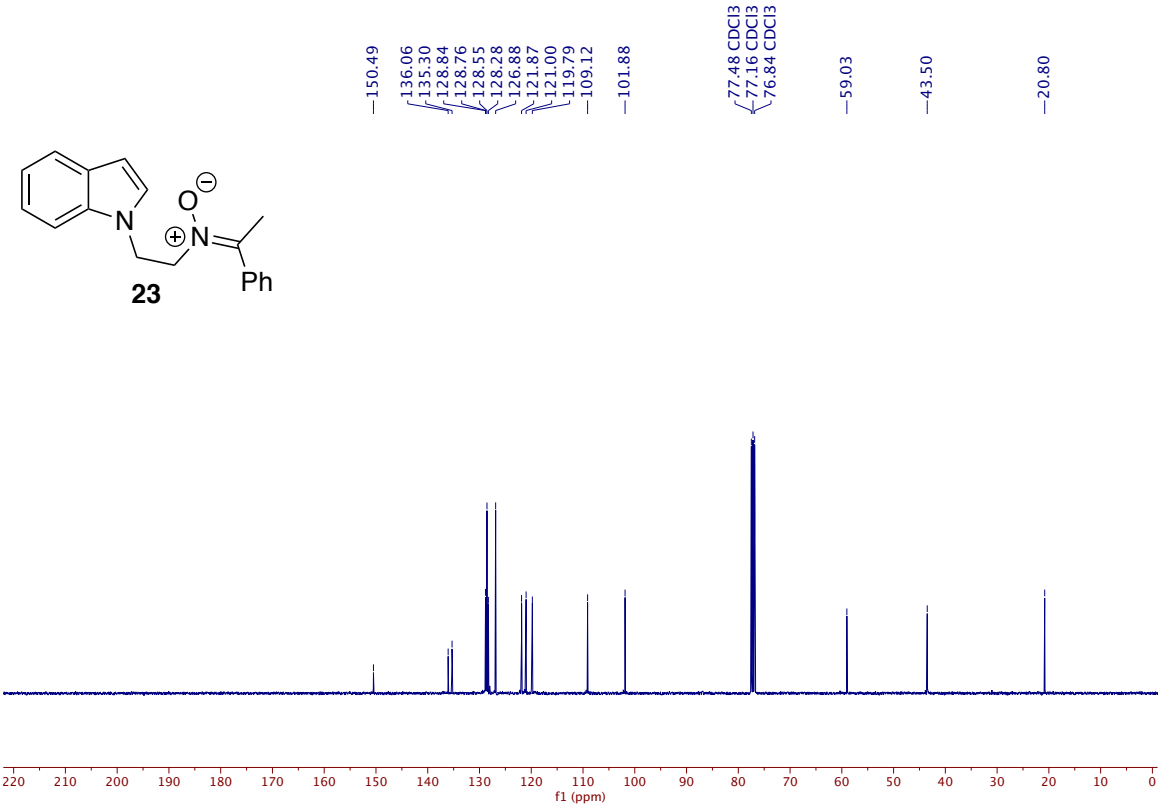
150.49
136.06
135.30
128.84
128.76
128.55
128.28
126.88
121.87
121.00
119.79
109.12
101.88
77.48 CDCl3
77.16 CDCl3
76.84 CDCl3
59.03
43.50
20.80
O
N
N
Ph
23
220
210
200
190
180
170
160
150
140
130
120
110
100
90
80
70
60
50
40
30
20
10
0
f1 (ppm)

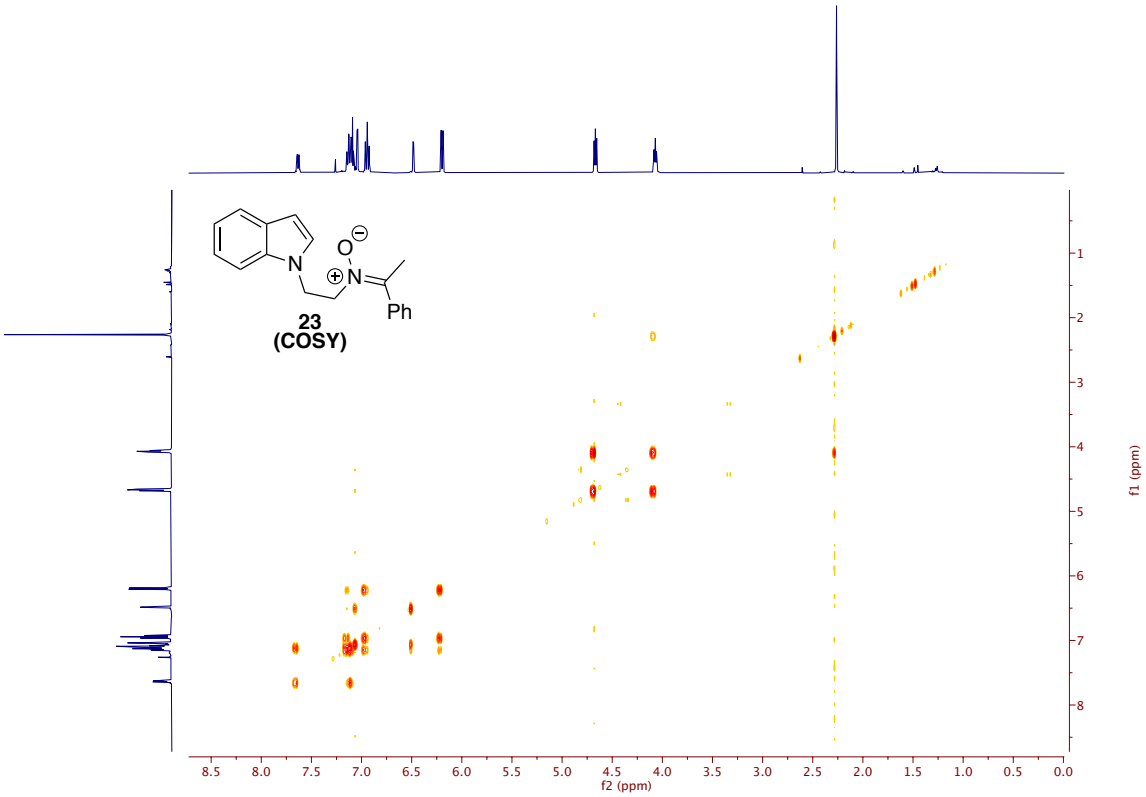
23
(COSY)
f2 (ppm)
f1 (ppm)

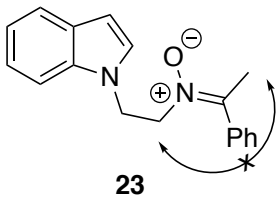
Ph
23

23
(NOESY)
f2 (ppm)
f1 (ppm)

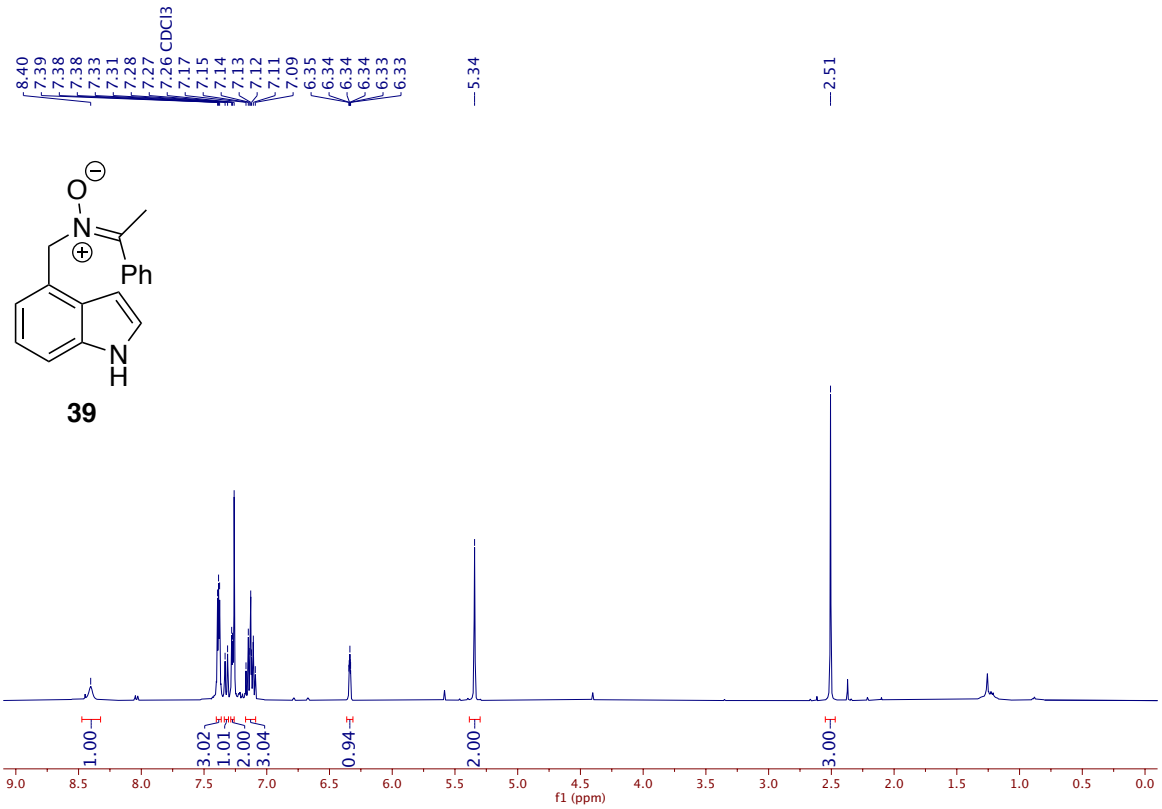
8.40
7.39
7.38
7.38
7.33
7.31
7.28
7.27
7.26 CDCl3
7.17
7.15
7.14
7.13
7.12
7.11
7.09
6.35
6.34
6.34
6.34
6.33
6.33
5.34
2.51
O
N
Ph
N
H
1.00
3.02
1.01
2.00
3.04
0.94
2.00
3.00
9.0
8.5
8.0
7.5
7.0
6.5
6.0
5.5
5.0
4.5
4.0
3.5
3.0
2.5
2.0
1.5
1.0
0.5
0.0
f1 (ppm)

39

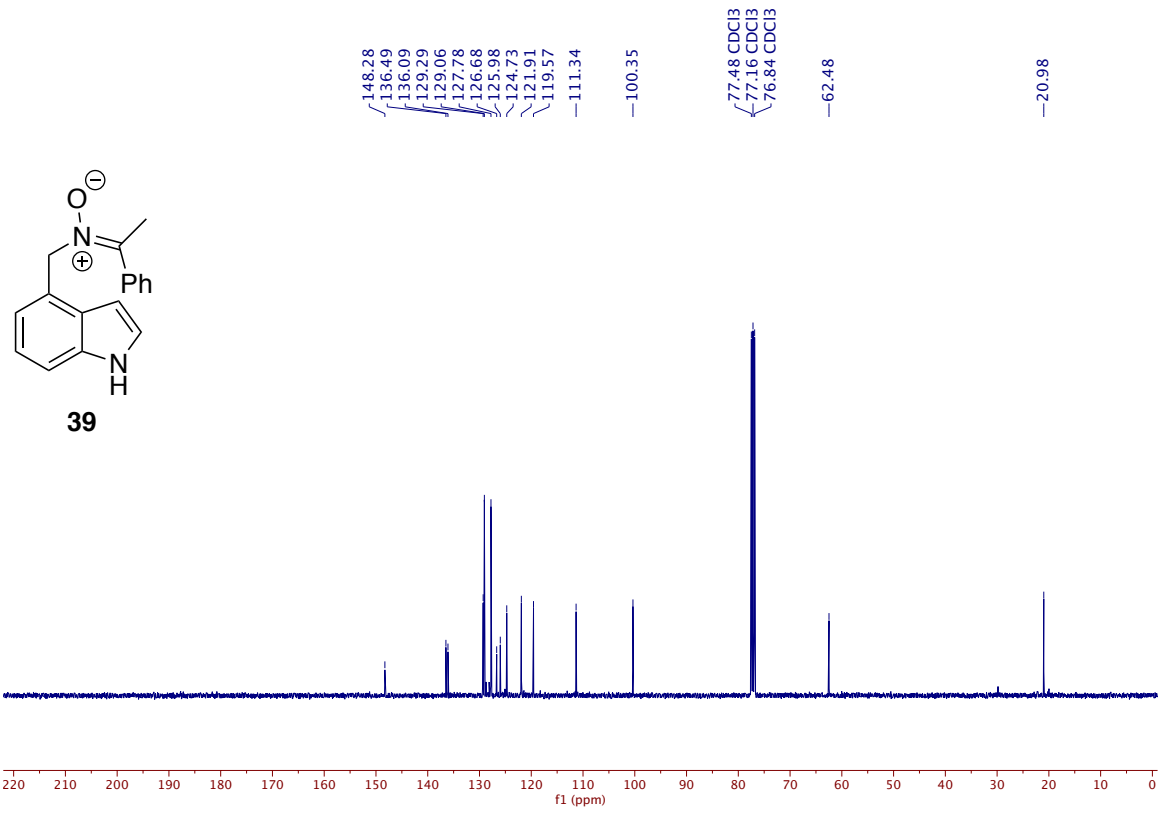
148.28
136.49
136.09
129.29
129.06
127.78
126.68
125.98
124.73
121.91
119.57
111.34
100.35
77.48 CDCl3
77.16 CDCl3
76.84 CDCl3
62.48
20.98
O
N
Ph
N
H
220
210
200
190
180
170
160
150
140
130
120
110
100
90
80
70
60
50
40
30
20
10
0
f1 (ppm)

39

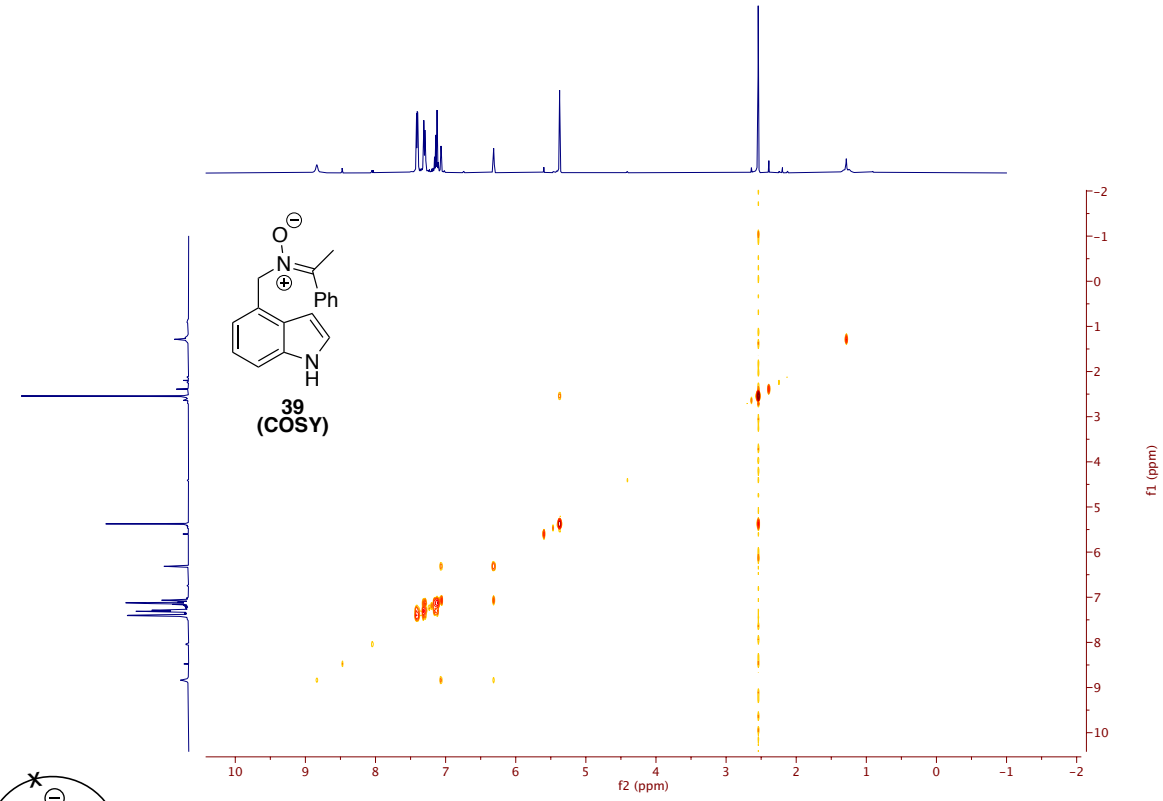

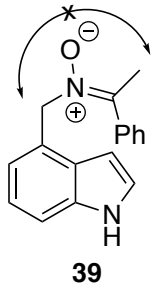

39

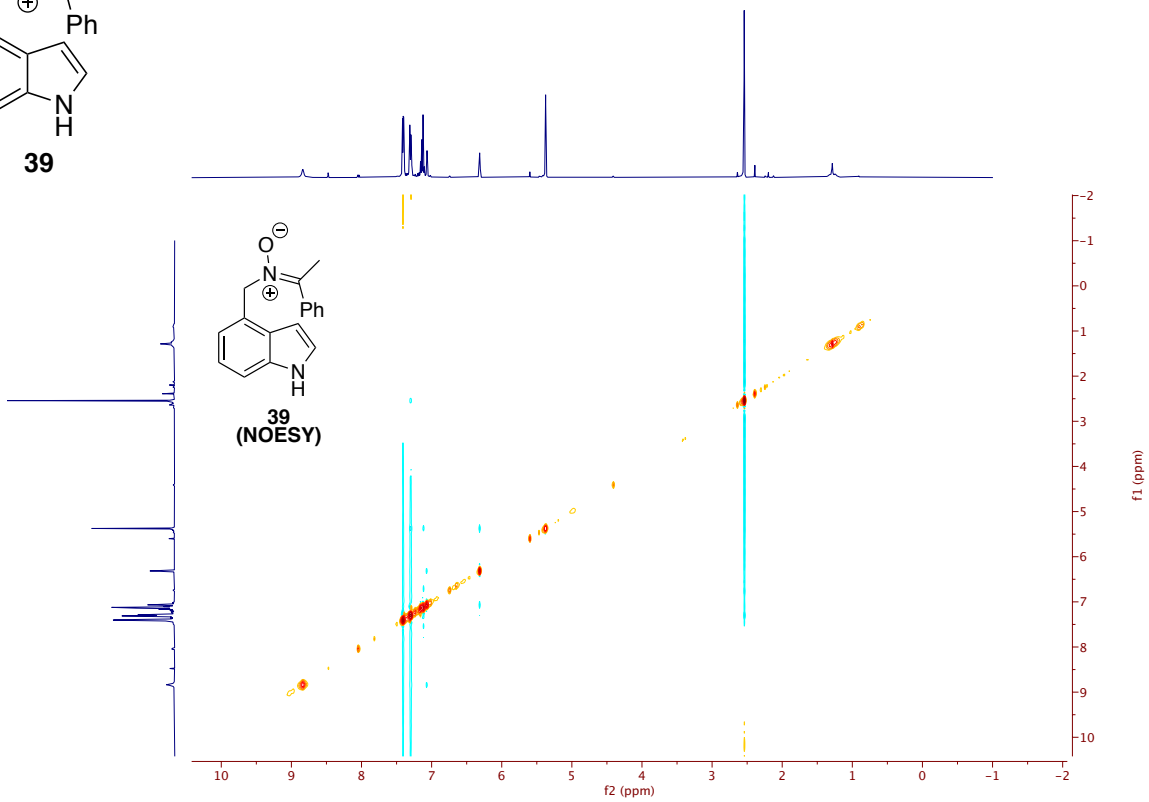

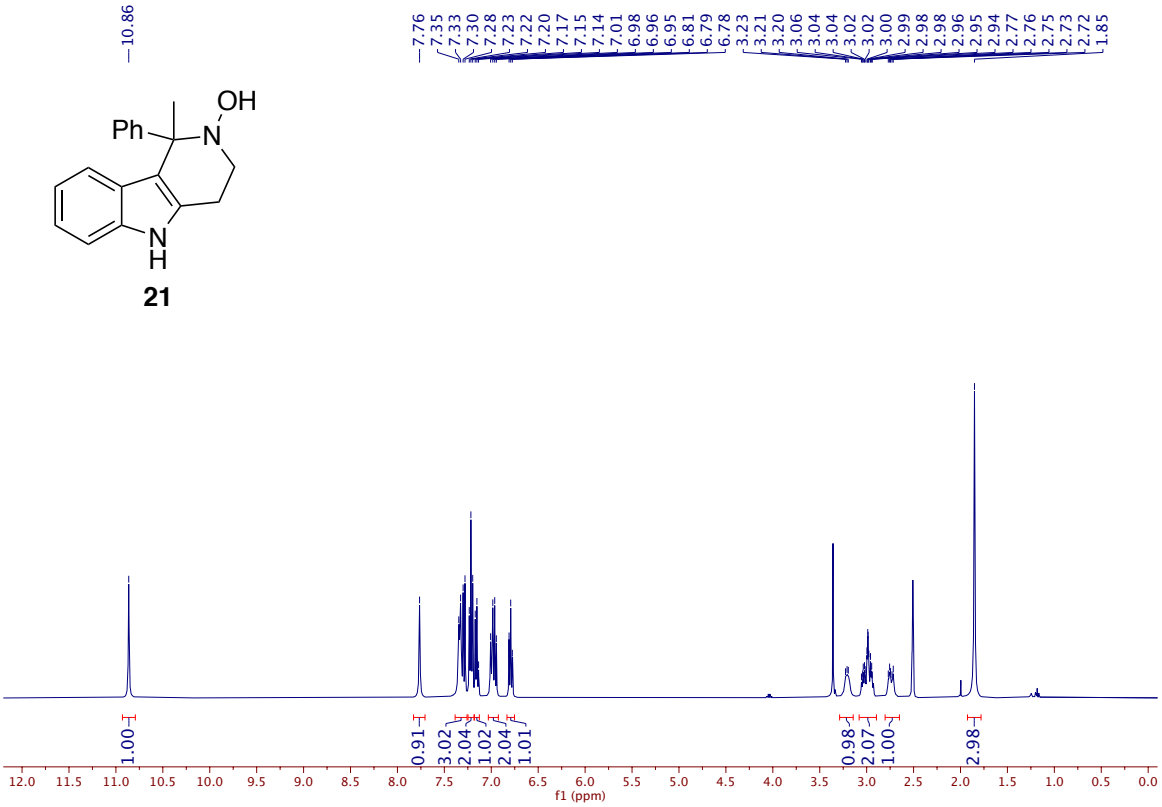
10.86
7.76
7.35
7.33
7.30
7.28
7.23
7.22
7.20
7.17
7.15
7.14
7.01
6.98
6.96
6.95
6.81
6.79
6.78
3.23
3.21
3.20
3.06
3.04
3.02
3.02
3.00
2.99
2.98
2.98
2.96
2.95
2.94
2.77
2.76
2.75
2.73
2.72
1.85
OH
Ph
N
N
H
21
1.00
0.91
3.02
2.04
1.02
2.04
1.01
0.98
2.07
1.00
2.98
f1 (ppm)

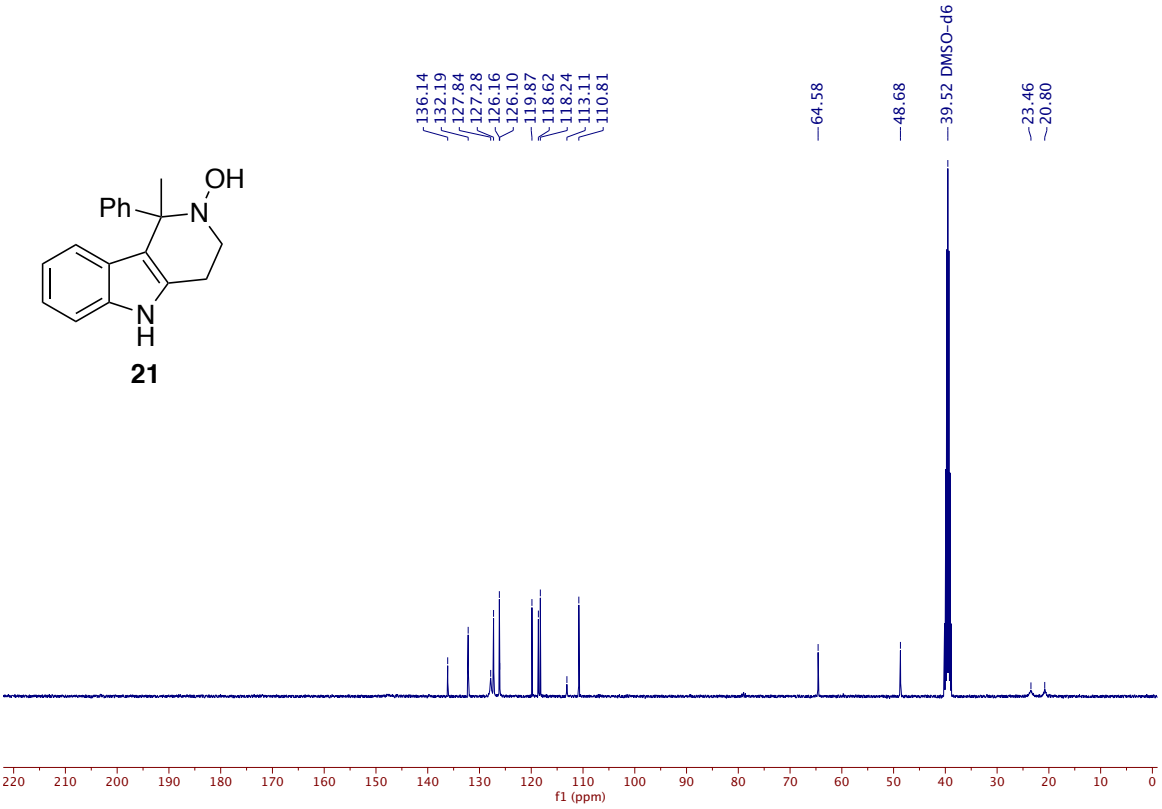
136.14
132.19
127.84
127.28
126.16
126.10
119.87
118.62
118.24
113.11
110.81
64.58
48.68
39.52 DMSO-d6
23.46
20.80
OH
Ph
N
N
H
21
f1 (ppm)

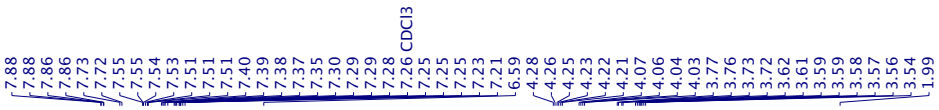
7.88
7.88
7.86
7.86
7.73
7.72
7.55
7.54
7.53
7.51
7.51
7.51
7.40
7.39
7.38
7.37
7.35
7.30
7.29
7.29
7.28
7.26 CDCl3
7.25
7.25
7.25
7.23
7.21
6.59
4.28
4.26
4.25
4.23
4.22
4.21
4.07
4.06
4.04
4.03
3.77
3.76
3.73
3.72
3.62
3.61
3.59
3.59
3.58
3.57
3.56
3.54
1.99

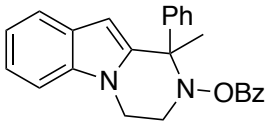
Ph
N
N–OBz

24

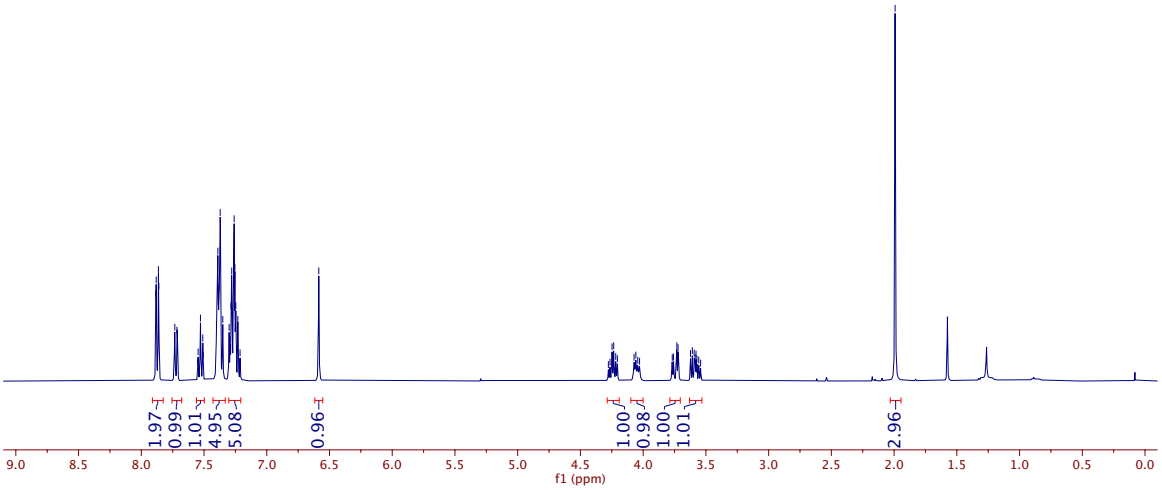
1.97
0.99
1.01
4.95
5.08
0.96
1.00
0.98
1.00
1.01
2.96
9.0
8.5
8.0
7.5
7.0
6.5
6.0
5.5
5.0
4.5
4.0
3.5
3.0
2.5
2.0
1.5
1.0
0.5
0.0
f1 (ppm)


165.31
144.85
138.01
137.07
133.44
129.67
128.93
128.70
128.51
128.10
127.88
127.29
121.58
120.71
120.49
109.44
101.27
77.48 CDCl3
77.16 CDCl3
76.84 CDCl3
66.80
46.69
37.32
27.90

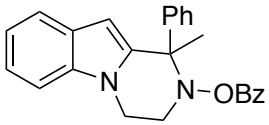
Ph
N
N–OBz

24

220
210
200
190
180
170
160
150
140
130
120
110
100
90
80
70
60
50
40
30
20
10
0
f1 (ppm)

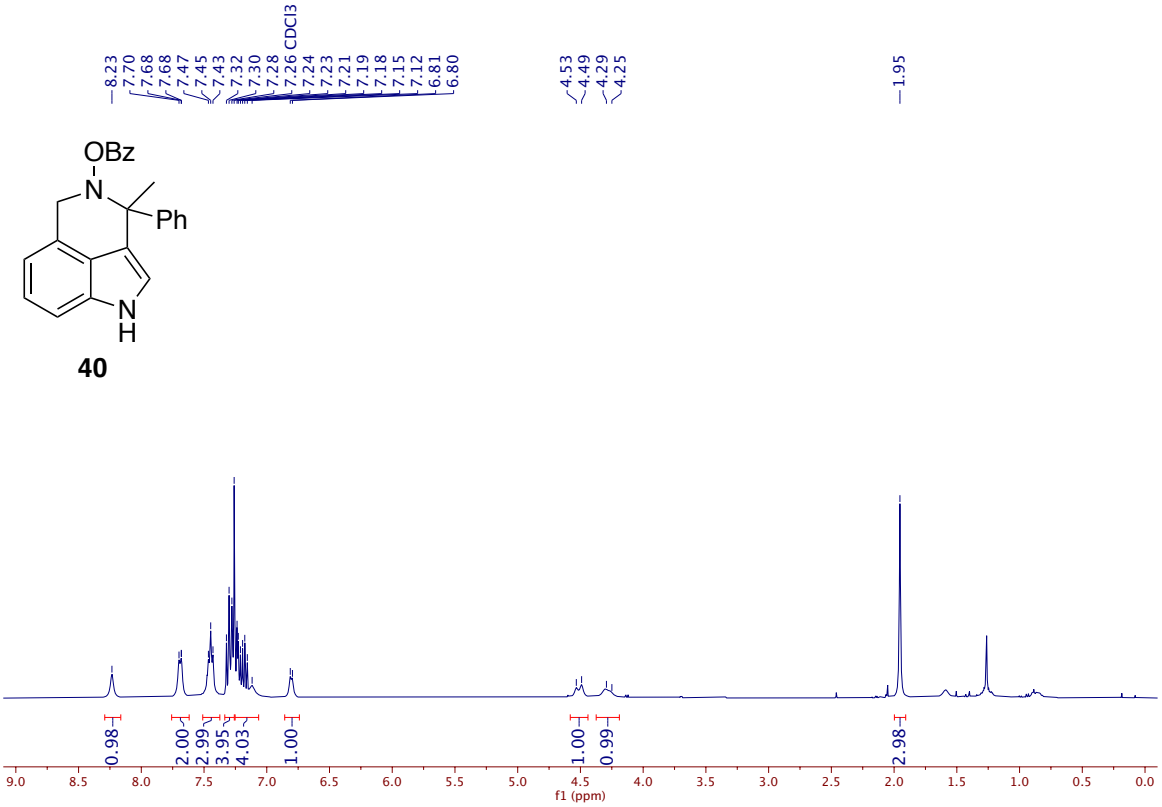
8.23
7.70
7.68
7.68
7.47
7.45
7.43
7.32
7.30
7.28
7.26 CDCl3
7.24
7.23
7.21
7.19
7.18
7.15
7.12
6.81
6.80
4.53
4.49
4.29
4.25
1.95
OBz
N
Ph
N
H
0.98
2.00
2.99
3.95
4.03
1.00
1.00
0.99
2.98
f1 (ppm)

40

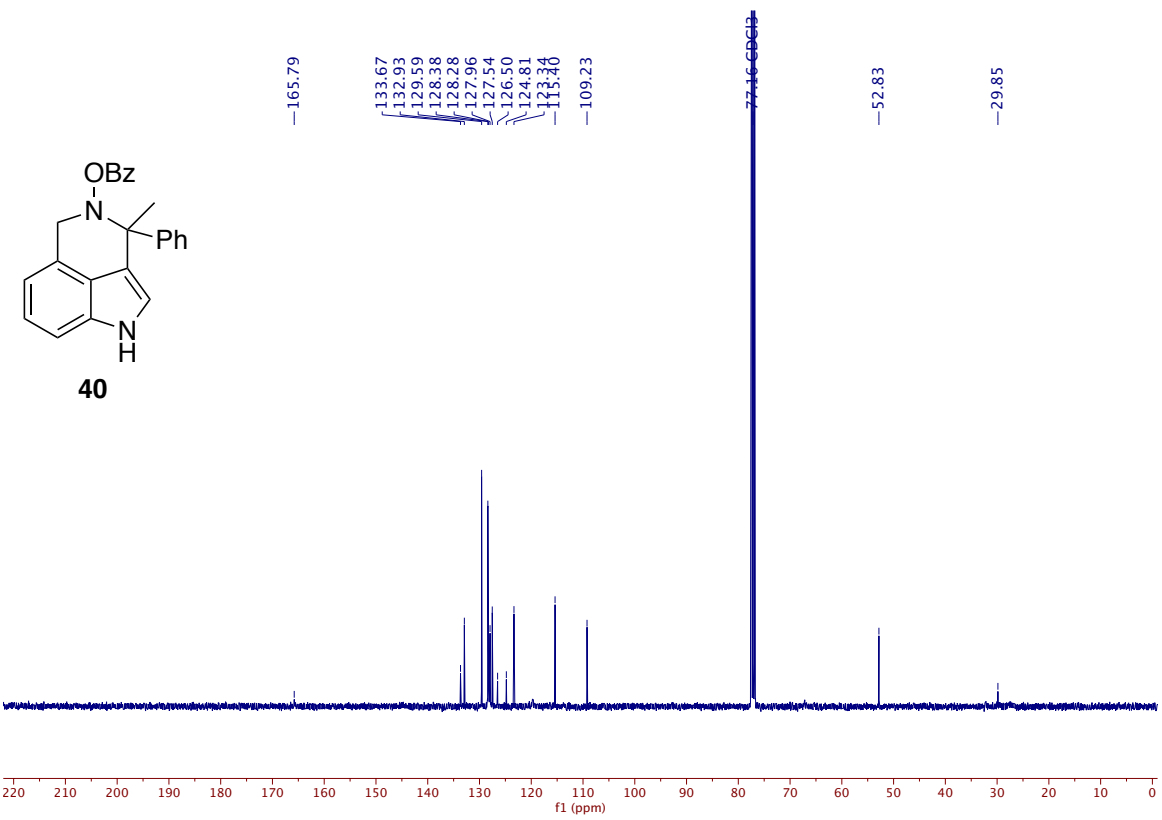
165.79
133.67
132.93
129.59
128.38
128.28
127.96
127.54
126.50
124.81
123.34
115.40
109.23
77.16 CDCl3
52.83
29.85
OBz
N
Ph
N
H
f1 (ppm)

40